Mathematics

A Conceptual Approach

Alison Chapman

Mathematics: A Conceptual Approach

Mathematics: A Conceptual Approach

Edited by
Alison Chapman

Published by The English Press,
5 Penn Plaza,
19th Floor,
New York, NY 10001, USA

ISBN: 978-1-9789-7438-8

Cataloging-in-Publication Data

Mathematics : a conceptual approach / edited by Alison Chapman.
p. cm.
Includes bibliographical references and index.
ISBN 978-1-9789-7438-8
1. Mathematics. I. Chapman, Alison.

QA37.3 .M38 2021

510--dc23

Contents

Preface

Every book is a source of knowledge and this one is no exception. The idea that led to the conceptualization of this book was the fact that the world is advancing rapidly; which makes it crucial to document the progress in every field. I am aware that a lot of data is already available, yet, there is a lot more to learn. Hence, I accepted the responsibility of editing this book and contributing my knowledge to the community.

The discipline that focuses on the study of the topics like space, quantity, change and structure is referred to as mathematics. It plays an essential role in various important fields including finance, social science, engineering, medicine and natural science. The main branches of mathematics are applied mathematics and pure mathematics. Applied mathematics is a combination of specialized knowledge and mathematical science. It focuses on the application of mathematical methods through different fields like computer science, engineering, science, and business. Pure mathematics focuses on the study of the mathematical concepts. Algebra, number theory, arithmetic, mathematical analysis and geometry are a few of the most important areas of mathematics. This book is a valuable compilation of topics, ranging from the basic to the most complex advancements in the field of mathematics. Some of the diverse topics covered in this book address the varied branches that fall under this category. It is appropriate for students seeking detailed information in this area as well as for experts.

While editing this book, I had multiple visions for it. Then I finally narrowed down to make every chapter a sole standing text explaining a particular topic, so that they can be used independently. However, the umbrella subject sinews them into a common theme. This makes the book a unique platform of knowledge.

I would like to give the major credit of this book to the experts from every corner of the world, who took the time to share their expertise with us. Also, I owe the completion of this book to the never-ending support of my family, who supported me throughout the project.

Editor

WT

A Mathematical Model for Coinfection of Listeriosis and Anthrax Diseases

Shaibu Osman [1] **and Oluwole Daniel Makinde** [2]

[1] *Department of Mathematics, Pan African University, Institute for Basic Sciences, Technology and Innovations, Box 62000-00200, Nairobi, Kenya*
[2] *Faculty of Military Science, Stellenbosch University, Private Bag X2, Saldanha 7395, South Africa*

Correspondence should be addressed to Shaibu Osman; shaibuo@yahoo.com

Academic Editor: Ram N. Mohapatra

Listeriosis and Anthrax are fatal zoonotic diseases caused by Listeria monocytogene and Bacillus Anthracis, respectively. In this paper, we proposed and analysed a compartmental Listeriosis-Anthrax coinfection model describing the transmission dynamics of Listeriosis and Anthrax epidemic in human population using the stability theory of differential equations. Our model revealed that the disease-free equilibrium of the Anthrax model only is locally stable when the basic reproduction number is less than one. Sensitivity analysis was carried out on the model parameters in order to determine their impact on the disease dynamics. Numerical simulation of the coinfection model was carried out and the results are displayed graphically and discussed. We simulate the Listeriosis-Anthrax coinfection model by varying the human contact rate to see its effects on infected Anthrax population, infected Listeriosis population, and Listeriosis-Anthrax coinfected population.

1. Introduction

Listeriosis and Anthrax are fatal zoonotic diseases caused by Listeria monocytogene and Bacillus Anthracis, respectively. Listeriosis in infants can be acquired in two forms. Mothers usually acquire it after eating foods that are contaminated with Listeria monocytogenes and can develop sepsis resulting in chorioamnionitis and delivering a septic infant or fetus. Moreover, mothers carrying the pathogens in the gastrointestinal tract can infect the skin and respiratory tract of their babies during childbirth. Listeria monocytogenes are among the commonest pathogens responsible for bacterial meningitis among neonates. Responsible factors for the disease include induced immune suppression linked with HIV infection, hemochromatosis hematologic malignancies, cirrhosis, diabetes, and renal failure with hemodialysis [1].

Authors in [2] developed a model for Anthrax transmission but never considered the transmissions in both animal and human populations. Our model is an improvement of the work done by authors in [2, 3]. Both formulated Anthrax models but only concentrated on the disease transmissions in animals cases only. Anthrax disease is caused by bacteria infections and it affects both humans and animals. Our model is an improvement of the two models as we considered Anthrax as a zoonotic disease and also looked at sensitivity analysis and the effects of the contact rate on the disease transmissions.

Authors in [4] published a paper on the effectiveness of constant and pulse vaccination policies using SIR model. The analysis of their results under constant vaccination showed that the dynamics of the disease model is similar to the dynamics without vaccination [5, 6]. There are some findings on the spread of zoonotic diseases but a number of these researches focused on the effect of vaccination on the spread and transmission of the diseases as in the case of the authors in [7]. Moreover, authors in [8] investigated a disease transmission model by considering the impact of a protective vaccine and came up with the optimal vaccine coverage threshold required for disease eradication. However, authors in [9] employed optimal control to study a nonlinear SIR epidemic model with a vaccination strategy. Several mathematical modeling techniques have been employed to

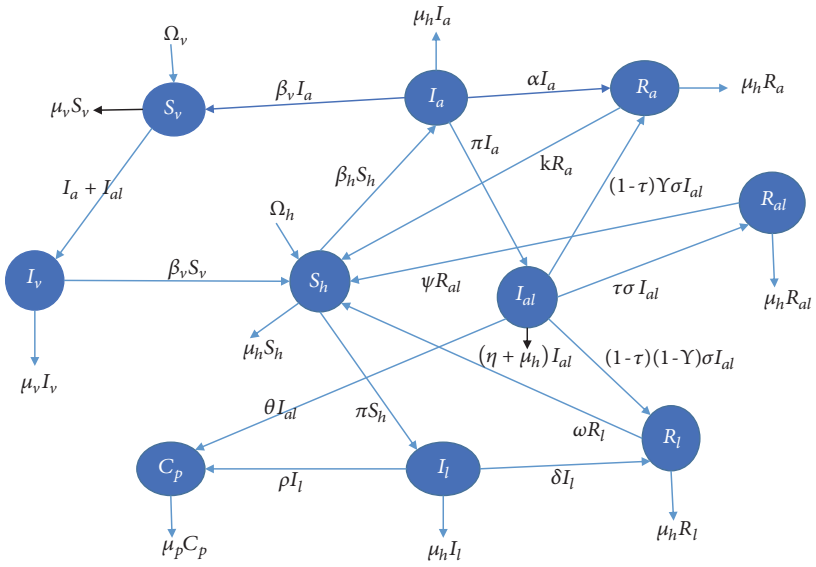

Figure 1: Flowchart for the coinfection model.

study the role of optimal control using SIR epidemic model [10–12]. Authors in [13] formulated an SIR epidemic model by considering vaccination as a control measure in their model analysis. Authors in [14] developed a mathematical model for the transmission dynamics of Listeriosis in animal and human populations but did not use optimal control as a control measure in fighting the disease. They divided the animal population into four compartments by introducing the vaccination compartment.

Authors in [15] formulated a model and employed optimal control to investigate the impact of chemotherapy on malaria disease with infection immigrants and [16] applied optimal control methods associated with preventing exogenous reinfection based on a exogenous reinfection tuberculosis model. Authors in [17] conducted a research on the identification and reservoirs of pathogens for effective control of sporadic disease and epidemics. Listeria monocytogenes is among the major zoonotic food borne pathogen that is responsible for approximately twenty-eight percent of most food-related deaths in the United States annually and a major cause of serious product recalls worldwide. The dairy farm has been observed as a potential point and reservoir for Listeria monocytogenes.

Models are widely used in the study of transmission dynamics of infectious diseases. In recent times, the application of mathematical models in the study of infectious diseases has increased tremendously. Hence the emergence of a branch called mathematical epidemiology. Frequent diagnostic tests, the availability of clinical data, and electronic surveillance have facilitated the applications of mathematical models to critical examining of scientific hypotheses and the design of real-life strategies of controlling diseases [18, 19].

Authors in [20] constructed a coinfection model of malaria and cholera diseases with optimal control but never considered sensitivity analysis and analysis of the force of infection. Sensitivity analysis determines the most sensitive parameters to the model and the analysis of the force of infections determines the effects of the contact rate on the disease transmissions.

2. Model Formulation

In this section, we divide the model into subcompartments (groups) as shown in Figure 1. The total human population (N_h) is divided into subcompartments consisting of susceptible humans (S_h), individuals that are infected with Anthrax(I_a), individuals that are infected with Listeriosis (I_l), individuals that are infected with both Anthrax and Listeriosis (I_{al}), and those that have recovered from Anthrax, Listeriosis, and both Anthrax and Listeriosis, respectively, (R_a), (R_l), and (R_{al}). The total vector population is represented by N_v; this is divided into subcompartments that consist of susceptible animals (S_v) and animals infected with Anthrax (I_v), where (C_p) is population of carcasses of animals in the soil that may have diet of Anthrax. Carcasses of animals which may have not been properly disposed of have the tendency of generating pathogens. The total vector and human populations are represented as

$$\begin{aligned} N_h &= S_h + I_a + I_l + I_{al} + R_a + R_l + R_{al}. \\ N_h &= S_v + I_v, \end{aligned} \tag{1}$$

where $\pi = C_p\nu/(k + C_p)$.

The concentration of carcasses and ingestion rate are denoted as K and ν, respectively. Listeriosis related death rates are m and η, respectively, and Anthrax related death rates are ϕ and n, respectively. Waning immunity rates are given by ω, k, and ψ.α, δ, and σ are the recovery rates, respectively, and $\tau(1-\sigma)$ are the bi-infected persons who have recovered from Anthrax only. The natural death rates of human and vector populations are μ_h and μ_v, respectively, and the modification parameter is given by θ. The coinfected persons who have

recovered from Listeriosis are denoted by $(1-\tau)(1-\sigma)$. This implies that

$$\sigma + \tau(1-\sigma) + (1-\tau)(1-\sigma) = 1. \tag{2}$$

The following differential equations were obtained from the flowchart diagram of the coinfection model in Figure 1:

$$\begin{aligned}
\frac{dS_h}{dt} &= \Omega_h + kR_a + \omega R_l + \psi R_{al} - \beta_h I_v S_h - \pi S_h - \mu_h S_h \\
\frac{dI_a}{dt} &= \beta_h I_v S_h - \pi I_a - (\alpha + \mu_h + \phi) I_a \\
\frac{dI_l}{dt} &= \pi S_h - \beta_l I_v I_l - (\delta + \mu_h + m + \rho) I_l \\
\frac{dI_{al}}{dt} &= \beta_h I_v I_l + \pi I_a + (\sigma + \mu_h + \eta + \theta) I_{al} \\
\frac{dR_a}{dt} &= \alpha I_a - (k + \mu_h) R_a + (1-\tau)\gamma\sigma I_{al} \\
\frac{dR_l}{dt} &= \delta I_l - (\omega + \mu_h) R_l + (1-\tau)(1-\gamma)\sigma I_{al} \\
\frac{dR_{al}}{dt} &= \tau\sigma I_{al} - (\psi + \mu_h) R_{al} \\
\frac{dC_p}{dt} &= \rho I_l + \theta I_{al} - \mu_b C_p \\
\frac{dS_v}{dt} &= \Omega_v - \beta_v (I_a + I_{al}) S_v - \mu_v S_v \\
\frac{dI_v}{dt} &= \beta_v (I_a + cI) S_v - \mu_v I_v
\end{aligned} \tag{3}$$

3. Analysis of Listeriosis Only Model

In this section, only the Listeriosis model is considered in the analysis of the transmission dynamics.

$$\begin{aligned}
\frac{dS_h}{dt} &= \Omega_h + \omega R_l - \pi S_h - \mu_h S_h \\
\frac{dI_l}{dt} &= \pi S_h - (\delta + \mu_h + m) I_l \\
\frac{dR_l}{dt} &= \delta I_l - (\omega + \mu_h) R_l \\
\frac{dC_p}{dt} &= \rho I_l - \mu_b C_p
\end{aligned} \tag{4}$$

3.1. Disease-Free Equilibrium. We obtain the disease-free equilibrium of the Listeriosis only model by setting the system of equations in (4) to zero. At disease-free equilibrium, there are no infections and recovery.

$$\begin{aligned}
&\Omega_h + \omega R_l - \pi S_h - \mu_h S_h = 0 \\
&S_h = \frac{\Omega_h}{\mu_h} \\
&\xi_{0l} = \left(S_h^*, I_l^*, R_l^*, C_p^*\right) = \left(\frac{\Omega_h}{\mu_h}, 0, 0, 0\right).
\end{aligned} \tag{5}$$

3.2. Basic Reproduction Number. In this section, the concept of the Next-Generation Matrix would be employed in computing the basic reproduction number. Using the theorem in Van den Driessche and Watmough [21] on the Listeriosis model in (4), the basic reproduction number of the Listeriosis only model, $(\mathfrak{R}_{0l})$, is given by

$$\mathfrak{R}_{0l} = \frac{\nu\rho\Omega_h}{\mu_b\mu_h K(\delta + \mu_h + m)} \tag{6}$$

3.3. Existence of the Disease-Free Equilibrium

3.4. Endemic Equilibrium. The endemic equilibrium points are computed by setting the system of differential equations in the Listeriosis only model (4) to zero. The endemic equilibrium points are as follows:

$$\begin{aligned}
S_h^* &= \frac{\Omega_h + \omega R_l^*}{\mu_h + \pi^*}, \\
I_l^* &= \frac{\pi^* S_h^*}{(\delta + \mu_h + m)}, \\
R_l^* &= \frac{\delta I_l^*}{\omega + \mu_h}, \\
C_p^* &= \frac{\rho I_l^*}{\mu_b}.
\end{aligned} \tag{7}$$

$$\begin{aligned}
\xi_{0l} &= \left(S_h^*, I_l^*, R_l^*, C_p^*\right) \\
&= \left(\frac{\Omega_h + \omega R_l^*}{\mu_h + \pi^*}, \frac{\pi^* S_h^*}{(\delta + \mu_h + m)}, \frac{\delta I_l^*}{\omega + \mu_h}, \frac{\rho I_l^*}{\mu_b}\right).
\end{aligned}$$

$$\begin{aligned}
S_h^* &= \frac{\Omega_h + \omega R_l^*}{\mu_h + \pi^*} \\
I_l^* &= \frac{\pi^* S_h^*}{(\delta + \mu_h + m)} \\
R_l^* &= \frac{\delta I_l^*}{\omega + \mu_h} \\
C_p^* &= \frac{\rho I_l^*}{\mu_b}
\end{aligned} \tag{8}$$

3.5. Existence of the Endemic Equilibrium

Lemma 1. *The Listeriosis only model has a unique endemic equilibrium if and only if the basic reproduction number* $\mathfrak{R}_{0l} > 1$.

Proof. The Listeriosis force of infection, $(\pi = C_p\nu/(K + C_p))$, satisfies the polynomial;

$$P(\pi^*) = A(\pi^*)^2 + B(\pi^*) = 0 \tag{9}$$

where $A = \Omega_h\rho(\omega + \mu_h) + \mu_b K(m(\omega + \mu_h) + \mu_h(\delta + \mu_h + \omega))$, and

$$B = (\omega + \mu_h)(1 - R_{0l}). \tag{10}$$

By mathematical induction, $A > 0$ and $B > 0$ whenever the basic reproduction number is less than one ($\mathfrak{R}_{0l} < 1$). This implies that $\pi^* = -B/A \leq 0$. In conclusion, the Listeriosis model has no endemic equilibrium and the basic reproductive number is less than one ($\mathfrak{R}_{0l} < 1$). □

The analysis illustrates the impossibility of backward bifurcation in the Listeriosis model, because there is no existence of endemic equilibrium whenever the basic reproduction number is less than one ($\mathfrak{R}_{0l} < 1$).

4. Analysis of Anthrax Only Model

In this section, only the Anthrax model is considered in the analysis of the transmission dynamics.

$$\begin{aligned}
\frac{dS_h}{dt} &= \Omega_h + kR_a - \beta_h I_v S_h - \mu_h S_h \\
\frac{dI_a}{dt} &= \beta I_v S_h - (\alpha + \mu_h + \phi) I_a \\
\frac{dR_a}{dt} &= \alpha I_a - (k + \mu_h) R_a \\
\frac{dS_v}{dt} &= \Omega_v - \beta_v I_a S_v - \mu_v S_v \\
\frac{dI_v}{dt} &= \beta_v I_a S_v - \mu_v I_v
\end{aligned} \tag{11}$$

4.1. Disease-Free Equilibrium. The disease-free equilibrium of the Anthrax only model is obtained by setting the system of equations in model (11) to zero. At disease-free equilibrium, there are no infections and recovery.

$$\begin{aligned}
&\Omega_h + kR_a - \beta_h I_v S_h - \mu_h S_h = 0 \\
&S_h = \frac{\Omega_h}{\mu_h}. \\
&\Omega_v - \beta_v I_a S_v - \mu_v S_v = 0 \\
&S_v = \frac{\Omega_v}{\mu_v}.
\end{aligned} \tag{12}$$

$$\xi_{0a} = (S_h^*, I_a^*, R_a^*, S_v^*, I_v^*) = \left(\frac{\Omega_h}{\mu_h}, 0, 0, \frac{\Omega_v}{\mu_v}, 0\right). \tag{13}$$

4.2. Basic Reproduction Number. In this section, the concept of the Next-Generation Matrix would be employed in computing the basic reproduction number. Using the theorem in Van den Driessche and Watmough [21] on the Anthrax model in (11), the basic reproduction number of the Anthrax only model, ($\mathfrak{R}_{0a}$), is given by

$$\mathfrak{R}_{0a} = \sqrt{\frac{\Omega_h \Omega_v \beta_h \beta_v}{\mu_h \mu_v^2 (\alpha + \mu_h + \phi)}} \tag{14}$$

4.3. Stability of the Disease-Free Equilibrium. Using the next-generation operator concept in Van den Driessche and Watmough [21] on the systems of equations in model (11), the linear stability of the disease-free equilibrium, (ξ_{0a}), can be ascertained. The disease-free equilibrium is locally asymptotically stable whenever the basic reproduction number is less than one ($\mathfrak{R}_{0a} < 1$). And it is unstable whenever the basic reproduction number is greater than one ($\mathfrak{R}_{0a} > 1$). The disease-free equilibrium is the state at which there are no infections in the system. At disease-free equilibrium, there are no infections in the system.

4.4. Endemic Equilibrium. The endemic equilibrium points are computed by setting the system of differential equations in the Anthrax only model (11) to zero. The endemic equilibrium points are as follows:

$$\begin{aligned}
S_h &= \frac{\Omega_h + kR_a^*}{\mu_h + \beta_h I_v^*}, \\
I_a^* &= \frac{\beta_v S_h^* I_v^*}{(\alpha + \mu_h + \phi)}, \\
R_a^* &= \frac{\alpha I_a^*}{k + \mu_h}, \\
S_v^* &= \frac{\Omega_v}{\mu_v + \beta_v I_a^*}, \\
I_v^* &= \frac{\beta_v S_v^* I_a^*}{\mu_v}.
\end{aligned} \tag{15}$$

The endemic equilibrium of the Anthrax only model is given by

$$\begin{aligned}
\xi_{0a} = (S_h^*, I_a^*, R_a^*, S_v^*, I_v^*) = \Bigg(&\frac{\Omega_h + kR_a^*}{\mu_h + \beta_h I_v^*}, \frac{\beta_v S_h^* I_v^*}{(\alpha + \mu_h + \phi)}, \\
&\frac{\alpha I_a^*}{k + \mu_h}, \frac{\Omega_v}{\mu_v + \beta_v I_a^*}, \frac{\beta_v S_v^* I_a^*}{\mu_v}.\Bigg)
\end{aligned} \tag{16}$$

$$\begin{aligned}
\xi_{0a} = \Bigg(&\frac{\Omega_h + kR_a^*}{\mu_h + \beta_h I_v^*}, \frac{\beta_v S_h^* I_v^*}{(\alpha + \mu_h + \phi)}, \frac{\alpha I_a^*}{k + \mu_h}, \frac{\Omega_v}{\mu_v + \beta_v I_a^*}, \\
&\frac{\beta_v S_v^* I_a^*}{\mu_v}.\Bigg)
\end{aligned} \tag{17}$$

4.5. Existence of the Endemic Equilibrium

Lemma 2. *The Anthrax only model has a unique endemic equilibrium whenever the basic reproduction number* ($\mathfrak{R}_{0a}$) *is greater than one* ($\mathfrak{R}_{0a} > 1$).

Proof. Considering the endemic equilibrium points of the Anthrax only model,

$$\begin{aligned}
\xi_{0a} = \Bigg(&\frac{\Omega_h + kR_a^*}{\mu_h + \beta_h I_v^*}, \frac{\beta_v S_h^* I_v^*}{(\alpha + \mu_h + \phi)}, \frac{\alpha I_a^*}{k + \mu_h}, \frac{\Omega_v}{\mu_v + \beta_v I_a^*}, \\
&\frac{\beta_v S_v^* I_a^*}{\mu_v}\Bigg).
\end{aligned} \tag{18}$$

The endemic equilibrium point satisfies the given polynomial

$$P\left(I_a^*\right) = A_1\left(I_a^*\right)^2 + B_1\left(I_a^*\right) = 0 \tag{19}$$

where

$$\begin{aligned} A_1 = {} & \beta_v\left(\Omega_v\beta_h\left(k\phi + \mu_h\left(\alpha + k + \phi + \mu_h\right)\right)\right. \\ & \left. + \mu_h\left(k + \mu_h\right)\left(\alpha + \phi + \mu_h\right)\mu_v\right) \end{aligned} \tag{20}$$

and

$$B_1 = \left(k + \mu_h\right)\left(1 - R_{0a}^2\right). \tag{21}$$

By mathematical induction, $A_1 > 0$ and $B_1 > 0$ whenever the basic reproduction number is less than one ($\mathfrak{R}_{0a} < 1$). This implies that $I_a^* = -B_1/A_1 \leq 0$. In conclusion, the Anthrax only model has no endemic any time the basic reproductive number is less than one ($\mathfrak{R}_{0a} < 1$). □

The analysis illustrates the impossibility of backward bifurcation in the Anthrax only model. Because there is no existence of endemic equilibrium whenever the basic reproduction number is less than one ($\mathfrak{R}_{0a} < 1$).

5. Anthrax-Listeriosis Coinfection Model

In this section, the dynamics of the Anthrax-Listeriosis coinfection model in (3) is considered in the analysis of the transmission dynamics.

5.1. Disease-Free Equilibrium. The disease-free equilibrium of the Anthrax-Listeriosis model is obtained by setting the system of equations of model (3) to zero. At disease-free equilibrium, there are no infections and recovery.

$$\begin{aligned} \Omega_h + kR_a + \omega R_l + \psi R_{al} - \beta_h I_v S_h - \pi S_h - \mu_h S_h = 0 \\ S_h^* = \frac{\Omega_h}{\mu_h} \\ \Omega_v - \beta_v\left(I_a + cI_{al}\right)S_v - \mu_v S_v = 0 \\ S_v^* = \frac{\Omega_v}{\mu_v} \end{aligned} \tag{22}$$

The disease-free equilibrium is given by

$$\xi_{0al} = \left(S_h^*, I_l^*, I_a^*, I_{al}^*, R_l^*, R_a^*, R_{al}^*, C_p^*, S_v^*, I_v^*\right) \tag{23}$$

$$\xi_{0al} = \left(\frac{\Omega_h}{\mu_h}, 0, 0, 0, 0, 0, 0, 0, \frac{\Omega_v}{\mu_v}, 0\right) \tag{24}$$

5.2. Basic Reproduction Number. The concept of the next-generation operator method in Van den Driessche and Watmough [21] was employed on the system of differential equations in model (3) to compute the basic reproduction number of the Anthrax-Listeriosis coinfection model. The Anthrax-Listeriosis coinfection model has a reproduction number ($\mathfrak{R}_{al}$) given by

$$\mathfrak{R}_{al} = \max\left\{\mathfrak{R}_a, \mathfrak{R}_l\right\} \tag{25}$$

where $\mathfrak{R}_a$ and $\mathfrak{R}_l$ are the basic reproduction numbers of Anthrax and Listeriosis, respectively.

$$\mathfrak{R}_a = \sqrt{\frac{\Omega_h\Omega_v\beta_h\beta_v}{\mu_h\mu_v^2\left(\alpha + \mu_h + \phi\right)}} \tag{26}$$

and

$$\mathfrak{R}_l = \frac{\nu\rho\Omega_h}{\mu_b\mu_h K}\left(\frac{\left(\sigma + \mu_h + \eta + \theta\right) + \theta\left(\delta + \mu_h + m\right)}{\left(\delta + \mu_h + m\right)\left(\sigma + \mu_h + \eta + \theta\right)}\right) \tag{27}$$

Theorem 3. *The disease-free equilibrium (ξ_{0al}) is locally asymptotically stable whenever the basic reproduction number is less than one ($\mathfrak{R}_{al} < 1$) and unstable otherwise.*

5.3. Impact of Listeriosis on Anthrax. In this section, the impact of Listeriosis on Anthrax and vice versa is analysed. This is done by expressing the reproduction number of one in terms of the other by expressing the basic reproduction number of Listeriosis on Anthrax, that is, expressing $\mathfrak{R}_l$ in terms of $\mathfrak{R}_a$

from $\mathfrak{R}_a = \sqrt{\Omega_h\Omega_v\beta_h\beta_v/\mu_h\mu_v^2(\alpha + \mu_h + \phi)}$.

Solving for μ_h in the above,

$$\mu_h = \frac{-G_1\mathfrak{R}_a + \sqrt{G_1^2\mathfrak{R}_a^2 + 4G_2}}{2\mu_v\mathfrak{R}_a}, \tag{28}$$

where

$$\begin{aligned} G_1 &= \mu_v\left(\alpha + \phi\right) \\ \text{and } G_2 &= \Omega_h\Omega_v\beta_h\beta_v \end{aligned} \tag{29}$$

Also, letting

$$\sqrt{G_1^2\mathfrak{R}_a^2 + 4G_2} = G_3\mathfrak{R}_a + G_4, \tag{30}$$

this implies

$$\mu_h = \frac{\mathfrak{R}_a\left(G_3 - G_1\right) + G_4}{2\mu_v\mathfrak{R}_a} \tag{31}$$

By substituting μ_h into the basic reproduction number of Listeriosis ($\mathfrak{R}_l$),

$$\mathfrak{R}_l = \frac{\mathfrak{R}_{0l}\left(G_4 + \left(G_3 - G_1\right)\mathfrak{R}_a + 2\left(\sigma + \eta + \theta\right)\mu_v\mathfrak{R}_a + \theta\left(G_4 + \left(G_3 - G_1\right)\mathfrak{R}_a + 2\left(m + \delta\right)\mu_v\mathfrak{R}_a\right)\right)}{G_4 + \left(G_3 - G_1\right)\mathfrak{R}_a + 2\left(\sigma + \eta + \theta\right)\mu_v\mathfrak{R}_a} \tag{32}$$

where the basic reproduction number of Listeriosis only model (R_{0l}) is given in the relation

$$\mathfrak{R}_{0l} = \frac{\nu\rho\Omega_h}{\mu_b\mu_h K\left(\delta+\mu_h+m\right)}. \tag{33}$$

Now, taking the partial derivative of $\mathfrak{R}_l$ with respect to $\mathfrak{R}_a$ in (32) gives

$$\frac{\partial\mathfrak{R}_l}{\partial\mathfrak{R}_a} = \frac{2G_4\theta\left(m+\delta-\left(\sigma+\eta+\theta\right)\right)\mu_v\mathfrak{R}_{0l}}{\left[G_4+\left(G_3-G_1+2\left(\sigma+\eta+\theta\right)\mu_v\mathfrak{R}_a\right)\right]^2}. \tag{34}$$

If $(m+\delta)\geq(\sigma+\eta+\theta)$, the derivative $(\partial\mathfrak{R}_l/\partial\mathfrak{R}_a)$, is strictly positive. Two scenarios can be deduced from the derivative $(\partial\mathfrak{R}_l/\partial\mathfrak{R}_a)$, depending on the values of the parameters:

$$\begin{aligned}&\frac{\partial\mathfrak{R}_l}{\partial\mathfrak{R}_a}=0,\\ \text{and }&\frac{\partial\mathfrak{R}_l}{\partial\mathfrak{R}_a}\geq 0.\end{aligned} \tag{35}$$

(1) If $\partial\mathfrak{R}_l/\partial\mathfrak{R}_a=0$, it implies that $(m+\delta)=(\sigma+\eta+\theta)$ and the epidemiological implication is that Anthrax has no significance effect on the transmission dynamics of Listeriosis.

(2) If $\partial\mathfrak{R}_l/\partial\mathfrak{R}_a>0$, it implies that $(m+\delta)\geq(\sigma+\eta+\theta)$, and the epidemiological implication is that an increase in Anthrax cases would result in an increase Listeriosis cases in the environment. That is Anthrax enhances Listeriosis infections in the environment.

However, by expressing the basic reproduction number of Anthrax on Listeriosis, that is expressing $\mathfrak{R}_a$ in terms of $\mathfrak{R}_l$,

$$\mu_h = \frac{H_1-H_2\mathfrak{R}_l+\sqrt{H_3\mathfrak{R}_l^2+H_4\mathfrak{R}_l+H_5}}{2\mathfrak{R}_l}, \tag{36}$$

where

$$\begin{aligned}H_1&=(1+\theta)\,\mathfrak{R}_{0l},\\ H_2&=\left(m+\delta+\sigma+\eta+\theta\right)\\ H_3&=\left(\sigma+\eta+\theta-m-\delta\right),\\ H_4&=2\left(\theta-1\right)\left(m+\delta-\sigma-\eta-\theta\right)\mathfrak{R}_{0l}\\ H_1&=(1+\theta)^2\,\mathfrak{R}_{0l}^2.\end{aligned} \tag{37}$$

By letting

$$\sqrt{H_3\mathfrak{R}_l^2+H_4\mathfrak{R}_l+H_5}=H_6\mathfrak{R}_l+H_7, \tag{38}$$

it implies that

$$\mu_h=\frac{\left(H_6-H_2\right)\mathfrak{R}_l+H_7+H_1}{2\mathfrak{R}_l}. \tag{39}$$

Therefore,

$$\mathfrak{R}_a^2=\frac{4\Omega_h\Omega_v\beta_h\beta_v\mathfrak{R}_l^2}{\left[\left(H_6-H_2\right)\mathfrak{R}_l+H_7+H_1\right]\left[H_7+H_1+2\left(\alpha+\phi\right)\mathfrak{R}_l+\left(H_6-H_2\right)\mathfrak{R}_l\right]\mu_v} \tag{40}$$

Now, taking the partial derivative of $\mathfrak{R}_a$ with respect to $\mathfrak{R}_l$ in equation (40) gives

$$\frac{\partial\mathfrak{R}_a}{\partial\mathfrak{R}_l}=\frac{4\left(H_7+H_1\right)\left[H_7+H_1+\left(\alpha+\phi+H_6-H_2\right)\mathfrak{R}_l\right]\Omega_h\Omega_v\beta_h\beta_v\mathfrak{R}_l}{\left[\left(H_6-H_2\right)\mathfrak{R}_l+H_7+H_1\right]^2\left[H_7+H_1+\left(2\left(\alpha+\phi\right)+H_6-H_2\right)\mathfrak{R}_l\right]^2\mu_v} \tag{41}$$

If the partial derivative of $\mathfrak{R}_a$ with respect to $\mathfrak{R}_l$ is greater than zero, $(\partial\mathfrak{R}_a/\partial\mathfrak{R}_l>0)$, the biological implication is that an increase in the number of cases of Listeriosis would result in an increase in the number of cases of Anthrax in the environment. Moreover, the impact of Anthrax treatment on Listeriosis can also be analysed by taking the partial derivative of $\mathfrak{R}_a$ with respect to α, $(\partial\mathfrak{R}_a/\partial\alpha)$.

$$\frac{\partial\mathfrak{R}_a}{\partial\alpha}=-\frac{\alpha}{\alpha+\phi+\mu_h}. \tag{42}$$

Clearly, $\mathfrak{R}_a$ is a decreasing function of α; the epidemiological implication is that the treatment of Listeriosis would have an impact on the transmission dynamics of Anthrax.

5.4. Analysis of Backward Bifurcation. In this section, the phenomenon of backward bifurcation is carried out by employing the center manifold theory on the system of differential equations in model (3). Bifurcation analysis was carried out by employing the center manifold theory in Castillo-Chavez and Song [22]. Considering the human transmission rate (β_h) and ν as the bifurcation parameters, it implies that $\mathfrak{R}_a=1$ and $\mathfrak{R}_l=1$ if and only if

$$\beta_h=\beta_h^*=\frac{\mu_h\mu_v^2\left(\alpha+\phi+\mu_h\right)}{\Omega_h\Omega_v\beta_v}, \tag{43}$$

and

$$v = v^* = \frac{\mu_b \mu_h K (\delta + \mu_h + m)(\sigma + \mu_h + \eta + \theta)}{\rho \Omega_h (\sigma + \mu_h + \eta + \theta + \theta (m + \delta + \mu_h))}. \quad (44)$$

By considering the following change of variables,

$$\begin{aligned} S_h &= x_1, \\ I_a &= x_2, \\ I_l &= x_3, \\ I_{al} &= x_4, \\ R_a &= x_5, \\ R_l &= x_6, \\ R_{al} &= x_7, \\ C_p &= x_8, \\ S_v &= x_9, \\ I_v &= x_{10}. \end{aligned} \quad (45)$$

This would give the total population as

$$N = x_1 + x_2 + x_3 + x_4 + x_5 + x_6 + x_7 + x_8 + x_9 + x_{10}. \quad (46)$$

By applying vector notation

$$X = (x_1, x_2, x_3, x_4, x_5, x_6, x_7, x_8, x_9, x_{10})^T. \quad (47)$$

The Anthrax-Listeriosis coinfection model can be expressed as

$$\frac{dX}{dt} = F(X), \quad \text{where } F = (f_1, f_2, f_3, f_4, f_5, f_6, f_7, f_8, f_9, f_{10})^T. \quad (48)$$

The following system of differential equations is obtained:

$$\begin{aligned} \frac{dx_1}{dt} &= \Omega_h + k x_5 + \omega x_6 + \psi x_7 - \beta_h x_{10} x_1 - \pi x_1 - \mu_h x_1 \\ \frac{dx_2}{dt} &= \beta_h x_{10} x_1 - \pi x_2 - (\alpha + \mu_h + \phi) x_2 \\ \frac{dx_3}{dt} &= \pi x_1 - \beta_l x_{10} x_3 - (\delta + \mu_h + m + \rho) x_3 \\ \frac{dx_4}{dt} &= \beta_l x_{10} x_3 + \pi x_2 + (\sigma + \mu_h + \eta + \theta) x_4 \\ \frac{dx_5}{dt} &= \alpha x_2 - (k + \mu_h) x_5 + (1 - \tau) \gamma \sigma x_4 \\ \frac{dx_6}{dt} &= \delta x_3 - (\omega + \mu_h) x_6 + (1 - \tau)(1 - \gamma) \sigma x_4 \\ \frac{dx_7}{dt} &= \tau \sigma x_4 - (\psi + \mu_h) x_7 \\ \frac{dx_8}{dt} &= \rho x_3 + \theta x_4 - \mu_b x_8 \\ \frac{dx_9}{dt} &= \Omega_v - \beta_v (x_2 + x_4) x_9 - \mu_v x_9 \\ \frac{dx_{10}}{dt} &= \beta_v (x_2 + x_4) x_9 - \mu_v x_{10} \end{aligned} \quad (49)$$

Backward bifurcation is carried out by employing the center manifold theory on the system of differential equations in model (3). This concept involves the computation of the Jacobian of the system of differential equations in (49) at the disease-free equilibrium (ξ_0). The Jacobian matrix at disease-free equilibrium is given by

$$J(\xi_0) = \begin{bmatrix} -\mu_h & 0 & 0 & J_1 & k & \omega & \psi & J_2 & 0 & J_3 \\ 0 & -J_4 & 0 & 0 & 0 & 0 & 0 & 0 & 0 & J_3 \\ 0 & 0 & -J_5 & J_1 & 0 & 0 & 0 & J_2 & 0 & 0 \\ 0 & 0 & 0 & -J_6 & 0 & 0 & 0 & 0 & 0 & 0 \\ 0 & \alpha & 0 & J_7 & -J_8 & 0 & 0 & 0 & 0 & 0 \\ 0 & 0 & \delta & J_9 & 0 & -J_{10} & 0 & 0 & 0 & 0 \\ 0 & 0 & 0 & \sigma & 0 & 0 & -J_{11} & 0 & 0 & 0 \\ 0 & 0 & \rho & \theta & 0 & 0 & 0 & -\mu_b & 0 & 0 \\ 0 & -J_{12} & 0 & -J_{12} & 0 & 0 & 0 & 0 & -\mu_v & 0 \\ 0 & J_{12} & 0 & J_{12} & 0 & 0 & 0 & 0 & 0 & -\mu_v \end{bmatrix} \quad (50)$$

where

$$\begin{aligned} J_1 &= \frac{\rho \Omega_h}{\mu_h}, \\ J_2 &= \frac{\mu_b (\delta + \mu_h + m)(\sigma + \mu_h + \eta + \theta)}{\rho (\sigma + \mu_h + \eta + \theta + \theta (\delta + \mu_h + m))}, \\ J_3 &= \frac{\mu_v^3 (\alpha + \phi + \mu_h)}{\Omega_v \beta_v}, \\ J_4 &= (\alpha + \phi + \mu_h), \\ J_5 &= (\delta + \mu_h + m), \\ J_6 &= (\sigma + \mu_h + \eta + \theta), \\ J_7 &= (1 - \tau) \gamma \sigma, \\ J_8 &= (k + \mu_h), \end{aligned}$$

$$J_9 = (1-\tau)(1-\gamma)\sigma,$$
$$J_{10} = (\omega + \mu_h),$$
$$J_{11} = (\psi + \mu_h)$$
$$\text{and } J_{12} = \frac{\Omega_v \beta_v}{\mu_v}. \tag{51}$$

Clearly, the Jacobian matrix at disease-free equilibrium has a case of simple zero eigenvalue as well as other eigenvalues with negative real parts. This is an indication that the center manifold theorem is applicable. By applying the center manifold theorem in Castillo-Chavez and Song [22], the left and right eigenvectors of the Jacobian matrix $J(\xi_0)$ are computed first. Letting the left and right eigenvector represented by

$$y = [y_1, y_2, y_3, y_4, y_5, y_6, y_7, y_8, y_9, y_{10}]$$
$$\text{and } w = [w_1, w_2, w_3, w_4, w_5, w_6, w_7, w_8, w_9, w_{10}]^T, \tag{52}$$

respectively, the following were obtained:

$$w_1 = \frac{K w_5}{\mu_h} + \frac{w_2 \mu_v^2 (\alpha + \phi + \mu_h)}{\mu_h},$$
$$w_2 = \frac{\mu_v^2}{\Omega_v \beta_v},$$
$$w_3 = w_4 = w_6 = w_7 = w_8 = 0,$$
$$w_5 = \frac{\alpha \mu_v^2}{\Omega_v \beta_v (k + \mu_h)}, \tag{53}$$
$$w_9 = -w_{10},$$
$$w_{10} = 1.$$

And

$$y_1 = y_3 = y_5 = y_6 = y_7 = y_8 = y_9 = 0,$$
$$y_2 = \frac{v_{10} \Omega_v \beta_v}{\mu_v (\alpha + \phi + \mu_h)},$$
$$y_2 = y_4, \tag{54}$$
$$y_{10} = \frac{-\mu_v (\sigma + \mu_h + \eta + \theta)}{\Omega_v \beta_v}.$$

Moreover, by further simplifications, it can be shown that

$$a = \frac{\tau w_{10} \mu_v^3 (\sigma + \mu_h + \eta + \theta)}{\Omega_v \beta_v} - 2 w_{10} \beta_v \left[\frac{\mu_v^2 (\sigma + \mu_h + \eta + \theta)}{\mu_h \Omega_v \beta_v} + \frac{\alpha K \mu_v^2 (\sigma + \mu_h + \eta + \theta)}{\mu_h \Omega_v \beta_v (k + \mu_h)(\alpha + \phi + \mu_h)} \right], \tag{55}$$
$$b = y_2 w_{10} \frac{\Omega_h}{\mu_h} > 0.$$

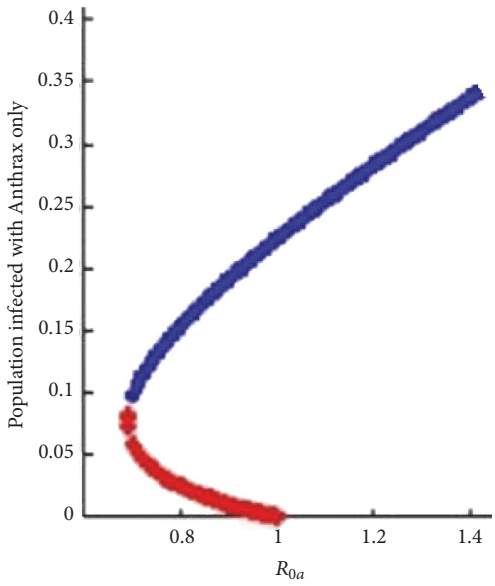

FIGURE 2: Simulation of the coinfection model showing the existence of backward bifurcation.

It can be deduced that the coefficient b would always be positive. Backward bifurcation will take place in the system of differential equations in (3) if the coefficient a is positive. In conclusion, it implies that the disease-free equilibrium is not globally stable.

Figure 2 shows the simulation of the coinfection model indicating the phenomenon of backward bifurcation as evidence to the model analysis. This phenomenon usually exists in cases where the disease-free equilibrium and the endemic equilibrium coexist. Epidemically, the implication is that the concept of whenever the basic reproduction number is less than unity, the ability to control the disease is no longer sufficient. Figure 2 confirms the analytical results which shows that endemic equilibrium exists when the basic reproduction number is greater than unity.

6. Sensitivity Analysis of the Coinfection Model

In this section, we performed the sensitivity analysis of the basic reproduction number of the coinfection model to each of the parameter values. This is to determine the significance or contribution of each parameter on the basic reproduction number. The sensitivity index of the basic reproduction number ($\mathfrak{R}_0$) to a parameter P is given by the relation

$$\Pi_P^{\mathfrak{R}_0} = \left(\frac{\partial \mathfrak{R}_0}{\partial P} \right) \left(\frac{P}{\mathfrak{R}_0} \right). \tag{56}$$

Sensitivity analysis of the basic reproduction number of Anthrax $\mathfrak{R}_{0a}$ and Listeriosis $\mathfrak{R}_{0a}$ to each of the parameter values was computed separately, since the basic reproduction number of the coinfection model is usually

$$\mathfrak{R}_0 = \max \{\mathfrak{R}_{0a}, \mathfrak{R}_{0l}\}. \tag{57}$$

Table 1: Sensitivity indices of $\mathfrak{R}_{0a}$ to each of the parameter values.

Parameter	Description	Sensitivity Index
Ω_h	Human recruitment rate	1.2164
Ω_v	Vector recruitment rate	0.2433
β_h	Human transmission rate	0.1216
β_v	Vector transmission rate	0.0243
α	Anthrax recovery rate	−0.0037
μ_h	Human natural death rate	−0.0122
μ_v	Vector natural death rate	−0.0061
ϕ	Anthrax related death rate	−0.0065
θ	Modification parameter	$3.42913 * 10^{-}6$

6.1. Sensitivity Indices of $\mathfrak{R}_{0a}$. In this section, we derive the sensitivity of $\mathfrak{R}_{0a}$, to each of the parameters. Table 1 shows the detailed sensitivity indices of the basic reproduction number of Anthrax ($\mathfrak{R}_{0a}$) to each of the parameter values. From the values in Table 1, it can be observed that the most sensitive parameters are human transmission rate, vector transmission rate, human recruitment rate, and vector recruitment rate. Since the basic reproduction number is less than one, increasing the human recruitment rate by 10% would increase the basic reproduction number of Anthrax by 12.164%. However, decreasing the human recruitment rate by 10% would decrease the basic reproduction number of Anthrax by 12.164%. Moreover, decreasing human and vector transmission rates by 10% would decrease the basic reproduction number of Anthrax by 1.216% and 0.243%, respectively. However, increasing human and vector transmission rates by 10% would increase the basic reproduction number of Anthrax by 1.216% and 0.243%, respectively. The sensitivity analysis determines the contribution of each parameter to the basic reproduction number. This is an improvement of the work done by authors in [2, 3].

6.2. Sensitivity Indices of $\mathfrak{R}_{0l}$. In this section, we derive the sensitivity of $\mathfrak{R}_{0l}$ to each of the parameters. The detailed sensitivity indices of the basic reproduction number of Listeriosis ($\mathfrak{R}_{0l}$) to each of the parameter values are shown in Table 2. We observe from the values in Table 2 that the most sensitive parameters are bacteria ingestion rate, Listeriosis related death, human recruitment rate, and Listeriosis contribution to environment. Decreasing the human recruitment rate by 10% would cause a decrease in the basic reproduction number of Listeriosis by 0.201487%. However, increasing the human recruitment rate by 10% would cause an increase in the basic reproduction number of Listeriosis by 0.201487%. Moreover, decreasing Listeriosis contribution to environment and bacteria ingestion rate by 10% would cause a decrease in the basic reproduction number of Listeriosis. Increasing Listeriosis contribution to environment and bacteria ingestion rate by 10% would cause an increase in the basic reproduction number of Listeriosis.

7. Numerical Methods and Results

In this section, we carried out the numerical simulations of the coinfection model to illustrate the results of the qualitative analysis of the model which has already been performed. The variable and parameter values in Table 3 were used in the simulation of the coinfection model in (3). For the purposes of illustrations, we assumed some of the parameter values. Table 3 shows the detailed description of parameters and values that were used in the simulations of model (3). We used a Range-Kutta fourth-order scheme in the numerical solutions of the system of differential equations in model (3) by using matlab program.

7.1. Simulation of Model Showing the Effects of Increasing Force of Infection on Infectious Anthrax and Listeriosis Populations Only. In this section, we simulate the system of differential equations in model (3) by varying the human contact rate to see its effects on infected Anthrax population, infected Listeriosis population, and Anthrax-Listeriosis coinfected population. This was done by setting the values of human contact rate as $\beta_h = 0.01, \beta_h = 0.02, \beta_h = 0.03$, and $\beta_h = 0.04$. Figure 3 shows an increase in the infected Anthrax population as the value of contact rate increases. Moreover, as the value of the human contact rate decreases, the number of Anthrax infected population decreases with time. However, an increase or decrease in the human contact rate increases or decreases the Listeriosis infected population with time as confirmed in Figure 4. The number of Anthrax-Listeriosis coinfected population shows a sharp reduction in the number of individuals infected with both diseases but the there is an increase in the number of infectious population as shown in Figure 5. An increase or decrease in the human contact rate shows an increase or decrease in the number of Anthrax-Listeriosis coinfected population as indicated in Figure 5. Analysis of force of infection gives a better understanding of the effects of the contact rate which was not considered by the work of authors in [2, 3, 20].

7.2. Simulation of Model Showing Infected Anthrax, Listeriosis, and Coinfected Populations. In this section, we simulate the model (3) to see the behaviour of Anthrax infected population, Listeriosis infected population, and Anthrax-Listeriosis coinfected population. Figure 6 shows an increase in the number of Anthrax infected individuals and a sharp increase in the number of Listeriosis infected individuals. Figure 7 shows a sharp reduction in the number of Anthrax-Listeriosis coinfected population from the beginning and it increases steadily at a point in time. Since the number of susceptible human populations increases in the system with time, there are higher chances of individuals being infected with Anthrax, Listeriosis, and Anthrax-Listeriosis coinfection. This is because the concept of mass action was one of the assumptions that was incorporated in our model.

7.3. Simulation of Model Showing Susceptible Human Bacteria Populations. In this section, we simulate model (3), to observe the behaviour of the susceptible human population and how the bacteria (carcasses) growth behaves with time in the epidemics. Figure 8 shows an increase in both the susceptible and bacteria growth. An increase in the number of susceptible from the beginning confirms the increase in

Table 2: Sensitivity indices of $\mathfrak{R}_{0l}$ to each of the parameter values.

Parameter	Description	Sensitivity Index
Ω_h	Human recruitment rate	0.0201487
σ	Co-infected human recovery rate	$-5.41441 * 10^{-}6$
μ_h	Human natural death rate	−0.00014638
η	Listeriosis death rate among co-infected	$-5.41441 * 10^{-}6$
θ	Modification parameter	$3.42913 * 10^{-}6$
ν	Bacteria ingestion rate	0.0000402975
ρ	Listeriosis contribution to environment	0.0000309981
K	Concentration of carcasses	$-2.01487 * 10^{-}10$
δ	Listeriosis recovery rate	−0.0000402218
μ_b	Carcasses mortality rate	−0.0080595
m	Listeriosis related death	−0.0000402218

Table 3: Variable and parameter values of the coinfection model.

Parameter	Description	Value	Reference
ϕ	Anthrax related death rate	0.2	(Health line, Dec., 2015)
m	Listeriosis related death rate	0.2	Adak et al., 2002.
q	Anthrax death rate among co-infected	0.04	assumed
η	Listeriosis death rate among co-infected	0.08	assumed
β_h	Human transmission rate	0.01	[23]
β_v	Vector transmission rate	0.05	assumed
k	Anthrax waning immunity	0.02	assumed
μ_v	Vector natural death rate	0.0004	[23]
Ω_h	Human recruitment rate	0.001	assumed
Ω_v	Vector recruitment rate	0.005	[23]
α	Anthrax recovery rate	0.33	[24]
δ	Listeriosis recovery rate	0.002	assumed
ψ	Anthrax-Listeriosis waning immunity	0.07	assumed
ρ	Listeriosis contribution to environment	0.65	assumed
σ	Co-infected recovery rate	0.005	assumed
μ_b	Bacteria death rate	0.0025	assumed
μ_h	Human natural death rate	0.2	[23]
ω	Listeriosis waning immunity	0.001	assumed
θ	Modification parameter	0.45	assumed
ε	Co-infected who recover from Anthrax only	0.025	assumed
K	Concentration of carcasses	10000	[20]
ν	Bacteria ingestion rate	0.5	[20]

the number of Anthrax infection and Listeriosis infection in Figure 6. The increase in the number of susceptible human populations could be attributed to our model being an open system.

8. Conclusion

In this paper, we analysed the transmission dynamics of Anthrax-Listeriosis coinfection model. The compartmental model was analysed qualitatively and quantitatively to fully understand the transmission mechanism of Anthrax-Listeriosis coinfection. Our model revealed that the disease-free equilibrium of the Anthrax model only is locally stable when the basic reproduction number is less than one and a unique endemic equilibrium whenever the basic reproduction number is greater than one. The disease-free equilibrium of the Listeriosis model only is locally stable when the basic reproduction number is less than one and a unique endemic equilibrium whenever the basic reproduction number is greater than one. Our model analysis

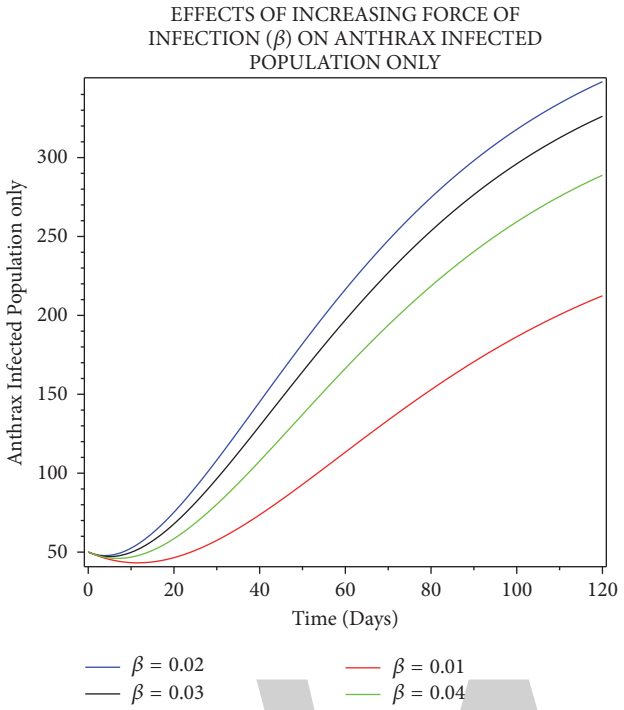

Figure 3: Simulation showing the effects of increasing the force of infection on Anthrax infected population only.

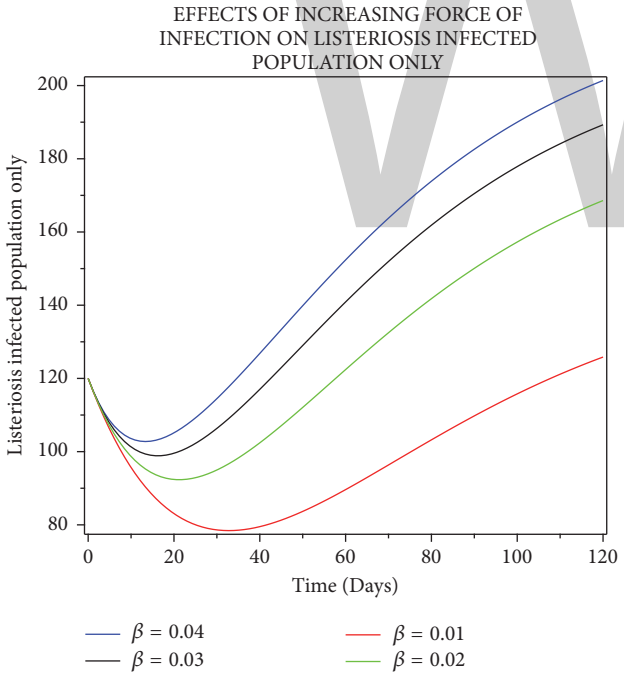

Figure 4: Simulation showing the effects of increasing the force of infection on Anthrax infected population only.

also reveals that the disease-free equilibrium of the Anthrax-Listeriosis coinfection model is locally stable whenever the basic reproduction number is less than one. The phenomenon of backward bifurcation was exhibited by our model. The biological implication is that the idea of the model been locally stable whenever the reproduction number is less than

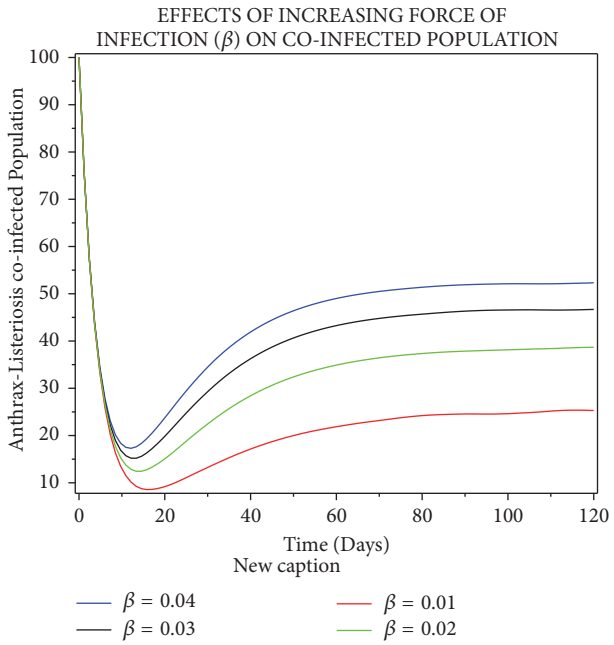

Figure 5: Simulation showing the effects of increasing the force of infection on Anthrax infected population only.

unity and unstable otherwise does not apply. This means that the Anthrax-Listeriosis coinfection model shows a case of coexistence of the disease-free equilibrium and the endemic equilibrium whenever the basic reproduction number is less than one.

We performed the sensitivity analysis of the basic reproductive number to each of the parameters to determine which parameter is more sensitive. The sensitivity indices of the basic reproduction number of Anthrax to each of the parameter values revealed that the most sensitive parameters are human transmission rate, vector transmission rate, human recruitment rate, and vector recruitment rate. Since the basic reproduction number is less than one, increasing the human recruitment rate would increase the basic reproduction number. This analysis is an improvement of the work done by [2, 3]. They considered the dynamics of Anthrax in animal population but never considered sensitivity analysis to determine the most sensitive parameter to the model.

The sensitivity indices of the basic reproduction number of Listeriosis to each of the parameter values shows that the most sensitive parameters are bacteria ingestion rate, Listeriosis related death, human recruitment rate, and Listeriosis contribution to environment.

We simulate the Anthrax-Listeriosis coinfection model by varying the human contact rate to see its effects on infected Anthrax population, infected Listeriosis population, and Anthrax-Listeriosis coinfected population. This analysis is an improvement of the work done by authors in [2, 3, 20]. Our simulation shows an increase in the infected Anthrax population, an increase the number Listeriosis infected population, and an increase in the number of Anthrax-Listeriosis

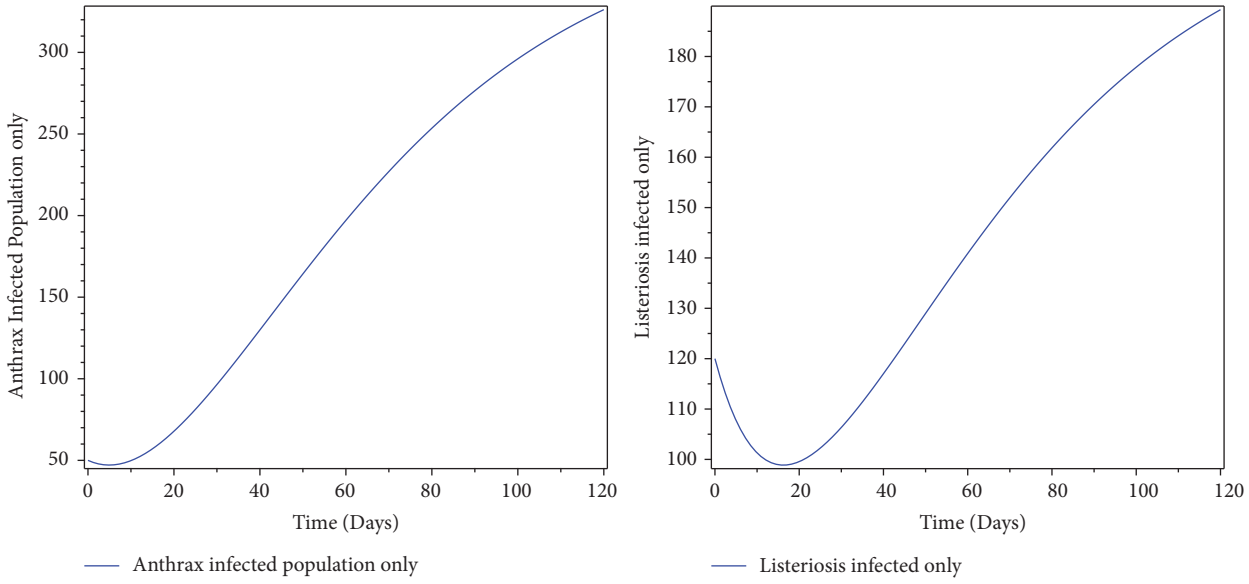

Figure 6: Simulation showing infected Anthrax and infected Listeriosis population.

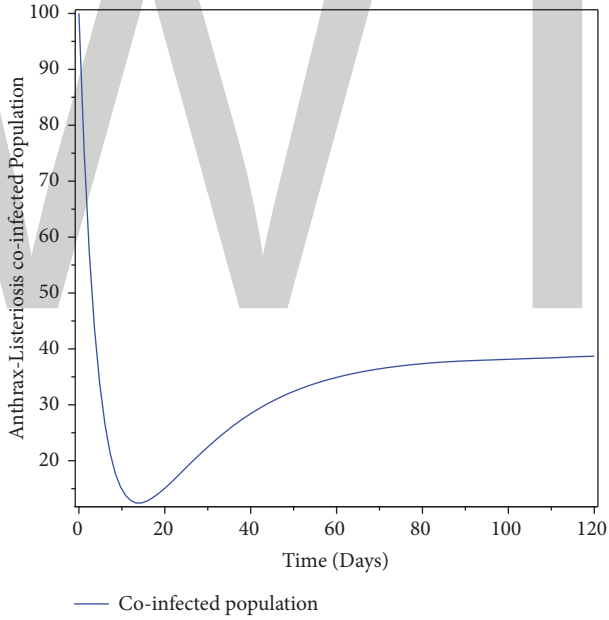

Figure 7: Simulation of model showing Anthrax-Listeriosis coinfection population.

coinfected population as the value of the human contact rate increases.

Conflicts of Interest

The authors declare that there are no conflicts of interest regarding the publication of this paper.

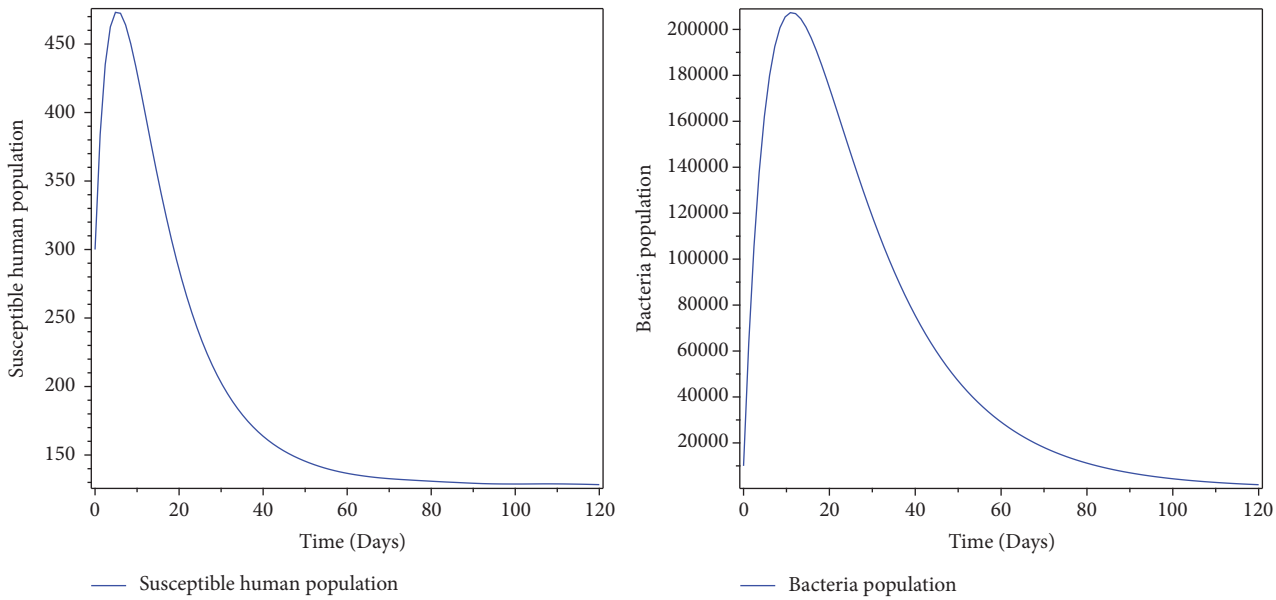

Figure 8: Simulation of model showing susceptible human and bacteria populations.

References

[1] W. F. Schlech and D. Acheson, "Foodborne listeriosis," *Clinical Infectious Diseases*, vol. 31, no. 3, pp. 770–775, 2000.

[2] C. M. Saad-Roy, P. van den Driessche, and A.-A. Yakubu, "A mathematical model of anthrax transmission in animal populations," *Bulletin of Mathematical Biology*, vol. 79, no. 2, pp. 303–324, 2017.

[3] A. Friedman and A. A. Yakubu, "Anthrax epizootic and migration: persistence or extinction," *Mathematical Biosciences*, vol. 241, no. 1, pp. 137–144, 2013.

[4] Z. Lu, X. Chi, and L. Chen, "The effect of constant and pulse vaccination on SIR epidemic model with horizontal and vertical transmission," *Mathematical and Computer Modelling*, vol. 36, no. 9-10, pp. 1039–1057, 2002.

[5] A. A. Lashari and G. Zaman, "Optimal control of a vector borne disease with horizontal transmission," *Nonlinear Analysis: Real World Applications*, vol. 13, no. 1, pp. 203–212, 2012.

[6] A. A. Lashari, "Optimal control of an SIR epidemic model with a saturated treatment," *Applied Mathematics & Information Sciences*, vol. 10, no. 1, pp. 185–191, 2016.

[7] S. Mushayabasa and C. P. Bhunu, "Is HIV infection associated with an increased risk for cholera? Insights from a mathematical model," *BioSystems*, vol. 109, no. 2, pp. 203–213, 2012.

[8] A. B. Gumel and S. M. Moghadas, "A qualitative study of a vaccination model with non-linear incidence," *Applied Mathematics and Computation*, vol. 143, no. 2-3, pp. 409–419, 2003.

[9] T. K. Kar and A. Batabyal, "Stability analysis and optimal control of an SIR epidemic model with vaccination," *BioSystems*, vol. 104, no. 2-3, pp. 127–135, 2011.

[10] O. D. Makinde, "Adomian decomposition approach to a SIR epidemic model with constant vaccination strategy," *Applied Mathematics and Computation*, vol. 184, no. 2, pp. 842–848, 2007.

[11] T. T. Yusuf and F. Benyah, "Optimal control of vaccination and treatment for an SIR epidemiological model," *World Journal of Modelling and Simulation*, vol. 8, no. 3, pp. 194–204, 2012.

[12] G. Zaman, Y. H. Kang, and I. H. Jung, "Optimal treatment of an SIR epidemic model with time delay," *BioSystems*, vol. 98, no. 1, pp. 43–50, 2009.

[13] G. Zaman, Y. Han Kang, and I. H. Jung, "Stability analysis and optimal vaccination of an SIR epidemic model," *BioSystems*, vol. 93, no. 3, pp. 240–249, 2008.

[14] O. Shaibu, D. M. Oluwole, and M. T. David, "Stability analysis and modelling of listeriosis dynamics in human and animal populations," *The Global Journal of Pure and Applied Mathematics (GJPAM)*, vol. 14, no. 1, pp. 115–137, 2018.

[15] O. D. Makinde and K. O. Okosun, "Impact of chemo-therapy on optimal control of malaria disease with infected immigrants," *BioSystems*, vol. 104, no. 1, pp. 32–41, 2011.

[16] K. Hattaf, M. Rachik, S. Saadi, Y. Tabit, and N. Yousfi, "Optimal control of tuberculosis with exogenous reinfection," *Applied Mathematical Sciences*, vol. 3, no. 5-8, pp. 231–240, 2009.

[17] M. K. Borucki, J. Reynolds, C. C. Gay et al., "Dairy farm reservoir of Listeria monocytogenes sporadic and epidemic strains," *Journal of Food Protection*, vol. 67, no. 11, pp. 2496–2499, 2004.

[18] H. W. Hethcote, "Qualitative analyses of communicable disease models," *Mathematical Biosciences*, vol. 28, no. 3-4, pp. 335–356, 1976.

[19] N. C. Grassly and C. Fraser, "Mathematical models of infectious disease transmission," *Nature Reviews Microbiology*, vol. 6, no. 6, pp. 477–487, 2008.

[20] K. O. Okosun and O. D. Makinde, "A co-infection model of malaria and cholera diseases with optimal control," *Mathematical Biosciences*, vol. 258, pp. 19–32, 2014.

[21] P. van den Driessche and J. Watmough, "Reproduction numbers and sub-threshold endemic equilibria for compartmental models of disease transmission," *Mathematical Biosciences*, vol. 180, pp. 29–48, 2002.

[22] C. Castillo-Chavez and B. Song, "Dynamical models of tuberculosis and their applications," *Mathematical Biosciences and Engineering*, vol. 1, no. 2, pp. 361–404, 2004.

[23] S. Mushayabasa, T. Marijani, and M. Masocha, "Dynamical analysis and control strategies in modeling anthrax," *Computational and Applied Mathematics*, vol. 36, no. 3, pp. 1333–1348, 2017.

[24] R. Brookmeyer, E. Johnson, and R. Bollinger, "Modeling the optimum duration of antibiotic prophylaxis in an anthrax outbreak," *Proceedings of the National Acadamy of Sciences of the United States of America*, vol. 100, no. 17, pp. 10129–10132, 2003.

On the Locating Chromatic Number of Certain Barbell Graphs

Asmiati,[1] **I. Ketut Sadha Gunce Yana**,[1] **and Lyra Yulianti**[2]

[1]*Mathematics Department, Faculty of Mathematics and Natural Sciences, Lampung University, Jl. Brodjonegoro No.1 Bandar Lampung, Indonesia*
[2]*Mathematics Department, Faculty of Mathematics and Natural Sciences, Andalas University, Kampus UNAND Limau Manis, Padang 25163, Indonesia*

Correspondence should be addressed to Asmiati; asmiati308@yahoo.com

Academic Editor: Dalibor Froncek

The locating chromatic number of a graph G is defined as the cardinality of a minimum resolving partition of the vertex set $V(G)$ such that all vertices have distinct coordinates with respect to this partition and every two adjacent vertices in G are not contained in the same partition class. In this case, the coordinate of a vertex v in G is expressed in terms of the distances of v to all partition classes. This concept is a special case of the graph partition dimension notion. In this paper we investigate the locating chromatic number for two families of barbell graphs.

1. Introduction

The partition dimension was introduced by Chartrand et al. [1] as the development of the concept of metric dimension. The application of metric dimension plays a role in robotic navigation [2], the optimization of threat detecting sensors [3], and chemical data classification [4]. The concept of locating chromatic number is a marriage between the partition dimension and coloring of a graph, first introduced by Chartrand et al in 2002 [5]. The locating chromatic number of a graph is a newly interesting topic to study because there is no general theorem for determining the locating chromatic number of any graph.

Let $G = (V, E)$ be a connected graph. We define the *distance* as the minimum length of path connecting vertices u and v in G, denoted by $d(u, v)$. A k-coloring of G is a function $c : V(G) \longrightarrow \{1, 2, \ldots, k\}$, where $c(u) \neq c(v)$ for any two adjacent vertices u and v in G. Thus, the coloring c induces a partition Π of $V(G)$ into k color classes (independent sets) $C_1, C_2, \ldots, C_k$, where C_i is the set of all vertices colored by the color i for $1 \leq i \leq k$. The *color code* $c_\Pi(v)$ of a vertex v in G is defined as the k-vector $(d(v, C_1), d(v, C_2), \ldots, d(v, C_k))$, where $d(v, C_i) = \min\{d(v, x) : x \in C_i\}$ for $1 \leq i \leq k$. The k-coloring c of G such that all vertices have different color codes is called a *locating coloring* of G. The *locating chromatic number* of G, denoted by $\chi_L(G)$, is the minimum k such that G has a locating coloring.

The following theorem is a basic theorem proved by Chartrand et al. [5]. The neighborhood of vertex u in a connected graph G, denoted by $N(u)$, is the set of vertices adjacent to u.

Theorem 1 (see [5]). *Let c be a locating coloring in a connected graph G. If u and v are distinct vertices of G such that $d(u, t) = d(v, t)$ for all $t \in V(G) - \{u, v\}$, then $c(u) \neq c(v)$. In particular, if u and v are non-adjacent vertices of G such that $N(u) = N(v)$, then $c(u) \neq c(v)$.*

The following corollary gives the lower bound of the locating chromatic number for every connected graph G.

Corollary 2 (see [5]). *If G is a connected graph and there is a vertex adjacent to k leaves, then $\chi_L(G) \geq k + 1$.*

There are some interesting results related to the determination of the locating chromatic number of some graphs. The results are obtained by focusing on certain families of graphs. Chartrand et al. in [5] have determined all graphs of order n with locating chromatic number n, namely, a complete multipartite graph of n vertices. Moreover, Chartrand et

al. [6] have succeeded in constructing tree on n vertices, $n \geq 5$, with locating chromatic numbers varying from 3 to n, except for $(n-1)$. Then Behtoei and Omoomi [7] have obtained the locating chromatic number of the Kneser graphs. Recently, Asmiati et al. [8] obtained the locating chromatic number of the generalized Petersen graph $P(n,1)$ for $n \geq 3$. Baskoro and Asmiati [9] have characterized all trees with locating chromatic number 3. In [10] all trees of order n with locating chromatic number $n-1$ were characterized, for any integers n and t, where $n > t+3$ and $2 \leq t < n/2$. Asmiati et al. in [11] have succeeded in determining the locating chromatic number of homogeneous amalgamation of stars and their monotonicity properties and in [12] for firecracker graphs. Next, Wellyyanti et al. [13] determined the locating chromatic number for complete n-ary trees.

The generalized Petersen graph $P(n,m)$, $n \geq 3$ and $1 \leq m \leq \lfloor (n-1)/2 \rfloor$, consists of an outer n-cycle $y_1, y_2, \ldots, y_n$, a set of n spokes $y_i x_i$, $1 \leq i \leq n$, and n edges $x_i x_{i+m}$, $1 \leq i \leq n$, with indices taken modulo n. The generalized Petersen graph was introduced by Watkins in [14]. Let us note that the generalized Petersen graph $P(n,1)$ is a prism defined as Cartesian product of a cycle C_n and a path P_2.

Next theorems give the locating chromatic numbers for complete graph K_n and generalized Petersen graph $P(n,1)$.

Theorem 3 (see [6]). *For $n \geq 2$, the locating chromatic number of complete graph K_n is n.*

Theorem 4 (see [8]). *The locating chromatic number of generalized Petersen graph $P(n,1)$ is 4 for odd $n \geq 3$ or 5 for even $n \geq 4$.*

The *barbell graph* is constructed by connecting two arbitrary connected graphs G and H by a bridge. In this paper, firstly we discuss the locating chromatic number for barbell graph $B_{m,n}$ for $m, n \geq 3$, where G and H are complete graphs on m and n vertices, respectively. Secondly, we determine the locating chromatic number of barbell graph $B_{P(n,1)}$ for $n \geq 3$, where G and H are two isomorphic copies of the generalized Petersen graph $P(n,1)$.

2. Results and Discussion

Next theorem proves the exact value of the locating chromatic number for barbell graph $B_{n,n}$.

Theorem 5. *Let $B_{n,n}$ be a barbell graph for $n \geq 3$. Then the locating chromatic number of $B_{n,n}$ is $\chi_L(B_{n,n}) = n+1$.*

Proof. Let $B_{n,n}$, $n \geq 3$, be the barbell graph with the vertex set $V(B_{n,n}) = \{u_i, v_i : 1 \leq i \leq n\}$ and the edge set $E(B_{n,n}) = \bigcup_{i=1}^{n-1} \{u_i u_{i+j} : 1 \leq j \leq n-i\} \cup \bigcup_{i=1}^{n-1} \{v_i v_{i+j} : 1 \leq j \leq n-i\} \cup \{u_n v_n\}$.

First, we determine the lower bound of the locating chromatic number for barbell graph $B_{n,n}$ for $n \geq 3$. Since the barbell graph $B_{n,n}$ contains two isomorphic copies of a complete graph K_n, then with respect to Theorem 3 we have $\chi_L(B_{n,n}) \geq n$. Next, suppose that c is a locating coloring using n colors. It is easy to see that the barbell graph $B_{n,n}$ contains two vertices with the same color codes, which is a contradiction. Thus, we have that $\chi_L(B_{n,n}) \geq n+1$.

To show that $n+1$ is an upper bound for the locating chromatic number of barbell graph $B_{n,n}$ it suffices to prove the existence of an optimal locating coloring $c : V(B_{n,n}) \longrightarrow \{1, 2, \ldots, n+1\}$. For $n \geq 3$ we construct the function c in the following way:

$$c(u_i) = i, \quad 1 \leq i \leq n$$
$$c(v_i) = \begin{cases} n, & \text{for } i = 1 \\ i, & \text{for } 2 \leq i \leq n-1 \\ n+1, & \text{otherwise.} \end{cases} \tag{1}$$

By using the coloring c, we obtain the color codes of $V(B_{n,n})$ as follows:

$$c_\Pi(u_i) = \begin{cases} 0, & \text{for } i^{th} \text{ component, } 1 \leq i \leq n \\ 2, & \text{for } (n+1)^{th} \text{ component, } 1 \leq i \leq n-1 \\ 1, & \text{otherwise,} \end{cases}$$

$$c_\Pi(v_i) = \begin{cases} 0, & \text{for } i^{th} \text{ component, } 2 \leq i \leq n-1 \\ & \text{for } n^{th} \text{ component, } i = 1, \text{ and} \\ & \text{for } (n+1)^{th} \text{ component, } i = n, \\ 3, & \text{for } 1^{st} \text{ component, } 1 \leq i \leq n-1 \\ 2, & \text{for } 1^{st} \text{ component, } i = n \\ 1, & \text{otherwise.} \end{cases} \tag{2}$$

Since all vertices in $V(B_{n,n})$ have distinct color codes, then the coloring c is desired locating coloring. Thus, $\chi_L(B_{n,n}) = n+1$. □

Corollary 6. *For $n, m \geq 3$, and $m \neq n$, the locating chromatic number of barbell graph $B_{m,n}$ is*

$$\chi_L(B_{m,n}) = \max\{m, n\}. \tag{3}$$

Next theorem provides the exact value of the locating chromatic number for barbell graph $B_{P(n,1)}$.

Theorem 7. *Let $B_{P(n,1)}$ be a barbell graph for $n \geq 3$. Then the locating chromatic number of $B_{P(n,1)}$ is*

$$\chi_L\left(B_{P(n,1)}\right) = \begin{cases} 4, & \text{for odd } n \\ 5, & \text{for even } n. \end{cases} \tag{4}$$

Proof. Let $B_{P(n,1)}$, $n \geq 3$, be the barbell graph with the vertex set $V(B_{P(n,1)}) = \{u_i, u_{n+i}, w_i, w_{n+i} : 1 \leq i \leq n\}$ and the edge set $E(B_{P(n,1)}) = \{u_iu_{i+1}, u_{n+i}u_{n+i+1}, w_iw_{i+1}, w_{n+i}w_{n+i+1} : 1 \leq i \leq n-1\} \cup \{u_nu_1, u_{2n}u_{n+1}, w_nw_1, w_{2n}w_{n+1}\} \cup \{u_iu_{n+i}, w_iw_{n+i} : 1 \leq i \leq n\} \cup \{u_nw_n\}$.

Let us distinguish two cases.

Case 1 (n odd). According to Theorem 4 for n odd we have $\chi_L(B_{P(n,1)}) \geq 4$. To show that 4 is an upper bound for the locating chromatic number of the barbell graph $B_{P(n,1)}$ we describe an locating coloring c using 4 colors as follows:

$$c\left(u_i\right) = \begin{cases} 1, & \text{for } i = 1 \\ 3, & \text{for even } i,\ i \geq 2 \\ 4, & \text{for odd } i,\ i \geq 3. \end{cases}$$

$$c\left(u_{n+i}\right) = \begin{cases} 2, & \text{for } i = 1 \\ 3, & \text{for odd } i,\ i \geq 3 \\ 4, & \text{for even } i,\ i \geq 2. \end{cases}$$

$$c\left(w_i\right) = \begin{cases} 1, & \text{for odd } i,\ i \leq n-2 \\ 2, & \text{for even } i,\ i \leq n-1 \\ 3, & \text{for } i = n. \end{cases}$$

$$c\left(w_{n+i}\right) = \begin{cases} 1, & \text{for even } i,\ i \leq n-1 \\ 2, & \text{for odd } i,\ i \leq n-2 \\ 4, & \text{for } i = n. \end{cases} \tag{5}$$

For n odd the color codes of $V(B_{P(n,1)})$ are

$$c_\Pi\left(u_i\right) = \begin{cases} i, & \text{for } 2^{nd} \text{ component, } i \leq \dfrac{n+1}{2} \\ i-1, & \text{for } 1^{st} \text{ component, } i \leq \dfrac{n+1}{2} \\ n-i+1, & \text{for } 1^{st} \text{ component, } i > \dfrac{n+1}{2} \\ n-i+2, & \text{for } 2^{nd} \text{ component, } i > \dfrac{n+1}{2} \\ 0, & \text{for } 3^{th} \text{ component, } i \text{ even, } i \geq 2 \\ & \text{for } 4^{th} \text{ component, } i \text{ odd, } i \geq 3 \\ 1, & \text{otherwise.} \end{cases}$$

$$c_\Pi\left(u_{n+i}\right) = \begin{cases} i, & \text{for } 1^{st} \text{ component, } i \leq \dfrac{n+1}{2} \\ i-1, & \text{for } 2^{nd} \text{ component, } i \leq \dfrac{n+1}{2} \\ n-i+1, & \text{for } 2^{nd} \text{ component, } i > \dfrac{n+1}{2} \\ n-i+2, & \text{for } 1^{st} \text{ component, } i > \dfrac{n+1}{2} \\ 0, & \text{for } 4^{th} \text{ component, } i \text{ even, } i \geq 2 \\ & \text{for } 3^{th} \text{ component, } i \text{ odd, } i \geq 3 \\ 1, & \text{otherwise.} \end{cases}$$

$$c_\Pi\left(w_i\right) = \begin{cases} i, & \text{for } 3^{th} \text{ component, } i \leq \dfrac{n-1}{2} \\ i+1, & \text{for } 4^{th} \text{ component, } i \leq \dfrac{n-1}{2} \\ n-i, & \text{for } 3^{th} \text{ component, } i \geq \dfrac{n+1}{2} \\ n-i+1, & \text{for } 4^{th} \text{ component, } i \geq \dfrac{n+1}{2} \\ 0, & \text{for } 2^{nd} \text{ component, } i \text{ even, } i \leq n-1 \\ & \text{for } 1^{st} \text{ component, } i \text{ odd, } i \leq n-2 \\ 1, & \text{otherwise.} \end{cases}$$

$$c_\Pi\left(w_{n+i}\right) = \begin{cases} i, & \text{for } 4^{th} \text{ component, } i \leq \dfrac{n-1}{2} \\ i+1, & \text{for } 3^{th} \text{ component, } i \leq \dfrac{n-1}{2} \\ n-i, & \text{for } 4^{th} \text{ component, } i \geq \dfrac{n+1}{2} \\ n-i+1, & \text{for } 3^{th} \text{ component, } i \geq \dfrac{n+1}{2} \\ 0, & \text{for } 1^{st} \text{ component, } i \text{ even, } i \leq n-1 \\ & \text{for } 2^{nd} \text{ component, } i \text{ odd, } i \leq n-2 \\ 1, & \text{otherwise.} \end{cases} \tag{6}$$

Since all vertices in $B_{P(n,1)}$ have distinct color codes, then the coloring c with 4 colors is an optimal locating coloring and it proves that $\chi_L(B_{P(n,1)}) \leq 4$.

Case 2 (n even). In view of the lower bound from Theorem 7 it suffices to prove the existence of a locating coloring $c : V(B_{P(n,1)}) \longrightarrow \{1, 2, \ldots, 5\}$ such that all vertices in $B_{P(n,1)}$ have distinct color codes. For n even, $n \geq 4$, we describe the locating coloring in the following way:

$$c\left(u_i\right) = \begin{cases} 1, & \text{for } i = 1 \\ 3, & \text{for even } i,\ 2 \leq i \leq n-2 \\ 4, & \text{for odd } i,\ 3 \leq i \leq n-1 \\ 5, & \text{for } i = n. \end{cases}$$

$$c(u_{n+i}) = \begin{cases} 2, & \text{for } i = 1 \\ 3, & \text{for odd } i,\ i \geq 3 \\ 4, & \text{for even } i,\ i \geq 2. \end{cases}$$

$$c(w_i) = \begin{cases} 1, & \text{for odd } i,\ i \leq n-3 \\ 2, & \text{for even } i,\ i \leq n-2 \\ 3, & \text{for } i = n-1 \\ 4, & \text{for } i = n. \end{cases}$$

$$c(w_{n+i}) = \begin{cases} 1, & \text{for even } i,\ i \leq n-2 \\ 2, & \text{for odd } i,\ i \leq n-1 \\ 5, & \text{for } i = n. \end{cases} \tag{7}$$

In fact, our locating coloring of $B_{P(n,1)}$, n even, has been chosen in such a way that the color codes are

$c_\Pi(u_i)$

$$= \begin{cases} i, & \text{for } 2^{nd} \text{ and } 5^{th} \text{ components, } i \leq \frac{n}{2} \\ i-1, & \text{for } 1^{st} \text{ component, } i \leq \frac{n}{2} \\ n-i, & \text{for } 5^{th} \text{ component, } i > \frac{n}{2} \\ n-i+1, & \text{for } 1^{st} \text{ component, } i > \frac{n}{2} \\ n-i+2, & \text{for } 2^{nd} \text{ component, } i > \frac{n}{2} \\ 0, & \text{for } 3^{th} \text{ component, } i \text{ even, } 2 \leq i \leq n-2 \\ & \text{for } 4^{th} \text{ component, } i \text{ odd, } 3 \leq i \leq n-1 \\ 2, & \text{for } 4^{th} \text{ component, } i = 1 \\ & \text{for } 3^{th} \text{ component, } i = n \\ 1, & \text{otherwise.} \end{cases}$$

$c_\Pi(u_{n+i})$

$$= \begin{cases} i, & \text{for } 1^{st} \text{ component, } i \leq \frac{n}{2} \\ i-1, & \text{for } 2^{nd} \text{ component, } i \leq \frac{n}{2} \\ n+i, & \text{for } 5^{th} \text{ component, } i \leq \frac{n}{2} \\ n-i+1, & \text{for } 2^{nd} \text{ and } 5^{th} \text{ components, } i > \frac{n}{2} \\ n-i+2, & \text{for } 1^{th} \text{ component, } i > \frac{n}{2} \\ 0, & \text{for } 3^{th} \text{ component, } i \text{ odd, } 3 \leq i \leq n-1 \\ & \text{for } 4^{th} \text{ component, } i \text{ even, } 2 \leq i \leq n \\ 2, & \text{for } 3^{th} \text{ component, } i = 1 \\ 1, & \text{otherwise.} \end{cases}$$

$c_\Pi(w_i)$

$$= \begin{cases} i, & \text{for } 4^{th} \text{ component, } i \leq \frac{n}{2} \\ i+1, & \text{for } 5^{th} \text{ component, } i \leq \frac{n}{2} \\ & \text{for } 3^{th} \text{ component, } i \leq \frac{n}{2}-1 \\ n-i, & \text{for } 4^{th} \text{ component, } i > \frac{n}{2} \\ n-i+1, & \text{for } 5^{th} \text{ component, } i > \frac{n}{2} \\ n-i-1, & \text{for } 3^{th} \text{ component, } \frac{n}{2} \leq i \leq n-1 \\ 0, & \text{for } 1^{st} \text{ component, } i \text{ odd, } i \leq n-3 \\ & \text{for } 2^{nd} \text{ component, } i \text{ even, } i \leq n-2 \\ 2, & \text{for } 1^{st} \text{ component, } i = n-1 \\ & \text{for } 2^{nd} \text{ component, } i = n \\ 1, & \text{otherwise.} \end{cases}$$

$c_\Pi(w_{n+i})$

$$= \begin{cases} i, & \text{for } 5^{th} \text{ component, } i \leq \frac{n}{2} \\ i+1, & \text{for } 4^{th} \text{ component, } i \leq \frac{n}{2} \\ i+2 & \text{for } 3^{th} \text{ component, } i \leq \frac{n}{2}-1 \\ n-i, & \text{for } 3^{th} \text{ component, } \frac{n}{2} \leq i \leq n-1 \\ & \text{for } 5^{th} \text{ component, } i > \frac{n}{2} \\ n-i+1, & \text{for } 4^{th} \text{ component, } i > \frac{n}{2} \\ 0, & \text{for } 1^{st} \text{ component, } i \text{ even, } i \leq n-2 \\ & \text{for } 2^{nd} \text{ component, } i \text{ odd, } i \leq n-1 \\ 2, & \text{for } 1^{st} \text{ and } 3^{th} \text{ components, } i = n \\ 1, & \text{otherwise.} \end{cases} \tag{8}$$

Since for n even all vertices of $B_{P(n,1)}$ have distinct color codes then our locating coloring has the required properties and $\chi_L(B_{P(n,1)}) \leq 5$. This concludes the proof. □

Conflicts of Interest

The authors declare that they have no conflicts of interest.

Acknowledgments

The authors are thankful to DRPM Dikti for the Fundamental Grant 2018.

References

[1] G. Chartrand, P. Zhang, and E. Salehi, "On the partition dimension of a graph," *Congressus Numerantium*, vol. 130, pp. 157–168, 1998.

[2] V. Saenpholphat and P. Zhang, "Conditional resolvability: a survey," *International Journal of Mathematics and Mathematical Sciences*, vol. 38, pp. 1997–2017, 2004.

[3] M. Johnson, "Structure-activity maps for visualizing the graph variables arising in drug design," *Journal of Biopharmaceutical Statistics*, vol. 3, no. 2, pp. 203–236, 1993.

[4] G. Chartrand and P. Zhang, "THE theory and applications of resolvability in graphs. A survey," vol. 160, pp. 47–68.

[5] G. Chartrand, D. Erwin, M. A. Henning, P. J. Slater, and P. Zhang, "The locating-chromatic number of a graph," *Bulletin of the Institute of Combinatorics and Its Applications*, vol. 36, pp. 89–101, 2002.

[6] G. Chartrand, D. Erwin, M. A. Henning, P. J. Slater, and P. Zhang, "Graphs of order *n*-1," *Discrete Mathematics*, vol. 269, no. 1-3, pp. 65–79, 2003.

[7] A. Behtoei and B. Omoomi, "On the locating chromatic number of Kneser graphs," *Discrete Applied Mathematics: The Journal of Combinatorial Algorithms, Informatics and Computational Sciences*, vol. 159, no. 18, pp. 2214–2221, 2011.

[8] Asmiati, Wamiliana, Devriyadi, and L. Yulianti, "On some petersen graphs having locating chromatic number four or five," *Far East Journal of Mathematical Sciences*, vol. 102, no. 4, pp. 769–778, 2017.

[9] E. T. Baskoro and Asmiati, "Characterizing all trees with locating-chromatic number 3," *Electronic Journal of Graph Theory and Applications. EJGTA*, vol. 1, no. 2, pp. 109–117, 2013.

[10] D. K. Syofyan, E. T. Baskoro, and H. Assiyatun, "Trees with certain locating-chromatic number," *Journal of Mathematical and Fundamental Sciences*, vol. 48, no. 1, pp. 39–47, 2016.

[11] Asmiati, H. Assiyatun, and E. T. Baskoro, "Locating-chromatic number of amalgamation of stars," *ITB Journal of Science*, vol. 43A, no. 1, pp. 1–8, 2011.

[12] Asmiati, H. Assiyatun, E. T. Baskoro, D. Suprijanto, R. Simanjuntak, and S. Uttunggadewa, "The locating-chromatic number of firecracker graphs," *Far East Journal of Mathematical Sciences (FJMS)*, vol. 63, no. 1, pp. 11–23, 2012.

[13] D. Welyyanti, E. T. Baskoro, R. Simanjuntak, and S. Uttunggadewa, "On locating-chromatic number of complete *n*-ary tree," *AKCE International Journal of Graphs and Combinatorics*, vol. 10, no. 3, pp. 309–315, 2013.

[14] M. E. Watkins, "A theorem on tait colorings with an application to the generalized Petersen graphs," *Journal of Combinatorial Theory*, vol. 6, no. 2, pp. 152–164, 1969.

3

A Formulation of L-Isothermic Surfaces in Three-Dimensional Minkowski Space

Paul Bracken

Department of Mathematics, University of Texas, Edinburg, TX 78540, USA

Correspondence should be addressed to Paul Bracken; paul.bracken@utrgv.edu

Academic Editor: Ilya M. Spitkovsky

The Cartan structure equations are used to study space-like and time-like isothermic surfaces in three-dimensional Minkowski space in a unified framework. When the lines of curvature of a surface constitute an isothermal system, the surface is called isothermic. This condition serves to define a system of one-forms such that, by means of the structure equations, the Gauss-Codazzi equations for the surface are determined explicitly. A Lax pair can also be obtained from these one-forms for both cases, and, moreover, a nonhomogeneous Schrödinger equation can be associated with the set of space-like surfaces.

1. Introduction

The study of isothermic surfaces can be traced back to the work of Bianchi and Bour [**1, 2**], as well as to Darboux [**3**]. These surfaces seem to have their origin in work by Lamé motivated by problems in heat conduction. An important subclass of isothermic surfaces was subsequently investigated by Bonnet. The study of these surfaces has seen renewed interest recently with the work of Rogers and Schief [**4–6**]. Rogers established that a Bäcklund transformation for isothermic surfaces is associated with a nonhomogeneous linear Schrödinger equation. This is largely due to the fact that the classical Gauss-Mainardi-Codazzi equations which are associated with surfaces in general are integrable in the sense they possess soliton solutions. Thus, these surfaces can be put in correspondence with solitonic solutions of certain nonlinear partial differential equations. Thus they have a strong appeal to those with interests that range from integrable equations to their associated Bäcklund transformations [**7–9**]. Thus, integrable systems theory can be applied to isothermic surfaces and used to study transformations of these surfaces as well. Consequently, isothermic surfaces constitute an important subclass of surfaces with a connection to solitons.

It is the purpose of this work to study the cases of both space-like and time-like surfaces as well as their immersion in three-dimensional Minkowski space $\mathbb{E}_1^3$ in a unified manner by basing the approach on the structure equations of Cartan and the associated moving frame [**10**]. Suppose that $\Sigma \subset \mathbb{E}_1^3$ is such a surface or manifold to which a first fundamental form is associated. With respect to the larger space $\mathbb{E}_1^3$, there exist both space-like and time-like surfaces residing in this larger space. Thus, a particular Σ could be either one of these two types of object. This is expressed by the fact that there are two ways in which the metric or first fundamental form can be specified intrinsically on the surface. In terms of two local coordinates, the metric may be written with two positive signs, hence a positive signature, or it may be written with a negative signature or alternating signs. In the former case, the surface Σ is referred to as space-like and in the latter case it is called time-like.

To start, let us outline the approach used here. Cartan's equations of structure are formulated in such a way that they are adapted to the signature of the flat metric of the ambient background space $\mathbb{E}_1^3$. These equations are defined in terms of a set of one-forms. By selecting these one-forms in a particular way along with the appropriate choice of signs, the system of structure equations can be restricted to study one of the classes of surface already described. In fact, a set of partial differential equations can be obtained which can be used to describe each of these types of surface. Therefore, the solutions of these equations can be used to describe a corresponding type of surface immersed in E_1^3.

In fact, it can be mentioned quite generally that new integrable equations have been obtained in the case of purely Euclidean space from the Cartan system by exploiting the one-to-one correspondence between the Ablowitz-Kaup-Newell-Segur (AKNS) program **[11, 12]** and the classical theory of surfaces in three dimensions. Its relationship to the problem of embedding surfaces in three-dimensional Euclidean space arises from the fact that the Gauss-Codazzi equations are in this case equivalent to Cartan's equations of structure for $SO(3)$. This correspondence suggests that the soliton connection can be given a deeper structure at the Riemannian level. In fact, in Euclidean space, much effort has been expended to exploit the equivalence between the AKNS systems and surface theory at the metric level in order to construct new nonlinear equations.

Once the structure equations have been formulated in this context, the one-forms can then be chosen for the case of isothermic surfaces. Classically, when the lines of curvature of a surface form an isothermal system, the surface is referred to as isothermic. The case studied here will be the one in which the third fundamental form is conformally flat in the manifold coordinates:

$$III = e^{2\vartheta}\left(du^2 + dv^2\right). \tag{1}$$

When the surface has a third fundamental form diagonal as in (1), it is often called L-isothermic. The prefix will be omitted here. This will lead to an equation whose solutions can be used to express the three fundamental forms which characterize surface. For each type of surface, the function in (1) turns out to be specified by a nonlinear second-order equation. It will be shown finally that Lax pairs can subsequently be formulated for each of the two second-order systems. Out of these results, further equations of physical interest can be developed which are relevant to both types of surface. One way in which these auxiliary equations arise is through compatibility conditions. Moreover, an interesting result is presented by showing that there is an important link between a nonhomogeneous Schrödinger equation and a combination of surface variables which are relevant to the more physical case of space-like isothermic surfaces. Investigations into this area have appeared **[13–15]**. Here the idea is to show how these geometries can be studied consistently by using the moving frame approach by simply altering some of the parameters in the metric.

2. Cartan Formulation of Structure Equations in Three-Space

A Darboux frame $(\mathbf{x}; e_1, e_2, e_3)$ is established on Σ such that the vectors (e_1, e_2) are tangent to surface Σ and e_3 is a normal vector to Σ; hence (e_1, e_2) determines an orientation for Σ. At a point $x \in M$, it is the case that

$$d\mathbf{x} = \omega_i e_i, \tag{2}$$

where $\mathbf{x}$ denotes a position vector in (2), ω_i constitute a basis of one-forms, and index i goes from 1 to 3. A surface Σ can be established by taking

$$\omega_3 = 0, \tag{3}$$

with e_3 a normal vector to Σ. The metric on the ambient background space is taken to have the following form **[13]:**

$$g = \begin{pmatrix} 1 & 0 & 0 \\ 0 & \epsilon & 0 \\ 0 & 0 & \eta \end{pmatrix} \tag{4}$$

so there is no loss of generality in defining the surface by means of (3). Moreover, the quantities ϵ and η in (4) can assume one of the two values $\epsilon = \pm 1$ and $\eta = \pm 1$. In the case in which $\epsilon = \eta = 1$, metric g specifies a three-dimensional Euclidean space $\mathbb{E}^3$ as usual. However, it is the intention here to study the cases in which only one of the quantities ϵ or η is taken to be negative. On the one hand, if $\epsilon = -1$ and $\eta = 1$ the surface metric is space-like, and if $\epsilon = 1$ and $\eta = -1$, the surface metric is time-like.

The surfaces immersed in $\mathbb{E}_1^3$ which are studied here have first fundamental form or metric on the surface defined by

$$I = \omega_1^2 + \epsilon\omega_2^2. \tag{5}$$

The two choices of sign for ϵ account for two classes of surface just introduced. For the basis vectors of the Darboux frame, Cartan's structure equations must hold and they are given as follows:

$$\begin{aligned} de_1 &= \omega_{12}e_2 + \omega_{13}e_3, \\ de_2 &= \omega_{21}e_1 + \omega_{23}e_3, \\ de_3 &= \omega_{31}e_1 + \omega_{32}e_2, \end{aligned} \tag{6}$$

$$\omega_{ij} + \omega_{ji} = 0. \tag{7}$$

As in Chern **[12]**, we suppose the relative components of the frame field are ω_i and ω_{ij}. These are differential one-forms which depend on the two independent surface coordinates (u, v). To be able to discuss the embedding problem, the second fundamental form for Σ has to be defined as well. It is given by

$$II = \omega_1 \otimes \omega_{13} + \epsilon\omega_2 \otimes \omega_{23}. \tag{8}$$

To formulate and study the case of isothermic surfaces, the complete system of Cartan structure equations is required. Under the convention adopted for g given in (4), these equations can be presented in the notation of Chern **[12]** as

$$\begin{aligned} d\omega_1 &= \omega_2 \wedge \omega_{21}, \\ d\omega_2 &= \omega_1 \wedge \omega_{12}, \end{aligned} \tag{9}$$

$$\omega_1 \wedge \omega_{13} + \epsilon\omega_2 \wedge \omega_{23} = 0, \tag{10}$$

$$\begin{aligned} d\omega_{12} &= \epsilon\eta\omega_{13} \wedge \omega_{32}, \\ d\omega_{13} &= \omega_{12} \wedge \omega_{23}, \\ d\omega_{23} &= \epsilon\omega_{21} \wedge \omega_{13}. \end{aligned} \tag{11}$$

In the case of a space-like Σ, we take $\epsilon = 1$ and $\eta = -1$, so a space-like metric (5) results. For the time-like case $\epsilon = -1$

and $\eta = 1$, and a time-like metric (5) results. Each of these two cases will be studied by defining the one-forms which appear in (9)-(11) appropriately.

Theorem 1. *The Gauss-Codazzi equations (11) for embedding Σ can be expressed in the form of Cartan's structure equations for the group $SL(2,\mathbb{R})$ as*

$$d\sigma^i + \frac{1}{2}c^i_{jk}\sigma^j \wedge \sigma^k = 0. \tag{12}$$

The one-forms σ^i, where $i = 0, 1, 2$, are defined to be

$$\begin{aligned}
\sigma^0 &= -\frac{\epsilon^{1/2}}{2i}\omega_{12},\\
\sigma^1 &= \frac{1}{2\epsilon^{1/2}\eta^{1/2}}\left(i\epsilon^{1/2}\omega_{13} + \omega_{23}\right),\\
\sigma^2 &= -\frac{1}{2\epsilon^{1/2}\eta^{1/2}}\left(i\epsilon^{1/2}\omega_{13} - \omega_{23}\right).
\end{aligned} \tag{13}$$

The structure constants of $SL(2,\mathbb{R})$ which appear in (13) are $c^0_{12} = 1$, $c^1_{01} = -c^2_{02} = -2$.

The proof is straightforward, simply substitute the forms (13) into (12), and solve for $d\omega_{12}$, $d\omega_{13}$ and $d\omega_{23}$. Upon carrying this out, system (11) appears directly.

3. Surfaces with Space-Like Metric

To obtain a metric which has a positive signature on surface Σ, the parameters which appear in g in (4) are set to the values $\epsilon = 1$ and $\eta = -1$. Metric g assumes the following form:

$$g = \begin{pmatrix} 1 & 0 & 0\\ 0 & 1 & 0\\ 0 & 0 & -1 \end{pmatrix}. \tag{14}$$

The structure equations (9)-(11) then take the following form:

$$\begin{aligned}
d\omega_1 &= \omega_2 \wedge \omega_{21},\\
d\omega_2 &= \omega_1 \wedge \omega_{12},
\end{aligned} \tag{15}$$

$$\omega_1 \wedge \omega_{13} + \omega_2 \wedge \omega_{23} = 0, \tag{16}$$

$$\begin{aligned}
d\omega_{12} &= -\omega_{13} \wedge \omega_{32},\\
d\omega_{13} &= \omega_{12} \wedge \omega_{23},\\
d\omega_{23} &= \omega_{21} \wedge \omega_{13},
\end{aligned} \tag{17}$$

$$\omega_{ij} + \omega_{ji} = 0. \tag{18}$$

These equations constitute the Gauss-Codazzi system for the space-like surface.

In order to study isothermic surfaces, the one-forms which are to be used in (15)-(17) are defined in such a way that the third fundamental form is proportional to a flat metric on Σ (1). Given a coordinate chart (u, v) for Σ, the one-forms ω_1 and ω_2 are taken to depend on functions of the coordinate parameters as

$$\begin{aligned}
\omega_1 &= A du,\\
\omega_2 &= B dv.
\end{aligned} \tag{19}$$

The functions $A = A(u, v)$ and $B = B(u, v)$ depend on both (u, v) in general. Further, define the one-forms as follows:

$$\begin{aligned}
\omega_{13} &= \kappa_1 A du,\\
\omega_{23} &= \kappa_2 B dv.
\end{aligned} \tag{20}$$

Equations (19) and (20) imply that the first three fundamental forms of the surface can be constructed in the following way:

$$\begin{aligned}
I &= A^2 du^2 + B^2 dv^2,\\
II &= \kappa_1 A^2 du^2 + \kappa_2 B^2 dv^2,\\
III &= \kappa_1^2 A^2 du^2 + \kappa_2^2 B^2 dv^2.
\end{aligned} \tag{21}$$

From the fact that the mean and Gaussian curvatures are given by

$$\begin{aligned}
H &= -\mathrm{tr}\left(II \cdot I^{-1}\right),\\
K &= \det\left(II \cdot I^{-1}\right),
\end{aligned} \tag{22}$$

κ_1 and κ_2 in (20) can be interpreted as the principal curvatures of the surface. To obtain an expression for ω_{12} in terms of A and B from (19), let us suppose $\omega_{12} = \alpha du + \beta dv$, where functions α and β depend on both coordinates as do A and B. Substituting this ω_{12} into (15), we can solve for α and β and (15) reduces to a pair of identities provided that ω_{12} has the following form"

$$\omega_{12} = -\frac{A_v}{B}du + \frac{B_u}{A}dv. \tag{23}$$

Clearly, forms (19), (20) clearly satisfy (16) automatically. Finally, putting the set of forms into the remaining equations in (17) produces a system which can be used to determine the two functions A and B. In fact, doing so produces a coupled system of partial differential equations which must hold when expressed in terms of all the relevant functions κ_1, κ_2, A and B.

Differentiating ω_{12} in (23) gives

$$d\omega_{12} = \left(\left(\frac{A_v}{B}\right)_v + \left(\frac{B_u}{A}\right)_u\right) du \wedge dv, \tag{24}$$

Thus the first equation in (17) implies that A and B satisfy a second-order equation:

$$\left(\frac{A_v}{B}\right)_v + \left(\frac{B_u}{A}\right)_u - \kappa_1\kappa_2 AB = 0. \tag{25}$$

The next two equations of (17) yield the following pair:

$$\begin{aligned}
\kappa_{1,v} + (\log A)_v(\kappa_1 - \kappa_2) &= 0,\\
\kappa_{2,u} + (\log B)_u(\kappa_2 - \kappa_1) &= 0.
\end{aligned} \tag{26}$$

Therefore, (25) and (26) constitute the relevant system to be studied.

The condition that the space-like surface Σ be isothermic is that the third fundamental form be conformally flat in terms of the (u, v)-coordinate system like (1). In order to ensure this, it suffices to take

$$A\kappa_1 = B\kappa_2 = e^{\vartheta}. \tag{27}$$

This parameterization can now be used to transform the system of (25)-(26) into a set which depends on only variable $\vartheta = \vartheta(u, v)$.

To this end, differentiate $B\kappa_2$ in (27) with respect to u:

$$\left(B\kappa_2\right)_u = B_u\kappa_2 + B\kappa_{2,u} = \vartheta_u e^{\vartheta}. \tag{28}$$

Substituting (28) into the second equation of (26) simplifies to the following form:

$$\vartheta_u e^{\vartheta} - \kappa_1 B_u = 0. \tag{29}$$

By using (27) to eliminate e^{ϑ}, (29) becomes

$$B_u = A\vartheta_u. \tag{30}$$

Similarly, differentiate $A\kappa_1 = e^{\vartheta}$ with respect to v to obtain

$$\left(A\kappa_1\right)_v = A_v\kappa_1 + A\kappa_{1,v} = \vartheta_v e^{\vartheta}. \tag{31}$$

Substituting (31) into the first equation in (26) simplifies to

$$A_v = B\vartheta_v. \tag{32}$$

Using (30) and (32) in the second-order equation (25) as well as the fact that $\kappa_1\kappa_2 AB = e^{2\vartheta}$ becomes an equation in terms of only the ϑ variable:

$$\vartheta_{uu} + \vartheta_{vv} - e^{2\vartheta} = 0. \tag{33}$$

To summarize then, the Gauss-Mainardi-Codazzi equations reduce to the following form under (27):

$$\begin{aligned} A_v &= B\vartheta_v, \\ B_u &= A\vartheta_u, \\ \vartheta_{uu} + \vartheta_{vv} - e^{2\vartheta} &= 0. \end{aligned} \tag{34}$$

Based on the results in (34), it is possible to make further links to other types of equations which are of importance in mathematics and physics. These arise by working out the compatibility conditions between them. Suppose two independent functions F and G and related to A and B in the following way:

$$\begin{aligned} 2A &= F + G, \\ 2B &= G - F. \end{aligned} \tag{35}$$

Putting these in the first equation of (34) and collecting like functions on opposite sides and multiplying by $e^{-\vartheta}$ give

$$e^{-\vartheta}\left(G_u - G\vartheta_u\right) = \left(F_u + F\vartheta_u\right)e^{-\vartheta}. \tag{36}$$

Doing the same thing to the second equation gives

$$-\vartheta_v G e^{-\vartheta} + G_v e^{-\vartheta} = -e^{-2\vartheta}\left(F_v e^{\vartheta} + F\vartheta_v e^{\vartheta}\right). \tag{37}$$

Using the product rule on (36) and (37), the following pair of equations has been obtained:

$$\begin{aligned} \left(e^{-\vartheta}G\right)_u &= e^{-2\vartheta}\left(Fe^{\vartheta}\right)_u, \\ \left(e^{-\vartheta}G\right)_v &= -e^{-2\vartheta}\left(Fe^{\vartheta}\right)_v. \end{aligned} \tag{38}$$

Finally, the desired compatibility condition for F can be obtained by differentiating $(e^{-\vartheta}G)_u$ with respect to v, then $(e^{-\vartheta}G)_v$ with respect to u, and finally equating the results. After multiplying the result by $e^{-\vartheta}$, this simplifies to the following:

$$e^{-\vartheta}F_{uv} = \left(e^{-\vartheta}\right)_{uv}F. \tag{39}$$

To obtain an analogous equation for G, $(e^{\vartheta}F)_u$ is differentiated with respect to v and $(e^{\vartheta}F)_v$ with respect to u. Upon equating them, one obtains

$$e^{\vartheta}G_{uv} = \left(e^{\vartheta}\right)_{uv}G. \tag{40}$$

These steps have proved the following theorem.

Theorem 2. *The compatibility conditions for functions F and G defined in terms of A and B by (35) are specified in terms of the following Moutard equations:*

$$\begin{aligned} e^{-\vartheta}F_{uv} &= \left(e^{-\vartheta}\right)_{uv}F, \\ e^{\vartheta}G_{uv} &= \left(e^{\vartheta}\right)_{uv}G. \end{aligned} \tag{41}$$

Normally, there exists a close connection between the Moutard equation and a transformation called the fundamental transformation between surfaces. We show that a Lax pair exists for the second-order system in (34). Let $\mathbf{X}$, $\mathbf{Y}$ be unit space-like tangent vectors to Σ in $\mathbb{E}_1^3$.

Theorem 3. *Let $\mathbf{X}$, $\mathbf{Y}$ be unit tangent vectors and $\mathbf{N}$ a unit normal to the space-like surface Σ. Define the following matrix system which depends on function ϑ:*

$$\begin{aligned} \begin{pmatrix} \mathbf{X} \\ \mathbf{Y} \\ \mathbf{N} \end{pmatrix}_u &= \begin{pmatrix} 0 & -\vartheta_v & \lambda e^{\vartheta} \\ \vartheta_v & 0 & 0 \\ \frac{1}{\lambda}e^{\vartheta} & 0 & 0 \end{pmatrix} \begin{pmatrix} \mathbf{X} \\ \mathbf{Y} \\ \mathbf{N} \end{pmatrix}, \\ \begin{pmatrix} \mathbf{X} \\ \mathbf{Y} \\ \mathbf{N} \end{pmatrix}_v &= \begin{pmatrix} 0 & \vartheta_u & 0 \\ -\vartheta_u & 0 & \lambda e^{\vartheta} \\ 0 & \frac{1}{\lambda}e^{\vartheta} & 0 \end{pmatrix} \begin{pmatrix} \mathbf{X} \\ \mathbf{Y} \\ \mathbf{N} \end{pmatrix}. \end{aligned} \tag{42}$$

In (42), λ is a spectral parameter. The zero curvature condition for system (42) is satisfied if and only if function ϑ satisfies the second-order equation of (34), namely,

$$\vartheta_{uu} + \vartheta_{vv} - e^{2\vartheta} = 0. \tag{43}$$

Proof. It suffices to differentiate the first matrix equation in (42) with respect to v, and the second with respect to u and require that the results agree identically. In other words, (42) is equivalent to the first-order system:

$$\begin{aligned}
\mathbf{X}_u &= -\vartheta_v \mathbf{Y} + \lambda e^{\vartheta} \mathbf{N}, \\
\mathbf{Y}_u &= \vartheta_v \mathbf{X}, \\
\mathbf{N}_u &= \frac{1}{\lambda} e^{\vartheta} \mathbf{X}, \\
\mathbf{X}_v &= \vartheta_u \mathbf{Y}, \\
\mathbf{Y}_v &= -\vartheta_u \mathbf{X} + \lambda e^{\vartheta} \mathbf{N}, \\
\mathbf{N}_v &= \frac{1}{\lambda} e^{\vartheta} \mathbf{Y}.
\end{aligned} \tag{44}$$

Condition $\mathbf{X}_{uv} = \mathbf{X}_{vu}$ under (44) reduces to

$$\begin{aligned}
&-\vartheta_{vv}\mathbf{Y} - \vartheta_v \left(-\vartheta_u \mathbf{X} + \lambda e^{\vartheta} \mathbf{N}\right) + \lambda \vartheta_v e^{\vartheta} \mathbf{N} + e^{2\vartheta} \mathbf{Y} \\
&\quad = \vartheta_{uu} \mathbf{Y} + \vartheta_u \vartheta_v \mathbf{X}.
\end{aligned} \tag{45}$$

Simplifying this, the spectral parameter disappears and equality holds exactly when the function ϑ satisfies the second-order equation, $\vartheta_{uu} + \vartheta_{vv} - e^{2\vartheta} = 0$. Similarly, the condition $\mathbf{Y}_{uv} = \mathbf{Y}_{vu}$ is

$$\begin{aligned}
\vartheta_{vv}\mathbf{X} + \vartheta_v \vartheta_u \mathbf{Y} &= -\vartheta_{uu}\mathbf{X} - \vartheta_u \left(-\vartheta_v \mathbf{Y} + \lambda e^{\vartheta} \mathbf{N}\right) \\
&\quad + \lambda \vartheta_u e^{\vartheta} \mathbf{N} + e^{2\vartheta} \mathbf{X}.
\end{aligned} \tag{46}$$

This holds whenever ϑ satisfies this partial differential equation. Finally, $\mathbf{N}_{uv} = \mathbf{N}_{vu}$ simply reduces to

$$\frac{1}{\lambda}\left(\vartheta_v e^{\vartheta} \mathbf{X} + \vartheta_u e^{\vartheta} \mathbf{Y}\right) = \frac{1}{\lambda}\left(\vartheta_u e^{\vartheta} \mathbf{Y} + \vartheta_v e^{\vartheta} \mathbf{X}\right) \tag{47}$$

which is an identity. □

To write the position vector of the surface, it is useful to define the new variable $\mathbf{S}$ in terms of $\mathbf{X}$, $\mathbf{Y}$ as follows:

$$\mathbf{S} = \mathbf{X} + i\mathbf{Y}. \tag{48}$$

Taking $z = u + iv$ to be complex, the following complex derivatives are defined:

$$\begin{aligned}
\partial &= \frac{1}{2}\left(\partial_u - i\partial_v\right), \\
\bar{\partial} &= \frac{1}{2}\left(\partial_u + i\partial_v\right).
\end{aligned} \tag{49}$$

In terms of $\mathbf{S}$ and these derivatives, (44) can be abbreviated to the following form:

$$\begin{aligned}
\partial \mathbf{S} &= -(\partial\vartheta)\,\mathbf{S} + e^{\vartheta}\mathbf{N}, \\
\bar{\partial}\mathbf{S} &= \left(\bar{\partial}\vartheta\right)\mathbf{S}, \\
\partial \mathbf{N} &= \frac{1}{2} e^{\vartheta} \bar{\mathbf{S}}, \\
\bar{\partial}\mathbf{N} &= \frac{1}{2} e^{\vartheta} \mathbf{S}.
\end{aligned} \tag{50}$$

The position vector $\mathbf{r}$ of the space-like surface will be obtained by integration of the following equation:

$$\mathbf{r}_z = \frac{1}{4}\left(P\mathbf{S} + R\bar{\mathbf{S}}\right). \tag{51}$$

To this end, introduce the scalar quantity:

$$\tau = \mathbf{r} \cdot \mathbf{N}, \tag{52}$$

which can be regarded as the distance from the origin to the tangent plane on the space-like surface at the point $\mathbf{r}$. Differentiating τ with respect to z and $\bar{z}$, we find that

$$\begin{aligned}
\partial\tau &= \frac{1}{2} e^{\vartheta} \mathbf{r} \cdot \bar{\mathbf{S}}, \\
\bar{\partial}\tau &= \frac{1}{2} e^{\vartheta} \mathbf{r} \cdot \mathbf{S}.
\end{aligned} \tag{53}$$

The position vector $\mathbf{r}$ of the space-like surface therefore admits a decomposition of the following form:

$$\mathbf{r} = e^{-\vartheta}(\partial\tau)\,\mathbf{S} + e^{-\vartheta}\left(\bar{\partial}\tau\right)\bar{\mathbf{S}} - \tau\mathbf{N}. \tag{54}$$

To obtain $\partial\mathbf{r}$ in terms of τ and ϑ, differentiate $\mathbf{r}$ with respect to z and substitute (50):

$$\begin{aligned}
\mathbf{r}_z &= -\vartheta_z e^{-\vartheta}\tau_z \mathbf{S} + e^{-\vartheta}\tau_{zz}\mathbf{S} + e^{-\vartheta}\tau_z \mathbf{S}_z - \vartheta_z e^{-\vartheta}\tau_{\bar{z}}\bar{\mathbf{S}} \\
&\quad + e^{-\vartheta}\tau_{\bar{z}z}\bar{\mathbf{S}} + e^{-\vartheta}\tau_{\bar{z}}\bar{\mathbf{S}}_z - \tau_z\mathbf{N} - \tau\mathbf{N}_z.
\end{aligned} \tag{55}$$

Replacing the first derivatives from (44), this derivative simplifies to

$$\begin{aligned}
\mathbf{r}_z &= e^{-\vartheta}\left(-\vartheta_z\tau_z + \tau_{zz} - \vartheta_z\tau_z\right)\mathbf{S} \\
&\quad + e^{-\vartheta}\left(-\vartheta_z\tau_{\bar{z}} + \tau_{z\bar{z}} + \vartheta_z\tau_{\bar{z}} - \frac{1}{2}\tau e^{2\vartheta}\right)\bar{\mathbf{S}} \\
&\quad + \left(\tau_z - \tau_z\right)\mathbf{N} \\
&= e^{\vartheta}\left(e^{-2\vartheta}\tau_z\right)_z \mathbf{S} + \frac{1}{2}e^{-\vartheta}\left(2\tau_{z\bar{z}} - \tau e^{2\vartheta}\right)\bar{\mathbf{S}}.
\end{aligned} \tag{56}$$

Comparing this result with (51), this procedure allows us to write P and R in terms of ϑ and τ:

$$\begin{aligned}
P &= 4e^{\vartheta}\left(e^{-2\vartheta}\tau_z\right)_z, \\
R &= e^{-\vartheta}\left(4\tau_{z\bar{z}} - 2\tau e^{2\vartheta}\right).
\end{aligned} \tag{57}$$

It has been found that the position vector of the space-like surface is given by $\mathbf{r}$ where the real function τ is a solution of the following equation:

$$\tau_{zz} - 2\vartheta_z \tau_z = \frac{1}{4} e^{\vartheta} P. \tag{58}$$

Finally, it can be shown that (58) is equivalent to an inhomogeneous Schrödinger equation. To do so, a new variable $\Psi(z, \overline{z})$ is introduced and defined as

$$\Psi = e^{-\vartheta} \tau. \tag{59}$$

Differentiating both sides of Ψ with respect to z gives

$$e^{-2\vartheta} \tau_z = e^{-\vartheta} \left(\vartheta_z \Psi + \Psi_z \right), \tag{60}$$

and, after a second time, we have

$$\begin{aligned} \left(e^{-2\vartheta} \tau_z \right)_z = & -\vartheta_z e^{-\vartheta} \left(\vartheta_z \Psi + \Psi_z \right) \\ & + e^{-\vartheta} \left(\vartheta_{zz} \Psi + \vartheta_z \Psi_z + \Psi_{zz} \right). \end{aligned} \tag{61}$$

Substituting this second derivative on the left of (58), the following second-order equation for Ψ results after dividing out $e^{-\vartheta}$ is

$$\Psi_{zz} + \left(\vartheta_{zz} - \vartheta_z^2 \right) \Psi = \frac{1}{4} P. \tag{62}$$

Introducing the potential function which is defined in terms of ϑ as $V = \vartheta_{zz} - \vartheta_z^2$, (62) assumes the following form:

$$\Psi_{zz} + V\Psi = \frac{1}{4} P. \tag{63}$$

4. Surfaces with Time-like Metric

To obtain a metric for this case with a time-like structure on Σ it must be that $\epsilon = 1$ and $\eta = -1$ in (4). The metric g then assumes the following form:

$$g = \begin{pmatrix} 1 & 0 & 0 \\ 0 & 1 & 0 \\ 0 & 0 & -1 \end{pmatrix} \tag{64}$$

Structure equations (9)-(11) then differ by signs and are given by

$$\begin{aligned} d\omega_1 &= \omega_2 \wedge \omega_{21}, \\ d\omega_2 &= \omega_1 \wedge \omega_{12}, \end{aligned} \tag{65}$$

$$\omega_1 \wedge \omega_{13} - \omega_2 \wedge \omega_{23} = 0, \tag{66}$$

$$\begin{aligned} d\omega_{12} &= -\omega_{13} \wedge \omega_{32}, \\ d\omega_{13} &= \omega_{12} \wedge \omega_{23}, \\ d\omega_{23} &= -\omega_{21} \wedge \omega_{13}, \end{aligned} \tag{67}$$

$$\omega_{ij} + \omega_{ji} = 0. \tag{68}$$

The one-forms ω_1 and ω_2 required to define the first fundamental form (5) are taken to be

$$\begin{aligned} \omega_1 &= -A du, \\ \omega_2 &= B dv, \end{aligned} \tag{69}$$

where A, B are functions of the coordinates (u, v). Furthermore, the one-forms ω_{13} and ω_{23} take the following form:

$$\begin{aligned} \omega_{13} &= -\kappa_1 A du, \\ \omega_{23} &= \kappa_2 B dv. \end{aligned} \tag{70}$$

Based on the one-forms (69)-(70), the three fundamental forms for Σ can be written as

$$\begin{aligned} I &= A^2 du^2 - B^2 dv^2, \\ II &= \kappa_1 A^2 du^2 - \kappa_2 B^2 dv^2, \\ III &= \kappa_1^2 A^2 du^2 - \kappa^2 B^2 dv^2. \end{aligned} \tag{71}$$

Since both ω_1 and ω_{13} differ from the previous case, ω_{12} has to be determined again, and it is given by

$$\omega_{12} = \frac{A_v}{B} du + \frac{B_u}{A} dv. \tag{72}$$

Equation (66) is satisfied automatically by this system of forms as well. The remaining three equations (67) can now be computed exactly as before. The conclusion is that a second-order equation results, namely,

$$\left(\frac{B_u}{A} \right)_u - \left(\frac{A_v}{B} \right)_v + \kappa_1 \kappa_2 AB = 0, \tag{73}$$

as in the previous case, and the pair

$$\begin{aligned} \kappa_{1,v} + \left(\log A \right)_v \left(\kappa_1 - \kappa_2 \right) &= 0, \\ \kappa_{2,u} + \left(\log B \right)_u \left(\kappa_2 - \kappa_1 \right) &= 0. \end{aligned} \tag{74}$$

Both equations in (74) are seen to be identical to their corresponding counterparts in (74). In this case as well, the equations in (73) and (74) can be written in such a way that the fundamental form III is conformally flat assuming the form (1), $A\kappa_1 = B\kappa_2 = e^{\vartheta}$. Since the steps are identical to the previous case, the results are summarized as follows:

$$\begin{aligned} A_v &= B\vartheta_v, \\ B_u &= A\vartheta_u, \\ \vartheta_{uu} - \vartheta_{vv} + e^{2\vartheta} &= 0. \end{aligned} \tag{75}$$

These are exactly analogous to (34), the first two being identical to those of the space-like case. The second-order equation differs by signs from the case (34). Since the first two equations are exactly the same, similar functions F and G can be introduced which are related to A and B as in (35). All the steps which lead to Theorem 2 are unchanged as they involve only the first two equations and are independent of the second-order equation. Thus, a version of Theorem 2 can be formulated here as well. The Lax pair however has to be different since the second-order equation is different.

Theorem 4. *Let* $\mathbf{X}$, $\mathbf{Y}$ *be unit tangent vectors to time-like surface* Σ *and* $\mathbf{N}$ *a unit normal vector to* Σ. *Define the following matrix system in terms of function* ϑ *as*

$$\begin{pmatrix}\mathbf{X}\\ \mathbf{Y}\\ \mathbf{N}\end{pmatrix}_u = \begin{pmatrix}0 & -\vartheta_v & e^{\vartheta}\\ \vartheta_v & 0 & 0\\ e^{\vartheta} & 0 & 0\end{pmatrix}\begin{pmatrix}\mathbf{X}\\ \mathbf{Y}\\ \mathbf{N}\end{pmatrix},$$
$$\begin{pmatrix}\mathbf{X}\\ \mathbf{Y}\\ \mathbf{N}\end{pmatrix}_v = \begin{pmatrix}0 & \vartheta_u & 0\\ -\vartheta_u & 0 & e^{\vartheta}\\ 0 & e^{\vartheta} & 0\end{pmatrix}\begin{pmatrix}\mathbf{X}\\ \mathbf{Y}\\ \mathbf{N}\end{pmatrix} \tag{76}$$

The compatibility condition in (u, v) *for this system holds if and only if function* ϑ *satisfies the second-order equation in (75), namely,*

$$\vartheta_{uu} - \vartheta_{vv} + e^{2\vartheta} = 0. \tag{77}$$

The proof of Theorem 4 goes exactly as the proof of (42). To illustrate, the details for the $\mathbf{X}$ *equations will be given. Differentiating the first matrix equation by* v *and the second by* u *and substituting (76) for the first derivatives, it is found that*

$$\begin{aligned}\mathbf{X}_{uv} &= -\vartheta_{vv}\mathbf{Y} - \vartheta_v\left(-\vartheta_u\mathbf{X} + e^{\vartheta}\mathbf{N}\right) + \vartheta_v e^{\vartheta}\mathbf{N} + e^{2\vartheta}\mathbf{Y}\\ &= -\vartheta_{uu}\mathbf{Y} + \vartheta_u\vartheta_v\mathbf{X} = \mathbf{X}_{vu}.\end{aligned} \tag{78}$$

This will be satisfied provided that ϑ *satisfies the second-order equation in (75). A similar result is found to hold for the* $\mathbf{Y}$ *equation and* $\mathbf{N}_{uv} = \mathbf{N}_{vu}$ *holds as an identity.*

Again, if $\mathbf{S}$ is defined exactly as in the previous case, then, in terms of complex derivatives, and using the equations of (76), the system corresponding to (50) is

$$\begin{aligned}\overline{\partial}\mathbf{S} &= -\left(\overline{\partial}\vartheta\right)\overline{\mathbf{S}} + e^{\vartheta}\mathbf{N},\\ \overline{\partial}\mathbf{S} &= (\partial\vartheta)\,\overline{\mathbf{S}},\\ \partial\mathbf{N} &= -\frac{1}{2}e^{\vartheta}\mathbf{S},\\ \overline{\partial}\mathbf{N} &= -\frac{1}{2}e^{\vartheta}\overline{\mathbf{S}}.\end{aligned} \tag{79}$$

Taking $\mathbf{r}_z$ to have the same form (51) and $\mathbf{r}$ given by (54), then differentiating (54) with respect to z and comparing to (51), it is found that

$$\begin{aligned}b_{zz} - \vartheta_z b_z + \vartheta_{\overline{z}} b_{\overline{z}} + \frac{1}{2}e^{2\vartheta}b &= \frac{1}{4}Pe^{\vartheta},\\ b_{z\overline{z}} - \vartheta_z b_{\overline{z}} - \vartheta_{\overline{z}} b_z &= \frac{1}{4}Re^{\vartheta}.\end{aligned} \tag{80}$$

Supposing τ has the form (35), then the first equation in (80) becomes a second-order partial differential equation for the function $\Psi(z, \overline{z})$, namely,

$$\Psi_{zz} + \vartheta_z\Psi_z + \vartheta_{\overline{z}}\Psi_{\overline{z}} + \left(\vartheta_{zz} + \vartheta_z^2 + \frac{1}{2}e^{2\vartheta}\right)\Psi = \frac{1}{4}P. \tag{81}$$

5. Conclusions and Summary

In the Cartan framework, we can discuss isothermic surfaces in Minkowski three-space for both space-like and time-like cases. As Theorems 2 and 4 show, the classical Gauss-Mainardi-Codazzi system associated with isothermic surfaces is integrable in the modern solitonic sense. Bäcklund transformations will exist for both types of surface. The appearance of the Moutard equations (41) in both cases is remarkable, and, subsequently, Sturm-Liouville or Schrödinger equation (62). This leads to the final proposition.

Proposition 5. *Let* V *and* P *satisfy the compatibility condition* $P_{\alpha\beta} = 2P\,\mathrm{Im}\,V$ *and let* Ψ *be a real solution of the inhomogeneous Schrödinger equation (63). Then with* $\tau = e^{\vartheta}\Psi$, *(54) provides a position vector for a space-like isothermic surface.*

Conflicts of Interest

The author declares that they have no conflicts of interest.

References

[1] L. Bianchi, "Ricerche sulle superficie isoterme e sulla deformazione delle quadriche," *Annali di Matematica Pura ed Applicata*, vol. 11, no. 1, pp. 93–157, 1905.

[2] E. Bour, "Theories de la deformation des surfaces," *J. lEcole Imperiale Polytech*, vol. 19, p. 48, 1862.

[3] G. Darboux, "Sur les surfaces isothermiques," *Comptes Rendus de l'Académie des Sciences*, vol. 128, pp. 1299–1305, 1899.

[4] C. Rogers and W. K. Schief, *Bäcklund and Darboux Transformations, Geometry and Modern Applications in Soliton Theory*, Cambridge Texts in Applied Mathematics, Cambridge University Press, Cambridge, UK, 2002.

[5] C. Rogers and A. Szereszewski, "A Bäcklund transformation for L-isothermic surfaces," *Journal of Physics A: Mathematical and General*, vol. 42, no. 40, Article ID 404015, 12 pages, 2009.

[6] W. K. Schief, A. Szereszewski, and C. Rogers, "The Lamé-type equation in shell membrane theory," *Journal of Mathematical Physics*, vol. 48, no. 7, Article ID 073510, 23 pages, 2007.

[7] R. Hermann, *The geometry of non-linear differential equations, Bäcklund Transformations and Solitons, Part A*, Math Sci Press, Brookline, Mass, USA, 1976.

[8] L. P. Eisenhart, *Transformations of surfaces*, Chelsea Publishing Co., NY, USA, 1962.

[9] M. P. do Carmo, *Differential Geometry of Curves and Surfaces*, Prentice Hall, Englewood Cliffs, NJ, USA, 1976.

[10] P. Bracken, "Determination of surfaces in three-dimensional Minkowski and Euclidean spaces based on solutions of the sinh-Laplace equation," *International Journal of Mathematics and Mathematical Sciences*, vol. 2005, no. 9, pp. 1393–1404, 2005.

[11] M. J. Ablowitz, D. J. Kaup, A. C. Newell, and H. Segur, "The inverse scattering transform-Fourier analysis for nonlinear problems," *Studies in Applied Mathematics*, vol. 53, no. 4, pp. 249–315, 1974.

[12] S. S. Chern, W. H. Chen, and K. S. Lam, *Lectures on Differential Geometry*, World Scientific, Singapore, 1999.

[13] K. Alkan and S. C. Anco, "Integrable systems from inelastic curve flows in 2- and 3- dimensional space," *Journal of Nonlinear Mathematical Physics*, vol. 23, no. 2, pp. 256–299, 2016.

[14] N. Gürbüz, "Inextensible flows of spacelike, timelike and null curves," *International Journal of Contemporary Mathematical Sciences*, vol. 4, no. 29-32, pp. 1599–1604, 2009.

[15] P. Bracken and J. Hayes, "On a formulation of certain integrable systems using hyperbolic numbers," *Physics Letters A*, vol. 301, no. 3-4, pp. 191–194, 2002.

4

Mass Renormalization in the Nelson Model

Fumio Hiroshima[1] and Susumu Osawa[2]

[1]*Faculty of Mathematics, Kyushu University, Fukuoka 819-0385, Japan*
[2]*Faculty of Science, Department of Mathematics, Hokkaido University, Sapporo, Hokkaido 060-0810, Japan*

Correspondence should be addressed to Susumu Osawa; susumu_osawa@kyudai.jp

Academic Editor: Rodica D. Costin

The asymptotic behavior of the effective mass $m_{\mathrm{eff}}(\Lambda)$ of the so-called Nelson model in quantum field theory is considered, where Λ is an ultraviolet cutoff parameter of the model. Let m be the bare mass of the model. It is shown that for sufficiently small coupling constant $|\alpha|$ of the model, $m_{\mathrm{eff}}(\Lambda)/m$ can be expanded as $m_{\mathrm{eff}}(\Lambda)/m = 1 + \sum_{n=1}^{\infty} a_n(\Lambda)\alpha^{2n}$. A physical folklore is that $a_n(\Lambda) = O([\log\Lambda]^{(n-1)})$ as $\Lambda \to \infty$. It is rigorously shown that $0 < \lim_{\Lambda\to\infty} a_1(\Lambda) < C$, $C_1 \le \lim_{\Lambda\to\infty} a_2(\Lambda)/\log\Lambda \le C_2$ with some constants C, C_1, and C_2.

1. Introduction and Main Results

The model considered in this paper is the so-called Nelson model [1], which describes a nonrelativistic nucleon with bare mass $m > 0$ interacting with a quantized scalar field with mass $\nu > 0$. The nucleon is governed by a Schrödinger operator. Let us first define the Nelson Hamiltonian. We use relativistic unit and employ the total momentum representation. Then the Hilbert space of states is the boson Fock space over $L^2(\mathbb{R}^3)$ which is given by

$$\mathscr{F} = \bigoplus_{n=0}^{\infty} \left[\bigotimes_{s}^{n} L^2\left(\mathbb{R}^3\right) \right], \tag{1}$$

where $\bigotimes_s^n$ denotes the n-fold symmetric tensor product and $\bigotimes_s^0 L^2(\mathbb{R}^3) = \mathbb{C}$. Then $\Phi \in \mathscr{F}$ can be written as $\Phi = \{\Phi^{(0)}, \Phi^{(1)}, \Phi^{(2)}, \ldots\}$, where $\Phi^{(n)} \in \bigotimes_s^n L^2(\mathbb{R}^3)$. The Fock vacuum $\Omega \in \mathscr{F}$ is defined by $\Omega = \{1, 0, 0, \ldots\}$. Let $a(f)$, $f \in L^2(\mathbb{R}^3)$, be the annihilation operator and $a(f)^*$, $f \in L^2(\mathbb{R}^3)$, the creation operator on $\mathscr{F}$, which are defined by

$$\begin{aligned} &D\left(a(f)^*\right) \\ &= \left\{ \Psi \in \mathscr{F} \mid \sum_{n=0}^{\infty} (n+1) \left\| S_{n+1}\left(f \otimes \Psi^{(n)}\right) \right\|_{\otimes^n L^2(\mathbb{R}^3)}^2 < \infty \right\}, \\ &\left(a(f)^* \Psi\right)^{(0)} = 0, \\ &\left(a(f)^* \Psi\right)^{(n+1)} = \sqrt{n+1}\, S_{n+1}\left(f \otimes \Psi^{(n)}\right), \end{aligned} \tag{2}$$

and $a(f) = (a(f)^*)^*$, where S_n is the symmetrizer, $D(X)$ the domain of operator X, and $\|\cdot\|_{\mathscr{K}}$ the norm on $\mathscr{K}$. They satisfy canonical commutation relations as follows:

$$\begin{aligned} \left[a(f), a(g)^*\right] &= (f, g), \\ [a(f), a(g)] &= 0, \\ \left[a(f)^*, a(g)^*\right] &= 0 \end{aligned} \tag{3}$$

on a suitable dense domain, where $[X, Y] = XY - YX$ and $(\cdot,\cdot)$ is the inner product on $\mathscr{K}$ (linear in the second variable). Let T be a self-adjoint operator on $L^2(\mathbb{R}^3)$. Then we define the self-adjoint operator $d\Gamma(T)$ on $\mathscr{F}$ by $d\Gamma(T) = \bigoplus_{n=0}^{\infty} T^{(n)}$, where

$$T^{(n)} = \overline{\left(\sum_{j=1}^{n} I \otimes \cdots \otimes I \otimes \overset{j\text{th}}{\check{T}} \otimes I \otimes \cdots \otimes I \right) \Bigg\lceil \overline{\bigotimes^{n} D(T)}} \tag{4}$$

$$(n \ge 1)$$

with $T^{(0)} = 0$. Here, for a closable operator T, $\overline{T}$ denotes the closure of T. The operator $d\Gamma(T)$ is called the second quantization of T. The free energy of the scalar field is given by $H_f = d\Gamma(\omega)$, where $\omega(k) = \sqrt{|k|^2 + \nu^2}$ ($k = (k_1, k_2, k_3) \in \mathbb{R}^3$, $\nu > 0$) is considered as a multiplication operator on $L^2(\mathbb{R}^3)$. Similarly the momentum of the scalar field is given by $P_{f\mu} = \mathrm{d}\Gamma(k_\mu)$ ($\mu = 1, 2, 3$). The coupling of the nucleon and a scalar field is mediated through the Segal field operator $\Phi_s(g)$ defined by

$$\Phi_s(g) = \frac{1}{\sqrt{2}}\left(a(g) + a(g)^*\right), \tag{5}$$

where g is a cutoff function given by $g(k) = \widehat{\phi}(k)/\sqrt{\omega(k)}$. Here $\widehat{\phi}$ is the form factor with infrared cutoff $\kappa > 0$ and ultraviolet cutoff $\Lambda > 0$, which are defined by

$$\widehat{\phi}(k) = \begin{cases} 0 & |k| < \kappa, \\ (2\pi)^{-3/2} & \kappa \le |k| \le \Lambda, \\ 0 & |k| > \Lambda. \end{cases} \tag{6}$$

The Nelson Hamiltonian with total momentum $p \in \mathbb{R}^3$ is given by a self-adjoint operator on $\mathcal{F}$ as follows:

$$H(p) = \frac{1}{2m}\left(p - P_f\right)^2 + H_f + \alpha\Phi_s(g), \tag{7}$$

where $\alpha \in \mathbb{R}$ is a coupling constant. Let $E(p, \alpha)$ be the energy-momentum relation (the infimum of the spectrum $\sigma(H(p))$) defined by

$$E(p, \alpha) = \inf \sigma(H(p)). \tag{8}$$

Then the effective mass $m_{\mathrm{eff}} = m_{\mathrm{eff}}(\Lambda)$ is defined by

$$\frac{1}{m_{\mathrm{eff}}} = \frac{1}{3}\Delta_p E(p, \alpha)\restriction_{p=0}. \tag{9}$$

Here Δ_p denotes the three-dimensional Laplacian in the variable p. We are concerned with the asymptotic behavior of m_{eff} as the ultraviolet cutoff goes to infinity. It is however a subtle problem. Removal of the ultraviolet cutoff Λ through mass renormalization means finding sequences $\{m\}$ and $\{\Lambda\}$ such that $m \to 0$, $\Lambda \to \infty$, and m_{eff} converges. Since we can see that m_{eff}/m is a function of Λ/m, to achieve this, we want to find constants $0 < \gamma < 1$ and $0 < b_0 < \infty$ such that

$$\lim_{\Lambda\to\infty} \frac{m_{\mathrm{eff}}/m}{(\Lambda/m)^\gamma} = b_0. \tag{10}$$

If we succeed in finding constants γ and b_0 such as in (10), scaling the bare mass m as

$$m = \frac{1}{\Lambda^{\gamma/(1-\gamma)}} M, \tag{11}$$

where $M = (m^*/b_0)^{1/(1-\gamma)}$ with an arbitrary positive constant m^*, we have

$$\lim_{\Lambda\to\infty} m_{\mathrm{eff}}(\Lambda) = m^*. \tag{12}$$

The mass renormalization is, however, a subtle problem, and unfortunately, we cannot yet find constants γ and b_0 such as in (10). For that reason we turn to perturbative renormalization, by which we try to guess the proper value of γ. Main results obtained in this paper are summarized as follows.

Theorem 1. *Let $\kappa > 0$. Then m_{eff} is an analytic function of α^2 and can be expanded in the following power series for sufficiently small $|\alpha|$:*

$$\frac{m_{\mathrm{eff}}}{m} = 1 + \sum_{n=1}^{\infty} a_n(\Lambda)\,\alpha^{2n}. \tag{13}$$

Theorem 2. *There exists a strictly positive constant C such that*

$$\lim_{\Lambda\to\infty} a_1(\Lambda) = C. \tag{14}$$

Theorem 3. *There exist some constants C_1 and C_2 such that*

$$C_1 \le \lim_{\Lambda\to\infty} \frac{a_2(\Lambda)}{\log\Lambda} \le C_2. \tag{15}$$

From Theorems 2 and 3, if $D = \lim_{\Lambda\to\infty} a_2(\Lambda)/\log\Lambda > 0$, it is suggested that $\gamma = D\alpha^2/C$. So, the mass of the Nelson model is renormalizable for sufficiently small $|\alpha|$.

The effective mass and energy-momentum relation have been studied mainly in nonrelativistic electrodynamics. Spohn [2] investigates the upper and lower bound of the effective mass of the polaron model from a functional integral point of view. Hiroshima and Spohn [3] study a perturbative mass renormalization including fourth order in the coupling constant in the case of a spinless electron. Hiroshima and Ito [4, 5] study it in the case of an electron with spin 1/2. Bach et al. [6] show that the energy-momentum relation is equal to the infimum of the essential spectrum of the Hamiltonian for $\kappa \ge 0$. Fröhlich and Pizzo [7] investigate energy-momentum relation when infrared cutoff goes to 0.

2. Analytic Properties

In order to investigate the effective mass in a perturbation theory we have to check the analytic properties of $E(p, \alpha)$.

2.1. Analytic Family in the Sense of Kato

Lemma 4. *$H(p)$ is an analytic family in the sense of Kato.*

Proof. We prove $H(p)$ is an analytic family of type (A). We see that

$$H(p) = H_0 + \sum_{\mu=1}^{3} p_\mu \frac{1}{2m}\left(p_\mu - 2P_{f\mu}\right) + \alpha H_I, \tag{16}$$

where $H_0 = (1/2m)P_f^2 + H_f$ and $H_I = \Phi_s(g)$. Hence all we have to do is to prove the following facts.

(a) $D(H_0) \subset \bigcap_{\mu=1}^{3} D(P_{f\mu}) \cap D(H_I)$.

(b) There exist real constants a_μ, b_μ $(\mu = 1,2,3)$, c, and d such that for any $\Psi \in D(H_0)$

$$\left\| \frac{1}{2m}\left(p_\mu - 2P_{f\mu}\right)\Psi \right\|_{\mathscr{F}} \le a_\mu \left\| H_0\Psi \right\|_{\mathscr{F}} + b_\mu \left\|\Psi\right\|_{\mathscr{F}} \quad (\mu = 1,2,3), \qquad \left\| H_I\Psi \right\|_{\mathscr{F}} \le c\left\| H_0\Psi \right\|_{\mathscr{F}} + d\left\|\Psi\right\|_{\mathscr{F}}. \tag{17}$$

We prove (a) at first. Since $\bigcap_{\mu=1}^{3} D(P_{f\mu}^2) \subset D(P_{f\mu})$, we have $D(H_0) = \bigcap_{\mu=1}^{3} D(P_{f\mu}^2) \cap D(H_f) \subset \bigcap_{\mu=1}^{3} D(P_{f\mu})$. Additionally, since $\|\omega^{-1/2} g\|_{L^2(\mathbb{R}^3)} < \infty$, we have $g \in D(\omega^{-1/2})$. Furthermore, since ω is a nonnegative and injective self-adjoint operator on $L^2(\mathbb{R}^3)$, it follows that $D(d\Gamma(\omega)^{1/2}) \subset D(a(g)) \cap D(a(g)^*) = D(H_I)$. Hence we have $D(H_0) \subset D(d\Gamma(\omega)) \subset D(d\Gamma(\omega)^{1/2})$. Together with them, (a) is proven. Next we prove (b). Let Ψ be an arbitrary vector in $D(H_0)$. Then we have

$$\left\| \frac{1}{2m}\left(p_\mu - 2P_{f\mu}\right)\Psi \right\|_{\mathscr{F}} \le \frac{|p_\mu|}{2m}\left\|\Psi\right\|_{\mathscr{F}} + \frac{1}{m}\left\| P_{f\mu}\Psi \right\|_{\mathscr{F}}. \tag{18}$$

Since $\|P_{f\mu}\Psi\|_{\mathscr{F}}^2 \le 2m\|H_0^{1/2}\Psi\|_{\mathscr{F}}^2$, we have $\|H_0^{1/2}\Psi\|_{\mathscr{F}}^2 \le \|(H_0+1)\Psi\|_{\mathscr{F}}^2$. Hence

$$\left\| \frac{1}{2m}\left(p_\mu - 2P_{f\mu}\right)\Psi \right\|_{\mathscr{F}} \le \sqrt{\frac{2}{m}}\left\| H_0\Psi \right\|_{\mathscr{F}} + \left(\frac{|p_\mu|}{2m} + \sqrt{\frac{2}{m}} \right)\left\|\Psi\right\|_{\mathscr{F}}. \tag{19}$$

Since $D(H_0) \subset D(d\Gamma(\omega)^{1/2})$,

$$\left\| a(g)\Psi \right\|_{\mathscr{F}} \le \left\| \omega^{-1/2} g \right\|_{L^2(\mathbb{R}^3)} \left\| H_f^{1/2}\Psi \right\|_{\mathscr{F}}, \qquad \left\| a(g)^*\Psi \right\|_{\mathscr{F}} \le \left\| \omega^{-1/2} g \right\|_{L^2(\mathbb{R}^3)} \left\| H_f^{1/2}\Psi \right\|_{\mathscr{F}} + \left\| g \right\|_{L^2(\mathbb{R}^3)} \left\|\Psi\right\|_{\mathscr{F}} \tag{20}$$

hold. Hence

$$\left\| H_I\Psi \right\|_{\mathscr{F}} \le \sqrt{2}\left\| \omega^{-1/2} g \right\|_{L^2(\mathbb{R}^3)} \left\| H_f^{1/2}\Psi \right\|_{\mathscr{F}} + \frac{1}{\sqrt{2}}\left\| g \right\|_{L^2(\mathbb{R}^3)} \left\|\Psi\right\|_{\mathscr{F}}. \tag{21}$$

From triangle inequality, we have $\|H_f^{1/2}\Psi\|_{\mathscr{F}} \le \|H_f\Psi\|_{\mathscr{F}} + \|\Psi\|_{\mathscr{F}}$. In addition,

$$\left\| H_0\Psi \right\|_{\mathscr{F}}^2 - \left\| H_f\Psi \right\|_{\mathscr{F}}^2 = \left\| \frac{1}{2m} P_f^2\Psi \right\|_{\mathscr{F}}^2 + \frac{1}{m}\Re\left(P_f^2\Psi, H_f\Psi \right). \tag{22}$$

Since P_f^2 and H_f are strongly commutative and nonnegative self-adjoint operators on $\mathscr{F}$, $(P_f^2\Psi, H_f\Psi) \ge 0$ holds. Hence $\|H_f\Psi\|_{\mathscr{F}} \le \|H_0\Psi\|_{\mathscr{F}}$. Then we have

$$\left\| H_I\Psi \right\|_{\mathscr{F}} \le \sqrt{2}\left\| \omega^{-1/2} g \right\|_{L^2(\mathbb{R}^3)} \left\| H_0\Psi \right\|_{\mathscr{F}} + \left(\sqrt{2}\left\| \omega^{-1/2} g \right\|_{L^2(\mathbb{R}^3)} + \frac{1}{\sqrt{2}}\left\| g \right\|_{L^2(\mathbb{R}^3)} \right)\left\|\Psi\right\|_{\mathscr{F}}. \tag{23}$$

From (19) and (23), (b) is proven. Hence $H(p)$ is an analytic family of type (A). Since every analytic family of type (A) is an analytic family of in the sense of Kato, it is an analytic family in the sense of Kato. □

We denote the ground state of $H(p)$ by $\psi_g(p)$.

Lemma 5. (1) *$E(p,\alpha)$ is analytic in p and α if $|p|$ and $|\alpha|$ are sufficiently small.* (2) *$\psi_g(p)$ is strongly analytic in p and α if $|p|$ and $|\alpha|$ are sufficiently small.*

Proof. From [8, Theorem XII.9], (1) follows, and from [8, Theorem XII.8], (2) follows. □

2.2. Formula. In this section we expand m/m_{eff} with respect to α.

Lemma 6. *The ratio m/m_{eff} can be expressed as*

$$\frac{m}{m_{eff}} = 1 - \frac{2}{3}\sum_{\mu=1}^{3} \frac{\left(P_{f\mu}\psi_g(0), \psi'_{g_\mu}(0) \right)}{\left(\psi_g(0), \psi_g(0) \right)}, \tag{24}$$

where $\psi'_{g_\mu}(0) = s - \partial p_\mu \psi_g(p)\restriction_{p=0}$.

Proof. Since $E(p,\alpha)$ is symmetry, $E(p,\alpha) = E(-p,\alpha)$, we have

$$\partial p_\mu E(p,\alpha)\restriction_{p=0} = 0, \quad \mu = 1,2,3. \tag{25}$$

Since $H(p)\psi_g(p) = E(p,\alpha)\psi_g(p)$, for any $\Psi \in D(H(p))$,

$$\left(H(p)\Psi, \psi_g(p) \right) = E(p,\alpha)\left(\Psi, \psi_g(p) \right) \tag{26}$$

holds. Taking a derivative with respect to p_μ on both sides above, we have

$$\begin{aligned} &\left(H'_\mu(p)\Psi, \psi_g(p) \right) + \left(H(p)\Psi, \psi'_{g_\mu}(p) \right) = E'_\mu(p,\alpha)\left(\Psi, \psi_g(p) \right) + E(p,\alpha)\left(\Psi, \psi'_{g_\mu}(p) \right), \\ &\left(H''_\mu(p)\Psi, \psi_g(p) \right) + 2\left(H'_\mu(p)\Psi, \psi'_{g_\mu}(p) \right) + \left(H(p)\Psi, \psi''_{g_\mu}(p) \right) = E''_\mu(p,\alpha)\left(\Psi, \psi_g(p) \right) \\ &\quad + 2E'_\mu(p,\alpha)\left(\Psi, \psi'_{g_\mu}(p) \right) + E(p,\alpha)\left(\Psi, \psi''_{g_\mu}(p) \right). \end{aligned} \tag{27}$$

Here $'$ denotes the derivative or strong derivative with respect to p_μ, and $H'_\mu(p) = (1/m)(p_\mu - P_{f\mu})$, $H''_\mu(p) = 1/m$. Setting $\Psi = \psi_g(0)$ and $p = 0$, we have

$$E''_\mu(0,\alpha) = \frac{1}{m}\frac{\left(\psi_g(0),\psi_g(0)\right) - 2\left(P_{f\mu}\psi_g(0),\psi'_{g\mu}(0)\right)}{\left(\psi_g(0),\psi_g(0)\right)}. \tag{28}$$

This expression and the definition of the effective mass prove the lemma. □

2.3. Perturbative Expansions. We define operators A^+ and A^- by $A^+ = (1/\sqrt{2})a(g)^*$ and $A^- = (1/\sqrt{2})a(g)$. Then $H_I = A^+ + A^-$. Moreover, let $\mathscr{F}^{(n)} = \bigotimes_s^n L^2(\mathbb{R}^3)$ and

$$\psi_g(0) = \sum_{n=0}^{\infty}\frac{\alpha^n}{n!}\varphi_n. \tag{29}$$

Since $E(p,\alpha)$ is symmetry $E(p,-\alpha) = E(p,\alpha)$, we have

$$E(0,\alpha) = \sum_{n=0}^{\infty}\frac{\alpha^{2n}}{(2n)!}E_{2n}. \tag{30}$$

Since $\ker H_0 \neq \{0\}$, H_0 is not injective. However, we define the operator $1/H_0$ (for notational simplicity we write $1/H_0$ for H_0^{-1} in what follows) on $\mathscr{F}$ as follows.

$$\begin{aligned} &D\left(\frac{1}{H_0}\right) \\ &\quad= \left\{\Psi = \bigoplus_{n=0}^{\infty}\Psi^{(n)} \in \mathscr{F} \mid \sum_{n=1}^{\infty}\left\|\beta^n\Psi^{(n)}\right\|^2 < \infty\right\}, \\ &\left(\frac{1}{H_0}\Psi\right)^{(0)} = 0, \\ &\left(\frac{1}{H_0}\Psi\right)^{(n)}(k_1,\dots,k_n) \\ &\quad= \beta^n(k_1,\dots,k_n)\Psi^{(n)}(k_1,\dots,k_n) \quad (n \geq 1). \end{aligned} \tag{31}$$

Here

$$\begin{aligned} \beta^n &= \beta^n(k_1,\dots,k_n) \\ &= \frac{1}{(1/2m)\left|k_1+\cdots+k_n\right|^2 + \sum_{i=1}^n \omega(k_i)}. \end{aligned} \tag{32}$$

We define the subspace $\mathscr{F}_{\text{fin}}$ of $\mathscr{F}$ as $\mathscr{F}_{\text{fin}} = \{\{\Psi^{(n)}\}_{n=0}^{\infty} \in \mathscr{F} \mid \Psi^{(l)} = 0 \text{ for } l \geq q \text{ with some } q\}$.

Lemma 7. *It holds that $\mathscr{F}_{fin} \subset D(1/H_0)$.*

Proof. Let $\Psi \in \mathscr{F}_{\text{fin}}$. Then $\|(1/H_0)\Psi\|^2 = \sum_{n=1}^{\infty}\|((1/H_0)\Psi)^{(n)}\|^2 < \infty$. Hence the lemma follows. □

Lemma 8. *Let $\psi_g(0) = \sum_{n=0}^{\infty}(\alpha^n/n!)\varphi_n$. Then $\varphi_0 = \Omega$, $\varphi_1 = -(1/H_0)H_I\Omega$, and the recurrence formulas*

$$\varphi_{2l} = \frac{1}{H_0}\left\{-2lH_I\varphi_{2l-1} + \sum_{j=1}^{l}\binom{2l}{2j}E_{2j}\varphi_{2l-2j}\right\} \quad (l \geq 1), \tag{33}$$

$$\varphi_{2l+1} = \frac{1}{H_0}\left\{-(2l+1)H_I\varphi_{2l} + \sum_{j=1}^{l}\binom{2l+1}{2j}E_{2j}\varphi_{2l+1-2j}\right\} \quad (l \geq 0) \tag{34}$$

follow, with

$$\begin{aligned} \varphi_{2l} &\in \mathscr{F}^{(2)} \oplus \mathscr{F}^{(4)} \oplus \cdots \oplus \mathscr{F}^{(2l)} \quad (l \geq 1), \\ \varphi_{2l+1} &\in \mathscr{F}^{(1)} \oplus \mathscr{F}^{(3)} \oplus \cdots \oplus \mathscr{F}^{(2l+1)} \quad (l \geq 0), \end{aligned} \tag{35}$$

and E_{2l} is given by

$$E_{2l} = 2l\left(\Omega, H_I\varphi_{2l-1}\right) \quad (l \geq 1). \tag{36}$$

Proof. We have $E(0,0) = E_0$ by substituting $\alpha = 0$ in (30). Since $E(0,0)$ is the ground state energy of H_0, $E(0,0) = 0$. Hence $E_0 = 0$. Since φ_0 is the ground state of H_0, φ_0 can be Ω. We can find that $(\varphi_n,\Omega) = \delta_{0n}$ for $n = 0,1,\dots$ holds in the same way as [3]. From now we set $H = H(p)$, $\psi_g = \psi_g(0)$, $E = E(p,\alpha)$, and $'$ means (strong)derivative with respect to α.

$$\left(H\Psi,\psi_g\right) = E\left(\Psi,\psi_g\right) \tag{37}$$

holds for $\Psi \in D(H)$. Differentiating (37) with respect to α, we have

$$\left(H_I\Psi,\psi_g\right) + \left(H\Psi,\psi'_g\right) = E'\left(\Psi,\psi_g\right) + E\left(\Psi,\psi'_g\right). \tag{38}$$

Hence $\psi'_g \in D(H)$ and we have

$$H_I\psi_g + H\psi'_g = E'\psi_g + E\psi'_g. \tag{39}$$

Substituting $p = 0$ and $\alpha = 0$ into (39) and taking into account $(\varphi_n,\Omega) = \delta_{0n}$, we have $\varphi_1 = -(1/H_0)H_I\Omega$. Differentiating (37) n times with respect to α, we also have

$$\begin{aligned} &\left(H\Psi,\psi_g^{(n)}\right) + n\left(\Psi,H_I\psi_g^{(n-1)}\right) \\ &\quad= \sum_{j=1}^{n}\binom{n}{j}E^{(j)}\left(\Psi,\psi_g^{(n-j)}\right). \end{aligned} \tag{40}$$

By the induction on n, we have $\psi_g^{(n)} \in D(H)$ and

$$H\psi_g^{(n)} + nH_I\psi_g^{(n-1)} = \sum_{j=1}^{n}\binom{n}{j}E^{(j)}\psi_g^{(n-j)}. \tag{41}$$

Substituting $p = 0$ and $\alpha = 0$ into both sides above, we have

$$H_0\varphi_{2l} + 2lH_I\varphi_{2l-1} = \sum_{j=1}^{l}\binom{2l}{2j}E_{2j}\varphi_{2l-2j} \quad (l \geq 1),$$
$$H_0\varphi_{2l+1} + (2l+1)H_I\varphi_{2l} = \sum_{j=1}^{l}\binom{2l+1}{2j}E_{2j}\varphi_{2l+1-2j} \quad (l \geq 0). \tag{42}$$

From now on, we shall prove

$$\begin{aligned}
&\varphi_n^{(i)} = 0, \quad (i > n,\ i = 0),\\
&\varphi_{2l}^{(2i+1)} = 0, \quad (l \geq 1,\ 0 \leq i \leq l-1),\\
&\operatorname*{supp}_{k\in\mathbb{R}^{3\cdot 2i}}\varphi_{2l}^{(2i)}(k) = S_{2i} \text{ or } \emptyset, \quad (l \geq 1,\ 1 \leq i \leq l),\\
&\varphi_{2l+1}^{(2i)} = 0, \quad (l \geq 0,\ 0 \leq i \leq l),\\
&\operatorname*{supp}_{k\in\mathbb{R}^{3(2i+1)}}\varphi_{2l+1}^{(2i+1)}(k) = S_{2i+1} \text{ or } \emptyset, \quad (l \geq 0,\ 0 \leq i \leq l),
\end{aligned} \tag{43}$$

where we set $\varphi_n = \{\varphi_n^{(i)}\}_{i=0}^{\infty}$ by induction for $n \geq 1$, and

$$S_i = \left\{(k_1,\ldots,k_i) \in \mathbb{R}^{3i} \mid \kappa \leq |k_1| \leq \Lambda, \ldots, \kappa \leq |k_i| \leq \Lambda\right\}. \tag{44}$$

Since $\varphi_1 = -(1/H_0)H_I\Omega \in \mathscr{F}^{(1)}$, $\varphi_1^{(i)} = 0$, $i > 1$, $i = 0$. Moreover, since

$$\varphi_1^{(1)}(k_1) = -\frac{1}{\sqrt{2}(2\pi)^{3/2}\sqrt{\omega(k_1)E(k_1)}}\chi_{[\kappa,\Lambda]}(|k_1|), \tag{45}$$

we have $\operatorname{supp}_{k_1\in\mathbb{R}^3}\varphi_1^{(1)}(k_1) = S_1$, where $E(k) = |k|^2/2m + \omega(k)$. Assume that the assumption of the induction holds when $n \leq 2l+1$, $(l \geq 0)$. Then

$$\begin{aligned}
&H_0\varphi_{2l+2} + (2l+2)H_I\varphi_{2l+1}\\
&\quad = \sum_{j=1}^{l+1}\binom{2l+2}{2j}E_{2j}\varphi_{2l+2-2j}.
\end{aligned} \tag{46}$$

It is derived that $\varphi_{2l+2}^{(i)} = 0$, $i > 2l+2$, $i = 0$, by $(\varphi_n, \Omega) = \delta_{0n}$ and (46). By the assumption of the induction, $(H_I\varphi_{2l+1})^{(2i+1)} = 0$, $0 \leq i \leq l$, holds. When $1 \leq q \leq l$, it holds that

$$\begin{aligned}
&\left(H_0\varphi_{2l+2}\right)^{(2q)} = -2(l+1)\left(H_I\varphi_{2l+1}\right)^{(2q)}\\
&\quad + \sum_{j=1}^{l+1}\binom{2l+2}{2j}E_{2j}\varphi_{2l+2-2j}^{(2q)} = -\sqrt{2}(l+1)\left\{\frac{1}{\sqrt{2q}}\right.\\
&\quad \cdot \sum_{i=1}^{2q}\frac{1}{(2\pi)^{3/2}}\frac{\chi_{[\kappa,\Lambda]}(|k_i|)}{\sqrt{2}\sqrt{\omega(k_i)}}\varphi_{2l+1}^{(2q-1)}\left(k_1,\ldots,\widehat{k_i},\ldots,k_{2q}\right)\\
&\quad + \sqrt{2q+1}\int\frac{1}{(2\pi)^{3/2}}\frac{\chi_{[\kappa,\Lambda]}(|k|)}{\sqrt{2}\sqrt{\omega(k)}}\varphi_{2l+1}^{(2q+1)}\left(k,k_1,\ldots,\right.\\
&\quad \left.\left.k_{2q}\right)dk\right\} + \sum_{j=1}^{l+1}\binom{2l+2}{2j}E_{2j}\varphi_{2l+1-2j}^{(2q)},
\end{aligned} \tag{47}$$

where $\widehat{k_i}$ means that k_i is omitted. By the assumption of the induction, the supports of the functions

$$\begin{aligned}
&\frac{1}{(2\pi)^{3/2}}\frac{\chi_{[\kappa,\Lambda]}(|k_i|)}{\sqrt{2}\sqrt{\omega(k_i)}}\varphi_{2l+1}^{(2q-1)}\left(k_1,\ldots,\widehat{k_i},\ldots,k_{2q}\right),\\
&\int\frac{1}{(2\pi)^{3/2}}\frac{\chi_{[\kappa,\Lambda]}(|k|)}{\sqrt{2}\sqrt{\omega(k)}}\varphi_{2l+1}^{(2q+1)}\left(k,k_1,\ldots,k_{2q}\right)dk
\end{aligned} \tag{48}$$

and $\varphi_{2l+1-2j}^{(2q)}$ are S_{2q} or $\emptyset$. Furthermore,

$$\begin{aligned}
&\left(H_0\varphi_{2l+2}\right)^{(2l+2)}(k_1,\ldots,k_{2l+2}) = -2(l+1)\\
&\quad \cdot\left(A^+\varphi_{2l+1}\right)^{(2l+2)}(k_1,\ldots,k_{2l+2})\\
&\quad = -\sqrt{2(l+1)}\sum_{i=1}^{2l+2}\frac{1}{(2\pi)^{3/2}}\frac{\chi_{[\kappa,\Lambda]}(|k_i|)}{\sqrt{2}\sqrt{\omega(k_i)}}\\
&\quad \cdot\varphi_{2l+1}^{(2l+1)}\left(k_1,\ldots,\widehat{k_i},\ldots,k_{2l+2}\right)
\end{aligned} \tag{49}$$

holds. By the assumption of the induction, the support of the right hand side is S_{2l+2} or $\emptyset$. Hence we have $\operatorname{supp}_{k\in\mathbb{R}^{3\cdot 2i}}\varphi_{2l+2}^{(2i)}(k) = S_{2i}$ or $\emptyset$, $1 \leq i \leq l+1$. We can prove $\varphi_{2l+3}^{(i)} = 0$, $i > 2l+3$, $i = 0$, $\varphi_{2l+3}^{(2i)} = 0$, $1 \leq i \leq l+1$, and $\operatorname{supp}_{k\in\mathbb{R}^{3(2i+1)}}\varphi_{2l+3}^{(2i+1)}(k) = S_{2i+1}$ or $\emptyset$, $0 \leq i \leq l+1$, in a similar way. From the discussion so far, we have

$$\begin{aligned}
&-2lH_I\varphi_{2l-1} + \sum_{j=1}^{l}\binom{2l}{2j}E_{2j}\varphi_{2l-2j} \in \mathscr{F}_{\text{fin}} \quad (l \geq 1),\\
&-(2l+1)H_I\varphi_{2l} + \sum_{j=1}^{l}\binom{2l+1}{2j}E_{2j}\varphi_{2l+1-2j} \in \mathscr{F}_{\text{fin}} \quad (l \geq 0).
\end{aligned} \tag{50}$$

Hence we have

$$\begin{aligned}
&\varphi_{2l} = \frac{1}{H_0}\left\{-2lH_I\varphi_{2l-1} + \sum_{j=1}^{l}\binom{2l}{2j}E_{2j}\varphi_{2l-2j}\right\} + b_{2l}\Omega \quad (l \geq 1),\\
&\varphi_{2l+1}\\
&\quad = \frac{1}{H_0}\left\{-(2l+1)H_I\varphi_l + \sum_{j=1}^{l}\binom{2l+1}{2j}E_{2j}\varphi_{2l+1-2j}\right\}\\
&\quad + b_{2l+1}\Omega \quad (l \geq 0),
\end{aligned} \tag{51}$$

where b_{2l} and b_{2l+1} are some constants. Since $(\varphi_{2l}, \Omega) = 0$, $l \geq 1$, and $(\varphi_{2l+1}, \Omega) = 0$, $l \geq 0$, $b_{2l} = b_{2l+1} = 0$. Hence (33) and (34) are proven. By the discussion so far, (35) are also proven. We can derive (36) by (33) and $(\varphi_n, \Omega) = \delta_{0n}$. □

3. Main Theorems

For notational simplicity we set $\widehat{\phi}_j = \widehat{\phi}(k_j)$ and $\omega_j = \omega(k_j)$ for $k_j \in \mathbb{R}^3$, $j = 1, 2$. Let

$$\begin{aligned} E_j &= \frac{|k_j|^2}{2m} + \omega_j, \quad j = 1, 2, \\ E_{12} &= \frac{|k_1 + k_2|^2}{2m} + \omega_1 + \omega_2, \\ \omega(r) &= \sqrt{r^2 + \nu^2}, \\ F(r) &= \frac{r^2}{2m} + \omega(r). \end{aligned} \tag{52}$$

Theorem 9. *Let $\kappa > 0$. Then m_{eff} is an analytic function of α^2 and can be expanded in the following power series for sufficiently small $|\alpha|$:*

$$\frac{m_{eff}}{m} = 1 + \sum_{n=1}^{\infty} a_n(\Lambda)\, \alpha^{2n}. \tag{53}$$

Proof. By the power series (29), we have

$$\begin{aligned} \left(\psi_g, \psi_g\right) &= \left(\sum_{n=0}^{\infty} \frac{\alpha^n}{n!} \varphi_n, \sum_{m=0}^{\infty} \frac{\alpha^m}{m!} \varphi_m\right) \\ &= \sum_{n=0}^{\infty} \sum_{m=0}^{\infty} \frac{\alpha^{n+m}}{n!m!} (\varphi_n, \varphi_m). \end{aligned} \tag{54}$$

By Lemma 8, $(\varphi_n, \varphi_m) \neq 0$ if and only if both n and m are even or odd. Then we have

$$\left(\psi_g, \psi_g\right) = 1 + \sum_{n=1}^{\infty} b_n(\Lambda)\, \alpha^{2n}. \tag{55}$$

From the fact that both m_{eff}^{-1} and (ψ_g, ψ_g) are analytic functions of α^2 and Lemma 6, we have the following power series:

$$-\frac{2}{3} \sum_{\mu=1}^{3} \left(P_{f\mu} \psi_g, \psi'_{g_\mu}(0)\right) = \sum_{n=0}^{\infty} c_n(\Lambda)\, \alpha^{2n}. \tag{56}$$

Since $\psi'_{g_\mu}(0)$ is an analytic function of α, we can write

$$\psi'_{g_\mu}(0) = \sum_{n=0}^{\infty} \frac{\alpha^n}{n!} \Phi_n^\mu. \tag{57}$$

We note that

$$\begin{aligned} c_0(\Lambda) &= -\frac{2}{3} \sum_{\mu=1}^{3} \left(P_{f\mu} \varphi_0, \Phi_0^\mu\right) \\ &= -\frac{2}{3} \sum_{\mu=1}^{3} \left(d\Gamma\left(k_\mu\right) \varphi_0, \Phi_0^\mu\right) = 0. \end{aligned} \tag{58}$$

Hence if $|\alpha|$ is sufficiently small, then we have the following power series:

$$\begin{aligned} \frac{m_{\text{eff}}}{m} &= \frac{\left(\psi_g, \psi_g\right)}{\left(\psi_g, \psi_g\right) - (2/3) \sum_{\mu=1}^{3} \left(P_{f\mu} \psi_g(0), \psi'_{g_\mu}(0)\right)} \\ &= \frac{1 + \sum_{n=1}^{\infty} b_n(\Lambda)\, \alpha^{2n}}{1 + \sum_{n=1}^{\infty} \left(b_n(\Lambda) + c_n(\Lambda)\right) \alpha^{2n}} \\ &= \left(1 + \sum_{n=1}^{\infty} b_n(\Lambda)\, \alpha^{2n}\right) \\ &\quad \cdot \sum_{n=0}^{\infty} \left(-\sum_{l=1}^{\infty} \left(b_l(\Lambda) + c_l(\Lambda)\right) \alpha^{2l}\right)^n. \end{aligned} \tag{59}$$

This proves the theorem. □

Theorem 10. *There exists strictly positive constant C such that $\lim_{\Lambda \to \infty} a_1(\Lambda) = C$.*

Proof. From (59), we have

$$\begin{aligned} \frac{m_{\text{eff}}}{m} &= \left\{1 + b_1(\Lambda)\, \alpha^2 + O\left(\alpha^4\right)\right\} \\ &\quad \cdot \left[1 - \left\{b_1(\Lambda) + c_1(\Lambda)\right\} \alpha^2 + O\left(\alpha^4\right)\right] = 1 - c_1(\Lambda) \\ &\quad \cdot \alpha^2 + O\left(\alpha^4\right). \end{aligned} \tag{60}$$

Therefore $a_1(\Lambda) = -c_1(\Lambda)$. Since

$$\begin{aligned} \sum_{n=1}^{\infty} c_n(\Lambda)\, \alpha^{2n} &= -\frac{2}{3} \sum_{\mu=1}^{3} \left(P_{f\mu} \psi_g, \psi'_{g_\mu}(0)\right) \\ &= -\frac{2}{3} \sum_{\mu=1}^{3} \left(P_{f\mu} \sum_{n=0}^{\infty} \frac{\alpha^n}{n!} \varphi_n, \sum_{n=0}^{\infty} \frac{\alpha^n}{n!} \Phi_n^\mu\right), \end{aligned} \tag{61}$$

we have

$$\begin{aligned} c_1(\Lambda) &= -\frac{2}{3} \sum_{\mu=1}^{3} \left\{\frac{1}{0!2!} \left(P_{f\mu} \varphi_0, \Phi_2^\mu\right) + \frac{1}{1!1!} \left(P_{f\mu} \varphi_1, \Phi_1^\mu\right)\right. \\ &\quad \left. + \frac{1}{2!0!} \left(P_{f\mu} \varphi_2, \Phi_0^\mu\right)\right\} = -\frac{2}{3} \sum_{\mu=1}^{3} \left\{\left(P_{f\mu} \varphi_1, \Phi_1^\mu\right)\right. \\ &\quad \left. + \frac{1}{2} \left(P_{f\mu} \varphi_2, \Phi_0^\mu\right)\right\}. \end{aligned} \tag{62}$$

Substituting $p = 0$ into (27) and using (25), we have

$$\begin{aligned} -\frac{1}{m} \left(P_{f\mu} \Psi, \psi_g\right) + \left(\left(H_0 + \alpha H_I\right) \Psi, \psi'_{g_\mu}(0)\right) \\ = E(0, \alpha) \left(\Psi, \psi'_{g_\mu}(0)\right). \end{aligned} \tag{63}$$

In addition, by setting $\alpha = 0$, we have $-(P_{f\mu}/m)\varphi_0 + H_0 \Phi_0^\mu = 0$. Since $P_{f\mu} \varphi_0 = d\Gamma(k_\mu)\Omega = 0$, $H_0 \Phi_0^\mu = 0$ holds. Hence we have

$$\Phi_0^\mu = c_0 \Omega, \quad \left(c_0 \text{ is some constant}\right). \tag{64}$$

Differentiating both sides of (63) with respect to α, we have

$$\begin{aligned}
&-\frac{1}{m}\left(P_{f\mu}\Psi, s-\frac{d}{d\alpha}\psi_g\right)+\left(H(0)\Psi, s-\frac{d}{d\alpha}\psi'_{g_\mu}(0)\right)\\
&\quad+\left(H_I\Psi, \psi'_{g_\mu}(0)\right)\\
&=E(0,\alpha)\left(\Psi, s-\frac{d}{d\alpha}\psi'_{g_\mu}(0)\right)\\
&\quad+\frac{d}{d\alpha}E(0,\alpha)\left(\Psi, \psi'_{g_\mu}(0)\right).
\end{aligned} \tag{65}$$

Substituting $\alpha = 0$ into both sides, we have

$$\left(H_0\Psi, \Phi_1^\mu\right)=\frac{1}{m}\left(\Psi, P_{f\mu}\varphi_1\right)-\left(\Psi, H_I\Phi_0^\mu\right). \tag{66}$$

Therefore $\Phi_1^\mu \in D(H_0)$ and

$$\begin{aligned}
H_0\Phi_1^\mu&=\frac{1}{m}P_{f\mu}\varphi_1-H_I\Phi_0^\mu\\
&=-\frac{1}{m}P_{f\mu}\frac{1}{H_0}H_I\Omega-c_0H_I\Omega.
\end{aligned} \tag{67}$$

Since $-(1/m)P_{f\mu}(1/H_0)H_I\Omega - c_0H_I\Omega \in \mathscr{F}_{\text{fin}}$, we have

$$\Phi_1^\mu=-\frac{1}{m}\frac{1}{H_0}P_{f\mu}\frac{1}{H_0}H_I\Omega-c_0\frac{1}{H_0}H_I\Omega+c_1\Omega, \tag{68}$$

where c_1 is some constant. By $a_1(\Lambda) = -c_1(\Lambda)$, (62), (64), and (68), we have

$$\begin{aligned}
a_1(\Lambda)&=\frac{2}{3}\sum_{\mu=1}^{3}\left(P_{f\mu}\varphi_1, \Phi_1^\mu\right)\\
&=\frac{2}{3m}\sum_{\mu=1}^{3}\left(P_{f\mu}\frac{1}{H_0}H_I\Omega, \frac{1}{H_0}P_{f\mu}\frac{1}{H_0}H_I\Omega\right)\\
&\quad-\frac{2c_0}{3}\sum_{\mu=1}^{3}\left(P_{f\mu}\frac{1}{H_0}H_I\Omega, \frac{1}{H_0}H_I\Omega\right)\\
&\quad-\frac{2c_1}{3}\sum_{\mu=1}^{3}\left(P_{f\mu}\frac{1}{H_0}H_I\Omega, \Omega\right).
\end{aligned} \tag{69}$$

It is also seen that

$$\begin{aligned}
&\sum_{\mu=1}^{3}\left(P_{f\mu}\frac{1}{H_0}H_I\Omega, \frac{1}{H_0}H_I\Omega\right)=\sum_{\mu=1}^{3}\left(P_{f\mu}\frac{1}{H_0}H_I\Omega, \Omega\right)\\
&\quad=0.
\end{aligned} \tag{70}$$

Thus we have

$$\begin{aligned}
a_1(\Lambda)&=\frac{2}{3m}\sum_{\mu=1}^{3}\left(P_{f\mu}\frac{1}{H_0}H_I\Omega, \frac{1}{H_0}P_{f\mu}\frac{1}{H_0}H_I\Omega\right)\\
&=\frac{2}{3m}\sum_{\mu=1}^{3}\left(P_{f\mu}\frac{1}{H_0}A^+\Omega, \frac{1}{H_0}P_{f_\mu}\frac{1}{H_0}A^+\Omega\right)\\
&=\frac{2}{3m}\int\frac{\left|\widehat{\phi}(k)\right|^2}{\omega(k)}\frac{|k|^2}{E(k)^3}dk.
\end{aligned} \tag{71}$$

Changing variables into polar coordinate, we have

$$\begin{aligned}
&\frac{2}{3m}\int\frac{\left|\widehat{\phi}(k)\right|^2}{\omega(k)}\frac{|k|^2}{E(k)^3}dk\\
&\quad=\frac{8\pi}{3m(2\pi)^3}\int_\kappa^\Lambda\frac{r^4}{\omega(r)F(r)^3}dr.
\end{aligned} \tag{72}$$

Since $r^4/\omega(r)F(r)^3 = O(r^{-3})$ $(r \to \infty)$, the improper integral $\int_\kappa^\infty (r^4/\omega(r)F(r)^3)dr$ converges. It is trivial to see that $\lim_{\Lambda\to\infty} a_1(\Lambda) > 0$. Thus the theorem follows. □

Lemma 11. *It follows that $\Phi_n^\mu \in \mathscr{F}_{fin}$ for $n \in \mathbb{N} \cup \{0\}$.*

Proof. By (64), we have $\Phi_0^\mu \in \mathscr{F}_{\text{fin}}$. Assume that $\Phi_n^\mu \in \mathscr{F}_{\text{fin}}$ holds when $n \le k-1$. Differentiating both sides of (63) k times with respect to α and substituting $\alpha = 0$, we have

$$\begin{aligned}
&-\frac{1}{m}\left(P_{f\mu}\Psi, \varphi_k\right)+\left(H_0\Psi, \Phi_k^\mu\right)+k\left(H_I\Psi, \Phi_{k-1}^\mu\right)\\
&=\sum_{j=1}^{k}\binom{k}{j}E_j\left(\Psi, \Phi_{k-j}^\mu\right);
\end{aligned} \tag{73}$$

however, $E_j = 0$ when j is odd. Since $\Phi_{k-1}^\mu \in \mathscr{F}_{\text{fin}}$, $\Phi_{k-1}^\mu \in D(H_I)$ and

$$\begin{aligned}
\left(H_0\Psi, \Phi_k^\mu\right)&=\frac{1}{m}\left(\Psi, P_{f\mu}\varphi_k\right)-k\left(\Psi, H_I\Phi_{k-1}^\mu\right)\\
&\quad+\left(\Psi, \sum_{j=1}^{k}\binom{k}{j}E_j\Phi_{k-j}^\mu\right).
\end{aligned} \tag{74}$$

Thus $\Phi_k^\mu \in D(H_0)$ and

$$H_0\Phi_k^\mu=\frac{1}{m}P_{f\mu}\varphi_k-kH_I\Phi_{k-1}^\mu+\sum_{j=1}^{k}\binom{k}{j}E_j\Phi_{k-j}^\mu. \tag{75}$$

Since $\varphi_k \in \mathscr{F}_{\text{fin}}$, $H_I\Phi_{k-1}^\mu \in \mathscr{F}_{\text{fin}}$, and $\Phi_{k-j}^\mu \in \mathscr{F}_{\text{fin}}$ $(j = 1, \ldots, k)$, by the assumption of induction, $H_0\Phi_k^\mu \in \mathscr{F}_{\text{fin}}$. Hence $\Phi_n^\mu \in \mathscr{F}_{\text{fin}}$ holds when $n = k$. □

Lemma 12. *It holds that $\Phi_0^\mu = c_0\Omega$, $\Phi_1^\mu = -(1/m)(1/H_0)P_{f\mu}(1/H_0)H_I\Omega - c_0(1/H_0)H_I\Omega + c_1\Omega$, and the recurrence formulas*

$$\begin{aligned}
\Phi_{2l}^\mu&=\frac{1}{H_0}\left\{\frac{1}{m}P_{f\mu}\varphi_{2l}-2lH_I\Phi_{2l-1}^\mu\right.\\
&\quad\left.+\sum_{j=1}^{l}\binom{2l}{2j}E_{2j}\Phi_{2l-2j}^\mu\right\}+c_{2l}\Omega\\
&\qquad\left(l \ge 1,\ c_{2l}\ \textit{is some constant}\right).
\end{aligned}$$

$$\Phi_{2l+1}^{\mu} = \frac{1}{H_0}\left\{\frac{1}{m}P_{f\mu}\varphi_{2l+1} - (2l+1)\,H_I\Phi_{2l}^{\mu} + \sum_{j=1}^{l}\binom{2l+1}{2j}E_{2j}\Phi_{2l+1-2j}^{\mu}\right\} + c_{2l+1}\Omega, \quad (l \geq 0,\ c_{2l+1}\ \textit{is some constant.}) \tag{76}$$

Proof. The first and second expressions are proven in Theorem 10. From (75), it follows that

$$\begin{aligned} H_0\Phi_{2l}^{\mu} &= \frac{1}{m}P_{f\mu}\varphi_{2l} - 2lH_I\Phi_{2l-1}^{\mu} + \sum_{j=1}^{l}\binom{2l}{2j}E_{2j}\Phi_{2l-2j}^{\mu} \quad (l \geq 1) \\ H_0\Phi_{2l+1}^{\mu} &= \frac{1}{m}P_{f\mu}\varphi_{2l+1} - (2l+1)\,H_I\Phi_{2l}^{\mu} + \sum_{j=1}^{l}\binom{2l+1}{2j}E_{2j}\Phi_{2l+1-2j}^{\mu} \quad (l \geq 0). \end{aligned} \tag{77}$$

These prove the lemma. □

Lemma 13. *It is proven that $a_2(\Lambda)$ can be expanded as*

$$a_2(\Lambda) = \frac{2}{3m}\sum_{j=1}^{8}I_j(\Lambda) + \frac{E_2(\Lambda)}{m}I_9(\Lambda) - a_1(\Lambda)\,I_{10}(\Lambda) + a_1(\Lambda)^2, \tag{78}$$

where I_j are given by

$$\begin{aligned} I_1(\Lambda) &= \frac{1}{4}\iint \frac{\left|\widehat{\phi}_1\right|^2\left|\widehat{\phi}_2\right|^2}{\omega_1\omega_2}\left(\frac{|k_1|^2}{E_1^3} + \frac{|k_2|^2}{E_2^3}\right)\cdot\left(\frac{1}{E_1}+\frac{1}{E_2}\right)\frac{1}{E_{12}}dk_1dk_2, \\ I_2(\Lambda) &= \frac{1}{8}\iint \frac{\left|\widehat{\phi}_1\right|^2\left|\widehat{\phi}_2\right|^2}{\omega_1\omega_2}\left(\frac{|k_1|^2}{E_1^4} + \frac{|k_2|^2}{E_2^4}\right)\frac{1}{E_{12}}dk_1dk_2, \\ I_3(\Lambda) &= \frac{1}{8}\iint \frac{\left|\widehat{\phi}_1\right|^2\left|\widehat{\phi}_2\right|^2}{\omega_1\omega_2}\left(\frac{1}{E_1^2} + \frac{1}{E_2^2}\right)\left(\frac{1}{E_1}+\frac{1}{E_2}\right)\cdot\frac{(k_1,k_2)}{E_{12}^2}dk_1dk_2, \\ I_4(\Lambda) &= \frac{1}{4}\iint \frac{\left|\widehat{\phi}_1\right|^2\left|\widehat{\phi}_2\right|^2}{\omega_1\omega_2}\left(\frac{|k_1|^2}{E_1^2} + \frac{|k_2|^2}{E_2^2}\right)\cdot\left(\frac{1}{E_1}+\frac{1}{E_2}\right)\frac{1}{E_{12}^2}dk_1dk_2, \\ I_5(\Lambda) &= \frac{1}{4}\iint \frac{\left|\widehat{\phi}_1\right|^2\left|\widehat{\phi}_2\right|^2}{\omega_1\omega_2E_1^2E_2^2}\frac{(k_1,k_2)}{E_{12}}dk_1dk_2, \\ I_6(\Lambda) &= \frac{1}{8}\iint \frac{\left|\widehat{\phi}_1\right|^2\left|\widehat{\phi}_2\right|^2}{\omega_1\omega_2}\left(\frac{1}{E_1}+\frac{1}{E_2}\right)^2\cdot\frac{|k_1|^2+|k_2|^2}{E_{12}^3}dk_1dk_2, \\ I_7(\Lambda) &= \frac{1}{4}\iint \frac{\left|\widehat{\phi}_1\right|^2\left|\widehat{\phi}_2\right|^2}{\omega_1\omega_2}\left(\frac{1}{E_1}+\frac{1}{E_2}\right)^2\cdot\frac{(k_1,k_2)}{E_{12}^3}dk_1dk_2, \\ I_8(\Lambda) &= \frac{1}{4}\iint \frac{\left|\widehat{\phi}_1\right|^2\left|\widehat{\phi}_2\right|^2}{\omega_1\omega_2}\left(\frac{1}{E_1}+\frac{1}{E_2}\right)\frac{(k_1,k_2)}{E_{12}^4}dk_1dk_2, \\ I_9(\Lambda) &= \frac{1}{2}\int \frac{\left|\widehat{\phi}(k)\right|^2|k|^2}{\omega(k)\,E(k)^4}dk, \\ I_{10}(\Lambda) &= \frac{1}{2}\int \frac{\left|\widehat{\phi}(k)\right|^2}{\omega(k)\,E(k)^2}dk. \end{aligned} \tag{79}$$

The proof of Lemma 13 is given in the next section. The asymptotic behaviors of terms $I_j(\Lambda)$ as $\Lambda \to \infty$ is given in the lemma below. Only two terms $I_1(\Lambda)$ and $I_2(\Lambda)$ logarithmically diverge, and other terms converge as $\Lambda \to \infty$.

Lemma 14. *(1)–(3) follow the following:*

(1) *There exist some constants C_3 and C_4 such that $C_3 \leq \lim_{\Lambda\to\infty}(I_1(\Lambda)/\log\Lambda) \leq C_4$.*

(2) *There exist some constants C_5 and C_6 such that $C_5 \leq \lim_{\Lambda\to\infty}(I_2(\Lambda)/\log\Lambda) \leq C_6$.*

(3) *For $j = 3,4,5,6,7,8$ $\lim_{\Lambda\to\infty}|I_j(\Lambda)| < \infty$.*

The proof of Lemma 14 is technical and also given in the next section.

Lemma 15. *It holds that*

$$\lim_{\Lambda\to\infty}\frac{E_2(\Lambda)}{\log\Lambda} = -\frac{m}{\pi^2}. \tag{80}$$

Proof. From (36), we have $E_2(\Lambda) = -(1/2\pi^2)\int_{\kappa}^{\Lambda}(r^2/\omega(r)F(r))dr$ and $\lim_{r\to\infty}((r^2/\omega(r)F(r))/(1/r)) = 2m$. It implies (80). □

Now we are in the position to state the main theorem in this paper.

Theorem 16. *There exist some constants C_1 and C_2 such that*

$$C_1 \leq \lim_{\Lambda\to\infty}\frac{a_2(\Lambda)}{\log\Lambda} \leq C_2. \tag{81}$$

Proof. We have $I_9(\Lambda) = (1/4\pi^2)\int_\kappa^\Lambda (r^4/\omega(r)F(r)^4)dr$. Since $r^4/\omega(r)F(r)^4 = O(r^{-5})$ $(r \to \infty)$, we have

$$\lim_{\Lambda\to\infty} \left|I_9(\Lambda)\right| < \infty. \tag{82}$$

We also have $I_{10}(\Lambda) = (1/4\pi^2)\int_\kappa^\Lambda (r^2/\omega(r)F(r)^2)dr$. Then $r^2/\omega(r)F(r)^2 = O(r^{-3})$ $(r \to \infty)$ and we also have

$$\lim_{\Lambda\to\infty} \left|I_{10}(\Lambda)\right| < \infty. \tag{83}$$

By (82) and (83), Theorem 10, and Lemmas 13, 14, and 15 we can conclude the theorem. □

4. Proof of Lemmas 13 and 14

In this section we prove Lemmas 13 and 14.

4.1. Proof of Lemma 13. From (59) and $a_1(\Lambda) = -c_1(\Lambda)$, we have $a_2(\Lambda) = -c_2(\Lambda) - b_1(\Lambda)a_1(\Lambda) + a_1(\Lambda)^2$. Here

$$b_1(\Lambda) = (\varphi_1, \varphi_1) = \frac{1}{2}\int \frac{\left|\widehat{\phi}(k)\right|^2}{\omega(k)E(k)^2}dk, \tag{84}$$

$$\begin{aligned} c_2(\Lambda) = &-\frac{2}{3}\left\{\frac{1}{0!4!}\sum_{\mu=1}^{3}\left(P_{f\mu}\varphi_0, \Phi_4^\mu\right)\right. \\ &+ \frac{1}{1!3!}\sum_{\mu=1}^{3}\left(P_{f\mu}\varphi_1, \Phi_3^\mu\right) + \frac{1}{2!2!}\sum_{\mu=1}^{3}\left(P_{f\mu}\varphi_2, \Phi_2^\mu\right) \\ &\left.+ \frac{1}{3!1!}\sum_{\mu=1}^{3}\left(P_{f\mu}\varphi_3, \Phi_1^\mu\right) + \frac{1}{4!0!}\sum_{\mu=1}^{3}\left(P_{f_\mu}\varphi_4, \Phi_0^\mu\right)\right\} \\ = &-\frac{1}{9}\sum_{\mu=1}^{3}\left(P_{f\mu}\varphi_1, \Phi_3^\mu\right) - \frac{1}{6}\sum_{\mu=1}^{3}\left(P_{f\mu}\varphi_2, \Phi_2^\mu\right) - \frac{1}{9} \\ &\cdot \sum_{\mu=1}^{3}\left(P_{f_\mu}\varphi_3, \Phi_1^\mu\right). \end{aligned} \tag{85}$$

Using recurrence formulas (33), (34), and (76), we have

$$\begin{aligned} \varphi_2 &= 2\left(\frac{1}{H_0}H_I\right)^2\Omega, \\ \varphi_3 &= -6\left(\frac{1}{H_0}H_I\right)^3\Omega - 3E_2\left(\frac{1}{H_0}\right)^2 H_I\Omega, \\ \Phi_2^\mu &= \frac{2}{m}\frac{1}{H_0}P_{f\mu}\left(\frac{1}{H_0}H_I\right)^2\Omega \\ &\quad + \frac{2}{m}\frac{1}{H_0}H_I\frac{1}{H_0}P_{f\mu}\frac{1}{H_0}H_I\Omega \\ &\quad + 2c_0\left(\frac{1}{H_0}H_I\right)^2\Omega - 2c_1\frac{1}{H_0}H_I\Omega + c_2\Omega, \end{aligned}$$

$$\begin{aligned} \Phi_3^\mu = &-\frac{6}{m}\frac{1}{H_0}P_{f\mu}\left(\frac{1}{H_0}H_I\right)^3\Omega \\ &- \frac{6}{m}\frac{1}{H_0}H_I\frac{1}{H_0}P_{f\mu}\left(\frac{1}{H_0}H_I\right)^2\Omega \\ &- \frac{6}{m}\left(\frac{1}{H_0}H_I\right)^2\frac{1}{H_0}P_{f\mu}\frac{1}{H_0}H_I\Omega \\ &- \frac{3}{m}E_2\frac{1}{H_0}P_{f\mu}\left(\frac{1}{H_0}\right)^2 H_I\Omega \\ &- \frac{3}{m}E_2\left(\frac{1}{H_0}\right)^2 P_{f_\mu}\frac{1}{H_0}H_I\Omega \\ &- 6c_0\left(\frac{1}{H_0}H_I\right)^3\Omega + 6c_1\left(\frac{1}{H_0}H_I\right)^2\Omega \\ &- 3c_2\frac{1}{H_0}H_I\Omega - 3c_0E_2\left(\frac{1}{H_0}\right)^2 H_I\Omega + c_3\Omega. \end{aligned} \tag{86}$$

Substituting them into (85), we have

$$\begin{aligned} c_2(\Lambda) = &-\frac{2}{3m}\left\{\sum_{\mu=1}^{3}\left(P_{f\mu}\frac{1}{H_0}H_I\Omega, \frac{1}{H_0}P_{f_\mu}\left(\frac{1}{H_0}H_I\right)^3\Omega\right)\right. \\ &+ \sum_{\mu=1}^{3}\left(P_{f\mu}\frac{1}{H_0}H_I\Omega, \frac{1}{H_0}H_I\frac{1}{H_0}P_{f\mu}\left(\frac{1}{H_0}H_I\right)^2\Omega\right) \\ &+ \sum_{\mu=1}^{3}\left(P_{f\mu}\frac{1}{H_0}H_I\Omega, \left(\frac{1}{H_0}H_I\right)^2\frac{1}{H_0}P_{f_\mu}\frac{1}{H_0}H_I\Omega\right) \\ &+ \sum_{\mu=1}^{3}\left(P_{f\mu}\left(\frac{1}{H_0}H_I\right)^2\Omega, \frac{1}{H_0}P_{f_\mu}\left(\frac{1}{H_0}H_I\right)^2\Omega\right) \\ &+ \sum_{\mu=1}^{3}\left(P_{f_\mu}\left(\frac{1}{H_0}H_I\right)^2\Omega, \frac{1}{H_0}H_I\frac{1}{H_0}P_{f_\mu}\frac{1}{H_0}H_I\Omega\right) \\ &\left.+ \sum_{\mu=1}^{3}\left(P_{f_\mu}\left(\frac{1}{H_0}H_I\right)^3\Omega, \frac{1}{H_0}P_{f\mu}\frac{1}{H_0}H_I\Omega\right)\right\} \\ &- \frac{E_2}{3m}\left\{\sum_{\mu=1}^{3}\left(P_{f\mu}\frac{1}{H_0}H_I\Omega, \frac{1}{H_0}P_{f\mu}\left(\frac{1}{H_0}\right)^2 H_I\Omega\right)\right. \\ &+ \sum_{\mu=1}^{3}\left(P_{f\mu}\frac{1}{H_0}H_I\Omega, \left(\frac{1}{H_0}\right)^2 P_{f\mu}\frac{1}{H_0}H_I\Omega\right) \\ &\left.+ \sum_{\mu=1}^{3}\left(P_{f\mu}\left(\frac{1}{H_0}\right)^2 H_I\Omega, \frac{1}{H_0}P_{f\mu}\frac{1}{H_0}H_I\Omega\right)\right\} - \frac{2c_0}{3} \\ &\cdot \sum_{\mu=1}^{3}\left(P_{f\mu}\frac{1}{H_0}H_I\Omega, \left(\frac{1}{H_0}H_I\right)^3\Omega\right) + \frac{2c_1}{3} \end{aligned}$$

$$
\begin{aligned}
&\cdot \sum_{\mu=1}^{3}\left(P_{f\mu}\frac{1}{H_0}H_I\Omega,\left(\frac{1}{H_0}H_I\right)^2\Omega\right)-\frac{c_2}{3}\\
&\cdot \sum_{\mu=1}^{3}\left(P_{f\mu}\frac{1}{H_0}H_I\Omega,\frac{1}{H_0}H_I\Omega\right)-\frac{c_0E_2}{3}\\
&\cdot \sum_{\mu=1}^{3}\left(P_{f\mu}\frac{1}{H_0}H_I\Omega,\left(\frac{1}{H_0}\right)^2H_I\Omega\right)+\frac{c_3}{9}\\
&\cdot \sum_{\mu=1}^{3}\left(P_{f\mu}\frac{1}{H_0}H_I\Omega,\Omega\right)-\frac{2c_0}{3}\\
&\cdot \sum_{\mu=1}^{3}\left(P_{f\mu}\left(\frac{1}{H_0}H_I\right)^2\Omega,\left(\frac{1}{H_0}H_I\right)^2\Omega\right)+\frac{2c_1}{3}\\
&\cdot \sum_{\mu=1}^{3}\left(P_{f\mu}\left(\frac{1}{H_0}H_I\right)^2\Omega,\frac{1}{H_0}H_I\Omega\right)-\frac{c_2}{3}\\
&\cdot \sum_{\mu=1}^{3}\left(P_{f\mu}\left(\frac{1}{H_0}H_I\right)^2\Omega,\Omega\right)-\frac{2c_0}{3}\\
&\cdot \sum_{\mu=1}^{3}\left(P_{f\mu}\left(\frac{1}{H_0}H_I\right)^3\Omega,\frac{1}{H_0}H_I\Omega\right)+\frac{2c_1}{3}\\
&\cdot \sum_{\mu=1}^{3}\left(P_{f\mu}\left(\frac{1}{H_0}H_I\right)^3\Omega,\Omega\right)-\frac{c_0E_2}{3}\\
&\cdot \sum_{\mu=1}^{3}\left(P_{f\mu}\left(\frac{1}{H_0}\right)^2H_I\Omega,\frac{1}{H_0}H_I\Omega\right)+\frac{c_1E_2}{3}\\
&\cdot \sum_{\mu=1}^{3}\left(P_{f\mu}\left(\frac{1}{H_0}\right)^2H_I\Omega,\Omega\right)=\sum_{j=1}^{21}(j).
\end{aligned}
\tag{87}
$$

We estimate 21 terms (1)–(21) above. We can however directly see that $0=(10)=\cdots=(21)$ as follows:

$$
\begin{aligned}
&\sum_{\mu=1}^{3}\left(P_{f\mu}\frac{1}{H_0}H_I\Omega,\left(\frac{1}{H_0}H_I\right)^3\Omega\right)\\
&\quad=\sum_{\mu=1}^{3}\left(P_{f\mu}\frac{1}{H_0}H_I\Omega,\left(\frac{1}{H_0}H_I\right)^2\Omega\right)\\
&\quad=\sum_{\mu=1}^{3}\left(P_{f\mu}\frac{1}{H_0}H_I\Omega,\frac{1}{H_0}H_I\Omega\right)\\
&\quad=\sum_{\mu=1}^{3}\left(P_{f\mu}\frac{1}{H_0}H_I\Omega,\left(\frac{1}{H_0}\right)^2H_I\Omega\right)\\
&\quad=\sum_{\mu=1}^{3}\left(P_{f\mu}\frac{1}{H_0}H_I\Omega,\Omega\right)\\
&\quad=\sum_{\mu=1}^{3}\left(P_{f\mu}\left(\frac{1}{H_0}H_I\right)^2\Omega,\left(\frac{1}{H_0}H_I\right)^2\Omega\right)\\
&\quad=\sum_{\mu=1}^{3}\left(P_{f\mu}\left(\frac{1}{H_0}H_I\right)^2\Omega,\frac{1}{H_0}H_I\Omega\right)\\
&\quad=\sum_{\mu=1}^{3}\left(P_{f\mu}\left(\frac{1}{H_0}H_I\right)^2\Omega,\Omega\right)\\
&\quad=\sum_{\mu=1}^{3}\left(P_{f\mu}\left(\frac{1}{H_0}H_I\right)^3\Omega,\frac{1}{H_0}H_I\Omega\right)\\
&\quad=\sum_{\mu=1}^{3}\left(P_{f\mu}\left(\frac{1}{H_0}H_I\right)^3\Omega,\Omega\right)\\
&\quad=\sum_{\mu=1}^{3}\left(P_{f\mu}\left(\frac{1}{H_0}\right)^2H_I\Omega,\frac{1}{H_0}H_I\Omega\right)\\
&\quad=\sum_{\mu=1}^{3}\left(P_{f\mu}\left(\frac{1}{H_0}\right)^2H_I\Omega,\Omega\right)=0.
\end{aligned}
\tag{88}
$$

We can compute remaining terms (1)–(9) as

$$
\begin{aligned}
(1)\ &\sum_{\mu=1}^{3}\left(P_{f\mu}\frac{1}{H_0}H_I\Omega,\frac{1}{H_0}P_{f\mu}\left(\frac{1}{H_0}H_I\right)^3\Omega\right)\\
&=\sum_{\mu=1}^{3}\left(A^+\frac{1}{H_0}P_{f\mu}\frac{1}{H_0}P_{f\mu}\frac{1}{H_0}A^+\Omega,\left(\frac{1}{H_0}A^+\right)^2\Omega\right)\\
&=\frac{1}{8}\iint\frac{\left|\widehat{\phi}_1\right|^2\left|\widehat{\phi}_2\right|^2}{\omega_1\omega_2}\left(\frac{|k_1|^2}{E_1^3}+\frac{|k_2|^2}{E_2^3}\right)\left(\frac{1}{E_1}+\frac{1}{E_2}\right)\\
&\cdot\frac{1}{E_{12}}dk_1dk_2,\\
(2)\ &\sum_{\mu=1}^{3}\left(P_{f\mu}\frac{1}{H_0}H_I\Omega,\frac{1}{H_0}H_I\frac{1}{H_0}P_{f\mu}\left(\frac{1}{H_0}H_I\right)^2\Omega\right)\\
&=\sum_{\mu=1}^{3}\left(A^+\frac{1}{H_0}P_{f\mu}\frac{1}{H_0}A^+\Omega,\frac{1}{H_0}P_{f\mu}\left(\frac{1}{H_0}A^+\right)^2\Omega\right)\\
&=\frac{1}{8}\iint\frac{\left|\widehat{\phi}_1\right|^2\left|\widehat{\phi}_2\right|^2}{\omega_1\omega_2}\left(\frac{|k_1|^2}{E_1^2}+\frac{|k_2|^2}{E_2^2}\right)\left(\frac{1}{E_1}+\frac{1}{E_2}\right)\\
&\cdot\frac{1}{E_{12}^2}dk_1dk_2+\frac{1}{8}\iint\frac{\left|\widehat{\phi}_1\right|^2\left|\widehat{\phi}_2\right|^2}{\omega_1\omega_2}\left(\frac{1}{E_1^2}+\frac{1}{E_2^2}\right)\\
&\cdot\left(\frac{1}{E_1}+\frac{1}{E_2}\right)\frac{(k_1,k_2)}{E_{12}^2}dk_1dk_2,
\end{aligned}
$$

$$(3)\ \sum_{\mu=1}^{3}\left(P_{f\mu}\frac{1}{H_0}H_I\Omega,\left(\frac{1}{H_0}H_I\right)^2\frac{1}{H_0}P_{f\mu}\frac{1}{H_0}H_I\Omega\right)$$
$$=\sum_{\mu=1}^{3}\left(A^+\frac{1}{H_0}P_{f\mu}\frac{1}{H_0}A^+\Omega,\frac{1}{H_0}A^+\frac{1}{H_0}P_{f\mu}\frac{1}{H_0}A^+\Omega\right)$$
$$=\frac{1}{8}\iint\frac{\left|\widehat{\phi}_1\right|^2\left|\widehat{\phi}_2\right|^2}{\omega_1\omega_2}\left(\frac{|k_1|^2}{E_1^4}+\frac{|k_2|^2}{E_2^4}\right)\frac{1}{E_{12}}dk_1dk_2$$
$$+\frac{1}{4}\iint\frac{\left|\widehat{\phi}_1\right|^2\left|\widehat{\phi}_2\right|^2}{\omega_1\omega_2E_1^2E_2^2}\frac{(k_1,k_2)}{E_{12}}dk_1dk_2,$$

$$(4)\ \sum_{\mu=1}^{3}\left(P_{f\mu}\left(\frac{1}{H_0}H_I\right)^2\Omega,\frac{1}{H_0}P_{f\mu}\left(\frac{1}{H_0}H_I\right)^2\Omega\right)$$
$$=\sum_{\mu=1}^{3}\left(P_{f\mu}\left(\frac{1}{H_0}A^+\right)^2\Omega,\frac{1}{H_0}P_{f\mu}\left(\frac{1}{H_0}A^+\right)^2\Omega\right)$$
$$=\frac{1}{8}\iint\frac{\left|\widehat{\phi}_1\right|^2\left|\widehat{\phi}_2\right|^2}{\omega_1\omega_2}\left(\frac{1}{E_1}+\frac{1}{E_2}\right)^2$$
$$\cdot\frac{|k_1|^2+|k_2|^2}{E_{12}^3}dk_1dk_2+\frac{1}{4}$$
$$\cdot\iint\frac{\left|\widehat{\phi}_1\right|^2\left|\widehat{\phi}_2\right|^2}{\omega_1\omega_2}\left(\frac{1}{E_1}+\frac{1}{E_2}\right)^2\frac{(k_1,k_2)}{E_{12}^3}dk_1dk_2,$$

$$(5)\ \sum_{\mu=1}^{3}\left(P_{f\mu}\left(\frac{1}{H_0}H_I\right)^2\Omega,\frac{1}{H_0}H_I\frac{1}{H_0}P_{f\mu}\frac{1}{H_0}H_I\Omega\right)$$
$$=\sum_{\mu=1}^{3}\left(P_{f\mu}\left(\frac{1}{H_0}A^+\right)^2\Omega,\frac{1}{H_0}A^+\frac{1}{H_0}P_{f\mu}\frac{1}{H_0}A^+\Omega\right)$$
$$=\frac{1}{8}\iint\frac{\left|\widehat{\phi}_1\right|^2\left|\widehat{\phi}_2\right|^2}{\omega_1\omega_2}\left(\frac{|k_1|^2}{E_1^2}+\frac{|k_2|^2}{E_2^2}\right)\left(\frac{1}{E_1}+\frac{1}{E_2}\right)$$
$$\cdot\frac{1}{E_{12}^2}dk_1dk_2+\frac{1}{4}\iint\frac{\left|\widehat{\phi}_1\right|^2\left|\widehat{\phi}_2\right|^2}{\omega_1\omega_2}\left(\frac{1}{E_1}+\frac{1}{E_2}\right)$$
$$\cdot\frac{(k_1,k_2)}{E_{12}^4}dk_1dk_2,$$

$$(6)\ \sum_{\mu=1}^{3}\left(P_{f\mu}\left(\frac{1}{H_0}H_I\right)^3\Omega,\frac{1}{H_0}P_{f\mu}\frac{1}{H_0}H_I\Omega\right)$$
$$=\sum_{\mu=1}^{3}\left(\left(\frac{1}{H_0}A^+\right)^2\Omega,A^+\frac{1}{H_0}P_{f\mu}\frac{1}{H_0}P_{f\mu}\frac{1}{H_0}A^+\Omega\right)$$
$$=\frac{1}{8}\iint\frac{\left|\widehat{\phi}_1\right|^2\left|\widehat{\phi}_2\right|^2}{\omega_1\omega_2}\left(\frac{|k_1|^2}{E_1^3}+\frac{|k_2|^2}{E_2^3}\right)\left(\frac{1}{E_1}+\frac{1}{E_2}\right)$$
$$\cdot\frac{1}{E_{12}}dk_1dk_2,$$

$$(7)\ \sum_{\mu=1}^{3}\left(P_{f\mu}\frac{1}{H_0}H_I\Omega,\frac{1}{H_0}P_{f\mu}\left(\frac{1}{H_0}\right)^2H_I\Omega\right)$$
$$=\frac{1}{2}\int\frac{\left|\widehat{\phi}(k)\right|^2|k|^2}{\omega(k)E(k)^4}dk,$$

$$(8)\ \sum_{\mu=1}^{3}\left(P_{f\mu}\frac{1}{H_0}H_I\Omega,\left(\frac{1}{H_0}\right)^2P_{f\mu}\frac{1}{H_0}H_I\Omega\right)$$
$$=\frac{1}{2}\int\frac{\left|\widehat{\phi}(k)\right|^2|k|^2}{\omega(k)E(k)^4}dk,$$

$$(9)\ \sum_{\mu=1}^{3}\left(P_{f\mu}\left(\frac{1}{H_0}\right)^2H_I\Omega,\frac{1}{H_0}P_{f\mu}\frac{1}{H_0}H_I\Omega\right)$$
$$=\frac{1}{2}\int\frac{\left|\widehat{\phi}(k)\right|^2|k|^2}{\omega(k)E(k)^4}dk.\tag{89}$$

Thus the lemma follows.

4.2. Proof of Lemma 14

Proof of $C_3\le\lim_{\Lambda\to\infty}(I_1(\Lambda)/\log\Lambda)$ *and* $C_5\le\lim_{\Lambda\to\infty}(I_2(\Lambda)/\log\Lambda)$. Changing variables to polar coordinates, we have

$$I_1(\Lambda)=\frac{2\pi^2}{(2\pi)^6}\cdot\int_{-1}^{1}\int_{\kappa}^{\Lambda}\int_{\kappa}^{\Lambda}\frac{r_1^2r_2^2}{\omega(r_1)\omega(r_2)}\left(\frac{r_1^2}{F(r_1)^3}+\frac{r_2^2}{F(r_2)^3}\right)\cdot\left(\frac{1}{F(r_1)}+\frac{1}{F(r_2)}\right)\frac{1}{L(r_1,r_2,z)}dz\,dr_1dr_2,\tag{90}$$

where

$$L(r_1,r_2,z)=\frac{r_1^2+r_2^2+2r_1r_2z}{2m}+\omega(r_1)+\omega(r_2).\tag{91}$$

We define $h(r_1,r_2)$, $h_1(r_1,r_2)$, $h_2(r_1,r_2)$, $S(\Lambda)$, $S_1(\Lambda)$ and $S_2(\Lambda)$ as

$$h(r_1,r_2)=\frac{r_1^2r_2^2}{\omega(r_1)\omega(r_2)}\left(\frac{r_1^2}{F(r_1)^3}+\frac{r_2^2}{F(r_2)^3}\right)\cdot\left(\frac{1}{F(r_1)}+\frac{1}{F(r_2)}\right)\frac{1}{L(r_1,r_2,1)},$$
$$h_1(r_1,r_2)=\frac{r_1^2r_2^4}{\omega(r_1)\omega(r_2)F(r_2)^4L(r_1,r_2,1)},$$
$$h_2(r_1,r_2)=h(r_1,r_2)-h_1(r_1,r_2),$$

$$
\begin{aligned}
S(\Lambda) &= \int_{\kappa}^{\Lambda}\int_{\kappa}^{\Lambda} h(r_1,r_2)\,dr_1dr_2,\\
S_1(\Lambda) &= \int_{\kappa}^{\kappa+1}\int_{\kappa+1+\nu+m}^{\Lambda} h_1(r_1,r_2)\,dr_2dr_1,\\
S_2(\Lambda) &= \int_{\kappa}^{\kappa+1}\int_{\kappa}^{\kappa+1+\nu+m} h_1(r_1,r_2)\,dr_2dr_1\\
&\quad+\int_{\kappa+1}^{\Lambda}\int_{\kappa}^{\Lambda} h_1(r_1,r_2)\,dr_1dr_2\\
&\quad+\int_{\kappa}^{\Lambda}\int_{\kappa}^{\Lambda} h_2(r_1,r_2)\,dr_1dr_2.
\end{aligned}
\tag{92}
$$

Then

$$
\frac{4\pi^2}{(2\pi)^6}S(\Lambda)\le I_1(\Lambda). \tag{93}
$$

In addition, $S(\Lambda)=S_1(\Lambda)+S_2(\Lambda)$ follows. Since $h_1(r_1,r_2)>0$ and $h_2(r_1,r_2)>0$, $S_2(\Lambda)>0$. Hence

$$
S(\Lambda)>S_1(\Lambda). \tag{94}
$$

Let r_2 satisfy $\kappa\le r_2\le\kappa+1$. Suppose that $\kappa+1+\nu+m\le r_1\le\Lambda$. Since $\nu<r_1$, $r_1^2+\nu^2<2r_1^2$ holds. Therefore we have $\omega(r_1)<\sqrt{2}r_1$. Since $r_2<r_1$, we have $r_1r_2<r_1^2$ and $r_2^2<r_1^2$. Thus $L(r_1,r_2,1)<2(1/m+\sqrt{2})r_1^2$. So,

$$
\begin{aligned}
&\int_{\kappa+1+\nu+m}^{\Lambda}\frac{r_1^2}{\omega(r_1)L(r_1,r_2,1)}dr_1\\
&>\frac{1}{2\sqrt{2}\left(1/m+\sqrt{2}\right)}\int_{\kappa+1+\nu+m}^{\Lambda} r_1^{-1}dr_1\\
&=\frac{1}{2\sqrt{2}\,(1/m+2)}\left(\log\Lambda-\log(\kappa+1+\nu+m)\right)
\end{aligned}
\tag{95}
$$

follows. When $\kappa\le r_2\le\kappa+1$, we have

$$
\begin{aligned}
\omega(r_2)&\le\sqrt{(\kappa+1)^2+\nu^2},\\
F(r_2)&\le\frac{(\kappa+1)^2}{2m}+\sqrt{(\kappa+1)^2+\nu^2}.
\end{aligned}
\tag{96}
$$

Then

$$
\begin{aligned}
S_1(\Lambda) &= \int_{\kappa}^{\kappa+1}\frac{r_2^4}{\omega(r_2)F(r_2)^4}dr_2\\
&\quad\cdot\int_{\kappa+1+\nu+m}^{\Lambda}\frac{r_1^2}{\omega(r_1)L(r_1,r_2,1)}dr_1\\
&>\frac{K}{2\sqrt{2}\left(1/m+\sqrt{2}\right)}\left(\log\Lambda-\log(\kappa+1+\nu+m)\right)\\
&\quad\cdot\int_{\kappa}^{\kappa+1} r_2^4dr_2=\frac{K\left\{(\kappa+1)^5-\kappa^5\right\}}{10\sqrt{2}\left(1/m+\sqrt{2}\right)}\left(\log\Lambda\right.\\
&\quad\left.-\log(\kappa+1+\nu+m)\right),
\end{aligned}
\tag{97}
$$

where

$$
\begin{aligned}
&K\\
&=\frac{1}{\sqrt{(\kappa+1)^2+\nu^2}\left((\kappa+1)^2/2m+\sqrt{(\kappa+1)^2+\nu^2}\right)^4}.
\end{aligned}
\tag{98}
$$

From (93), (94), and (97), $C_3\le\lim_{\Lambda\to\infty}(I_1(\Lambda)/\log\Lambda)$ follows.

The proof of $C_5\le\lim_{\Lambda\to\infty}(I_2(\Lambda)/\log\Lambda)$ is similar to that of $C_3\le\lim_{\Lambda\to\infty}(I_1(\Lambda)/\log\Lambda)$. Then we omit it. □

Proof of $\lim_{\Lambda\to\infty}(I_1(\Lambda)/\log\Lambda)\le C_4$. We redefine $h(r_1,r_2)$, $h_1(r_1,r_2)$, $h_2(r_1,r_2)$, $S_1(\Lambda)$, $S_2(\Lambda)$, and $S(\Lambda)$ as

$$
\begin{aligned}
h(r_1,r_2) &= \frac{r_1^2r_2^2}{\omega(r_1)\omega(r_2)}\left(\frac{r_1^2}{F(r_1)^3}+\frac{r_2^2}{F(r_2)^3}\right)\\
&\quad\cdot\left(\frac{1}{F(r_1)}+\frac{1}{F(r_2)}\right)\frac{1}{L(r_1,r_2,-1)},\\
h_1(r_1,r_2) &= \frac{r_1^2r_2^4}{\omega(r_1)\omega(r_2)F(r_2)^4L(r_1,r_2,-1)},\\
h_2(r_1,r_2) &= \frac{r_1^2r_2^4}{\omega(r_1)\omega(r_2)F(r_1)F(r_2)^3L(r_1,r_2,-1)},\\
S_1(\Lambda) &= \int_{\kappa}^{\Lambda}\int_{\kappa}^{\Lambda} h_1(r_1,r_2)\,dr_1dr_2,\\
S_2(\Lambda) &= \int_{\kappa}^{\Lambda}\int_{\kappa}^{\Lambda} h_2(r_1,r_2)\,dr_1dr_2,\\
S(\Lambda) &= \int_{\kappa}^{\Lambda}\int_{\kappa}^{\Lambda} h(r_1,r_2)\,dr_1dr_2.
\end{aligned}
\tag{99}
$$

Then we have

$$
I_1(\Lambda)\le\frac{4\pi^2}{(2\pi)^6}S(\Lambda). \tag{100}
$$

Since $h(r_1,r_2)=h_1(r_1,r_2)+h_1(r_2,r_1)+h_2(r_1,r_2)+h_2(r_2,r_1)$, we have

$$
S(\Lambda)=2\left(S_1(\Lambda)+S_2(\Lambda)\right). \tag{101}
$$

Let B be $B=((\kappa+1)^3-\kappa^3)/6\nu^2$. Since $\nu<\omega(r_1)$ and $2\nu<L(r_1,r_2,-1)$,

$$
\int_{\kappa}^{\kappa+1}\frac{r_1^2}{\omega(r_1)L(r_1,r_2,-1)}dr_1<B \tag{102}
$$

follows. Let Y be $Y=2r_2+\kappa+1$. Since $r_1<\omega(r_1)$ and $r_1<L(r_1,r_2,-1)$,

$$
\int_{\kappa+1}^{Y}\frac{r_1^2}{\omega(r_1)L(r_1,r_2,-1)}dr_1<2r_2 \tag{103}
$$

holds. When $Y \le r_1$, since $2r_2 < r_1$, we have $r_1 - r_2 > r_1/2$. Then $L(r_1, r_2, -1) > (r_1 - r_2)^2/2m > r_1^2/8m$. So,

$$\int_Y^\Lambda \frac{r_1^2}{\omega(r_1) L(r_1, r_2, -1)} dr_1 < 8m \int_Y^\Lambda \frac{dr_1}{r_1} < 8m \log \Lambda \quad (104)$$

follows. From (102), (103), and (104), we have

$$\int_\kappa^\Lambda \frac{r_1^2}{\omega(r_1) L(r_1, r_2, -1)} dr_1 < B + 2r_2 + 8m \log \Lambda. \quad (105)$$

Using this, we see that $S_1(\Lambda) < \int_\kappa^\Lambda (B + 2r_2 + 8m \log \Lambda)(r_2^4/\omega(r_2) F(r_2)^4) dr_2$. Since $r_2 < \omega(r_2)$ and $r_2^2/2m < F(r_2)$, we have

$$\begin{aligned} S_1(\Lambda) &< \int_\kappa^\Lambda (2r_2 + B + 8m \log \Lambda) \frac{16m^4}{r_2^5} dr_2 \\ &= \frac{32m^4}{3} \left(\frac{1}{\kappa^3} - \frac{1}{\Lambda^3} \right) \\ &\quad + 4m^4 (B + 8m \log \Lambda) \left(\frac{1}{\kappa^4} - \frac{1}{\Lambda^4} \right) \\ &< \frac{32m^5}{\kappa^4} \log \Lambda + \frac{32m^4}{3\kappa^3} + \frac{4m^4 B}{\kappa^4}. \end{aligned} \quad (106)$$

Since $r_1 < L(r_1, r_2, -1)$,

$$\begin{aligned} \int_\kappa^\Lambda \frac{r_1^2}{\omega(r_1) F(r_1) L(r_1, r_2, -1)} dr_1 &< 2m \int_\kappa^\Lambda \frac{dr_1}{r_1^2} \\ &< \frac{2m}{\kappa}. \end{aligned} \quad (107)$$

Then we have

$$\begin{aligned} S_2(\Lambda) &= \int_\kappa^\Lambda \frac{r_2^4}{\omega(r_2) F(r_2)^3} dr_2 \\ &\cdot \int_\kappa^\Lambda \frac{r_1^2}{\omega(r_1) F(r_1) L(r_1, r_2, -1)} dr_1 < \frac{2m}{\kappa} \\ &\cdot \int_\kappa^\Lambda \frac{r_2^4}{\omega(r_2) F(r_2)^3} dr_2 < \frac{16m^4}{\kappa} \int_\kappa^\Lambda \frac{dr_2}{r_2^3} < \frac{8m^4}{\kappa^3}. \end{aligned} \quad (108)$$

From (101), (106), and (108), it follows that

$$S(\Lambda) < \frac{64m^5}{\kappa^4} \log \Lambda + \frac{112m^4}{3\kappa^3} + \frac{8m^2 B}{\kappa^4}. \quad (109)$$

From (100) and (109), the lemma follows. □

Proof of $\lim_{\Lambda \to \infty} (I_2(\Lambda)/\log \Lambda) \le C_6$. We redefine $h(r_1, r_2)$, $h_1(r_1, r_2)$, $S(\Lambda)$, and $S_1(\Lambda)$ as

$$\begin{aligned} &h(r_1, r_2) \\ &= \frac{r_1^2 r_2^2}{\omega(r_1) \omega(r_2)} \left(\frac{r_1^2}{F(r_1)^4} + \frac{r_2^2}{F(r_2)^4} \right) \frac{1}{L(r_1, r_2, -1)}, \\ &h_1(r_1, r_2) = \frac{r_1^2 r_2^4}{\omega(r_1) \omega(r_2) F(r_2)^4 L(r_1, r_2, -1)}, \\ &S(\Lambda) = \int_\kappa^\Lambda \int_\kappa^\Lambda h(r_1, r_2) dr_1 dr_2, \\ &S_1(\Lambda) = \int_\kappa^\Lambda \int_\kappa^\Lambda h_1(r_1, r_2) dr_1 dr_2. \end{aligned} \quad (110)$$

We have

$$\begin{aligned} I_2(\Lambda) &= \frac{\pi^2}{(2\pi)^6} \\ &\cdot \int_{-1}^1 \int_\kappa^\Lambda \int_\kappa^\Lambda \frac{r_1^2 r_2^2}{\omega(r_1) \omega(r_2)} \left(\frac{r_1^2}{F(r_1)^4} + \frac{r_2^2}{F(r_2)^4} \right) \\ &\cdot \frac{1}{L(r_1, r_2, z)} dz\, dr_1 dr_2. \end{aligned} \quad (111)$$

Then

$$I_2(\Lambda) \le \frac{2\pi^2}{(2\pi)^6} S(\Lambda) \quad (112)$$

holds. Since $h(r_1, r_2) = h_1(r_1, r_2) + h_1(r_2, r_1)$, we have

$$S(\Lambda) = 2S_1(\Lambda). \quad (113)$$

We have

$$\int_\kappa^\Lambda \frac{r_1^2}{\omega(r_1) L(r_1, r_2, -1)} dr_1 < B + 2r_2 + 8m \log \Lambda \quad (114)$$

in the same way as the proof of $\lim_{\Lambda \to \infty} (I_1(\Lambda)/\log \Lambda) \le C_4$. Since $r_2 < \omega(r_2)$ and $r_2^2/2m < F(r_2)$, we have

$$\begin{aligned} S_1(\Lambda) &< \int_\kappa^\Lambda (B + 2r_2 + 8m \log \Lambda) \frac{r_2^4}{\omega(r_2) F(r_2)^4} dr_2 \\ &< 32m^4 \int_\kappa^\Lambda \frac{dr_2}{r_2^4} \\ &\quad + 16m^4 (B + 8m \log \Lambda) \int_\kappa^\Lambda \frac{dr_2}{r_2^5} \\ &< \frac{32m^5}{\kappa^4} \log \Lambda + \frac{32m^4}{3\kappa^3} + \frac{4m^4 B}{\kappa^4}. \end{aligned} \quad (115)$$

From (112), (113), and (115), the lemma follows. □

Proof of $\lim_{\Lambda\to\infty}(I_3(\Lambda)/\log\Lambda) = 0$. We define $h(r_1, r_2, z)$ as

$$h(r_1,r_2,z) = \frac{z r_1^3 r_2^3}{\omega(r_1)\,\omega(r_2)}\left(\frac{1}{F(r_1)^2}+\frac{1}{F(r_2)^2}\right) \cdot\left(\frac{1}{F(r_1)}+\frac{1}{F(r_2)}\right)\frac{1}{L(r_1,r_2,z)^2} \tag{116}$$

and redefine $S(\Lambda)$ as

$$S(\Lambda) = \int_{-1}^{1}\int_{\kappa}^{\Lambda}\int_{\kappa}^{\Lambda} h(r_1,r_2,z)\,dz\,dr_2dr_1. \tag{117}$$

Then we have $I_3(\Lambda) = (\pi^2/(2\pi)^6)S(\Lambda)$. We divide $S(\Lambda)$ in the following way.

$$\begin{aligned} &S(\Lambda)\\ &= \int_{-1}^{0}\int_{\kappa}^{\Lambda}\int_{\kappa}^{\Lambda} h(r_1,r_2,z)\,dz\,dr_2dr_1\\ &\quad+\int_{0}^{1}\int_{\kappa}^{\Lambda}\int_{\kappa}^{\Lambda} h(r_1,r_2,z)\,dz\,dr_2dr_1\\ &= -\int_{1}^{0}\int_{\kappa}^{\Lambda}\int_{\kappa}^{\Lambda} h(r_1,r_2,-z)\,dz\,dr_2dr_1\\ &\quad+\int_{0}^{1}\int_{\kappa}^{\Lambda}\int_{\kappa}^{\Lambda} h(r_1,r_2,z)\,dz\,dr_2dr_1\\ &= \int_{0}^{1}\int_{\kappa}^{\Lambda}\int_{\kappa}^{\Lambda} \left(h(r_1,r_2,z)+h(r_1,r_2,-z)\right)dz\,dr_2dr_1\\ &= \int_{0}^{1}\int_{\kappa}^{\Lambda}\int_{\kappa}^{\Lambda} g(r_1,r_2,z)\,dz\,dr_2dr_1, \end{aligned} \tag{118}$$

where

$$\begin{aligned} g(r_1,r_2,z) &= h(r_1,r_2,z)+h(r_1,r_2,-z)\\ &= -\frac{2z^2 r_1^4 r_2^4}{m\omega(r_1)\,\omega(r_2)}\left(\frac{1}{F(r_1)^2}+\frac{1}{F(r_2)^2}\right)\\ &\quad\cdot\left(\frac{1}{F(r_1)}+\frac{1}{F(r_2)}\right)\\ &\quad\cdot\frac{\left(\left(r_1^2+r_2^2\right)/m+2\omega(r_1)+2\omega(r_2)\right)}{L(r_1,r_2,z)^2\,L(r_1,r_2,-z)^2}. \end{aligned} \tag{119}$$

Since $g(r_1, r_2, z) \le 0$, $S(\Lambda)$ is decreasing in Λ.

$$\begin{aligned} S(\Lambda) &= \int_0^1\int_{\kappa}^{\Lambda}\int_{r_2}^{\Lambda} g(r_1,r_2,z)\,dz\,dr_2dr_1\\ &\quad+\int_0^1\int_{\kappa}^{\Lambda}\int_{r_1}^{\Lambda} g(r_1,r_2,z)\,dz\,dr_1dr_2\\ &= 2\int_0^1\int_{\kappa}^{\Lambda}\int_{r_2}^{\Lambda} g(r_1,r_2,z)\,dz\,dr_2dr_1\\ &= 2\int_0^1\int_{\kappa}^{\Lambda}\int_{r_2}^{2r_2} g(r_1,r_2,z)\,dz\,dr_2dr_1\\ &\quad+2\int_0^1\int_{\kappa}^{\Lambda}\int_{2r_2}^{\Lambda} g(r_1,r_2,z)\,dz\,dr_2dr_1. \end{aligned} \tag{120}$$

Since $\kappa \le r_1$, we have $1 \le r_1/\kappa$. Hence $r_1^2+\nu^2 \le ((\kappa^2+\nu^2)/\kappa^2)r_1^2$. Therefore we have $\omega(r_1) \le (\sqrt{\kappa^2+\nu^2}/\kappa)r_1$, and similarly $\omega(r_2) \le (\sqrt{\kappa^2+\nu^2}/\kappa)r_2$. When $0 \le z \le 1$, we have

$$L(r_1,r_2,z) > \frac{r_1^2}{2m}. \tag{121}$$

Then

$$\begin{aligned} L(r_1,r_2,-z) &= \frac{(r_1-r_2)^2+2r_1r_2(1-z)}{2m}+\omega(r_1)\\ &\quad+\omega(r_2) > \omega(r_1) > r_1. \end{aligned} \tag{122}$$

When $r_2 \le r_1$, we have $r_2^2/m \le r_1^2/m$. Then it holds that

$$\begin{aligned} 2\omega(r_1) &\le \frac{2r_1^2}{\kappa^2}\sqrt{\kappa^2+\nu^2},\\ 2\omega(r_2) &\le \frac{2r_2}{\kappa}\sqrt{\kappa^2+\nu^2} \le \frac{2r_1^2}{\kappa^2}\sqrt{\kappa^2+\nu^2}. \end{aligned} \tag{123}$$

Thus we have

$$\begin{aligned} &\frac{r_1^2}{m}+\frac{r_2^2}{m}+2\omega(r_1)+2\omega(r_2)\\ &\quad\le 2\left(\frac{1}{m}+\frac{2\sqrt{\kappa^2+\nu^2}}{\kappa^2}\right)r_1^2. \end{aligned} \tag{124}$$

When $r_2 \le r_1 \le 2r_2$, we have

$$\begin{aligned} \frac{1}{F(r_1)}+\frac{1}{F(r_2)} &< \frac{10m}{r_1^2},\\ \frac{1}{F(r_1)^2}+\frac{1}{F(r_2)^2} &< \frac{68m^2}{r_1^4}. \end{aligned} \tag{125}$$

From (119), (121), (122), (124), and (125), it follows that

$$\begin{aligned} -g(r_1,r_2,z) &\le \frac{2}{m}\frac{z^2r_1^4r_2^4}{r_1r_2}\frac{68m^2}{r_1^4}\frac{10m}{r_1^2} \\ &\cdot 2\left(\frac{1}{m}+\frac{2\sqrt{\kappa^2+\nu^2}}{\kappa^2}\right)r_1^2\left(\frac{2m}{r_1^2}\right)^2\frac{1}{r_1^2} \\ &= 68\cdot 10\cdot 16m^4\left(\frac{1}{m}+\frac{2\sqrt{\kappa^2+\nu^2}}{\kappa^2}\right)\frac{z^2r_2^3}{r_1^7}. \end{aligned} \tag{126}$$

Hence

$$\begin{aligned} &-2\int_0^1\int_\kappa^\Lambda\int_{r_2}^{2r_2} g(r_1,r_2,z)\,dz\,dr_2dr_1 \\ &\le 1190\frac{m^4}{\kappa^2}\left(\frac{1}{m}+\frac{2\sqrt{\kappa^2+\nu^2}}{\kappa^2}\right). \end{aligned} \tag{127}$$

When $2r_2 \le r_1$, we have

$$\begin{aligned} &\frac{1}{F(r_1)}+\frac{1}{F(r_2)} < \frac{5m}{2r_2^2}, \\ &\frac{1}{F(r_1)^2}+\frac{1}{F(r_2)^2} < \frac{17m^2}{4r_2^4}. \end{aligned} \tag{128}$$

Since $r_2 \le r_1/2$, we have $r_1/2 \le r_1 - r_2$. Then we have

$$\begin{aligned} L(r_1,r_2,\pm z) &= \frac{(r_1-r_2)^2+2r_1r_2(1\pm z)}{2m}+\omega(r_1) \\ &+\omega(r_2) > \frac{(r_1-r_2)^2}{2m} \ge \frac{r_1^2}{8m}. \end{aligned} \tag{129}$$

From (119), (124), (128), and (129), it follows that

$$\begin{aligned} -g(r_1,r_2,z) &\le \frac{2}{m}\frac{z^2r_1^4r_2^4}{r_1r_2}\frac{17m^2}{4r_2^4}\frac{5m}{2r_2^2} \\ &\cdot 2\left(\frac{1}{m}+\frac{2\sqrt{\kappa^2+\nu^2}}{\kappa^2}\right)r_1^2\left(\frac{8m}{r_1^2}\right)^4 = 2^{11}\cdot 5 \\ &\cdot 17m^6\left(\frac{1}{m}+\frac{2\sqrt{\kappa^2+\nu^2}}{\kappa^2}\right)\frac{z^2}{r_1^3r_2^3}. \end{aligned} \tag{130}$$

Hence

$$\begin{aligned} &-2\int_0^1\int_\kappa^\Lambda\int_{2r_2}^{\Lambda} g(r_1,r_2,z)\,dz\,dr_2dr_1 \\ &\le 2^7\cdot 5\cdot 17\frac{m^6}{\kappa^4}\left(\frac{1}{m}+\frac{2\sqrt{\kappa^2+\nu^2}}{\kappa^2}\right). \end{aligned} \tag{131}$$

Then by (120), (127), and (131), we have

$$\begin{aligned} -S(\Lambda) &\le \frac{1190m^4}{\kappa^2}\left(\frac{1}{m}+\frac{2\sqrt{\kappa^2+\nu^2}}{\kappa^2}\right) \\ &+ 2^7\cdot 5\cdot 17\frac{m^6}{\kappa^4}\left(\frac{1}{m}+\frac{2\sqrt{\kappa^2+\nu^2}}{\kappa^2}\right). \end{aligned} \tag{132}$$

Since $S(\Lambda)$ is decreasing and bounded below, it converges as $\Lambda \to \infty$. This fact proves the lemma. □

Proof of $\lim_{\Lambda\to\infty}(I_4(\Lambda)/\log\Lambda) = 0$. We redefine $h(r_1,r_2,z)$ as

$$\begin{aligned} h(r_1,r_2,z) &= \frac{r_1^2r_2^2}{\omega(r_1)\omega(r_2)}\left(\frac{r_1^2}{F(r_1)^2}+\frac{r_2^2}{F(r_2)^2}\right) \\ &\cdot\left(\frac{1}{F(r_1)}+\frac{1}{F(r_2)}\right)\frac{1}{L(r_1,r_2,z)^2}. \end{aligned} \tag{133}$$

Then we have $I_4(\Lambda) = (2\pi^2/(2\pi)^6)\int_{-1}^1\int_\kappa^\Lambda\int_\kappa^\Lambda h(r_1,r_2,z)dz\,dr_1dr_2$. We define $J(\Lambda)$ as

$$J(\Lambda) = \int_{-1}^1\int_\kappa^\Lambda\int_\kappa^\Lambda h(r_1,r_2,z)\,dz\,dr_1dr_2. \tag{134}$$

Step 1. We define $S(\Lambda,z)$ as

$$S(\Lambda,z) = \int_\kappa^\Lambda\int_\kappa^\Lambda h(r_1,r_2,z)\,dr_1dr_2. \tag{135}$$

Our first task is to prove that $\lim_{\Lambda\to\infty}S(\Lambda,z)$ exists for all $z \in I = [-1,1]$. Since $h(r_1,r_2,z) > 0$, $S(\Lambda,z)$ is increasing in Λ. Let

$$\begin{aligned} S_1(\Lambda,z) &= 2\int_\kappa^\Lambda\int_{r_2}^{2r_2} h(r_1,r_2,z)\,dr_2dr_1, \\ S_2(\Lambda,z) &= 2\int_\kappa^\Lambda\int_{2r_2}^{\Lambda} h(r_1,r_2,z)\,dr_2dr_1. \end{aligned} \tag{136}$$

Then

$$\begin{aligned} S(\Lambda,z) &= \int_\kappa^\Lambda\int_{r_2}^\Lambda h(r_1,r_2,z)\,dr_2dr_1 \\ &+\int_\kappa^\Lambda\int_{r_1}^\Lambda h(r_1,r_2,z)\,dr_1dr_2 \\ &= 2\int_\kappa^\Lambda\int_{r_2}^\Lambda h(r_1,r_2,z)\,dr_2dr_1 \\ &= 2\int_\kappa^\Lambda\int_{r_2}^{2r_2} h(r_1,r_2,z)\,dr_2dr_1 \\ &+2\int_\kappa^\Lambda\int_{2r_2}^\Lambda h(r_1,r_2,z)\,dr_2dr_1 \\ &= S_1(\Lambda,z)+S_2(\Lambda,z) \end{aligned} \tag{137}$$

holds. We have

$$\begin{aligned} &\frac{1}{F(r_1)}+\frac{1}{F(r_2)} < 2m\left(\frac{1}{r_1^2}+\frac{1}{r_2^2}\right), \\ &\frac{r_1^2}{F(r_1)^2}+\frac{r_2^2}{F(r_2)^2} < 4m^2\left(\frac{1}{r_1^2}+\frac{1}{r_2^2}\right), \end{aligned} \tag{138}$$

$$r_1 < L(r_1,r_2,z). \tag{139}$$

Let $r_2 \le r_1 \le 2r_2$. Since $1/r_2^2 \le 4/r_1^2$, it holds that

$$\frac{1}{r_1^2} + \frac{1}{r_2^2} \le \frac{5}{r_1^2}. \tag{140}$$

Then from (138) and (140), it follows that

$$\begin{aligned} \frac{1}{F(r_1)} + \frac{1}{F(r_2)} &< \frac{10m}{r_1^2}, \\ \frac{r_1^2}{F(r_1)^2} + \frac{r_2^2}{F(r_2)^2} &< \frac{20m^2}{r_1^2}. \end{aligned} \tag{141}$$

Hence from (139) and (141), it follows that $h(r_1, r_2, z) < 200m^3 r_2/r_1^5$. Therefore we have

$$\begin{aligned} S_1(\Lambda, z) &< 400m^3 \int_\kappa^\Lambda r_2 dr_2 \int_{r_2}^{2r_2} \frac{dr_1}{r_1^5} \\ &= \frac{375m^3}{8}\left(\frac{1}{\kappa^2} - \frac{1}{\Lambda^2}\right) < \frac{375m^3}{8\kappa^2}. \end{aligned} \tag{142}$$

Let $2r_2 \le r_1$. Since $r_1/2 \le r_1 - r_2$, we have

$$\frac{r_1^2}{8m} \le \frac{(r_1 - r_2)^2}{2m} < L(r_1, r_2, z). \tag{143}$$

Since $r_2^2 \le r_1^2$, we have

$$\begin{aligned} \frac{1}{F(r_1)} + \frac{1}{F(r_2)} &< \frac{4m}{r_2^2}, \\ \frac{r_1^2}{F(r_1)^2} + \frac{r_2^2}{F(r_2)^2} &< \frac{8m^2}{r_2^2}. \end{aligned} \tag{144}$$

Hence from (143) and (144), it follows that $h(r_1, r_2, z) < 2048m^5/r_1^3 r_2^3$. Therefore we have

$$\begin{aligned} S_2(\Lambda, z) &< 4096m^5 \int_\kappa^\Lambda \frac{dr_2}{r_2^3} \int_{2r_2}^\Lambda \frac{dr_1}{r_1^3} \\ &< 512m^5 \int_\kappa^\Lambda \frac{dr_2}{r_2^5} < \frac{128m^5}{\kappa^4}. \end{aligned} \tag{145}$$

From (137), (142), and (145), it follows that

$$S(\Lambda, z) < \frac{375m^3}{8\kappa^2} + \frac{128m^5}{\kappa^4}. \tag{146}$$

Since $S(\Lambda, z)$ is increasing in Λ and bounded above for all $z \in I$, it converges as Λ goes to infinity.

Step 2. Our second task is to prove that $J(\Lambda)$ converges when Λ goes to infinity. Let $M(r_1, r_2)$ be

$$\begin{aligned} M(r_1, r_2) = \frac{r_1^2 r_2^2}{\omega(r_1)\omega(r_2)} &\left(\frac{r_1^2}{F(r_1)^2} + \frac{r_2^2}{F(r_2)^2}\right) \\ &\cdot \left(\frac{1}{F(r_1)} + \frac{1}{F(r_2)}\right) \frac{1}{L(r_1, r_2, -1)^2}. \end{aligned} \tag{147}$$

$|h(r_1, r_2, z)| \le M(r_1, r_2)$ holds for all $(r_1, r_2, z) \in [\kappa, \Lambda]^2 \times I$, and by Step 1 there exists

$$\lim_{\Lambda\to\infty} \int_\kappa^\Lambda \int_\kappa^\Lambda M(r_1, r_2)\, dr_1 dr_2. \tag{148}$$

Since

$$\begin{aligned} M_\Lambda &= \int_\kappa^\Lambda \int_\kappa^\Lambda M(r_1, r_2)\, dr_1 dr_2 \longrightarrow \\ M_\infty &= \lim_{\Lambda\to\infty} \int_\kappa^\Lambda \int_\kappa^\Lambda M(r_1, r_2)\, dr_1 dr_2, \end{aligned} \tag{149}$$

from Cauchy convergence condition, for any $\epsilon > 0$, there exists $\Lambda_0 \in [\kappa, \infty)$ such that if $\Lambda_0 < \Lambda_1 \le \Lambda_2$, $|M_{\Lambda_2} - M_{\Lambda_1}| < \epsilon$. Then for $\Lambda_0 < \Lambda_1 \le \Lambda_2$ and all $z \in I$,

$$\begin{aligned} &\left|S(\Lambda_2, z) - S(\Lambda_1, z)\right| \\ &= \left| \int_\kappa^{\Lambda_1} \int_{\Lambda_1}^{\Lambda_2} h(r_1, r_2, z)\, dr_1 dr_2 \right. \\ &\quad + \int_\kappa^{\Lambda_1} \int_{\Lambda_1}^{\Lambda_2} h(r_1, r_2, z)\, dr_2 dr_1 \\ &\quad \left. + \int_{\Lambda_1}^{\Lambda_2} \int_{\Lambda_1}^{\Lambda_2} h(r_1, r_2, z)\, dr_1 dr_2 \right| \\ &\le \int_\kappa^{\Lambda_1} \int_{\Lambda_1}^{\Lambda_2} M(r_1, r_2)\, dr_1 dr_2 \\ &\quad + \int_\kappa^{\Lambda_1} \int_{\Lambda_1}^{\Lambda_2} M(r_1, r_2)\, dr_2 dr_1 \\ &\quad + \int_{\Lambda_1}^{\Lambda_2} \int_{\Lambda_1}^{\Lambda_2} M(r_1, r_2)\, dr_1 dr_2 = \left|M_{\Lambda_2} - M_{\Lambda_1}\right| < \epsilon. \end{aligned} \tag{150}$$

Therefore $\sup_{z\in I}|S(\Lambda_2, z) - S(\Lambda_1, z)| \le |M_{\Lambda_2} - M_{\Lambda_1}| < \epsilon$ holds. Since family of functions $(S(\Lambda, \cdot))_{\Lambda\in[\kappa,\infty)}$ on I satisfies uniform Cauchy conditions, it converges uniformly on I. Since $[\kappa, \Lambda]^2$ is a Jordan measurable bounded closed set of $\mathbb{R}^2$, the function $S(\Lambda, z)$ is continuous on I. Hence

$$S(\infty, z) = \lim_{\Lambda\to\infty} \int_\kappa^\Lambda \int_\kappa^\Lambda h(r_1, r_2, z)\, dr_1 dr_2 \tag{151}$$

is continuous on I. Since both $S(\Lambda, z)$ and $S(\infty, z)$ are integrable on Jordan measurable set I, by uniform convergence theorem, we have

$$\lim_{\Lambda\to\infty} \int_{-1}^1 S(\Lambda, z)\, dz = \int_{-1}^1 S(\infty, z)\, dz. \tag{152}$$

It implies that $J(\Lambda)$ converges as $\Lambda \to \infty$. □

Proof of $\lim_{\Lambda\to\infty}(I_5(\Lambda)/\log\Lambda) = 0$. We redefine $h(r_1, r_2, z)$, $g(r_1, r_2, z)$, and $S(\Lambda)$ as

$$\begin{aligned} &h(r_1, r_2, z) \\ &\quad = \frac{z r_1^3 r_2^3}{\omega(r_1)\,\omega(r_2)\,F(r_1)^2\,F(r_2)^2\,L(r_1, r_2, z)}, \\ &g(r_1, r_2, z) = h(r_1, r_2, z) + h(r_1, r_2, -z), \\ &S(\Lambda) = \int_{-1}^{1}\int_{\kappa}^{\Lambda}\int_{\kappa}^{\Lambda} h(r_1, r_2, z)\,dz\,dr_1 dr_2. \end{aligned} \tag{153}$$

Then $I_5(\Lambda) = (2\pi^2/(2\pi)^6)S(\Lambda)$. We have

$$S(\Lambda) = \int_{0}^{1}\int_{\kappa}^{\Lambda}\int_{\kappa}^{\Lambda} g(r_1, r_2, z)\,dz\,dr_2 dr_1 \tag{154}$$

in the same way as (118). Since

$$\begin{aligned} &g(r_1, r_2, z) \\ &= -\frac{2z^2 r_1^4 r_2^4}{m^2\omega(r_1)\,\omega(r_2)\,F(r_1)^2\,F(r_2)^2\,L(r_1, r_2, z)\,L(r_1, r_2, -z)} \\ &\le 0, \end{aligned} \tag{155}$$

$S(\Lambda)$ is decreasing in Λ. Since $r_1 < L(r_1, r_2, z)$, we have

$$\frac{r_1^4}{\omega(r_1)\,F(r_1)^2\,L(r_1, r_2, z)} < \frac{4m^2}{r_1^2}. \tag{156}$$

Similarly, we have

$$\frac{r_2^4}{\omega(r_2)\,F(r_2)^2\,L(r_1, r_2, -z)} < \frac{4m^2}{r_2^2}. \tag{157}$$

Hence

$$\begin{aligned} -S(\Lambda) &= \frac{2}{m^2}\int_{0}^{1} z^2 dz \\ &\cdot \int_{\kappa}^{\Lambda} \frac{r_2^4}{\omega(r_2)\,F(r_2)^2\,L(r_1, r_2, -z)} dr_2 \\ &\cdot \int_{\kappa}^{\Lambda} \frac{r_1^4}{\omega(r_1)\,F(r_1)^2\,L(r_1, r_2, z)} dr_1 < \frac{2}{3m^2} \\ &\cdot \int_{\kappa}^{\Lambda} \frac{4m^2}{r_2^2} dr_2 \int_{\kappa}^{\Lambda} \frac{4m^2}{r_1^2} dr_1 < \frac{32m^2}{3\kappa^2}. \end{aligned} \tag{158}$$

Since $S(\Lambda)$ is decreasing and bounded below, it converges as $\Lambda \to \infty$. □

Proof of $\lim_{\Lambda\to\infty}(I_6(\Lambda)/\log\Lambda) = 0$. We redefine $h(r_1, r_2, z)$, $J(\Lambda)$, $S(\Lambda, z)$, $S_1(\Lambda, z)$, and $S_2(\Lambda, z)$ as

$$\begin{aligned} &h(r_1, r_2, z) \\ &\quad = \frac{r_1^2 r_2^2}{\omega(r_1)\,\omega(r_2)}\left(\frac{1}{F(r_1)} + \frac{1}{F(r_2)}\right)^2 \frac{r_1^2 + r_2^2}{L(r_1, r_2, z)^3}, \\ &J(\Lambda) = \int_{-1}^{1}\int_{\kappa}^{\Lambda}\int_{\kappa}^{\Lambda} h(r_1, r_2, z)\,dz\,dr_2 dr_1, \\ &S(\Lambda, z) = \int_{\kappa}^{\Lambda}\int_{\kappa}^{\Lambda} h(r_1, r_2, z)\,dr_1 dr_2, \\ &S_1(\Lambda, z) = 2\int_{\kappa}^{\Lambda}\int_{r_2}^{2r_2} h(r_1, r_2, z)\,dr_2 dr_1, \\ &S_2(\Lambda, z) = 2\int_{\kappa}^{\Lambda}\int_{2r_2}^{\Lambda} h(r_1, r_2, z)\,dr_2 dr_1. \end{aligned} \tag{159}$$

We have $I_6(\Lambda) = (\pi^2/(2\pi)^6)J(\Lambda)$.

Step 1. Our first task is to prove that $\lim_{\Lambda\to\infty}S(\Lambda, z)$ exists for all $z \in I$. Since $h(r_1, r_2, z) > 0$, $S(\Lambda, z)$ is increasing in Λ. We have

$$S(\Lambda, z) = S_1(\Lambda, z) + S_2(\Lambda, z) \tag{160}$$

in the same way as (137). When $r_2 \le r_1$, it holds that

$$\begin{aligned} r_1^2 + r_2^2 &\le 2r_1^2, \\ \frac{1}{F(r_1)} + \frac{1}{F(r_2)} &< \frac{4m}{r_2^2}. \end{aligned} \tag{161}$$

When $r_2 \le r_1 \le 2r_2$, it also holds that

$$\frac{1}{F(r_1)} + \frac{1}{F(r_2)} < \frac{10m}{r_1^2}. \tag{162}$$

Then we have

$$\begin{aligned} \int_{r_2}^{2r_2} h(r_1, r_2, z)\,dr_1 &< \int_{r_2}^{2r_2} \frac{r_1^2 r_2^2}{r_1 r_2}\left(\frac{10m}{r_1^2}\right)^2 \frac{2r_1^2}{r_1^3} dr_1 \\ &= \frac{175m^2}{3r_2^2}. \end{aligned} \tag{163}$$

Hence

$$S_1(\Lambda, z) < \frac{350m^2}{3}\int_{\kappa}^{\Lambda}\frac{dr_2}{r_2^2} < \frac{350m^2}{3\kappa}. \tag{164}$$

Let $2r_2 \le r_1$. Since $r_1/2 \le r_1 - r_2$, we have

$$\frac{r_1^2}{8m} \le \frac{(r_1 - r_2)^2}{2m} < L(r_1, r_2, z). \tag{165}$$

Then

$$\begin{aligned}&\int_{2r_2}^{\Lambda} h\left(r_1, r_2, \right) dr_1 \\ &< \int_{2r_2}^{\Lambda} \frac{r_1^2 r_2^2}{r_1 r_2} \left(\frac{4m}{r_2^2}\right)^2 \left(\frac{8m}{r_1^2}\right)^3 2r_1^2 dr_1 \\ &= \frac{16384m^5}{r_2^3} \int_{2r_2}^{\Lambda} \frac{dr_1}{r_1^3} < \frac{2048m^5}{r_2^5}.\end{aligned} \tag{166}$$

Therefore

$$S_2(\Lambda, z) < 4096m^5 \int_{\kappa}^{\Lambda} \frac{dr_2}{r_2^5} < \frac{1024m^5}{\kappa^4}. \tag{167}$$

From (160), (164), and (167), it follows that $S(\Lambda, z) < 350m^2/3\kappa + 1024m^5/\kappa^4$. Since $S(\Lambda, z)$ is increasing in Λ and bounded above, it converges as Λ goes to infinity.

Step 2. Our second task is to prove $J(\Lambda)$ converges as Λ goes to infinity. This step is the same as that of $\lim_{\Lambda\to\infty}(I_4(\Lambda)/\log\Lambda) = 0$. □

Proof of $\lim_{\Lambda\to\infty}(I_7(\Lambda)/\log\Lambda) = 0$. We redefine $h(r_1, r_2, z)$, $g(r_1, r_2, z)$, and $S(\Lambda)$ as

$$\begin{aligned}&h\left(r_1, r_2, z\right) \\ &= \frac{z r_1^3 r_2^3}{\omega\left(r_1\right)\omega\left(r_2\right)} \left(\frac{1}{F\left(r_1\right)} + \frac{1}{F\left(r_2\right)}\right)^2 \frac{1}{L\left(r_1, r_2, z\right)^3}, \\ &g\left(r_1, r_2, z\right) = h\left(r_1, r_2, z\right) + h\left(r_1, r_2, -z\right), \\ &S(\Lambda) = \int_{-1}^{1} \int_{\kappa}^{\Lambda} \int_{\kappa}^{\Lambda} h\left(r_1, r_2, z\right) dz\, dr_1 dr_2.\end{aligned} \tag{168}$$

Then we have $I_7(\Lambda) = (2\pi^2/(2\pi)^6)S(\Lambda)$, and

$$S(\Lambda) = \int_0^1 \int_{\kappa}^{\Lambda} \int_{\kappa}^{\Lambda} g\left(r_1, r_2, z\right) dz\, dr_1 dr_2 \tag{169}$$

in the same way as $\lim_{\Lambda\to\infty}(I_3(\Lambda)/\log\Lambda) = 0$. We define $g_1(r_1, r_2, z)$ and $g_2(r_1, r_2, z)$ as

$$\begin{aligned}&g_1\left(r_1, r_2, z\right) = -\frac{6z^2 r_1^4 r_2^4}{m\omega\left(r_1\right)\omega\left(r_2\right)} \left(\frac{1}{F\left(r_1\right)} + \frac{1}{F\left(r_2\right)}\right)^2 \\ &\cdot \frac{\left(\left(r_1^2 + r_2^2\right)/2m + \omega\left(r_1\right) + \omega\left(r_2\right)\right)^2}{L\left(r_1, r_2, z\right)^3 L\left(r_1, r_2, -z\right)^3}, \\ &g_2\left(r_1, r_2, z\right) \\ &= -\frac{2z^4 r_1^6 r_2^6}{m^3\omega\left(r_1\right)\omega\left(r_2\right)} \left(\frac{1}{F\left(r_1\right)} + \frac{1}{F\left(r_2\right)}\right)^2 \\ &\cdot \frac{1}{L\left(r_1, r_2, z\right)^3 L\left(r_1, r_2, -z\right)^3}.\end{aligned} \tag{170}$$

Then we have $g(r_1, r_2, z) = g_1(r_1, r_2, z) + g_2(r_1, r_2, z)$. We redefine $S_1(\Lambda)$ and $S_2(\Lambda)$ by

$$\begin{aligned}S_1(\Lambda) &= \int_0^1 \int_{\kappa}^{\Lambda} \int_{\kappa}^{\Lambda} g_1\left(r_1, r_2, z\right) dz\, dr_1 dr_2, \\ S_2(\Lambda) &= \int_0^1 \int_{\kappa}^{\Lambda} \int_{\kappa}^{\Lambda} g_2\left(r_1, r_2, z\right) dz\, dr_1 dr_2.\end{aligned} \tag{171}$$

Then

$$S(\Lambda) = S_1(\Lambda) + S_2(\Lambda). \tag{172}$$

Since $g_1(r_1, r_2, z) \le 0$, $S_1(\Lambda)$ is decreasing in Λ. We divide $S_1(\Lambda)$ in the following way:

$$\begin{aligned}S_1(\Lambda) &= \int_0^1 \int_{\kappa}^{\Lambda} \int_{r_1}^{\Lambda} g_1\left(r_1, r_2, z\right) dz\, dr_1 dr_2 \\ &\quad + \int_0^1 \int_{\kappa}^{\Lambda} \int_{r_2}^{\Lambda} g_1\left(r_1, r_2, z\right) dz\, dr_2 dr_1 \\ &= \int_0^1 \int_{\kappa}^{\Lambda} \int_{r_1}^{\Lambda} g_1\left(r_1, r_2, z\right) dz\, dr_1 dr_2 \\ &\quad + \int_0^1 \int_{\kappa}^{\Lambda} \int_{r_1}^{\Lambda} g_1\left(r_2, r_1, z\right) dz\, dr_1 dr_2 \\ &= 2\int_0^1 \int_{\kappa}^{\Lambda} \int_{r_1}^{\Lambda} g_1\left(r_1, r_2, z\right) dz\, dr_1 dr_2.\end{aligned} \tag{173}$$

Let $\kappa \le r_1 \le r_2$. Then we have

$$\frac{r_1^2 + r_2^2}{2m} + \omega\left(r_1\right) + \omega\left(r_2\right) \le \left(\frac{1}{m} + \frac{2\sqrt{\kappa^2 + \nu^2}}{\kappa^2}\right) r_2^2 \tag{174}$$

in the same way as (124). Let $r_1 \le r_2 \le 2r_1$. Then we also have

$$\frac{1}{F\left(r_1\right)} + \frac{1}{F\left(r_2\right)} < \frac{10m}{r_2^2}. \tag{175}$$

Therefore

$$\begin{aligned}&-g_1\left(r_1, r_2, z\right) \le \frac{6}{m} \frac{z^2 r_1^4 r_2^4}{r_1 r_2} \left(\frac{10m}{r_2^2}\right)^2 \\ &\cdot \left\{\left(\frac{1}{m} + \frac{2\sqrt{\kappa^2 + \nu^2}}{\kappa^2}\right) r_2^2\right\}^2 \left(\frac{2m}{r_2^2}\right)^3 \frac{1}{r_2^3} \\ &= 4800m^4 \left(\frac{1}{m} + \frac{2\sqrt{\kappa^2 + \nu^2}}{\kappa^2}\right)^2 \frac{z^2 r_1^3}{r_2^6}, \\ &-\int_{r_1}^{2r_1} g_1\left(r_1, r_2, z\right) dr_2 \\ &\le 4800m^4 \left(\frac{1}{m} + \frac{2\sqrt{\kappa^2 + \nu^2}}{\kappa^2}\right)^2 z^2 r_1^3 \int_{r_1}^{2r_1} \frac{dr_2}{r_2^6} \\ &= 930m^4 \left(\frac{1}{m} + \frac{2\sqrt{\kappa^2 + \nu^2}}{\kappa^2}\right)^2 \frac{z^2}{r_1^2}.\end{aligned} \tag{176}$$

Hence

$$-2\int_0^1\int_\kappa^\Lambda\int_{r_1}^{2r_1} g_1(r_1,r_2,z)\,dz\,dr_1dr_2 \le 1860m^4\left(\frac{1}{m}+\frac{2\sqrt{\kappa^2+\nu^2}}{\kappa^2}\right)^2\int_0^1 z^2dz\int_\kappa^\Lambda\frac{dr_2}{r_2^2} < \frac{620m^4}{\kappa}\left(\frac{1}{m}+\frac{2\sqrt{\kappa^2+\nu^2}}{\kappa^2}\right)^2. \quad (177)$$

Let $2r_1 \le r_2$. Then we have

$$\frac{1}{F(r_1)}+\frac{1}{F(r_2)} < \frac{5m}{2r_1^2}. \quad (178)$$

In addition, since $r_2/2 \le r_2 - r_1$, we can see that

$$\frac{r_2^2}{8m} \le \frac{(r_2-r_1)^2}{2m} < L(r_1,r_2,-z). \quad (179)$$

Therefore

$$-g_1(r_1,r_2,z) \le \frac{6}{m}\frac{z^2r_1^4r_2^4}{r_1r_2}\left(\frac{5m^2}{2r_1^2}\right)^2 \cdot\left\{\left(\frac{1}{m}+\frac{2\sqrt{\kappa^2+\nu^2}}{\kappa^2}\right)r_2^2\right\}^2\left(\frac{2m}{r_2^2}\right)^3\left(\frac{8m}{r_2^2}\right)^3 = 153600m^9\left(\frac{1}{m}+\frac{2\sqrt{\kappa^2+\nu^2}}{\kappa^2}\right)^2\frac{z^2}{r_1r_2^5}. \quad (180)$$

Then we have

$$-\int_{2r_1}^\Lambda g_1(r_1,r_2,z)\,dr_2 \le \frac{153600m^9z^2}{r_1}\left(\frac{1}{m}+\frac{2\sqrt{\kappa^2+\nu^2}}{\kappa^2}\right)^2\int_{2r_1}^\Lambda\frac{dr_2}{r_2^5} \le 2400m^9\left(\frac{1}{m}+\frac{2\sqrt{\kappa^2+\nu^2}}{\kappa^2}\right)^2\frac{z^2}{r_1^5}. \quad (181)$$

Hence

$$-2\int_0^1\int_\kappa^\Lambda\int_{2r_1}^\Lambda g_1(r_1,r_2,z)\,dz\,dr_1dr_2 \le 4800m^9\left(\frac{1}{m}+\frac{2\sqrt{\kappa^2+\nu^2}}{\kappa^2}\right)^2\int_0^1 z^2dz\int_\kappa^\Lambda\frac{dr_1}{r_1^5} < \frac{400m^9}{\kappa^4}\left(\frac{1}{m}+\frac{2\sqrt{\kappa^2+\nu^2}}{\kappa^2}\right)^2. \quad (182)$$

Then we have

$$-S_1(\Lambda) < \frac{620m^4}{\kappa}\left(\frac{1}{m}+\frac{2\sqrt{\kappa^2+\nu^2}}{\kappa^2}\right)^2 + \frac{400m^9}{\kappa^4}\left(\frac{1}{m}+\frac{2\sqrt{\kappa^2+\nu^2}}{\kappa^2}\right)^2. \quad (183)$$

Since $S_1(\Lambda)$ is decreasing and bounded below, it converges as $\Lambda\to\infty$. Since $g_2(r_1,r_2,z)\le 0$, $S_2(\Lambda)$ is also decreasing in Λ. Let $r_1 \le r_2$. Then

$$\frac{1}{F(r_1)}+\frac{1}{F(r_2)} < \frac{4m}{r_1^2}. \quad (184)$$

Therefore

$$-g_2(r_1,r_2,z) \le \frac{2}{m^3}\frac{z^4r_1^6r_2^6}{r_1r_2}\left(\frac{4m}{r_1^2}\right)^2\frac{8m^3}{r_2^6}\frac{1}{r_2^3} = \frac{256m^2z^4r_1}{r_2^4}. \quad (185)$$

Then

$$-\int_{r_1}^\Lambda g_2(r_1,r_2,z)\,dr_2 \le 256m^2z^4r_1\int_{r_1}^\Lambda\frac{dr_2}{r_2^4} \le \frac{256m^2z^4}{3r_1^2}. \quad (186)$$

Hence

$$-S_2(\Lambda) \le \frac{512m^2}{3}\int_0^1 z^4dz\int_\kappa^\Lambda\frac{dr_1}{r_1^2} < \frac{512m^2}{15\kappa}. \quad (187)$$

Since $S_2(\Lambda)$ is decreasing in Λ and bounded below, it converges. Since both $S_1(\Lambda)$ and $S_2(\Lambda)$ converge, $S(\Lambda)$ converges. □

Proof of $\lim_{\Lambda\to\infty}(I_8(\Lambda)/\log\Lambda) = 0$. We redefine $h(r_1,r_2,z)$, $g(r_1,r_2,z)$, $g_1(r_1,r_2,z)$, $g_2(r_1,r_2,z)$, $S(\Lambda)$, $S_1(\Lambda)$, and $S_2(\Lambda)$ as

$$h(r_1,r_2,z) = \frac{zr_1^3r_2^3}{\omega(r_1)\omega(r_2)}\left(\frac{1}{F(r_1)}+\frac{1}{F(r_2)}\right)\cdot\frac{1}{L(r_1,r_2,z)^4}, \quad (188)$$

$$g(r_1,r_2,z) = h(r_1,r_2,z)+h(r_1,r_2,-z),$$

$$g_1(r_1,r_2,z) = -\frac{2z^2r_1^4r_2^4}{m\omega(r_1)\omega(r_2)}\left(\frac{1}{F(r_1)}+\frac{1}{F(r_2)}\right)\cdot\frac{1}{L(r_1,r_2,z)L(r_1,r_2,-z)^4}, \quad (189)$$

$$g_2(r_1,r_2,z) = -\frac{2z^2r_1^4r_2^4}{m\omega(r_1)\omega(r_2)}\left(\frac{1}{F(r_1)}+\frac{1}{F(r_2)}\right)\cdot G(r_1,r_2,z), \quad (190)$$

$$S(\Lambda) = \int_{-1}^1\int_\kappa^\Lambda\int_\kappa^\Lambda h(r_1,r_2,z)\,dz\,dr_2dr_1,$$

$$S_1(\Lambda) = \int_\kappa^\Lambda\int_{r_2}^\Lambda\int_0^{1-1/r_1^{1/4}r_2^{1/2}} g_1(r_1,r_2,z)\,dr_2dr_1dz, \quad (191)$$

$$S_2(\Lambda) = \int_\kappa^\Lambda\int_{r_2}^\Lambda\int_{1-1/r_1^{1/4}r_2^{1/2}}^1 g_1(r_1,r_2,z)\,dr_2dr_1dz,$$

where

$$G(r_1,r_2,z)=\frac{1}{L(r_1,r_2,z)^2L(r_1,r_2,-z)^3}+\frac{1}{L(r_1,r_2,z)^3L(r_1,r_2,-z)^2}+\frac{1}{L(r_1,r_2,z)^4L(r_1,r_2,-z)}. \tag{192}$$

Furthermore, we define $S_3(\Lambda)$ as

$$S_3(\Lambda)=\int_0^1\int_\kappa^\Lambda\int_{r_2}^\Lambda g_2(r_1,r_2,z)\,dz\,dr_2dr_1. \tag{193}$$

Then we have $I_8(\Lambda)=(2\pi^2/(2\pi)^6)S(\Lambda)$, and

$$S(\Lambda)=2\int_0^1\int_\kappa^\Lambda\int_{r_2}^\Lambda g(r_1,r_2,z)\,dz\,dr_2dr_1 \tag{194}$$

in the same way as the proof of $\lim_{\Lambda\to\infty}(I_3(\Lambda)/\log\Lambda)=0$. Since $g(r_1,r_2,z)=g_1(r_1,r_2,z)+g_2(r_1,r_2,z)$, it holds that

$$S(\Lambda)=2S_1(\Lambda)+2S_2(\Lambda)+2S_3(\Lambda). \tag{195}$$

Since $g_1(r_1,r_2,z)\le 0$ and $g_2(r_1,r_2,z)\le 0$, $S_i(\Lambda)$ $(i=1,2,3)$ are decreasing in Λ. Let $r_2\le r_1$. Then

$$\frac{1}{F(r_1)}+\frac{1}{F(r_2)}<\frac{4m}{r_2^2}. \tag{196}$$

Let $0\le z\le 1-1/r_1^{1/4}r_2^{1/2}$. Then we have

$$\frac{1}{(1-z)^4}\le r_1r_2^2. \tag{197}$$

We have

$$L(r_1,r_2,-z)=\frac{(r_1-r_2)^2+2r_1r_2(1-z)}{2m}+\omega(r_1)+\omega(r_2)>\frac{r_1r_2(1-z)}{m}. \tag{198}$$

Using (197) and (198), we have

$$\frac{1}{L(r_1,r_2,-z)^4}<\frac{m^4}{r_1^4r_2^4(1-z)^4}\le\frac{m^4}{r_1^3r_2^2}. \tag{199}$$

From (189), (196), and (199), it follows that

$$-g_1(r_1,r_2,z)\le\frac{2}{m}\frac{z^2r_1^4r_2^4}{r_1r_2}\frac{4m}{r_2^2}\frac{2m}{r_1^2}\frac{m^4}{r_1^3r_2^2}=\frac{16m^5}{r_1^2r_2}. \tag{200}$$

Hence we have

$$-S_1(\Lambda)\le 16m^5\int_\kappa^\Lambda\frac{dr_2}{r_2}\int_{r_2}^\Lambda\frac{1}{r_1^2}\left(1-\frac{1}{r_1^{1/4}r_2^{1/2}}\right)dr_1<16m^5\int_\kappa^\Lambda\frac{dr_2}{r_2}\int_{r_2}^\Lambda\frac{dr_1}{r_1^2}<\frac{16m^5}{\kappa}. \tag{201}$$

Since $S_1(\Lambda)$ is decreasing in Λ and bounded below, it converges. When $r_2\le r_1$ and $1-1/r_1^{1/4}r_2^{1/2}\le z\le 1$, from (189) and (196), it holds that

$$-g_1(r_1,r_2,z)<\frac{2}{m}\frac{r_1^4r_2^4}{r_1r_2}\frac{4m}{r_2^2}\frac{2m}{r_1^2}\frac{1}{r_1^4}=\frac{16mr_2}{r_1^3}. \tag{202}$$

Hence we have

$$\begin{aligned}-S_2(\Lambda)&<16m\int_\kappa^\Lambda\int_{r_2}^\Lambda\int_{1-1/r_1^{1/4}r_2^{1/2}}^1\frac{r_2}{r_1^3}dr_2dr_1dz\\&=16m\int_\kappa^\Lambda\int_{r_2}^\Lambda\frac{r_2}{r_1^3}r_1^{-1/4}r_2^{-1/2}dr_2dr_1\\&=16m\int_\kappa^\Lambda r_2^{1/2}dr_2\int_{r_2}^\Lambda r_1^{-13/4}dr_1\\&=\frac{64m}{9}\int_\kappa^\Lambda r_2^{1/2}\left(r_2^{-9/4}-\Lambda^{-9/4}\right)dr_2\\&<\frac{64m}{9}\int_\kappa^\Lambda r_2^{-7/4}dr_2\\&=\frac{256m}{27}\left(\kappa^{-3/4}-\Lambda^{-3/4}\right)<\frac{256m}{27\kappa^{3/4}}.\end{aligned} \tag{203}$$

Since $S_2(\Lambda)$ is decreasing in Λ and bounded below, it converges. We have

$$G(r_1,r_2,z)<\frac{4m^2}{r_1^7}+\frac{8m^3}{r_1^8}+\frac{16m^4}{r_1^9}. \tag{204}$$

From (190), (196), and (204), we have

$$\begin{aligned}&-g_2(r_1,r_2,z)\\&\le\frac{2}{m}\frac{z^2r_1^4r_2^4}{r_1r_2}\frac{4m}{r_2^2}\left(\frac{4m^2}{r_1^7}+\frac{8m^3}{r_1^8}+\frac{16m^4}{r_1^9}\right)\\&<8r_1^3r_2\left(\frac{4m^2}{r_1^7}+\frac{8m^3}{r_1^8}+\frac{16m^4}{r_1^9}\right)\\&=\frac{32m^2r_2}{r_1^4}+\frac{64m^3r_2}{r_1^5}+\frac{128m^4r_2}{r_1^6}.\end{aligned} \tag{205}$$

Hence

$$\begin{aligned}-S_3(\Lambda)&<32m^2\int_\kappa^\Lambda r_2dr_2\int_{r_2}^\Lambda\frac{dr_1}{r_1^4}\\&\quad+64m^3\int_\kappa^\Lambda r_2dr_2\int_{r_2}^\Lambda\frac{dr_1}{r_1^5}\\&\quad+128m^4\int_\kappa^\Lambda r_2dr_2\int_{r_2}^\Lambda\frac{dr_1}{r_1^6}\\&<\frac{32m^2}{3}\int_\kappa^\Lambda\frac{1}{r_2^2}dr_2+16m^3\int_\kappa^\Lambda\frac{1}{r_2^3}dr_2\end{aligned}$$

$$+\frac{128m^4}{5}\int_\kappa^\Lambda \frac{1}{r_2^4}dr_2$$
$$<\frac{32m^2}{3\kappa}+\frac{8m^3}{\kappa^2}+\frac{128m^4}{15\kappa^3}. \tag{206}$$

Since $S_3(\Lambda)$ is decreasing in Λ and bounded below, it converges. Since $S_i(\Lambda)$ $(i=1,2,3)$ converge, $I_8(\Lambda)$ converges by (195). □

5. Concluding Remarks

(1) The Nelson model is defined as the self-adjoint operator

$$H_V=\left(-\frac{1}{2}\Delta+V\right)\otimes 1+1\otimes H_f+\alpha\int_{\mathbb{R}^3}^{\oplus}\phi(x)\,dx, \tag{207}$$

acting in the Hilbert space $L^2(\mathbb{R})\otimes\mathcal{F}\cong\int_{\mathbb{R}^3}^{\oplus}\mathcal{F}\,dx$. Here $V:\mathbb{R}^3\to\mathbb{R}$ is an external potential and

$$\phi(x)=\frac{1}{\sqrt{2}}\int\left\{\frac{a^\dagger(k)\,e^{-ikx}\widehat{\varphi}(k)}{\sqrt{\omega(k)}}+\frac{a(k)\,e^{ikx}\widehat{\varphi}(-k)}{\sqrt{\omega(k)}}\right\}dk. \tag{208}$$

In the case of $V=0$, $H_{V=0}$ is translation invariant and the relationship between H_V and $H(p)$ is given by

$$H_{V=0}=\int_{\mathbb{R}^3}^{\oplus}H(p)\,dp. \tag{209}$$

Furthermore the ground state energy of $H(p=0)$ coincides with that of $H_{V=0}$.

(2) We show that $m_{\mathrm{eff}}(\Lambda)/m=1+\sum_{n=1}^{\infty}a_n(\Lambda)\alpha^{2n}$ and $\lim_{\Lambda\to\infty}a_2(\Lambda)=\pm\infty$. It is also expected that $\lim_{\Lambda\to\infty}a_n(\Lambda)$ diverges and the signatures are alternatively changed. Hence $\lim_{\Lambda\to\infty}m_{\mathrm{eff}}(\Lambda)/m$ may converge but it is not trivial to see it directly.

(3) The relativistic Nelson model is defined by replacing $-(1/2)\Delta+V$ with the semirelativistic Schrödinger operator $\sqrt{-\Delta+1}+V$ in (207); that is,

$$H_V^{\mathrm{rel}}=\left(\sqrt{-\Delta+1}+V\right)\otimes 1+1\otimes H_f+\int_{\mathbb{R}^3}^{\oplus}\phi(x)\,dx. \tag{210}$$

Then it follows that

$$H_{V=0}^{\mathrm{rel}}=\int_{\mathbb{R}^3}^{\oplus}H^{\mathrm{rel}}(p)\,dp, \tag{211}$$

where $H^{\mathrm{rel}}(p)=\sqrt{(p-P_f)^2+1}+H_f+\phi(0)$. Then the effective mass $m_{\mathrm{eff}}(\Lambda)$ of $H^{\mathrm{rel}}(p)$ is defined in the same way as that of $H(p)$. We are also interested in seeing the asymptotic behavior of $m_{\mathrm{eff}}(\Lambda)$ as $\Lambda\to\infty$. However $\sqrt{(p-P_f)^2+1}$ is a nonlocal operator and then estimates are rather complicated.

Another interesting nonlocal model is the so-called semirelativistic Pauli-Fierz model defined by

$$H_V^{\mathrm{PF}}=\sqrt{\left(-i\nabla\otimes-\alpha\int_{\mathbb{R}^3}^{\oplus}A(x)\,dx\right)^2+1}+V\otimes 1+1\otimes H_f, \tag{212}$$

where $A(x)$ is a quantized radiation field. See [9] for the detail. Then it follows that

$$H_{V=0}^{\mathrm{PF}}=\int_{\mathbb{R}^3}^{\oplus}H^{\mathrm{PF}}(p)\,dp, \tag{213}$$

where $H^{\mathrm{PF}}(p)=\sqrt{(p-P_f-\alpha A(0))^2+1}+H_f$. It is also interesting to investigate the asymptotic behavior of the effective mass of the semirelativistic Pauli-Fierz model.

Competing Interests

The authors declare that there is no conflict of interests regarding the publication of this paper.

Acknowledgments

Susumu Osawa is grateful to Asao Arai for helpful comments and financial support. This work is financially supported by Grant-in-Aid for Science Research(B) 16H03942 and Grant-in-Aid for challenging Exploratory Research 15K13445 from JSPS.

References

[1] E. Nelson, "Interaction of nonrelativistic particles with a quantized scalar field," *Journal of Mathematical Physics*, vol. 5, no. 9, pp. 1190–1197, 1964.

[2] H. Spohn, "Effective mass of the polaron: a functional integral approach," *Annals of Physics*, vol. 175, no. 2, pp. 278–318, 1987.

[3] F. Hiroshima and H. Spohn, "Mass renormalization in nonrelativistic quantum electrodynamics," *Journal of Mathematical Physics*, vol. 46, no. 4, Article ID 042302, pp. 42302–42328, 2005.

[4] F. Hiroshima and K. R. Ito, "Effective mass of nonrelativistic quantum electrodynamics," *RIMS Kokyuroku*, vol. 1492, pp. 22–48, 2006.

[5] F. Hiroshima and K. R. Ito, "Mass renormalization in nonrelativistic quantum electrodynamics with spin 1/2," *Reviews in Mathematical Physics*, vol. 19, no. 4, pp. 405–454, 2007.

[6] V. Bach, T. Chen, J. Fröhlich, and I. M. Sigal, "The renormalized electron mass in non-relativistic quantum electrodynamics," *Journal of Functional Analysis*, vol. 243, no. 2, pp. 426–535, 2007.

[7] J. Fröhlich and A. Pizzo, "Renormalized electron mass in nonrelativistic QED," *Communications in Mathematical Physics*, vol. 294, no. 2, pp. 439–470, 2010.

[8] M. Reed and B. Simon, *Methods of Modern Mathematical Physics IV*, Academic Press, 1978.

[9] F. Hiroshima, "Functional integral approach to semi-relativistic Pauli-Fierz models," *Advances in Mathematics*, vol. 259, pp. 784–840, 2014.

5

A New Special Function and its Application in Probability

Zeraoulia Rafik,[1] **Alvaro H. Salas**,[2] **and David L. Ocampo**[2,3]

[1] *University Batna, Algeria*
[2] *Universidad Nacional de Colombia, Colombia*
[3] *Universidad de Caldas-Colombia, Colombia*

Correspondence should be addressed to Zeraoulia Rafik; zeraouliarafik@gmail.com

Academic Editor: A. Zayed

In this note we present a new special function that behaves like the error function and we provide an approximated accurate closed form for its CDF in terms of both Chèbyshev polynomials of the first kind and the error function. Also we provide its series representation using Padé approximant. We show a convincing numerical evidence about an accuracy of 10^{-6} for the approximants in the sense of the quadratic mean norm. A similar approach may be applied to other probability distributions, for example, Maxwell–Boltzmann distribution and normal distribution, such that we show its application using both of those distributions.

1. Introduction

Integrals of the error function, see ([1]), occur in a great variety of applications usually in problems involving multiple integration where the integrand contains exponentials of the squares of the argument; an example of applications can be cited from atomic physics astrophysics and statistical analysis. It comes into our mind to seek for the integration of such functions $f(x)$ power its antiderivative $g(x)$. We have got example (1) where it is the power of two distributions related to normal distribution [1] as shown below such that $f(x) = e^{-x^2}$ and $g(x) = \operatorname{erf}(x)$

$$I(a) = \int_0^a \left(e^{-x^2}\right)^{\operatorname{erf}(x)} dx \tag{1}$$

with $\operatorname{erf}(x)$ is called error function and it is defined in (24).

$$\frac{2}{\sqrt{\pi}} \int_0^x e^{-t^2} dt = \operatorname{erf}(x) \tag{2}$$

1.1. Numerical Approximation of $\int_0^a (e^{-x^2})^{\operatorname{erf}(x)} dx$ in Some Ranges Values. Now, if we really need a simple expression for $I(a)$ in some range of values, there are ways to get various approximations.

The function is very nice. It goes to its limit at ∞ very fast. Figure 1 shows the plot of $I(a)$ for $a \in [0, 10]$.

Therefore (depending on the accuracy we need) we can easily take $I(a) = I(\infty)$ for $a > a_0$ with a_0 around 3 or 4.

Mathematica gives the following for the first 100 digits.

$$I(\infty) = 0.9721069927691785931510778754423911755542721833855699009722910408441888759958220033410678218401258734 \tag{3}$$

Now, what can we do for small a?

The function is so nice; we can just use the Taylor expansion around $a = 0$. The first term is as follows.

$$I(a) \approx a \tag{4}$$

The plot for $a \in [0, 1]$ is shown in Figure 2. The proof is simple. The Taylor series look like the following.

$$I(a) = I(0) + I'(0)\, a + \frac{I''(0)}{2!} a^2 + \frac{I'''(0)}{3!} a^3 + \cdots \tag{5}$$

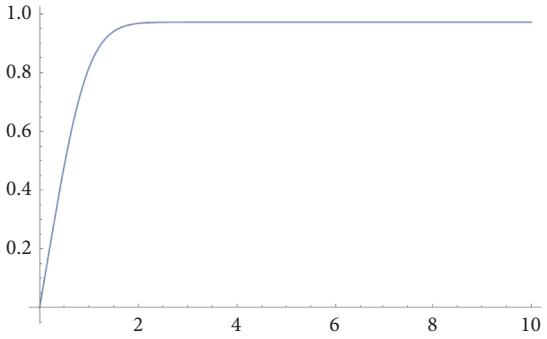

FIGURE 1: The plot of $I(a)$ for $a \in [0, 10]$.

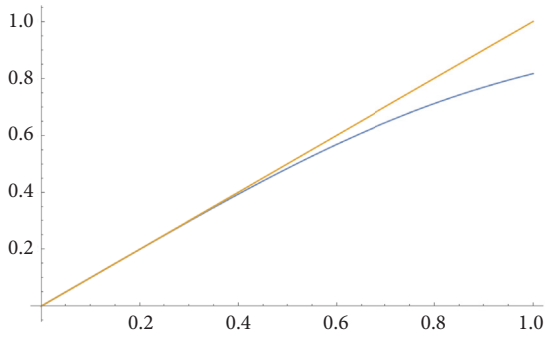

FIGURE 2: Approximation of $I(a)$ for $a \in [0, 1]$ using Taylor expansion.

We may see the following.

$$I(0) = 0$$
$$I'(0) = e^{-a^2 \operatorname{erf}(a)}\Big|_{a=0} = 1 \tag{6}$$

Now let us find a better approximation by computing the higher derivatives.

$$I''(a) = \left(e^{-a^2 \operatorname{erf}(a)}\right)'$$
$$= -\frac{2}{\sqrt{\pi}} a e^{-a^2(\operatorname{erf}(a)+1)} \left(\sqrt{\pi} e^{a^2} \operatorname{erf}(a) + a\right) \tag{7}$$
$$I''(0) = 0$$

We use Mathematica as a shortcut, but it is easy to do it by hand, if we remember that

$$\operatorname{erf}'(x) = \frac{2}{\sqrt{\pi}} e^{-x^2}$$
$$I'''(0) = 0 \tag{8}$$
$$I^{IV}(0) = -\frac{12}{\sqrt{\pi}}$$

so our next approximation is as follows.

$$I(a) \approx a - \frac{1}{2\sqrt{\pi}} a^4 \tag{9}$$

The plot with both approximations (orange, green) and the function itself (blue) is given in Figure 3 and we can continue in the same way for higher derivatives. Now we admit that it is possible that we need the values of $I(a)$ for all the possible a and with high precision, so the approximations will not do that. Then we need to turn to numerical integration (as Mathematica did for me to plot the function). Another way to approximate the function [2] is using its derivative:

$$\frac{dI}{da} = e^{-a^2 \operatorname{erf}(a)} \tag{10}$$

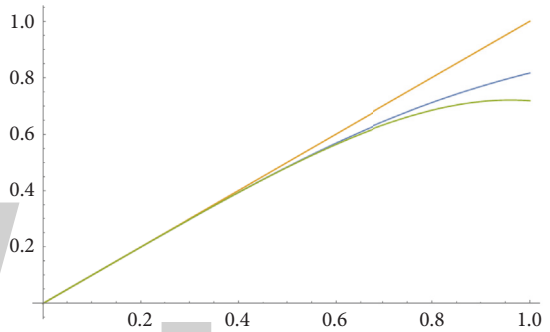

FIGURE 3: Plot of I(a) with both approximations.

but this is an ordinary differential equation, which can be solved numerically.

As an illustration, here is a simple explicit Euler scheme for the step size h.

$$\frac{I(a+h) - I(a)}{h} = e^{-a^2 \operatorname{erf}(a)}$$
$$I(a+h) = I(a) + h e^{-a^2 \operatorname{erf}(a)} \tag{11}$$

We can use an initial value $I(0) = 0$.

For $h = 1/10$, we have the following result (red dots) compared to the exact function (blue line) as shown in Figure 4.

For $h = 1/50$ see Figure 5.

This way can serve as a good alternative to numerical integration [3] (depending on the context and the application of course). Let us now show the relationship between this function and other standard special functions (integral of error function) [4] as error function and cumulative distribution function for normal distribution in the context of its use. Function (1) could be used to find values of complicated integral which are not available in any references of standard special functions and also it is not available to get their values in Wolfram Alpha, for example,

$$\int_0^{+\infty} e^{x^2(1-2\Phi(x\sqrt{2}))} dx, \tag{12}$$

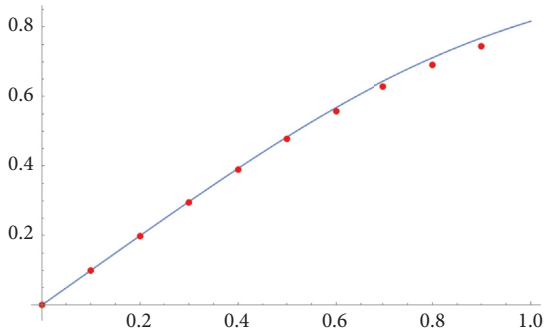

FIGURE 4: A simple explicit Euler scheme for the step size $h = 1/10$.

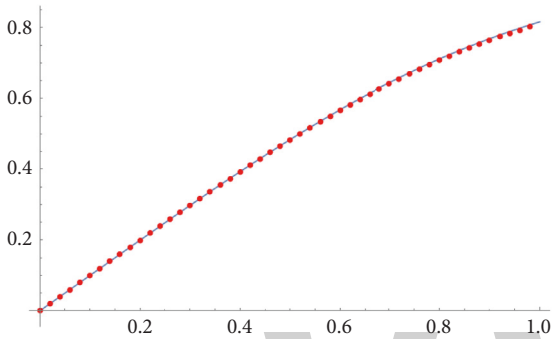

FIGURE 5: A simple explicit Euler scheme for the step size $h = 1/50$.

with $\Phi(x) = (1/\sqrt{2\pi})\int_{-\infty}^{x} e^{-z^2/2}dz$. It is CDF (cumulative distribution function for normal distribution); if someone was asked to find the value of this integral, he would be confused because it is very complicated; probably he cannot show whether it is convergent or not; even Wolfram Alpha as a best means of computation cannot recognize at a least that ϕ is a cumulative normal distribution, so no result would be obtained about the value of this integral. Let us compute (25) using (1) and we will conclude that they have the same value and both are identical function and identical integral.

The well-known formula which expresses the relationship between error function and cumulative density function, see ([2]), is defined as

$$\begin{aligned}\operatorname{Erf}(x) &= 2\left(\Phi\left(x\sqrt{2}\right) - \Phi(0)\right) = 2\left(\Phi\left(x\sqrt{2}\right) - \frac{1}{2}\right)\\ &= 2\Phi\left(x\sqrt{2}\right) - 1.\end{aligned} \tag{13}$$

And it is easy to check that it always holds for every real number by the following short proof.

Proof. By definition, the error function

$$\operatorname{Erf}(x) = \frac{2}{\sqrt{\pi}}\int_0^x e^{-t^2}dt. \tag{14}$$

Writing $t^2 = z^2/2$ implies $t = z/\sqrt{2}$ (because t is not negative), whence $dt = dz/\sqrt{2}$. The endpoints $t = 0$ and $t = x$ become $z = 0$ and $z = x\sqrt{2}$. To convert the resulting integral into something that looks like a cumulative distribution function (CDF), it must be expressed in terms of integrals that have lower limits of $-\infty$; thus

$$\begin{aligned}\operatorname{Erf}(x) &= \frac{2}{\sqrt{2\pi}}\int_0^{x\sqrt{2}} e^{-z^2/2}dz\\ &= 2\left(\frac{1}{\sqrt{2\pi}}\int_{-\infty}^{x\sqrt{2}} e^{-z^2/2}dz - \frac{1}{\sqrt{2\pi}}\int_{-\infty}^{0} e^{-z^2/2}dz\right).\end{aligned} \tag{15}$$

Those integrals on the right hand size are both values of the CDF of the standard normal distribution:

$$\Phi(x) = \frac{1}{\sqrt{2\pi}}\int_{-\infty}^{x} e^{-z^2/2}dz. \tag{16}$$

Specifically,

$$\begin{aligned}\operatorname{Erf}(x) &= 2\left(\Phi\left(x\sqrt{2}\right) - \Phi(0)\right) = 2\left(\Phi\left(x\sqrt{2}\right) - \frac{1}{2}\right)\\ &= 2\Phi\left(x\sqrt{2}\right) - 1.\end{aligned} \tag{17}$$

Now since the LHS of (18) has a known value which is $0.97210699\cdots$, then the right hand side also equals $0.97210699\cdots$; hence we came up with the following identity:

$$\int_0^a \left(e^{-x^2}\right)^{\operatorname{Erf}(x)} dx = \int_0^a e^{x^2(1-2\Phi(x\sqrt{2}))}dx. \tag{18}$$

Now we shall call the function defined in (1) $T(x) = \int_0^X (e^{-t^2})^{\operatorname{erf}(t)}dt$ since it does not refer to anyone and it has unknown analytic representation as elementary function using standard special functions and the RHS of (18) presents another representation of $T(x)$ function using CDF of the normal distribution. □

Lemma 1. *$T(x) = \int_0^X (e^{-t^2})^{\operatorname{erf}(t)}dt$ cannot be expressed in terms of elementary function.*

Proof. It is a theorem of Liouville [5], reproven later with purely algebraic methods, that for rational functions f and g, g is nonconstant, the antiderivative

$$\int [f(x)\exp(g(x))]\,dx \tag{19}$$

can be expressed in terms of elementary functions if and only if there exists some rational function h such that it is a solution to the differential equation:

$$f = h' + hg. \tag{20}$$

```
In[338]:=
α =
  (π^(1/6) Gamma[4/3] / 2^(1/3))^Hypergeometric1F1[0.5,1.5,-E^2 π] ;
β = NIntegrate[Exp[-x^2 Erf[x]], {x, 0, ∞}];
γ = α;
error = β - γ
Out[340]=
-0.0000616497
```

Figure 6: Error approximation for T(+∞).

Now if we apply Liouville theorem we can come up with the following ODE: $1 = h'(x) + h(x)(-x^2 \operatorname{erf}(x))$ with $g(x) = -x^2 \operatorname{erf}(x))$ and $f(x) = 1$. It is first ordinary differential equation. The computation we made with Wolfram Alpha gives the following solution:

$$\exp\left(\frac{e^{-x^2}\left(e^{x^2}\left(\sqrt{\pi}x^3 \operatorname{erf}(x)-1\right)+x^2+1\right)}{3\sqrt{\pi}}\right)\cdot\left(e^{1/3\sqrt{\pi}}\left(\int_1^x \exp\left(\frac{1}{3}\left(t^3(-\operatorname{erf}(t))-\frac{e^{-t^2}\left(t^2+1\right)}{\sqrt{\pi}}\right)\right)dt - \int_1^0 \exp\left(\frac{1}{3}\left(t^3(-\operatorname{erf}(t))-\frac{e^{-t^2}\left(t^2+1\right)}{\sqrt{\pi}}\right)\right)dt\right)+1\right) \quad (21)$$

with $h(0) = 1$. Really the function h can be written follows.

$$h(x) = l(x)\left[c_1 + \int_1^x l(-\xi)\,d\xi\right] \quad (22)$$

Now it is clear that $l(x)$ is a transcendental function and the defined integral in the right hand side of the $h(x)$ expression is also transcendental function because we have **derivatives of rational functions being rational functions. Therefore, if the antiderivative is rational, then the original function was rational.** The function h is rational only at $x = 0$, and since $h(x) \neq 0$, then the sum of two transcendental functions is always transcendental function. According to definition of the rational function, $h(x)$ cannot be called a rational function; then we are done. □

2. A Possible Approach Formula for $T(+\infty)$

We may give here a possible approach formula for T(+∞) which is defined as follows.

$$T(+\infty) = \int_0^{+\infty} \exp\left(-x^2 \operatorname{erf}(x)\right)dx = 0.97210699\cdots \quad (23)$$

The inverse symbolic calculator is unable to give us the representation of $0.97210699\cdots$ using standard special functions, but we have tried to give its representation using error function representation as hypergeometric function [6]; we have

$$\operatorname{erf}(x) = \frac{2}{\sqrt{\pi}}x1F1\left(\frac{1}{2};\frac{3}{2};-x^2\right) \quad (24)$$

with $1F1$ being the Kummer confluent hypergeometric function [6]. Now we have from (24) the following.

$$\int_0^{+\infty} \exp\left(-x^2 \operatorname{erf}(x)\right)dx = \int_0^{+\infty} \exp\left(-\frac{2}{\sqrt{\pi}}x^3\right)^{1F1(1/2;3/2;-x^2)}dx \quad (25)$$

The RHS of (25) using (24) gives $((\pi)^{1/6}\Gamma(4/3)/2^{1/3})^{1F1(0.5;1.5;-x^2)}$. Hence we may choose $x = e\sqrt{\pi}$ and we can get finally the following.

$$T(+\infty) \sim \frac{(\pi)^{1/6}\,\Gamma(4/3)}{2^{1/3}}^{1F1(0.5;1.5;-\pi e^2))} = 0.97216864\cdots \quad (26)$$

Mathematica gives the nice approximation of (25) as shown in Figure 6.

3. Series Representation of $T(x)$ Function

We may try to find a series expansion in powers of t of

$$I(t) = \int_0^t \exp\left(-x^2 \operatorname{erf}(x)\right)dx = \sum_{p=1}^{\infty} c_p t^p. \quad (27)$$

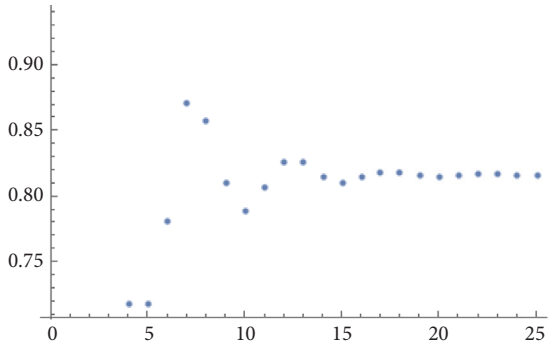

FIGURE 7: Convergence of $I_N = \sum_{p=0}^{N} c_p$ as a function of N up to $N = 25$.

The coefficients $c_p = p^{-1}d_{p-1}$ follow from the series expansion $e^{-x^2}\operatorname{erf} x = \sum_{p=0}^{\infty} d_p x^p$, resulting in

$$\begin{aligned} I(t) &= \sum_{p=1}^{\infty} c_p t^p \\ &= t - \frac{t^4}{2\sqrt{\pi}} + \frac{t^6}{9\sqrt{\pi}} + \frac{2t^7}{7\pi} - \frac{t^8}{40\sqrt{\pi}} - \frac{4t^9}{27\pi} \\ &\quad + \frac{(\pi - 28)\, t^{10}}{210\pi^{3/2}} + O\left(t^{11}\right). \end{aligned} \tag{28}$$

The series $I(1) = \sum_{p=1}^{\infty} c_p$ seems to converge. See Figure 7: The value of $I_{25} = 0.8162$ agrees with $I(1) = 0.816377$ to three decimal places. For $N = 50$ the agreement is up to six decimal places, but this did not give us the power series closed form for nth term. We should use some approximations using approximation of error function and Padé approximant as shown in the following sections.

4. Series Expansion of the n-th Derivative of $T(x) = \int_0^x e^{-\xi^2 erf(\xi)} d\xi$

Lemma 2. *Series expansion of* $T(x) = \int_0^x e^{-\xi^2 \operatorname{erf}(\xi)} d\xi$ *is defined by this identity:*

$$\begin{aligned} &\int_0^x e^{-\xi^2 \operatorname{erf}(\xi) d\xi} \\ &= \sum_{n=0}^{\infty} \lim_{\varepsilon -> 0} \left(\sum_{\substack{k_1 + 2k_2 + \cdots + nk_n = n \\ k_1 \geq 0, k_2 \geq 0, \ldots, k_n \geq 0}} \prod_{j=1}^{n} \frac{A_{j,\varepsilon}^{k_j}}{k_j!} \right) \frac{x^{n+1}}{n+1} \end{aligned} \tag{29}$$

where

$$\begin{aligned} A_{j,\epsilon} &= \frac{2(-1)^{(j-1)/2}}{(j-2)\left((1/2)(j-3)\right)!\sqrt{\pi}} \\ &\qquad \text{if } j \geq 3 \text{ and } j \text{ an odd integer;} \\ A_{j,\epsilon} &= \varepsilon \quad \text{otherwise } (0 < \varepsilon < 1) \end{aligned} \tag{30}$$

which is the key idea to get.

Proof. Suppose that we have the Taylor expansions:

$$f(x) = \sum_{n=1}^{\infty} \frac{a_n}{n!} x^n \tag{31}$$

and

$$g(x) = \sum_{n=1}^{\infty} \frac{b_n}{n!} x^n. \tag{32}$$

Then we have the standard result:

$$g(f(x)) = \sum_{n=1}^{\infty} \left(\sum_{k=1}^{n} b_k B_{n,k}(a_1, \ldots, a_{n-k+1}) \right) \frac{x^n}{n!} \tag{33}$$

where $B_{n,k}(\cdot)$ are the partial Bell polynomials, which are defined by the following formula.

$$\begin{aligned} &\widehat{B}_{m,j}\left(x_1, x_2, \ldots, x_{m-j+1}\right) \\ &= \sum_{\substack{k_0 + k_1 + \cdots + k_N = j \\ k_1 + 2k_2 + \cdots + Nk_N = m}} \binom{j}{k_0, k_1, \ldots, k_N} \prod_{i=1}^{N} x_i^{k_i} \end{aligned} \tag{34}$$

The key idea to get series expansion of the n-th derivative of $T(x)$ which is defined in (29) is to use Taylor expansion of $g(x) = \exp(-x)$ and $f(x) = -x^2 \operatorname{erf}(x)$ coming up for using one of the important formulas in mathematics called Bruno-Fadi formula such as that defined above in (33) using (34). It is well known that the Taylor expansion of $\exp(-x)$ is given by the following.

$$g(x) = \exp(-x) = \sum_{n=0}^{\infty} \frac{(-1)^n x^n}{n!} \tag{35}$$

Probably the interesting here for readers to know is Taylor expansion of $\operatorname{erf}(x)$; we give a simple proof about its expansion series using Hermite polynomial. □

Lemma 3. *Taylor expansion of* $\operatorname{erf}(x)$ *at each point a is given by this identity:*

$$\operatorname{erf}_a(x) = e^{-a^2} \sum_{n=0}^{\infty} (-1)^n \frac{H_n(a)}{n!} (x-a)^n \tag{36}$$

with $H_n(a)$ *is Hermite polynomial of degree n.*

Proof. $f^{(n)}(a)$ can be written in terms of Hermite polynomials H_n.

$$\begin{aligned} H_0(x) &= 1, \\ H_1(x) &= 2x, \\ H_2(x) &= 4x^2 - 2, \\ H_3(x) &= 8x^3 - 12x, \\ H_4(x) &= 16x^4 - 48x^2 + 12, \\ H_5(x) &= \cdots \end{aligned} \tag{37}$$

We may recognize that $H_{2n-1}(0) = 0$, which gives the power series for e^{-x^2} at $a = 0$.

$$e^{-x^2} = 1 - \frac{2}{2!}x^2 + \frac{12}{4!}x^4 - \frac{120}{6!}x^6 + \cdots \tag{38}$$

After multiplying by $2/\sqrt{\pi}$, this integrates to

$$\operatorname{erf}(z) = \frac{2}{\sqrt{\pi}}\left(z - \frac{z^3}{3} + \frac{z^5}{10} - \frac{z^7}{42} + \frac{z^9}{216} - \cdots\right). \tag{39}$$

Since $(d^n/dx^n)e^{-x^2} = (-1)^n e^{-x^2} H_n(x)$, one can do a Taylor Series for every a.

$$\operatorname{erf}_a(x) = e^{-a^2}\sum_{n=0}^{\infty}(-1)^n \frac{H_n(a)}{n!}(x-a)^n \tag{40}$$

Then we are done.

Now by composition of (40) with (35) after multiplying (40) by the term $-x^2$, we come up to Bruno-Fadi formula which is defined as

$$e^{-x^2\operatorname{erf}(x)}\sum_{n=0}^{\infty}\lim_{\varepsilon->0}\left(\sum_{\substack{k_1+2k_2+\cdots+nk_n=n \\ k_1\geq 0,k_2\geq 0,\ldots,k_n\geq 0}}\prod_{j=1}^{n}\frac{A_{j,\varepsilon}^{k_j}}{k_j!}\right)x^n, \tag{41}$$

where

$$A_{j,\varepsilon} = \frac{2(-1)^{(j-1)/2}}{(j-2)((1/2)(j-3))!\sqrt{\pi}} \tag{42}$$

if $j \geq 3$ and j an odd integer;

$$A_{j,\varepsilon} = \varepsilon \quad \text{otherwise } (0 < \varepsilon < 1). \tag{43}$$

Integrating this equation term by term gives

$$\begin{aligned} &\int_0^x e^{-\xi^2\operatorname{erf}(\xi)}d\xi \\ &= \sum_{n=0}^{\infty}\lim_{\varepsilon->0}\left(\sum_{\substack{k_1+2k_2+\cdots+nk_n=n \\ k_1\geq 0,k_2\geq 0,\ldots,k_n\geq 0}}\prod_{j=1}^{n}\frac{A_{j,\varepsilon}^{k_j}}{k_j!}\right)\frac{x^{n+1}}{n+1} \end{aligned} \tag{44}$$

which gives the series expansion for the new special function. Using Mathematica as a shortcut, it shows that (44) holds and also it shows the incrementation of π as shown in Figure 8. We may add also the series expansion of $T(x)$, the new special function, using Mathematica code as shown in Figure 9. □

```
In[70]:= Clear[m];
jthderivative[i_] := If[IntegerQ[1/2 (i - 3)] && i ≥ 3,
  (2 (-1)^(1/2 (i-1)) i!)/((i - 2) Sqrt[π] (1/2 (i - 3))!), 0];
TableForm[Join[{{j, "d^j/dx^j (-x^2 erf(x))"}},
  Table[{j, jthderivative[j]}, {j, 1, 10}]], TableAlignments → Center] //
 TraditionalForm
```

Out[72]//TraditionalForm=

j	$\frac{d^j}{dx^j}(-x^2\operatorname{erf}(x))$
1	0
2	0
3	$-\frac{12}{\sqrt{\pi}}$
4	0
5	$\frac{80}{\sqrt{\pi}}$
6	0
7	$-\frac{1008}{\sqrt{\pi}}$
8	0
9	$\frac{17280}{\sqrt{\pi}}$
10	0

FIGURE 8: n-th derivative of new special function $T(x)$.

```
In[140]:= Clear[x];
{Sum[coeff[j] * x^j, {j, 0, 12}],
  Normal[Series[Exp[-x^2 Erf[x]], {x, 0, 12}]]} // Simplify
```

Out[140]=

$$\left\{\frac{1}{3780\pi^2}\left(3780\pi^2 + 2520x^{12} + 5040\sqrt{\pi}\,x^9(-1+x^2) - 24\pi x^6(-315 + 210x^2 - 98x^4 + 36x^6) + \pi^{3/2}x^3(-7560 + 2520x^2 - 756x^4 + 180x^6 - 35x^8)\right),\right.$$
$$\left.\frac{1}{3780\pi^2}\left(3780\pi^2 + 2520x^{12} + 5040\sqrt{\pi}\,x^9(-1+x^2) - 24\pi x^6(-315 + 210x^2 - 98x^4 + 36x^6) + \pi^{3/2}x^3(-7560 + 2520x^2 - 756x^4 + 180x^6 - 35x^8)\right)\right\}$$

FIGURE 9: Series expansion of new special function $T(x)$ around $x = 0$.

5. Series Representation of $\int_{-1}^{1} erf(x)^n dx$ Using Error Function Approximation

We have the power series of

$$e^{-x^2\operatorname{erf}(x)} = \sum_{k=0}^{\infty}\frac{(-1)^k x^{2k}\operatorname{erf}^k(x)}{k!} \tag{45}$$

and then from (45) we have the following.

$$\int_{-1}^{1} e^{-x^2\operatorname{erf}(x)}dx = \sum_{k=0}^{\infty}\frac{(-1)^k}{k!}\int_{-1}^{1} x^{2k}\operatorname{erf}^k(x)\,dx \tag{46}$$

Now it is hard so much to evaluate the integral in RHS of (46) using error function expression; then we should use the following nice approximation.

$$(\operatorname{erf}(x))^2 \approx 1 - e^{-ax^2} \quad \text{with } a = (1+\pi)^{2/3}\log^2(2) \tag{47}$$

Here we can give a short proof to show that the error function squared was approximated as well with the value of $a = (1+\pi)^{2/3}\log^2(2)$.

Proof. We fully agree that

$$F(a) = \int_0^{\infty} \left(\operatorname{erf}(x)^2 - \left(1 - e^{-ax^2}\right) dx\right)^2 \tag{48}$$

is minimum for $a \approx 1.23907$. According to *RIES*, this number seems to be much closer to

$$a = (1+\pi)^{2/3} \log^2(2) \approx 1.23907 \tag{49}$$

than to $\pi^2/8 \approx 1.23370$ even if this does make very large difference (the maximum error is reduced from 0.006 to 0.004 and the value of the integral $F(a)$ changes from 0.00002769 to 0.00002572). If we look for a still better approximation, we could consider $\log(1 - \operatorname{erf}(x)^2)$ (which, for sure, introduces a bias in the problem), establish a Padé approximant, and finally arrive to

$$\operatorname{erf}(x)^2 \approx 1 - \exp\left(-\frac{4}{\pi}\frac{1+\alpha x^2}{1+\beta x^2}x^2\right) \tag{50}$$

where

$$\begin{aligned} \alpha &= \frac{10-\pi^2}{5(\pi-3)\pi} \\ \beta &= \frac{120-60\pi+7\pi^2}{15(\pi-3)\pi}. \end{aligned} \tag{51}$$

The value of the corresponding error function is 1.1568×10^{-7}, that is to say, almost 250 times smaller than that with the initial formulation; the maximum error is 0.00035.

Now we are ready to approximate

$$I_n = \int_{-1}^{1} (\operatorname{erf}(x))^{2n} dx \tag{52}$$

$$J_n = \int_{-1}^{1} \left(1 - e^{-ax^2}\right)^n dx \tag{53}$$

for which the binomial expansion would be required (easy). This would give you things like the following.

$$J_1 = 2 - \frac{\sqrt{\pi}\operatorname{erf}\left(\sqrt{a}\right)}{\sqrt{a}} \tag{54}$$

$$J_2 = 2 - \frac{2\sqrt{\pi}\operatorname{erf}\left(\sqrt{a}\right)}{\sqrt{a}} + \frac{\sqrt{\pi/2}\operatorname{erf}\left(\sqrt{2a}\right)}{\sqrt{a}} \tag{55}$$

$$\begin{aligned} J_3 = 2 &- \frac{3\sqrt{\pi}\operatorname{erf}\left(\sqrt{a}\right)}{\sqrt{a}} + \frac{3\sqrt{\pi/2}\operatorname{erf}\left(\sqrt{2a}\right)}{\sqrt{a}} \\ &- \frac{\sqrt{\pi/3}\operatorname{erf}\left(\sqrt{3a}\right)}{\sqrt{a}} \end{aligned} \tag{56}$$

Now it is easy to get recurrence relation for J_n in (53); we take $t = \sqrt{ak}x \Longrightarrow dx = dt/(\sqrt{ak})$ and we come up to $\operatorname{erf}(\sqrt{ak})$ which gives the following general formula.

$$J_n = 2 + \sqrt{\frac{\pi}{a}} \sum_{k=1}^{n} (-1)^k \frac{\binom{n}{k}}{\sqrt{k}} \operatorname{erf}\left(\sqrt{ak}\right) \tag{57}$$

Table 1: Short table for approximation comparison.

n	approximation	exact
1	0.591506	0.596751
2	0.279674	0.283168
3	0.151067	0.153256
4	0.0870954	0.0884650
5	0.0522216	0.0530855
6	0.0321485	0.0326982
7	0.0201718	0.0205243
8	0.0128409	0.0130686
9	0.00826756	0.00841548
10	0.00537202	0.00546863

We produce in Table 1 a short table for comparison; we reused for this problem our approach with the same Padé approximants and obtained the following as approximations.

$$I_n = \frac{2}{2n+1}\left(\frac{4}{\pi}\right)^n {}_2F_1\left(2n, \frac{2n+1}{2}; \frac{2n+3}{2}; -\frac{1}{3}\right) \tag{58}$$

$$\begin{aligned} I_n = &\frac{2}{2n+1}\left(\frac{4}{\pi}\right)^n \\ &\cdot F_1\left(\frac{2n+1}{2}; -2n, 2n; \frac{2n+3}{2}; \frac{1}{30}, -\frac{3}{10}\right) \end{aligned} \tag{59}$$

Really we are ready to give the series representation of $T(x)$ over $[-1;1]$ using error function approximation and Padé approximant. □

6. Series Representation of $T(x)$ Function over $[-1;1]$ Using Error Function Approximation and Padé Approximant

Recall

$$I_k = \int_{-1}^{1} x^{2k} [\operatorname{erf}(x)]^k dx \tag{60}$$

is 0 if k is odd. Thus, we need to focus on

$$I_{2k} = \int_{-1}^{1} x^{4k} [\operatorname{erf}(x)]^{2k} dx \tag{61}$$

which could be approximated, as we showed above in Section 3 to get (57) using

$$[\operatorname{erf}(x)]^2 \approx 1 - e^{-ax^2} \quad \text{with } a = (1+\pi)^{2/3}\log^2(2) \tag{62}$$

making

$$I_{2k} = \int_{-1}^{1} x^{4k}\left(1 - e^{-ax^2}\right)^k dx \tag{63}$$

to be developed using the binomial expansion. Therefore, in practice, we face the problem of

$$J_{n,k} = \int_{-1}^{1} x^{4k} e^{-nax^2} dx \tag{64}$$

Table 2: Reasonable approximation using bounds.

k	approximation	exact
1	0.22870436048	0.22959937502
2	0.08960938943	0.08997882179
3	0.04400808083	0.04418398568
4	0.02389675159	0.02398719298
5	0.01374034121	0.01378897319
6	0.00819869354	0.00822557475
7	0.00502074798	0.00503586007
8	0.00313428854	0.00314286515
9	0.00198581489	0.00199069974
10	0.00127304507	0.00127582211

and the antiderivative

$$\int x^{4k} e^{-nax^2}\,dx = -\frac{1}{2}x^{4k+1}E_{1/2-2k}\left(anx^2\right) \tag{65}$$

where the exponential integral function appears. Using the bounds, this reduces to

$$J_{n,k} = -E_{1/2-2k}\,(an) \tag{66}$$

and leads to "reasonable" approximation as shown in Table 2. Another approximation could be obtained using the simplest Padé approximant [7] of the error function

$$\operatorname{erf}(x) = \frac{2x}{\sqrt{\pi}\left(1 + x^2/3\right)} \tag{67}$$

which would lead to

$$\begin{aligned} I_{2k} &= \int_{-1}^{1} x^{4k}\left[\operatorname{erf}(x)\right]^{2k} dx \\ &= \frac{2}{6k+1}\left(\frac{4}{\pi}\right)^{k} {}_2F_1\left(2k, \frac{6k+1}{2}; \frac{6k+3}{2}; -\frac{1}{3}\right) \end{aligned} \tag{68}$$

slightly less accurate than the previous one. Continuing with Padé approximant

$$\operatorname{erf}(x) = \frac{2x/\sqrt{\pi} - x^3/15\sqrt{\pi}}{1 + 3x^2/10} \tag{69}$$

we should get

$$\begin{aligned} I_{2k} = \int_{-1}^{1} x^{4k}\left[\operatorname{erf}(x)\right]^{2k} dx &= \frac{2}{6k+1}\left(\frac{4}{\pi}\right)^{k} \\ &\cdot F_1\left(\frac{6k+1}{2}; -2k, 2k; \frac{6k+3}{2}; \frac{1}{30}, -\frac{3}{10}\right) \end{aligned} \tag{70}$$

where the Appell hypergeometric function of two variables appears. Finally we conclude the series representation as follows.

$$I(t) = \int_{-1}^{1} \exp\left(-x^2 \operatorname{erf}(x)\right) dx. \sim \sum_{k=0}^{+\infty} \frac{(-1)^k}{k!} I_{2k} \tag{71}$$

7. Approximation of $T(x)$ Function by Means of a Polynomial

Lemma 4. *The function f which is defined as*

$$f(x) = T\left(\frac{b+a}{2} + \frac{b-a}{2}x\right), \quad -1 \le x \le 1 \tag{72}$$

could be approximated by means of Chebytchev polynomial.

Proof. We may approximate the function f on the interval $[-1, 1]$ by using Chèbyshev polynomials [8] of the first kind. To this end, we choose some positive integer n and we define the coefficients c_n by the formula

$$c_j = \frac{2}{\pi}\int_{-1}^{1} \frac{T_j(x)}{\sqrt{1-x^2}} f(x)\,dx \quad \text{for } j = 0, 1, \ldots, n. \tag{73}$$

Then the polynomial

$$P_n(x) = \frac{1}{2}c_0 + \sum_{j=1}^{n} c_j T_j(x) \tag{74}$$

approximates $f(x)$ in the best possible way. Since

$$T(x) = f\left(\frac{a+b-2x}{a-b}\right) \quad \text{for } a \le x \le b \tag{75}$$

we see that the polynomial $Q_n(a, b, x) = P_n((a+b-2x)/(a-b))$ is an approximant to $T(x)$ function on $[a, b]$. Calculations give

$$\begin{aligned} Q_{11}\left(0, \frac{3}{2}, x\right) = {} & 0.0137936039435x^{11} \\ & - 0.135129528505x^{10} \\ & + 0.548169602543x^{9} \\ & - 1.16161653976x^{8} \\ & + 1.31691631085x^{7} \\ & - 0.746480407376x^{6} \\ & + 0.338453415662x^{5} \\ & - 0.370071852413x^{4} \\ & + 0.0133517048763x^{3} \\ & - 0.00104123958376x^{2} \\ & + 1.00003172454x \end{aligned} \tag{76}$$

and

$$\begin{aligned} Q_{11}\left(\frac{3}{2},3,x\right) = {} & -0.0000675632422240x^{11} \\ & + 0.00188305739843x^{10} \\ & - 0.0239397852528x^{9} \\ & + 0.183255163671x^{8} \\ & - 0.937675010268x^{7} \\ & + 3.35913844398x^{6} \\ & - 8.55140470408x^{5} \\ & + 15.3046428836x^{4} \\ & - 18.4622672665x^{3} \\ & + 13.5920479951x^{2} \\ & - 4.69093970289x \\ & + 1.04191571066. \end{aligned} \tag{77}$$

For both approximations the error is less than 10^{-6}. Indeed, numerical integration gives

$$\begin{aligned} &\left\| T(x) - Q_{11}\left(0,\frac{3}{2},x\right)\right\| \\ &= \sqrt{\int_0^{3/2}\left(T(x) - Q_{11}\left(0,\frac{3}{2},x\right)\right)^2 dx} \\ &\approx 2.26\times 10^{-7} \end{aligned} \tag{78}$$

and

$$\begin{aligned} &\left\| T(x) - Q_{11}\left(\frac{3}{2},3,x\right)\right\| \\ &= \sqrt{\int_{3/2}^{3}\left(T(x) - Q_{11}\left(\frac{3}{2},3,x\right)\right)^2 dx} \\ &\approx 3.66\times 10^{-10}. \end{aligned} \tag{79}$$

Thus, we may evaluate the $T(x)$ function with high accuracy on the interval $[0,3]$. For $x > 3$ we may use the following approximation formula in terms of the error function:

$$\begin{aligned} T(x) &\approx \varphi(x) \\ &\overset{def}{=\!=} \int_0^3 \exp\left(-t^2\operatorname{erf}(t)\right)dt + \frac{\sqrt{\pi}}{2}\left(\operatorname{erf}(x) - \operatorname{erf}(3)\right), \quad x \geq 3. \end{aligned} \tag{80}$$

The quadratic mean error on $[3,100]$ is

$$\begin{aligned} \left\| T(x) - \varphi(x)\ \right\| &= \sqrt{\int_3^{100}\left(T(x) - \varphi(x)\right)^2 dx} \\ &\approx 2.02\times 10^{-8}. \end{aligned} \tag{81}$$

Now we are ready to present application of $T(x)$ in probability and thermodynamics using one of the most important distributions which is called Maxwell–Boltzmann distribution □

8. Application of $T(x)$ in Probability

Let

$$F_{\lambda,\mu}(x) = \int_0^x e^{-\xi^2(\lambda+\mu\operatorname{erf}(\xi))}d\xi \quad (\lambda > 0). \tag{82}$$

Define

$$c = \int_0^\infty e^{-\xi^2(\lambda+\mu\operatorname{erf}(\xi))}d\xi \tag{83}$$

and let

$$T_{\lambda,\mu}(x) \coloneqq c^{-1}F_{\lambda,\mu}(x) \quad (x \geq 0). \tag{84}$$

The function $T(x)$ is the new special function we have studied in this paper. This function defines a cumulative probability distribution function (CDF) with probability distribution function (PDF).

$$f_{\lambda,\mu}(x) = e^{-x^2(\lambda+\mu\operatorname{erf}(x))} \quad (x \geq 0) \tag{85}$$

Indeed, we have

$$\begin{aligned} T'_{\lambda,\mu}(x) &= e^{-x^2(\lambda+\mu\operatorname{erf}(x))} > 0, \\ T_{\lambda,\mu}(+\infty) &= 1. \end{aligned} \tag{86}$$

The ODE for this function not involving the error function erf may be obtained by differentiating (84) twice and eliminating the expression containing that error function. This gives us the following ODE.

$$\sqrt{\pi}xy''(x) = 2e^{-x^2}y'(x)\left(\sqrt{\pi}e^{x^2}\log\left(y'(x)\right) - \mu x^3\right) \tag{87}$$

Letting $\mu = 0$ gives the ODE

$$xy''(x) = 2y'(x)\log\left(y'(x)\right) \tag{88}$$

whose general solution is as follows.

$$y(x) = \frac{1}{2}e^{-c_1/2}\sqrt{\pi}\operatorname{erfi}\left(e^{c_1/2}x\right) + c_2 \tag{89}$$

If we compare (89) with

$$\begin{aligned} c\,F_{\lambda,0}(x) &= c\int_0^x e^{-\lambda\xi^2}d\xi \\ &= \left(\int_0^\infty e^{-\lambda\xi^2}d\xi\right)^{-1}\int_0^x e^{-\lambda\xi^2}d\xi = \operatorname{erf}\left(\sqrt{\lambda}x\right) \end{aligned} \tag{90}$$

we must have

$$\frac{1}{2}e^{-c_1/2}\sqrt{\pi}\operatorname{erfi}\left(e^{c_1/2}x\right) + c_2 = \operatorname{erf}\left(\sqrt{\lambda}x\right) \tag{91}$$

so that

$$c_1 = i\pi + \log\left(\frac{\pi}{4}\right), \qquad c_2 = 0. \tag{92}$$

We showed that in the case when $\mu = 0$ our function $T_{\lambda,0}(x)$ coincides with the error function $\operatorname{erf}(\sqrt{\lambda}x)$ with the value $\lambda = \pi/4$. When $\mu \neq 0$ we cannot obtain the solution to the ODE (87) in closed form. We may try a numerical procedure or another method to solve it. Our aim is to show how we may apply the new special function $T_{\lambda,\mu}(x)$ in probability and physics.

8.1. Example. We look for λ and μ in order to adjust the error function by means of the function $y(x) = T_{\lambda,\mu}(x)$. To this end, we impose the following conditions.

$$\operatorname{erf}(1) = T_{\lambda,\mu}(x), \qquad \operatorname{erf}'(1) = T'_{\lambda,\mu}(1) \tag{93}$$

Solving this system gives

$$\lambda = 0.1671645, \qquad \mu = 0.8449657. \tag{94}$$

The function $T_{\lambda,\mu}(x)$ converts into

$$T_{\lambda,\mu}(x) = 1.05021 \int_0^x \exp\left(-\xi^2 \left(0.167164 + 0.844966 \operatorname{erf}(\xi)\right)\right) d\xi. \tag{95}$$

Plotting the two functions gives following picture as shown in Figure 10

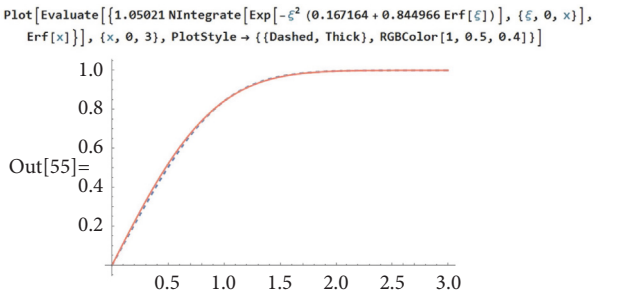

FIGURE 10: Adjusting the error function by means of the new special function.

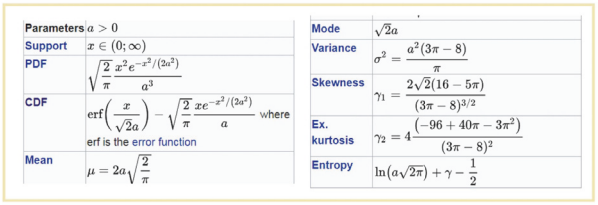

FIGURE 11: Maxwell–Boltzmann distribution.

9. Application of $T(x)$ in Thermodynamics

In physics (in particular in statistical mechanics), the Maxwell–Boltzmann distribution is a particular probability distribution named after James Clerk Maxwell and Ludwig Boltzmann. It was first defined and used for describing particle speeds in idealized gases, where the particles move freely inside a stationary container without interacting with one another, except for very brief collisions in which they exchange energy and momentum with each other or with their thermal environment. The term "particle" in this context refers to gaseous particles (atoms or molecules), and the system of particles is assumed to have reached thermodynamic equilibrium. The energies of such particles follow what is known as Maxwell–Boltzmann statistics, and the statistical distribution of speeds is derived by equating particle energies with kinetic energy. Mathematically, the Maxwell–Boltzmann distribution is the chi distribution with three degrees of freedom (the components of the velocity vector in Euclidean space), with a scale parameter measuring speeds in units proportional to the square root of T/m (the ratio of temperature and particle mass); see Figure 10. The CDF for the Boltzmann distribution may be approximated by means of the new special function $T_{\kappa,\mu}(x)$ as follows:

$$\operatorname{erf}\left(\frac{x}{\sqrt{2}a}\right) - \sqrt{\frac{2}{\pi}}\frac{x}{a}\exp\left(-\frac{x^2}{2a^2}\right) \approx T_{\lambda,\mu}(x) - \sqrt{\frac{2}{\pi}}\frac{x}{a}\exp\left(-\frac{x^2}{2a^2}\right), \tag{96}$$

where $T_{\lambda,\mu}(x)$ is an approximation to $\operatorname{erf}(x/\sqrt{2}a)$ for some parameters λ and μ depending on a. This approximation may be obtained in a similar way to what we illustrated in Example 1, Figure 11. On the other hand, in the case when $0 < a \leq 1$ we may approximate the CDF for the Maxwell–Boltzmann distribution as shown in Figure 12 for the value $a = 0.75$.

Finally this approximation by new special function showed that it may also be applied in thermodynamics to evaluate the average energy per particle in the circumstance where there is no energy-dependent density of states to skew the distribution, and the representation of probability for a given energy must be normalized to a probability of 1 which holds using our new special function with two parameters as shown in (86).

10. Conclusion

We have studied A new probability distribution defined on $[0, +\infty)$ and we gave series representations for $T(x)$ function using Padé approximant. Really we approximated the CDF for that distribution by means of Chèbyshev polynomials and the error function. The methods we applied are suitable for approximating other CDF for probability distributions, since their CDF are bounded and they take values from 0 to 1. And it is well known that Chèbyshev polynomials are the optimal

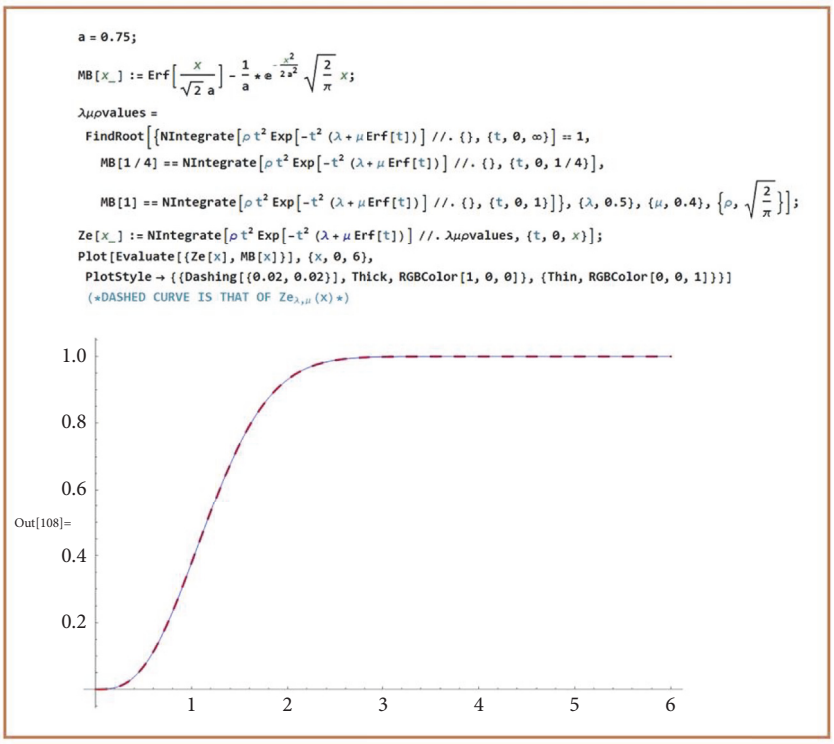

Figure 12: Approximation of the CDF for the Maxwell–Boltzmann distribution for $a = 0.75$.

ones for approximating continuous functions. On the other hand, it is also possible to approximate such functions by means of rational Chèbyshev approximants. This technique may be used in future works.

Disclosure

Zeraoulia Rafik present address is Department of Mathematics, High school-Timgad, Batna, Algeria.

Conflicts of Interest

There are no conflicts of interest regarding the publication of this paper.

Authors' Contributions

Zeraoulia Rafik, Alvaro H. Salas, and David L. Ocampo are equally contributing authors.

Acknowledgments

Alvaro H. Salas, Universidad Nacional de Colombia, Colombia, has received the Grant/Award Number 283, http://agenciadenoticias.unal.edu.co/detalle/article/profesor-de-la-un-gano-premio-scopus-en-el-area-de-matematicas.html. We would like to express our deep gratitude to Professor **David L. Ocampo** for improving the quality of the paper. My great salutation to Professor **Alvaro H. Salas** and to my parents and all my great salutations to my wife and to my second heart my son **Taha Abd-Aldjalil**. We would also like to thank **Yuriy S and Claude Leibovici** from Stack Exchange Math and **Prof. Carlo Beenakker** from MathOverflow for their contributions to the paper.

Endnotes

1. In mathematics, the error function (also called the Gauss error function) is a special function (nonelementary) of sigmoid shape that occurs in probability, statistics, and partial differential equations describing diffusion. It is defined as $\mathrm{Erf}(x) = (2/\sqrt{\pi}) \int_0^x e^{-t^2} dt$. Of course, it is closely related to the normal CDF $\Phi(x) = P(N < x) = (1/\sqrt{2\pi}) \int_{-\infty}^x e^{-t^2/2} dt$ (where $N \sim N(0,1)$ is a standard normal) by the expression $\mathrm{Erf} = 2\Phi(x\sqrt{2}) - 1$.
2. Cumulative distribution function for the normal distribution. In probability theory and statistics, the cumulative distribution function (CDF, also cumulative density

function) of a real-valued random variable X, or just distribution function of X, evaluated at x, is the probability that X will take a value less than or equal to x.If we have a quantity A that takes some value at random, the cumulative density function $F(x)$ gives the probability that X is less than or equal to x; that is,

$$F(x) = P(A \leq x) \qquad (*)$$

In the case of a continuous distribution, it gives the area under the probability density function from minus infinity to x. Cumulative distribution functions are also used to specify the distribution of multivariate random variables.

References

[1] J. L. Teugels and B. Sundt, *Encyclopedia of Actuarial Science*, vol. 1, Wiley, 2004.

[2] N. Mai-Duy and T. Tran-Cong, "Approximation of function and its derivatives using radial basis function networks," *Applied Mathematical Modelling*, vol. 27, no. 3, pp. 197–220, 2003.

[3] T. Suzuki and T. Suzuki, "Numerical integration error method for zeros of analytic functions," *Journal of Computational and Applied Mathematics*, vol. 152, no. 1-2, pp. 493–505, 2003.

[4] E. W. Ng and M. Geller, "A table of integrals of the error functions," *Journal of Research of the National Bureau of Standards*, vol. 73B, pp. 1–20, 1969.

[5] J. Liouville, "Suite du Mémoire sur la classification des Transcendantes, et sur l'impossibilité d'exprimer les racines de certaines équations en fonction finie explicite des coefficients," *Journal de Mathématiques Pures et Appliquées*, vol. 3, pp. 523–546, 1838.

[6] https://arxiv.org/pdf/1702.08438.pdf.

[7] A. Khani and S. Shahmorad, "An operational approach with Pade approximant for the numerical solution of non-linear Fredholm integro-differential equations," *Scientia Iranica*, vol. 19, no. 6, pp. 1691–1698, 2012.

[8] H. N. Soloklo and M. M. Farsangi, "Chebyshev rational functions approximation for model order reduction using harmony search," *Scientia Iranica*, vol. 20, no. 3, pp. 771–777, 2013.

6

Asymptotic Theory in Model Diagnostic for General Multivariate Spatial Regression

Wayan Somayasa,[1] Gusti N. Adhi Wibawa,[1] La Hamimu,[2] and La Ode Ngkoimani[2]

[1]*Department of Mathematics, Haluoleo University, Kendari, Indonesia*
[2]*Department of Geological Engineering, Haluoleo University, Kendari, Indonesia*

Correspondence should be addressed to Wayan Somayasa; wayan.somayasa@uho.ac.id

Academic Editor: Andrei I. Volodin

We establish an asymptotic approach for checking the appropriateness of an assumed multivariate spatial regression model by considering the set-indexed partial sums process of the least squares residuals of the vector of observations. In this work, we assume that the components of the observation, whose mean is generated by a certain basis, are correlated. By this reason we need more effort in deriving the results. To get the limit process we apply the multivariate analog of the well-known Prohorov's theorem. To test the hypothesis we define tests which are given by Kolmogorov-Smirnov (KS) and Cramér-von Mises (CvM) functionals of the partial sums processes. The calibration of the probability distribution of the tests is conducted by proposing bootstrap resampling technique based on the residuals. We studied the finite sample size performance of the KS and CvM tests by simulation. The application of the proposed test procedure to real data is also discussed.

1. Introduction

As mentioned in the literatures of model checks for multivariate regression, the appropriateness of an assumed model is mostly verified by analyzing the least squares residual of the observations; see, for example, Zellner [1], Christensen [2], pp. 1–22, Anderson [3], pp. 187–191, and Johnson and Wichern [4], pp. 395–398. A common feature of these works is the comparison between the length of the matrix of the residuals under the null hypothesis and that of the residuals under a proposed alternative.

Instead of considering the residuals directly MacNeill [5] and MacNeill [6] proposed a method in model check for univariate polynomial regression based on the partial sums process of the residuals. These popular approaches are generalized to the spatial case by MacNeill and Jandhyala [7] for ordinary partial sums and Xie and MacNeill [8] for set-indexed partial sums process of the residuals. Bischoff and Somayasa [9] and Somayasa et al. [10] derived the limit process in the spatial case by a geometric method generalizing a univariate approach due to Bischoff [11] and Bischoff [12]. These results can be used to establish asymptotic test of Cramér-von Mises and Kolmogorov-Smirnov type for model checks and change-point problems. Model checks for univariate regression with random design using the empirical process of the explanatory variable marked by the residuals was established in Stute [13] and Stute et al. [14]. In the papers mentioned above the limit processes were explicitly expressed as complicated functions of the univariate Brownian motion (sheet).

The purpose of the present article is to study the application of set-indexed partial sums technique to simultaneously check the goodness-of-fit of a multivariate spatial linear regression defined on high-dimensional compact rectangle. In contrast to the normal multivariate model studied in the standard literatures such as in Christensen [2], Anderson [3], and Johnson and Wichern [4] or in the references of model selection such as in Bedrick and Tsai [15] and Fujikoshi and Satoh [16], in this paper we will consider a multivariate regression model in which the components of the mean of the response vector are assumed to lie in different spaces and the underlying distribution model of the vector of random errors is unknown.

To see the problem in more detail let $n_1 \geq 1, \ldots, n_d \geq 1$ be fixed. Let a p-dimensional random vector $\mathbf{Z} \coloneqq (Z_i)_{i=1}^p$ be observed independently over an experimental design given by a regular lattice:

$$\Xi_{n_1 \cdots n_d} \coloneqq \left\{ \left(\frac{j_k}{n_k} \right)_{k=1}^d \in \mathbf{I}^d : 1 \leq j_k \leq n_k,\ k = 1, \ldots, d \right\}, \tag{1}$$

where $\mathbf{I}^d \coloneqq \prod_{k=1}^d [0,1]$ is the d-dimensional unit cube. Let $\mathbf{g} \coloneqq (g_i)_{i=1}^p$ be the true but unknown $\mathbb{R}^p$-valued regression function on $\mathbf{I}^d$ which represents the mean function of the observations. Let $\mathbf{Z}_{j_1 \cdots j_d} \coloneqq (Z_{i,j_1 \cdots j_d})_{i=1}^p$ and $\mathbf{g} \coloneqq (g_{i,j_1 \cdots j_d})_{i=1}^p$ be the observation and the corresponding mean in the experimental condition $(j_k/n_k)_{k=1}^d$. Under the null hypothesis H_0 we assume that $\mathbf{Z}_{j_1 \cdots j_d}$ follows a multivariate linear model. That is, we assume a model

$$H_0 : \mathbf{Z}_{j_1 \cdots j_d} = \left(\sum_{w=1}^{d_i} \beta_{iw} f_{iw} \left(\frac{j_k}{n_k} \right)_{k=1}^d \right)_{i=1}^p + \mathscr{E}_{j_1 \cdots j_d}, \quad 1 \leq j_1 \leq n_1, \ldots, 1 \leq j_d \leq n_d, \tag{2}$$

where, for $i = 1, \ldots, p$, $\beta_i \coloneqq (\beta_{iw})_{w=1}^{d_i} \in \mathbb{R}^{d_i}$ is a d_i-dimensional vector of unknown parameters; $\mathbf{f}_i \coloneqq (f_{iw})_{w=1}^{d_i}$ is a d_i-dimensional vector of known regression functions whose components are assumed to be square integrable with respect to the Lebesgue measure $\lambda_{\mathbf{I}}^d$ on $\mathbf{I}^d$, that is, $f_{iw} \in L_2(\lambda_{\mathbf{I}}^d)$, for all i and w. $\mathscr{E}_{j_1 \cdots j_d} \coloneqq (\varepsilon_{i,j_1 \cdots j_d})_{i=1}^p$ is the mutually independent p-dimensional vector of random errors defined on a common probability space $(\Omega, \mathscr{F}, \mathbb{P})$. We assume that, for all $1 \leq j_1 \leq n_1, \ldots, 1 \leq j_d \leq n_d$, $E(\mathscr{E}_{j_1 \cdots j_d}) = \mathbf{0} \in \mathbb{R}^p$, and $\mathrm{Cov}(\mathscr{E}_{j_1 \cdots j_d}) = \boldsymbol{\Sigma} = (\sigma_{uv})_{u,v=1}^{p,p}$. Let $\mathbf{Z}_{n_1 \cdots n_d} \coloneqq (\mathbf{Z}_{j_1 \cdots j_d})_{j_1=1,\ldots,j_d=1}^{n_1,\ldots,n_d}$ be the p-dimensional pyramidal array of random observations and let $\mathscr{E}_{n_1 \cdots n_d} \coloneqq (\mathscr{E}_{j_1 \cdots j_d})_{j_1=1,\ldots,j_d=1}^{n_1,\ldots,n_d}$ be the p-dimensional pyramidal array of random errors taking values in the Euclidean space $\prod_{i=1}^p \mathbb{R}^{n_1 \times \cdots \times n_d}$. Then under H_0 the observations can be represented by

$$\mathbf{Z}_{n_1 \cdots n_d} = \left(\sum_{w=1}^{d_i} \beta_{iw} f_{iw} \left(\Xi_{n_1 \cdots n_d} \right) \right)_{i=1}^p + \mathscr{E}_{n_1 \cdots n_d}, \tag{3}$$

where $f_{iw}(\Xi_{n_1 \cdots n_d}) \coloneqq (f_{iw}((j_k/n_k)_{k=1}^d))_{j_1=1,\ldots,j_d=1}^{n_1,\ldots,n_d}$. Under the alternative H_1 a multivariate nonparametric regression model

$$\mathbf{Z}_{n_1 \cdots n_d} = \mathbf{g}\left(\Xi_{n_1 \cdots n_d} \right) + \mathscr{E}_{n_1 \cdots n_d} \tag{4}$$

is assumed, where $\mathbf{g}(\Xi_{n_1 \cdots n_d}) \coloneqq (\mathbf{g}((j_k/n_k)_{k=1}^d))_{j_1=1,\ldots,j_d=1}^{n_1,\ldots,n_d} \in \prod_{i=1}^p \mathbb{R}^{n_1 \times \cdots \times n_d}$. By applying the similar argument as in Christensen [2] and Johnson and Wichern [4], the p-dimensional array of the least squares residuals of the observations is given by the following component-wise projection:

$$\begin{aligned} \mathbf{R}_{n_1 \cdots n_d} &\coloneqq \left(\mathbf{r}_{j_1 \cdots j_d} \right)_{j_1,\ldots,j_d=1}^{n_1,\ldots,n_d} \\ &\coloneqq \mathbf{Z}_{n_1 \cdots n_d} - \mathrm{pr}_{\prod_{i=1}^p \mathbf{W}_{i,n_1 \cdots n_d}} \mathbf{Z}_{n_1 \cdots n_d}, \end{aligned} \tag{5}$$

with $\mathbf{r}_{j_1 \cdots j_d} \coloneqq (r_{i,j_1 \cdots j_d})_{i=1}^p$, for $1 \leq j_k \leq n_k$, and $k = 1, \ldots, d$. Thereby, for $i = 1, \ldots, p$, we define $\mathbf{W}_{i,n_1 \cdots n_d} \coloneqq [f_{i1}(\Xi_{n_1 \cdots n_d}), \ldots, f_{id_i}(\Xi_{n_1 \cdots n_d})]$ as the subspace of $\mathbb{R}^{n_1 \times \cdots \times n_d}$ spanned by the arrays $\{f_{i1}(\Xi_{n_1 \cdots n_d}), \ldots, f_{id_i}(\Xi_{n_1 \cdots n_d})\}$. It is worth mentioning that the Euclidean space $\mathbb{R}^{n_1 \times \cdots \times n_d}$ is furnished with the inner product denoted by $\langle \cdot, \cdot \rangle_{\mathbb{R}^{n_1 \times \cdots \times n_d}}$ and defined by

$$\left\langle \mathbf{A}_{n_1 \cdots n_d}, \mathbf{B}_{n_1 \cdots n_d} \right\rangle_{\mathbb{R}^{n_1 \times \cdots \times n_d}} \coloneqq \sum_{j_1=1}^{n_1} \cdots \sum_{j_d=1}^{n_d} a_{j_1 \cdots j_d} b_{j_1 \cdots j_d}, \tag{6}$$

for every $\mathbf{A}_{n_1 \cdots n_d} \coloneqq (a_{j_1 \cdots j_d})_{j_1=1,\ldots,j_d=1}^{n_1,\ldots,n_d}$, and $\mathbf{B}_{n_1 \cdots n_d} \coloneqq (b_{j_1 \cdots j_d})_{j_1=1,\ldots,j_d=1}^{n_1,\ldots,n_d} \in \mathbb{R}^{n_1 \times \cdots \times n_d}$.

Next we define the set-indexed partial sums operator. Let $\mathscr{A}$ be the family of convex subset of $\mathbf{I}^d$, and let $\eta_{\lambda_{\mathbf{I}}^d}$ be the Lebesgue pseudometric on $\mathscr{A}$ defined by $\eta_{\lambda_{\mathbf{I}}^d}(A_1, A_2) \coloneqq \lambda_{\mathbf{I}}^d(A_1 \Delta A_2)$, for $A_1, A_2 \in \mathscr{A}$. Let $\mathscr{C}(\mathscr{A})$ be the set of continuous functions on $\mathscr{A}$ under $\eta_{\lambda_{\mathbf{I}}^d}$. We embed the array of the residual $\mathbf{R}_{n_1 \cdots n_d}$ into a p-dimensional stochastic process indexed by $\mathscr{A}$ by using the component-wise set-indexed partial sums operator

$$\mathbf{V}_{n_1 \cdots n_d} : \prod_{i=1}^p \mathbb{R}^{n_1 \times \cdots \times n_d} \longmapsto \mathscr{C}^p(\mathscr{A}) \coloneqq \prod_{i=1}^p \mathscr{C}(\mathscr{A}), \tag{7}$$

such that, for any $B \in \mathscr{A}$,

$$\begin{aligned} &\mathbf{V}_{n_1 \cdots n_d}\left(\mathbf{R}_{n_1 \cdots n_d} \right)(B) \\ &\quad \coloneqq \sum_{j_1=1}^{n_1} \cdots \sum_{j_d=1}^{n_d} \sqrt{n_1 \cdots n_d} \lambda_{\mathbf{I}}^d\left(B \cap C_{j_1 \cdots j_d} \right) \mathbf{r}_{j_1 \cdots j_d}, \end{aligned} \tag{8}$$

where, for $1 \leq j_1 \leq n_1, \ldots, 1 \leq j_d \leq n_d$, $C_{j_1 \cdots j_d} \coloneqq \prod_{k=1}^d ((j_k - 1)/n_k, j_k/n_k]$. Let us call this process the p-dimensional set-indexed least squares residual partial sums process. The space $\mathscr{C}^p(\mathscr{A})$ is furnished with the uniform topology induced by the metric φ defined by

$$\varphi(\mathbf{u}, \mathbf{w}) \coloneqq \sum_{i=1}^p \left\| u_i - w_i \right\|_{\mathscr{A}} = \sum_{i=1}^p \sup_{A \in \mathscr{A}} \left| u_i(A) - w_i(A) \right|, \tag{9}$$

for $\mathbf{u} \coloneqq (u_i)_{i=1}^p$ and $\mathbf{w} \coloneqq (w_i)_{i=1}^p \in \mathscr{C}^p(\mathscr{A})$.

We notice that, in the works of Bischoff and Somayasa [9], Bischoff and Gegg [17], and Somayasa and Adhi Wibawa [18], the limit process of the partial sums process of the least squares residuals has been investigated by applying the existing geometric method of Bischoff [11, 12]. However, the method becomes not applicable anymore in deriving the limit process of $\mathbf{V}_{n_1 \cdots n_d}(\mathbf{R}_{n_1 \cdots n_d})$ as the dimension of $\mathbf{W}_{i,n_1 \cdots n_d}$ varies. Therefore, in this work, we attempt to adopt the vectorial analog of Prohorov's theorem; see, for example, Theorem 6.1 in Billingsley [19] for obtaining the limit process. For our result we need to extend the ordinary partial sums formula to p-dimensional case defined on $\mathbf{I}^d$ as follows. Let $K \coloneqq \{1, 2, \ldots, d\}$ and C_k^K be the set of all k-combinations of the set K, with $k = 1, \ldots, d$. For a chosen value of k, we denote

the ith element of C_k^K by a k-tuple $(i(k_1), i(k_2), \ldots, i(k_k))$, for $1 \le i \le |C_k^K|$, where $|C_k^K|$ is the number of elements of C_k^K which is clearly given by

$$\left|C_k^K\right| = \frac{d\,(d-1)\,(d-2)\cdots(d-k+1)}{k\,(k-1)\,(k-2)\cdots 1}. \tag{10}$$

For example, let $K = \{1, 2, 3\}$. Then, for $k = 1$, we denote the elements of C_1^K as $1(k_1) := 1$, $2(k_1) := 2$, and $3(k_1) := 3$. In a similar way, we denote the elements of C_2^K which consists of $\{(1,2), (1,3), (2,3)\}$, respectively, by $(1(k_1), 1(k_2)) := (1,2)$, $(2(k_1), 2(k_2)) := (1,3)$, and $(3(k_1), 3(k_2)) := (2,3)$. Finally the element of $C_3^K = \{(1,2,3)\}$ is sufficiently written by $(1(k_1), 1(k_2), 1(k_3))$. Hence the p-dimensional ordinary partial sums operator transforms any p-dimensional array $\mathbf{A}_{n_1\cdots n_d} = (\mathbf{a}_{j_1\cdots j_d})_{j_1=1,\ldots,j_d=1}^{n_1,\ldots,n_d} \in \prod_{i=1}^{p} \mathbb{R}^{n_1\times\cdots\times n_d}$ to a continuous function on $\mathbf{I}^d$ defined by

$$\begin{aligned}
\mathbf{T}_{n_1\cdots n_d}\left(\mathbf{A}_{n_1\cdots n_d}\right)(\mathbf{t}) &:= \frac{1}{\sqrt{n_1\cdots n_d}} \sum_{j_1=1\cdots j_d=1}^{[n_1t_1]\cdots[n_dt_d]} \mathbf{a}_{j_1\cdots j_d} \\
&+ \sum_{k=1}^{d}\sum_{i=1}^{|C_2^K|}\left(\prod_{u=1}^{k}\left(t_{i(k_u)} - \frac{\left[n_{i(k_u)}t_{i(k_u)}\right]}{n_{i(k_u)}}\right)\right) \\
&\cdot \frac{\sqrt{n_1\cdots n_d}}{\left(n_1\cdots n_d\right)/\left(n_{i(k_1)}\cdots n_{i(k_d)}\right)} \\
&\cdot \sum_{\{j_1=1,\ldots,j_d=1\}/\{j_{i(k_1)},\ldots,j_{i(k_d)}\}}^{[n_1t_1],\ldots,[n_dt_d]} \mathbf{a}_{j_1\cdots j_d \mid j_{i(k_1)}=[n_{i(k_1)}t_{i(k_1)}]+1,\ldots,j_{i(k_d)}=[n_{i(k_d)}t_{i(k_d)}]+1},
\end{aligned} \tag{11}$$

for every $\mathbf{t} := (t_1, \ldots, t_d)^\top \in \mathbf{I}^d$, where for positive integers $b_u, b_{u+1}, \ldots, b_{u+m} \in \mathscr{Z}_+$ we define a notation

$$\begin{aligned}
&\mathbf{a}_{j_1\cdots j_d} \mid j_u = b_u, \ldots, j_{u+m} = b_{u+m} \\
&\qquad := \mathbf{a}_{j_1,\ldots,j_{u-1},b_u,\ldots,b_{u+m},j_{u+m+1},\ldots,j_d}.
\end{aligned} \tag{12}$$

It is clear that the partial sums process of the residuals obtained using (11) is a special case of (8) since for every $\mathbf{t} := (t_1, \ldots, t_d)^\top \in \mathbf{I}^d$ it holds

$$\mathbf{T}_{n_1\cdots n_d}\left(\mathbf{A}_{n_1\cdots n_d}\right)(\mathbf{t}) = \mathbf{V}_{n_1\cdots n_d}\left(\mathbf{A}_{n_1\cdots n_d}\right)\left(\prod_{k=1}^{d}[0, t_k]\right). \tag{13}$$

It is worth noting that the extension of the study from univariate to multivariate model and also the expansion of the dimension of the lattice points are strongly motivated by the prediction problem in mining industry and geosciences. As for an example recently Tahir [20] presented data provided by PT Antam Tbk (a mining industry in Southeast Sulawesi). The data consist of a joint measurement of the percentage of several chemical elements and substances such as Ni, Co, Fe, MgO, SiO_2, and CaO which are recorded in every point of a three-dimensional lattice defined over the exploration region of the company. Hence, by the inherent existence of the correlation among the variables, the statistical analysis for the involved variables must be conducted simultaneously.

There have been many methods proposed in the literatures for testing H_0. Most of them have been derived for the case of $\mathbf{W}_1 = \cdots = \mathbf{W}_p$ under normally distributed random error. Generalized likelihood ratio test which has been leading to Wilk's lambda statistic or variant of it can be found in Zellner [1], Christensen [2], pp. 1–22, Anderson [3], pp. 187–191, and Johnson and Wichern [4], pp. 395–398. Mardia and Goodall [21] derived the maximum likelihood estimation procedure for the parameters of the general normal spatial multivariate model with stationary observations. This approach can be straightforwardly extended for obtaining the associated likelihood ratio test in model check for the model. Unfortunately, in the practice especially when dealing with mining data, normal distribution is sometimes found to be not suitable for describing the distribution model of the observations, so that the test procedures mentioned above are consequently no longer applicable. Asymptotic method established in Arnold [22] for multivariate regression with $\mathbf{W}_1 = \cdots = \mathbf{W}_p$ can be generalized in such a way that it is valid for the general model. As a topic in statistics it must be well known. However, we cannot find literatures where the topic has been studied.

The rest of the paper is organized as follows. In Section 2 we show that when H_0 is true $\mathbf{\Sigma}^{-1/2}\mathbf{V}_{n_1\cdots n_d}(\mathbf{R}_{n_1\cdots n_d})$ converges weakly to a projection of the p-dimensional set-indexed Brownian sheet. The limit process is shown to be useful for testing H_0 asymptotically based on the Kolmogorov-Smirnov (KS-test) and Cramér-von Mises (CvM-test) functionals of the set-indexed p-dimensional least squares residual partial sum processes, defined, respectively, by

$$\begin{aligned}
\mathrm{KS}_{n_1\cdots n_d,\mathscr{A}} &:= \sup_{A\in\mathscr{A}} \left\|\mathbf{\Sigma}^{-1/2}\mathbf{V}_{n_1\cdots n_d}\left(\mathbf{R}_{n_1\cdots n_d}\right)(A)\right\|_{\mathbb{R}^p} \\
\mathrm{CvM}_{n_1\cdots n_d,\mathscr{A}} &:= \frac{1}{n_1\cdots n_d}\sum_{A\in\mathscr{A}} \left\|\mathbf{\Sigma}^{-1/2}\mathbf{V}_{n_1\cdots n_d}\left(\mathbf{R}_{n_1\cdots n_d}\right)(A)\right\|_{\mathbb{R}^p}^2.
\end{aligned} \tag{14}$$

For both tests the rejection of H_0 is for large value of the KS and CvM statistics, respectively. Under localized alternative the above sequence of random processes converges weakly to the above limit process with an additional deterministic trend (see Section 3). In Section 4, we define a consistent estimator for $\mathbf{\Sigma}$. In Section 5 we investigate a residual based bootstrap method for the calibration of the tests. Monte Carlo simulation for the purpose of studying the finite sample behavior of the KS and CvM tests is reported in Section 6. Application of the test procedure in real data is presented in Section 7. The paper is closed in Section 8 with conclusion and some remarks for future research. Auxiliary results needed for deriving the limit process are presented in the appendix. We note that all convergence results derived throughout this paper which hold for $n_1, \ldots, n_d$ simultaneously go to infinity, that is, for $n_k \to \infty$, for all $k = 1, \ldots, d$; otherwise they will be stated in some way. The notion of convergence in distribution and convergence in probability will be conventionally denoted by $\xrightarrow{\mathscr{D}}$ and $\xrightarrow{\mathscr{P}}$, respectively.

2. The Limit of $\mathbf{V}_{n_1\cdots n_d}(\mathbf{R}_{n_1\cdots n_d})$ under H_0

Let $B := \{B(A) : A \in \mathscr{A}\}$ be the one-dimensional set-indexed Brownian sheet having sample path in $\mathscr{C}(\mathscr{A})$. We refer the reader to Pyke [23], Bass and Pyke [24], and Alexander and Pyke [25] for the definition and the existence of B. Let us consider a subspace of $\mathscr{C}(\mathscr{A})$ which is closely related to B, defined by

$$\mathscr{H}_B := \left\{h_v : \mathscr{A} \longrightarrow \mathbb{R},\ \exists v \in L_2\left(\lambda_{\mathbf{I}}^d\right),\ \text{s.t. } h_v(A) := \int_A v(\mathbf{t})\,\lambda^d(\mathbf{t})\right\}. \tag{15}$$

Under the inner product and the norm defined by

$$\left\langle h_v, h_w\right\rangle_{\mathscr{H}_B} := \int_{\mathbf{I}^d} v(\mathbf{t})\,w(\mathbf{t})\,\lambda_{\mathbf{I}}^d(\mathbf{t}),$$
$$\left\|h_v\right\|^2 := \int_{\mathbf{I}^d} v^2(\mathbf{t})\,\lambda_{\mathbf{I}}^d(\mathbf{t}), \tag{16}$$

it is clear that $\mathscr{H}_B$ and $L_2(\lambda_{\mathbf{I}}^d)$ are isometric. For our result we need to define subspaces $\mathbf{W}_i$ and $\mathbf{W}_{i\mathscr{H}_B}$ associated with the regression functions $f_{i1},\ldots,f_{id_i}$, where $\mathbf{W}_i := [f_{i1},\ldots,f_{id_i}] \subset L_2(\lambda_{\mathbf{I}}^d)$ and $\mathbf{W}_{i\mathscr{H}_B} := [h_{f_{i1}},\ldots,h_{f_{id_i}}] \subset \mathscr{H}_B$, for $i = 1,\ldots,p$.

Now we are ready to state the limit process of the sequence of p-dimensional set-indexed residual partial sums processes for the model specified under H_0.

Theorem 1. *For $i = 1,\ldots,p$, let $\{f_{i1},\ldots,f_{id_i}\}$ be an orthonormal basis (ONB) of $\mathbf{W}_i$. We assume that $\mathbf{W}_i \subseteq \mathbf{W}_{i+1}$, for $i = 1,\ldots,p-1$. Let $\mathbf{B}_p := \{(B_i(A))_{i=1}^p : A \in \mathscr{A}\}$ be the p-dimensional set-indexed Brownian sheet with the covariance function $\mathrm{Cov}(\mathbf{B}_p(A),\mathbf{B}_p(A')) := \lambda_{\mathbf{I}}^d(A\cap A')\mathbf{I}_p$, for $A, A' \in \mathscr{A}$, where $\mathbf{I}_p$ is the $p\times p$ identity matrix. Suppose $\{f_{i1},\ldots,f_{id_i}\}$ are in $\mathscr{C}(\mathbf{I}^d)\cap \mathrm{BV}_H(\mathbf{I}^d)$, where $\mathscr{C}(\mathbf{I}^d)$ is the space of continuous functions on $\mathbf{I}^d$ (see Definition A.4 for the definition of $\mathrm{BV}_H(\mathbf{I}^d)$). Then under H_0 it holds that*

$$\boldsymbol{\Sigma}^{-1/2}\mathbf{V}_{n_1\cdots n_d}\left(\mathbf{R}_{n_1\cdots n_d}\right) \xrightarrow{\mathscr{D}} \mathbf{B}_{p,\mathbf{f}}^{H_0} := \mathbf{B}_p - pr^*_{\prod_{i=1}^p \mathbf{W}_{i\mathscr{H}_B}}\mathbf{B}_p, \tag{17}$$

where

$$pr^*_{\prod_{i=1}^p \mathbf{W}_{i\mathscr{H}_B}}\mathbf{B}_p := \left(pr^*_{\mathbf{W}_{i\mathscr{H}_B}}B_i\right)_{i=1}^p. \tag{18}$$

Thereby $pr^*_{\mathbf{W}_{i\mathscr{H}_B}}$ is a projector such that, for every $u \in \mathscr{C}(\mathscr{A})$ and $A \in \mathscr{A}$,

$$\left(pr^*_{\mathbf{W}_{i\mathscr{H}_B}}u\right)(A) := \sum_{j=1}^{d_i}\left\langle h_{f_{ij}}, u\right\rangle h_{f_{ij}}(A),$$
$$\text{where } \left\langle h_{f_{ij}}, u\right\rangle := \int_{\mathbf{I}^d}^{(R)} f_{ij}(\mathbf{t})\,du(\mathbf{t}). \tag{19}$$

For $\mathbf{t} := (t_k)_{k=1}^d \in \mathbf{I}^d$, we set $u(\mathbf{t})$ for $u(\prod_{k=1}^d[0,t_k])$, and $\int^{(R)}$ stands for the integral in the sense of Riemann-Stieltjes. Moreover, the limit process $\mathbf{B}_{p,\mathbf{f}}^{H_0}$ is a centered Gaussian process with the covariance function given by

$$K(A,C) := \mathrm{diag}\Bigg(\lambda(A\cap C) - \sum_{j=1}^{d_1}h_{f_{1j}}(A)\,h_{f_{1j}}(C),\ldots,\lambda(A\cap C) - \sum_{j=1}^{d_p}h_{f_{pj}}(A)\,h_{f_{pj}}(C)\Bigg). \tag{20}$$

Proof. By applying the linear property of $\mathbf{V}_{n_1\cdots n_d}$ and Lemma C.2, we have under H_0,

$$\mathbf{V}_{n_1\cdots n_d}\left(\mathbf{R}_{n_1\cdots n_d}\right) = \mathbf{V}_{n_1\cdots n_d}\left(\mathscr{E}_{n_1\cdots n_d}\right) - \mathrm{pr}_{\prod_{i=1}^p \mathbf{W}_{i,n_1\cdots n_d\mathscr{H}_B}}\mathbf{V}_{n_1\cdots n_d}\left(\mathscr{E}_{n_1\cdots n_d}\right). \tag{21}$$

It can be shown by extending the uniform central limit theorem studied in Pyke [23], Bass and Pyke [24], and Alexander and Pyke [25] to its vectorial analog that the term $\boldsymbol{\Sigma}^{-1/2}\mathbf{V}_{n_1\cdots n_d}(\mathscr{E}_{n_1\cdots n_d})$ on the right-hand side of (21) converges weakly to $\mathbf{B}_p$. Therefore we only need to show that the second term satisfies the weak convergence:

$$\mathscr{Z}_{n_1\cdots n_d} := \boldsymbol{\Sigma}^{-1/2}\mathrm{pr}_{\prod_{i=1}^p \mathbf{W}_{i,n_1\cdots n_d\mathscr{H}_\mathbf{B}}}\mathbf{V}_{n_1\cdots n_d}\left(\mathscr{E}_{n_1\cdots n_d}\right) \xrightarrow{\mathscr{D}} U := \mathrm{pr}^*_{\prod_{i=1}^p \mathbf{W}_{i\mathscr{H}_B}}\mathbf{B}_p, \tag{22}$$

where U is a p-dimensional centered Gaussian process with the covariance matrix given by

$$K_U(A_1,A_2) = \mathrm{diag}\Bigg(\sum_{j=1}^{d_1}h_{f_{1j}}(A_1)\,h_{f_{1j}}(A_2),\ldots,\sum_{j=1}^{d_p}h_{f_{pj}}(A_1)\,h_{f_{pj}}(A_2)\Bigg),\quad \text{for } A_1,A_2 \in \mathscr{A}. \tag{23}$$

By Prohorov's theorem it is sufficient to show that, for any finite collection of convex sets $A_1,\ldots,A_r$ in $\mathscr{A}$ and real numbers $c_1,\ldots,c_r$, with $r \geq 1$, it holds that

$$\sum_{k=1}^r c_k\mathscr{Z}_{n_1\cdots n_d}(A_k) \xrightarrow{\mathscr{D}} \sum_{k=1}^r c_k U(A_k), \tag{24}$$

where the left-hand side has the covariance which can be expressed as

$$\mathrm{Cov}\left(\sum_{k=1}^r c_k\mathscr{Z}_{n_1\cdots n_d}(A_k)\right) = \sum_{k=1}^r\sum_{\ell=1}^r c_k c_\ell\boldsymbol{\Sigma}^{-1/2}\left(E\left(B_i(A_k)\,B_j(A_\ell)\right)\right)_{i,j=1}^p\boldsymbol{\Sigma}^{-1/2}, \tag{25}$$

where $B_i(A_k) := \mathrm{pr}_{\mathbf{W}_{i,n_1\cdots n_d}\mathscr{K}_B}\mathbf{V}_{n_1\cdots n_d}(\varepsilon_{i,n_1\cdots n_d})(A_k)$, for $i = 1,\ldots,p$ and $k = 1,\ldots,r$. Let k and ℓ be fixed. Then by a simultaneous application of the definition of $\mathrm{pr}_{\mathbf{W}_{i,n_1\cdots n_d}\mathscr{K}_B}$ (see Lemma C.3), (11), the definition of the Riemann-Stieljes integral (cf. Stroock [26], pp. 7–17), and the independence of the array $\{\varepsilon_{i,j_1\cdots j_d} : 1 \le j_k \le n_k\}$, we further get

$$\begin{aligned}
E\left(B_i(A_k)B_j(A_\ell)\right) &= \sum_{w=1}^{d_i}\sum_{w'=1}^{d_j}\int_{A_k}\widetilde{s}_{iw}^{(n_1\cdots n_d)}(\mathbf{t})\,\lambda_{\mathbf{I}}^d(d\mathbf{t}) \\
&\cdot\int_{A_\ell}\widetilde{s}_{jw'}^{(n_1\cdots n_d)}(\mathbf{t})\,\lambda_{\mathbf{I}}^d(d\mathbf{t})\,E\left(\int_{\mathbf{I}^d}^{(R)}\widetilde{s}_{iw}^{(n_1\cdots n_d)}(\mathbf{t})\,d\mathbf{V}_{n_1\cdots n_d}\right. \\
&\left.\cdot\left(\varepsilon_{i,n_1\cdots n_d}\right)(\mathbf{t})\int_{\mathbf{I}^d}^{(R)}\widetilde{s}_{jw'}^{(n_1\cdots n_d)}(\mathbf{t})\,d\mathbf{V}_{n_1\cdots n_d}\left(\varepsilon_{j,n_1\cdots n_d}\right)(\mathbf{t})\right) \\
&= \sum_{w=1}^{d_i}\sum_{w'=1}^{d_j}\int_{A_k}\widetilde{s}_{iw}^{(n_1\cdots n_d)}(\mathbf{t})\,\lambda_{\mathbf{I}}^d(d\mathbf{t})\int_{A_\ell}\widetilde{s}_{jw'}^{(n_1\cdots n_d)}(\mathbf{t}) \\
&\cdot\lambda_{\mathbf{I}}^d(d\mathbf{t})\,\frac{\sigma_{ij}}{n_1\cdots n_d}\sum_{j_1=1,\ldots,j_d=1}^{n_1,\ldots,n_d}\widetilde{s}_{iw}^{(n_1\cdots n_d)}\left(\frac{j_1}{n_1},\ldots,\frac{j_d}{n_d}\right) \\
&\cdot\widetilde{s}_{jw'}^{(n_1\cdots n_d)}\left(\frac{j_1}{n_1},\ldots,\frac{j_d}{n_d}\right).
\end{aligned} \tag{26}$$

By recalling Lemma C.3 the last expression clearly converges to

$$\begin{aligned}
&\sigma_{ij}\sum_{w=1}^{d_i}\sum_{w'=1}^{d_j}\left\langle f_{iw}, f_{jw'}\right\rangle_{L_2(\lambda_{\mathbf{I}}^d)}h_{f_{iw}}(A_k)\,h_{f_{jw'}}(A_\ell) \\
&\quad = \sigma_{ij}\sum_{w=1}^{d_i}h_{f_{iw}}(A_k)\,h_{f_{jw}}(A_\ell).
\end{aligned} \tag{27}$$

Hence the matrix $(E(B_i(A_k)B_j(A_\ell)))_{i,j=1}^p$ converges element wise to the symmetric matrix which can be represented as $\boldsymbol{\Sigma}\odot\mathbf{D}$, for a matrix $\mathbf{D}$ defined by

$$\mathbf{D} := \begin{pmatrix}
\kappa_{11}(A_k,A_\ell) & \kappa_{12}(A_k,A_\ell) & \cdots & \kappa_{1p}(A_k,A_\ell) \\
\kappa_{21}(A_k,A_\ell) & \kappa_{22}(A_k,A_\ell) & \cdots & \kappa_{2p}(A_k,A_\ell) \\
\vdots & \vdots & \vdots & \vdots \\
\kappa_{p1}(A_k,A_\ell) & \kappa_{p2}(A_k,A_\ell) & \cdots & \kappa_{pp}(A_k,A_\ell)
\end{pmatrix} \tag{28}$$

with $\kappa_{ij}(A_k,A_\ell) := \sum_{w=1}^{d_{\min\{i,j\}}}h_{f_{iw}}(A_k)h_{f_{jw}}(A_\ell)$, for $i,j = 1,\ldots,p$. Thereby $\odot$ denotes the Hadarmard product defined, for example, in Magnus and Neudecker [27], pp. 53-54. Since $\boldsymbol{\Sigma}^{-1/2}(\boldsymbol{\Sigma}\odot\mathbf{D})\boldsymbol{\Sigma}^{-1/2} = \mathbf{D}\odot\mathbf{I}_p$, we successfully have shown that $\mathrm{Cov}(\sum_{k=1}^r c_k\mathscr{Z}_{n_1\cdots n_d}(A_k))$ converges to the following general linear combination:

$$\begin{aligned}
&\sum_{k=1}^r\sum_{\ell=1}^r c_k c_\ell \\
&\cdot\mathrm{diag}\left(\sum_{w=1}^{d_1}h_{f_{1w}}(A_k)\,h_{f_{1w}}(A_\ell),\ldots,\sum_{w=1}^{d_p}h_{f_{pw}}(A_k)\,h_{f_{pw}}(A_\ell)\right),
\end{aligned} \tag{29}$$

which is actually the covariance of $\sum_{k=1}^r c_k U(A_k)$. Next we observe that, by applying the definition of $\mathbf{V}_{n_1\cdots n_d}$ and the definition of the Riemann-Stieltjes integral, we can also write $\sum_{k=1}^r c_k\mathscr{Z}_{n_1\cdots n_d}(A_k)$ as follows:

$$\begin{aligned}
&\sum_{k=1}^r c_k\mathscr{Z}_{n_1\cdots n_d}(A_k) \\
&\quad = \sum_{j_1=1}^{n_1}\cdots\sum_{j_d=1}^{n_d}\boldsymbol{\Sigma}^{-1/2}\left(\sum_{k=1}^r\Lambda_i\left(\frac{j_1}{n_1},\ldots,\frac{j_d}{n_d};A_k\right)\right)_{i=1}^p,
\end{aligned} \tag{30}$$

where

$$\begin{aligned}
\Lambda_i\left(\frac{j_1}{n_1},\ldots,\frac{j_d}{n_d};A_k\right) &:= \sum_{w=1}^{d_i}\frac{c_k}{\sqrt{n_1\cdots n_d}} \\
&\cdot\widetilde{s}_{iw}^{(n_1\cdots n_d)}\left(\frac{j_1}{n_1},\ldots,\frac{j_d}{n_d}\right)\varepsilon_{i,j_1\cdots j_d}h_{\widetilde{s}_{iw}^{(n_1\cdots n_d)}}(A_k).
\end{aligned} \tag{31}$$

Let $\Gamma_f := \max_{1\le w\le d_i;1\le i\le p}\|f_{iw}\|_\infty$, $M := \max_{1\le k\le r}|c_k|$, and $\|\boldsymbol{\Sigma}^{-1/2}\|$ be the Euclidean norm of $\boldsymbol{\Sigma}^{-1/2}$. Then by considering the stochastic independence of the array of the p-vector of the random errors, it holds that

$$\begin{aligned}
0 \le \mathbb{L}_{\mathscr{Z}_{n_1\cdots n_d}}(\epsilon) &:= \sum_{j_1=1}^{n_1}\cdots\sum_{j_d=1}^{n_d}E \\
&\cdot\left(\left\|\left(\sum_{k=1}^r\Lambda_i\left(\frac{j_1}{n_1},\ldots,\frac{j_d}{n_d};A_k\right)\right)_{i=1}^p\right\|_{\mathbb{R}^p}^2\right. \\
&\left.\cdot\mathbf{1}\left\{\left\|\left(\sum_{k=1}^r\Lambda_i\left(\frac{j_1}{n_1},\ldots,\frac{j_d}{n_d};A_k\right)\right)_{i=1}^p\right\|_{\mathbb{R}^p}^2\ge\epsilon\right\}\right) \\
&\le (rM)^2\left(d_p\Gamma_f^2\right)^2\left\|\boldsymbol{\Sigma}^{-\frac{1}{2}}\right\|^2E\left(\left\|\mathscr{E}_{j_1\cdots j_d}\right\|_{\mathbb{R}^p}^2\right. \\
&\left.\cdot\mathbf{1}\left\{\left\|\mathscr{E}_{j_1\cdots j_d}\right\|_{\mathbb{R}^p}\ge\frac{\epsilon\sqrt{n_1\cdots n_d}}{(rM)\left(d_p\Gamma_f^2\right)}\right\}\right)\quad\forall\epsilon>0,
\end{aligned} \tag{32}$$

in which by the well-known bounded convergence theorem (cf. Athreya and Lahiri [28], pp. 57-58) the last term converges to zero. Thus the Lindeberg condition is satisfied. Therefore by the Lindeberg-Levy multivariate central limit theorem studied, for example, in van der Vaart [29], pp. 16, it can be concluded that $\sum_{k=1}^r c_k\mathscr{Z}_{n_1\cdots n_d}(A_k)$ converges in distribution to $\sum_{k=1}^r c_k U(A_k)$, where $\sum_{k=1}^r c_k U(A_k)$ has the p-variate normal distribution with mean zero and the covariance given by (29).

The tightness of $\mathscr{Z}_{n_1\cdots n_d}$ can be shown as follows. By the definition $\mathscr{Z}_{n_1\cdots n_d}$ can also be expressed as

$$\begin{aligned}
&\mathscr{Z}_{n_1\cdots n_d} \\
&\quad = \boldsymbol{\Sigma}^{-1/2}\mathrm{pr}_{\prod_{i=1}^p\mathbf{W}_{i,n_1\cdots n_d}\mathscr{K}_B}\boldsymbol{\Sigma}^{1/2}\boldsymbol{\Sigma}^{-1/2}\mathbf{V}_{n_1\cdots n_d}\left(\mathscr{E}_{n_1\cdots n_d}\right).
\end{aligned} \tag{33}$$

Since $\boldsymbol{\Sigma}^{-1/2}\mathbf{V}_{n_1\cdots n_d}(\mathscr{E}_{n_1\cdots n_d})$ is tight, hence by recalling Lemma 1 in Billingsley [19], pp. 38–40, it is sufficient to show that the mapping $\boldsymbol{\Sigma}^{-1/2}\mathrm{pr}_{\prod_{i=1}^{p}\mathbf{W}_{i,n_1\cdots n_d\mathscr{K}_B}}\boldsymbol{\Sigma}^{1/2}$ is continuous on $\mathscr{C}^p(\mathscr{A})$ for every $n_1 \geq 1, \ldots, n_d \geq 1$. Proposition C.4 finishes the proof. □

Corollary 2. *By Theorem 1 and the well-known continuous mapping theorem (cf. Theorem* 5.1 *in Billingsley [19]) the distribution of the statistics $KS_{n_1\cdots n_d,\mathscr{A}}$ and $CvM_{n_1\cdots n_d,\mathscr{A}}$ can be approximated, respectively, by those of*

$$\begin{aligned} KS &\coloneqq \sup_{A\in\mathscr{A}}\left\|\left(\mathbf{B}_p - pr^*_{\prod_{i=1}^{p}\mathbf{W}_{i\mathscr{K}_B}}\mathbf{B}_p\right)(A)\right\|_{\mathbb{R}^p} \\ CvM &\coloneqq \int_{\mathbf{I}^d}\left\|\left(\mathbf{B}_p - pr^*_{\prod_{i=1}^{p}\mathbf{W}_{i\mathscr{K}_B}}\mathbf{B}_p\right)(A)\right\|^2_{\mathbb{R}^p} dA. \end{aligned} \tag{34}$$

Let $\widetilde{t}_{1-\alpha}$ and $\widetilde{c}_{1-\alpha}$ be the $(1-\alpha)$th quantile of the distributions of KS and CvM, respectively. When $KS_{n_1\cdots n_d,\mathscr{A}}$ is used, H_0 will be rejected at level α if and only if $KS_{n_1\cdots n_d,\mathscr{A}} \geq \widetilde{t}_{1-\alpha}$. Likewise if $CvM_{n_1\cdots n_d,\mathscr{A}}$ is used, then H_0 will be rejected at level α if and only if $CvM_{n_1\cdots n_d,\mathscr{A}} \geq \widetilde{c}_{1-\alpha}$.

3. The Limit of $\mathbf{V}_{n_1\cdots n_d}(\mathbf{R}_{n_1\cdots n_d})$ under H_1

The test procedures derived above are consistent in the sense of Definition 11.1.3 in Lehmann and Romano [30]. That is, the probability of rejection of H_0 under the competing alternative converges to 1. As an immediate consequence we cannot observe the performance of the tests when the model moves away from H_0. Therefore, to be able to investigate the behavior of the tests, we consider the localized model defined as follows:

$$\mathbf{Z}_{n_1\cdots n_d} = \frac{1}{\sqrt{n_1\cdots n_d}}\mathbf{g}\left(\Xi_{n_1\cdots n_d}\right) + \mathscr{E}_{n_1\cdots n_d}. \tag{35}$$

When H_0 is true we get the similar least squares residuals as given in Section 1. Therefore, observing Model (35), the test problem will not be altered.

In the following theorem, we present the limit process of the p-dimensional set-indexed partial sums process of the residuals under H_1 associated with Model (35).

Theorem 3. *For $i = 1, \ldots, p$, let $\{f_{i1}, \ldots, f_{id_i}\}$ be an ONB of $\mathbf{W}_i$ with $\mathbf{W}_i \subseteq \mathbf{W}_{i+1}$, for $i = 1, \ldots, p-1$. If $\mathbf{g} = (g_i)_{i=1}^p \in \prod_{i=1}^p \mathrm{BVV}(\mathbf{I}^d)$ and $\{f_{i1}, \ldots, f_{id_i}\} \in \mathscr{C}(\mathbf{I}^d) \cap \mathrm{BV}_H(\mathbf{I}^d)$ (see Definition A.3 for the notion of $\mathrm{BVV}(\mathbf{I}^d)$), then, observing (35), we have under H_1 that*

$$\begin{aligned} \boldsymbol{\Sigma}^{-1/2}\mathbf{V}_{n_1\cdots n_d}\left(\mathbf{R}_{n_1\cdots n_d}\right) \xrightarrow{\mathscr{D}} \boldsymbol{\Sigma}^{-1/2}\left(\mathbf{I}_p - pr^*_{\prod_{i=1}^{p}\mathbf{W}_{i\mathscr{K}_B}}\right)\mathbf{h}_{\mathbf{g}} \\ + \mathbf{B}^{H_0}_{p,\mathbf{f}}, \end{aligned} \tag{36}$$

where $\mathbf{h}_{\mathbf{g}} \coloneqq (h_{g_i})_{i=1}^p : \mathscr{A} \to \mathscr{C}^p(\mathscr{A})$, with $h_{g_i}(A) \coloneqq \int_A g_i(\mathbf{t})\lambda^d_{\mathbf{I}}(d\mathbf{t})$.

Proof. Considering the linearity of $\mathbf{V}_{n_1\cdots n_d}$ and Lemma C.2, when H_1 is true we have

$$\begin{aligned} \boldsymbol{\Sigma}^{-1/2}\mathbf{V}_{n_1\cdots n_d}\left(\mathbf{R}_{n_1\cdots n_d}\right) &= \boldsymbol{\Sigma}^{-1/2}\frac{1}{\sqrt{n_1\cdots n_d}} \\ &\cdot \mathbf{V}_{n_1\cdots n_d}\left(\mathbf{g}\left(\Xi_{n_1\cdots n_d}\right)\right) - \boldsymbol{\Sigma}^{-1/2}\mathrm{pr}_{\prod_{i=1}^{p}\mathbf{W}_{i,n_1\cdots n_d\mathscr{K}_B}} \\ &\cdot \frac{1}{\sqrt{n_1\cdots n_d}}\mathbf{V}_{n_1\cdots n_d}\left(\mathbf{g}\left(\Xi_{n_1\cdots n_d}\right)\right) \\ &+ \boldsymbol{\Sigma}^{-1/2}\mathbf{V}_{n_1\cdots n_d}\left(\mathscr{E}_{n_1\cdots n_d}\right) \\ &- \boldsymbol{\Sigma}^{-1/2}\mathrm{pr}_{\prod_{i=1}^{p}\mathbf{W}_{i,n_1\cdots n_d\mathscr{K}_B}}\mathbf{V}_{n_1\cdots n_d}\left(\mathscr{E}_{n_1\cdots n_d}\right). \end{aligned} \tag{37}$$

Since, for $i = 1, \ldots, p$, g_i is in $\mathrm{BVV}(\mathbf{I}^d)$, it can be shown that $(1/\sqrt{n_1\cdots n_d})\mathbf{V}_{n_1\cdots n_d}(\mathbf{g}(\Xi_{n_1\cdots n_d}))(B)$ converges uniformly to $\mathbf{h}_{\mathbf{g}}(B)$, for every $B \in \mathscr{A}$. Also the last two terms on the right-hand side of the preceding equation converge in distribution to $\mathbf{B}^{H_0}_{p,\mathbf{f}}$ by Theorem 1. Thus to the rest we only need to show that $\mathrm{pr}_{\prod_{i=1}^{p}\mathbf{W}_{i,n_1\cdots n_d\mathscr{K}_B}}(1/\sqrt{n_1\cdots n_d})\mathbf{V}_{n_1\cdots n_d}(\mathbf{g}_{n_1\cdots n_d})$ converges to $\mathrm{pr}^*_{\prod_{i=1}^{p}\mathbf{W}_{i\mathscr{K}_{\mathbf{B}_{\mathrm{BV}(\mathbf{I}^d)}}}}\mathbf{h}_{\mathbf{g}}$. By the definition of component-wise projection we have

$$\begin{aligned} \mathrm{pr}_{\prod_{i=1}^{p}\mathbf{W}_{i,n_1\cdots n_d\mathscr{K}_B}}\frac{1}{\sqrt{n_1\cdots n_d}}\mathbf{V}_{n_1\cdots n_d}\left(\mathbf{g}\left(\Xi_{n_1\cdots n_d}\right)\right) &= \left(\mathrm{pr}_{\mathbf{W}_{i,n_1\cdots n_d\mathscr{K}_B}}\frac{1}{\sqrt{n_1\cdots n_d}}\mathbf{V}^{(i)}_{n_1\cdots n_d}\left(\mathbf{g}_i\left(\Xi_{n_1\cdots n_d}\right)\right)\right)_{i=1}^p \\ &= \left(\sum_{j=1}^{d_i}\left(\int^{(R)}_{\mathbf{I}^d}\widetilde{s}^{(n_1\cdots n_d)}_{ij}(\mathbf{t})\,d\frac{1}{\sqrt{n_1\cdots n_d}}\mathbf{V}^{(i)}_{n_1\cdots n_d}\left(\mathbf{g}_i\left(\Xi_{n_1\cdots n_d}\right)\right)(\mathbf{t})\right)h_{\widetilde{s}^{(n_1\cdots n_d)}_{ij}}\right)_{i=1}^p \\ &= \left(\sum_{j=1}^{d_i}\left(\frac{1}{n_1\cdots n_d}\sum_{j_1=1}^{n_1}\cdots\sum_{j_d=1}^{n_d}\widetilde{s}^{(n_1\cdots n_d)}_{ij}\left(\frac{j_1}{n_1},\ldots,\frac{j_d}{n_d}\right)g_i\left(\frac{j_1}{n_1},\ldots,\frac{j_d}{n_d}\right)\right)h_{\widetilde{s}^{(n_1\cdots n_d)}_{ij}}\right)_{i=1}^p. \end{aligned} \tag{38}$$

The right-hand side of the last expression is obtained directly from the definition of the ordinary partial sums (11) and the definition of the Riemann-Stieltjes integral on $\mathbf{I}^d$. Since $\widetilde{s}^{(n_1\cdots n_d)}_{ij}$ converges uniformly to f_{ij} and g_i has bounded variation

on $\mathbf{I}^d$ for all i and j, then the last expression clearly converges component-wise to $(\sum_{j=1}^{d_i}(\int_{\mathbf{I}^d}^{(R)} f_{ij}(\mathbf{t})dh_{g_i}(\mathbf{t}))h_{f_{ij}})_{i=1}^p$, which can be written as $\mathrm{pr}^*_{\prod_{i=1}^p \mathbf{W}_{i\mathscr{K}_\mathbf{B}}}\mathbf{h}_\mathbf{g}$. We are done. □

Corollary 4. *By Theorem 3 the power function of the KS and CvM tests at a level α can now be approximated by computing the probabilities of the form*

$$\begin{aligned}
&\mathbf{P}\left\{\sup_{A\in\mathscr{A}}\left\|\boldsymbol{\Sigma}^{-1/2}\left(\mathbf{h}_\mathbf{g}-pr^*_{\prod_{i=1}^p \mathbf{W}_{i\mathscr{K}_{\mathbf{B}_{\mathrm{BV}(\mathbf{I}^d)}}}}\mathbf{h}_\mathbf{g}\right)+\mathbf{B}^{H_0}_{p,\mathbf{f}}\right\|_{\mathbb{R}^p}\right.\\
&\qquad\left.\geq \widetilde{t}_{1-\alpha}\right\}\\
&\mathbf{P}\left\{\int_\mathbf{I}\left\|\boldsymbol{\Sigma}^{-1/2}\left(\mathbf{h}_\mathbf{g}-pr^*_{\prod_{i=1}^p \mathbf{W}_{i\mathscr{K}_{\mathbf{B}_{\mathrm{BV}(\mathbf{I}^d)}}}}\mathbf{h}_\mathbf{g}\right)+\mathbf{B}^{H_0}_{p,\mathbf{f}}\right\|^2_{\mathbb{R}^p}dA\right.\\
&\qquad\left.\geq \widetilde{c}_{1-\alpha}\right\},
\end{aligned}\tag{39}$$

for a fixed $\mathbf{g}\in\prod_{i=1}^p \mathrm{BVV}(\mathbf{I}^d)$, respectively. In Section 5 we investigate the empirical power functions of the KS and CvM tests by simulation.

4. Estimating the Population Covariance Matrix

If the covariance matrix $\boldsymbol{\Sigma}$ is unknown, as it usually is, it is impossible to use $\mathrm{KS}_{n_1\cdots n_d;\mathscr{A}}$ and $\mathrm{CvM}_{n_1\cdots n_d;\mathscr{A}}$ in practice. What we propose to do is to employ a consistent estimate of $\boldsymbol{\Sigma}$. We need some further notations for expressing the residuals of the model. For $i=1,\ldots,p$, let $Z_i^{(n_1\cdots n_d)}$, $g_i^{(n_1\cdots n_d)}$, and $\varepsilon_i^{(n_1\cdots n_d)}$ be $(n_1\cdots n_d)$-dimensional column vectors defined by

$$\begin{aligned}
Z_i^{(n_1\cdots n_d)} &:= \left(Z_i\left(\frac{j_1}{n_1},\ldots,\frac{j_d}{n_d}\right)\right)_{j_1=1,\ldots,j_d=1}^{n_1,\ldots,n_d}\in\mathbb{R}^{n_1\cdots n_d}\\
g_i^{(n_1\cdots n_d)} &:= \left(g_i\left(\frac{j_1}{n_1},\ldots,\frac{j_d}{n_d}\right)\right)_{j_1=1,\ldots,j_d=1}^{n_1,\ldots,n_d}\in\mathbb{R}^{n_1\cdots n_d}\\
\varepsilon_i^{(n_1\cdots n_d)} &:= \left(\varepsilon_i\left(\frac{j_1}{n_1},\ldots,\frac{j_d}{n_d}\right)\right)_{j_1=1,\ldots,j_d=1}^{n_1,\ldots,n_d}\in\mathbb{R}^{n_1\cdots n_d}.
\end{aligned}\tag{40}$$

Furthermore, let $\mathbf{Z}^{(n_1\cdots n_d)}$, $\mathbf{g}^{(n_1\cdots n_d)}$, and $\mathscr{E}^{(n_1\cdots n_d)}$ be $(n_1\cdots n_d)\times p$-dimensional matrices whose ith column is given, respectively, by the column vectors $Z_i^{(n_1\cdots n_d)}$, $g_i^{(n_1\cdots n_d)}$, and $\varepsilon_i^{(n_1\cdots n_d)}$, $i=1,\ldots,p$. Then Model (35) can also be represented as follows:

$$\mathbf{Z}^{(n_1\cdots n_d)} = \frac{1}{\sqrt{n_1\cdots n_d}}\mathbf{g}^{(n_1\cdots n_d)}+\mathscr{E}^{(n_1\cdots n_d)},\tag{41}$$

where, for $u,v=1,\ldots,p$, $\mathrm{Cov}(\varepsilon_u^{(n_1\cdots n_d)},\varepsilon_v^{(n_1\cdots n_d)})=\sigma_{uv}\mathbf{I}_{n_1\cdots n_d}$, with $\mathbf{I}_{n_1\cdots n_d}$ being the identity matrix in $\mathbb{R}^{(n_1\cdots n_d)\times(n_1\cdots n_d)}$.

Associated with the subspace $\mathbf{W}_{i,n_1\cdots n_d}$ we define the design matrix $\mathbf{X}_i^{(n_1\cdots n_d)}$ as an element of $\mathbb{R}^{(n_1\cdots n_d)\times d_i}$ whose uth column is given by the $(n_1\cdots n_d)$-dimensional column vector:

$$\left(f_{iu}\left(\frac{j_1}{n_1},\ldots,\frac{j_d}{n_d}\right)\right)_{j_1=1,\ldots,j_d=1}^{n_1,\ldots,n_d}\in\mathbb{R}^{n_1\cdots n_d},\quad u=1,\ldots,d_i,\ i=1,\ldots,p.\tag{42}$$

We denote the column space of $\mathbf{X}_i^{(n_1\cdots n_d)}$ by $\mathscr{C}(\mathbf{X}_i^{(n_1\cdots n_d)})\subset\mathbb{R}^{(n_1\cdots n_d)\times d_i}$ for the sake of brevity. We also define the column-wise projection of any matrix $\mathbf{U}^{(n_1\cdots n_d)}:=(U_1^{(n_1\cdots n_d)},\ldots,U_p^{(n_1\cdots n_d)})$ in $\mathbb{R}^{n_1\cdots n_d\times p}$ into the product space $\prod_{i=1}^p\mathscr{C}(\mathbf{X}_i^{(n_1\cdots n_d)})$ by

$$\begin{aligned}
&\mathrm{pr}_{\prod_{i=1}^p\mathscr{C}(\mathbf{X}_i^{(n_1\cdots n_d)})}\mathbf{U}^{(n_1\cdots n_d)}\\
&\quad:=\left(\mathrm{pr}_{\mathscr{C}(\mathbf{X}_1^{(n_1\cdots n_d)})}U_1^{(n_1\cdots n_d)},\ldots,\mathrm{pr}_{\mathscr{C}(\mathbf{X}_p^{(n_1\cdots n_d)})}U_p^{(n_1\cdots n_d)}\right).
\end{aligned}\tag{43}$$

A reasonable estimator of the covariance matrix $\boldsymbol{\Sigma}$ is denoted by $\widehat{\boldsymbol{\Sigma}}_{n_1\cdots n_d}$, defined by

$$\begin{aligned}
\widehat{\boldsymbol{\Sigma}}_{n_1\cdots n_d} &:= \frac{1}{n_1\cdots n_d}\left(\mathrm{pr}_{\prod_{i=1}^p\mathscr{C}(\mathbf{X}_i^{(n_1\cdots n_d)})^\perp}\mathbf{Z}^{(n_1\cdots n_d)}\right)^\top\\
&\quad\cdot\left(\mathrm{pr}_{\prod_{i=1}^p\mathscr{C}(\mathbf{X}_i^{(n_1\cdots n_d)})^\perp}\mathbf{Z}^{(n_1\cdots n_d)}\right),
\end{aligned}\tag{44}$$

where

$$\mathrm{pr}_{\prod_{i=1}^p\mathscr{C}(\mathbf{X}_i^{(n_1\cdots n_d)})^\perp}:=\mathbf{I}_{n_1\cdots n_d}-\mathrm{pr}_{\prod_{i=1}^p\mathscr{C}(\mathbf{X}_i^{(n_1\cdots n_d)})}\tag{45}$$

constitutes the component-wise orthogonal projector into the orthogonal complement of the product space $\prod_{i=1}^p\mathscr{C}(\mathbf{X}_i^{(n_1\cdots n_d)})$.

Zellner [1] and Arnold [22] investigated the consistency of $\widehat{\boldsymbol{\Sigma}}_{n_1\cdots n_d}$ toward $\boldsymbol{\Sigma}$ in the case of the multivariate regression model with $\mathbf{W}_1=\cdots=\mathbf{W}_p$. Some difficulties appear when the situation is extended to the case of $\mathbf{W}_1\neq\cdots\neq\mathbf{W}_p$, since it involves the problem of finding the limit of matrices with the components given by inner products of two vectors.

Theorem 5. *Suppose the localized model (41) is observed. If H_0 is true, then, under the conditions of Theorem 1, we have $\widehat{\boldsymbol{\Sigma}}_{n_1\cdots n_d}\xrightarrow{\mathscr{P}}\boldsymbol{\Sigma}$.*

Proof. If H_0 is true, it can be easily shown that

$$\begin{aligned}
(n_1\cdots n_d)\,\widehat{\boldsymbol{\Sigma}}_{n_1\cdots n_d} &= \left(\mathrm{pr}_{\prod_{i=1}^p\mathscr{C}(\mathbf{X}_i^{(n_1\cdots n_d)})^\perp}\mathscr{E}^{(n_1\cdots n_d)}\right)^\top\\
&\quad\cdot\left(\mathrm{pr}_{\prod_{i=1}^p\mathscr{C}(\mathbf{X}_i^{(n_1\cdots n_d)})^\perp}\mathscr{E}^{(n_1\cdots n_d)}\right).
\end{aligned}\tag{46}$$

For technical reason we assume without lost of generality that $\mathbf{X}_i^{(n_1\cdots n_d)}$ is an orthogonal matrix, for $i = 1,\ldots,p$. Hence we further get the representation

$$\begin{aligned}
&(n_1\cdots n_d)\,\widehat{\boldsymbol{\Sigma}}_{n_1\cdots n_d}\\
&= \left(\boldsymbol{\varepsilon}_u^{(n_1\cdots n_d)\top}\boldsymbol{\varepsilon}_v^{(n_1\cdots n_d)}\right)_{u,v=1}^{p,p}\\
&\quad - \left(\left(\mathbf{X}_v^{(n_1\cdots n_d)\top}\boldsymbol{\varepsilon}_u^{(n_1\cdots n_d)}\right)^{\top}\left(\mathbf{X}_v^{(n_1\cdots n_d)\top}\boldsymbol{\varepsilon}_v^{(n_1\cdots n_d)}\right)\right)_{u,v=1}^{p,p}\\
&\quad - \left(\left(\mathbf{X}_u^{(n_1\cdots n_d)\top}\boldsymbol{\varepsilon}_u^{(n_1\cdots n_d)}\right)^{\top}\left(\mathbf{X}_u^{n_1\cdots n_d\top}\boldsymbol{\varepsilon}_v^{(n_1\cdots n_d)}\right)\right)_{u,v=1}^{p,p}\\
&\quad + \left(\left(\mathbf{X}_u^{(n_1\cdots n_d)\top}\boldsymbol{\varepsilon}_u^{(n_1\cdots n_d)}\right)^{\top}\left(\mathbf{X}_v^{(n_1\cdots n_d)\top}\boldsymbol{\varepsilon}_v^{(n_1\cdots n_d)}\right)\right)_{u,v=1}^{p,p}.
\end{aligned} \tag{47}$$

Since $(\boldsymbol{\varepsilon}_u(j_1/n_1,\ldots,j_d/n_d)\boldsymbol{\varepsilon}_v(j_1/n_1,\ldots,j_d/n_d))_{u,v=1}^{p,p}$ are independent and identically distributed random matrices with mean $\boldsymbol{\Sigma}$, by the well-known weak law of large numbers, we get

$$\begin{aligned}
&\frac{1}{n_1\cdots n_d}\sum_{j_1=1}^{n_1}\cdots\sum_{j_d=1}^{n_d}\left(\boldsymbol{\varepsilon}_u\left(\frac{j_1}{n_1},\ldots,\frac{j_d}{n_d}\right)\right.\\
&\left.\cdot\,\boldsymbol{\varepsilon}_v\left(\frac{j_1}{n_1},\ldots,\frac{j_d}{n_d}\right)\right)_{u,v=1}^{p,p}\xrightarrow{\mathscr{P}}\boldsymbol{\Sigma}.
\end{aligned} \tag{48}$$

Note that in the practice we consider the polynomial regression model. Hence, for every $v = 1,\ldots,p$, the design matrix $\mathbf{X}_v^{(n_1\cdots n_d)}$ satisfies the so-called Huber condition (cf. Pruscha [31], pp. 115–117). By this reason, for the rest of the terms, we can immediately apply the technique proposed in Arnold [22] to show $\mathbf{X}_v^{(n_1\cdots n_d)\top}\boldsymbol{\varepsilon}_u^{(n_1\cdots n_d)}\xrightarrow{\mathscr{D}}N_{d_v}(\mathbf{0},\sigma_{uu}\mathbf{I}_{d_v})$, for all $u,v = 1,\ldots,p$. Therefore, we finally get the following component-wise convergence:

$$\begin{aligned}
&\frac{1}{n_1\cdots n_d}\left(\left(\mathbf{X}_v^{(n_1\cdots n_d)\top}\boldsymbol{\varepsilon}_u^{(n_1\cdots n_d)}\right)^{\top}\right.\\
&\left.\cdot\left(\mathbf{X}_v^{(n_1\cdots n_d)\top}\boldsymbol{\varepsilon}_v^{(n_1\cdots n_d)}\right)\right)_{u,v=1}^{p,p}\xrightarrow{\mathscr{P}}\mathbf{O}_{p\times p}\\
&\frac{1}{n_1\cdots n_d}\left(\left(\mathbf{X}_u^{(n_1\cdots n_d)\top}\boldsymbol{\varepsilon}_u^{(n_1\cdots n_d)}\right)^{\top}\right.\\
&\left.\cdot\left(\mathbf{X}_u^{(n_1\cdots n_d)\top}\boldsymbol{\varepsilon}_v^{(n_1\cdots n_d)}\right)\right)_{u,v=1}^{p,p}\xrightarrow{\mathscr{P}}\mathbf{O}_{p\times p}\\
&\frac{1}{n_1\cdots n_d}\left(\left(\mathbf{X}_u^{(n_1\cdots n_d)\top}\boldsymbol{\varepsilon}_u^{(n_1\cdots n_d)}\right)^{\top}\right.\\
&\left.\cdot\left(\mathbf{X}_v^{(n_1\cdots n_d)\top}\boldsymbol{\varepsilon}_v^{(n_1\cdots n_d)}\right)\right)_{u,v=1}^{p,p}\xrightarrow{\mathscr{P}}\mathbf{O}_{p\times p},
\end{aligned} \tag{49}$$

where $\mathbf{O}_{p\times p}$ is the $p\times p$-zero matrix. □

Remark 6. Since $\widehat{\boldsymbol{\Sigma}}_{n_1\cdots n_d}^{-1/2}\mathbf{V}_{n_1\cdots n_d}(\mathbf{R}_{n_1\cdots n_d}) = \widehat{\boldsymbol{\Sigma}}_{n_1\cdots n_d}^{-1/2}\boldsymbol{\Sigma}^{1/2}\boldsymbol{\Sigma}^{-1/2}\mathbf{V}_{n_1\cdots n_d}(\mathbf{R}_{n_1\cdots n_d})$, without altering the convergence result presented in Theorem 1, the population variance-covariance matrix $\boldsymbol{\Sigma}$ can be directly replaced by the consistence estimator $\widehat{\boldsymbol{\Sigma}}_{n_1\cdots n_d}$.

5. Calibration of the Tests

The limits of the test statistics are not distribution-free and we need therefore calibration for the distribution of the statistical tests. For the calibration we adapted the idea of residual based bootstrap for multivariate regression studied in Shao and Tu [32] for approximating the distributions of $\mathrm{KS}_{n_1\cdots n_d,\mathscr{A}}$ and $\mathrm{CvM}_{n_1\cdots n_d,\mathscr{A}}$.

For fixed $n_1,\ldots,n_d$, let $F_{n_1\cdots n_d}$ be the empirical distribution function of the vectors of least squares residuals $\{\mathbf{r}_{j_1\cdots j_d}-\overline{\mathbf{R}}_{n_1\cdots n_d} : 1\le j_k\le n_k,\ k = 1,\ldots,d\}$ centered at zero vector, where $\overline{\mathbf{R}}_{n_1\cdots n_d} := (1/(n_1\cdots n_d))\sum_{j_1=1}^{n_1}\cdots\sum_{j_d=1}^{n_d}\mathbf{r}_{j_1\cdots j_d}$. Let $\mathscr{E}_{n_1\cdots n_d}^* := (\mathscr{E}_{j_1\cdots j_d}^*)_{j_1=1,\ldots,j_d=1}^{n_1,\ldots,n_d}$ be an array of independent and identically distributed random vectors sampled from $F_{n_1\cdots n_d}$ and let $\widehat{\mathbf{g}}(\Xi_{n_1\cdots n_d})$ be the ordinary LSE of $\mathbf{g}(\Xi_{n_1\cdots n_d})$, where $\widehat{\mathbf{g}}(\Xi_{n_1\cdots n_d}) = \mathrm{pr}_{\prod_{i=1}^p\mathbf{w}_i}\mathbf{Z}_{n_1\cdots n_d}$. Then we generate the array of p-dimensional bootstrap observations which is denoted in this paper by $\mathbf{Z}_{n_1\cdots n_d}^* := (\mathbf{Z}_{j_1\cdots j_d}^*)_{j_1=1,\ldots,j_d=1}^{n_1,\ldots,n_d}$ through the model:

$$\mathbf{Z}_{n_1\cdots n_d}^* = \mathrm{pr}_{\prod_{i=1}^p\mathbf{w}_i}\mathbf{Z}_{n_1\cdots n_d} + \mathscr{E}_{n_1\cdots n_d}^*. \tag{50}$$

Based on this model we get the array of p-dimensional bootstrap least squares residuals which is given by the component-wise projection of the bootstrap observations:

$$\begin{aligned}
\mathbf{R}_{n_1\cdots n_d}^* &:= \left(\mathbf{r}_{j_1\cdots j_d}^*\right)_{j_1=1,\ldots,j_d=1}^{n_1,\ldots,n_d}\\
&= \mathbf{Z}_{n_1\cdots n_d}^* - \mathrm{pr}_{\prod_{i=1}^p\mathbf{w}_i}\mathbf{Z}_{n_1\cdots n_d}^*.
\end{aligned} \tag{51}$$

Hence, the bootstrap analog of $\mathrm{KS}_{n_1\cdots n_d,\mathscr{A}}$ and $\mathrm{CvM}_{n_1\cdots n_d,\mathscr{A}}$ is

$$\begin{aligned}
&\mathrm{KS}_{n_1\cdots n_d,\mathscr{A}}^* := \sup_{A\in\mathscr{A}}\left\|\widehat{\boldsymbol{\Sigma}}_{n_1\cdots n_d}^{*-1/2}\mathbf{V}_{n_1\cdots n_d}\left(\mathbf{R}_{n_1\cdots n_d}^*\right)(A)\right\|_{\mathbb{R}^p}\\
&\mathrm{CvM}_{n_1\cdots n_d,\mathscr{A}}^*\\
&\quad := \frac{1}{n_1\cdots n_d}\sum_{A\in\mathscr{A}}\left\|\widehat{\boldsymbol{\Sigma}}_{n_1\cdots n_d}^{*-1/2}\mathbf{V}_{n_1\cdots n_d}\left(\mathbf{R}_{n_1\cdots n_d}^*\right)(A)\right\|_{\mathbb{R}^p}^2,
\end{aligned} \tag{52}$$

where

$$\begin{aligned}
\widehat{\boldsymbol{\Sigma}}_{n_1\cdots n_d}^* &:= \frac{1}{n_1\cdots n_d}\left(\mathrm{pr}_{\prod_{i=1}^p\mathscr{C}(\mathbf{x}_i^{(n_1\cdots n_d)})^{\perp}}\mathbf{Z}^{*(n_1\cdots n_d)}\right)^{\top}\\
&\quad\cdot\left(\mathrm{pr}_{\prod_{i=1}^p\mathscr{C}(\mathbf{x}_i^{(n_1\cdots n_d)})^{\perp}}\mathbf{Z}^{*(n_1\cdots n_d)}\right).
\end{aligned} \tag{53}$$

The question regarding the consistency of the bootstrap approximation of the p-dimensional processes $\widehat{\boldsymbol{\Sigma}}_{n_1\cdots n_d}^{*-1/2}\mathbf{V}_{n_1\cdots n_d}(\mathbf{R}_{n_1\cdots n_d}^*)(A)$ for $\widehat{\boldsymbol{\Sigma}}_{n_1\cdots n_d}^{-1/2}\mathbf{V}_{n_1\cdots n_d}(\mathbf{R}_{n_1\cdots n_d})(A)$ is summarized in the following theorem.

Theorem 7. *Let $\{f_{i1}, \ldots, f_{id_i}\}$ be an ONB of $\mathbf{W}_i$, for $i = 1, \ldots, p$. Suppose the conditions of Theorem 1 are fulfilled. Then under H_0 it holds that*

$$\boldsymbol{\Sigma}^{*-1/2}\mathbf{V}_{n_1\cdots n_d}\left(\mathbf{R}^*_{n_1\cdots n_d}\right) \xrightarrow{\mathscr{D}} \mathbf{B}_p - pr^*_{\prod_{i=1}^p \mathbf{W}_{i\mathscr{K}_B}}\mathbf{B}_p, \tag{54}$$

where $pr^*_{\prod_{i=1}^p \mathbf{W}_{i\mathscr{K}_B}}\mathbf{B}_p$ is defined in Theorem 1.

Proof. We notice that $\{\mathscr{E}^*_{j_1\cdots j_d} : 1 \le j_k \le n_k, k = 1, \ldots, d\}$ are independent and identically distributed with $E_*(\mathscr{E}^*_{1\cdots 1}) = \mathbf{0}$ and $\mathrm{Cov}_*(\mathscr{E}^*_{1\cdots 1}) = \widehat{\boldsymbol{\Sigma}}_{n_1\cdots n_d} - \overline{\mathbf{R}}_{n_1\cdots n_d}\overline{\mathbf{R}}^\top_{n_1\cdots n_d}$. Hence, the invariance principle implies that $(\widehat{\boldsymbol{\Sigma}}_{n_1\cdots n_d} - \overline{\mathbf{R}}_{n_1\cdots n_d}\overline{\mathbf{R}}^\top_{n_1\cdots n_d})^{-1/2}\mathbf{V}_{n_1\cdots n_d}(\mathscr{E}^*_{n_1\cdots n_d})$ converges in distribution to $\mathbf{B}_p$. Hence under H_0 we have $\mathbf{R}^*_{n_1\cdots n_d} = \mathscr{E}^*_{n_1\cdots n_d} - \mathrm{pr}_{\prod_{i=1}^p \mathbf{W}_i}\mathscr{E}^*_{n_1\cdots n_d}$ and $\boldsymbol{\Sigma}^{*-1/2}_{n_1\cdots n_d}$ can be written as

$$\begin{aligned}\boldsymbol{\Sigma}^{*-1/2}_{n_1\cdots n_d} = \boldsymbol{\Sigma}^{*-1/2}_{n_1\cdots n_d}&\left(\widehat{\boldsymbol{\Sigma}}_{n_1\cdots n_d} - \overline{\mathbf{R}}_{n_1\cdots n_d}\overline{\mathbf{R}}^\top_{n_1\cdots n_d}\right)^{1/2}\\ &\cdot\left(\widehat{\boldsymbol{\Sigma}}_{n_1\cdots n_d} - \overline{\mathbf{R}}_{n_1\cdots n_d}\overline{\mathbf{R}}^\top_{n_1\cdots n_d}\right)^{-1/2},\end{aligned} \tag{55}$$

where it can be shown easily that

$$\begin{aligned}\overline{\mathbf{R}}_{n_1\cdots n_d}\overline{\mathbf{R}}^\top_{n_1\cdots n_d} &= o_{\mathscr{P}}(1),\\ E_*\left(\widehat{\boldsymbol{\Sigma}}^*_{n_1\cdots n_d}\right) &= \widehat{\boldsymbol{\Sigma}}_{n_1\cdots n_d} + o_{\mathscr{P}}(1),\end{aligned} \tag{56}$$

with $o_{\mathscr{P}}(1)$ being the collection of the terms converging in probability to $\mathbf{O}_{p\times p}$. Then by recalling Theorem 5 and the linearity of $\mathbf{V}_{n_1\cdots n_d}$ we only need to show that

$$\left(\widehat{\boldsymbol{\Sigma}}_{n_1\cdots n_d} - \overline{\mathbf{R}}_{n_1\cdots n_d}\overline{\mathbf{R}}^\top_{n_1\cdots n_d}\right)^{-1/2}\mathbf{V}_{n_1\cdots n_d}\left(\mathrm{pr}_{\prod_{i=1}^p \mathbf{W}_i}\mathscr{E}^*_{n_1\cdots n_d}\right) \xrightarrow{\mathscr{D}} \mathrm{pr}^*_{\prod_{i=1}^p \mathbf{W}_{i\mathscr{K}_B}}\mathbf{B}_p. \tag{57}$$

The proof is established by imitating the steps of proving convergence result of Theorem 1. We are done. □

6. Simulation Study

In this section, we report on a simulation study designed to investigate the finite sample size behavior of the KS and CvM tests. We simulate a multivariate model with four components defined on the unit rectangle $\mathbf{I}^2$. The hypothesis under study is $H_0 : \mathbf{g} \in \prod_{i=1}^4 \mathbf{W}_i$ against $H_1 : \mathbf{g} \notin \prod_{i=1}^4 \mathbf{W}_i$, where $\mathbf{W}_1 := [f_1]$, $\mathbf{W}_2 := [f_1, f_2, f_3]$, $\mathbf{W}_3 := [f_1, f_2, f_3, f_4, f_5, f_6]$, and $\mathbf{W}_4 := [f_1, f_2, f_3, f_4, f_5, f_6, f_7]$. Thereby we define $f_1(t,s) := 1$, $f_2(t,s) = t$, $f_3(t,s) = s$, $f_4(t,s) = t^2$, $f_5(t,s) = s^2$, $f_6(t,s) = ts$, and $f_7(t,s) = t^3$, for $(t,s) \in \mathbf{I}^2$. The samples are generated from a localized model $\mathbf{Y}(\ell/n_1, k/n_2) = (1/\sqrt{n_1 n_2})\mathbf{g}(\ell/n_1, k/n_2) + \mathscr{E}(\ell/n_1, k/n_2)$ under the experimental design given by $\Xi_{n_1\times n_2} = \{(\ell/n_1, k/n_2) \in \mathbf{I}^2 : 1 \le \ell \le n_1,\ 1 \le k \le n_2\}$, where $\mathbf{g}(\ell/n_1, k/n_2)$ is defined as

$$\mathbf{g}\left(\frac{\ell}{n_1}, \frac{k}{n_2}\right) := \begin{pmatrix} 5 + \rho\exp\left\{\dfrac{\ell}{n_1}\dfrac{k}{n_2}\right\} \\ 10 - 5\dfrac{\ell}{n_1} + 10\dfrac{k}{n_2} + \gamma\exp\left\{\dfrac{\ell}{n_1}\dfrac{k}{n_2}\right\} \\ 10 + 20\dfrac{\ell}{n_1} - 25\dfrac{k}{n_2} + 10\dfrac{\ell^2}{n_1^2} - 5\dfrac{k^2}{n_2^2} + 20\dfrac{\ell}{n_1}\dfrac{k}{n_2} + \delta\exp\left\{\dfrac{\ell}{n_1}\dfrac{k}{n_2}\right\} \\ 30 - 30\dfrac{\ell}{n_1} - 5\dfrac{k}{n_2} + 20\dfrac{\ell^2}{n_1^2} - 15\dfrac{k^2}{n_2^2} + 10\dfrac{\ell}{n_1}\dfrac{k}{n_2} + 10\dfrac{\ell^3}{n_1^3} + \kappa\exp\left\{\dfrac{\ell}{n_1}\dfrac{k}{n_2}\right\} \end{pmatrix}, \tag{58}$$

for constants ρ, γ, δ, and κ determined prior to the generation of the samples. For fixed n_1 and n_2 and $1 \le \ell \le n_1$ and $1 \le k \le n_2$ the vector of random errors $\mathscr{E}(\ell/n_1, k/n_2)$ is generated independently from the 4-variate normal distribution with mean zero and variance-covariance matrix given by

$$\boldsymbol{\Sigma}_{4\times 4} := \begin{pmatrix} 9 & 3 & -6 & 12 \\ 3 & 26 & -7 & -11 \\ -6 & -7 & 9 & 7 \\ 12 & -11 & 7 & 65 \end{pmatrix}; \tag{59}$$

however, we assume in the computation that $\boldsymbol{\Sigma}_{4\times 4}$ is unknown. It is therefore estimated using $\widehat{\boldsymbol{\Sigma}}_{n_1 n_2}$ defined in Section 4. It is important to note that for computational reason we restricted the index set to the Vapnick Chervonenkis Classes (VCC) of subsets of $\mathbf{I}^2$ which is given by the family of closed rectangle with the point $(0,0)$ as the essential point. That is, the family $\{[0,t]\times[0,s] : 0 \le t, s \le 1\}$.

When ρ, γ, δ, and κ are set simultaneously to zero then we get the samples which coincide to the model specified under H_0. Conversely, when at least one of them takes a nonzero value then we obtain the samples which can be regarded as from the alternative whose corresponding samples are generated by assigning nonzero values to either one of the constants, ρ, γ, δ, and κ, or the combinations of them.

Table 1 presents the empirical probabilities of rejection of H_0 for $\alpha = 0.05$ and some selected values of ρ, γ, δ, and κ. The empirical powers of the KS and CvM tests are denoted by $\widehat{\alpha}_{\mathrm{KS}}$ and $\widehat{\alpha}_{\mathrm{CvM}}$, respectively. The notations $\widehat{\sigma}_{\mathrm{KS}}$ and $\widehat{\sigma}_{\mathrm{CvM}}$ stand, respectively, for the standard deviation of the samples. The critical values of the statistics $\mathrm{KS}_{n_1,n_2;\mathscr{A}}$ and $\mathrm{CvM}_{n_1,n_2;\mathscr{A}}$ are

Table 1: The empirical probabilities of rejection of the KS and CvM tests for several selected values of ρ, γ, δ, and κ. The sample sizes are selected to 35×40 and 50×60. The simulation results are based on 10000 runs.

Sample size	ρ	γ	δ	κ	$\widehat{\alpha}_{\mathrm{KS}}$	$\widehat{\sigma}_{\mathrm{KS}}$	$\widehat{\alpha}_{\mathrm{CvM}}$	$\widehat{\sigma}_{\mathrm{CvM}}$
	0	0	0	0	4.90%	1.31299	4.60%	2.52127
	10	0	0	0	10.60%	1.52902	11.28%	4.11538
	20	0	0	0	32.80%	1.71455	33.40%	6.26419
	40	0	0	0	88.64%	1.86015	87.22%	10.37546
	0	50	0	0	5.03%	1.28540	5.33%	2.63926
	0	200	0	0	4.43%	1.22630	5.90%	2.57881
	0	300	0	0	4.60%	1.18783	7.03%	2.52180
	0	500	0	0	4.63%	0.90516	11.00%	2.32439
	0	0	50	0	4.83%	1.27888	5.03%	2.59347
	0	0	100	0	5.17%	1.29476	5.20%	2.68005
	0	0	200	0	6.03%	1.28627	5.23%	2.53931
	0	0	500	0	8.23%	1.27694	7.73%	2.71275
	0	0	0	50	5.00%	1.27241	5.03%	2.69462
35×40	0	0	0	100	4.77%	1.23645	4.63%	2.56912
	0	0	0	300	4.77%	1.27318	5.07%	2.53470
	0	0	0	500	4.97%	1.26322	4.97%	2.55223
	10	50	0	0	11.34%	1.55144	12.22%	3.82300
	10	100	0	0	11.12%	1.49017	12.70%	3.81009
	10	200	0	0	11.20%	1.52118	12.06%	3.71303
	10	500	0	0	12.46%	1.10222	22.44%	2.87591
	20	50	50	50	32.78%	1.76263	33.62%	5.75683
	20	50	100	50	31.80%	1.71323	32.52%	5.98971
	20	50	200	50	28.16%	1.68594	29.16%	5.79669
	20	50	500	50	27.08%	1.52512	28.86%	4.92925
	50	50	50	20	98.60%	1.86506	97.60%	13.43552
	50	50	50	40	98.60%	1.83424	97.95%	13.10968
	50	50	50	60	98.55%	1.91241	98.25%	13.49794
	0	0	0	0	4.75%	1.26388	4.55%	2.52770
	10	0	0	0	11.35%	1.48925	11.40%	3.70839
	20	0	0	0	33.65%	1.75109	33.40%	5.82381
	30	0	0	0	65.70%	1.82802	64.90%	8.31756
	0	50	0	0	4.70%	1.26907	4.95%	2.60854
	0	200	0	0	4.75%	1.23471	5.90%	2.53725
	0	300	0	0	5.35%	1.19808	7.35%	2.62291
	0	0	50	0	0.0485	1.27867	5.15%	2.57206
	0	0	100	0	4.35%	1.23893	4.45%	2.40576
	0	0	200	0	5.80%	1.27524	5.50%	2.62313
	0	0	500	0	8.45%	1.28708	6.50%	2.64556
	0	0	0	50	5.00%	1.28525	4.85%	2.71581
50×60	0	0	0	100	4.50%	1.25700	4.70%	2.57227
	0	0	0	500	4.70%	1.25102	5.10%	2.51076
	20	50	0	0	32.10%	1.70264	32.30%	5.72887
	20	100	0	0	33.55%	1.74878	32.50%	5.76105
	20	200	0	0	33.30%	1.72065	34.35%	5.71531
	20	500	0	0	33.90%	1.61848	46.30%	5.77714
	30	50	100	0	62.55%	1.78912	61.80%	8.08037
	30	50	200	0	60.50%	1.79929	58.60%	7.76765
	30	50	500	0	56.35%	1.78203	54.00%	7.76498
	20	20	20	20	32.55%	1.70930	33.05%	5.60510
	30	50	50	50	63.10%	1.86549	61.65%	8.63149
	50	50	50	50	97.75%	1.88146	97.10%	13.27029
	50	100	50	50	97.60%	1.89668	96.90%	13.30456

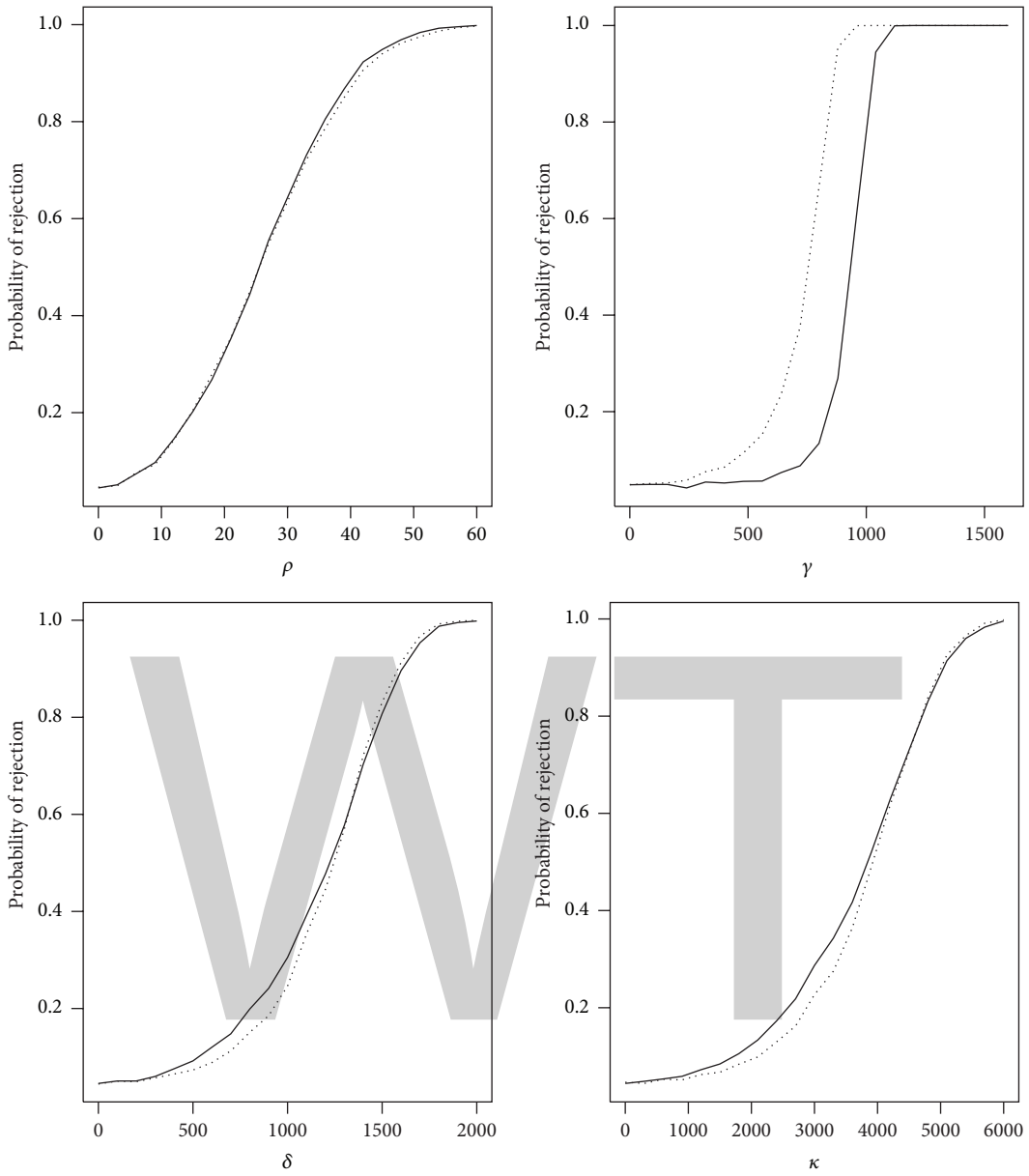

Figure 1: The empirical power functions of the KS test (smooth line) and CvM test (dotted line) for the 4-variate model using 50×60-point regular lattice. The simulation is under 10000 runs.

6.0742 and 7.9910 which are approximated by simulation. For $\rho = \gamma = \delta = \kappa = 0$ the values of $\widehat{\alpha}_{\mathrm{KS}}$ and $\widehat{\alpha}_{\mathrm{CvM}}$ fluctuate around 0.05 as it should be. This means that, independent of the selected number of the lattice points, both tests attain the specified level of significance.

Furthermore, Figure 1 exhibits the graphs of the empirical power function of the KS and CvM tests for $\alpha = 0.05$ associated with hypothesis H_0 specified above against $H_1 : g_i \notin \mathbf{W}_i$, for $i = 1, 2, 3, 4$. For the four cases we generate the error vectors independently from the same 4-variate normal distribution mentioned above. In the clockwise direction the left-top panel presents the graphs of the power function for testing H_0 against $H_1 : g_1 \notin \mathbf{W}_1$, the right-top panel is for H_0 against $H_1 : g_2 \notin \mathbf{W}_2$, the right-bottom is for H_0 against $H_1 : g_3 \notin \mathbf{W}_3$, and left-bottom is for H_0 against $H_1 : g_4 \notin \mathbf{W}_4$. The common characteristic of the tests is that the power gets larger as the the model moves away from H_0. The KS tests represented by smooth line tend to have slightly larger power. However, somewhat unexpectedly, in the second case, the CvM test has much larger power.

7. Example of Application

In this example, the proposed method is applied to a mining data studied in Tahir [20]. As introduced in Section 1, the data consist of a simultaneous measurement of the percentages of Nickel (Ni), Cobalt (Co), Ferum (Fe), and other substances like Calcium-Monoxide (CaO), Silicon-Dioxide (SiO_2), and

Table 2: Pearson's correlation matrix of the percentages of CaO, log SiO_2, log MgO, Ni, log Fe, and Co observed over a regular lattice of size 7×14. Source of data: Tahir [20].

	CaO	log SiO_2	log MgO	Ni	log Fe	Co
CaO	1.0000	0.3949	0.4045	−0.1285	−0.1167	−0.0665
log SiO_2	0.3949	1.0000	0.8459	−0.0003	−0.5414	−0.4556
log MgO	0.4045	0.8459	1.0000	−0.1331	−0.4968	−0.3134
Ni	−0.1285	−0.0003	−0.1331	1.0000	0.1652	0.1068
log Fe	−0.1166	−0.5414	−0.4968	0.1652	1.0000	0.5937
Co	−0.0665	−0.4556	−0.3134	0.1068	0.5937	1.0000

Magnesium-Monoxide (MgO). The sample was obtained by drilling bores set according to a three-dimensional lattice of size $7 \times 14 \times 10$ with 7 equidistance rows running west to east, 14 equidistance columns running south to north, and 10 equidistance depths from the surface of the earth to the bottom. To simplify the computation of the test statistics we consider the experimental design as a two-dimensional lattice of size 7×14 by taking the average value of the samples measured in the same position. We further assume that the exploration region is given by a closed rectangle so that by suitable rescaling it can be transformed into a closed unit rectangle $\mathbf{I}^2$. Table 2 exhibits, respectively, the pairs scatter plot and Pearson's correlation coefficient among the percentages of Ni, CaO, Co, the logarithm of the percentages of SiO_2 (log SiO_2), MgO (log MgO), and Fe (log Fe). By this reason a multivariate analysis must be conducted in the statistical modelling taking into account the unknown covariance matrix of the vector of the variables. Furthermore, based on the individual scatter plot of the samples which are not presented in this work, it can be inferred that polynomials of lower order seem to be adequate to approximate the population model. More precisely, let $\mathbf{Y} := (Y_1, Y_2, Y_3, Y_4, Y_5, Y_6)^\top$ be the vector of observations representing the observed percentages of CaO, log SiO_2, log MgO, Co, Ni, and log Fe, respectively. We aim to test the hypothesis

$$H_0 : \mathbf{E}(Y) = \begin{pmatrix} \beta_{11} \\ \beta_{21} + \beta_{22}t + \beta_{23}s \\ \beta_{31} + \beta_{32}t + \beta_{33}s \\ \beta_{41} + \beta_{42}t + \beta_{43}s \\ \beta_{51} + \beta_{52}t + \beta_{53}s + \beta_{54}t^2 + \beta_{55}ts + \beta_{56}s^2 \\ \beta_{61} + \beta_{62}t + \beta_{63}s + \beta_{64}t^2 + \beta_{65}ts + \beta_{66}s^2 \end{pmatrix}, \quad (60)$$
$$0 \le t, s \le 1,$$

for some unknown constants β_{ij}, $i = 1, 2, 3, 4, 5, 6$ and $j = 1, \ldots, d_i$, with $d_1 = 1$, $d_2 = d_3 = d_4 = 3$ and $d_5 = d_6 = 6$. For this case we have $\mathbf{W}_1 := [f_1]$, $\mathbf{W}_2 = \mathbf{W}_3 = \mathbf{W}_4 := [f_1, f_2, f_3]$, and $\mathbf{W}_5 = \mathbf{W}_6 := [f_1, f_2, f_3, f_4, f_5, f_6]$, with $f_1(t, s) := 1$, $f_2(t, s) = t$, $f_3(t, s) = s$, $f_4(t, s) = t^2$, $f_5(t, s) = ts$, and $f_6(t, s) = s^2$.

We obtained the values $\mathrm{KS}_{7\times14;\mathscr{A}} = 1.44109$ and $\mathrm{CvM}_{7\times14;\mathscr{A}} = 0.936687$ with the associated simulated p values of 0.98350 and 0.93670, respectively. We notice that in the computation we consider the VCC $\{[0, t] \times [0, s] : 0 \le t, s \le 1\}$ as the index sets instead of $\mathscr{A}$. Hence when using the KS test as well as CvM test the hypothesis will be not rejected for almost all commonly used values of α. There exists a significant evidence that the assumed model is appropriate for describing the functional relationship between the experimental conditional and the percentages of those elements.

In the practice some computational difficulties appear for testing using our proposed method. First, to the knowledge of the authors, the analytical formula for computing the critical and p values of the tests have been not yet available in the literatures; therefore we need to approximate them by simulation using computer. Second, although the test procedures are established for a much larger family of sets $\mathscr{A}$, in the application the computation is always restricted to the VCC of subsets of $\mathbf{I}^d$ like that of $\{\prod_{i=1}^d [0, t_i] \subset \mathbf{I}^d : 0 < t_i \le 1,\ i = 1, \ldots, d\}$ or $\{\prod_{i=1}^d [s_i, t_i] \subset \mathbf{I}^d : 0 \le s_i < t_i \le 1,\ i = 1, \ldots, d\}$.

8. Concluding Remark

In this article we have developed an asymptotic method for checking the validity of a general multivariate spatial regression model by considering the multidimensional set-indexed partial sums of the residuals. For the calibration of the distribution of the test statistics we propose the residual based bootstrap for multivariate regression. It is shown by applying imitation technique that the residual bootstrap resampling technique is consistent. In a simulation study the finite sample size behavior of the KS and CvM statistics is investigated in greater detail. For the first-order model CvM test has much larger power, whereas for constant, second-order, and third-order models the powers of the two tests are almost the same.

Other possibilities of tests for multidimensional case can be obtained by incorporating a sampling technique according to an arbitrary experimental design. Sometimes because of technical, economic, or ecological reason, practitioners will not or cannot sample the observations equidistantly. One possible approach is to sample according to a continuous probability measure; see, for example, the sampling method

proposed in Bischoff [11]. Under this concern we get the so-called weighted KS and CvM tests which can be viewed as generalization of the KS and CvM tests studied in this paper.

Instead of considering the least squares residuals of the observations we can also define a test by directly investigating the partial sums of the observations. The limit process will be given by a type of signal plus a noise which is given by the multidimensional set-indexed Brownian sheet. Observing the limit process we can formulate likelihood ratio test based on the Cameron-Matrin-Girsanov density formula of the limit process. Establishing such type of test will be of our concern in our future research project.

Appendix

A. Function of Bounded Variation on $\mathbf{I}^d$

Definition A.1. Let $f : \mathbb{R}^d \to \mathbb{R}$ be a real-valued function with d variables. For $\alpha_k, \beta_k \in \mathbb{R}$, let $\Delta_{\alpha_k}^{\beta_k} f$ be a real-value function defined on $\mathbb{R}^d$, given by

$$\begin{aligned}\Delta_{\alpha_k}^{\beta_k} f &:= f\left(x_1, \ldots, x_{k-1}, \beta_k, x_{k+1}, \ldots, x_d\right) \\ &\quad - f\left(x_1, \ldots, x_{k-1}, \alpha_k, x_{k+1}, \ldots, x_d\right),\end{aligned} \tag{A.1}$$

for $k = 1, \ldots, d$. Furthermore, for $\alpha := (\alpha_k)_{k=1}^d$ and $\beta := (\beta_k)_{k=1}^d \in \mathbb{R}^d$, $\Delta_\alpha^\beta f$ is defined on $\mathbb{R}^d$ recursively starting from the last components of α and β. More precisely,

$$\Delta_\alpha^\beta f := \Delta_{\alpha_1}^{\beta_1}\left(\cdots\left(\Delta_{\alpha_{d-1}}^{\beta_{d-1}}\left(\Delta_{\alpha_d}^{\beta_d} f\right)\right)\cdots\right). \tag{A.2}$$

Let $\{j_1, \ldots, j_d\}$ be permutation of $\{1, 2, \ldots, d\}$; then it holds that

$$\begin{aligned}\Delta_\alpha^\beta f &= \Delta_{\alpha_{j_1}}^{\beta_{j_1}}\left(\cdots\left(\Delta_{\alpha_{j_{d-1}}}^{\beta_{j_{d-1}}}\left(\Delta_{\alpha_{j_d}}^{\beta_{j_d}} f\right)\right)\cdots\right) \\ &= \Delta_{\alpha_1}^{\beta_1}\left(\cdots\left(\Delta_{\alpha_{d-1}}^{\beta_{d-1}}\left(\Delta_{\alpha_d}^{\beta_d} f\right)\right)\cdots\right).\end{aligned} \tag{A.3}$$

This means that the operation of $\Delta_\alpha^\beta f$ does not depend on the order. By this reason we write $\Delta_\alpha^\beta f$ by $\Delta_{\alpha_1}^{\beta_1} \cdots \Delta_{\alpha_{d-1}}^{\beta_{d-1}} \Delta_{\alpha_d}^{\beta_d} f$ ignoring the brackets. The reader is referred to Yeh [33] and Elstrodt [34], pp. 44-45.

Definition A.2 (see Yeh [33]). Let $\Gamma_k := \{[x_{k_0}, x_{k_1}], [x_{k_1}, x_{k_2}], \ldots, [x_{k_{M_k-1}}, x_{k_{M_k}}]\}$ be a collection of M_k rectangles on the unit interval $[0, 1]$ with $0 = x_{k_0} \le x_{k_1} \le \cdots \le x_{k_{M_k}} = 1$, for $k = 1, \ldots, d$. The Cartesian product $\mathcal{K} := \prod_{k=1}^d \Gamma_k$ which consists of $M_1 \times M_2 \times \cdots \times M_d$ rectangles is called a nonoverlapping finite exact cover of $\mathbf{I}^d$. The family of all nonoverlapping finite exact cover of $\mathbf{I}^d$ is denoted by $\mathcal{J}(\mathcal{K})$.

Definition A.3 (see Yeh [33]). For $1 \le w_k \le M_k$, with $k = 1, \ldots, d$, let $\mathbf{J}_{w_1 \cdots w_d}$ be the element of $\mathcal{K}$ defined by $\mathbf{J}_{w_1 \cdots w_d} := \prod_{k=1}^d [x_{k_{w_k-1}}, x_{k_{w_k}}]$. Let $\psi : \mathbf{I}^d \to \mathbb{R}$ be a real-valued function on $\mathbf{I}^d$. Operator $\Delta_{\mathbf{J}_{w_1 \cdots w_d}}$ acting on a function ψ is defined by

$$\Delta_{\mathbf{J}_{w_1 \cdots w_d}} \psi := \Delta_{x_{1_{w_1-1}}}^{x_{1_{w_1}}} \Delta_{x_{2_{w_2-1}}}^{x_{2_{w_2}}} \cdots \Delta_{x_{d_{w_d-1}}}^{x_{d_{w_d}}} \psi. \tag{A.4}$$

The variation of ψ over the finite exact cover $\mathcal{K}$ is defined by

$$v(\psi; \mathcal{K}) := \sum_{w_1=1}^{M_1} \cdots \sum_{w_d=1}^{M_d} \left|\Delta_{\mathbf{J}_{w_1 \cdots w_d}} \psi\right|. \tag{A.5}$$

Accordingly, the total variation of ψ over $\mathbf{I}^d$ is defined by

$$V\left(\psi; \mathbf{I}^d\right) := \sup_{\mathcal{K} \in \mathcal{J}(\mathcal{K})} v(\psi; \mathcal{K}). \tag{A.6}$$

Furthermore, function ψ is said to have bounded variation in the sense of Vitaly on $\mathbf{I}^d$ if there exists a real number $M > 0$ such that $V(\psi; \mathbf{I}^d) \le M$ for some real number $M > 0$. The class of such functions is denoted by $\mathrm{BVV}(\mathbf{I}^d)$.

Definition A.4 (see Yeh [33]). Let $(x_k)_{k=1}^d$ be a variable in $\mathbf{I}^d$. For fixed k, let $\mathbf{I}^k := [0, 1]^k$ be a k-dimensional unit closed rectangle constructed in the following way. We choose $d - k$ components of the variable $(x_k)_{k=1}^d$. For each choice from all possible elements of the set C_{d-k}^d, we set each x_i with 0 or 1 and let the remaining k variables satisfy $0 \le x_i \le 1$. Then for each k we get $2^{d-k}|C_{d-k}^d|$ unit closed rectangles $\mathbf{I}^k$. For convention we denote the collection of all $2^{d-k}|C_{d-k}^d|$ of closed rectangles $\mathbf{I}^k$ by $\mathcal{B}^k$ and the jth element of $\mathcal{B}^k$ will be denoted by $\mathbf{I}_j^k$. Function ψ is said to have bounded variation in the sense of Hardy on $\mathbf{I}^d$, if and only if for each $k = 1, \ldots, d$ and $j = 1, \ldots, 2^{d-k}|C_{d-k}^d|$ there exists a real number $M_{jk} > 0$ such that $V(\psi_{\mathbf{I}_j^k}(\cdot); \mathbf{I}_j^k) \le M_{jk}$, where, for $k = 1, \ldots, d$ and $j = 1, \ldots, 2^{d-k}|C_{d-k}^d|$, $\psi_{\mathbf{I}_j^k}(\cdot)$ is a function with k variables obtained from the function $\psi(x_1, x_2 \ldots, x_d)$ by setting the $d-k$ selected variables with 0 or 1, whereas the remaining k variables lie in the interval $[0, 1]$. The class of such functions will be denoted by $\mathrm{BV}_H(\mathbf{I}^d)$.

B. Integration by Parts on $\mathbf{I}^d$

For family $\mathcal{B}^k$ defined in Definition A.4, let $\mathcal{J} := \bigcup_{k=0}^d \mathcal{B}^k$, where, for $k = 0$, the family $\mathcal{B}^0$ is a collection of 2^d different points in $\mathbf{I}^d$. As an example, for $d = 2$, we have $\mathcal{B}^0 = \{\mathbf{I}_1^0 = (0, 0), \mathbf{I}_2^0 = (0, 1), \mathbf{I}_3^0 = (1, 0), \mathbf{I}_4^0 = (1, 1)\}$. For each $k = 1, \ldots, d$ and $j = 1, \ldots, 2^{d-k}|C_{k-d}^d|$, let $\sharp(\mathbf{I}_j^k)$ be the number of 1's appearing in $\mathbf{I}_j^k$. Next, let φ and ψ be defined on $\mathbf{I}^d$. If φ is Riemann-Stieltjes integrable with respect to ψ on $\mathbf{I}_j^k \in \mathcal{B}^k$, we denote the integral by $\int_{\mathbf{I}_j^k}^{(R)} \varphi \, d^k\psi$. For $k = 0$, it is understood that $\int_{\mathbf{I}_j^0}^{(R)} \varphi \, d^0\psi$ is defined as the product of φ and ψ at that point of $\mathbf{I}_j^0$ (see Yeh [33]).

Theorem B.1 (integration by parts (see Yeh [33])). *Let φ be Riemann-Stieltjes integrable with respect to ψ on each member*

of $\mathcal{I}$. Then ψ is Riemann-Stieltjes integrable with respect to φ on $\mathbf{I}^d$, and we have the formula

$$\int_{\mathbf{I}^d}^{(R)} \psi(x_1,\ldots,x_d)\, d\varphi(x_1,\ldots,x_d) = \sum_{k=0}^{d} \sum_{j=1}^{2^{d-k}|C_{d-k}^d|} (-1)^{(d-\sharp(\mathbf{I}_j^k))} \int_{\mathbf{I}_j^k}^{(R)} \varphi\, d^k\psi. \tag{B.1}$$

Moreover, if ψ have bounded variation in the sense of Hardy on $\mathbf{I}^d$ and φ is continuous on $\mathbf{I}^d$, then we have the inequality

$$\left|\int_{\mathbf{I}^d}^{(R)} \psi(x_1,\ldots,x_d)\, d\varphi(x_1,\ldots,x_d)\right| \le \|\varphi\|_\infty \left(2^d \|\psi\|_\infty + \sum_{k=1}^{d} \sum_{j=1}^{2^{d-k}|C_{d-k}^d|} V\left(\psi_{\mathbf{I}_j^k}(\cdot);\mathbf{I}_j^k\right)\right). \tag{B.2}$$

C. Some Property of the Partial Sums Operator

Lemma C.1 (see Bischoff and Somayasa [9]). *For every one-dimensional pyramidal array $A_{n_1\cdots n_d} := (a_{j_1\cdots j_d})_{j_1=1,\ldots,j_d=1}^{n_1,\ldots,n_d}$, it holds that $\mathbf{V}_{n_1\cdots n_d}^{(i)}(A_{n_1\cdots n_d}) \in \mathscr{H}_B$, where $\mathscr{H}_B$ is the subspace defined in (15). Furthermore, for any arrays $A_{n_1\cdots n_d} := (a_{j_1\cdots j_d})_{j_1=1,\ldots,j_d=1}^{n_1,\ldots,n_d}$ and $B_{n_1\cdots n_d} := (b_{j_1\cdots j_d})_{j_1=1,\ldots,j_d=1}^{n_1,\ldots,n_d}$, we have*

$$\left\langle V_{n_1\cdots n_d}^{(i)}\left(A_{n_1\cdots n_d}\right), V_{n_1\cdots n_d}^{(i)}\left(B_{n_1\cdots n_d}\right)\right\rangle_{\mathscr{H}_B} = \left\langle A_{n_1\cdots n_d}, B_{n_1\cdots n_d}\right\rangle_{\mathbb{R}^{n_1\times\cdots\times n_d}}, \tag{C.1}$$

where $V_{n_1\cdots n_d}^{(i)}$ is the one-dimensional component of the partial sums operator $\mathbf{V}_{n_1\cdots n_d}$.

Proof. Associated with $A_{n_1\cdots n_d}$ we can construct a step function $s_{A_{n_1\cdots n_d}} : \mathbf{I}^d \to \mathbb{R}$ defined by

$$s_{A_{n_1\cdots n_d}}(\mathbf{t}) := \sum_{j_1=1}^{n_1} \cdots \sum_{j_d=1}^{n_d} a_{j_1\cdots j_d} \mathbf{1}_{C_{j_1\cdots j_d}}(\mathbf{t}), \quad \mathbf{t} \in \mathbf{I}^d, \tag{C.2}$$

where $C_{j_1\cdots j_d} = \prod_{k=1}^{d}((j_k-1)/n_k, j_k/n_k]$, for $1 \le j_k \le n_k$. For any $B \in \mathscr{A}$, it holds that

$$h_{s_{A_{n_1\cdots n_d}}}(B) := \int_B s_{A_{n_1\cdots n_d}}(\mathbf{t})\, \lambda_{\mathbf{I}}^d(d\mathbf{t}) = \frac{1}{\sqrt{n_1\cdots n_d}} V_{n_1\cdots n_d}^{(i)}\left(A_{n_1\cdots n_d}\right)(B). \tag{C.3}$$

Hence, $V_{n_1\cdots n_d}^{(i)}(A_{n_1\cdots n_d}) \in \mathscr{H}_B$ having $\sqrt{n_1\cdots n_d}\, s_{A_{n_1\cdots n_d}}$ as the $L_2(\lambda_{\mathbf{I}}^d)$ density. By the definition of the inner product $\langle\cdot,\cdot\rangle_{\mathscr{H}_B}$, we further get

$$\begin{aligned}\left\langle V_{n_1\cdots n_d}^{(i)}\left(A_{n_1\cdots n_d}\right), V_{n_1\cdots n_d}^{(i)}\left(B_{n_1\cdots n_d}\right)\right\rangle_{\mathscr{H}_B} &= \int_{\mathbf{I}^d} \sqrt{n_1\cdots n_d}\, s_{A_{n_1\cdots n_d}}(\mathbf{t})\, \sqrt{n_1\cdots n_d}\, s_{B_{n_1\cdots n_d}}(\mathbf{t}) \\ &\cdot \lambda_{\mathbf{I}}^d(d\mathbf{t}) = \sum_{j_1=1}^{n_1}\cdots\sum_{j_d=1}^{n_d} a_{j_1\cdots j_d} b_{j_1\cdots j_d} \\ &= \left\langle A_{n_1\cdots n_d}, B_{n_1\cdots n_d}\right\rangle_{\mathbb{R}^{n_1\times\cdots\times n_d}}.\end{aligned} \tag{C.4}$$

□

Lemma C.2 (see Bischoff and Somayasa [9]). *For any $A_{n_1\cdots n_d} := (a_{j_1\cdots j_d})_{j_1=1,\ldots,j_d=1}^{n_1,\ldots,n_d}$ in $\mathbb{R}^{n_1\times\cdots\times n_d}$ it holds that, for $i = 1,\ldots,p$,*

$$V_{n_1\cdots n_d}^{(i)}\left(pr_{\mathbf{W}_{i,n_1\cdots n_d}} A_{n_1\cdots n_d}\right) = pr_{\mathbf{W}_{i,n_1\cdots n_d\mathscr{H}_B}} V_{n_1\cdots n_d}^{(i)}\left(A_{n_1\cdots n_d}\right), \tag{C.5}$$

where

$$\mathbf{W}_{i,n_1\cdots n_d\mathscr{H}_B} := \left\{V_{n_1\cdots n_d}^{(i)}\left(B_{n_1\cdots n_d}\right) \mid B_{n_1\cdots n_d} \in \mathbf{W}_{i,n_1\cdots n_d}\right\} \subset \mathscr{H}_B. \tag{C.6}$$

Furthermore, by the definition of the component-wise projection, we finally get

$$\mathbf{V}_{n_1\cdots n_d}\left(pr_{\prod_{i=1}^p \mathbf{W}_{i,n_1\cdots n_d}} \mathbf{A}_{n_1\cdots n_d}\right) = \left(pr_{\mathbf{W}_{i,n_1\cdots n_d\mathscr{H}_B}} V_{n_1\cdots n_d}^{(i)}\left(A_{n_1\cdots n_d}\right)\right)_{i=1}^{p}, \tag{C.7}$$

for every p-dimensional array $\mathbf{A}_{n_1\cdots n_d} \in \prod_{i=1}^p \mathbb{R}^{n_1\times\cdots\times n_d}$.

Proof. For fixed i, let $\{f_{i1}(\Xi_{n_1\cdots n_d}),\ldots,f_{id_i}(\Xi_{n_1\cdots n_d})\}$ be an ONB of $\mathbf{W}_{i,n_1\cdots n_d}$. Then by Lemma C.1 the corresponding ONB of $\mathbf{W}_{i,n_1\cdots n_d\mathscr{H}_B}$ is given by the set

$$\left\{\mathbf{V}_{n_1\cdots n_d}^{(i)}\left(f_{i1}\left(\Xi_{n_1\cdots n_d}\right)\right),\ldots,\mathbf{V}_{n_1\cdots n_d}^{(i)}\left(f_{id_i}\left(\Xi_{n_1\cdots n_d}\right)\right)\right\}. \tag{C.8}$$

Hence, by the linearity of $\mathbf{V}_{n_1\cdots n_d}^{(i)}$ and by Lemma C.1, we get

$$V_{n_1\cdots n_d}^{(i)}\left(\mathrm{pr}_{\mathbf{W}_{i,n_1\cdots n_d}} A_{n_1\cdots n_d}\right) = V_{n_1\cdots n_d}^{(i)}\left(\sum_{j=1}^{d_i}\left\langle f_{ij}\left(\Xi_{n_1\cdots n_d}\right), A_{n_1\cdots n_d}\right\rangle_{\mathbb{R}^{n_1\times\cdots\times n_d}} \cdot f_{ij}\left(\Xi_{n_1\cdots n_d}\right)\right)$$

$$
\begin{aligned}
&= \sum_{j=1}^{d_i} \left\langle f_{ij}\left(\Xi_{n_1\cdots n_d}\right), A_{n_1\cdots n_d}\right\rangle_{\mathbb{R}^{n_1\times\cdots\times n_d}} \\
&\cdot V^{(i)}_{n_1\cdots n_d}\left(f_{ij}\left(\Xi_{n_1\cdots n_d}\right)\right) \\
&= \sum_{j=1}^{d_i} \left\langle V^{(i)}_{n_1\cdots n_d}\left(f_{ij}\left(\Xi_{n_1\cdots n_d}\right)\right), V^{(i)}_{n_1\cdots n_d}\left(A_{n_1\cdots n_d}\right)\right\rangle_{\mathscr{H}_B} \\
&\cdot V^{(i)}_{n_1\cdots n_d}\left(f_{ij}\left(\Xi_{n_1\cdots n_d}\right)\right) \\
&= \mathrm{pr}_{\mathbf{W}_{i,n_1\cdots n_d\mathscr{H}_B}} V^{(i)}_{n_1\cdots n_d}\left(A_{n_1\cdots n_d}\right).
\end{aligned} \tag{C.9}
$$

□

Lemma C.3 (see Bischoff and Somayasa [9]). *Let* $\{\widetilde{s}_{i1}^{(n_1\cdots n_d)},\ldots,\widetilde{s}_{id_i}^{(n_1\cdots n_d)}\}$ *be an orthonormal set in* $L_2(\lambda_{\mathbf{I}}^d)$ *obtained by the Gram-Schmidt procedure from the step functions:*

$$
\begin{aligned}
&s_{ij}^{(n_1\cdots n_d)}(\mathbf{t}) \\
&\quad := \sum_{j_1=1}^{n_1}\cdots\sum_{j_d=1}^{n_d} f_{ij}\left(\frac{j_1}{n_1},\ldots,\frac{j_d}{n_d}\right)\mathbf{1}_{C_{j_1\cdots j_d}}(\mathbf{t}),
\end{aligned} \tag{C.10}
$$

$$\mathbf{t}\in\mathbf{I}^d,$$

for $i=1,\ldots,p$, *and* $j=1,\ldots,d_i$. *Then* $\{h_{\widetilde{s}_{i1}^{(n_1\cdots n_d)}},\ldots,h_{\widetilde{s}_{id_i}^{(n_1\cdots n_d)}}\}$ *is an ONB of* $\mathbf{W}_{i,n_1\cdots n_d\mathscr{H}_B}$. *The projection of any function* $u_n\in\mathscr{H}_B$ *into* $\mathbf{W}_{i,n_1\cdots n_d\mathscr{H}_B}$ *with respect to this basis is given by*

$$
\begin{aligned}
pr_{\mathbf{W}_{i,n_1\cdots n_d\mathscr{H}_B}} u_n &= \sum_{j=1}^{d_i}\left\langle h_{\widetilde{s}_{ij}^{(n_1\cdots n_d)}}, u_n\right\rangle_{\mathscr{H}_B} h_{\widetilde{s}_{ij}^{(n_1\cdots n_d)}} \\
&= \sum_{j=1}^{d_i}\int_{\mathbf{I}^d}^{(R)} \widetilde{s}_{ij}^{(n_1\cdots n_d)}(\mathbf{t})\,du(\mathbf{t})\,h_{\widetilde{s}_{ij}^{(n_1\cdots n_d)}}.
\end{aligned} \tag{C.11}
$$

Moreover, if, for $i=1,\ldots,p$ *and* $j=1,\ldots,d_i$, f_{ij} *is continuous on* $\mathbf{I}^d$ *and* $\{f_{i1},\ldots,f_{id_i}\}$ *is an ONB of* $\mathbf{W}_i$, *then* $\|\widetilde{s}_{ij}^{(n_1\cdots n_d)}-f_{ij}\|_\infty\to 0$ *as* $n_1,\ldots,n_d\to\infty$. *Consequently, it also holds that* $\|h_{\widetilde{s}_{ij}^{(n_1\cdots n_d)}}-h_{f_{ij}}\|_{\mathscr{A}}\to 0$, *for* $n_1,\ldots,n_d\to\infty$.

Proof. Since $h_{s_{ij}^{(n_1\cdots n_d)}} = (1/\sqrt{n_1\cdots n_d})V^{(i)}_{n_1\cdots n_d}(f_{ij}(\Xi_{n_1\cdots n_d}))$, by the linearity of $V^{(i)}_{n_1\cdots n_d}$ it follows that $\{h_{s_{i1}^{(n_1\cdots n_d)}},\ldots,h_{s_{id_i}^{(n_1\cdots n_d)}}\}$ builds a basis for $\mathbf{W}_{i,n_1\cdots n_d\mathscr{H}_B}$ whenever the set $\{f_{i1}(\Xi_{n_1\cdots n_d}),\ldots,f_{id_i}(\Xi_{n_1\cdots n_d})\}$ is a basis of $\mathbf{W}_{i,n_1\cdots n_d}$. Furthermore, if f_{ij} is continuous on $\mathbf{I}^d$, it can be shown that $\|s_{ij}^{(n_1\cdots n_d)}-f_{ij}\|_\infty\to 0$ as $n_1,\ldots,n_d\to\infty$. Hence, by the definition of the Gram-Schmidt process and also by the continuity of $\|\cdot\|_{L_2(\lambda_{\mathbf{I}}^d)}$, we can further show that $\|h_{\widetilde{s}_{ij}^{(n_1\cdots n_d)}}-h_{f_{ij}}\|_{\mathscr{A}}\to 0$ as $n_1,\ldots,n_d\to\infty$. The last assertion is immediately obtained from the definition of $h_{\widetilde{s}_{ij}^{(n_1\cdots n_d)}}$ and $h_{f_{ij}}$. □

Proposition C.4. *The p-dimensional projection* $pr_{\prod_{i=1}^p \mathbf{W}_{i,n_1\cdots n_d\mathscr{H}_B}}$ *is continuous uniformly on the space of continuous function* $\mathscr{C}^p(\mathscr{A})$ *for all* $n_1\geq 1,\ldots,n_d\geq 1$.

Proof. Let $\mathbf{w}_1 := (w_{1i})_{i=1}^p$ and $\mathbf{w}_2 := (w_{2i})_{i=1}^p$ be any functions in $\mathscr{C}^p(\mathscr{A})$. Then, by the definition and the inequality presented in Theorem B.1, for any $A\in\mathscr{A}$ we have

$$
\begin{aligned}
&\left|\left(\mathrm{pr}_{\prod_{i=1}^p \mathbf{W}_{i,n_1\cdots n_d\mathscr{H}_B}}\mathbf{w}_1\right)(A) - \left(\mathrm{pr}_{\prod_{i=1}^p \mathbf{W}_{i,n_1\cdots n_d\mathscr{H}_B}}\mathbf{w}_2\right)\cdot(A)\right| \\
&\leq \sum_{i=1}^p\sum_{j=1}^{d_i}\left|\left\langle h_{\widetilde{s}_{ij}^{(n_1\cdots n_d)}}, w_{1i}\right\rangle h_{\widetilde{s}_{ij}^{(n_1\cdots n_d)}}(A) - \left\langle h_{\widetilde{s}_{ij}^{(n_1\cdots n_d)}}, w_{2i}\right\rangle h_{\widetilde{s}_{ij}^{(n_1\cdots n_d)}}(A)\right| \\
&= \sum_{i=1}^p\sum_{j=1}^{d_i}\left|\left\langle h_{\widetilde{s}_{ij}^{(n_1\cdots n_d)}}, w_{1i}-w_{2i}\right\rangle\right|\left|h_{\widetilde{s}_{ij}^{(n_1\cdots n_d)}}(A)\right| \\
&\leq \sum_{i=1}^p\sum_{j=1}^{d_i}\|w_{1i}-w_{2i}\|_{\mathscr{A}}\|f_{ij}\|_\infty\left(2^d\|f_{ij}\|_\infty\right. \\
&\left.+\sum_{k=1}^d\sum_{\ell=1}^{2^{d-k}|C_{d-k}^d|} V\left(f_{ij_{\mathbf{I}_\ell^k}}(\cdot);\mathbf{I}_\ell^k\right)\right) \leq \|\mathbf{w}_1-\mathbf{w}_2\|_{\mathscr{A}} K,
\end{aligned} \tag{C.12}
$$

for some constant K defined by

$$
\begin{aligned}
K &:= \sum_{i=1}^p\sum_{j=1}^{d_i}\|f_{ij}\|_\infty \\
&\cdot\left(2^d\|f_{ij}\|_\infty + \sum_{k=1}^d\sum_{\ell=1}^{2^{d-k}|C_{d-k}^d|} V\left(f_{ij_{\mathbf{I}_\ell^k}}(\cdot);\mathbf{I}_\ell^k\right)\right).
\end{aligned} \tag{C.13}
$$

Hence we get

$$
\begin{aligned}
&\left\|\mathrm{pr}_{\prod_{i=1}^p \mathbf{W}_{i,n_1\cdots n_d\mathscr{H}_B}}\mathbf{w}_1 - \mathrm{pr}_{\prod_{i=1}^p \mathbf{W}_{i,n_1\cdots n_d\mathscr{H}_B}}\mathbf{w}_2\right\|_{\mathscr{A}} \\
&\quad\leq \|\mathbf{w}_1-\mathbf{w}_2\|_{\mathscr{A}} K.
\end{aligned} \tag{C.14}
$$

Given any positive small number ϵ, there exists a small number $\delta := \varepsilon/K$, such that, for any $\mathbf{w}_1,\mathbf{w}_2\in\mathscr{C}^p(\mathscr{A})$, if $\|\mathbf{w}_1-\mathbf{w}_2\|_{\mathscr{A}}\leq\delta$, then

$$
\left\|\mathrm{pr}_{\prod_{i=1}^p \mathbf{W}_{i,n_1\cdots n_d\mathscr{H}_B}}\mathbf{w}_1 - \mathrm{pr}_{\prod_{i=1}^p \mathbf{W}_{i,n_1\cdots n_d\mathscr{H}_B}}\mathbf{w}_2\right\|_{\mathscr{A}} \leq \varepsilon. \tag{C.15}
$$

□

Competing Interests

The authors declare that they have no competing interests.

Acknowledgments

The authors wish to thank the Ministry of Research, Technology and Higher Education (RISTEK-DIKTI) for the financial

support. They also thank Karlsruher Institut für Technologie (KIT) Institut für Stochastik for hospitality. Special thanks are addressed to Professor Andrei I. Volodin for his constructive comments for the improvement of the paper.

References

[1] A. Zellner, "An efficient method of estimating seemingly unrelated regressions and tests for aggregation bias," *Journal of the American Statistical Association*, vol. 57, no. 298, pp. 348–368, 1962.

[2] R. Christensen, *Advanced Linear Modeling: Multivariate, Time Series, and Spatial Data; Nonparametric Regression and Response Surface Maximization*, Springer, New York, NY, USA, 2001.

[3] D. W. Anderson, *An Introduction to Multivariate Statistical Analysis*, John Wiley & Sons, New York, NY, USA, 3rd edition, 2003.

[4] R. A. Johnson and D. W. Wichern, *Applied Multivariate Statistical Analysis*, Prentice Hall, New York, NY, USA, 3rd edition, 2007.

[5] I. B. MacNeill, "Properties of partial sums of polynomial regression residuals with applications to test for change of regression at unknown times," *The Annals of Statistics*, vol. 6, no. 2, pp. 422–433, 1978.

[6] I. B. MacNeill, "Limit processes for sequences of partial sums of regression residuals," *The Annals of Probability*, vol. 6, no. 4, pp. 695–698, 1978.

[7] I. B. MacNeill and V. K. Jandhyala, "Change-point methods for spatial data," in *Multivariate Environmental Statistics*, G. P. Patil and C. R. Rao, Eds., pp. 298–306, Elevier Science, Berlin, Germany, 1993.

[8] L. Xie and I. B. MacNeill, "Spatial residual processes and boundary detection," *South African Statistical Journal*, vol. 40, no. 1, pp. 33–53, 2006.

[9] W. Bischoff and W. Somayasa, "The limit of the partial sums process of spatial least squares residuals," *Journal of Multivariate Analysis*, vol. 100, no. 10, pp. 2167–2177, 2009.

[10] W. Somayasa, Ruslan, E. Cahyono, and L. O. Ngkoimani, "Checking adequateness of spatial regressions using set-indexed partial sums technique," *Far East Journal of Mathematical Sciences*, vol. 96, no. 8, pp. 933–966, 2015.

[11] W. Bischoff, "A functional central limit theorem for regression models," *The Annals of Statistics*, vol. 26, no. 4, pp. 1398–1410, 1998.

[12] W. Bischoff, "The structure of residual partial sums limit processes of linear regression models," *Theory of Stochastic Processes*, vol. 2, pp. 23–28, 2002.

[13] W. Stute, "Nonparametric model checks for regression," *The Annals of Statistics*, vol. 25, no. 2, pp. 613–641, 1997.

[14] W. Stute, W. González Manteiga, and M. Presedo Quindimil, "Bootstrap approximations in model checks for regression," *Journal of the American Statistical Association*, vol. 93, no. 441, pp. 141–149, 1998.

[15] E. J. Bedrick and C.-L. Tsai, "Model selection for multivariate regression in small samples," *Biometrics*, vol. 50, no. 1, pp. 226–231, 1994.

[16] Y. Fujikoshi and K. Satoh, "Modified AIC and C_p in multivariate linear regression," *Biometrika*, vol. 84, no. 3, pp. 707–716, 1997.

[17] W. Bischoff and A. Gegg, "Partial sum process to check regression models with multiple correlated response: with an application for testing a change-point in profile data," *Journal of Multivariate Analysis*, vol. 102, no. 2, pp. 281–291, 2011.

[18] W. Somayasa and G. N. Adhi Wibawa, "Asymptotic model-check for multivariate spatial regression with correlated responses," *Far East Journal of Mathematical Sciences*, vol. 98, no. 5, pp. 613–639, 2015.

[19] P. Billingsley, *Convergence of Probability Measures*, John Wiley & Sons, New York, NY, USA, 1968.

[20] M. Tahir, "Prediction of the amount of nickel deposit based on the results of drilling bores on several points (case study: south mining region of PT. Aneka Tambang Tbk., Pomalaa, Southeast Sulawesi)," Research Report, Halu Oleo University, Kendari, Indonesia, 2010.

[21] K. V. Mardia and C. R. Goodall, "Spatial-temporal analysis of multivariate environmental monitoring data," in *Multivariate Environmental Statistics*, G. P. Patil and C. R. Rao, Eds., pp. 347–386, North-Holland, Amsterdam, The Netherlands, 1993.

[22] S. Arnold, "The asymptotic validity of invariant procedures for the repeated measures model and multivariate linear model," *Journal of Multivariate Analysis*, vol. 15, no. 3, pp. 325–335, 1984.

[23] R. Pyke, "A uniform central limit theorem for partial sum processes indexed by sets," in *London Mathematical Society Lecture Note Series*, vol. 79, pp. 219–240, 1983.

[24] R. F. Bass and R. Pyke, "Functional law of the iterated logarithm and uniform central limit theorem for partial-sum processes indexed by sets," *The Annals of Probability*, vol. 12, no. 1, pp. 13–34, 1984.

[25] K. S. Alexander and R. Pyke, "A uniform central limit theorem for set-indexed partial-sum processes with finite variance," *The Annals of Probability*, vol. 14, no. 2, pp. 582–597, 1986.

[26] D. W. Stroock, *A Concise Introduction to the Theory of Integration*, Birkhäuser, Berlin, Germany, 3rd edition, 1999.

[27] J. N. Magnus and H. Neudecker, *Matrix Differential Calculus with Applications in Statistics and Econometrics*, John Wiley & Sons, New York, NY, USA, 3rd edition, 2007.

[28] K. B. Athreya and S. N. Lahiri, *Measure Theory and Probability Theory*, Springer, New York, NY, USA, 2006.

[29] A. W. van der Vaart, *Asymptotic Statistics*, vol. 3, Cambridge University Press, London, UK, 1998.

[30] E. L. Lehmann and J. P. Romano, *Testing Statitical Hypotheses*, Springer, New York, NY, USA, 3rd edition, 2005.

[31] H. Pruscha, *Vorlesungen über Mathematische Statistik*, B.G. Teubner, Stuttgart, Germany, 2000.

[32] J. Shao and D. S. Tu, *The Jackknife and Bootstrap*, Springer, New York, NY, USA, 1995.

[33] J. Yeh, "Cameron-Martin translation theorems in the Wiener space of functions of two variables," *Transactions of the American Mathematical Society*, vol. 107, no. 3, pp. 409–420, 1963.

[34] J. Elstrodt, *Maß- und Integrationstheorie*, vol. 7 of *Korregierte und Aktualisierte Auflage*, Springer, Berlin, Germany, 2011.

7

Graphs with Bounded Maximum Average Degree and their Neighbor Sum Distinguishing Total-Choice Numbers

Patcharapan Jumnongnit and Kittikorn Nakprasit

Department of Mathematics, Faculty of Science, Khon Kaen University, Khon Kaen 40002, Thailand

Correspondence should be addressed to Kittikorn Nakprasit; kitnak@hotmail.com

Academic Editor: Daniel Simson

Let G be a graph and $\phi : V(G) \cup E(G) \to \{1, 2, 3, \ldots, k\}$ be a k-total coloring. Let $w(v)$ denote the sum of color on a vertex v and colors assigned to edges incident to v. If $w(u) \neq w(v)$ whenever $uv \in E(G)$, then ϕ is called a neighbor sum distinguishing total coloring. The smallest integer k such that G has a neighbor sum distinguishing k-total coloring is denoted by $\text{tndi}_{\sum}(G)$. In 2014, Dong and Wang obtained the results about $\text{tndi}_{\sum}(G)$ depending on the value of maximum average degree. A k-assignment L of G is a list assignment L of integers to vertices and edges with $|L(v)| = k$ for each vertex v and $|L(e)| = k$ for each edge e. A *total-L-coloring* is a total coloring ϕ of G such that $\phi(v) \in L(v)$ whenever $v \in V(G)$ and $\phi(e) \in L(e)$ whenever $e \in E(G)$. We state that G has a *neighbor sum distinguishing total-L-coloring* if G has a total-L-coloring such that $w(u) \neq w(v)$ for all $uv \in E(G)$. The smallest integer k such that G has a neighbor sum distinguishing total-L-coloring for every k-assignment L is denoted by $\text{Ch}''_{\sum}(G)$. In this paper, we strengthen results by Dong and Wang by giving analogous results for $\text{Ch}''_{\sum}(G)$.

1. Introduction

Let G be a simple, finite, and undirected graph. We use $V(G)$, $E(G)$, and $\Delta(G)$ to denote the vertex set, edge set, and maximum degree of a graph G, respectively. A vertex v is called a k-vertex if $d(v) = k$. The length of a shortest cycle in G is called the *girth* of a graph G, denoted by $g(G)$. The *maximum average degree* of G is defined by $\text{mad}(G) = \max_{H \subseteq G}(2|E(H)|/|V(H)|)$. The well-known observation for a planar graph G is $\text{mad}(G) < 2g(G)/(g(G) - 2)$. Let $\phi : V(G) \cup E(G) \to \{1, 2, 3, \ldots, k\}$ be a k-total coloring. We denote the sum (set, resp.) of colors assigned to edges incident to v and the color on the vertex v by $w(v)$ ($C(v)$, resp.); that is, $w(v) = \sum_{uv \in E(G)} \phi(uv) + \phi(v)$ and $C(v) = \{\phi(v)\} \cup \{\phi(uv) \mid uv \in E(G)\}$. The total coloring ϕ of G is a *neighbor sum distinguishing* (*neighbor distinguishing*, resp.) total coloring if $w(u) \neq w(v)$ ($C(u) \neq C(v)$, resp.) for each edge $uv \in E(G)$. The smallest integer k such that G has a neighbor sum distinguishing (neighbor distinguishing, resp.) total coloring is called the *neighbor sum distinguishing total chromatic number* (*neighbor distinguishing total chromatic number*, resp.), denoted by $\text{tndi}_{\sum}(G)$ ($\text{tndi}(G)$, resp.). In 2005, a neighbor distinguishing total coloring of graphs was introduced by Zhang et al. [1]. They obtained $\text{tndi}(G)$ for many basic graphs and brought forward the following conjecture.

Conjecture 1 (see [1]). *If G is a graph with order at least two, then* $\text{tndi}(G) \leq \Delta(G) + 3$.

Conjecture 1 has been confirmed for subcubic graphs, K_4-minor free graphs, and planar graphs with large maximum degree [2–4].

In 2015, Pilśniak and Woźniak [5] obtained $\text{tndi}_{\sum}(G)$ for cycles, cubic graphs, bipartite graphs, and complete graphs. Moreover, they posed the following conjecture.

Conjecture 2 (see [5]). *If G is a graph with at least two vertices, then* $\text{tndi}_{\sum}(G) \leq \Delta(G) + 3$.

Li et al. verified this conjecture for K_4-minor free graphs [6] and planar graphs with the large maximum degree [7]. Wang et al. [8] confirmed this conjecture by using the famous Combinatorial Nullstellensatz that holds for any triangle free planar graph with maximum degree of at least 7. Several

results about $\mathrm{tndi}_{\sum}(G)$ for planar graphs can be found in [9–11].

In 2014, Dong and Wang [12] proved the following results.

Theorem 3. *If G is a graph with* $\mathrm{mad}(G) < 3$, *then* $\mathrm{tndi}_{\sum}(G) \leq \max\{\Delta(G) + 2, 7\}$.

Corollary 4. *If G is a graph with* $\mathrm{mad}(G) < 3$ *and* $\Delta(G) \geq 5$, *then* $\mathrm{tndi}_{\sum}(G) \leq \max \Delta(G) + 2$.

Corollary 5. *Let G be a planar graph. If $g(G) \geq 6$ and $\Delta(G) \geq 5$, then* $\mathrm{tndi}_{\sum}(G) \leq \Delta(G) + 2$; *and* $\mathrm{tndi}_{\sum}(G) = \Delta(G) + 2$ *if and only if G has two adjacent vertices of maximum degree.*

The concept of list coloring was introduced by Vizing [13] and by Erdös et al. [14]. A k-assignment L of G is a list assignment L of integers to vertices and edges with $|L(v)| = k$ for each vertex v and $|L(e)| = k$ for each edge e. A *total-L-coloring* is a total coloring ϕ of G such that $\phi(v) \in L(v)$ whenever $v \in V(G)$ and $\phi(e) \in L(e)$ whenever $e \in E(G)$. We state that G has a *neighbor sum distinguishing total-L-coloring* if G has a total-L-coloring such that $w(u) \neq w(v)$ for all $uv \in E(G)$. The smallest integer k such that G has a neighbor sum distinguishing total-L-coloring for every k-assignment L, denoted by $\mathrm{Ch}''_{\sum}(G)$, is called the *neighbor sum distinguishing total-choice number*.

Qu et al. [15] proved that $\mathrm{Ch}''_{\sum}(G) \leq \Delta(G) + 3$ for any planar graph G with $\Delta(G) \geq 13$. Yao et al. [16] studied $\mathrm{Ch}''_{\sum}(G)$ of d-degenerate graphs. Later, Wang et al. [17] confirmed Conjecture 2 true for planar graphs without 4-cycles. For $H \subseteq G$, we let L_H denote a list L restricted to any proper subgraph H of G. In this paper, we strengthen Theorem 3 by giving analogous results for $\mathrm{Ch}''_{\sum}(G)$.

2. Main Results

The following lemma is obvious, so we omit the proof.

Lemma 6. *Let $|S_1| = |S_2| = \cdots = |S_k| = k + 1$ and $S^* = \{a_1 + a_2 + \cdots + a_k \mid a_i \in S_i,\ a_i \neq a_j,\ 1 \leq i < j \leq k\}$. Then $|S^*| \geq k + 1$.*

Proof. We proceed by induction on k.

If $k = 1$, then $|S_1| = 2$; then Lemma 6 holds. Assume that $k > 1$. Suppose that Lemma 6 holds for $k - 1$. Let $a = \min(S_1 \cup S_2 \cup \cdots \cup S_k)$. Without loss of generality, let $a \in S_1$. Let $T_i \subseteq S_i$ be such that $|T_i| = k$ and $a \notin T_i$ for $i = 1, 2, \ldots, k$. By induction hypothesis, we have $|T^*| \geq k$. Thus $\{a + t_2 + t_3 + \cdots + t_k\} \subseteq S^*$, where $t_i \in T_i$, $t_j \in T_j$ for $2 \leq i,\ j \leq k$ and $t_i \neq t_j$ for $i \neq j$. So $|S^*| \geq k$. Let $t'_2 + \cdots + t'_k = \max T^*$ with $t'_i \in T_i$, $t'_j \in T_j$ for $2 \leq i,\ j \leq k$ and $t'_i \neq t'_j$ for $i \neq j$ and $b \in S_1 \setminus \{a, t'_2, t'_3, \ldots, t'_k\}$. Thus $b + t'_2 + t'_3 + \ldots + t'_k > \max\{a + t_2 + t_3 + \cdots + t_k\}$ and $b + t'_2 + t'_3 + \cdots + t'_k \in S^*$. Therefore, we obtain $|S^*| \geq k + 1$. □

Lemma 7 (see [12]). *Let S_1, S_2 be two sets and let $S_3 = \{a + b \mid a \in S_1,\ b \in S_2,\ a \neq b\}$. If $|S_1| \geq 2$ and $S_2 \geq 3$, then $|S_3| \geq 3$.*

Theorem 8. *If G is a graph with* $\mathrm{mad}(G) < 3$, *then* $\mathrm{Ch}''_{\sum}(G) \leq k$, *where* $k = \max\{\Delta(G) + 2, 7\}$.

Proof. The proof is proceeded by contradiction. Assume that G is a minimum counterexample. Let $|L(v)| \geq k$ for each vertex v and $|L(e)| \geq k$ for each edge e in G. For any proper subgraph G' of G, we always assume that there is a neighbor sum distinguishing total-$L_{G'}$-coloring ϕ of G' by minimality of G. For convenience, we use a total-$L_{G'}$-coloring ϕ of G' to denote a neighbor sum distinguishing total-$L_{G'}$-coloring ϕ of G' and we use $F(v) = \{\phi(u), \phi(uv) \mid uv \in E(G')\}$ for $v \in V(G)$ and $F(uv) = \{\phi(u), \phi(v), \phi(ur), \phi(vs) \mid ur \in E(G'), vs \in E(G')\}$ for $uv \in E(G)$.

Let H be the graph obtained by removing all leaves of G. Then H is a connected graph with $\mathrm{mad}(H) \leq \mathrm{mad}(G) < 3$. The properties of the graph H are collected in the following claims.

Claim 1. Each vertex in H has degree of at least 2.

Proof. Suppose to the contrary that H contains a vertex v with $d_H(v) \leq 1$. If $d_H(v) = 0$, then G is the star $K_{1,\Delta(G)-1}$ and $\mathrm{Ch}''_{\sum}(G) = \Delta(G)$; then we obtain a total-L_G-coloring ϕ of G, a contradiction to the choice of G. Assume that $d_H(v) = 1$. Let u and v_i be the neighbors of v where $i = 1, 2, \ldots, l = \Delta(G) - 1$ and $d_G(v_i) = 1$. Let $G' = G - vv_1$. First, we uncolor v_i where $i = 1, 2, \ldots, \Delta(G) - 1$. Then we color vv_1 with a color in $L(vv_1) \setminus (F(vv_1) \cup \{w(u) - w(v)\})$. Next, we color v_i with a color in $L(v_i) \setminus (F(v_i) \cup \{(w(v) - w(v_i)\})$ for $i = 1, 2, \ldots, \Delta(G) - 1$; then we obtain a total-L_G-coloring ϕ of G, a contradiction to the choice of G. □

Claim 2. If $d_H(u) = 2$, then $d_G(u) = 2$.

Proof. Suppose to the contrary that $d_G(u) = k \geq 3$. Let u_1, u_2 be the neighbors of u and v_i be all neighbors of u which are leaves in G for $i = 1, 2, \ldots, l = d_G(u) - 2$.

Case 1 ($d_G(u) = 3$). Let $G' = G - v_1$ and $L'(uv_1) = L(uv_1) \setminus (F(uv_1) \cup \{w(u_1) - w(u), w(u_2) - w(u)\})$. We color uv_1 with a color in $L'(uv_1)$ and color v_1 with a color in $L(v_1) \setminus (F(v_1) \cup \{w(u) - w(v_1)\})$. Thus we obtain a total-L_G-coloring ϕ of G, which is a contradiction to the choice of G.

Case 2 ($d_G(u) \geq 4$). Let $G' = G - \{v_1, \ldots, v_l\}$, where $l = d_G(u) - 2$. Let $A_i = L(uv_i) - \{\phi(u), \phi(uu_1), \phi(uu_2)\}$, where $i = 1, 2, \ldots, l$. Then $|A_i| \geq \Delta(G) - 1 \geq l + 1 \geq 3$, where $i = 1, 2, \ldots, l$. By Lemma 6, we have at least $l + 1 \geq 3$ color sets available for the edge set $\{uv_i \mid i = 1, 2, \ldots, l\}$ to guarantee $w(u) = w(u_i)$ for $i = 1, 2$. Since at most two color sets may cause $w(u) = w(u_1)$ or $w(u) = w(u_2)$, we have at least one color set available for the edge set $\{uv_i \mid i = 1, 2, \ldots, l\}$. Finally, we color v_i with the color in $L(v_i) \setminus (F(v_i) \cup \{w(u) - w(v_i)\})$ for $i = 1, 2, \ldots, l = d_G(u) - 2$; then we obtain a total-L_G-coloring ϕ of G, which is a contradiction to the choice of G. □

Claim 3. A 2-vertex u is not adjacent to a 3-vertex.

Proof. Suppose to the contrary that u is adjacent to a 3-vertex v in H. Let v_1, v_2 be the neighbors of v and s be the other neighbor of u.

Case 1 ($d_G(v) = 3$). Let $G' = G - uv$. First, we uncolor u. Next, we color uv with a color in $L(uv) \setminus (F(uv) \cup \{w(v_1) - w(v), w(v_2) - w(v)\})$. Later, we color u with a color in $L(u) \setminus (F(u) \cup \{w(v) - w(u), w(s) - w(u)\})$; then we obtain a total-L_G-coloring ϕ of G, which is a contradiction to the choice of G.

Case 2 ($d_G(v) \geq 4$). Let $x_1, x_2, \ldots, x_t$ be the other neighbors of v such that $d_G(x_i) = 1$ for all $i = 1, 2, \ldots, t = d_G(u) - 3$. Let $G' = G - \{uv, vx_1\}$. First, we uncolor all vertices u and x_i, $i = 1, 2, \ldots, t$. Consider $L'(vx_1) = L(vx_1) \setminus F(vx_1)$ and $L'(uv) = L(uv) \setminus F(uv)$. We can see that $|L'(vx_1)| \geq 3$ and $|L'(uv)| \geq 2$. By Lemma 7, we can choose $\phi(vx_1) \in L'(vx_1)$ and $\phi(uv) \in L'(uv)$ such that $w(v) \neq w(v_1)$ and $w(v) \neq w(v_2)$. Next, we color u with a color in $L(u) \setminus (F(u) \cup \{w(v) - w(u), w(s) - w(u)\})$ and color x_i with a color in $L(x_i) \setminus (F(x_i) \cup \{w(v) - w(x_i)\})$ for $i = 1, 2, \ldots, t$; then we obtain a total-L_G-coloring ϕ of G, which is a contradiction to the choice of G. □

Claim 4. A 4-vertex u is adjacent to at most two 2-vertices.

Proof. Suppose to the contrary that u is adjacent to three 2-vertices v_1, v_2, v_3 and the other vertex v. Let v_i' be the neighbor of v_i for $i = 1, 2, 3$.

Case 1 ($d_G(u) = 4$). Let $G' = G - uv_1$ and $L'(uv_1) = L(uv_1) \setminus (F(uv_1) \cup \{w(v) - w(u)\})$. First, we uncolor all vertices v_1, v_2, v_3. Next, we color uv_1 with a color in $L'(uv_1)$ and color v_i with a color in $L(v_i) \setminus (F(v_i) \cup \{w(u) - w(v_i), w(v_i') - w(v_i)\})$ for $i = 1, 2, 3$. Thus we obtain a total-L_G-coloring ϕ of G, which is a contradiction to the choice of G.

Case 2 ($d_G(u) \geq 5$). Let $x_1, x_2, \ldots, x_t$ be the neighbors of u such that $d_G(x_i) = 1$ for all $i = 1, 2, \ldots, t = d_G(u) - 4$. Let $G' = G - ux_1$. First, we uncolor vertices v_i and x_j where $1 \leq i \leq 3$, $1 \leq j \leq t$. Next, we choose $\phi(ux_1) \in L(ux_1) \setminus (F(ux_1) \cup \{w(v) - w(u)\})$. After that, we color v_i with a color in $L(v_i) \setminus (F(v_i) \cup \{w(u) - w(v_i), w(v_i') - w(v_i)\})$ for $i = 1, 2, 3$ and color x_j with a color in $L(x_j) \setminus (F(x_j) \cup \{w(u) - w(x_j)\})$ for $j = 1, 2, \ldots, t$. Thus we obtain a total-L_G-coloring ϕ of G, which is a contradiction to the choice of G. □

Claim 5. A 5-vertex u is adjacent to at most four 2-vertices.

Proof. Suppose to the contrary that u is adjacent to five 2-vertices v_1, v_2, v_3, v_4, v_5. Let $x_1, x_2, \ldots, x_t$ be the other neighbors of u (if they exist) such that $d_G(x_i) = 1$ for all $i = 1, 2, \ldots, t = d_G(u) - 5$ and v_i' be the neighbor of v_i for $i = 1, 2, 3, 4, 5$. Let $i = 1, 2, 3, 4, 5$ and $j = 1, 2, \ldots, t = d_G(u) - 5$ and $G' = G - uv_1$. First, we uncolor vertices v_i and x_j. Next, we color uv_1 with a color in $L(uv_1) \setminus F(uv_1)$. After that, we color v_i with a color in $L(v_i) \setminus (F(v_i) \cup \{w(u) - w(v_i), w(v_i') - w(v_i)\})$. Finally, we color x_j with a color in $L(x_j) \setminus (F(x_j) \cup \{w(u) - w(x_j)\})$. Thus we obtain a total-L_G-coloring ϕ of G, which is a contradiction to the choice of G. □

By Claim 1, we have $\Delta(H) \geq 2$.

Suppose that $\Delta(H) = 2$. By Claims 1 and 2, G is a cycle. One can obtain that $\mathrm{Ch}''_{\sum}(G) \leq 7$, a contradiction to the choice of G.

Suppose that $\Delta(H) = 3$. By Claim 3, H is a 3-regular graph. Thus we have $\mathrm{mad}(H) = 3$, which is a contradiction.

Suppose that $\Delta(H) \geq 4$. We complete the proof by using the discharging method. Define an initial charge function $\mathrm{ch}(v) = d_H(v)$ for every $v \in V(H)$. Next, rearrange the weights according to the designed rule. When the discharging is finished, we have a new charge $\mathrm{ch}'(v)$. However, the sum of all charges is kept fixed. Finally, we want to show that $\mathrm{ch}'(v) \geq 3$ for all $v \in V(H)$. This leads to the following contradiction:

$$\begin{aligned} 3 &= \frac{3\,|V(H)|}{|V(H)|} \leq \frac{\sum_{v \in V(H)} w'(v)}{|V(H)|} = \frac{\sum_{v \in V(H)} w(v)}{|V(H)|} \\ &= \frac{2\,|E(H)|}{|V(H)|} \leq \mathrm{mad}(H) < 3. \end{aligned} \tag{1}$$

Let $v \in V(H)$. Assume that $d_H(v) = 2$ and $uv \in E(H)$. Then vertex u gives charge $1/2$ to v.

Consider a vertex $v \in V(H)$. By Claim 1, we have $d_H(v) \geq 2$.

If $d_H(v) = 2$, then v is adjacent to at least two 4-vertices by Claim 3. Hence $\mathrm{ch}'(v) \geq \mathrm{ch}(v) + (2 \times (1/2)) = 3$.

If $d_H(v) = 3$, then $\mathrm{ch}'(v) = \mathrm{ch}(v) = 3$.

If $d_H(v) = 4$, then v is adjacent to at most two 2-vertices by Claim 4. Hence $\mathrm{ch}'(v) \geq \mathrm{ch}(v) - (2 \times (1/2)) = 3$.

If $d_H(v) = 5$, then v is adjacent to at most four 2-vertices by Claim 5. Hence $\mathrm{ch}'(v) \geq \mathrm{ch}(v) - (4 \times (1/2)) = 3$.

If $d_H(v) \geq 6$, then $\mathrm{ch}'(v) \geq \mathrm{ch}(v) - ((1/2)d_H(v)) = (1/2)d_H(v) \geq 3$.

From the above discussion, we have $\sum_{v \in V(H)} \mathrm{ch}'(v) \geq 3$, which is a contradiction. This completes the proof of Theorem 8.

Conflicts of Interest

The authors declare that there are no conflicts of interest regarding the publication of this paper.

Acknowledgments

The first author is supported by University of Phayao, Thailand. In addition, the authors would like to thank Dr. Keaitsuda Nakprasit for her helpful comments.

References

[1] Z. Zhang, X. E. Chen, J. Li, B. Yao, X. Lu, and J. Wang, "On adjacent-vertex-distinguishing total coloring of graphs," *Science China Mathematics*, vol. 48, no. 3, pp. 289–299, 2005.

[2] X. Chen, "On the adjacent vertex distinguishing total coloring numbers of graphs with $\Delta = 3$," *Discrete Mathematics*, vol. 308, no. 17, pp. 4003–4007, 2008.

[3] W. Wang and D. Huang, "The adjacent vertex distinguishing total coloring of planar graphs," *Journal of Combinatorial Optimization*, vol. 27, no. 2, pp. 379–396, 2014.

[4] W. Wang and P. Wang, "On adjacent-vertex-distinguishing total coloring of K4-minor free graphs," *Sci. China Ser. A*, vol. 39, no. 12, pp. 1462–1472, 2009.

[5] M. Pilśniak and M. Woźniak, "On the total-neighbor-distinguishing index by sums," *Graphs and Combinatorics*, vol. 31, no. 3, pp. 771–782, 2015.

[6] H. Li, B. Liu, and G. Wang, "Neighbor sum distinguishing total colorings of K_4-minor free graphs," *Frontiers of Mathematics in China*, vol. 8, no. 6, pp. 1351–1366, 2013.

[7] H. Li, L. Ding, B. Liu, and G. Wang, "Neighbor sum distinguishing total colorings of planar graphs," *Journal of Combinatorial Optimization*, vol. 30, no. 3, pp. 675–688, 2015.

[8] J. H. Wang, Q. L. Ma, and X. Han, "Neighbor sum distinguishing total colorings of triangle free planar graphs," *Acta Mathematica Sinica*, vol. 31, no. 2, pp. 216–224, 2015.

[9] X. Cheng, D. Huang, G. Wang, and J. Wu, "Neighbor sum distinguishing total colorings of planar graphs with maximum degree Δ," *Discrete Applied Mathematics: The Journal of Combinatorial Algorithms, Informatics and Computational Sciences*, vol. 190-191, pp. 34–41, 2015.

[10] C. Qu, G. Wang, J. Wu, and X. Yu, "On the neighbor sum distinguishing total coloring of planar graphs," *Theoretical Computer Science*, vol. 609, no. part 1, pp. 162–170, 2016.

[11] H. J. Song, W. H. Pan, X. N. Gong, and C. Q. Xu, "A note on the neighbor sum distinguishing total coloring of planar graphs," *Theoretical Computer Science*, vol. 640, pp. 125–129, 2016.

[12] A. J. Dong and G. H. Wang, "Neighbor sum distinguishing total colorings of graphs with bounded maximum average degree," *Acta Mathematica Sinica*, vol. 30, no. 4, pp. 703–709, 2014.

[13] V. G. Vizing, "Vertex colorings with given colors" (Russian), Metody Diskret. Analiz., 29, 3–10.

[14] P. Erdös, A. L. Rubin, and H. Taylor, "Choosability in graphs," in *In Proceedings of the West Coast Conference on Combinatorics, Graph Theory and Computing, Arcata, Congr. Num.*, vol. 26, pp. 125–157, 1979.

[15] C. Qu, G. Wang, G. Yan, and X. Yu, "Neighbor sum distinguishing total choosability of planar graphs," *Journal of Combinatorial Optimization*, vol. 32, no. 3, pp. 906–916, 2016.

[16] J. Yao, X. Yu, G. Wang, and C. Xu, "Neighbor sum (set) distinguishing total choosability of d-degenerate graphs," *Graphs and Combinatorics*, vol. 32, no. 4, pp. 1611–1620, 2016.

[17] J. Wang, J. Cai, and Q. Ma, "Neighbor sum distinguishing total choosability of planar graphs without 4-cycles," *Discrete Applied Mathematics: The Journal of Combinatorial Algorithms, Informatics and Computational Sciences*, vol. 206, pp. 215–219, 2016.

8

Optimal Control Techniques on a Mathematical Model for the Dynamics of Tungiasis in a Community

Jairos Kahuru,[1] Livingstone S. Luboobi,[1,2] and Yaw Nkansah-Gyekye[1]

[1]*School of Computational and Communication Science and Engineering, Nelson Mandela African Institution of Science and Technology, P.O. Box 447, Arusha, Tanzania*
[2]*Department of Mathematics, Makerere University, P.O. Box 7062, Kampala, Uganda*

Correspondence should be addressed to Jairos Kahuru; shinzehk@nm-aist.ac.tz

Academic Editor: Nawab Hussain

Tungiasis is a permanent penetration of female sand flea *"Tunga penetrans"* into the epidermis of its host. It affects human beings and domestic and sylvatic animals. In this paper, we apply optimal control techniques to a Tungiasis controlled mathematical model to determine the optimal control strategy in order to minimize the number of infested humans, infested animals, and sand flea populations. In an attempt to reduce Tungiasis infestation in human population, the control strategies based on personal protection, personal treatment, educational campaign, environmental sanitation, and insecticidal treatments on the affected parts as well as on animal fur are considered. We prove the existence of optimal control problem, determine the necessary conditions for optimality, and then perform numerical simulations. The numerical results showed that the control strategy comprises all five control measures and that which involves the three control measures of insecticide control, insecticidal dusting on animal furs, and environmental hygiene has the significant impact on Tungiasis transmission. Therefore, fighting against Tungiasis infestation in endemic settings, multidimensional control process should be employed in order to achieve the maximum benefits.

1. Introduction

Tungiasis is a skin disease caused by the sand flea *"Tunga penetrans"*; the disease is endemic in some poor resource communities where various domestic and sylvatic animals act as reservoirs for this zoonosis [1]. The flea infestation is associated with poverty and occurs in many resource-poor communities in the Caribbean, South America, and sub-Saharan Africa [2]. Transmission of Tungiasis is strictly by infestation of humans and animal reservoirs by *"Tunga penetrans"* when they are in contact with sandy soil in which female fleas are present or when in contact with infested animal reservoirs as it is known that the animal reservoirs harbor the fleas [3]. Tungiasis results in significant morbidity, manifesting itself in a number of symptoms such as severe local inflammation, autoamputation of digits, deformation and loss of nails, formation of fissures and ulcers, gangrene, and walking difficulties [4]. Moreover it may result into secondary infection caused by transmission of blood-borne pathogens such as hepatitis B and C virus and possibly also HIV/AIDS when a single nonsterile instrument is used to remove the jiggers from different affected individuals [5].

Mathematical models have played a major role in increasing understanding of the underlying mechanisms which influence the spread of the diseases and provide guidelines as to how the spread can be controlled [6, 7]. Optimal control theory is a powerful mathematical tool which makes the decision involving complex dynamical systems. It is a standard method for solving dynamic optimization problems, when those problems are expressed in continuous time [8]. Optimal control theory was developed by the Russian mathematician Lev S. Pontryagin (1908–1988) and his coworkers with the formulation and proof of the Pontryagin Maximum Principle (Pontryagin et al., 1962). Optimal control is the process of determining control and state trajectories for a dynamic system over a period of time to minimize a performance index [9]. Optimal control problem is represented by a set of differential equations describing the paths of the control variables that minimize the cost functional and has been used successfully to make decisions involving biological or

medical models [10]. The formulation of an optimal control problem requires a mathematical model of the system to be controlled, a specification of the performance index (cost function), and a specification of all boundary conditions on states and constraints to be satisfied by states and controls [11]. Pontryagin's maximum (or minimum) principle of optimal control gives the fundamental necessary conditions for a controlled trajectory to be optimal [12]. The principle technique is to transform the constrained dynamic optimization problem into an unconstrained problem, by allowing each of the adjoint variables to correspond to each of the state variables accordingly and combining the results with the objective functional [13]. The resulting function is known as the Hamiltonian, which is used to solve a set of necessary conditions that an optimal control and corresponding state variables must satisfy. The necessary conditions are the optimality solutions and adjoint equations which form the optimality system. The optimality system consists of the state system and adjoint system with initial and transversal conditions together with characterization of optimal control.

To the best of our knowledge Tungiasis dynamical model with application of optimal control technique has not been done. Therefore we are going to refer to other infectious diseases with similar characteristics where the optimal control theory has been applied. Bonyah et al. [20] applied optimal control theory to a Buruli ulcer model that takes into account human, water bug, and fish populations as well as *Microbacterium ulcerans* in the environment. The control measures were applied on mass treatment, insecticide, and mass education to minimize the number of infected hosts, vectors, and infected fishes. The optimality system was determined and computed numerically for several scenarios. The results showed that the combination of all the control measures, mass treatment, insecticide, and mass education, is capable of helping reduce the number of infected humans, water bugs, small fishes, and *Mycobacterium ulcerans* in the environment. Isere et al. [21] developed the optimal control model that includes two time dependent control functions with one minimizing the contact between the susceptible and the bacteria and the others, the population of bacteria in water. The results from the numerical solutions showed that increasing the susceptible pool and the infected populations above some threshold values were responsible for reducing cholera epidemic and the difference between the growth rate and the loss rate of the bacteria played a huge role in the outbreak of the disease. Devipriya and Kalaivani [22] conducted the study on "Optimal Control of Multiple Transmission of Water-Borne Disease." A controlled SIWR model was considered. The control measures represented an immune boosting and pathogen suppressing drugs. Their objective function was based on a combination of minimizing the number of infected individuals and the cost of the drugs dose. The numerical results have shown that both the vaccines resulted in minimizing the number of infected individuals and at the same time in a reduction of the budget related to the disease.

In this paper, the Tungiasis dynamical model with control measures is presented and a detailed qualitative optimal control model that minimizes the number of infested individuals (humans and animals) and sand fleas with minimal cost of implementing the control measures is developed. We establish the proof for existence of the optimal control and analyze the optimal control problem in order to determine the necessary conditions for optimality using the Pontryagin's maximum principle (Pontryagins et al., 1962). We then determine numerically the optimality system for several scenarios. Our paper is arranged as follows. In Section 2, we formulate an optimal control model. In Section 3, we analyze the optimal control model by determining the conditions for existence of optimal control and the necessary conditions for optimality. In Section 4, we carry out numerical simulations and discussion of the results and Section 5 is the conclusion.

2. Formulation of Optimal Control Problem

We formulate an optimal control model for Tungiasis disease in order to derive five optimal control measures with minimal implementation cost to eradicate the disease after a defined period of time. We employ the control efforts $w_i(t)$ in human, animal reservoirs, and adult flea populations and $(1 - w_i(t))$ is the failure rate for the control efforts $w_i(t)$ for $i = 1, \ldots, 5$. We let $w_1(t)$ be the effort of controlling the flea infested soil environment with insecticides spraying, $w_2(t)$ be the efforts of controlling the flea infested animal reservoir through dusting them with ant-flea compounds, $w_3(t)$ be the efforts of controlling the transmission from flea infested environment to susceptible animals (this can be achieved by environmental hygiene and cementing the floors), $w_4(t)$ be the efforts of controlling the transmission from flea infested animals to susceptible humans (this can be achieved by educating people not to live with animals in the same quarters or sharing common resting places), and $w_5(t)$ be the efforts of controlling transmission from flea infested environment to susceptible humans (this can be achieved by environmental hygiene, cementing the floors, covering of feet with solid shoes, and application of plant based repellent (Zanzarin) within the time interval of $[0, T]$). Therefore we assume that the mortality rate of jigger fleas in the soil environment is increased by the factor $(\mu_F + w_1(t))$, on-host spraying of infested animals will reduce the shedding rate ε_A of adult jigger fleas into the environment by a fraction $(1 - w_2(t))$, and the animal to animal effective contact rate ρ_A is reduced at the same fraction $(1 - w_2(t))$ because spraying insecticides on animal fur will reduce the transmission of infestation within animal population. The transmission rate from the soil environment to animal hosts is reduced by the factor $(1-w_3(t))$, the factor $(1-w_4(t))$ reduces the transmission from severely infested animal reservoirs to susceptible humans, and the factor $(1 - w_5(t))$ reduces the transmission from flea infested soil environment to susceptible humans. Here, we consider the model developed by Kahuru et al. [19] whereby we add a distinct epidemiological compartment T_H which represents human beings under treatment and incorporate the five control measures w_1, w_2, w_3, w_4, and w_5 as defined above. In the submodel of human population, the total human population N_H is subdivided into susceptible population S_H mildly infested population I_{Hl}, the severely infested population I_{Hh}, and the human treatment class denoted by

T_H; therefore we have $N_H = S_H + I_{Hl} + I_{Hh} + T_H$. We assume that the humans are recruited into S_H through birth by the adults at a rate b_H. Individuals in class S_H acquire infestation from the severely infested animal reservoirs I_{Ah} and move to class I_{Hl} at a rate $(1 - w_4(t))\rho_{AH}I_{Ah}/N_H$ and may also acquire infestation from the flea infested soil environment and move to class I_{Hh} at a rate $(1-w_5(t))\alpha_{EH}\beta_{EH}r_F F_E/(k+F_E)$. I_{Hl} may as well acquire infestation from the flea infested soil environment and progresses to class I_{Hh} at a rate $(1 - w_5(t))\alpha_{EH}\beta_{EH}r_F F_E/(k + F_E)$. Classes I_{Hh} and I_{Hl} seek treatment at the respective rates p_1 and p_2 and join T_H class, and eventually the treated individuals revert back to join S_H at a progression rate ω. Individuals in compartments S_H, I_{Hl}, and T_H suffer a natural mortality rate μ_H and for the compartment I_{Hh} they suffer a natural mortality at a rate μ_H and the disease induced mortality at a rate σ_H. In the submodel of animal reservoir population, the total animal reservoir population N_A is subdivided into susceptible population S_A mildly infested population I_{Al} and the severely infested population I_{Ah}; therefore we have $N_A = S_A + I_{Al} + I_{Ah}$. We assume that the animals are recruited into S_A through birth by the adults at a rate b_A. Individuals in class S_A acquire infestation from the severely infested animal reservoirs I_{Ah} and move to I_{Al} at a rate $(1 - w_2(t))\rho_A I_{Ah}/N_A$ and also may acquire infestation from the flea infested environment and move to class I_{Ah} at a rate $(1 - w_3(t))\alpha_{EA}\beta_{EA}r_F F_E/(k + F_E)$. I_{Al} may as well acquire infestation from the flea infested soil environment and progresses to class I_{Ah} at a rate $(1 - w_3(t))\alpha_{EA}\beta_{EA}r_F F_E/(k + F_E)$. Individuals in compartments S_A and I_{Al} suffer a natural mortality rate μ_A and for the compartment I_{Ah} they suffer a natural mortality at a rate μ_A and a disease induced mortality at a rate σ_A. The submodel of environmental component consists of two compartments, a compartment of larvae denoted by L_E and a compartment of adult sand fleas denoted by F_E. The larvae population are recruited into L_E through shedding of jigger eggs by I_{Hh} and I_{Ah} at a constant rate δ_e; therefore we have the total contribution of $\delta_e I_{Hh}$ and $\delta_e I_{Ah}$ from infested humans and animal reservoir populations, respectively. The larvae in compartment L_E mature into adult jigger fleas at a maturation rate γ_L and undergo a natural death at a rate μ_L. The adult jigger flea population are recruited into F_E through maturation by larvae at a rate γ_L and from infested animal reservoirs who contributes the fleas into the soil environment at a rate $(1 - w_2(t))\varepsilon_A$. The adult fleas leave the compartment F_E when they attack the hosts at a rate $r_F F_E/(k+F_E)$ and when they undergo a natural death at a rate μ_F and the additional death due to insecticides control at a rate $w_1(t)$, therefore we have the flea total death rate of $(\mu_F + w_1(t))F_E$.

The variables and parameters that describe the flow rates between compartments are given, respectively, in Notations. The possible interactions between humans, animal reservoirs, and flea infested environment with control measures are presented by the model flow diagram in Figure 1 and the differential equations describing the model are given in system (1).

2.1. Model Flow Chart with Control Measures. The dynamical model with submodels of humans, animal reservoirs, and flea infested environment that incorporates time dependent control measures is presented hereunder.

2.2. Equations of the Model with Control Measures. From compartmental flow chart in Figure 1 the nonlinear differential equations representing the controlled system of Tungiasis dynamical model are given by

Dynamics in human population

$$\begin{aligned}
&\frac{dS_H(t)}{dt} \\
&= b_H N_H + \omega T_H - (1 - w_5(t))\psi_{EH}S_H \\
&\quad - (1 - w_4(t))\psi_{AH}S_H - \mu_H S_H \\
&\frac{dI_{Hl}(t)}{dt} \\
&= (1 - w_4(t))\psi_{AH}S_H - (1 - w_5(t))\psi_{EH}I_{Hl} \\
&\quad - (p_1 + \mu_H)I_{Hl} \\
&\frac{dI_{Hh}(t)}{dt} \\
&= (1 - w_5(t))\psi_{EH}S_H + (1 - w_5(t))\psi_{EH}I_{Hl} \\
&\quad - (p_2 + \mu_H + \sigma_H)I_{Hh} \\
&\frac{dT_H(t)}{dt} = p_1 I_{Hl} + p_2 I_{Hh} - (\omega + \mu_H)T_H
\end{aligned}$$

Dynamics in animal reservoir population

$$\begin{aligned}
&\frac{dS_A(t)}{dt} \\
&= b_A N_A - (1 - w_2(t))\psi_{AA}S_A - (1 - w_3(t))\psi_{EA}S_A \\
&\quad - \mu_A S_A \\
&\frac{dI_{Al}(t)}{dt} \\
&= (1 - w_2(t))\psi_{AA}S_A - (1 - w_3(t))\psi_{EA}I_{Al} - \mu_A I_{Al} \\
&\frac{dI_{Ah}(t)}{dt} \\
&= (1 - w_3(t))\psi_{EA}S_A + (1 - w_3(t))\psi_{EA}I_{Al} \\
&\quad - (\mu_A + \sigma_A)I_{Ah}
\end{aligned} \tag{1}$$

Dynamics in jigger flea population

$$\begin{aligned}
&\frac{dL_E(t)}{dt} = \delta_e\left(1 - \frac{L_E}{K}\right)(I_{Hh} + I_{Ah}) - (\gamma_L + \mu_L)L_E \\
&\frac{dF_E(t)}{dt} \\
&= \gamma_L L_E + (1 - w_2(t))\varepsilon_A I_{Ah} - (\mu_F + w_1(t))F_E \\
&\quad - r_F\frac{F_E}{k + F_E}
\end{aligned}$$

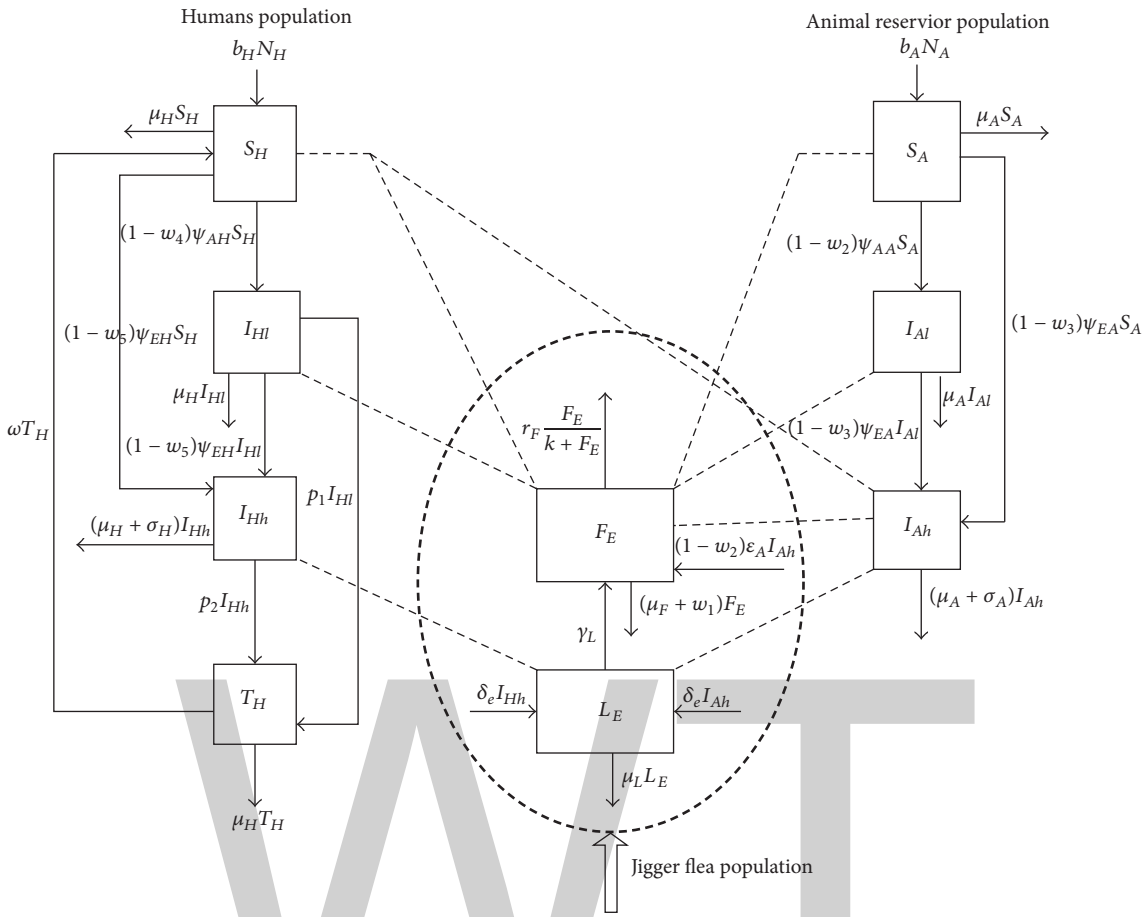

Figure 1: The flow chart showing the dynamics of Tungiasis with control measures incorporated.

with initial condition

$$\begin{aligned}
S_H(0) &> 0,\\
I_{Hl}(0) &\geq 0,\\
I_{Hh}(0) &\geq 0,\\
T_H(0) &\geq 0,\\
S_A(0) &> 0,\\
I_{Al}(0) &\geq 0,\\
I_{Ah}(0) &\geq 0,\\
L_E(0) &\geq 0,\\
F_E(0) &> 0,\\
w_1(t) &\geq 0,\\
w_2(t) &\geq 0,\\
w_3(t) &\geq 0,\\
w_4(t) &\geq 0,\\
w_5(t) &\geq 0,
\end{aligned} \tag{2}$$

where

$$\begin{aligned}
\psi_{AA} &= \rho_A \frac{I_{Ah}}{N_A},\\
\psi_{EA} &= \alpha_{EA}\beta_{EA} r_F \frac{F_E}{k+F_E},\\
\psi_{EH} &= \alpha_{EH}\beta_{EH} r_F \frac{F_E}{k+F_E},\\
\psi_{AH} &= \rho_{AH} \frac{I_{Ah}}{N_H}\\
0 \leq w_1(t), w_2(t), w_3(t), w_4(t), w_5(t) &\leq 1.
\end{aligned} \tag{3}$$

2.3. Optimal Control Problem for Tungiasis Epidemic. In this section, we present the optimal control problem considering the performance index and the controlled model equations with initial state conditions whereby the goal is to find the optimal levels of the control measures needed to minimize the number of infested humans, animal reservoirs, and fleas as well as the cost of implementing the control strategies (w_i for $i = 1, \ldots, 5$). The objective functional $J(w)$ to be minimized is given by

$$J(w) = \min \int_0^T \left\{ R_1 I_{Hh} + R_2 I_{Hl} + R_3 I_{Ah} + R_4 I_{Al} + R_5 F_E + \frac{1}{2} \sum_{i=1}^{5} Z_i w_i^2 \right\} dt. \tag{4}$$

The terms I_{Hh}, I_{Hl}, I_{Ah}, I_{Al}, F_E in the objective functional $J(w)$ are the number of infested populations that need to be minimized. The terms $Z_1 w_1^2$ represents the cost of off-host insecticides spraying, $Z_2 w_2^2$ represents the cost of on-host spraying of infested domestic animals, $Z_3 w_3^2$ represent the cost of implementing environmental hygiene, $Z_4 w_4^2$ represents the cost of education campaign, and $Z_5 w_5^2$ represents the cost of personal protection. R_1, R_2, R_3, R_4, R_5, Z_1, Z_2, Z_3, Z_4, and Z_5 are positive balancing coefficients (weights) which regularize the optimal control. Quadratic expressions of the controls are included to indicate nonlinear costs potentially arising at high intervention levels [23].

The optimal control problem is formulated to obtain the minimum number of infested populations I_{Hh}, I_{Hl}, I_{Ah}, I_{Al}, F_E under minimum cost. Therefore the objective function in (4) is minimized subject to the model equations in (1). We seek the optimal controls $w_1^*, w_2^*, w_3^*, w_4^*, w_5^*$ such that

$$\begin{aligned} &J(w_1^*, w_2^*, w_3^*, w_4^*, w_5^*) \\ &\quad = \min J\{(w_1, w_2, w_3, w_4, w_5) \mid w_i \in \Pi \text{ for } i \\ &\quad = 1, \ldots, 5\} \\ &\text{subject to the dynamical system in (1)} \\ &\quad \text{and the control set given by} \\ &\Pi = \{(w_1, w_2, w_3, w_4, w_5) \text{ such that; } 0 \le w_i \le 1, \text{ for } i \\ &\quad = 1, \ldots, 5; \ \forall t \in [0, T]\}. \end{aligned} \tag{5}$$

3. Model Analysis

The basic framework of an optimal control is to prove the existence of the optimal control and then characterize the optimal control through optimality system [24]. Given the optimal control problem in (5) we prove the existence of optimal control problem using the approach by Fleming and Rishel [25] and by Lukes [26] and then characterizing it for optimality.

3.1. The Existence of Optimal Control Problem. To prove the existence of optimal control the following conditions should be satisfied:

(i) The set of controls and corresponding state variables are nonempty.

(ii) The control set is convex and closed.

(iii) The right-hand side of the state system is bounded by a linear function in the state and control variables.

(iv) The integrand of the objective functional is convex.

(v) The integrand of the objective functional is bounded below by $\tau_1(\sum_{i=1}^{5} |w_i|^2)^{\varpi/2} - \tau_2$, where $\tau_1, \tau_2 > 0$ and $\varpi > 1$.

Given that, S_H, I_{Hl}, I_{Hh}, T_H, S_A, I_{Al}, I_{Ah}, L_E, and F_E are the state variables of the controlled model system (1) and w_1, w_2, w_3, w_4, w_5 are the control variables. We state and prove Theorem 1 as follows.

Theorem 1. *There exists an optimal control variables set* $w^* = (w_1^*, w_2^*, w_3^*, w_4^*, w_5^*) \in \Pi$ *such that*

$$J(w_1^*, w_2^*, w_3^*, w_4^*, w_5^*) = \min J\{(w_1, w_2, w_3, w_4, w_5) \mid w_i \in \Pi \text{ for } i = 1, \ldots, 5\}. \tag{6}$$

Proof. Using the results in Fleming and Rishel [25] and by Lukes [26], the control and the state variables are nonnegative values. In this minimization problem, the necessary convexity of the objective functional in w_1, w_2, w_3, w_4, w_5 is satisfied. The set of admissible Lebesgue measurable control variables $(w_1, w_2, w_3, w_4, w_5) \in \Pi$ is also convex and closed by the definition. The optimal system is bounded which determines the compactness needed for the existence of optimal control. In order to verify this argument we use the approach adopted by Sadiq et al. [27] and Namawejje et al. [28], whereby system (1) is put in the following form:

$$Y' = BY + G(Y), \tag{7}$$

where

$$Y = (S_H, I_{Hl}, I_{Hh}, T_H, S_A, I_{Al}, I_{Ah}, L_E, F_E)^T. \tag{7a}$$

B is the 9×9 matrix

$$G(Y) = \begin{bmatrix} b_H N_H - (1 - w_5(t))\psi_{EH} S_H - (1 - w_4(t))\psi_{AH} S_H \\ (1 - w_4(t))\psi_{AH} S_H - (1 - w_5(t))\psi_{EH} I_{Hl} \\ (1 - w_5(t))\psi_{EH} S_H + (1 - w_5(t))\psi_{EH} I_{Hl} \\ 0 \\ b_A N_A - (1 - w_2(t))\psi_{AA} S_A - (1 - w_3(t))\psi_{EA} S_A \\ (1 - w_2(t))\psi_{AA} S_A - (1 - w_3(t))\psi_{EA} I_{Al} \\ (1 - w_3(t))\psi_{EA} S_A + (1 - w_3(t))\psi_{EA} I_{Al} \\ 0 \\ 0 \end{bmatrix} \tag{7b}$$

$$B = \begin{bmatrix} -\mu_H & 0 & 0 & \omega & 0 & 0 & 0 & 0 & 0 \\ 0 & -\Psi_1 & 0 & 0 & 0 & 0 & 0 & 0 & 0 \\ 0 & 0 & -\Psi_2 & 0 & 0 & 0 & 0 & 0 & 0 \\ 0 & p_1 & p_2 & -\Psi_3 & 0 & 0 & 0 & 0 & 0 \\ 0 & 0 & 0 & 0 & -\mu_A & 0 & 0 & 0 & 0 \\ 0 & 0 & 0 & 0 & 0 & -\mu_A & 0 & 0 & 0 \\ 0 & 0 & 0 & 0 & 0 & 0 & -(\mu_A + \sigma_A) & 0 & 0 \\ 0 & 0 & \delta_e & 0 & 0 & 0 & \delta_e & -\Psi_5 & 0 \\ 0 & 0 & 0 & 0 & 0 & 0 & \Psi_4 & \gamma_L & -\Psi_6 \end{bmatrix}, \quad (7c)$$

where

$$\begin{aligned} \Psi_1 &= (p_1 + \mu_H), \\ \Psi_2 &= (p_2 + \mu_H + \sigma_H), \\ \Psi_3 &= (\omega + \mu_H), \\ \Psi_4 &= (1 - w_2)\varepsilon_A, \\ \Psi_5 &= \left\{ \frac{\delta_e}{K} (I_{Hh} + I_{Ah}) + (\gamma_L + \mu_L) \right\}, \\ \Psi_6 &= \left(\mu_F + w_1 + \frac{r_F}{k + F_E} \right) \end{aligned} \quad (8)$$

and Y' denotes the derivative of Y with respect to time t. System (4) is a nonlinear system with a bounded coefficient. We set

$$R(Y) = BY + G(Y). \quad (7d)$$

The second term on the right-hand side of (7d), $G(Y)$, satisfies

$$\begin{aligned} &|G(Y_1) - G(Y_2)| \le H_1 (|S_{1H}(t) - S_{2H}(t)|) \\ &\quad + H_2 (|I_{1Hl}(t) - I_{2Hl}(t)|) \\ &\quad + H_3 (|I_{1Hh}(t) - I_{2Hh}(t)|) \\ &\quad + H_4 (|T_{1H}(t) - T_{2H}(t)|) + H_5 (|S_{1A}(t) - S_{2A}(t)|) \\ &\quad + H_6 (|I_{1Al}(t) - I_{2Al}(t)|) + H_7 (|I_{1Ah}(t) - I_{2Ah}(t)|) \\ &\quad + H_8 (|L_{1E}(t) - L_{2E}(t)|) + H_9 (|F_{1E}(t) - F_{2E}(t)|) \\ &\quad \le H ((|S_{1H}(t) - S_{2H}(t)|) + (|I_{1Hl}(t) - I_{2Hl}(t)|) \\ &\quad + (|I_{1Hh}(t) - I_{2Hh}(t)|) + (|T_{1H}(t) - T_{2H}(t)|) \\ &\quad + (|S_{1A}(t) - S_{2A}(t)|) + (|I_{1Al}(t) - I_{2Al}(t)|) \\ &\quad + (|I_{1Ah}(t) - I_{2Ah}(t)|) + (|L_{1E}(t) - L_{2E}(t)|) \\ &\quad - (|F_{1E}(t) + F_{2E}(t)|)), \end{aligned} \quad (9)$$

where the positive constant $H = \max(H_i \text{ for } i = 1, \ldots, 9)$ is independent of the state variables. Also we have $|R(Y_1) - R(Y_2)| \le H|Y_1 - Y_2|$, where $H = \sum_{i=1}^{9} H_i + \|M\| < \infty$. So, it follows that the function R is uniformly Lipchitz continuous.

From the definition of control variables and nonnegative initial conditions we can see that a solution of the system (1) exists [29].

The integrand in the objective functional (4) which is given by the following equation $L(t, y, w) = R_1 I_{Hh} + R_2 I_{Hl} + R_3 I_{Ah} + R_4 I_{Al} + R_5 F_E + (1/2) \sum_{i=1}^{5} Z_i w_i^2$ is convex in the control set Π.

We must verify the condition that there exist a constant $\varpi > 1$ and positive numbers τ_1 and τ_2 such that

$$\begin{aligned} &L(t, y, w) \ge \tau_1 \left(\sum_{i=1}^{5} |w_i|^2 \right)^{\varpi/2} - \tau_2, \\ &R_1 I_{Hh} + R_2 I_{Hl} + R_3 I_{Ah} + R_4 I_{Al} + R_5 F_E + \frac{1}{2} \sum_{i=1}^{5} Z_i w_i^2 \\ &\quad \ge \frac{1}{2} \sum_{i=1}^{5} Z_i w_i^2 \\ &\frac{1}{2} \sum_{i=1}^{5} Z_i w_i^2 \ge \tau_1 \left(\sum_{i=1}^{5} |w_i|^2 \right)^{\varpi/2} - \tau_2. \end{aligned} \quad (10)$$

The last condition is satisfied when $\varpi = 2$, $\tau_2 > 0$, and $\tau_1 = \min\{Z_1, Z_2, Z_3, Z_4, Z_5\}$. This ends the proof. □

3.2. Determination of the Necessary Conditions for Optimality. The necessary conditions include the optimality solutions and the adjoint equations that an optimal control must satisfy which come from Pontryagin's maximum principle (Pontryagin's et al., 1962). This principle converts systems (1) and (4) into a problem of minimizing pointwise Hamiltonian function H, which is formed by allowing each of the adjoint variables to correspond to each of the state variables accordingly and combining the results with the objective functional [21]. The resulting equation is as given by

$$\begin{aligned} H(t, y, w, \lambda) &= R_1 I_{Hh} + R_2 I_{Hl} + R_3 I_{Ah} + R_4 I_{Al} \\ &\quad + R_5 F_E + \frac{1}{2} \sum_{i=1}^{5} Z_i w_i^2 + \sum_{i=1}^{9} \lambda_i Q_i, \end{aligned} \quad (11)$$

where

λ_i for $i = 1, \ldots, 9$ are the adjoint functions associated with the state equations in (1),

Q_i for $i = 1, \ldots, 9$ is the right-hand side of the differential equations of ith state variable in system (1).

The expanded form of Hamiltonian function in (11) is given by

$$\begin{aligned} H(t, y, w, \lambda) &= R_1 I_{Hh} + R_2 I_{Hl} + R_3 I_{Ah} + R_4 I_{Al} \\ &\quad + R_5 F_E + \frac{1}{2} \sum_{i=1}^{5} Z_i w_i^2 + \lambda_1 \{ b_H N_H + \omega T_H \end{aligned}$$

$$
\begin{aligned}
&- (1 - w_5)\,\psi_{EH} S_H - (1 - w_4)\,\psi_{AH} S_H - \mu_H S_H\} \\
&+ \lambda_2 \{(1 - w_4)\,\psi_{AH} S_H - (1 - w_5)\,\psi_{EH} I_{Hl} - p_1 I_{Hl} \\
&- \mu_H I_{Hl}\} + \lambda_3 \{(1 - w_5)\,\psi_{EH} S_H + (1 - w_5)\,\psi_{EH} I_{Hl} \\
&- p_2 I_{Hh} - (\mu_H + \sigma_H)\, I_{Hh}\} + \lambda_4 \{p_1 I_{Hl} + p_2 I_{Hh} \\
&- \omega T_H - \mu_H T_H\} + \lambda_5 \{b_A N_A - (1 - w_2)\,\psi_{AA} S_A \\
&- (1 - w_3)\,\psi_{EA} S_A - \mu_A S_A\} + \lambda_6 \{(1 - w_2)\,\psi_{AA} S_A \\
&- (1 - w_3)\,\psi_{EA} I_{Al} - \mu_A I_{Al}\} + \lambda_7 \{(1 - w_3)\,\psi_{EA} S_A \\
&+ (1 - w_3)\,\psi_{EA} I_{Al} - (\mu_A + \sigma_A)\, I_{Ah}\} \\
&+ \lambda_8 \left\{\delta_e \left(1 - \frac{L_E}{K}\right)(I_{Hh} + I_{Ah}) - (\gamma_L + \mu_L)\, L_E\right\} \\
&+ \lambda_9 \left\{\gamma_L L_E + (1 - w_2)\,\varepsilon_A I_{Ah} - (\mu_F + w_1)\, F_E \right. \\
&\left. - \frac{r_F F_E}{(k + F_E)}\right\}.
\end{aligned} \tag{12}
$$

The optimality equations are obtained when taking the partial derivative of the Hamiltonian function H with respect to the control variables $(w_1, w_2, w_3, w_4, w_5)$, respectively, and the time derivative of adjoint equation λ' which is obtained by taking the negative partial derivative of H with respect to the model state variables $y(t)$ such that $\lambda' = -H_y$.

Theorem 2. *There exist an optimal control set* $(w_1^*, w_2^*, w_3^*, w_4^*, w_5^*)$ *and their corresponding state solutions* S_H^*, I_{Hl}^*, I_{Hh}^*, T_H^*, S_A^*, I_{Al}^*, I_{Ah}^*, L_E^*, *and* F_E^* *that minimize* $J(w_1, w_2, w_3, w_4, w_5)$, *and therefore there exist adjoint functions* $\lambda_1, \lambda_2, \ldots, \lambda_9$ *such that*

$$
\begin{aligned}
&\frac{d\lambda_1}{dt} \\
&\quad = \lambda_1 \mu_H - (1 - w_4(t))\,(\lambda_2 - \lambda_1)\,\psi_{AH} \\
&\qquad - (1 - w_5(t))\,(\lambda_3 - \lambda_1)\,\psi_{EH} \\
&\frac{d\lambda_2}{dt} \\
&\quad = (1 - w_5(t))\,\psi_{EH}\,(\lambda_2 - \lambda_3) + \lambda_2\,(p_1 + \mu_H) \\
&\qquad - \lambda_4 p_1 - R_2 \\
&\frac{d\lambda_3}{dt} \\
&\quad = \lambda_3\,(p_2 + \mu_H + \sigma_H) - \lambda_8 \delta_e \left(1 - \frac{L_E}{K}\right) - \lambda_4 p_2 \\
&\qquad - R_1 \\
&\frac{d\lambda_4}{dt} = \lambda_4\,(\omega + \mu_H) - \lambda_1 \omega \\
&\frac{d\lambda_5}{dt} \\
&\quad = \lambda_5 \mu_A - (1 - w_2(t))\,(\lambda_6 - \lambda_5)\,\psi_{AA} \\
&\qquad - (1 - w_3(t))\,(\lambda_7 - \lambda_5)\,\psi_{EA} \\
&\frac{d\lambda_6}{dt} = (\lambda_6 - \lambda_7)\,(1 - w_3(t))\,\psi_{EA} + \lambda_6 \mu_A - R_4 \\
&\frac{d\lambda_7}{dt} \\
&\quad = \lambda_7\,(\mu_A + \sigma_A) - \frac{(1 - w_4(t))\,(\lambda_2 - \lambda_1)\,\rho_{AH} S_H}{N_H} \\
&\qquad - \lambda_8 \delta_e \left(1 - \frac{L_E}{K}\right) \\
&\qquad - \left\{\lambda_9 \varepsilon_A + \frac{(\lambda_6 - \lambda_5)\,\rho_A S_A}{N_A}\right\}(1 - w_2(t)) - R_3 \\
&\frac{d\lambda_8}{dt} = \frac{\lambda_8\,(I_{Hh} + I_{Ah})\,\delta_e}{K} + \lambda_8\,(\gamma_L + \mu_L) - \lambda_9 \gamma_L \\
&\frac{d\lambda_9}{dt} \\
&\quad = \lambda_9 \left\{(\mu_F + w_1(t)) + \frac{r_F k}{(k + F_E)^2}\right\} - R_5 \\
&\qquad - \chi_H\,(1 - w_5(t))\,\{S_H\,(\lambda_3 - \lambda_1) + I_{Hl}\,(\lambda_3 - \lambda_2)\} \\
&\qquad - \chi_A\,(1 - w_3(t))\,\{S_A\,(\lambda_7 - \lambda_5) + I_{Al}\,(\lambda_7 - \lambda_6)\},
\end{aligned} \tag{13}
$$

where $\chi_H = \alpha_{EH}\beta_{EH} r_F k/(k + F_E)^2$ *and* $\chi_A = \alpha_{EA}\beta_{EA} r_F k/(k + F_E)^2$ *with transversality conditions,* $\{\lambda_i(T)$ *for* $i = 1, 2, \ldots, 9\} = 0$, *and the control variables* $(w_1^*, w_2^*, w_3^*, w_4^*, w_5^*)$ *satisfy the following optimality conditions:*

$$
\begin{aligned}
w_1^* &= \min \left\{\max\left\{0, \frac{\lambda_9 F_E}{Z_1}\right\}, 1\right\}, \\
w_2^* &= \min \left\{\max\left\{0, \frac{\{\psi_{AA} S_A\,(\lambda_6 - \lambda_5) + \lambda_9 \varepsilon_A I_{Ah}\}}{Z_2}\right\}, 1\right\}, \\
w_3^* &= \min \left\{\max\left\{0, \frac{\psi_{EA}\,\{S_A\,(\lambda_7 - \lambda_5) + I_{Al}\,(\lambda_7 - \lambda_6)\}}{Z_3}\right\}, 1\right\},
\end{aligned}
$$

$$w_4^* = \min \left\{ \max \left\{ 0, \frac{\psi_{AH} S_H (\lambda_2 - \lambda_1)}{Z_4} \right\}, 1 \right\},$$
$$w_5^* = \min \left\{ \max \left\{ 0, \frac{\psi_{EH} \{S_H (\lambda_3 - \lambda_1) + I_{Hl} (\lambda_3 - \lambda_2)\}}{Z_5} \right\}, 1 \right\}. \tag{14}$$

Proof. The differential equations for the adjoints are standard results from Pontryagin's maximum principle (1962). Given the Hamiltonian function in (12) the adjoint equations can be easily computed by

$$\begin{aligned}
\frac{d\lambda_1}{dt} &= -\frac{dH}{dS_H}, \\
\frac{d\lambda_2}{dt} &= -\frac{dH}{dI_{Hl}}, \\
\frac{d\lambda_3}{dt} &= -\frac{dH}{dI_{Hh}}, \\
\frac{d\lambda_4}{dt} &= -\frac{dH}{dT_H}, \\
\frac{d\lambda_5}{dt} &= -\frac{dH}{dS_A}, \\
\frac{d\lambda_6}{dt} &= -\frac{dH}{dI_{Al}}, \\
\frac{d\lambda_7}{dt} &= -\frac{dH}{dI_{Ah}}, \\
\frac{d\lambda_8}{dt} &= -\frac{dH}{dL_E}, \\
\frac{d\lambda_9}{dt} &= -\frac{dH}{dF_E}.
\end{aligned} \tag{15}$$

Therefore, the adjoint system evaluated at optimal controls w_1, w_2, w_3, w_4, and w_5 and the corresponding model state variables S_H, I_{Hl}, I_{Hh}, T_H, S_A, I_{Al}, I_{Ah}, L_E, F_E is as given by

$$\begin{aligned}
&\frac{d\lambda_1}{dt} \\
&\quad = \lambda_1 \mu_H - (1 - w_4(t))(\lambda_2 - \lambda_1)\psi_{AH} \\
&\qquad - (1 - w_5(t))(\lambda_3 - \lambda_1)\psi_{EH} \\
&\frac{d\lambda_2}{dt} \\
&\quad = (1 - w_5(t))\psi_{EH}(\lambda_2 - \lambda_3) + \lambda_2(p_1 + \mu_H) \\
&\qquad - \lambda_4 p_1 - R_2 \\
&\frac{d\lambda_3}{dt} \\
&\quad = \lambda_3(p_2 + \mu_H + \sigma_H) - \lambda_8 \delta_e \left(1 - \frac{L_E}{K}\right) - \lambda_4 p_2 \\
&\qquad - R_1 \\
&\frac{d\lambda_4}{dt} = \lambda_4(\omega + \mu_H) - \lambda_1 \omega \\
&\frac{d\lambda_5}{dt} \\
&\quad = \lambda_5 \mu_A - (1 - w_2(t))(\lambda_6 - \lambda_5)\psi_{AA} \\
&\qquad - (1 - w_3(t))(\lambda_7 - \lambda_5)\psi_{EA} \\
&\frac{d\lambda_6}{dt} = (\lambda_6 - \lambda_7)(1 - w_3(t))\psi_{EA} + \lambda_6 \mu_A - R_4 \\
&\frac{d\lambda_7}{dt} \\
&\quad = \lambda_7(\mu_A + \sigma_A) - \frac{(1 - w_4(t))(\lambda_2 - \lambda_1)\rho_{AH} S_H}{N_H} \\
&\qquad - \lambda_8 \delta_e \left(1 - \frac{L_E}{K}\right) \\
&\qquad - \left\{ \lambda_9 \varepsilon_A + \frac{(\lambda_6 - \lambda_5)\rho_A S_A}{N_A} \right\}(1 - w_2(t)) - R_3 \\
&\frac{d\lambda_8}{dt} = \frac{\lambda_8 (I_{Hh} + I_{Ah}) \delta_e}{K} + \lambda_8(\gamma_L + \mu_L) - \lambda_9 \gamma_L \\
&\frac{d\lambda_9}{dt} \\
&\quad = \lambda_9 \left\{ (\mu_F + w_1(t)) + \frac{r_F k}{(k + F_E)^2} \right\} - R_5 \\
&\qquad - \chi_H (1 - w_5(t)) \{S_H(\lambda_3 - \lambda_1) + I_{Hl}(\lambda_3 - \lambda_2)\} \\
&\qquad - \chi_A (1 - w_3(t)) \{S_A(\lambda_7 - \lambda_5) + I_{Al}(\lambda_7 - \lambda_6)\},
\end{aligned} \tag{16}$$

where $\chi_H = \alpha_{EH}\beta_{EH} r_F k/(k + F_E)^2$ and $\chi_A = \alpha_{EA}\beta_{EA} r_F k/(k + F_E)^2$ with transversality conditions, $\{\lambda_i(T) \text{ for } i = 1, 2, \ldots, 9\} = 0$, and the characterization of optimal controls $w_1^*, w_2^*, w_3^*, w_4^*, w_5^*$; that is, the optimality equations are based on the conditions:

$$\frac{\partial H}{\partial w_1} = \frac{\partial H}{\partial w_2} = \frac{\partial H}{\partial w_3} = \frac{\partial H}{\partial w_4} = \frac{\partial H}{\partial w_5} = 0. \tag{17}$$

Subject to (17) the optimality condition given the Lebesgue measurable control set $\Pi = \{0 \le w_i(t) \le 1$, for

$i = 1, 2, \ldots, 5$ and $t \in [0, T]\}$, where the control variables w_1, w_2, w_3, w_4, w_5 are measurable functions, is given by

$$\begin{aligned}
\frac{\partial H}{\partial w_1} &= Z_1 w_1 - \lambda_9 F_E \\
\frac{\partial H}{\partial w_2} &= Z_2 w_2 + \lambda_5 \psi_{AA} S_A - \lambda_6 \psi_{AA} S_A - \lambda_9 \varepsilon_A I_{Ah} \\
\frac{\partial H}{\partial w_3} &= Z_3 w_3 + \lambda_5 \psi_{EA} S_A + \lambda_6 \psi_{EA} I_{Al} - \lambda_7 \psi_{EA} S_A \\
&\quad - \lambda_7 \psi_{EA} I_{Al} \\
\frac{\partial H}{\partial w_4} &= Z_4 w_4 + \lambda_1 \psi_{AH} S_H - \lambda_2 \psi_{AH} S_H \\
\frac{\partial H}{\partial w_5} &= Z_5 w_5 + \lambda_1 \psi_{EH} S_H + \lambda_2 \psi_{EH} I_{Hl} - \lambda_3 \psi_{EH} S_H \\
&\quad - \lambda_3 \psi_{EH} I_{Hl}.
\end{aligned} \tag{18}$$

If we set $\partial H / \partial w_i = 0$ at w_i^* the results are the same as in characterization in (14).

In order to satisfy the given bounds for the control functions (i.e., $0 \le w_i \le 1$ and $t \in [0, T]$) the optimal control is restricted to $w_i^* = \min\{\max(0, w_i), 1\}$. Therefore using the bounds for the controls w_1, w_2, w_3, w_4, w_5 we have the following.

The bounds and the impact notation for the control w_1 are, respectively, given as

$$w_1^* = \begin{cases} \dfrac{\lambda_9 F_E^*}{Z_1} & \text{if } 0 \le \dfrac{\lambda_9 F_E^*}{Z_1} \le 1, \\ 0 & \text{if } \dfrac{\lambda_9 F_E^*}{Z_1} \le 0, \\ 1 & \text{if } \dfrac{\lambda_9 F_E^*}{Z_1} \ge 1, \end{cases} \tag{19}$$

$$w_1^* = \min\left\{\max\left\{0, \frac{\lambda_9 F_E^*}{Z_1}\right\}, 1\right\}.$$

Similar four-step arguments hold for optimal control schedules w_2^*, w_3^*, w_4^*, and w_5^* in the same way as in (19) based on the characterization in (14). □

3.3. The Optimality System. The optimality system consists of the state system and adjoint system with initial and transversal conditions together with characterization of optimal control. Any optimal control pair must satisfy this optimality system as indicated in (20) and (22), respectively.

$$\begin{aligned}
\frac{dS_H(t)}{dt} &= b_H N_H - \Bigg(1 \\
&\quad - \min\left\{\max\left\{0, \frac{\psi_{EH}^* \{S_H(\lambda_3 - \lambda_1) + I_{Hl}(\lambda_3 - \lambda_2)\}}{Z_5}\right\}, \right. \\
&\quad \left. 1\right\}\Bigg) \psi_{EH}^* S_H + \omega T_H - \Bigg(1 \\
&\quad - \min\left\{\max\left\{0, \frac{\psi_{AH}^* S_H(\lambda_2 - \lambda_1)}{Z_4}\right\}, 1\right\}\Bigg) \psi_{AH}^* S_H \\
&\quad - \mu_H S_H \\
\frac{dI_{Hl}(t)}{dt} &= \left(1 - \min\left\{\max\left\{0, \frac{\psi_{AH}^* S_H(\lambda_2 - \lambda_1)}{Z_4}\right\}, 1\right\}\right) \\
&\quad \cdot \psi_{AH}^* S_H - \Bigg(1 \\
&\quad - \min\left\{\max\left\{0, \frac{\psi_{EH}^* \{S_H(\lambda_3 - \lambda_1) + I_{Hl}(\lambda_3 - \lambda_2)\}}{Z_5}\right\}, \right. \\
&\quad \left. 1\right\}\Bigg) \psi_{EH}^* I_{Hl} - p_1 I_{Hl} - \mu_H I_{Hl} \\
\frac{dI_{Hh}(t)}{dt} &= \Bigg(1 \\
&\quad - \min\left\{\max\left\{0, \frac{\psi_{EH}^* \{S_H(\lambda_3 - \lambda_1) + I_{Hl}(\lambda_3 - \lambda_2)\}}{Z_5}\right\}, \right. \\
&\quad \left. 1\right\}\Bigg) \psi_{EH}^* (S_H + I_{Hl}) - p_2 I_{Hh} - (\mu_H + \sigma_H) I_{Hh} \\
\frac{dT_H(t)}{dt} &= p_1 I_{Hl} + p_2 I_{Hh} - \omega T_H - \mu_H T_H \\
\frac{dS_A(t)}{dt} &= b_A N_A - \Bigg(1 \\
&\quad - \min\left\{\max\left\{0, \frac{\psi_{AA}^* S_A(\lambda_6 - \lambda_5) + \lambda_9 \varepsilon_A I_{Ah}}{Z_2}\right\}, 1\right\}\Bigg) \\
&\quad \cdot \psi_{AA}^* S_A - \Bigg(1 \\
&\quad - \min\left\{\max\left\{0, \frac{\psi_{EA}^* \{S_A(\lambda_7 - \lambda_5) + I_{Al}(\lambda_7 - \lambda_6)\}}{Z_3}\right\}, \right. \\
&\quad \left. 1\right\}\Bigg) \psi_{EA}^* S_A - \mu_A S_A \\
\frac{dI_{Al}(t)}{dt} &= \Bigg(1 \\
&\quad - \min\left\{\max\left\{0, \frac{\{\psi_{AA}^* S_A(\lambda_6 - \lambda_5) + \lambda_9 \varepsilon_A I_{Ah}\}}{Z_2}\right\}, 1\right\}\Bigg) \\
&\quad \cdot \psi_{AA}^* S_A - \Bigg(1 \\
&\quad - \min\left\{\max\left\{0, \frac{\psi_{EA}^* \{S_A(\lambda_7 - \lambda_5) + I_{Al}(\lambda_7 - \lambda_6)\}}{Z_3}\right\}, \right. \\
&\quad \left. 1\right\}\Bigg) \psi_{EA}^* I_{Al} - \mu_A I_{Al} \\
\frac{dI_{Ah}(t)}{dt} &= \Bigg(1
\end{aligned}$$

$$
\begin{aligned}
&- \min\left\{\max\left\{0, \frac{\psi_{EA}^{*}\left\{S_A\left(\lambda_7-\lambda_5\right)+I_{Al}\left(\lambda_7-\lambda_6\right)\right\}}{Z_3}\right\},\right.\\
&\left.1\right\}\Bigg)\psi_{EA}^{*}\left(S_A+I_{Al}\right)-\left(\mu_A+\sigma_A\right)I_{Ah}\\
&\frac{dL_E(t)}{dt}=\delta_e\left(1-\frac{L_E}{K}\right)\left(I_{Hh}+I_{Ah}\right)-\left(\gamma_L+\mu_L\right)L_E\\
&\frac{dF_E(t)}{dt}=\gamma_L L_E+\Bigg(1\\
&- \min\left\{\max\left\{0, \frac{\left\{\psi_{AA}^{*}S_A\left(\lambda_6-\lambda_5\right)+\lambda_9\varepsilon_A I_{Ah}\right\}}{Z_2}\right\},1\right\}\Bigg)\\
&\cdot\varepsilon_A I_{Ah}-\left(\mu_F+\min\left\{\max\left\{0, \frac{\lambda_9 F_E}{Z_1}\right\},1\right\}\right)F_E\\
&- \frac{r_F F_E}{\left(k+F_E\right)}
\end{aligned}
\tag{20}
$$

with initial conditions

$$
\begin{aligned}
&S_H(0)>0,\\
&I_{Hl}(0)\geq 0,\\
&I_{Hh}(0)\geq 0,\\
&T_H(0)\geq 0,\\
&S_A(0)>0,\\
&I_{Al}(0)\geq 0,\\
&I_{Ah}(0)\geq 0,\\
&L_E(0)\geq 0,\\
&F_E(0)>0,
\end{aligned}
\tag{21}
$$

$$
\begin{aligned}
&\frac{d\lambda_1}{dt}=\lambda_1\mu_H-\Bigg(1\\
&- \min\left\{\max\left\{0, \frac{\psi_{EA}^{*}\left\{S_A\left(\lambda_7-\lambda_5\right)+I_{Al}\left(\lambda_7-\lambda_6\right)\right\}}{Z_3}\right\},\right.\\
&\left.1\right\}\Bigg)\psi_{AH}^{*}\left(\lambda_2-\lambda_1\right)-\Bigg(1\\
&- \min\left\{\max\left\{0, \frac{\psi_{EH}^{*}\left\{S_H\left(\lambda_3-\lambda_1\right)+I_{Hl}\left(\lambda_3-\lambda_2\right)\right\}}{Z_5}\right\},\right.\\
&\left.1\right\}\Bigg)\psi_{EH}^{*}\left(\lambda_3-\lambda_1\right)\\
&\frac{d\lambda_2}{dt}=\Bigg(1\\
&- \min\left\{\max\left\{0, \frac{\psi_{EH}^{*}\left\{S_H\left(\lambda_3-\lambda_1\right)+I_{Hl}\left(\lambda_3-\lambda_2\right)\right\}}{Z_5}\right\},\right.\\
&\left.1\right\}\Bigg)\psi_{EH}^{*}\left(\lambda_2-\lambda_3\right)+\lambda_2\left(p_1+\mu_H\right)-\lambda_4 p_1-R_2\\
&\frac{d\lambda_3}{dt}=\lambda_3\left(p_2+\mu_H+\sigma_H\right)-R_1-\lambda_4 p_2-\lambda_8\delta_e\left(1-\frac{L_E}{K}\right)\\
&\frac{d\lambda_4}{dt}=\lambda_4\left(\omega+\mu_H\right)-\lambda_1\omega\\
&\frac{d\lambda_5}{dt}=\lambda_5\mu_A-\Bigg(1\\
&- \min\left\{\max\left\{0, \frac{\left\{\psi_{AA}^{*}S_A\left(\lambda_6-\lambda_5\right)+\lambda_9\varepsilon_A I_{Ah}\right\}}{Z_2}\right\},1\right\}\Bigg)\\
&\cdot\psi_{AA}^{*}\left(\lambda_6-\lambda_5\right)-\Bigg(1-\min\left\{\max\left\{0,\right.\right.\\
&\left.\left.\frac{\psi_{EA}^{*}\left\{S_A\left(\lambda_7-\lambda_5\right)+I_{Al}\left(\lambda_7-\lambda_6\right)\right\}}{Z_3}\right\},1\right\}\Bigg)\psi_{EA}^{*}\left(\lambda_7-\lambda_5\right)\\
&\frac{d\lambda_6}{dt}=\left(\lambda_6-\lambda_7\right)\Bigg(1\\
&- \min\left\{\max\left\{0, \frac{\psi_{EA}^{*}\left\{S_A\left(\lambda_7-\lambda_5\right)+I_{Al}\left(\lambda_7-\lambda_6\right)\right\}}{Z_3}\right\},\right.\\
&\left.1\right\}\Bigg)\psi_{EA}+\lambda_6\mu_A-R_4\\
&\frac{d\lambda_7}{dt}=\lambda_7\left(\mu_A+\sigma_A\right)-\Bigg(1\\
&- \min\left\{\max\left\{0, \frac{\psi_{AH}^{*}S_H\left(\lambda_2-\lambda_1\right)}{Z_4}\right\},1\right\}\Bigg)\\
&\cdot\frac{\left(\lambda_2-\lambda_1\right)\rho_{AH}S_H}{N_H}-\left\{\lambda_9\varepsilon_A+\frac{\left(\lambda_6-\lambda_5\right)\rho_A S_A}{N_A}\right\}\Bigg(1\\
&- \min\left\{\max\left\{0, \frac{\left\{\psi_{AA}^{*}S_A\left(\lambda_6-\lambda_5\right)+\lambda_9\varepsilon_A I_{Ah}\right\}}{Z_2}\right\},1\right\}\Bigg)\\
&- \lambda_8\delta_e\left(1-\frac{L_E}{K}\right)-R_3\\
&\frac{d\lambda_8}{dt}=\frac{\lambda_8\left(I_{Hh}+I_{Ah}\right)\delta_e}{K}+\lambda_8\left(\gamma_L+\mu_L\right)-\lambda_9\gamma_L\\
&\frac{d\lambda_9}{dt}=\lambda_9\left\{\left(\mu_F+\mu_F+\min\left\{\max\left(0, \frac{\lambda_9 F_E}{Z_1}\right),1\right\}\right)\right.\\
&\left.+\frac{r_F k}{\left(k+F_E\right)^2}\right\}-R_5-\chi_H\Bigg(1\\
&- \min\left\{\max\left\{0, \frac{\psi_{EH}^{*}\left\{S_H^{*}\left(\lambda_3-\lambda_1\right)+I_{Hl}^{*}\left(\lambda_3-\lambda_2\right)\right\}}{Z_5}\right\},\right.\\
&\left.1\right\}\Bigg)\left\{S_H\left(\lambda_3-\lambda_1\right)+I_{Hl}\left(\lambda_3-\lambda_2\right)\right\}-\chi_A\Bigg(1\\
&- \min\left\{\max\left\{0, \frac{\psi_{EA}^{*}\left\{S_A\left(\lambda_7-\lambda_5\right)+I_{Al}\left(\lambda_7-\lambda_6\right)\right\}}{Z_3}\right\},\right.\\
&\left.1\right\}\Bigg)\left\{S_A\left(\lambda_7-\lambda_5\right)+I_{Al}\left(\lambda_7-\lambda_6\right)\right\},
\end{aligned}
\tag{22}
$$

where $\chi_H=\alpha_{EH}\beta_{EH}r_F k/(k+F_E)^2$ and $\chi_A=\alpha_{EA}\beta_{EA}r_F k/(k+F_E)^2$ with transversality conditions $\{\lambda_i(T)$ for $i=1,2,\ldots,9\}=0$.

Table 1: Parameter values for numerical simulation of optimal control model.

Parameter	Value/range	Source/references
k	1×10^4 cell/m^3	Estimated
K	1×10^5 cell/m^3	Estimated
γ_L	0.0105 per day¡sup/¿	Estimated
σ_H	0.011 per day	Estimated
σ_A	0.037 per day	Estimated
μ_H	0.000045 per day	UNICEF. [14]
μ_A	0.0028 (360–3600)$^{-1}$ per day	Gaff et al. [15]; Radostits. (2001)
μ_F	0.04 per day	Eisele et al. [16],
r_F	0.58 per day	Estimated
μ_L	0.08 per day	Estimated
β_{EH}	0.19 per day	Estimated
β_{EA}	0.48 per day	Estimated
ρ_{AH}	0.052 per day	Gaff et al. [15]
ρ_A	0.26 (0.091–0.9) per day	Allerson et al. [17]
b_H	0.00011 per day	TP, [18].
b_A	0.022 per day	Gaff et al. [15]
ε_A	0.40 per day	Estimated
δ_e	0.12 per day	Estimated
α_{EH}	0.4	Estimated
α_{EA}	0.6	Estimated
p_1	0.15	Estimated
p_2	0.15	Estimated
ω	0.09	Estimated

Source: Kahuru et al. [19].

4. Numerical Simulation of the Optimal Control Model, Results, and Discussion

Sometimes it may not be possible to solve the optimality system analytically; instead numerical methods are used to approximate the solutions and display the results. The optimality system is a two-point boundary problem, because of the initial condition of the state system and the terminal condition of the adjoint system [30]. To solve the optimality system with initial conditions for the states and final time conditions for the adjoints, we use the Runge-Kutta fourth-order procedure which is more accurate and elaborative technique. A Runge-Kutta method is a multiple-step method, where the solution at time t_{k+1} is obtained from a defined set of previous values $t_{n-k}, \ldots, t_k$ and n is the number of steps. This method is described in a book by Lenhart and Workman [8] and it is known as forward-backward sweep method. The process begins with an initial guess on the control variable and given initial conditions for states, we approximate solutions for state equations using Runge-Kutta forward sweep method. Given the state solutions from previous step and the final time conditions for adjoints, we approximate solutions for adjoint equations using Runge-Kutta backward sweep method. The value of control variables is updated by averaging the previous value and the new value arising from the control characterization. The process is repeated for forward numerical scheme and updating of the controls until successive values of all states, adjoints, and controls are sufficiently close or converge.

4.1. Numerical Simulation of Optimal Control Model. We conduct numerical simulation in order to investigate the effects of the control strategies on the transmission dynamics of Tungiasis. The simulations are performed using MALAB, and we set time in days. The estimated initial values of model state variables are $S_H = 1000$, $I_{Hl} = 200$, $I_{Hh} = 300$, $T_H = 0$, $S_A = 900$, $I_{Al} = 200$, $I_{Ah} = 300$, $L_E = 10000$, and $F_E = 4000$ and for the adjoint system we have terminal conditions $\{\lambda_i(T)$ for $i = 1, \ldots, 9\} = 0$, where we set $T = 200$ days. The cost coefficients corresponding to state variables are estimated to be $R_1 = 20$, $R_2 = 10$, $R_3 = 15$, $R_4 = 20$, and $R_5 = 25$. The quadratic cost coefficient corresponding to control measures is as well estimated to be $Z_1 = 50$, $Z_2 = 60$, $Z_3 = 80$, $Z_4 = 10$, and $Z_5 = 15$. We use a set of parameter values whose sources are from literature and others are estimated as shown in Table 1.

We then plot the graphs to show the effects of the control measures when implemented under different combination options. We first illustrate the situation when no optimal control strategy is implemented as shown in Figures 2(a)–2(d) and then we suggest seven control strategies with different combinations of control measures and compare their performance in order to determine the best option to control the disease for maximum benefit.

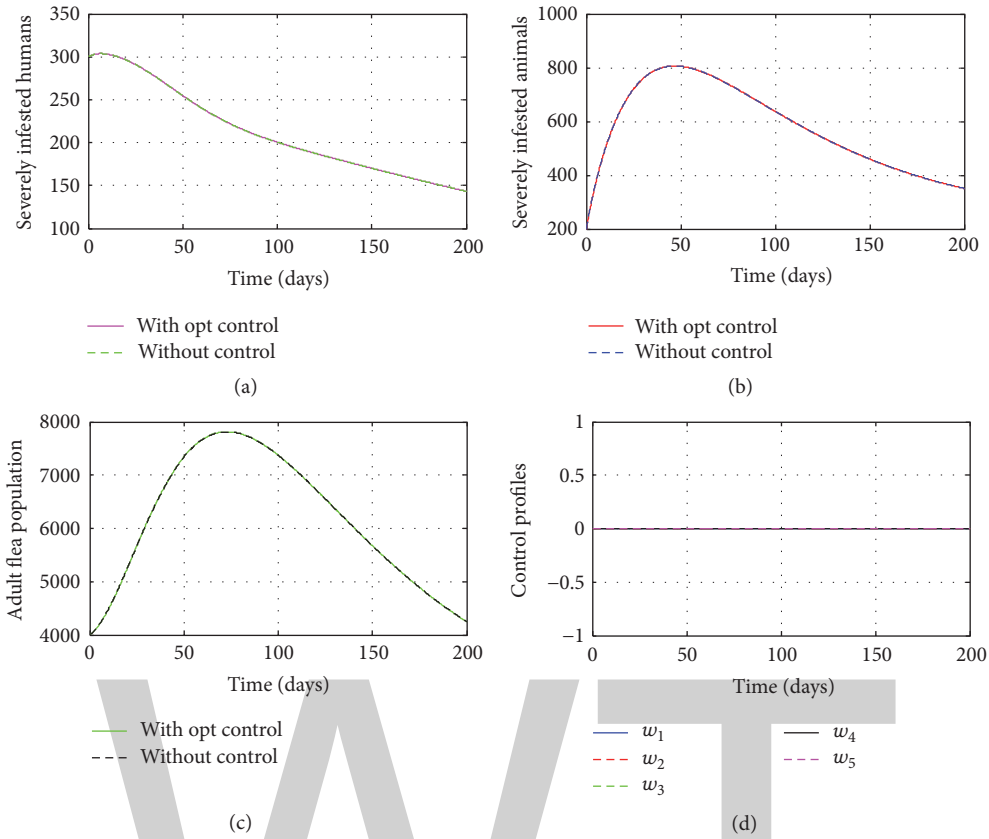

Figure 2: Simulations of model variables I_{Hh}, I_{Ah}, F_E without intervention.

4.2. Discussion of the Results. In this section, we present the results of the numerical simulation of our optimal control problem by discussing the implications of implementing the seven optimal control strategies on the Tungiasis dynamical model. To observe the effects of the optimal control strategies, we plot the results from simulation of the uncontrolled system and that from the controlled system together in Figures 3–9. To compare the effects of these options, we plot the results together in Figures 10(a)–10(c). Thus we consider the following seven combination options.

4.2.1. When All the Control Strategies Are Not Implemented (i.e., $w_1, w_2, w_3, w_4, w_5 = 0$). Figures 2(a)–2(c) show the situation where no control strategy is implemented to the dynamical system whereby the model trajectories represented by a dotted lines for severely infested humans, severely infested animal reservoir, and flea populations remain unchanged and the control profiles in Figure 2(d) show that all control measures are at the lower bound (i.e., $w_1, w_2, w_3, w_4, w_5 = 0$).

4.2.2. Strategy 1: All Control Measures Are Implemented (i.e., $w_1, w_2, w_3, w_4, w_5 \neq 0$). Under strategy 1, all the control measures $(w_1, w_2, w_3, w_4, w_5)$ are used to optimize the objective functional $J(w)$. In Figure 3(d), the control measure w_5 is at upper bound at the beginning and after 40 days it gradually drops to the lower bound at the final time. The control measure w_3 is at the upper bound at the beginning and after 45 days it gradually drops to the lower bound at the final time. The control measure w_1 is at the upper bound at the beginning and after 60 days it drops to the lower bound at the final time. The control measure w_4 is at the upper bound at the beginning and after 140 days it rapidly drops to the lower bound at the final time and the control measure w_2 starts at the upper bound at the beginning and remains there until it drops to the lower bound.

4.2.3. Strategy 2: The Control Measures (i.e., $w_2, w_3, w_4, w_5 \neq 0$ and $w_1 = 0$). Under strategy 2, the control measures (w_2, w_3, w_4, w_5) are used to optimize the objective functional $J(w)$. In Figure 4(d), the control measure w_4 is at upper bound at the beginning and after 140 days it rapidly drops to the lower bound at the final time. The control measure w_5 is at the upper bound at the beginning and after 175 days it rapidly drops to the lower bound at the final time. The control measure w_3 is at the upper bound at the beginning and after 195 days it drops to the lower bound at the final time. The control measure w_2 starts at the upper bound at the beginning and remains there until it drops to the lower bound at the final time. The control measure w_1 is at the lower bound at the beginning and remains there till the final time.

4.2.4. Strategy 3: The Control Measures (i.e., $w_3, w_4, w_5 \neq 0$ and $w_1, w_2 = 0$). Under strategy 3, the control measures (w_3, w_4, w_5) are used to optimize the objective functional

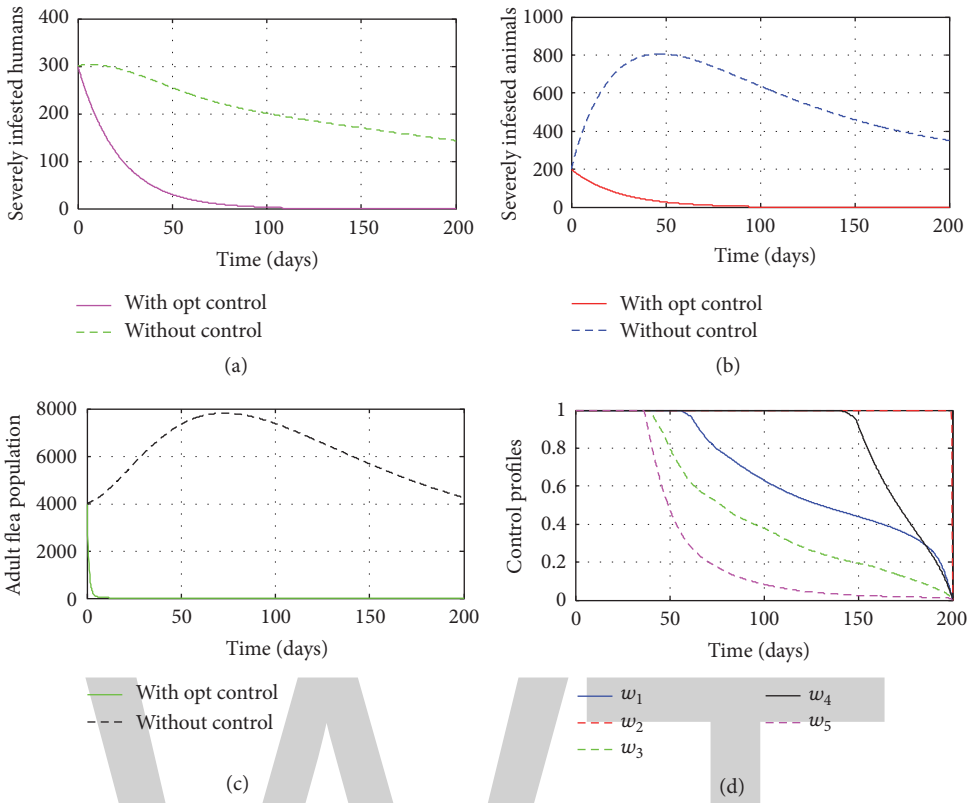

FIGURE 3: Optimal solutions for model variables I_{Hh}, I_{Ah}, F_E and the control profiles for w_1, w_2, w_3, w_4, w_5 with $(w_1, w_2, w_3, w_4, w_5 \neq 0)$.

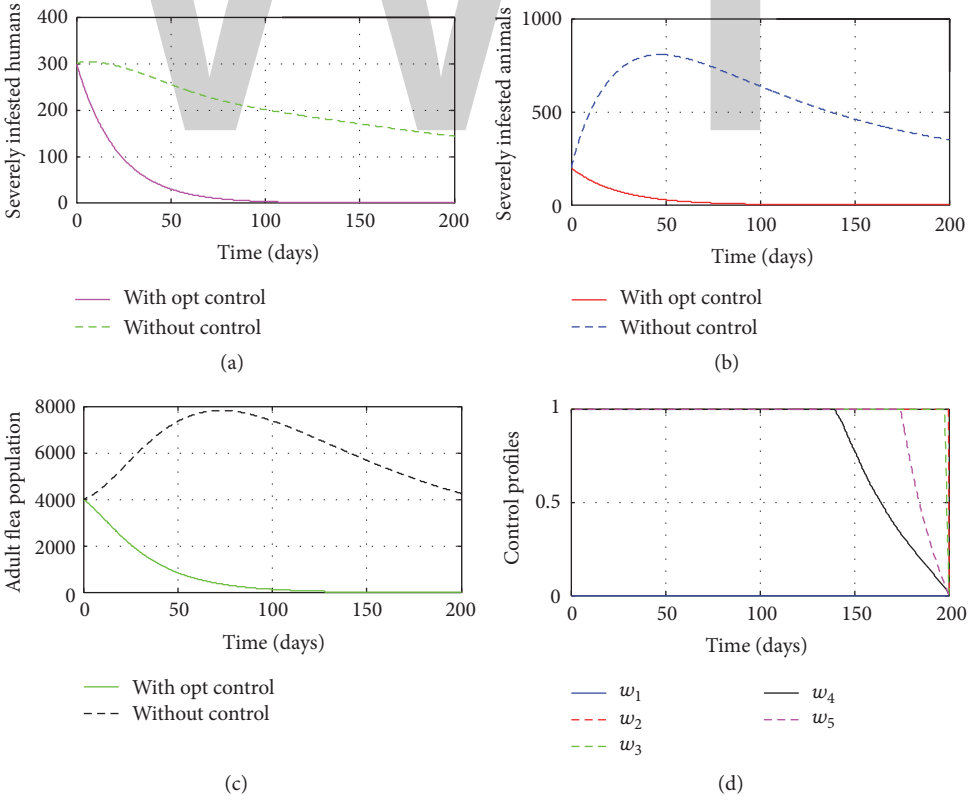

FIGURE 4: Optimal solutions for model variables I_{Hh}, I_{Ah}, F_E and the control profiles for w_1, w_2, w_3, w_4, w_5 with $(w_2, w_3, w_4, w_5 \neq 0)$.

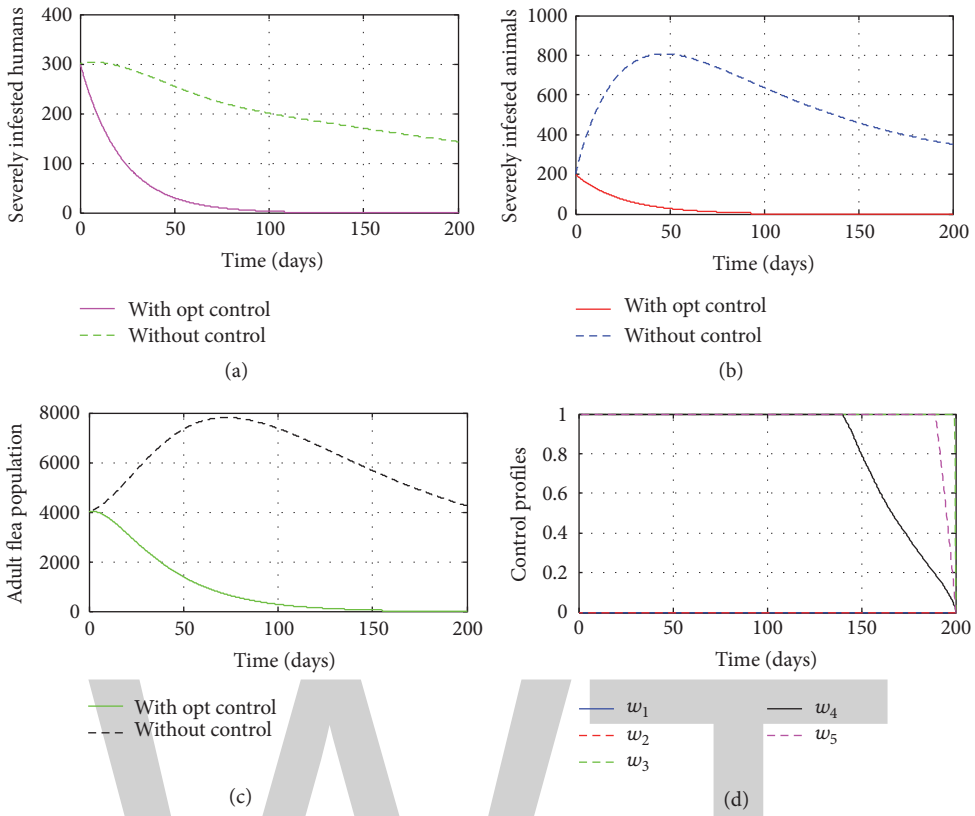

FIGURE 5: Optimal solutions for model variables I_{Hh}, I_{Ah}, F_E and the control profiles for w_1, w_2, w_3, w_4, w_5 with $(w_3, w_4, w_5 \neq 0)$.

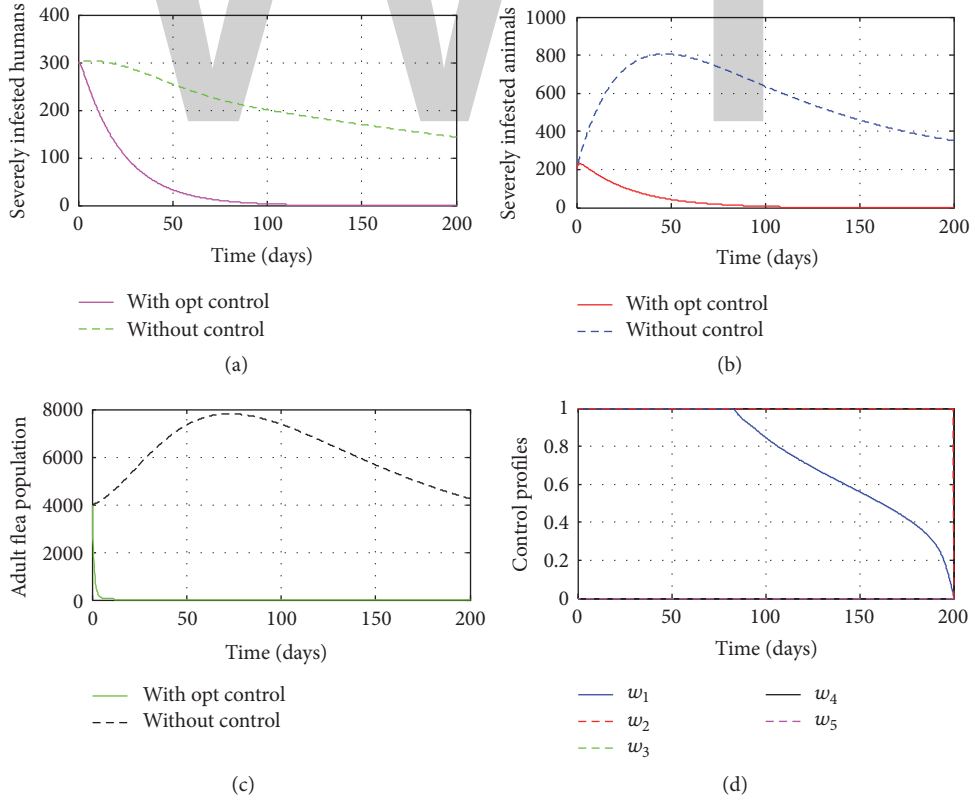

FIGURE 6: Optimal solutions for model variables I_{Hh}, I_{Ah}, F_E and the control profiles for w_1, w_2, w_3, w_4, w_5 with $(w_1, w_2 \neq 0)$.

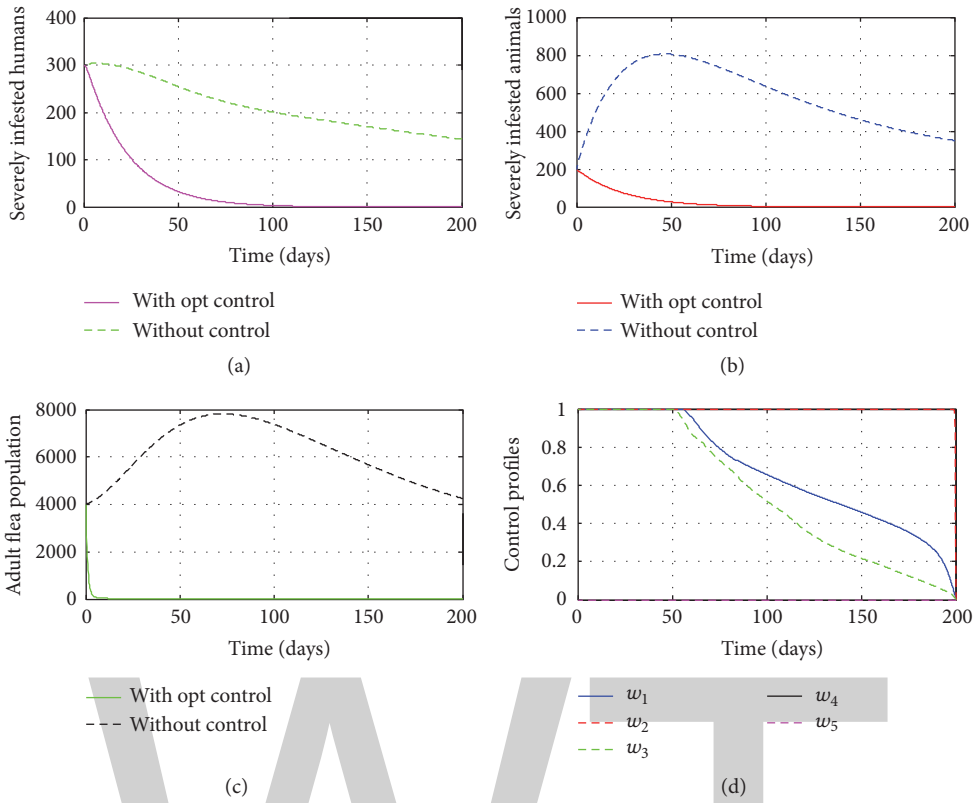

FIGURE 7: Optimal solutions for model variables I_{Hh}, I_{Ah}, F_E and the control profiles for w_1, w_2, w_3, w_4, w_5 with $(w_1, w_2, w_3 \neq 0)$.

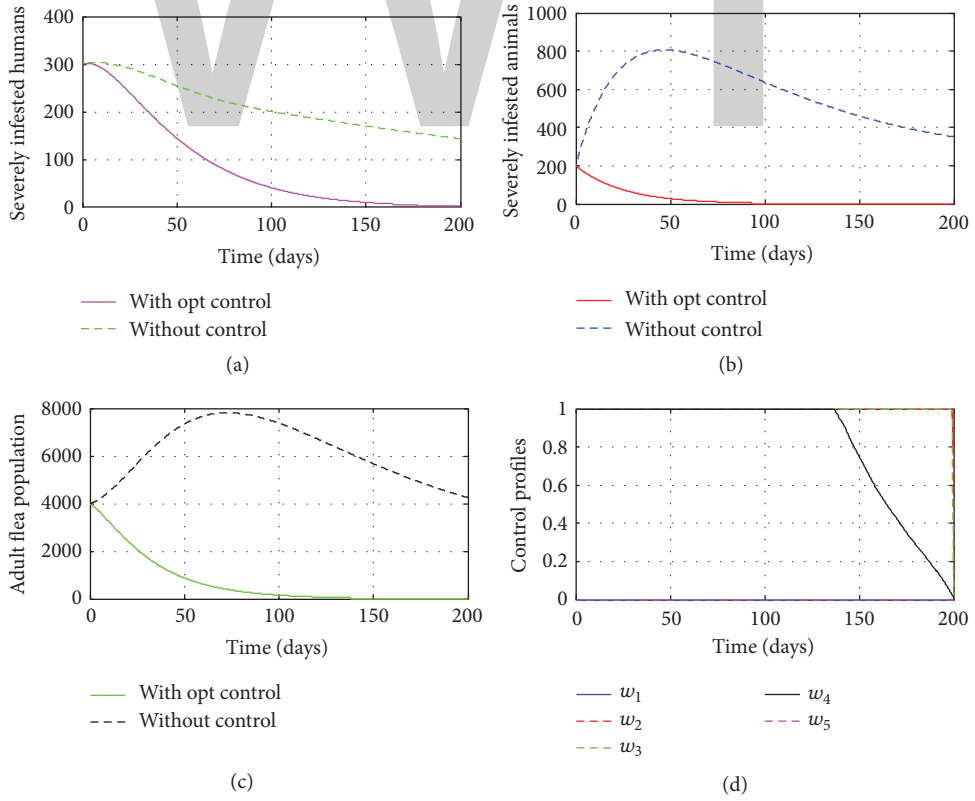

FIGURE 8: Optimal solutions for model variables I_{Hh}, I_{Ah}, F_E and the control profiles for w_1, w_2, w_3, w_4, w_5 with $(w_2, w_3, w_4 \neq 0)$.

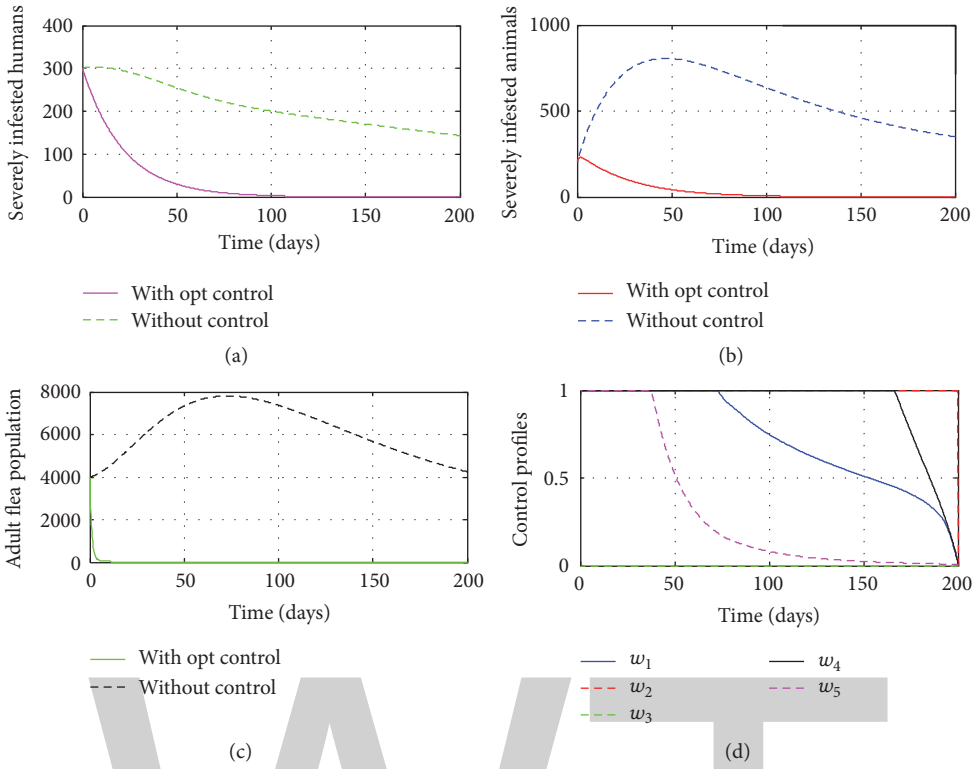

FIGURE 9: Optimal solutions for model variables I_{Hh}, I_{Ah}, F_E and the control profiles for w_1, w_2, w_3, w_4, w_5 with $(w_1, w_2, w_4, w_5 \neq 0)$.

$J(w)$. In Figure 5(d), the control measure w_4 is at upper bound at the beginning and after 140 days it rapidly drops to the lower bound at the final time. The control measure w_5 is at the upper bound at the beginning and after 190 days it rapidly drops to the lower bound at the final time. The control measure w_3 starts at the upper bound at the beginning and remains there until it drops to the lower bound. The control measures w_1 and w_2 start at the lower bound at the beginning and remains there till the final time.

4.2.5. Strategy 4: The Control Measures (i.e., $w_1, w_2 \neq 0$ and $w_3, w_4, w_5 = 0$). Under strategy 4, the control measures (w_1, w_2) are used to optimize the objective functional $J(w)$. In Figure 6(d), the control measure w_1 is at upper bound at the beginning and after 80 days it gradually drops to the lower bound at the final time. The control measure w_2 starts at the upper bound at the beginning and remains there until it drops to the lower bound. The control measures, w_3, w_4, and w_5, start at the lower bound at the beginning and remain there till the final time.

4.2.6. Strategy 5: The Control Strategies (i.e., $w_1, w_2, w_3 \neq 0$ and $w_4, w_5 = 0$). Under strategy 5, the control measures (w_1, w_2, w_3) are used to optimize the objective functional $J(w)$. In Figure 7(d), the control measure w_3 is at upper bound at the beginning and after 50 days it gradually drops to the lower bound at the final time. The control measure w_1 is at the upper bound at the beginning and after 60 days it gradually drops to the lower bound at the final time. The control measure w_2 starts at the upper bound at the beginning and remains there until it drops to the lower bound at the final time. The control measures w_4 and w_5 start at the lower bound at the beginning and remains there till the final time.

4.2.7. Strategy 6: The Control Measures (i.e., $w_2, w_3, w_4 \neq 0$ and $w_1, w_5 = 0$). Under strategy 6, the control measures (w_2, w_3, w_4) are used to optimize the objective functional $J(w)$. In Figure 8(d), the control measure w_4 is at upper bound at the beginning and after 140 days it rapidly drops to the lower bound at the final time. The control measures w_2 and w_3 start at the upper bound at the beginning and remain there until they drop to the lower bound. The control measures w_1 and w_5 start at the lower bound at the beginning and remain there till the final time.

4.2.8. Strategy 7: The Control Measures (i.e., $w_1, w_2, w_4, w_5 \neq 0$ and $w_3 = 0$). Under strategy 7, the control measures (w_1, w_2, w_4, w_5) are used to optimize the objective functional $J(w)$. In Figure 9(d), the control measure w_5 is at the upper bound at the beginning and after 40 days it gradually drops to the lower bound at the final time. The control measure w_1 is at the upper bound at the beginning and after 75 days it gradually drops to the lower bound at the final time. The control measure w_4 is at the upper bound at the beginning and after 170 days it rapidly drops to the lower bound at the final time. The control measure w_2 starts at the upper bound at the beginning and remains there until it drops to the lower bound at the final time and the control measure w_3 starts at the lower bound at the beginning and remains there till the final time.

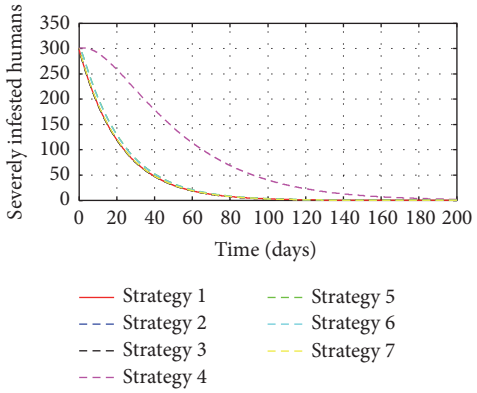

(a) The comparison of the control strategies on severely infested humans

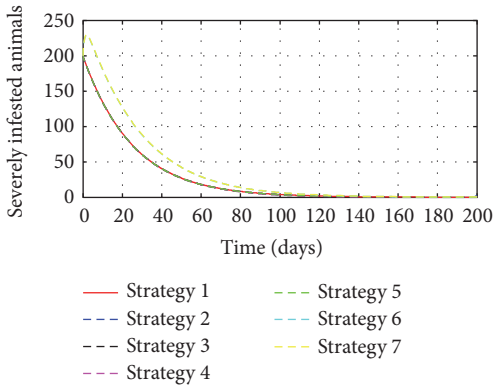

(b) The comparison of the control strategies on severely infested animals

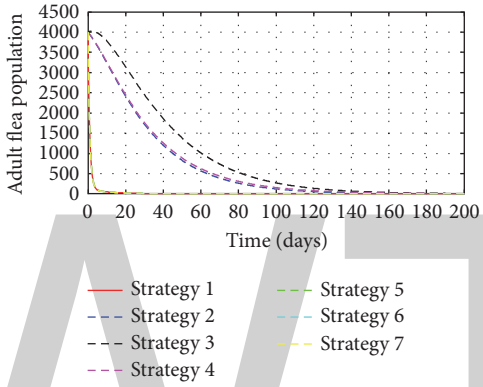

(c) The comparison of the control strategies on the adult flea population

Figure 10

Generally, it is observed in Figures 3(a)–3(c), 4(a)–4(c), 5(a)–5(c), 6(a)–6(c), 7(a)–7(c), 8(a)–8(c), and 9(a)–9(c) that the controlled trajectories represented by the solid lines decrease compared to uncontrolled trajectories represented by the dotted lines. This implies that the control strategies have the positive impacts which lead to a reduction in the number of infested humans and animals and also reduces the sand flea population in the soil environment.

4.2.9. The Comparison of the Control Strategies. To compare the performance of the control strategies under consideration, we plot the results on same graphs indicating the effects of the control strategies as indicated in Figures 10(a)–10(c).

From Figures 10(a)–10(c), it is observed that the control strategy involving the combination of all the five control measures w_1, w_2, w_3, w_4, w_5 has the significant impact on the reduction of disease transmission because it lowers the severely infested humans and animals and the sand flea populations to minimal levels compared to other control strategies. The red solid line as depicted in Figures 10(a), 10(b), and 10(c) represents the effect caused by the control strategy 1: with the combination of all five control measures. This is the best control strategy because it dominates both graphs as it decreases rapidly compared to other trajectories. Moreover we have observed that those control strategies, whose combinations involve the control measure based on insecticides applications to the premises (w_1), yield better results. These are control strategies 5, 6, and 7. But control strategy 5 denoted by the control measures (w_1, w_2, w_3) performs better in the same way as the control strategy 1 denoted by the control measures $(w_1, w_2, w_3, w_4, w_5)$.

5. Conclusion

In this paper, the optimal control techniques have been applied on Tungiasis dynamical model with control strategies. We defined the control set including controlling the transmission of infestation from flea infested soil environment to human population, from the flea infested soil environment to animal population, and from flea infested animal to human population, controlling flea infested soil environment, and controlling the flea infested animal population. We proved the existence of optimal control problem and determined the necessary conditions for optimality using Pontryagin's maximum principle which converts constrained optimization problem into unconstrained Hamiltonian function whereby optimality and adjoint equations are obtained. We, lastly, performed numerical simulations of the resulting control problem to investigate the effects of the control strategies under consideration and compare their

performances. The numerical results showed that the control strategy that comprises all five control measures and that with control measures (w_1, w_2, w_3) have the significant impact on reduced Tungiasis transmission and those control strategies involving insecticides control to the premises (w_1) yielded better results, which implies that the insecticides application control is more effective than other individual control measures. In poor rural communities where resources are always scarce, we suggest that the combination option involving the controls of focal insecticides spraying, insecticidal dusting on animal furs, and environmental hygiene should be adopted, having observed from the comparison of all seven control strategies in Figures 10(a), 10(b), and 10(c) that there is no significant difference between this strategy $(w_1, w_2, w_3 \neq 0)$ and the strategy that involves the combination of the five control measures $(w_1, w_2, w_3, w_4, w_5 \neq 0)$. Among others, poor housing conditions and the presence of domestic and sylvatic animals on the home compound are risk factors. Therefore, controlling of infested soils and animal reservoirs with insecticides control, ant-flea compounds or animal furs, environmental hygiene, and cementing the floors of houses may serve as a possible approach to control the epidemic and, thus, to fight against Tungiasis infestation in endemic settings multidimensional control process should be employed in order to achieve the maximum benefits.

Notations

The State Variables of the Model with Control Measures (Source: Kahuru et al. [19])

$S_H(t)$: Number of humans in a susceptible class at time t
$S_A(t)$: Number of animals in a susceptible class at time t
$I_{Hl}(t)$: Number of humans in mildly infested class at time t
$I_{Al}(t)$: Number of animals in mildly infested class at time t
$I_{Hh}(t)$: Number of humans in severely infested class at time t
$I_{Ah}(t)$: Number of animals in severely infested class at time t
$T_H(t)$: Number of humans who are receiving treatments at time t
$F_E(t)$: The density of fleas population in the environment at time t
$L_E(t)$: The density of larvae population in the environment at time t
$N_H(t)$, $N_A(t)$: Total human and animal reservoirs populations at time t

The Parameters of the Model with Control Measures (Source: Kahuru et al. [19])

K: Maximal larval carrying capacity
k: Half saturation constant
γ_L: Maturation (transition) rate from larvae to adult jigger fleas
σ_H, σ_A: Disease induced death rates for humans and animal reservoirs, respectively
μ_H, μ_A, μ_F, μ_L: Natural mortality rates for humans, animals, fleas, and larvae, respectively
r_F: The rate of removal of jigger fleas that leaves the soil to attack the hosts
β_{EH}: Effective contact rate between environment and humans
β_{EA}: Effective contact rate between environment and animal reservoirs
ρ_{AH}: Effective contact rate between infested animals and susceptible humans
ρ_A: Effective contact rate between infested animals and susceptible animals
b_H, b_A: Recruitment birth rates for humans and animal reservoirs, respectively
δ_e: The rate of flea eggs deposit on the ground
ε_A: Shedding rates for adult fleas into the environment
α_{EH}, α_{EA}: The proportions of infestation for humans and animals, respectively
ω: Progression rate of treated humans to susceptible class
p_1, p_2: Progression rates from infested human classes to the treatment class.

Conflicts of Interest

The authors declare that there are no conflicts of interest.

References

[1] D. Pilger, S. Schwalfenberg, J. Heukelbach et al., "Controlling tungiasis in an impoverished community: an intervention study," *PLoS Neglected Tropical Diseases*, vol. 2, no. 10, article e324, 2008.

[2] J. Heukelbach, T. Wilcke, G. Harms, and H. Feldmeier, "Seasonal variation of tungiasis in an endemic community," *American Journal of Tropical Medicine and Hygiene*, vol. 72, no. 2, pp. 145–149, 2005.

[3] J. Heukelbach, A. M. L. Costa, T. Wilcke, N. Mencke, and H. Feldmeier, "The animal reservoir of Tunga penetrans in severely affected communities of north-east Brazil," *Medical and Veterinary Entomology*, vol. 18, no. 4, pp. 329–335, 2004.

[4] G. Collins, T. McLeod, N. I. Konfor, C. B. Lamnyam, L. Ngarka, and N. L. Njamnshi, "Tungiasis: a neglected health problem in rural cameroon," *International Journal of Collaborative Research on Internal Medicine and Public Health*, vol. 1, no. 1, pp. 2–10, 2009.

[5] P. Nordin, M. Thielecke, N. Ngomi, G. M. Mudanga, I. Krantz, and H. Feldmeier, "Treatment of tungiasis with a two-component dimeticone: a comparison between moistening the whole foot and directly targeting the embedded sand fleas," *Tropical Medicine and Health*, vol. 45, no. 1, 2017.

[6] M. Ozair, A. A. Lashari, I. H. Jung, and K. O. Okosun, "Stability analysis and optimal control of a vector-borne disease with nonlinear incidence," *Discrete Dynamics in Nature and Society*, vol. 2012, Article ID 595487, 21 pages, 2012.

[7] B. Seidu and O. D. Makinde, "Optimal control of HIV/AIDS in the workplace in the presence of careless individuals,"

Computational and Mathematical Methods in Medicine, Article ID 831506, 19 pages, 2014.

[8] S. M. Lenhart and J. T. Workman, *Optimal Control Applied to Biological Models*, CRC Press, 2007.

[9] H. S. Rodrigues, M. T. T. Monteiro, and D. F. Torres, "Optimal control and numerical software: an overview," https://arxiv.org/abs/1401.7279.

[10] H. R. Joshi, S. Lenhart, M. Y. Li, and L. Wang, "Optimal control methods applied to disease models," in *Mathematical studies on human disease dynamics*, vol. 410 of *Contemp. Math.*, pp. 187–207, Amer. Math. Soc., Providence, RI, 2006.

[11] P. D. Roberts and V. M. Becerra, "Optimal control of a class of discrete-continuous non-linear systems—decomposition and hierarchical structure," *Automatica. A Journal of IFAC, the International Federation of Automatic Control*, vol. 37, no. 11, pp. 1757–1769, 2001.

[12] H. Schättler and U. Ledzewicz, "The Pontryagin Maximum Principle: From Necessary Conditions to the Construction of an Optimal Solution," in *Geometric Optimal Control*, vol. 38 of *Interdisciplinary Applied Mathematics*, pp. 83–194, Springer New York, New York, NY, 2012.

[13] P. Ruhnau and C. Schnörr, "Optical stokes flow estimation: an imaging-based control approach," *PAMM*, vol. 6, no. 1, pp. 863-864, 2006.

[14] UNICEF, "State of The World's Children 2015 Country Statistical Information," 2015.

[15] H. D. Gaff, D. M. Hartley, and N. P. Leahy, "An epidemiological model of rift valley fever," *Electronic Journal of Differential Equations*, vol. 115, pp. 1–12, 2007.

[16] M. Eisele, J. Heukelbach, E. Van Marck et al., "Investigations on the biology, epidemiology, pathology and control of Tunga penetrans in Brazil: I. Natural history of tungiasis in man," *Parasitology Research*, vol. 90, no. 2, pp. 87–99, 2003.

[17] M. Allerson, J. Deen, S. E. Detmer et al., "The impact of maternally derived immunity on influenza A virus transmission in neonatal pig populations," *Vaccine*, vol. 31, no. 3, pp. 500–505, 2013.

[18] Tanzania population 2016, "Tanzania Population 2017," http://worldpopulationreview.com/countries/tanzania-population/.

[19] J. Kahuru, L. Luboobi, and Y. Nkansah-Gyekye, "Modelling the dynamics of Tungiasis transmission in zoonotic areas," *Journal of Mathematical and Computational Science*, vol. 7, no. 2, pp. 375–399, 2017.

[20] E. Bonyah, I. Dontwi, and F. Nyabadza, "Optimal control applied to the spread of buruli uclcer disease," *American Journal of Computational and Applied Mathematics*, vol. 4, no. 3, pp. 61–67, 2014.

[21] A. O. Isere, J. E. Osemwenkhae, and D. Okuonghae, "Optimal control model for the outbreak of cholera in Nigeria," *African Journal of Mathematics and Computer Science Research*, vol. 7, no. 2, pp. 24–30, 2014.

[22] G. Devipriya and K. Kalaivani, "Optimal control of multiple transmission of water-borne diseases," *International Journal of Mathematics and Mathematical Sciences*, vol. 2012, Article ID 421419, 2012.

[23] R. L. M. Neilan, *Optimal Control Applied to Population and Disease Models [Ph.D. Dissertation]*, University of Tennessee, Knoxville, Tennessee, Tenn, USA, 2009.

[24] D. Kirschner, S. Lenhart, and S. Serbin, "Optimal control of the chemotherapy of HIV," *Journal of Mathematical Biology*, vol. 35, no. 7, pp. 775–792, 1997.

[25] W. H. Fleming and R. W. Rishel, *Deterministic and Stochastic Optimal Control*, vol. 1, Springer, New York, NY, USA, 1975.

[26] D. L. Lukes, *Differential Equations: Classical to Controlled*, Mathematics in Science and Engineering, Academic Press, New York, NY, USA, 1982.

[27] S. F. Sadiq, M. A. Khan, S. Islam, G. Zaman, H. Jung, and S. A. Khan, "Optimal control of an epidemic model of leptospirosis with nonlinear saturated incidences," *Annual Research & Review in Biology*, vol. 4, no. 3, pp. 560–576, 2014.

[28] H. Namawejje, L. S. Luboobi, D. Kuznetsov, and E. Wobudeya, "Modeling optimal control of rotavirus disease with different control strategies," *Journal of Mathematical and Computational Science*, vol. 4, no. 5, p. 892, 2014.

[29] G. Birkhoff and G. Rota, *Ordinary Differential Equations*, John Wiley & Sons, New York, NY, USA, 4th edition, 1989.

[30] K. Blayneh, Y. Cao, and H.-D. Kwon, "Optimal control of vector-borne diseases: treatment and prevention," *Discrete and Continuous Dynamical Systems B*, vol. 11, no. 3, pp. 587–611, 2009.

9

Analysis of Fractional Order Mathematical Model of *Hematopoietic Stem Cell* Gene-Based Therapy

Mohammad Imam Utoyo, Windarto, and Aminatus Sa'adah

Department of Mathematics, Faculty of Science and Technology, Universitas Airlangga, Indonesia

Correspondence should be addressed to Mohammad Imam Utoyo; m.i.utoyo@fst.unair.ac.id

Academic Editor: Hans Engler

Hematopoietic stem cell (HSC) has been discussed as a basis for gene-based therapy aiming to cure immune system infections, such as HIV. This therapy protects target cells from infections or specifying technic and immune responses to face virus by using genetically modified HSCs. A mathematical model approach could be used to predict the dynamics of HSC gene-based therapy of viral infections. In this paper, we present a fractional mathematical model of HSC gene-based therapy with the fractional order derivative $\alpha \in (0, 1]$. We determine the stability of fractional model equilibriums. Based on the model analysis, we obtained three equilibriums, namely, free virus equilibrium (FVE) E_0, CTL-Exhaustion Equilibrium (CEE) E_1, and control immune equilibrium (CIE) E_2. Besides, we obtained Basic Reproduction Number R_0 that determines the existence and stability of the equilibriums. These three equilibriums will be conditionally locally asymptotically stable. We also analyze the sensitivity of parameters to determine the most influence parameter to the spread of therapy. Furthermore, we perform numerical simulations with variations of α to illustrate the dynamical HSC gene-based therapy to virus-system immune interactions. Based on the numerical simulations, we obtained that HSC gene-based therapy can decrease the concentration of infected cells and increase the concentration of the immune cells.

1. Introduction

An immune system is body's primary defense system that has a function to fight against microbes. Humoral immunity consists of innate immunity and adaptive immunity. The main principle of innate immunity is an initial defense which responds quickly against microbes. Meanwhile, adaptive immunity would be activated when innate immunity failed to eradicate microbes. Adaptive immunity consists of B lymphocytes cells (B cells) and T lymphocytes cells (T cells). T cells consist of CD4+ T cells and cytotoxic T lymphocytes (CTL and CD8+ T cells). Adaptive immunity has some capabilities such as specificity, diversity, and memory, so it can eradicate microbes effectively [1].

Viruses are one of the microorganisms that infect the immune system. A virus will be detected and then eradicated by innate immunity. However, there are several viruses that can escape from innate immunity and infect CD4+ T cells. Infected CD4+ T cells will produce cytokines to stimulate proliferation and differentiation of precursor CTL cells to become effector CTL cells that would eradicate infected CD4+ T cells [2].

Hematopoiesis is the process to derive blood cells that are located in bone marrow. The first stage of hematopoietic is a stem cell. Hematopoietic stem cells (HSCs) have an ability to multipotency and self-renewing. While in embryonic phase, HSCs that migrate to thymus would be differentiated to mature T cells [1]. Gene-based therapy has been discussed to cure immune impairing infections, such as HIV. The therapy's concept is specifying technic and immune responses to face viruses by using genetically modified HSCs. In 2012, Kitchen et al. performed an in vivo experiment with HSCs gene-based therapy. Based on the experiment, engineered HSCs have the ability to establish functional antivirus responses that suppressed HIV replication. Hence, it will allow suppression of infected CD4+ T cells and prevent suppression of uninfected CD4+ T cells [3].

Korpusik [4] developed a mathematical model to study the influence of a constant influx of CTLs on the dynamic of the virus and immune system interactions, using a modification of the basic mathematical model of virus-induced impairment of help [2]. In addition, Korpusik and Kolev [5] developed a mathematical model to study the dynamical

virus-immune system interactions after a single injection of CD8+ T cells derived from HSCs.

Ordinary differential equation (ODE) system that consists of first-order differential equations can be generalized to fractional differential equation (FDE) system that consists of fractional order differential equations α, with a fractional order parameter $0 < \alpha \leq 1$ [6]. In most biological systems, FDE are naturally connected to systems with memory [7]. In addition, memory effect has an important role in the disease spread. The presence of memory effects on past events will affect the disease spread in the future. The distance of memory effect indicates the history of disease spread. Thus, memory effects on the spread of an infectious disease can be investigated using fractional derivatives [8–13].

In this paper, we extend the ODE model from Korpusik and Kolev [14] into a fractional differential equation system model. We also determined equilibria and stability of the equilibria from the proposed model. Finally, we perform numerical simulation to support the mathematical model interpretation.

2. Mathematical Model Formulation

In this section, we proposed a mathematical model of HSCs gene-based therapy based on [5]. The model was constructed under the following assumptions:

(1) The model consists of five compartments, namely, concentration of uninfected CD4+ T cells (X), concentration of infected CD4+ T cells (Y), concentration of precursor CTL (W), concentration of effector CTL (Z), and concentration of CD8+ T lymphocytes derived from HSCs (H).

(2) Uninfected CD4+ T cells are produced with constant rate.

(3) Viral infections occur only in a human body.

(4) Free virus particle only infected uninfected CD4+ T cells.

(5) Effector CTL only killed infected CD4+ T cells.

(6) Injected HSCs will be differentiated into a precursor CTL.

(7) The proliferation rate of precursor CTL cells depends on susceptible CD4+ T cells, infected CD4+ T cells, and CTL precursor cells at the current time.

The transmission diagram of the model is shown in Figure 1.

The basic model from Korpusik and Kolev [5] was given as follows:

$$\frac{dX}{dt} = \Lambda - \theta X - \beta XY \tag{1a}$$

$$\frac{dY}{dt} = \beta XY - aY - pYZ \tag{1b}$$

$$\frac{dW}{dt} = m\gamma H + cWXY - qWY - b_1 W \tag{1c}$$

$$\frac{dZ}{dt} = qWY - b_2 Z \tag{1d}$$

$$\frac{dH}{dt} = -\gamma H \tag{1e}$$

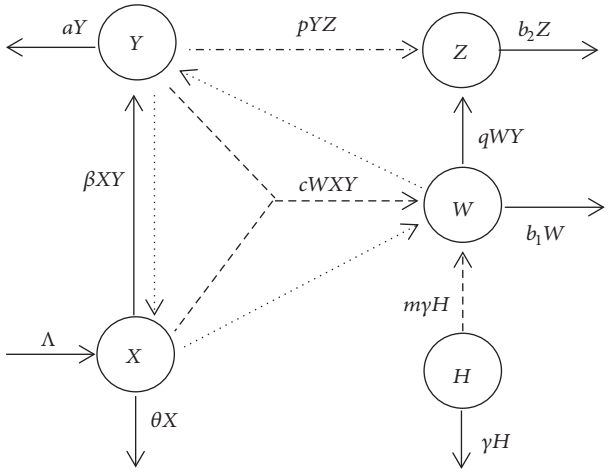

Figure 1: HSCs gene-based therapy transmission diagram.

Here, all parameters $\Lambda, \theta, \beta, a, p, c, b_1, b_2, \gamma > 0$, $0 \leq m, q \leq 1$ and $X(0), Y(0), W(0), Z(0), H(0) \geq 0$. The description of the parameter for the model is presented in Table 1.

The differential equation (1a) describes the dynamic of uninfected CD4+ T cells concentration. Concentrations of CD4+ T cells increase by production of bone marrow and decreased caused by natural death rate and infected by free virus particle. The differential equation (1b) shows the dynamic of infected CD4+ T cells concentrations. Concentrations of infected CD4+ T cells increase, caused by infection of free virus particle. Infected CD4+ T cells will be decreased because of natural death rate and it was killed by effector CTL cells.

The differential equation (1c) describes the dynamic of precursor CTL cells concentrations. Concentrations of precursor CTL cells increased by CTL proliferation process and HSCs were differentiated into CD8+ T cells that are parts of precursor CTL cells. Concentrations of precursor CTL cells are decreased, caused by differentiating into effector CTL, and decreased by natural death rate. Equation (1d) shows the dynamic of concentrations of effector CTL cells at time. Concentrations of effector CTL cells are increased, caused by differentiating of precursor CTL into effector CTL phase, and decreased, caused by natural death rate. The last equation (1e) shows the dynamic of CD8+ T cells concentrations that derived from HSCs. Concentrations of CD8+ T cells are decreased, caused by successfully passing the thymic selection and differentiating into functional precursor CTL cells.

Next, we consider a fractional order model of (1a)-(1e) above. The fractional model corresponding to system (1a)-(1e) is as follows:

$$\frac{d^\alpha X}{dt^\alpha} = \Lambda - \theta X - \beta XY$$

$$\frac{d^\alpha Y}{dt^\alpha} = \beta XY - aY - pYZ$$

$$\frac{d^\alpha W}{dt^\alpha} = m\gamma H + cWXY - qWY - b_1 W$$

Table 1: The description of parameters in the model.

Parameter	Description	Unit
Λ	Production rate of uninfected CD4+ T cells	Concentration cells/time unit
θ	Death rate of uninfected CD4+ T cells	1/ time unit
β	Infection rate	Concentration cells^{-1}/ time unit
a	Death rate of infected CD4+ T cells	1/ time unit
p	Effector CTL rate of killing infected CD4+ T cells	Concentration cells^{-1}/ time unit
m	Fractions of HSCs that successfully differentiated into functional CTL cells	-
c	Proliferation rate of precursor CTL	Concentration cells^{-2}/ time unit
q	Fraction of precursor CTL cells that differentiated into effector CTL cells	-
b_1	Death rate of precursor CTL	1/ time unit
b_2	Death rate of effector CTL	1/ time unit
γ	Differentiation rate of CD8+ T lymphocytes	1/ time unit

$$\frac{d^\alpha Z}{dt^\alpha} = qWY - b_2 Z$$
$$\frac{d^\alpha H}{dt^\alpha} = -\gamma H \tag{2}$$

where the fractional order derivative $0 < \alpha \leq 1$. Fractional derivative of the model (2) is adopted from Caputo's definition. The main advantages of Caputo approach are the initial values for fractional differential equations with the Caputo derivatives taking on the same form as for integer order differential equations [15]. The Caputo fractional derivative is defined as follows.

Definition 1 (see [15]). Let $\alpha > 0$, $t > 0$, and $n \in \mathbb{N}$. Caputo fractional derivative $D^\alpha := d^\alpha/dt^\alpha$, with fractional order α, of function $f(t)$ is defined by

$$D^\alpha f(t) = I^{n-\alpha} D^n f(t)$$
$$= \begin{cases} \dfrac{1}{\Gamma(n-\alpha)} \displaystyle\int_0^t \frac{f^{(n)}(s)}{(t-s)^{\alpha-n+1}} ds, & n-1 < \alpha < n \\ f^{(n)}(t), & \alpha = n, \end{cases} \tag{3}$$

where $\Gamma(\bullet)$ is the gamma function.

3. Stability Analysis

In this section, we study stability of the equilibriums of the fractional order model (2) above. We begin by computed the basic reproduction number R_0 of model (2). Basic reproduction number R_0 is defined as the average number of new cases of an infection caused by one typical infected individual, in a population consisting of susceptible only [16]. If $R_0 < 1$, then the infections will die out, while if $R_0 > 1$, then there is an epidemic case [17].

The stability theorem on fractional order system was given in the following theorem.

Theorem 2 (see [18]). *Consider a nonlinear fractional order system*

$$D^\alpha \boldsymbol{x}(\boldsymbol{t}) = \boldsymbol{f}(\boldsymbol{x}) \tag{4}$$

where $0 < \alpha \leq 1$, $\boldsymbol{x} \in \mathbb{R}^n$, and $\boldsymbol{f} \in \mathbb{R}^n$. The equilibrium points x^* of system (4) are calculated by solving equation $\boldsymbol{f}(\boldsymbol{x}) = \mathbf{0}$. The equilibrium points x^* are locally asymptotically stable if all the eigenvalues λ_j $(j = 1, 2, \ldots, n)$ of the Jacobian matrix $A = \partial \boldsymbol{f}/\partial \boldsymbol{x}$ evaluated at the equilibrium points x^* satisfy the following condition:

$$\left|\arg \lambda_j\right| > \frac{\alpha\pi}{2}. \tag{5}$$

The equilibriums of the fractional mathematical model in (2) satisfy the following equations:

$$\Lambda - \theta X - \beta XY = 0 \tag{6}$$
$$\beta XY - aY - pYZ = 0 \tag{7}$$
$$m\gamma H + cWXY - qWY - b_1 W = 0 \tag{8}$$
$$qWY - b_2 Z = 0 \tag{9}$$
$$-\gamma H = 0 \tag{10}$$

The fractional model in (2) has three equilibriums, namely, virus-free equilibrium (E_0), CTL-Exhaustion Equilibrium (E_1), and control immune equilibrium E_2. The virus-free equilibrium is condition when there is CD4+ T cells in human body ($X \neq 0$), no infected CD4+ T cells ($Y = 0$), and CTL precursor is not activated ($W = 0$). The virus-free equilibrium of model (2) above is given by $E_0 = (X_0, Y_0, W_0, Z_0, H_0) = (\Lambda/\theta, 0, 0, 0, 0)$.

Basic reproduction number (R_0) is an important parameter in epidemiological cases. Basic reproduction number R_0 is defined by average secondary infections caused by one primary infection in susceptible population. In this paper, we use Next Generation Matrix (NGM) that developed by [19] to determine R_0. By using the Next Generation method, we obtained the basic reproduction number $R_{01} = \beta\Lambda/\theta a$. Stability of virus-free equilibrium is presented in Theorem 3.

Theorem 3. *The virus-free equilibrium E_0 of model (2) is locally asymptotically stable if and only if $R_{01} < 1$.*

Proof. The Jacobi matrix that evaluated at the virus-free equilibrium (E_0) of the model (2) above is as follows:

$$J(E_0) = \begin{pmatrix} -\theta & -\frac{\beta\Lambda}{\theta} & 0 & 0 & 0 \\ 0 & \frac{\beta\Lambda}{\theta} - a & 0 & 0 & 0 \\ 0 & 0 & -b_1 & 0 & m\gamma \\ 0 & 0 & 0 & -b_2 & 0 \\ 0 & 0 & 0 & 0 & -\gamma \end{pmatrix}. \quad (11)$$

The eigenvalues of the Jacobi matrix $J(E_0)$ are $\lambda_1 = -\theta$, $\lambda_2 = \beta\Lambda/\theta - a$, $\lambda_3 = -b_1$, $\lambda_4 = -b_2$, and $\lambda_5 = -\gamma$. Hence, we have $|\arg(\lambda_1)| = |\arg(\lambda_3)| = |\arg(\lambda_4)| = |\arg(\lambda_5)| = \pi > \pi/2$. Meanwhile, $|\arg(\lambda_2)| = \pi > \pi/2$ if and only if $R_{01} = \beta\Lambda/a\theta < 1$. If the condition $R_{01} = \beta\Lambda/a\theta < 1$ is satisfied, then it is clear that all the eigenvalues satisfy the condition $|\arg\lambda_j| > \alpha\pi/2$, for $j = 1, 2, 3, 4, 5$. Hence, the virus-free equilibrium (E_0) of model (2) is locally asymptotically stable if $R_{01} < 1$. □

We continue with the stability analysis of the CTL-Exhaustion Equilibrium (E_1) of the model (2). The CTL-Exhaustion Equilibrium is condition when there is CD4+ T cells in human body ($X \neq 0$), there are infected CD4+ T cells ($Y \neq 0$), but CTL precursor is not activated yet ($W = 0$). The CTL-Exhaustion Equilibrium of the model in (2) is given by $E_1 = (a/\beta, (\beta\Lambda - a\theta)/\beta a, 0, 0, 0)$. This equilibrium will exist whenever $R_{01} > 1$.

Theorem 4. *Let $q\beta - ca < 0$ and $R_{02} = b_1 a\beta^2/(a\theta - \beta\Lambda)(q\beta - ca)$. The CTL-Exhaustion Equilibrium (E_1) of the model in (2) is locally asymptotically stable if and only if $R_{02} > 1$.*

Proof. The Jacobi matrix evaluated at the free virus equilibrium $E_1 = (a/\beta, (\beta\Lambda - a\theta)/\beta a, 0, 0, 0)$ of the model in (2) above is as follows:

$$J(E_1) = \begin{pmatrix} -\frac{\beta\Lambda}{a} & -a & 0 & 0 & 0 \\ \frac{\beta\Lambda}{a} - \theta & 0 & -p\left(\frac{\Lambda}{a} - \frac{\theta}{\beta}\right) & 0 & 0 \\ 0 & 0 & (a\theta - \beta\lambda)\left(\frac{-ca + q\beta}{a\beta^2}\right) - b_1 & 0 & m\gamma \\ 0 & 0 & q\left(\frac{\Lambda}{a} - \frac{\theta}{\beta}\right) & -b_2 & 0 \\ 0 & 0 & 0 & 0 & -\gamma \end{pmatrix}. \quad (12)$$

The eigenvalues of the Jacobi matrix $J(E_1)$ above are $\lambda_1 = -\gamma$, $\lambda_2 = -b_2$, $\lambda_3 = (a\theta - \beta\Lambda)((-ca + q\beta)/a\beta^2) - b_1$, and $\lambda_{4,5}$ is root of polynomial $\lambda^2 + b\lambda + c = 0$, where $b = \beta\Lambda/\theta$, and $c = \beta\Lambda - a\theta$. We have $|\arg(\lambda_1)| = |\arg(\lambda_2)| = \pi > \pi/2$. Then we determined the argument of λ_4 and λ_5. Based on the condition of existence of E_1 that $R_{01} = \beta\Lambda/a\theta > 1$, we obtained $c = \beta\Lambda - a\theta > 0$. By using Routh-Hurwitz criterion, we obtained $|\arg(\lambda_4)| = |\arg(\lambda_5)| > \pi/2$.

Since all parameters are assumed to have positive value, the third eigenvalue λ_3 is a real number. We obtained that $|\arg(\lambda_3)| = \pi > \pi/2$ if and only if the condition $((a\theta - \beta\Lambda)(q\beta - ca) < b_1 a\beta^2)$ is fulfilled. It is clear that all the eigenvalues satisfy the condition $|\arg\lambda_j| > \alpha\pi/2$, for $j = (1, 2, 3, 4, 5)$. Hence, the CTL-Exhaustion Equilibrium E_1 of model (2) is locally asymptotically stable if and only if $(a\theta - \beta\Lambda)(q\beta - ca) < b_1 a\beta^2$ or $R_{02} > 1$. This completes the proof □

Last, we analyze the stability of the control immune equilibrium (E_2). The control immune equilibrium is the condition when there are CD4+ T cells in human body ($X \neq 0$), there is infected CD4+ T cells ($Y \neq 0$), and CTL precursor is activated ($W \neq 0$) so that can give the immune response. The control immune equilibrium is given by $E_2(X^*, Y^*, W^*, Z^*, H^*)$, where

$$\begin{aligned} X^* &= \frac{\Lambda}{(\theta + \beta Y^*)} = \frac{qY^* + b_1}{cY^*}, \\ Y^* &= \frac{\theta q + \beta b_1 - \Lambda c \pm \sqrt{A}}{2\beta q}, \\ W^* &= \left(\frac{b_2}{qY^*}\right)\left(\frac{\beta\Lambda - a\theta + a\beta Y^*}{p\theta - p\beta Y^*}\right) \\ &= \frac{b_2\left(R_{01} + \beta Y^*/\theta - 1\right)}{pqY^*\left(\theta - \beta Y^*\right)}, \\ Z^* &= \frac{q}{b_2} W^* Y^* = \frac{\beta\Lambda - a\theta + a\beta Y^*}{p\theta - p\beta Y^*}, \end{aligned} \quad (13)$$

and $H^* = 0$.

The equilibriums will exist if the conditions $A = (\Lambda c - \theta q)^2 - 2\beta b_1(\Lambda c + \theta q) + (\beta b_1)^2 \geq 0$, $\theta > \beta Y^*$ and $R_{01} + \beta Y^*/\theta > 1$ are satisfied.

The Jacobi matrix of the model in (2) that evaluated in the equilibrium point E_2 is

$$J(E_2) = \begin{pmatrix} -\beta Y^* - \theta & -\beta X^* & 0 & 0 & 0 \\ \beta Y^* & \beta X^* - pZ^* - a & -pY^* & 0 & 0 \\ cW^*Y^* & cW^*X^* - qW^* & cXY^* - qY^* - b_1 & 0 & m\gamma \\ 0 & qW^* & qY^* & -b_2 & 0 \\ 0 & 0 & 0 & 0 & -\gamma \end{pmatrix}. \quad (14)$$

By using the control immune equilibrium condition, the Jacobi matrix $J(E_2)$ could be simplified into

$$J(E_2) = \begin{pmatrix} -\frac{\Lambda}{X^*} & -\beta X^* & 0 & 0 & 0 \\ \beta Y^* & 0 & -pY^* & 0 & 0 \\ cW^*Y^* & cW^*X^* - qW^* & 0 & 0 & m\gamma \\ 0 & qW^* & qY^* & -b_2 & 0 \\ 0 & 0 & 0 & 0 & -\gamma \end{pmatrix}. \quad (15)$$

From the Jacobi matrix $J(E_2)$ above, we get the polynomial characteristic equations as follows:

$$(\lambda + \gamma)(\lambda + b_2)\left(\lambda^3 + a_1\lambda^2 + a_2\lambda + a_3\right) = 0 \quad (16)$$

where $a_1 = \Lambda/X^*$, $a_2 = \beta^2 X^*Y^* + pY^*W^*(cX^* - q)$, and $a_3 = pY^*W^*(\Lambda c - \Lambda q/X^* - c\beta X^*Y^*)$.

Based on the characteristic equations (16) above, we obtain eigen values $\lambda_1 = -\gamma$, $\lambda_2 = -b_2$, and $\lambda_{3,4,5}$ is the roots of the following equation:

$$\lambda^3 + a_1\lambda^2 + a_2\lambda + a_3 = 0. \quad (17)$$

The argument of the first and second eigen values is π, $|\arg(\lambda_1)| = |\arg(\lambda_2)| = \pi$. Next, we will determine the argument of the third, fourth, and fifth eigen values. The third, fourth, and fifth eigen values are roots of polynomial with degree of three (17), satisfying the following conditions:

(i) $\lambda_3 + \lambda_4 + \lambda_5 = -a_1$

(ii) $\lambda_3\lambda_4 + \lambda_4\lambda_5 + \lambda_3\lambda_5 = a_2$

(iii) $\lambda_3\lambda_4\lambda_5 = -a_3$

Then, we will analyze two conditions when $a_3 < 0$ and $a_3 > 0$. If $a_3 < 0$, then we have Theorem 5. On the other hand, if $a_3 > 0$ then we obtain Theorem 6 below.

Theorem 5. *If $\Lambda(cX^* - q)/c\beta(X^*)^2Y^* < 1$, then the immune control equilibrium E_2 of model (2) is unstable.*

Proof. Let $a_3 = pY^*W^*(\Lambda c - \Lambda q/X^* - c\beta X^*Y^*) < 0$; we obtained $\Lambda(cX^* - q)/c\beta(X^*)^2Y^* < 1$. Since $a_3 < 0$, then based on the third condition (iii) above we have $\lambda_3\lambda_4\lambda_5 > 0$. There are two possibilities, either all the eigen values of the polynomial (17) are real number or one of the eigen values is real number and two other eigen values are complex numbers.

(1) Let all the eigen values $\lambda_3, \lambda_4, \lambda_5$ be real number. Because of $\lambda_3\lambda_4\lambda_5 > 0$, then there are two possibilities. First, all the eigen values are real positive number. If all the eigen values are real positive numbers, then it is clear that $|\arg(\lambda_3)| = |\arg(\lambda_4)| = |\arg(\lambda_5)| = 0 < \alpha\pi/2$. Second, one of the eigen values is real positive number and two others are real negative number. Let $\lambda_3 \in \mathbb{R}$, then $|\arg(\lambda_3)| = 0 < \alpha\pi/2$.

(2) Let one of the eigen values be real number, $\lambda_3 \in \mathbb{R}$, and two others eigen values are complex numbers, $\lambda_4 = a + bi$, $\lambda_5 = a - bi$, where $a, b \in \mathbb{R}$. Because $\lambda_3\lambda_4\lambda_5 > 0$ and $\lambda_4\lambda_5 > 0$, then we obtained $\lambda_3 > 0$. As a result, $|\arg(\lambda_3)| = 0 < \alpha\pi/2$.

From the two conditions above, we find that the immune control equilibrium E_2 of the model (2) is unstable whenever $\Lambda(cX^* - q)/c\beta(X^*)^2Y^* < 1$. □

Theorem 6. *The immune control equilibrium E_2 of the model (2) is asymptotically stable if $\Lambda(cX^* - q)/c\beta(X^*)^2Y^* > 1$ for some fractional order α.*

Proof. Let we consider the polynomial

$$\lambda^3 + a_1\lambda^2 + a_2\lambda + a_3 = 0 \quad (18)$$

where $a_1 = \Lambda/X^*$, $a_2 = \beta^2 X^*Y^* + pY^*W^*(cX^* - q)$, and $a_3 = pY^*W^*(\Lambda c - \Lambda q/X^* - c\beta X^*Y^*)$.

Let $a_3 = pY^*W^*(\Lambda c - \Lambda q/X^* - c\beta X^*Y^*) > 0$. Hence we obtained $\Lambda(cX^* - q)/c\beta(X^*)^2Y^* > 1$. If $a_3 > 0$, then based on the third condition (iii) above we have $\lambda_3\lambda_4\lambda_5 < 0$.

(i) Let the polynomial characteristic (18) above have complex number roots. Let one of the eigen values be real number, $\lambda_3 \in \mathbb{R}$, and two other eigen values are complex number, $\lambda_4 = a + bi$, $\lambda_5 = a - bi$, where $a, b \in \mathbb{R}$. Since $\lambda_3\lambda_4\lambda_5 < 0$ and $\lambda_4\lambda_5 > 0$, then we obtained $\lambda_3 < 0$. As a result, $|\arg(\lambda_3)| = \pi > \alpha\pi/2$. In addition, we can found a fractional order value $\alpha \in (0, 1]$ such that the arguments of the third and fourth eigen values satisfy $|\arg(\lambda_4)| > \alpha\pi/2$ and $|\arg(\lambda_5)| > \alpha\pi/2$. As a result, the immune control equilibrium E_2 of model (2) is asymptotically stable for some fractional order α.

(ii) Let all the eigen values of the polynomial characteristic (18) above λ_3, λ_4, λ_5 be real numbers. Then we will determine the conditions such that all roots of the polynomial (18) above are either negative or complex roots with negative real parts by using Routh-Hurwitz criterion.

Based on Routh-Hurwitz criteria, the polynomial (18) will have real negative or real negative parts roots if it satisfies $a_1, a_2, a_3 > 0$ and $a_1a_2 - a_3 > 0$. Hence, we obtained the following conditions:

(a) Since all parameters are assumed to be positive and $X^* \neq 0$, then it is clear that $a_1 > 0$.

(b) The coefficient a_2 will have positive value if a_3 is positive.

(c) The coefficient a_3 will have positive value if it satisfies $\Lambda(cX^* - q)/c\beta(X^*)^2Y^* > 1$.

(d) It is clear that the coefficients a_1, a_2, a_3 satisfy $a_1a_2 - a_3 > 0$.

Based on [20], for $\alpha \in (0, 1]$ these conditions are sufficient but not necessary. Therefore, the argument of $\lambda_3, \lambda_4, \lambda_5$ will satisfy $|\arg(\lambda_3)| = |\arg(\lambda_4)| = |\arg(\lambda_5)| = \pi > \pi/2$ if

Table 2: The sensitivity indices of $\boldsymbol{R_{01}}$.

Parameter	Sensitivity indices
$\boldsymbol{\beta}$	1
$\boldsymbol{\Lambda}$	1
$\boldsymbol{a}$	-1
$\boldsymbol{\theta}$	-1

Table 3: The sensitivity indices of $\boldsymbol{R_{02}}$.

Parameter	Sensitivity indices
β	0.945
Λ	1
a	-0.994
θ	-1
b_1	-0.049
q	-0.006
c	0.055

the condition $\Lambda(cX^* - q)/c\beta(X^*)^2Y^* > 1$ is satisfied. As a result, the immune control equilibrium E_2 of the model (2) is asymptotically stable. This completes the proof. □

4. Sensitivity Analysis

In this section, we will analyze the sensitivity of parameters of the model (2) above. Sensitivity analysis is used to determine the relative importance of model parameters to disease transmission and prevalence based on the sensitivity index of basic reproduction number R_0. The calculation of sensitivity index of R_0 follows the approach in Chitnis [21].

Definition 7 (see [21]). The normalized forward sensitivity index of a variable, m, that depends differentially on a parameter, k, is defined as

$$\Upsilon_k^m := \frac{\partial m}{\partial k} \times \frac{k}{m}. \tag{19}$$

Based on Definition 7, the sensitivity indices of R_{01} with respect to each parameter such as β, Λ, a, and θ can be computed in the same way as (19). The sensitivity indices of R_{01} are given in Table 2. Based on Table 2, it can be seen that parameters β and Λ positively affect the rate of model changed. Respectively, the parameters a and θ negatively affect the rate of model changed. But, we did not know what is the relative importance of model parameters of R_{01}. So, we also analyze the sensitivity parameters of R_{02}.

Based on Definition 7, the sensitivity indices of R_{02} with respect to each parameter such as $\beta, \Lambda, a, \theta, b_1, q$, and c can be computed in the same way as (19). The sensitivity indices of parameter Λ are $(\partial R_{02}/\partial\Lambda)(\Lambda/R_{02}) = \Lambda(ca - q\beta)/\beta(-ab_1 - \Lambda q) + ac\Lambda$; we next substituted the value of parameters of Table 4 so we obtain $(\partial R_{02}/\partial\Lambda)(\Lambda/R_{02}) = 1$. The sensitivity indices of R_{02} are given in Table 3.

Based on Table 3, it can be seen that if production rate of uninfected CD4+ T cells (Λ) is increased (decreased) about 10%, then R_{02} will increase (decrease) about 10%. Respectively, if death rate of infected CD4+ T cells (a) is increased (decreased) about 10%, then R_{02} will decrease (increase) about 9.94%, and the same for other parameters.

5. Numerical Simulation

In this section, we present numerical simulations to show the dynamics of the model at free virus condition, CTL-exhaustion condition, and control immune condition using MATLAB R2009a. The initial conditions of simulations of free virus condition are $X_0 = 3.6, Y_0 = 0.2, W_0 = 0.01, Z_0 = 0.01$, and $H_0 = 0.001$. The parameter values are presented in Table 4. Based on Table 4, we have that basic reproduction number R_0 is $R_{01} = \beta\Lambda/a\theta = (0.15)(0.2)/(0.8)(0.05) = 0.75 < 1$ that shows free virus condition or there is no spread of viral infection. This simulation used variations of fractional order α and time interval for 2500 time units.

The result of simulation of free virus condition can be seen in Figure 2. Based on Figure 2, greater the fractional order α leads to the increase of concentrations of uninfected CD4+ T cells but concentrations of infected CD4+ T cells are decreasing that show free virus conditions. Besides, concentrations of precursor CTL cells are decreasing caused by the decrease of CD4+ T cells. That also implies the decrease of effector CTL. Meanwhile, concentrations of CD8+ T cells are decreasing because they were differentiated into precursor CTL cells.

Next, we will interpret the simulation of CTL-exhaustion condition. The initial conditions of simulations of CTL-exhaustion condition are $X_0 = 1.5, Y_0 = 0.8, W_0 = 0.6, Z_0 = 0.3$, and $H_0 = 0.001$. The parameter values are presented in Table 4 except for β, a, and θ, which are $\beta = 0.216$, $a = 0.4$, and $\theta = 0.02$. Therefore, we have basic reproduction number $R_{01} = (0.216)(0.2)/(0.4)(0.02) = 5.4 > 1$ and $R_{02} = \beta\Lambda/a\theta + b_1\beta^2/\theta(q\beta - ca) = 10.1 > 1$ which is condition when there is spread of viral infections in the human body. This simulation used variations of fractional order α and time interval for 2500 time units.

Based on Figure 3, it can be seen that greater the fractional order α leads to the decrease of concentrations of uninfected CD4+ T cells but concentrations of infected CD4+ T cells are increasing. That implies the conditions of viral infections. But, concentrations of effector CTL cells are decreasing. That implies the CTL-exhaustion conditions where CTL are not activated yet so they cannot against the viral infections. Meanwhile, concentrations of CD8+ T cells were decreased because they differentiated into precursor CTL cells.

Last, we will show the simulation of control immune conditions. The initial conditions of simulations of CTL-exhaustion condition are $X_0 = 5, Y_0 = 1, W_0 = 2.5, Z_0 = 0.8$, and $H_0 = 0.001$. The parameter values are showed in Table 4 except for θ, that is, $\theta = 0.02$. Therefore, we have basic reproduction number $R_{01} = 1.87 > 1$ and $R_{02} = 1.01 > 1$ which is condition when there is spread of viral infections in the human body. This simulation used variations of fractional order α and time interval for 2500 time units. Based on Figure 4, it can be seen that greater the fractional order α leads to the increase of concentrations of uninfected CD4+ T cells but concentrations of infected CD4+ T cells

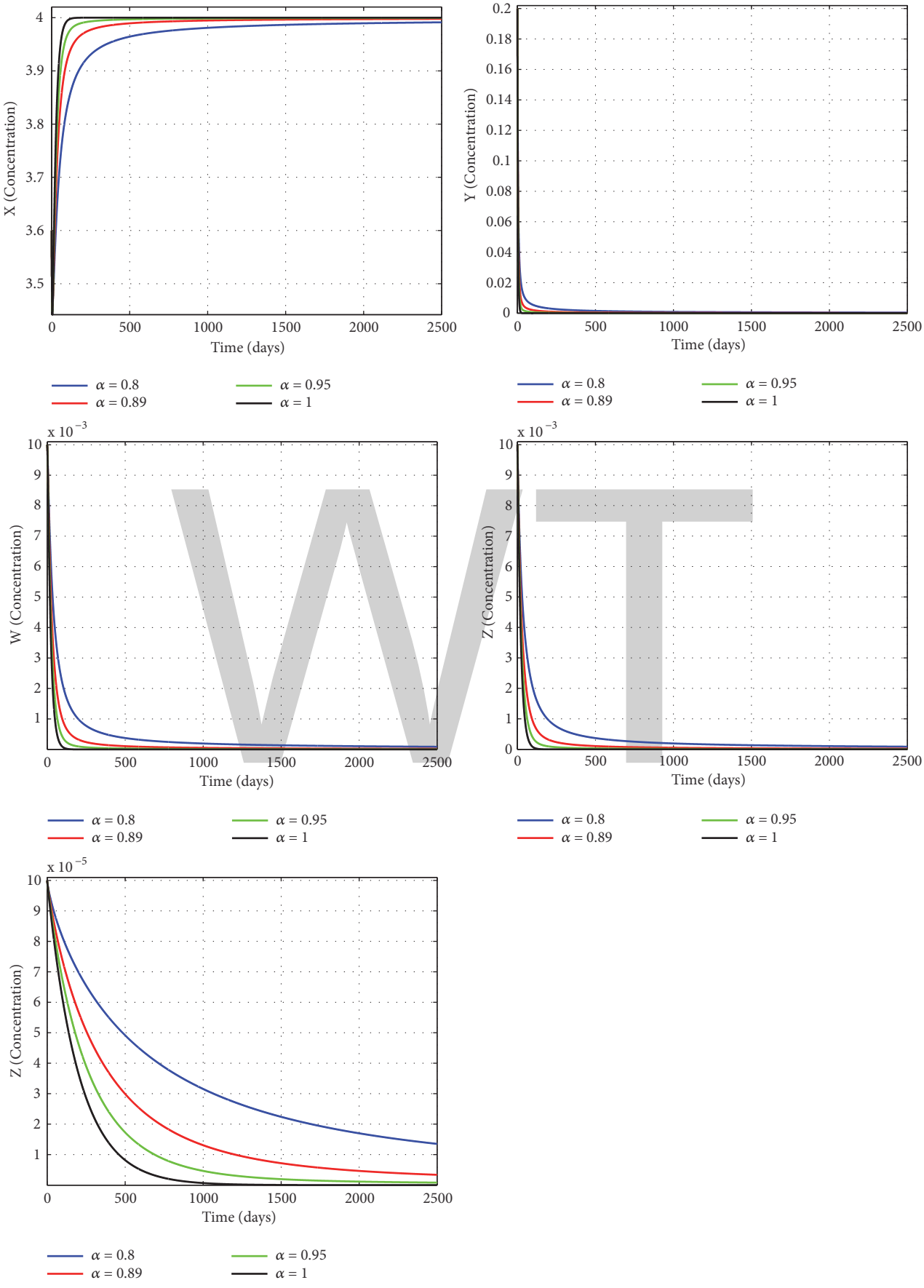

Figure 2: The dynamics of mathematical model of HSCs gene-based therapy for free virus conditions.

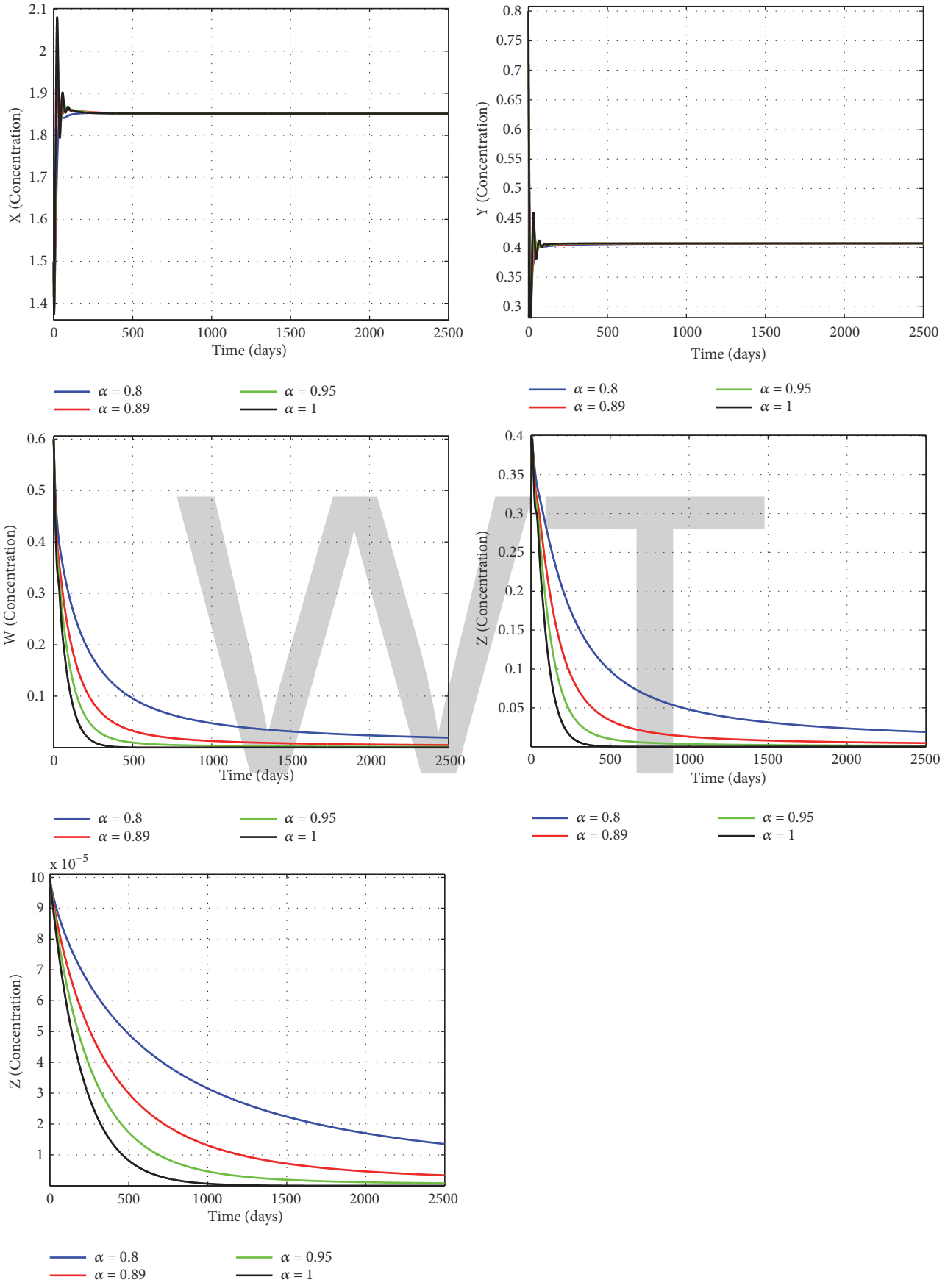

Figure 3: The dynamics of mathematical model of HSCs gene-based therapy for CTL-exhaustion conditions.

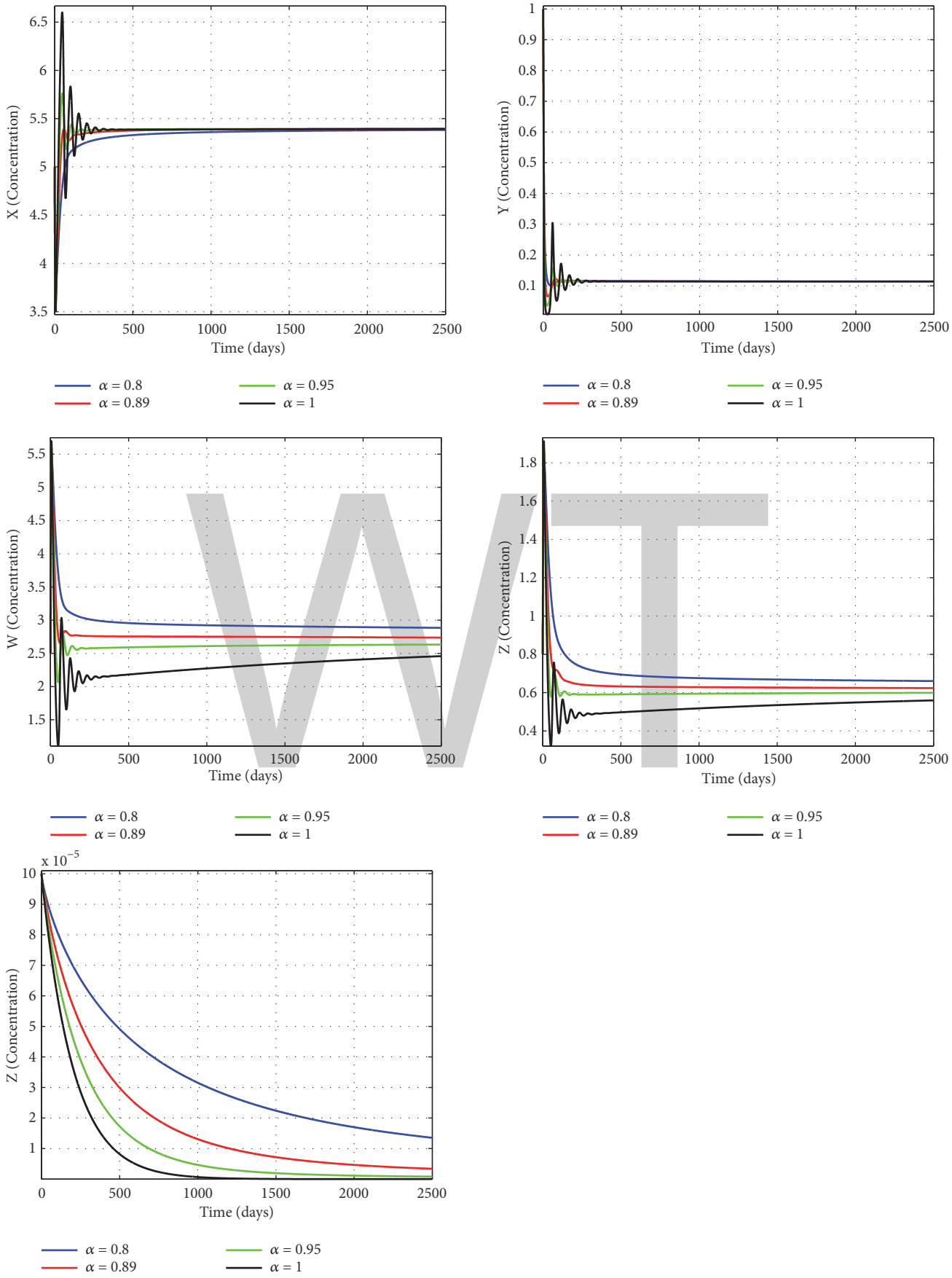

FIGURE 4: The dynamics of fractional order mathematical model of HSCs gene-based therapy for control immune conditions.

Table 4: Parameters value of the model.

Parameter	Description	Value	Source
Λ	Production rate of uninfected CD4+ T cells	0.2	[14]
θ	Death rate of uninfected CD4+ T cells	0.05	Assumption
β	Infection rate	0.15	[14].
a	Death rate of infected CD4+ T cells	0.8	[14]
p	Effector CTL rate of killing infected CD4+ T cells	0.016	[14]
m	Fractions of HSCs that successfully differentiated into functional CTL cells	0.01	Assumption
c	Proliferation rate of precursor CTL	0.1	Assumption
q	Fraction of precursor CTL cells that differentiated into effector CTL cells	0.1	Assumption
b_1	Death rate of precursor CTL	0.05	[14]
b_2	Death rate of effector CTL	0.05	[14]
γ	Differentiation rate of CD8+ T cells	0.005	Assumption

are decreasing. Meanwhile, concentrations of precursor and effector CTL cells are increasing, which means the precursor and effector CTL cells are activated so they can fight against the viral infections. That implies control immune conditions. Meanwhile, concentrations of CD8+ T cells were decreased because they differentiated into precursor CTL cells.

6. Conclusions

We were discussed about the stability analysis of fractional order mathematical model of HSCs gene-based therapy. The model has three equilibriums points. The existence and stability of the equilibriums were achieved. Based on the numerical simulations, we conclude that HSCs gene-based therapy has potential to reduce the viral infections because it can decrease the concentration of infection cells and increase the concentration of the immune cells.

Conflicts of Interest

The authors state that there are no conflicts of interest concerning the preparation and publication of the manuscript.

References

[1] R. Nairn and M. Helbert, *Immunology for Medical Students*, Mosby Elsevier, Philadelphia, 2nd edition, 2007.

[2] D. Wodarz, *Killer cell dynamics*, vol. 32 of *Interdisciplinary Applied Mathematics*, Springer-Verlag, New York, 2007.

[3] S. G. Kitchen, B. R. Levin, G. Bristol et al., "In vivo suppression of HIV by antigen specific T cells derived from engineered hematopoietic stem cells," *PLoS Pathogens*, vol. 8, no. 4, Article ID e1002649, 2012.

[4] A. Korpusik, "Hematopoietic stem cell based therapy of immunosuppressive viral infection - Numerical simulations," *Biocybernetics and Biomedical Engineering*, vol. 34, no. 2, pp. 125–131, 2014.

[5] A. Korpusik and M. Kolev, "Single injection of CD8+ T lymphocytes derived from hematopoietic stem cells - Mathematical and numerical insights," *BioSystems*, vol. 144, pp. 46–54, 2016.

[6] S. Das and P. K. Gupta, "A mathematical model on fractional Lotka-Volterra equations," *Journal of Theoretical Biology*, vol. 277, pp. 1–6, 2011.

[7] E. Ahmed and A. S. Elgazzar, "On fractional order differential equations model for nonlocal epidemics," *Physica A: Statistical Mechanics and its Applications*, vol. 379, no. 2, pp. 607–614, 2007.

[8] F. Fatmawati, E. M. Shaiful, and M. I. Utoyo, "A Fractional-Order Model for HIV Dynamics in a Two-Sex Population," *International Journal of Mathematics and Mathematical Sciences*, vol. 2018, Article ID 6801475, 11 pages, 2018.

[9] J. Huo and H. Zhao, "Dynamical analysis of a fractional SIR model with birth and death on heterogeneous complex networks," *Physica A: Statistical Mechanics and its Applications*, vol. 448, pp. 41–56, 2016.

[10] J. Huo, H. Zhao, and L. Zhu, "The effect of vaccines on backward bifurcation in a fractional order HIV model," *Nonlinear Analysis: Real World Applications*, vol. 26, pp. 289–305, 2015.

[11] C. M. A. Pinto and A. R. M. Carvalho, "The HIV/TB coinfection severity in the presence of TB multi-drug resistant strains," *Ecological Complexity*, vol. 32, pp. 1–20, 2017.

[12] M. Saeedian, M. Khalighi, N. Azimi-Tafreshi, G. R. Jafari, and M. Ausloos, "Memory effects on epidemic evolution: the susceptible-infected-recovered epidemic model," *Physical Review E: Statistical, Nonlinear, and Soft Matter Physics*, vol. 95, no. 2, 022409, 9 pages, 2017.

[13] T. Sardar, S. Rana, and J. Chattopadhyay, "A mathematical model of dengue transmission with memory," *Communications in Nonlinear Science and Numerical Simulation*, vol. 22, no. 1–3, pp. 511–525, 2015.

[14] G. Huang, Y. Takeuchi, and A. Korobeinikov, "HIV evolution and progression of the infection to AIDS," *Journal of Theoretical Biology*, vol. 307, pp. 149–159, 2012.

[15] S. Z. Rida and A. A. Arafa, "New method for solving linear fractional differential equations," *International Journal of Differential Equations*, Art. ID 814132, 8 pages, 2011.

[16] O. Diekmann, J. A. P. Heesterbeek, and M. G. Roberts, "The construction of next-generation matrices for compartmental epidemic models," *Journal of the Royal Society Interface*, vol. 7, no. 47, pp. 873–885, 2010.

[17] F. Brauer and C. Castillo-Chávez, *Mathematical Models in Population Biology and Epidemiology*, vol. 40 of *Texts in applied mathematics*, Springer, New York, NY, USA, 2001.

[18] M. S. Tavazoei and M. Haeri, "Chaotic attractors in incommensurate fractional order systems," *Physica D: Nonlinear Phenomena*, vol. 237, no. 20, pp. 2628–2637, 2008.

[19] P. van den Driessche and J. Watmough, "Reproduction numbers and sub-threshold endemic equilibria for compartmental models of disease transmission," *Mathematical Biosciences*, vol. 180, pp. 29–48, 2002.

[20] E. Ahmed, A. M. A. El-Sayed, and H. A. A. El-Saka, "On some Routh-Hurwitz conditions for fractional order differential equations and their applications in Lorenz, Rössler, Chua and Chen systems," *Physics Letters A*, vol. 358, no. 1, pp. 1–4, 2006.

[21] N. Chitnis, J. M. Hyman, and J. M. Cushing, "Determining important parameters in the spread of malaria through the sensitivity analysis of a mathematical model," *Bulletin of Mathematical Biology*, vol. 70, no. 5, pp. 1272–1296, 2008.

10

A Topology on Milnor's Group of a Topological Field and Continuous Joint Determinants

Sung Myung

Department of Mathematics Education, Inha University, 253 Yonghyun-dong, Nam-gu, Incheon 402-751, Republic of Korea

Correspondence should be addressed to Sung Myung; s-myung1@inha.ac.kr

Academic Editor: Daniel Simson

For the tuple set of commuting invertible matrices with coefficients in a given field, the joint determinants are defined as generalizations of the determinant map for the square matrices. We introduce a natural topology on Milnor's K-groups of a topological field as the quotient topology induced by the joint determinant map and investigate the existence of a nontrivial continuous joint determinant by utilizing this topology, generalizing the author's previous results on the continuous joint determinants for the commuting invertible matrices over $\mathbb{R}$ and $\mathbb{C}$.

1. Introduction

In [1], a joint determinant is introduced as a generalization of the determinant map for invertible matrices. More precisely, for a field k, a joint determinant D $(= D_l)$ $(l \geq 1)$ is defined as a map from the set of l-tuples of commuting matrices in $\mathrm{GL}_n(k)$ $(n \geq 1)$ into some abelian group $(G, +)$ which satisfies the following properties.

(i) Multilinearity: for $l + 1$ commuting matrices $A_1, \ldots, A_l$ and B in $\mathrm{GL}_n(k)$ for some $n \geq 1$, we have $D(A_1, \ldots, A_i B, \ldots, A_l) = D(A_1, \ldots, A_i, \ldots, A_l) + D(A_1, \ldots, B, \ldots, A_l)$.

(ii) Block diagonal matrices: for commuting $A_1, \ldots, A_l \in \mathrm{GL}_m(k)$ and commuting $B_1, \ldots, B_l \in \mathrm{GL}_n(k)$ for some $m, n \geq 1$, we have

$$D\left(\begin{pmatrix} A_1 & 0 \\ 0 & B_1 \end{pmatrix}, \ldots, \begin{pmatrix} A_l & 0 \\ 0 & B_l \end{pmatrix}\right) = D(A_1, \ldots, A_l) + D(B_1, \ldots, B_l). \tag{1}$$

(iii) Similar matrices: for commuting matrices $A_1, \ldots, A_l \in \mathrm{GL}_n(k)$ and any $S \in \mathrm{GL}_n(k)$, we have $D(SA_1S^{-1}, \ldots, SA_lS^{-1}) = D(A_1, \ldots, A_l)$.

(iv) Polynomial homotopy: for commuting $A_1(t), \ldots, A_l(t) \in \mathrm{GL}_n(k[t])$, we have $D(A_1(0), \ldots, A_l(0)) = D(A_1(1), \ldots, A_l(1))$.

Using the standard inclusion $\mathrm{GL}_n(k) \hookrightarrow \mathrm{GL}_{n+1}(k)$

$$\begin{pmatrix} a_{11} & \cdots & a_{1n} \\ \vdots & \ddots & \vdots \\ a_{n1} & \cdots & a_{nn} \end{pmatrix} \longmapsto \begin{pmatrix} a_{11} & \cdots & a_{1n} & 0 \\ \vdots & \ddots & \vdots & 0 \\ a_{n1} & \cdots & a_{nn} & 0 \\ 0 & \cdots & 0 & 1 \end{pmatrix}, \tag{2}$$

we define $\mathrm{GL}(k)$ as the direct limit of these groups $\mathrm{GL}(k) = \cup_{n\to\infty}\mathrm{GL}_n(k)$. Using the above inclusions, we may identify the direct limit $\mathrm{Comm}_l(k)$ of the set of l-tuples of commuting matrices in $\mathrm{GL}_n(k)^l = \mathrm{GL}_n(k) \times \cdots \times \mathrm{GL}_n(k)$ over n as a subset of $\mathrm{GL}(k)^l = \mathrm{GL}(k) \times \cdots \times \mathrm{GL}(k)$. Then, a joint determinant may be thought of as a map from $\mathrm{Comm}_l(k)$ into an abelian group G.

The main result in [1] about the joint determinants is that there exists a one-to-one correspondence between the set of joint determinants from $\mathrm{Comm}_l(k)$ into an abelian group G and the set of group homomorphisms from Milnor's K-group $K_l^M(k)$ into G. Milnor's K-group is introduced in [2] as the quotient group of the tensor product $k^* \otimes \cdots \otimes k^*$ by the subgroup generated by elements of the form $a_1 \otimes \cdots \otimes a_l$, where $a_i + a_j = 1$ for some i, j $(1 \leq i < j \leq l)$. It is a major object of study in algebraic K-theory and appears in numerous literatures. For example, Voevodsky's proof of

Bloch-Kato conjecture [3] relates Milnor's K-group of a field with its étale cohomology. The element of $K_l^M(k)$ represented by $a_1 \otimes \cdots \otimes a_l$ is typically denoted by a symbol $\{a_1, \ldots, a_l\}$.

To describe the "universal" joint determinant $\mathrm{Comm}_l(k) \to K_l^M(k)$, we need the Goodwillie group $\mathrm{GW}_l(k)$ which is defined to be the abelian group generated by l-tuples of commuting matrices $(A_1, \ldots, A_l)$ $(A_1, \ldots, A_l \in \mathrm{GL}_n(k)$ for various $n \geq 1)$, subject to the following 4 kinds of relations.

(i) Identity matrices: $(A_1, \ldots, A_l) = 0$ when A_i for some i is equal to the identity matrix $I_n \in \mathrm{GL}_n(k)$.

(ii) Similar matrices: $(A_1, \ldots, A_l) = (SA_1S^{-1}, \ldots, SA_lS^{-1})$ for commuting $A_1, \ldots, A_l \in \mathrm{GL}_n(k)$ and any $S \in \mathrm{GL}_n(k)$.

(iii) Direct sum: $(A_1, \ldots, A_l) + (B_1, \ldots, B_l) = \left(\begin{pmatrix} A_1 & 0 \\ 0 & B_1 \end{pmatrix}, \ldots, \begin{pmatrix} A_l & 0 \\ 0 & B_l \end{pmatrix}\right)$ for commuting $A_1, \ldots, A_l \in \mathrm{GL}_n(k)$ and commuting $B_1, \ldots, B_l \in \mathrm{GL}_m(k)$.

(iv) Polynomial homotopy: $(A_1(0), \ldots, A_l(0)) = (A_1(1), \ldots, A_l(1))$ for commuting matrices $A_1(t), \ldots, A_l(t)$ in $\mathrm{GL}_n(k[t])$, where $k[t]$ is the polynomial ring over k with the indeterminate t.

The universal joint determinant map $\Phi_l : \mathrm{Comm}_l(k) \to K_l^M(k)$ is then the composite of the natural map $\mathrm{Comm}_l(k) \to \mathrm{GW}_l(k)$, which sends an l-tuple of commuting matrices to a generator of $\mathrm{GW}_l(k)$ and the isomorphism $\phi_l : \mathrm{GW}_l(k) \xrightarrow{\sim} K_l^M(k)$, which is described in the proof of Theorem 6.7 of [1]. From the fact that ϕ is an isomorphism follows easily the one-to-one correspondence between the set of joint determinants from $\mathrm{Comm}_l(k)$ into an abelian group G and the set of group homomorphisms from Milnor's K-group $K_l^M(k)$ into G.

When $l = 1$, $\mathrm{GW}_l(k) \simeq k^*$ and the universal joint determinant is nothing but the traditional determinant map (Proposition 4.4 of [1]).

The definition of joint determinant maps is given in purely algebraic terms and so there are possibilities of very complicated joint determinants; for example, when k is the field $\mathbb{C}$ of complex numbers or $\mathbb{R}$ of real numbers, Milnor's K-groups $K_l^M(k)$ for $l \geq 2$ are known to be uniquely divisible or a direct sum of a cyclic group of order 2 and a uniquely divisible group, respectively [2].

Thus, if we disregard the topological continuity of a joint determinant map, the joint determinants are far from trivial, but if we require a joint determinant to be continuous, then the situation becomes drastically different. It is proven that, for $l \geq 2$, there exists only one nontrivial joint determinant from $\mathrm{Comm}_l(\mathbb{R})$ into $\mathbb{R}^\times$, which is continuous when restricted to the set of commuting matrices in $\mathrm{GL}_n(\mathbb{R})$, for each n, with the standard topology (Corollary 7.3 of [1]).

In the present article, we generalize this result to determine all possible continuous joint determinants from $\mathrm{Comm}_l(\mathbb{R})$ or $\mathrm{Comm}_l(\mathbb{C})$ to a topological abelian group G. For this purpose, we introduce a natural topology on Milnor's K-groups $K_l^M(k)$ for a topological field k as the quotient topology induced by the joint determinant map and show that, in case of $k = \mathbb{R}$ or $\mathbb{C}$, the natural topology on $K_l^M(k)$ is disjoint union of two indiscrete components or indiscrete topology, respectively. This indicates that, for $k = \mathbb{R}$ or $\mathbb{C}$, the "universal" continuous joint determinant turns out to be $\mathrm{Comm}_l(\mathbb{R}) \to \mathbb{Z}_2$ or $\mathrm{Comm}_l(\mathbb{C}) \to \{1\}$, respectively.

2. A Natural Topology on $K_l^M(k)$

For a topological field k, $\mathrm{GL}(k) = \cup_{n\to\infty}\mathrm{GL}_n(k)$ is a topological group with the direct limit topology, that is, a subset U of $\mathrm{GL}(k)$ is open if and only if $U \cap \mathrm{GL}_n(k)$ is open for each $n \geq 1$ (e.g., 3.1 of [4]). The topology on $\mathrm{Comm}_l(k)$ is given by the subspace topology regarding it as a subspace of the product space $\mathrm{GL}(k)^l = \mathrm{GL}(k) \times \cdots \times \mathrm{GL}(k)$. Then it coincides with the direct limit topology if we think of $\mathrm{Comm}_l(k)$ as the direct limit of the subspace of l-tuples of commuting matrices in the space $\mathrm{GL}_n(k)^l = \mathrm{GL}_n(k) \times \cdots \times \mathrm{GL}_n(k)$ over n.

Definition 1. For a topological field k, the topology on Milnor's K-group $K_l^M(k)$ is the quotient topology with respect to the map $\Phi_l : \mathrm{Comm}_l(k) \to K_l^M(k)$, which is the composite of a natural map $\mathrm{Comm}_l(k) \to \mathrm{GW}_l(k)$ followed by the group isomorphism $\phi_l : \mathrm{GW}_l(k) \xrightarrow{\sim} K_l^M(k)$ which is described in the proof of Theorem 6.7 of [1].

The obvious map $\mathrm{Comm}_l(k) \to \mathrm{GW}_l(k)$ is actually surjective by Corollary 4.3 of [1] and so Φ_l is a surjection.

Theorem 2. *$K_l^M(k)$ is a topological group with respect to the topology given in Definition 1.*

Proof. By the definition of the Goodwillie group $\mathrm{GW}_l(k)$, the group law on $K_l^M(k)$ is given via $\phi_l : \mathrm{GW}_l(k) \xrightarrow{\sim} K_l^M(k)$ by the direct sum rule: $(A_1, \ldots, A_l) + (B_1, \ldots, B_l) = \left(\begin{pmatrix} A_1 & 0 \\ 0 & B_1 \end{pmatrix}, \ldots, \begin{pmatrix} A_l & 0 \\ 0 & B_l \end{pmatrix}\right)$ for commuting $A_1, \ldots, A_l \in \mathrm{GL}_p(k)$ and commuting $B_1, \ldots, B_l \in \mathrm{GL}_q(k)$ $(p, q \geq 1)$. This addition rule is not expressed by a continuous map $\mathrm{Comm}_l(k) \times \mathrm{Comm}_l(k) \to \mathrm{Comm}_l(k)$, but the following continuous map $\mathrm{Comm}_l(k) \times \mathrm{Comm}_l(k) \to \mathrm{Comm}_l(k)$ actually induces the group operation on $K_l^M(k)$:

$$\left(\left(\begin{pmatrix} a_{11} & a_{12} & a_{13} & \cdots \\ a_{21} & a_{22} & a_{23} & \cdots \\ a_{31} & a_{32} & a_{33} & \cdots \\ \vdots & \vdots & \vdots & \ddots \end{pmatrix}, \cdots\right), \left(\begin{pmatrix} b_{11} & b_{12} & b_{13} & \cdots \\ b_{21} & b_{22} & b_{23} & \cdots \\ b_{31} & b_{32} & b_{33} & \cdots \\ \vdots & \vdots & \vdots & \ddots \end{pmatrix}, \cdots\right)\right)$$

$$\longmapsto \left(\begin{pmatrix} a_{11} & 0 & a_{12} & 0 & a_{13} & 0 & \cdots \\ 0 & b_{11} & 0 & b_{12} & 0 & b_{13} & \cdots \\ a_{21} & 0 & a_{22} & 0 & a_{23} & 0 & \cdots \\ 0 & b_{21} & 0 & b_{22} & 0 & b_{23} & \cdots \\ a_{31} & 0 & a_{32} & 0 & a_{33} & 0 & \cdots \\ 0 & b_{31} & 0 & b_{32} & 0 & b_{33} & \cdots \\ \vdots & \vdots & \vdots & \vdots & \vdots & \vdots & \ddots \end{pmatrix}, \cdots \right). \tag{3}$$

To prove that the two elements

$$\left(\begin{pmatrix} a_{11} & 0 & a_{12} & 0 & \cdots \\ 0 & b_{11} & 0 & b_{12} & \cdots \\ a_{21} & 0 & a_{22} & 0 & \cdots \\ 0 & b_{21} & 0 & b_{22} & \cdots \\ \vdots & \vdots & \vdots & \vdots & \ddots \end{pmatrix}, \cdots \right),$$

$$\left(\begin{pmatrix} a_{11} & a_{12} & \cdots & 0 & 0 & \cdots \\ a_{21} & a_{22} & \cdots & 0 & 0 & \cdots \\ \vdots & \vdots & \ddots & \vdots & \vdots & \vdots \\ 0 & 0 & \cdots & b_{11} & b_{12} & \cdots \\ 0 & 0 & \cdots & b_{21} & b_{22} & \cdots \\ \vdots & \vdots & \cdots & \vdots & \vdots & \ddots \end{pmatrix}, \cdots \right) \tag{4}$$

of $\mathrm{Comm}_l(k)$ map to the same element under $\Phi_l : \mathrm{Comm}_l(k) \to K_l^M(k)$, it is enough to verify that an l-tuple $(A_1, \ldots, A_l)$ of commuting matrices in $\mathrm{GL}_n(k)^l$ represents the same element in $\mathrm{GW}_l(k)$ which is represented by the l-tuple of matrices which is obtained by simultaneously changing ith and jth rows and also ith and jth columns of all l $n \times n$ matrices $A_1, \ldots, A_l$. For notational convenience, we will prove this for 1st and 2nd rows and columns of 2×2 matrices and the proof is easily generalized to $n \times n$ matrices. Let us write the (i, j)th entry of the matrix A_k as a_{ij}^k $(k = 1, 2, \ldots, l)$. In $\mathrm{GW}_l(k)$, we have

$$\begin{aligned} (A_1, \ldots, A_l) &= \left(\begin{pmatrix} a_{11}^1 & a_{12}^1 \\ a_{21}^1 & a_{22}^1 \end{pmatrix}, \ldots, \begin{pmatrix} a_{11}^l & a_{12}^l \\ a_{21}^l & a_{22}^l \end{pmatrix} \right) \\ &= \left(\begin{pmatrix} a_{11}^1 & a_{12}^1 & 0 & 0 \\ a_{21}^1 & a_{22}^1 & 0 & 0 \\ 0 & 0 & 1 & 0 \\ 0 & 0 & 0 & 1 \end{pmatrix}, \ldots, \right. \\ &\quad \left. \begin{pmatrix} a_{11}^l & a_{12}^l & 0 & 0 \\ a_{21}^l & a_{22}^l & 0 & 0 \\ 0 & 0 & 1 & 0 \\ 0 & 0 & 0 & 1 \end{pmatrix} \right). \end{aligned} \tag{5}$$

Using the polynomial homotopy

$$\left(\begin{pmatrix} 1-t^2 & 0 & 0 & t \\ 0 & 1 & 0 & 0 \\ 0 & 0 & 1 & 0 \\ t^3-2t & 0 & 0 & 1-t^2 \end{pmatrix} \begin{pmatrix} a_{11}^1 & a_{12}^1 & 0 & 0 \\ a_{21}^1 & a_{22}^1 & 0 & 0 \\ 0 & 0 & 1 & 0 \\ 0 & 0 & 0 & 1 \end{pmatrix} \begin{pmatrix} 1-t^2 & 0 & 0 & -t \\ 0 & 1 & 0 & 0 \\ 0 & 0 & 1 & 0 \\ 2t-t^3 & 0 & 0 & 1-t^2 \end{pmatrix}, \ldots, \right.$$

$$\left. \begin{pmatrix} 1-t^2 & 0 & 0 & t \\ 0 & 1 & 0 & 0 \\ 0 & 0 & 1 & 0 \\ t^3-2t & 0 & 0 & 1-t^2 \end{pmatrix} \begin{pmatrix} a_{11}^l & a_{12}^l & 0 & 0 \\ a_{21}^l & a_{22}^l & 0 & 0 \\ 0 & 0 & 1 & 0 \\ 0 & 0 & 0 & 1 \end{pmatrix} \begin{pmatrix} 1-t^2 & 0 & 0 & -t \\ 0 & 1 & 0 & 0 \\ 0 & 0 & 1 & 0 \\ 2t-t^3 & 0 & 0 & 1-t^2 \end{pmatrix} \right), \tag{6}$$

which results in interchanging the 1st and 4th rows with negative sign to the new 4th row and then interchanging 1st and 4th columns with negative sign to the new 4th column, we see that, in $\mathrm{GW}_l(k)$,

$$\left(\begin{pmatrix} a_{11}^1 & a_{12}^1 & 0 & 0 \\ a_{21}^1 & a_{22}^1 & 0 & 0 \\ 0 & 0 & 1 & 0 \\ 0 & 0 & 0 & 1 \end{pmatrix}, \ldots, \begin{pmatrix} a_{11}^l & a_{12}^l & 0 & 0 \\ a_{21}^l & a_{22}^l & 0 & 0 \\ 0 & 0 & 1 & 0 \\ 0 & 0 & 0 & 1 \end{pmatrix}\right)$$

$$= \left(\begin{pmatrix} 1 & 0 & 0 & 0 \\ 0 & a_{22}^1 & 0 & -a_{21}^1 \\ 0 & 0 & 1 & 0 \\ 0 & -a_{12}^1 & 0 & a_{11}^1 \end{pmatrix}, \ldots, \begin{pmatrix} 1 & 0 & 0 & 0 \\ 0 & a_{22}^l & 0 & -a_{21}^l \\ 0 & 0 & 1 & 0 \\ 0 & -a_{12}^l & 0 & a_{11}^l \end{pmatrix}\right). \tag{7}$$

Again, by applying the polynomial homotopy

$$\left(\begin{pmatrix} 1 & 0 & 0 & 0 \\ 0 & 1-t^2 & t & 0 \\ 0 & t^3-2t & 1-t^2 & 0 \\ 0 & 0 & 0 & 1 \end{pmatrix}\begin{pmatrix} 1 & 0 & 0 & 0 \\ 0 & a_{22}^1 & 0 & -a_{21}^1 \\ 0 & 0 & 1 & 0 \\ 0 & -a_{12}^1 & 0 & a_{11}^1 \end{pmatrix}\begin{pmatrix} 1 & 0 & 0 & 0 \\ 0 & 1-t^2 & -t & 0 \\ 0 & 2t-t^3 & 1-t^2 & 0 \\ 0 & 0 & 0 & 1 \end{pmatrix}, \ldots, \right.$$

$$\left.\begin{pmatrix} 1 & 0 & 0 & 0 \\ 0 & 1-t^2 & t & 0 \\ 0 & t^3-2t & 1-t^2 & 0 \\ 0 & 0 & 0 & 1 \end{pmatrix}\begin{pmatrix} 1 & 0 & 0 & 0 \\ 0 & a_{22}^l & 0 & -a_{21}^l \\ 0 & 0 & 1 & 0 \\ 0 & -a_{12}^l & 0 & a_{11}^l \end{pmatrix}\begin{pmatrix} 1 & 0 & 0 & 0 \\ 0 & 1-t^2 & -t & 0 \\ 0 & 2t-t^3 & 1-t^2 & 0 \\ 0 & 0 & 0 & 1 \end{pmatrix}\right), \tag{8}$$

which results in interchanging the 2nd and 3rd rows with negative sign to the new 3rd row and then interchanging 2nd and 3rd columns with negative sign to the new 3rd column, we have, in $\mathrm{GW}_l(k)$,

$$\left(\begin{pmatrix} 1 & 0 & 0 & 0 \\ 0 & a_{22}^1 & 0 & -a_{21}^1 \\ 0 & 0 & 1 & 0 \\ 0 & a_{12}^1 & 0 & a_{11}^1 \end{pmatrix}, \ldots, \begin{pmatrix} 1 & 0 & 0 & 0 \\ 0 & a_{22}^l & 0 & -a_{21}^l \\ 0 & 0 & 1 & 0 \\ 0 & a_{12}^l & 0 & a_{11}^l \end{pmatrix}\right)$$

$$= \left(\begin{pmatrix} 1 & 0 & 0 & 0 \\ 0 & 1 & 0 & 0 \\ 0 & 0 & a_{22}^1 & a_{21}^1 \\ 0 & 0 & a_{12}^1 & a_{11}^1 \end{pmatrix}, \ldots, \right. \tag{9}$$

$$\left.\begin{pmatrix} 1 & 0 & 0 & 0 \\ 0 & 1 & 0 & 0 \\ 0 & 0 & a_{22}^l & a_{21}^l \\ 0 & 0 & a_{12}^l & a_{11}^l \end{pmatrix}\right),$$

which is equal to $\left(\begin{pmatrix} a_{22}^1 & a_{21}^1 \\ a_{12}^1 & a_{11}^1 \end{pmatrix}, \ldots, \begin{pmatrix} a_{22}^l & a_{21}^l \\ a_{12}^l & a_{11}^l \end{pmatrix}\right)$ in $\mathrm{GW}_l(k)$. □

3. The Topological Structures of $K_l^M(\mathbb{R})$ and $K_l^M(\mathbb{C})$

Theorem 3. *For $l \geq 2$, the topological space $K_l^M(\mathbb{R})$ is a disjoint union of two indiscrete open sets.*

Proof. Note that we have $K_l^M(\mathbb{R}) \simeq (\mathbb{Z}/2) \oplus H$, where the first direct factor $\mathbb{Z}/2$ is generated by $\{-1, \ldots, -1\}$ and H is a uniquely divisible group [2]. For $\{a_1, \ldots, a_l\}$ where a_i are negative for all $i = 1, \ldots, l$, we have $\{a_1, \ldots, a_l\} = \{-1, a_2, \ldots, a_l\} + \{-a_1, a_2, \ldots, a_l\} = \{-1, -1, a_3, \ldots, a_l\} + \{-1, -a_2, \ldots, a_l\} + \{-a_1, a_2, \ldots, a_l\} = \cdots$ which is equal to the sum of $\{-1, -1, -1, \ldots, -1\}$ and various symbols of the form $\{b_1, \ldots, b_l\}$ where at least one of b_i is positive.

Every element of H can be written as a sum of symbols of the form $b_1, \ldots, b_l$, where at least one of b_i is positive. By writing a positive real number as a square of its square root, we may assume that b_i is positive for every $i = 1, \ldots, l$ (e.g., $\{b_1, b_2\} = \{b_1^2, \sqrt{b_2}\}$ in case $b_2 > 0$).

Let U be any open set of $K_l^M(\mathbb{R})$ containing the identity element and consider its inverse image $V = \Phi_l^{-1}(U)$ in $\mathrm{Comm}_l(\mathbb{R})$. Let $h \in H$ be any element. Then

$\Phi_l^{-1}(\{h\})$ contains an l-tuple of diagonal matrices of the form

$$\left(\begin{pmatrix} a_1^1 & & & \\ & a_2^1 & & \\ & & \ddots & \\ & & & a_n^1 \end{pmatrix}, \ldots, \begin{pmatrix} a_1^l & & & \\ & a_2^l & & \\ & & \ddots & \\ & & & a_n^l \end{pmatrix}\right), \quad (10)$$

where a_k^i is positive for every $k = 1, \ldots, n$ and $i = 1, \ldots, l$. By taking mth root of a_k^1 for sufficiently large m, we may assume that a_k^1 is arbitrarily close to 1. Then $\Phi_l^{-1}(\{h\})$ contains an element which is arbitrarily close to $(A_1, \ldots, A_l)$ with A_1 equal to the identity matrix. So, $\Phi_l^{-1}(\{h\})$ contains an element which is contained in the open set $V = \Phi_l^{-1}(U)$. Hence U must contain H.

Similarly, the coset $H + \{-1, -1, \ldots, -1\}$ is also an indiscrete subspace. In fact, H is the image under Φ_l of the set of l-tuples $(A_1, \ldots, A_l)$ of commuting matrices in $\mathrm{GL}_n(\mathbb{R})^l$ ($n \geq 1$) such that the determinants of A_i are positive for some $i \in \{1, \ldots, l\}$. On the other hand, $H + \{-1, -1, \ldots, -1\}$ is the image under Φ_l of the set of l-tuples $(A_1, \ldots, A_l)$ of commuting matrices where the determinants of A_i are negative for all $i = 1, \ldots, l$. Therefore, the proper open sets of $K_l^M(\mathbb{R})$ are H and $H + \{-1, -1, \ldots, -1\}$. □

Corollary 4. *For $l \geq 2$, the topological space $K_l^M(\mathbb{C})$ is indiscrete (trivial).*

Proof. Let U be an open set of $K_l^M(\mathbb{C})$ containing the identity element and let $V = \Phi^{-1}(U) \subset \mathrm{Comm}_l(\mathbb{C})$. For any element $h \in K_l^M(\mathbb{C})$, $\Phi^{-1}(\{h\})$ contains an l-tuple $(A_1, \ldots, A_l)$ of diagonal matrices. Write each diagonal element of A_i as a product of a positive real number and a complex number with absolute value 1. Any complex number with absolute value 1 is arbitrarily close to a root of unity and any symbol containing a root of unity is trivial since, for example, $\{\zeta, b\} = (1/m)\{\zeta^m, b\} = 0$ if ζ is an mth root of unity. Combining this fact with the arguments given in the proof of Theorem 3, we see that $\Phi^{-1}(\{h\})$ contains an element which is contained in $V = \Phi^{-1}(U)$. This shows that the natural topology on $K_l^M(\mathbb{C})$ is indiscrete. □

4. Applications to Joint Determinants

When k is a topological field, a joint determinant from $\mathrm{Comm}_l(k)$ into a topological abelian group G is called continuous if $\mathrm{Comm}_l(k)$ is given the subspace topology of $\mathrm{GL}(k) = \cup_{n\to\infty}\mathrm{GL}_n(k)$ with the direct limit topology as described in Section 2. Since the natural topology on $K_l^M(k)$ in Definition 1 is the quotient topology, any continuous joint determinant induces a continuous map from $K_l^M(k)$ into G and vice versa.

Corollary 5. *For $l \geq 2$ and any topological abelian group G which is T_0, any continuous joint determinant from $\mathrm{Comm}_l(\mathbb{R})$ into G factors through the discrete group $\mathbb{Z}_2$.*

Proof. This follows directly from Theorem 3. Note that a topological group is Hausdorff if it is T_0 (cf. Lemma 10.1 of [5]). □

The following is a direct consequence of Corollary 4.

Corollary 6. *For $l \geq 2$ and any topological abelian group G which is T_0, any continuous joint determinant from $\mathrm{Comm}_l(\mathbb{C})$ into G is trivial.*

We summarize our results on the continuous joint determinants for $k = \mathbb{R}$ and $k = \mathbb{C}$ in the following theorem, which is virtually equivalent to Theorem 3 and Corollary 4.

Theorem 7. *For $k = \mathbb{R}$ or $k = \mathbb{C}$ and a topological abelian group G, let $D : \mathrm{Comm}_l(k) \to G$ be a continuous surjective joint determinant. When $l = 1$, D is a composite of the usual determinant map followed by a canonical epimorphism $k^* \twoheadrightarrow G$ with G equipped with a coarser topology than the quotient topology induced by the epimorphism. When $k = \mathbb{R}$ and $l \geq 2$, G either is an indiscrete space or has an indiscrete subgroup of index 2. If $k = \mathbb{C}$, then G has the indiscrete topology.*

Conflicts of Interest

The author declares that they have no conflicts of interest.

Acknowledgments

This work was supported by the National Research Foundation of Korea (NRF) grant funded by the Korean government (MEST) (no. NRF-2010-0006083).

References

[1] S. Myung, "Transfer maps and nonexistence of joint determinant," *Linear Algebra and its Applications*, vol. 431, no. 9, pp. 1633–1651, 2009.

[2] J. Milnor, "Algebraic K-theory and quadratic forms," *Inventiones Mathematicae*, vol. 9, pp. 318–344, 1969/1970.

[3] V. Voevodsky, "On motivic cohomology with Z/l-coefficients," *Annals of Mathematics: Second Series*, vol. 174, no. 1, pp. 401–438, 2011.

[4] F. Paul, J. BaumRubén, and a. Sánchez-Garc, "K-theory for group C*-algebras," in *Topics in Algebraic and Topological K-Theory*, pp. 1–43, Springer, Berlin, Germany, 2008.

[5] M. F. Atiyah and I. G. Macdonald, *Introduction to Commutative Algebra*, Addison-Wesley Publishing Co., London, UK, 1969.

A Note on the Performance of Biased Estimators with Autocorrelated Errors

Gargi Tyagi and Shalini Chandra

Department of Mathematics & Statistics, Banasthali University, Rajasthan 304022, India

Correspondence should be addressed to Gargi Tyagi; tyagi.gargi@gmail.com

Academic Editor: Weimin Han

It is a well-established fact in regression analysis that multicollinearity and autocorrelated errors have adverse effects on the properties of the least squares estimator. Huang and Yang (2015) and Chandra and Tyagi (2016) studied the PCTP estimator and the $r-(k,d)$ class estimator, respectively, to deal with both problems simultaneously and compared their performances with the estimators obtained as their special cases. However, to the best of our knowledge, the performance of both estimators has not been compared so far. Hence, this paper is intended to compare the performance of these two estimators under mean squared error (MSE) matrix criterion. Further, a simulation study is conducted to evaluate superiority of the $r-(k,d)$ class estimator over the PCTP estimator by means of percentage relative efficiency. Furthermore, two numerical examples have been given to illustrate the performance of the estimators.

1. Introduction

Let us consider a linear regression model as

$$y = X\beta + u, \tag{1}$$

where y is an $n \times 1$ vector of observations on dependent variable, X is an $n \times p$ full column rank matrix of observations on p explanatory variables, β is a $p \times 1$ vector of unknown regression coefficients, and u is an $n \times 1$ vector of disturbance term with mean vector 0 and covariance matrix $\sigma^2 I_n$.

Ordinary least squares estimator (OLSE) is one of the most widely used estimator for β, given as

$$\widehat{\beta} = \left(X'X\right)^{-1} X'y. \tag{2}$$

In the presence of multicollinearity among explanatory variables, OLSE becomes unstable and shows undesirable properties, such as inflated variance, wide confidence intervals which leads to wrong inferences and sometimes it even produces wrong signs of the estimates.

Numerous alternative methods of estimation have been designed to lower the effects of multicollinearity in literature. For instance, Stein [1] proposed stein estimator; Hoerl and Kennard [2, 3] introduced the technique of ordinary ridge regression estimator (ORRE); Massy [4] suggested principal component regression estimator (PCRE) to deal with the problem. Several authors combined two techniques of estimation in the hope that the combination will contain the advantages of the both. Baye and Parker [5] gave $r-k$ class estimator by combining the PCRE and the ORRE, which includes the OLSE, ORRE, and PCRE as special cases. Nomura and Ohkubo [6] obtained conditions for dominance of the $r-k$ class estimator over its special cases under mean squared error (MSE) criterion. Liu [7] gave an estimator by combining the advantages of the stein and ORRE, known as Liu estimator (LE). Kaçiranlar and Sakallıoğlu [8] proposed $r-d$ class estimator which is a combination of the LE and PCRE and showed the superiority of the $r-d$ class estimator over the OLSE, LE, and PCRE. Özkale and Kaçıranlar [9] proposed two-parameter estimator (TPE) by utilizing the advantages of the ORRE and LE and obtained necessary and sufficient condition for dominance of the TPE over the OLSE in MSE matrix sense. Further, Yang and Chang [10] also combined the ORR and Liu estimator in a different way and introduced an another two-parameter estimator (ATPE) and

derived necessary and sufficient conditions for superiority of the ATPE over OLSE, ORRE, LE, and TPE under MSE matrix criterion. Özkale [11] put forward a general class of estimators, $r-(k,d)$ class estimator which is a mingle of the TPE [9] and PCRE; they evaluated the performance of the $r-(k,d)$ class estimator under MSE criterion. Chang and Yang [12] suggested another general class of estimators by merging the PCRE and ATPE [10] named as principal component two-parameter estimator (PCTPE) and analyzed its performance under MSE matrix sense.

In applied work, it is quite common to have autocorrelation in error terms; that is, $\operatorname{cov}(u)=\sigma^2\Omega$, where Ω is a known symmetric positive definite (p.d.) $n\times n$ matrix and it is well known to statisticians that autocorrelated errors reduce the efficiency of the OLSE. Now, since Ω is a symmetrical positive definite matrix there exists an orthogonal matrix E such that $EE'=\Omega$. On premultiplying model (1) by E^{-1}, we have

$$\begin{aligned} E^{-1}y &= E^{-1}X\beta + E^{-1}u \\ y^* &= X^*\beta + u^*. \end{aligned} \tag{3}$$

Note that $E(u^*)=0$ and $\operatorname{cov}(u^*)=\sigma^2 I$.

To overcome the effect of autocorrelated errors, Aitken [13] proposed the generalized least squares estimator (GLSE) for β in (1) which can be obtained by applying least squares technique in model (3) as

$$\widehat{\beta}_{\mathrm{GLS}} = \left(X'\Omega^{-1}X\right)^{-1}X'\Omega^{-1}y. \tag{4}$$

It has been observed that the problem of autocorrelation and multicollinearity arise simultaneously in several cases. Keeping this in mind, a good amount of literature has been devoted to study these problems simultaneously by Trenkler [14], Firinguetti [15], G. M. Bayhan and M. Bayhan [16], Alheety and Kibria [17], Özkale [18], Güler and Kaçiranlar [19], Alkhamisi [20], Yang and Wu [21], Eledum and Alkhalifa [22], Şiray [23], and Chandra and Sarkar [24], to name a few.

Further, to define the estimators, let $T=(t_1,t_2,\ldots,t_p)$ be a $p\times p$ orthogonal matrix with $T'X'\Omega^{-1}XT=\Lambda=\operatorname{diag}(\lambda_1,\lambda_2,\ldots,\lambda_p)$, where Λ is a $p\times p$ diagonal matrix of eigenvalues of $X'\Omega^{-1}X$ matrix such that $\lambda_1\geq\lambda_2\geq\cdots\geq\lambda_p$. Now, let $T_r=(t_1,t_2,\ldots,t_r)$ be $p\times r$ orthogonal matrix after deleting last $p-r$ columns from T matrix, where $r\leq p$. Thus, $T_r'X'\Omega^{-1}XT_r=\Lambda_r$ where $\Lambda_r=\operatorname{diag}(\lambda_1,\lambda_2,\ldots,\lambda_r)$ and $T_{p-r}'X'\Omega^{-1}XT_{p-r}=\Lambda_{p-r}$, where $\Lambda_{p-r}=\operatorname{diag}(\lambda_{r+1},\lambda_2,\ldots,\lambda_p)$. Also, $T'T=T_r'T_r+T_{p-r}'T_{p-r}$.

Chandra and Tyagi [25] modified the $r-(k,d)$ class estimator [11] to address multicollinearity and autocorrelated errors simultaneously, which is expressed as

$$\begin{aligned} \widehat{\beta}_r(k,d) &= T_r\left(T_r'X'\Omega^{-1}XT_r+kI_r\right)^{-1} \\ &\cdot\left(T_r'X'\Omega^{-1}XT_r\right)^{-1}\left(T_r'X'\Omega^{-1}XT_r+kdI_r\right) \\ &\cdot T_r'X'\Omega^{-1}y = T_rS_r(k)^{-1}\Lambda_r^{-1}S_r(kd)\,T_r'X'\Omega^{-1}y, \end{aligned} \tag{5}$$

where $S_r(q)=\Lambda_r+qI_r$, $q=1,k,d,kd$.

Huang and Yang [26] proposed PCTP estimator in the presence of autocorrelated errors as

$$\begin{aligned} \widetilde{\beta}_r(k,d) &= T_r\left(T_r'X'\Omega^{-1}XT_r+I_r\right)^{-1} \\ &\cdot\left(T_r'X'\Omega^{-1}XT_r+dI_r\right)\left(T_r'X'\Omega^{-1}XT_r+kI_r\right)^{-1} \\ &\cdot T_r'X'\Omega^{-1}y = T_rS_r(1)^{-1}S_r(d)\,S_r(k)^{-1}T_r'X'\Omega^{-1}y, \\ &\qquad k>0,\ 0<d<1. \end{aligned} \tag{6}$$

Some other biased estimators in the presence of multicollinearity and autocorrelation can be obtained as special cases. $\widehat{\beta}_r(k,0)=\widetilde{\beta}_r(k,1)=\widehat{\beta}_r(k)$ is the $r-k$ class estimator proposed by Şiray et al. [23]; $\widehat{\beta}_p(0,d)=\widetilde{\beta}_p(1,0)=\widehat{\beta}_{\mathrm{GLS}}$ is the GLSE by Aitken [13]; $\widehat{\beta}_p(k,0)=\widetilde{\beta}_p(k,1)=\widehat{\beta}(k)$ is the ridge regression estimator (RRE) given by Trenkler [14] and so forth. The special cases of the estimators have been compared with the $r-(k,d)$ class estimator and the PCTP estimator by Chandra and Tyagi [25] and Huang and Yang [26], respectively. Hence, this paper focuses on the comparison of the performance of the two general estimators.

Further, the rest of the paper is organized as follows: the necessary and sufficient condition for dominance of the PCTP estimator over the $r-(k,d)$ class estimator under the MSE matrix criterion has been derived in Section 2. Section 3 is devoted to simulation study to compare these estimators under MSE criterion. Some methods of selection of the unknown biasing parameters have been given in Section 4. Section 5 includes two numerical examples. Finally, the paper is summed up in Section 6 with some concluding remarks.

2. MSE Matrix Comparison of $\widehat{\beta}_r(k,d)$ and $\widetilde{\beta}_r(k,d)$

The MSE matrix criterion is a strong and one of the most widely used criteria for comparison of the estimators. Let $\breve{\beta}$ be an estimator of β; then the expression for the MSE matrix is given as

$$\begin{aligned} M\left(\breve{\beta}\right) &= E\left[\left(\breve{\beta}-\beta\right)\left(\breve{\beta}-\beta\right)'\right] \\ &= \operatorname{cov}\left(\breve{\beta}\right)-\operatorname{Bias}\left(\breve{\beta}\right)\operatorname{Bias}\left(\breve{\beta}\right)', \end{aligned} \tag{7}$$

where $\operatorname{cov}(\breve{\beta})$ and $\operatorname{Bias}(\breve{\beta})$ are the covariance matrix and bias vector of $\breve{\beta}$.

From (5) and (6), the covariance matrices and bias vectors of the $r-(k,d)$ estimator and PCTP estimator can be obtained as

$$\begin{aligned} \operatorname{cov}\left(\widehat{\beta}_r(k,d)\right) &= \sigma^2T_rS_r(k)^{-1}S_r(kd)\,\Lambda_r^{-1}S_r(kd) \\ &\cdot S_r(k)^{-1}T_r' \end{aligned}$$

$$\begin{aligned}
&\operatorname{cov}\left(\widetilde{\beta}_r(k,d)\right) = \sigma^2 T_r S_r(1)^{-1} S_r(d) S_r(k)^{-1} \Lambda_r S_r(k)^{-1} \\
&\quad \cdot S_r(d) S_r(1)^{-1} T_r' \\
&\operatorname{Bias}\left(\widehat{\beta}_r(k,d)\right) \\
&\quad = -\left(k(1-d) T_r S_r(k)^{-1} T_r' + T_{p-r} T_{p-r}'\right)\beta \\
&\quad = -TB_1T'\beta \\
&\operatorname{Bias}\left(\widetilde{\beta}_r(k,d)\right) \\
&\quad = \left(T_r S_r(1)^{-1} S_r(d) S_r(k)^{-1} \Lambda_r T_r' - I_p\right)\beta \\
&\quad = -TB_2T'\beta,
\end{aligned} \tag{8}$$

where $B_1 = \begin{pmatrix} k(1-d)S_r(k)^{-1} & 0 \\ 0 & I_{p-r} \end{pmatrix}$ and $B_2 = \begin{pmatrix} S_r(1)^{-1}(\Lambda_r(1+k-d)+kI_r)S_r(k)^{-1} & 0 \\ 0 & I_{p-r} \end{pmatrix}$.

Thus, the MSE matrices of the estimators can be given as

$$\begin{aligned}
&M\left(\widehat{\beta}_r(k,d)\right) = \sigma^2 T_r S_r(k)^{-1} S_r(kd) \Lambda_r^{-1} S_r(kd) \\
&\quad \cdot S_r(k)^{-1} T_r' + TB_1T'\beta\beta'TB_1T'
\end{aligned} \tag{9}$$

$$\begin{aligned}
&M\left(\widetilde{\beta}_r(k,d)\right) = \sigma^2 T_r S_r(1)^{-1} S_r(d) S_r(k)^{-1} \Lambda_r S_r(k)^{-1} \\
&\quad \cdot S_r(d) S_r(1)^{-1} T_r' + TB_2T'\beta\beta'TB_2T'.
\end{aligned} \tag{10}$$

To compare the performance of these estimators, the difference of the MSE matrices can be obtained as

$$\begin{aligned}
\Delta_M &= M\left(\widehat{\beta}_r(k,d)\right) - M\left(\widetilde{\beta}_r(k,d)\right) = \sigma^2 T_r S_r(k)^{-1} \\
&\cdot S_r(kd) \Lambda_r^{-1} S_r(kd) S_r(k)^{-1} T_r' + TB_1T'\beta\beta'TB_1T' \\
&- T_r S_r(1)^{-1} S_r(d) S_r(k)^{-1} \Lambda_r S_r(k)^{-1} S_r(d) S_r(1)^{-1} \\
&\cdot T_r' - TB_2T'\beta\beta'TB_2T' = D + a_1a_1' - a_2a_2',
\end{aligned} \tag{11}$$

where $D = \sigma^2 T_r S_r(k)^{-1}[S_r(kd)\Lambda_r^{-1}S_r(kd) - S_r(1)^{-1}S_r(d)\Lambda_r S_r(d)S_r(1)^{-1}]S_r(k)^{-1}T_r'$, $a_1 = TB_1T'\beta$, $a_2 = TB_2T'\beta$.

On further simplification, D can be written as

$$\begin{aligned}
D &= \sigma^2 T_r S_r(k)^{-1} S_r(1)^{-1} \left((kd+1-d) I_r + kd\Lambda_r^{-1}\right) \\
&\cdot \left(2\Lambda_r^2 + (kd+d+1)\Lambda_r + kdI_r\right) S_r(1)^{-1} \\
&\cdot S_r(k)^{-1} T_r'.
\end{aligned} \tag{12}$$

It is easy to note that D is positive definite. For the convenience of the derivation of the dominance conditions, we state the following Lemma.

Lemma 1. *Assume that $\widehat{\beta}_j = A_j y$, $j = 1, 2$, are two competing linear estimators of β. Suppose that $D = \operatorname{cov}(\widehat{\beta}_1) - \operatorname{cov}(\widehat{\beta}_2) > 0$, where $\operatorname{cov}(\widehat{\beta}_j)$, $j = 1, 2$, denotes the covariance matrix of $\widehat{\beta}_j$. Then $\Delta(\widehat{\beta}_1, \widehat{\beta}_2) = M(\widehat{\beta}_1) - M(\widehat{\beta}_2) \geq 0$ if and only if $d_2'(D + d_1d_1')^{-1}d_2 \leq 1$, where d_j denote the bias vector of $\widehat{\beta}_j$.*

From the expressions in (5) and (6), it is easy to verify that the $r - (k,d)$ class estimator and the PCTP estimator can be written as $\widehat{\beta}_r(k,d) = A_1\widehat{\beta}_{\mathrm{GLS}}$ and $\widetilde{\beta}_r(k,d) = A_2\widehat{\beta}_{\mathrm{GLS}}$, where $A_1 = T_r S_r(k)^{-1} S_r(kd) T_r'$ and $A_2 = T_r S_r(1)^{-1}\Lambda_r S_r(d) S_r(k)^{-1} T_r'$. Further, it is evident from (12) that $D = \operatorname{cov}(\widetilde{\beta}_r(k,d)) - \operatorname{cov}(\widetilde{\beta}_r(k,d))$ is a positive definite matrix. Thus from the above lemma, $\Delta_M \geq 0$ if and only if

$$a_2'\left(D + a_1a_1'\right)^{-1} a_2 \leq 1. \tag{13}$$

Hence, the comparison under MSE matrix can be concluded in the following theorem.

Theorem 2. *The PCTP estimator dominates the $r - (k,d)$ class estimator in MSE matrix sense if and only if $a_2'(D + a_1a_1')^{-1}a_2 \leq 1$.*

3. Selection of k and d

It is an important problem to find optimum value of the biasing parameters. A general approach to select an optimum value of the biasing parameters is to minimize the scalar MSE of the estimator.

3.1. For $\widehat{\beta}_r(k,d)$. The scalar MSE of the $r - (k,d)$ class estimator can be obtained by taking trace of the MSE matrix in (9), which is given as

$$\begin{aligned}
m_1(r,k,d) &= \sum_{i=1}^{r} \frac{\sigma^2(\lambda_i + kd)^2 + k^2(1-d)^2\lambda_i\alpha_i^2}{\lambda_i(\lambda_i + k)^2} \\
&+ \sum_{i=r+1}^{p} \alpha_i^2,
\end{aligned} \tag{14}$$

where α_i = ith component of $\alpha = T'\beta$. The optimum value of $k(d)$ for a fixed $d(k)$ and r can be obtained by differentiating $m_1(r,k,d)$ with respect to $k(d)$ and equating it to zero. Further, first derivative of $m_1(r,k,d)$ with respect to k for fixed r and d is obtained as

$$\begin{aligned}
&\frac{\partial m_1(r,k,d)}{\partial k} \\
&\quad = \sum_{i=1}^{r} \frac{2(1-d)\lambda_i\left\{\left(k\lambda_i\alpha_i^2 - \sigma^2\right) - kd\left(\sigma^2 + \lambda_i\alpha_i^2\right)\right\}}{(\lambda_i + k)^3}
\end{aligned} \tag{15}$$

On equating to zero, we get the value of k for the $r-(k,d)$ class estimator as

$$k_1\,(\text{say}) = \frac{\sigma^2}{\left(\alpha_i^2 - d\left(\sigma^2/\lambda_i + \alpha_i^2\right)\right)}, \quad \forall i = 1, 2, \ldots, r. \tag{16}$$

By taking harmonic mean as suggested by Hoerl et al. [27] and arithmetic mean and geometric mean [28] of the values in (16), we propose the following estimators:

$$\begin{aligned} k_{1_{\text{HM}}} &= \frac{r\sigma^2}{\sum_{i=1}^{r}\left(\alpha_i^2 - d\left(\sigma^2/\lambda_i + \alpha_i^2\right)\right)}, \\ k_{1_{\text{AM}}} &= \frac{1}{r}\sum_{i=1}^{r}\frac{\sigma^2}{\left(\alpha_i^2 - d\left(\sigma^2/\lambda_i + \alpha_i^2\right)\right)}, \\ k_{1_{\text{GM}}} &= \frac{\sigma^2}{\left(\prod_{i=1}^{r}\left(\alpha_i^2 - d\left(\sigma^2/\lambda_i + \alpha_i^2\right)\right)\right)^{1/r}}. \end{aligned} \tag{17}$$

Further, the positiveness of k_1 can be ensured when we have $d < \min_{i=1,2,\ldots,r}\{\alpha_i^2/(\sigma^2/\lambda_i + \alpha_i^2)\} = d_1(\text{say})$. It can be noted that when $d = \min_{i=1,2,\ldots,r}\{\alpha_i^2/(\sigma^2/\lambda_i + \alpha_i^2)\}$, $k_{1_{\text{GM}}}$ is not defined and $k_{1_{\text{GM}}}$ will give zero. This way we can choose a value of d satisfying $d < d_1$ and further the value of k is obtained by replacing d in (17).

Alternatively, for fixed r and k, the optimum value of d for the $r-(k,d)$ class estimator by minimizing $m_1(r,k,d)$ with respect to d is obtained as

$$d_{1_{\text{opt}}} = \frac{\sum_{i=1}^{r}\left(\left(k\alpha_i^2 - \sigma^2\right)/\left(\lambda_i + k\right)^2\right)}{\sum_{i=1}^{r}\left(k\left(\sigma^2 + \lambda_i\alpha_i^2\right)/\lambda_i\left(\lambda_i + k\right)^2\right)}. \tag{18}$$

Clearly, $d_{1_{\text{opt}}}$ is positive when $k > \sigma^2/\alpha_{\min}^2$. Hence, we can choose a value of $k > \sigma^2/\alpha_{\min}^2$ and making use of this value we can find optimum value $d_{1_{\text{opt}}}$.

3.2. For $\widetilde{\beta}_r(k,d)$. The scalar MSE of the PCTP estimator obtained by taking trace of the MSE matrix in (10) is given as

$$\begin{aligned} &m_2\,(r,k,d) \\ &\quad= \sum_{i=1}^{r}\frac{\sigma^2\lambda_i\left(\lambda_i + d\right)^2 + \left(\lambda_i\left(1 + k - d\right) + k\right)^2\alpha_i^2}{\left(\lambda_i + 1\right)^2\left(\lambda_i + k\right)^2} \\ &\qquad + \sum_{i=r+1}^{p}\alpha_i^2. \end{aligned} \tag{19}$$

The first order derivative of $m_2(r,k,d)$ is obtained as

$$\frac{\partial m_2\,(r,k,d)}{\partial k} = \sum_{i=1}^{r}\frac{\left(2\left(\lambda_i + 1\right)\left(\lambda_i + k\right)\left(\lambda_i\left(1 + k - d\right) + k\right)\alpha_i^2 - 2\lambda_i\left(\lambda_i + d\right)^2\sigma^2 - 2\left(\lambda_i\left(1 + k - d\right) + k\right)^2\alpha_i^2\right)}{\left(\lambda_i + 1\right)^2\left(\lambda_i + k\right)^3}. \tag{20}$$

The optimum value of k for the PCTP estimator is obtained as

$$k_2 = \frac{\left(\lambda_i + d\right)\sigma^2 - \left(1 - d\right)\lambda_i\alpha_i^2}{\left(\lambda_i + 1\right)\alpha_i^2}, \quad \forall i = 1, 2, \ldots, r. \tag{21}$$

Since k_2 depends on i, following Hoerl et al. [27] and Kibria [28], we propose the following estimators:

$$\begin{aligned} k_{2_{\text{HM}}} &= \frac{r}{\sum_{i=1}^{r}\left(\left(\left(\lambda_i + d\right)\sigma^2 - \left(1 - d\right)\lambda_i\alpha_i^2\right)/\left(\lambda_i + 1\right)\alpha_i^2\right)}, \\ k_{2_{\text{AM}}} &= \frac{1}{r}\sum_{i=1}^{r}\left(\frac{\left(\lambda_i + d\right)\sigma^2 - \left(1 - d\right)\lambda_i\alpha_i^2}{\left(\lambda_i + 1\right)\alpha_i^2}\right), \\ k_{2_{\text{GM}}} &= \left(\prod_{i=1}^{r}\frac{\left(\lambda_i + d\right)\sigma^2 - \left(1 - d\right)\lambda_i\alpha_i^2}{\left(\lambda_i + 1\right)\alpha_i^2}\right)^{1/r}. \end{aligned} \tag{22}$$

Further, the positiveness of k_2 can be ensured when we have $d > \max_{i=1,2,\ldots,r}\{(\alpha_i^2 - \sigma^2)/(\sigma^2/\lambda_i + \alpha_i^2)\} = d_2$. This way we can chose a value of d satisfying $d > d_2$ for the PCTP estimator and the value of k is then obtained by replacing d in (22).

Alternatively, for fixed r and k, the optimum values of d for the PCTP estimator by minimizing $m_2(r,k,d)$ with respect to d are obtained as

$$\begin{aligned} &d_{2_{\text{opt}}} \\ &\quad= \frac{\sum_{i=1}^{r}\left(\left(k\left(\lambda_i + 1\right)\alpha_i^2 - \lambda_i\left(\sigma^2 - \alpha_i^2\right)\right)/\left(\lambda_i + 1\right)^2\left(\lambda_i + k\right)^2\right)}{\sum_{i=1}^{r}\left(\left(\sigma^2 + \lambda_i\alpha_i^2\right)/\left(\lambda_i + 1\right)^2\left(\lambda_i + k\right)^2\right)}. \end{aligned} \tag{23}$$

When $\sigma^2 - \alpha_i^2 > 0$ for some $i = 1, 2, \ldots, r$, $0 < d_{2_{\text{opt}}} < 1$ for

$$\max_{i=1,2,\ldots,r}\left\{\frac{\lambda_i\left(\sigma^2 - \alpha_i^2\right)}{\left(\lambda_i + 1\right)\alpha_i^2}\right\} < k < \frac{\sigma^2}{\alpha_{\max}^2}. \tag{24}$$

When $\sigma^2 - \alpha_i^2 < 0$ for all $i = 1, 2, \ldots, r$, $0 < d_{2_{\text{opt}}} < 1$ for $0 < k < \sigma^2/\alpha_{\max}^2$.

Further, the values of k and d can be easily obtained by replacing the unknown parameters σ^2 and α with their unbiased estimators.

4. Monte Carlo Study

In this section, we will evaluate the performance of the estimators through Monte Carlo simulation. Following McDonald and Galarneau [29] and Gibbons [30], X matrix has been generated as follows:

$$x_{ij} = \left(1-\gamma^2\right)^{1/2} z_{ij} + \gamma z_{ip+1}, \quad i = 1,2,\ldots,n,\ \ j = 1,2,\ldots,p, \tag{25}$$

where z_{ij} are generated from standard normal pseudorandom numbers and x_{ij}'s are generated such that the correlation between any pair of X-variables is γ^2. In this study, we consider the values of γ to be 0.90, 0.95, and 0.99. Following McDonald and Galarneau [29], Gibbons [30], Kibria [28], and others, β has been chosen as the normalized eigenvector corresponding to the largest eigenvalue of the $X'X$ matrix. The dependent variable y is obtained by

$$y = X\beta + u. \tag{26}$$

Following Firinguetti [15], Judge et al. [31], and Chandra and Sarkar [24], u are generated from AR(1) process as

$$u_i = \rho u_{i-1} + e_i, \quad i = 1,2,\ldots,n, \tag{27}$$

where e_i are independent normal pseudorandom numbers with mean 0 and variance σ_e^2 and ρ is autoregressive coefficient such that $|\rho| < 1$. The covariance matrix Ω for AR(1) errors is given by

$$\Omega = \left(\omega_{ij}\right)_{n\times n}, \quad \omega_{ij} = \sigma^2\rho^{|i-j|}, \text{ where } \sigma^2 = \frac{\sigma_e^2}{1-\rho^2}. \tag{28}$$

The value of r is decided by a scree plot which is drawn between eigenvalues and components (see Johnson and Wichern [32]). In this simulation we chose $n = 20, 50, 100$, $p = 5, 10$, $\sigma_e^2 = 0.1, 1, 10$, $\rho = 0, 0.3, 0.9$, $k = 0.1, 0.5, 0.9, 2$, and $d = 0.1, 0.5, 0.9$. Then the experiment is repeated 2000 times by generating errors in every repetition and estimated MSE (EMSE) is calculated by the following formula:

$$\text{EMSE}\left(\widehat{\beta}\right) = \frac{1}{2000}\sum_{i=1}^{2000}\left(\widehat{\beta}_{(i)} - \beta\right)'\left(\widehat{\beta}_{(i)} - \beta\right), \tag{29}$$

where $\widehat{\beta}_{(i)}$ is the estimated value of β in ith iteration. To compare the performances of the estimators, percentage relative efficiency of the $r-(k,d)$ class estimator over the PCTP estimator has been calculated as follows:

$$\%\ \text{RE} = \frac{\text{EMSE}\left(\widetilde{\beta}_r(k,d)\right) - \text{EMSE}\left(\widehat{\beta}_r(k,d)\right)}{\text{EMSE}\left(\widehat{\beta}_r(k,d)\right)} \times 100. \tag{30}$$

For brevity, we have reported some selected results in Tables 1–3, where E_1, E_2, and E_3 give percent relative efficiency of the $r-(k,d)$ class estimator over the PCTP estimator when γ takes values 0.90, 0.95, and 0.99, respectively.

Since all the values of percent relative efficiency shown in Tables 1–3 are positive, it implies that the $r-(k,d)$ class estimator is more efficient than the PCTP estimator in all the cases considered in this study. However, when we examine the behavior of the percent relative efficiency for different parameters considered here, it is observed that the parameters n, p, ρ, and γ affect the percent relative efficiency negatively. That is, when these parameters take larger values, the percent relative efficiency decreases and approaches zero. Alternatively, we can say that there are some values of the parameters for which the value of percent relative efficiency is so low that it can be considered that both the estimators perform equally well, for example, when $\sigma_e^2 = 0.1$, $n = 20, 50, 100$, and $p = 10$ and $\sigma_e^2 = 0.1$, $n = 20, 50, 100$, $p = 5$, and $\rho = 0.9$ for most of the values of k and d.

5. Numerical Example

In this section we examine the performance of the two estimators, namely, the $r-(k,d)$ class estimator and the PCTP estimator in MSE sense using two numerical examples; one is for US GDP data and the other is the famous Hald data [33].

Example 1 (US GDP Data). The quarterly US data on GDP growth (y), personal disposable income (X_1), personal consumption expenditure (X_2), and corporate tax after profits (X_3) for the years 1970–1991 have been taken from Gujarati [34]. The data has also been used by Chandra and Sarkar [24]. The variables are standardized and the eigenvalues of $X'X$ matrix are obtained as 324.6527396, 21.8742084, 1.2365875, and 0.2364645, which shows high multicollinearity in the data. Further, the value of the DW statistic for the data is found to be 0.4784, which indicates the presence of positive autocorrelation at the significance level of 0.05 with the two limits of the critical value being $d_L = 1.429$ and $d_U = 1.611$ for $n = 88$. The error structure follows AR(1) process with estimated ρ to be 0.7530 and $\sigma_e^2 = 0.001118$. Thus the Ω matrix can be constructed using (28). The condition number of $X'\Omega^{-1}X$ is obtained to be 246.3951 which indicates high multicollinearity in the data. Although the GLSE is unstable in the presence of multicollinearity, several studies have suggested that the estimate of variance based on least squares estimator is superior to the estimates based on other shrinkage estimators, for instance, see Ohtani [35], Dube and Chandra [36], and Ünal [37]. Hence, we have estimated the value of σ^2 by using the GLSE of β, which comes out to be 0.00292. The eigenvalues of $X'\Omega^{-1}X$ are $\lambda_1 = 23.78081$, $\lambda_2 = 3.0276$, $\lambda_3 = 0.2420$, and $\lambda_4 = 0.0965$. We chose $r = 2$ which accounts for 99.57% of variation in the data. Now, we chose a value of k to be 0.2505 such that $k > \sigma^2/\alpha^2_{\min} = 0.1505$ for the $r-(k,d)$ class estimator and thus the optimum value $d_{1_{\text{opt}}}$ is obtained to be 0.4286. Further, since estimated σ^2 is smaller than $\alpha_r^2 = (0.258642223,\ 0.0194366)$, k is selected as 0.0056 which belongs to the interval $0 < k < \sigma^2/\alpha^2_{\max} = 0.01131$ and hence $d_{2_{\text{opt}}}$ is found to be 0.8501. The MSEs of the $r-(k,d)$ class estimator and the PCTP estimator for the obtained optimum values are 0.1396499 and 0.1396482, respectively. Clearly, the values are almost the same which suggests that both the estimators perform equally well for the corresponding optimum values. However, the difference can

Table 1: Percent relative efficiency of the $r-(k,d)$ class estimator over the PCTP estimator for $n=20$ and $p=5,10$.

			$p=5$										$p=10$								
	k	d	$\rho=0$			$\rho=0.3$			$\rho=0.9$			$\rho=0$			$\rho=0.3$			$\rho=0.9$		
			E_1	E_2	E_3	E_1	E_2	E_3	E_1	E_2	E_3	E_1	E_2	E_3	E_1	E_2	E_3	E_1	E_2	E_3
$\sigma_e^2=0.1$	0.1	0.1	2.60	2.39	2.24	2.28	2.09	1.96	1.11	1.02	0.96	0.89	0.81	0.75	0.78	0.71	0.66	0.41	0.37	0.35
		0.5	1.57	1.44	1.36	1.38	1.26	1.19	0.67	0.62	0.58	0.54	0.49	0.45	0.47	0.43	0.40	0.25	0.23	0.21
		0.9	0.55	0.50	0.47	0.48	0.44	0.41	0.23	0.21	0.20	0.19	0.17	0.16	0.16	0.15	0.14	0.09	0.08	0.07
	0.5	0.1	2.68	2.46	2.31	2.36	2.16	2.03	1.15	1.06	1.00	0.92	0.84	0.78	0.81	0.74	0.68	0.42	0.39	0.36
		0.5	2.13	1.96	1.84	1.87	1.72	1.61	0.91	0.84	0.79	0.73	0.67	0.62	0.64	0.58	0.54	0.34	0.31	0.29
		0.9	1.58	1.45	1.36	1.39	1.27	1.19	0.67	0.62	0.58	0.54	0.49	0.46	0.47	0.43	0.40	0.25	0.23	0.21
	0.9	0.1	2.76	2.54	2.38	2.43	2.23	2.09	1.19	1.10	1.04	0.96	0.87	0.81	0.84	0.76	0.71	0.44	0.40	0.38
		0.5	2.68	2.47	2.32	2.36	2.16	2.03	1.15	1.06	1.00	0.92	0.84	0.78	0.81	0.74	0.68	0.42	0.39	0.36
		0.9	2.60	2.39	2.25	2.29	2.10	1.96	1.11	1.02	0.96	0.89	0.81	0.75	0.78	0.71	0.66	0.41	0.37	0.35
	2	0.1	2.96	2.73	2.57	2.62	2.41	2.26	1.30	1.20	1.14	1.05	0.95	0.89	0.92	0.84	0.78	0.49	0.45	0.42
		0.5	4.14	3.81	3.58	3.65	3.35	3.14	1.80	1.66	1.56	1.44	1.31	1.22	1.27	1.15	1.07	0.67	0.61	0.57
		0.9	5.34	4.91	4.62	4.70	4.31	4.04	2.30	2.12	2.00	1.84	1.68	1.56	1.61	1.47	1.36	0.85	0.78	0.72
$\sigma_e^2=1$	0.1	0.1	8.02	7.65	7.53	7.21	6.85	6.71	3.51	3.32	3.22	4.18	3.92	3.73	3.68	3.45	3.28	1.75	1.64	1.56
		0.5	4.90	4.67	4.59	4.39	4.17	4.09	2.13	2.02	1.96	2.54	2.38	2.27	2.24	2.10	1.99	1.06	1.00	0.95
		0.9	1.82	1.73	1.69	1.62	1.53	1.50	0.77	0.72	0.70	0.91	0.85	0.81	0.80	0.75	0.71	0.37	0.35	0.33
	0.5	0.1	7.67	7.35	7.25	6.96	6.63	6.52	3.50	3.32	3.23	4.17	3.92	3.73	3.69	3.47	3.30	1.79	1.68	1.60
		0.5	6.45	6.16	6.07	5.81	5.52	5.42	2.86	2.70	2.63	3.40	3.19	3.04	3.00	2.81	2.67	1.43	1.35	1.28
		0.9	5.22	4.96	4.88	4.66	4.41	4.31	2.21	2.09	2.02	2.63	2.46	2.34	2.31	2.16	2.04	1.08	1.01	0.96
	0.9	0.1	7.38	7.09	7.02	6.74	6.45	6.36	3.49	3.32	3.24	4.15	3.91	3.74	3.70	3.48	3.31	1.82	1.71	1.63
		0.5	7.77	7.44	7.34	7.03	6.70	6.58	3.52	3.33	3.24	4.18	3.93	3.75	3.71	3.48	3.31	1.79	1.68	1.60
		0.9	8.18	7.79	7.66	7.33	6.95	6.81	3.55	3.35	3.25	4.22	3.96	3.76	3.71	3.48	3.30	1.76	1.65	1.57
	2	0.1	6.78	6.56	6.52	6.29	6.06	6.00	3.47	3.32	3.25	4.12	3.91	3.74	3.71	3.51	3.36	1.90	1.80	1.71
		0.5	10.55	10.15	10.05	9.66	9.26	9.13	5.08	4.83	4.72	6.04	5.70	5.45	5.40	5.09	4.85	2.69	2.53	2.41
		0.9	14.56	13.96	13.80	13.23	12.64	12.44	6.73	6.39	6.23	8.03	7.56	7.21	7.14	6.71	6.39	3.49	3.28	3.12
$\sigma_e^2=10$	0.1	0.1	7.04	7.00	7.49	6.91	6.85	7.26	4.79	4.69	4.87	6.14	6.00	5.89	5.82	5.67	5.55	3.50	3.38	3.28
		0.5	4.85	4.79	5.11	4.70	4.63	4.90	3.12	3.04	3.16	3.99	3.88	3.80	3.75	3.64	3.55	2.20	2.12	2.05
		0.9	2.77	2.69	2.84	2.59	2.51	2.62	1.49	1.44	1.47	1.89	1.82	1.76	1.73	1.65	1.60	0.92	0.87	0.84
	0.5	0.1	4.71	4.74	5.10	4.75	4.77	5.09	3.70	3.66	3.84	4.76	4.71	4.67	4.62	4.56	4.50	3.06	2.98	2.91
		0.5	5.71	5.65	6.03	5.56	5.50	5.81	3.80	3.72	3.87	4.87	4.76	4.67	4.61	4.50	4.40	2.79	2.70	2.62
		0.9	6.66	6.53	6.92	6.35	6.20	6.52	3.91	3.78	3.89	4.97	4.81	4.67	4.60	4.43	4.29	2.53	2.42	2.34
	0.9	0.1	3.74	3.77	4.06	3.80	3.83	4.10	3.10	3.09	3.26	4.00	3.99	3.96	3.94	3.91	3.88	2.75	2.69	2.65
		0.5	6.07	6.03	6.43	5.94	5.89	6.23	4.18	4.10	4.28	5.36	5.26	5.18	5.12	5.01	4.91	3.21	3.11	3.03
		0.9	8.34	8.22	8.75	8.05	7.92	8.36	5.25	5.12	5.30	6.73	6.54	6.39	6.30	6.11	5.96	3.67	3.53	3.42
	2	0.1	2.69	2.71	2.92	2.74	2.76	2.96	2.32	2.33	2.47	3.00	3.01	3.01	2.99	2.99	2.98	2.25	2.22	2.20
		0.5	6.46	6.43	6.87	6.37	6.33	6.72	4.67	4.62	4.84	6.02	5.94	5.87	5.82	5.73	5.65	3.89	3.80	3.73
		0.9	10.18	10.11	10.82	9.99	9.90	10.51	7.05	6.94	7.25	9.10	8.94	8.80	8.71	8.54	8.39	5.56	5.41	5.28

Table 2: Percent relative efficiency of the $r-(k,d)$ class estimator over the PCTP estimator for $n = 50$ and $p = 5, 10$.

			$p = 5$										$p = 10$								
	k	d	$\rho = 0$			$\rho = 0.3$			$\rho = 0.9$			$\rho = 0$			$\rho = 0.3$			$\rho = 0.9$		
			E_1	E_2	E_3	E_1	E_2	E_3	E_1	E_2	E_3	E_1	E_2	E_3	E_1	E_2	E_3	E_1	E_2	E_3
$\sigma_e^2 = 0.1$	0.1	0.1	2.11	1.86	1.69	1.79	1.60	1.46	0.64	0.59	0.55	0.85	0.73	0.65	0.73	0.63	0.57	0.29	0.26	0.24
		0.5	1.28	1.13	1.02	1.08	0.96	0.89	0.39	0.36	0.33	0.51	0.44	0.39	0.44	0.38	0.34	0.18	0.16	0.15
		0.9	0.44	0.39	0.36	0.38	0.34	0.31	0.13	0.12	0.12	0.18	0.15	0.14	0.15	0.13	0.12	0.06	0.05	0.05
	0.5	0.1	2.17	1.93	1.74	1.85	1.65	1.51	0.67	0.61	0.57	0.88	0.76	0.67	0.76	0.66	0.59	0.31	0.27	0.25
		0.5	1.73	1.53	1.39	1.47	1.31	1.20	0.53	0.48	0.45	0.70	0.60	0.53	0.60	0.52	0.47	0.24	0.22	0.20
		0.9	1.29	1.14	1.03	1.09	0.97	0.89	0.39	0.36	0.33	0.52	0.44	0.39	0.44	0.38	0.34	0.18	0.16	0.15
	0.9	0.1	2.24	1.98	1.80	1.90	1.70	1.56	0.69	0.63	0.59	0.92	0.79	0.70	0.78	0.68	0.61	0.32	0.28	0.26
		0.5	2.18	1.93	1.75	1.85	1.65	1.52	0.67	0.61	0.57	0.88	0.76	0.68	0.76	0.66	0.59	0.31	0.27	0.25
		0.9	2.11	1.87	1.69	1.79	1.60	1.47	0.64	0.59	0.55	0.85	0.73	0.65	0.73	0.63	0.57	0.29	0.26	0.24
	2	0.1	2.41	2.14	1.94	2.05	1.84	1.70	0.76	0.69	0.65	1.00	0.86	0.77	0.86	0.75	0.67	0.35	0.31	0.29
		0.5	3.35	2.98	2.70	2.86	2.56	2.35	1.04	0.95	0.90	1.38	1.19	1.06	1.18	1.03	0.92	0.48	0.43	0.39
		0.9	4.33	3.83	3.47	3.67	3.28	3.02	1.33	1.22	1.14	1.76	1.52	1.35	1.51	1.31	1.17	0.61	0.55	0.50
$\sigma_e^2 = 1$	0.1	0.1	5.35	4.95	4.58	4.62	4.30	4.05	1.73	1.61	1.55	2.94	2.69	2.48	2.53	2.31	2.15	0.94	0.85	0.80
		0.5	3.28	3.03	2.80	2.83	2.63	2.47	1.05	0.98	0.94	1.79	1.64	1.51	1.54	1.41	1.31	0.57	0.52	0.48
		0.9	1.23	1.13	1.04	1.05	0.97	0.91	0.38	0.35	0.34	0.65	0.59	0.54	0.55	0.50	0.47	0.20	0.18	0.17
	0.5	0.1	5.11	4.76	4.44	4.46	4.17	3.95	1.73	1.61	1.55	2.93	2.69	2.49	2.54	2.33	2.17	0.96	0.87	0.82
		0.5	4.31	4.00	3.71	3.73	3.48	3.28	1.41	1.31	1.26	2.40	2.19	2.02	2.07	1.89	1.75	0.77	0.70	0.66
		0.9	3.51	3.23	2.97	3.00	2.78	2.61	1.09	1.01	0.97	1.86	1.70	1.56	1.59	1.45	1.34	0.58	0.53	0.49
	0.9	0.1	4.92	4.61	4.31	4.33	4.07	3.86	1.72	1.62	1.56	2.92	2.69	2.49	2.54	2.34	2.18	0.97	0.89	0.84
		0.5	5.19	4.82	4.48	4.51	4.22	3.98	1.73	1.62	1.56	2.95	2.70	2.50	2.55	2.33	2.17	0.96	0.87	0.82
		0.9	5.46	5.04	4.66	4.70	4.36	4.11	1.75	1.63	1.56	2.97	2.72	2.50	2.56	2.33	2.16	0.94	0.86	0.80
	2	0.1	4.51	4.28	4.04	4.05	3.84	3.68	1.72	1.62	1.57	2.89	2.69	2.51	2.55	2.36	2.22	1.02	0.93	0.88
		0.5	6.99	6.57	6.15	6.18	5.82	5.53	2.50	2.35	2.26	4.23	3.91	3.63	3.69	3.41	3.19	1.44	1.31	1.24
		0.9	9.58	8.95	8.35	8.39	7.86	7.45	3.29	3.08	2.97	5.60	5.16	4.78	4.87	4.48	4.18	1.86	1.70	1.60
$\sigma_e^2 = 10$	0.1	0.1	4.82	4.74	4.46	4.52	4.44	4.32	2.38	2.31	2.34	3.98	3.99	3.85	3.73	3.64	3.51	1.80	1.67	1.61
		0.5	3.39	3.30	3.08	3.13	3.04	2.94	1.57	1.51	1.52	2.61	2.60	2.50	2.43	2.35	2.26	1.14	1.05	1.01
		0.9	2.01	1.90	1.73	1.78	1.68	1.59	0.76	0.72	0.72	1.28	1.24	1.16	1.14	1.08	1.02	0.48	0.44	0.42
	0.5	0.1	3.14	3.16	3.03	3.05	3.05	3.02	1.82	1.80	1.84	3.03	3.10	3.05	2.92	2.91	2.85	1.56	1.47	1.43
		0.5	3.92	3.84	3.60	3.65	3.57	3.46	1.90	1.84	1.86	3.16	3.17	3.06	2.96	2.89	2.79	1.44	1.34	1.29
		0.9	4.69	4.50	4.15	4.24	4.08	3.90	1.97	1.88	1.88	3.29	3.23	3.07	3.00	2.87	2.74	1.32	1.21	1.15
	0.9	0.1	2.47	2.50	2.42	2.42	2.44	2.43	1.52	1.52	1.56	2.52	2.61	2.59	2.47	2.48	2.45	1.40	1.33	1.30
		0.5	4.13	4.06	3.83	3.87	3.80	3.70	2.07	2.02	2.05	3.46	3.49	3.38	3.26	3.20	3.11	1.65	1.54	1.49
		0.9	5.78	5.60	5.22	5.31	5.15	4.97	2.62	2.53	2.54	4.39	4.36	4.18	4.06	3.93	3.78	1.90	1.75	1.68
	2	0.1	1.77	1.79	1.74	1.74	1.76	1.75	1.14	1.14	1.18	1.88	1.96	1.96	1.86	1.89	1.89	1.13	1.09	1.08
		0.5	4.36	4.30	4.08	4.11	4.07	3.98	2.30	2.26	2.31	3.83	3.91	3.83	3.67	3.64	3.57	1.98	1.87	1.82
		0.9	6.93	6.81	6.41	6.49	6.38	6.21	3.48	3.39	3.45	5.82	5.88	5.72	5.51	5.42	5.28	2.83	2.65	2.57

Table 3: Percent relative efficiency of the $r-(k,d)$ class estimator over the PCTP estimator for $n = 100$ and $p = 5, 10$.

			$p = 5$									$p = 10$								
			$\rho = 0$			$\rho = 0.3$			$\rho = 0.9$			$\rho = 0$			$\rho = 0.3$			$\rho = 0.9$		
	k	d	E_1	E_2	E_3	E_1	E_2	E_3	E_1	E_2	E_3	E_1	E_2	E_3	E_1	E_2	E_3	E_1	E_2	E_3
$\sigma_e^2 = 0.1$	0.1	0.1	1.50	1.36	1.26	1.32	1.21	1.13	0.42	0.39	0.37	0.67	0.59	0.53	0.59	0.53	0.48	0.21	0.19	0.17
		0.5	0.91	0.82	0.76	0.80	0.73	0.68	0.26	0.24	0.22	0.40	0.35	0.32	0.36	0.32	0.29	0.13	0.11	0.11
		0.9	0.32	0.29	0.27	0.28	0.25	0.24	0.09	0.08	0.08	0.14	0.12	0.11	0.12	0.11	0.10	0.04	0.04	0.04
	0.5	0.1	1.55	1.40	1.30	1.37	1.25	1.17	0.44	0.41	0.38	0.69	0.61	0.55	0.62	0.55	0.50	0.22	0.20	0.18
		0.5	1.23	1.12	1.04	1.09	0.99	0.93	0.35	0.32	0.30	0.55	0.48	0.44	0.49	0.43	0.39	0.17	0.16	0.14
		0.9	0.91	0.83	0.77	0.81	0.73	0.69	0.26	0.24	0.22	0.40	0.36	0.32	0.36	0.32	0.29	0.13	0.11	0.11
	0.9	0.1	1.57	1.43	1.33	1.39	1.27	1.18	0.45	0.41	0.39	0.70	0.62	0.56	0.63	0.56	0.51	0.22	0.20	0.19
		0.5	1.39	1.26	1.17	1.23	1.12	1.05	0.39	0.36	0.34	0.62	0.55	0.50	0.55	0.49	0.45	0.19	0.18	0.16
		0.9	1.21	1.10	1.02	1.07	0.97	0.91	0.34	0.32	0.30	0.54	0.47	0.43	0.48	0.42	0.39	0.17	0.15	0.14
	2	0.1	1.72	1.57	1.46	1.53	1.40	1.31	0.50	0.46	0.44	0.78	0.69	0.63	0.70	0.62	0.57	0.25	0.23	0.21
		0.5	2.39	2.17	2.02	2.12	1.94	1.81	0.69	0.64	0.60	1.08	0.95	0.86	0.96	0.86	0.78	0.34	0.31	0.29
		0.9	3.07	2.79	2.59	2.72	2.48	2.32	0.87	0.81	0.76	1.38	1.21	1.10	1.23	1.09	0.99	0.43	0.39	0.36
$\sigma_e^2 = 1$	0.1	0.1	3.62	3.38	3.21	3.24	3.04	2.89	1.12	1.05	1.00	2.05	1.87	1.75	1.83	1.67	1.57	0.61	0.56	0.53
		0.5	2.22	2.07	1.96	1.99	1.86	1.77	0.68	0.64	0.61	1.25	1.14	1.06	1.11	1.02	0.95	0.37	0.34	0.32
		0.9	0.83	0.77	0.73	0.74	0.69	0.65	0.25	0.23	0.22	0.45	0.41	0.38	0.40	0.37	0.34	0.13	0.12	0.11
	0.5	0.1	3.47	3.27	3.11	3.13	2.95	2.82	1.11	1.05	1.00	2.05	1.88	1.75	1.83	1.68	1.58	0.62	0.57	0.54
		0.5	2.92	2.74	2.60	2.62	2.46	2.35	0.91	0.85	0.81	1.67	1.53	1.42	1.49	1.37	1.28	0.50	0.46	0.43
		0.9	2.37	2.21	2.08	2.12	1.97	1.87	0.71	0.66	0.63	1.30	1.18	1.10	1.15	1.05	0.98	0.38	0.35	0.33
	0.9	0.1	3.35	3.17	3.03	3.04	2.88	2.76	1.11	1.05	1.00	2.04	1.88	1.76	1.83	1.69	1.59	0.64	0.59	0.55
		0.5	3.52	3.30	3.15	3.17	2.98	2.85	1.12	1.05	1.00	2.06	1.88	1.76	1.84	1.69	1.58	0.63	0.58	0.54
		0.9	3.69	3.44	3.26	3.30	3.09	2.94	1.13	1.06	1.01	2.07	1.89	1.76	1.85	1.69	1.58	0.62	0.57	0.53
	2	0.1	3.10	2.96	2.85	2.84	2.72	2.62	1.10	1.04	1.00	2.03	1.89	1.78	1.84	1.71	1.61	0.66	0.61	0.58
		0.5	4.76	4.51	4.32	4.33	4.11	3.94	1.60	1.51	1.45	2.96	2.73	2.56	2.66	2.46	2.32	0.93	0.86	0.81
		0.9	6.46	6.10	5.82	5.85	5.53	5.29	2.10	1.99	1.90	3.90	3.59	3.36	3.50	3.23	3.03	1.21	1.11	1.05
$\sigma_e^2 = 10$	0.1	0.1	3.31	3.27	3.23	3.15	3.11	3.07	1.51	1.47	1.45	2.86	2.76	2.67	2.67	2.57	2.49	1.14	1.08	1.04
		0.5	2.34	2.28	2.24	2.20	2.15	2.11	1.00	0.97	0.95	1.88	1.80	1.73	1.75	1.67	1.61	0.72	0.69	0.66
		0.9	1.39	1.32	1.26	1.27	1.21	1.16	0.50	0.47	0.46	0.92	0.85	0.81	0.83	0.78	0.74	0.31	0.29	0.27
	0.5	0.1	2.17	2.18	2.19	2.10	2.12	2.12	1.13	1.13	1.12	2.19	2.15	2.12	2.08	2.04	2.01	0.97	0.94	0.91
		0.5	2.70	2.65	2.60	2.55	2.51	2.47	1.20	1.17	1.15	2.27	2.19	2.12	2.12	2.04	1.98	0.91	0.87	0.83
		0.9	3.22	3.10	3.01	2.99	2.89	2.81	1.27	1.22	1.18	2.36	2.23	2.13	2.17	2.05	1.96	0.85	0.79	0.76
	0.9	0.1	1.71	1.73	1.74	1.67	1.69	1.70	0.94	0.94	0.94	1.83	1.81	1.80	1.75	1.73	1.72	0.86	0.84	0.82
		0.5	2.84	2.80	2.76	2.70	2.66	2.63	1.30	1.28	1.26	2.49	2.41	2.35	2.33	2.26	2.20	1.03	0.99	0.96
		0.9	3.96	3.86	3.78	3.72	3.63	3.56	1.67	1.62	1.58	3.15	3.01	2.90	2.92	2.79	2.69	1.20	1.14	1.09
	2	0.1	1.22	1.24	1.25	1.20	1.21	1.22	0.70	0.70	0.70	1.36	1.37	1.37	1.32	1.32	1.32	0.69	0.69	0.68
		0.5	2.99	2.96	2.94	2.86	2.83	2.81	1.44	1.42	1.41	2.76	2.70	2.65	2.61	2.56	2.51	1.23	1.19	1.16
		0.9	4.75	4.68	4.62	4.51	4.45	4.40	2.18	2.14	2.11	4.17	4.05	3.96	3.92	3.81	3.72	1.76	1.70	1.65

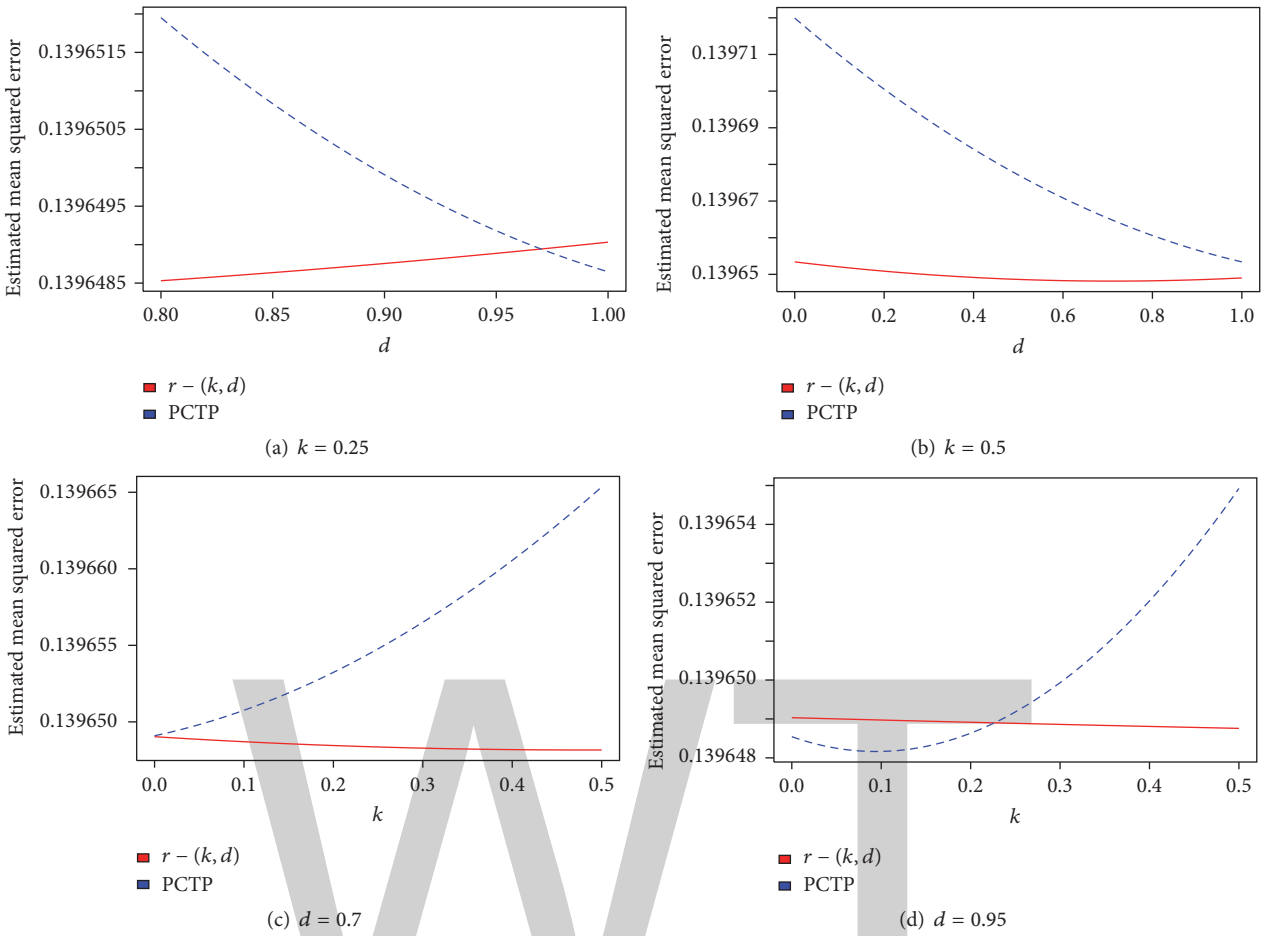

FIGURE 1: Estimated mean squared error of $r-(k,d)$ class and the PCTP estimators for US GDP data.

be noticed after 5 decimal places, indicating superiority of the PCTP estimator over the $r-(k,d)$ class estimator in MSE sense.

Further, the estimated MSEs of the $r-(k,d)$ class and the PCTP estimators with respect to d for fixed $k = 0.25,\ 0.5$ and with respect to k for $d = 0.7,\ 0.95$ are represented in Figure 1. The values of k and d are selected so that we can observe the behavior of estimators for k and d near and far from their respective optimum values. The figures depict superiority of the $r-(k,d)$ estimator over the PCTP estimator for larger range of k and d. Further, it can be seen from Figure 1(a) that the PCTP estimator starts dominating the $r-(k,d)$ class estimator after a point, whereas for $k = 0.5$ in Figure 1(b) we do not see a superiority of the PCTP estimator in the whole range of $0 < d < 1$. Similarly, we get a range of k in which the PCTP estimator dominates the $r-(k,d)$ class estimator for $d = 0.95$ and not for $d = 0.7$; see Figures 1(c) and 1(d).

Example 2 (Hald Data). Now, let us consider the data set on Portland cement originally due to Woods et al. [38] and then analyzed by Hald [33] and known as Hald data. The data is an outcome of an experiment conducted to investigate the heat evolved during setting and hardening of Portland cements of varied composition and the dependence of this heat on the percentages of four compounds in the clinkers from which the cement was produced. The data includes the heat evolved in calories per gram of cement (y) as dependent variable and four ingredients: tricalcium aluminate (X_1), tetracalcium silicate (X_2), tetracalcium aluminoferrite (X_3), and dicalcium silicate (X_4) as explanatory variables.

Following Özkale [11], the variables are standardized so that the $X'X$ matrix forms a correlation matrix and the eigenvalues obtained are $\lambda_1 = 2.235704$, $\lambda_2 = 1.576066$, $\lambda_3 = 0.186606$, and $\lambda_4 = 0.001623$. The value of Durbin-Watson test comes out to be 2.052597 resulting in the conclusion of no autocorrelation in error term at 5% level of significance with $d_L = 0.574$ and $d_U = 2.094$ for $n = 13$; hence we can consider $\Omega = I_n$. The estimated value of σ^2 is 0.00196 and the value of r has been chosen to be 2, which accounts for 95.29% of variation in data. The optimum value of d for a selected value of k is chosen for the $r-(k,d)$ class and PCTP estimators. For the $r-(k,d)$ class estimator, we chose value of k as 1.322 such that $k > \sigma^2/\alpha^2_{\min} = 1.222$, and for this value of k the optimum value $d_{1_{\text{opt}}}$ is obtained as 0.9899. Further, we obtain $\alpha_r^2 = (0.4348143,\ 0.0016061)$ which indicates that σ^2 is larger than the second value of α_r^2,

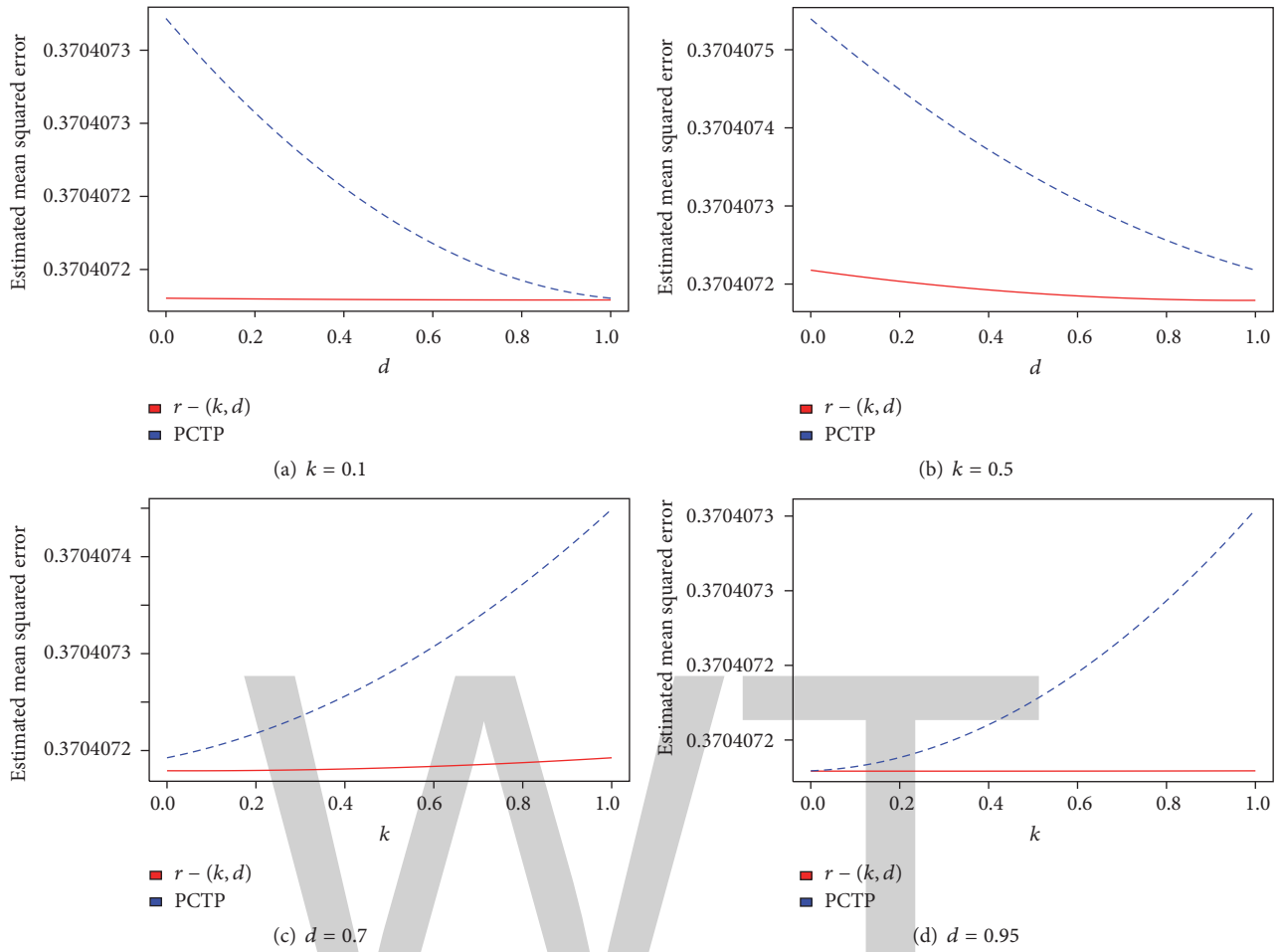

Figure 2: Estimated mean squared error of $r-(k,d)$ class and the PCTP estimators for Hald data.

hence we chose a value of k in the range $\max_{i=1,2,\ldots,r}\{\lambda_i(\sigma^2-\alpha_i^2)/(\lambda_i+1)\alpha_i^2\} < k < \sigma^2/\alpha^2_{\max}$. The value of lower bound is obtained as 0.000000574, which is approximately 0 and the upper bound is 0.004516; hence we chose a value k as 0.0022 and for this value $d_{2_{\text{opt}}}$ for the PCTP estimator is obtained as 0.9854. The MSEs of the $r-(k,d)$ class and PCTP estimators are obtained to be the same up to 7 decimal places, that is, 0.3704072, indicating the same performance at the optimum values.

Moreover, the performance of both estimators for various k and d is represented in Figures 2(a)–2(d). Clearly, the $r-(k,d)$ class estimator is exhibiting better performance for larger range of k and d. However, a careful examination of Figures 2(a) and 2(d) suggests that there may be some points of k and d where the PCTP may perform better. Figures 2(b) and 2(c) show that there is no value of d and k, respectively, for $k = 0.5$ and $d = 0.7$.

Looking at the results of both examples we observe that the $r-(k,d)$ class estimator performs better than the PCTP estimator in scalar MSE sense for most of the values of k and d under study. However, Figures 1(a), 1(d), 2(a), and 2(d) are showing a possibility of superiority of the PCTP estimator over the $r-(k,d)$ class estimator.

6. Conclusion

In this paper we have examined the performance of two biased estimators in the presence of multicollinearity with autocorrelated errors which include the same number of unknown parameters with same range. Further, a method of selection of k and d in both estimators has been suggested in terms of minimizing scalar MSE. The conditions of dominance of the PCTP estimator over the $r-(k,d)$ class estimator have been derived using MSE matrix as comparison criterion. Further, we have performed a simulation study and the percentage relative efficiency of the $r-(k,d)$ class estimator over the PCTP estimator has been evaluated. Moreover, two numerical examples are considered to compare the two estimators. The simulation study suggests that for all the parametric conditions considered here the $r-(k,d)$ class estimator performs better than the PCTP estimator in scalar MSE sense. The numerical examples give the results in favor of the simulation results; that is, the $r-(k,d)$ class estimator performed better than the PCTP estimator under scalar MSE criterion for most of the values of k and d. However, for optimum values of k and d the performance of both estimators is similar and the superiority of the PCTP estimator may be seen after the fourth or fifth decimal places.

Competing Interests

There are no conflicts of interest regarding the publication of this paper.

References

[1] C. Stein, "Inadmissibility of usual estimator for the mean of a multivariate normal distribution," in *Proceedings of the 3rd Berkeley Symposium on Mathematical Statistics and Probability*, pp. 197–206, University of California Press, 1956.

[2] A. E. Hoerl and R. W. Kennard, "Ridge regression: applications to nonorthogonal problems," *Technometrics*, vol. 12, no. 1, pp. 69–82, 1970.

[3] A. E. Hoerl and R. W. Kennard, "Ridge regression: biased estimation for nonorthogonal problems," *Technometrics*, vol. 12, no. 1, pp. 55–67, 1970.

[4] W. F. Massy, "Principal components regression in exploratory statistical research," *Journal of the American Statistical Association*, vol. 60, no. 309, pp. 234–256, 1965.

[5] M. R. Baye and D. F. Parker, "Combining ridge and principal component regression: a money demand illustration," *Communications in Statistics - Theory and Methods*, vol. 13, no. 2, pp. 197–205, 1984.

[6] M. Nomura and T. Ohkubo, "A note on combining ridge and principal component regression," *Communications in Statistics. Theory and Methods*, vol. 14, no. 10, pp. 2473–2487, 1985.

[7] K. J. Liu, "A new class of biased estimate in linear regression," *Communications in Statistics. Theory and Methods*, vol. 22, no. 2, pp. 393–402, 1993.

[8] S. Kaçiranlar and S. Sakallıoğlu, "Combining the liu estimator and the principal component regression estimator," *Communications in Statistics—Theory and Methods*, vol. 30, no. 12, pp. 2699–2705, 2001.

[9] M. R. Özkale and S. Kaçıranlar, "The restricted and unrestricted two-parameter estimators," *Communications in Statistics—Theory and Methods*, vol. 36, no. 15, pp. 2707–2725, 2007.

[10] H. Yang and X. Chang, "A new two-parameter estimator in linear regression," *Communications in Statistics—Theory and Methods*, vol. 39, no. 6, pp. 923–934, 2010.

[11] M. R. Özkale, "Combining the unrestricted estimators into a single estimator and a simulation study on the unrestricted estimators," *Journal of Statistical Computation and Simulation*, vol. 82, no. 5, pp. 653–688, 2012.

[12] X. Chang and H. Yang, "Combining two-parameter and principal component regression estimators," *Statistical Papers*, vol. 53, no. 3, pp. 549–562, 2012.

[13] A. C. Aitken, "IV.—on least squares and linear combination of observations," *Proceedings of the Royal Society of Edinburgh*, vol. 55, pp. 42–48, 1936.

[14] G. Trenkler, "On the performance of biased estimators in the linear regression model with correlated or heteroscedastic errors," *Journal of Econometrics*, vol. 25, no. 1-2, pp. 179–190, 1984.

[15] L. L. Firinguetti, "A simulation study of ridge regression estimators with autocorrelated errors," *Communications in Statistics. Simulation and Computation*, vol. 18, no. 2, pp. 673–702, 1989.

[16] G. M. Bayhan and M. Bayhan, "Forecasting using autocorrelated errors and multicollinear predictor variables," *Computers and Industrial Engineering*, vol. 34, no. 2-4, pp. 413–421, 1998.

[17] M. I. Alheety and B. M. G. Kibria, "On the liu and almost unbiased liu estimators in the presence of multicollinearity with heteroscedastic or correlated errors," *Surveys in Mathematics and its Applications*, vol. 4, pp. 155–167, 2009.

[18] M. R. Özkale, "Principal components regression estimator and a test for the restrictions," *Statistics. A Journal of Theoretical and Applied Statistics*, vol. 43, no. 6, pp. 541–551, 2009.

[19] H. Güler and S. Kaçiranlar, "A comparison of mixed and ridge estimators of linear models," *Communications in Statistics: Simulation and Computation*, vol. 38, no. 2, pp. 368–401, 2009.

[20] M. A. Alkhamisi, "Ridge estimation in linear models with autocorrelated errors," *Communications in Statistics. Theory and Methods*, vol. 39, no. 14, pp. 2630–2644, 2010.

[21] H. Yang and J. Wu, "Estimation in singular linear models with stochastic linear restrictions and linear equality restrictions," *Communications in Statistics—Theory and Methods*, vol. 40, no. 24, pp. 4364–4371, 2011.

[22] H. Y. A. Eledum and A. A. Alkhalifa, "Generalized two stages ridge regression estimator GTR for multicollinearity and autocorrelated errors," *Canadian Journal on Science and Engineering Mathematics*, vol. 3, pp. 79–85, 2012.

[23] G. Şiray, S. Kaçiranlar, and S. Sakallıoğlu, "r–k class estimator in the linear regression model with correlated errors," *Statistical Papers*, vol. 55, no. 2, pp. 393–407, 2014.

[24] S. Chandra and N. Sarkar, "A restricted r-k class estimator in the mixed regression model with autocorrelated disturbances," *Statistical Papers*, vol. 57, no. 2, pp. 429–449, 2016.

[25] S. Chandra and G. Tyagi, "A general class of biased estimators in the presence of multicollinearity with autocorrelated errors," *International Journal of Mathematics and Statistics*, vol. 18, no. 2, 2017.

[26] J. Huang and H. Yang, "On a principal component two-parameter estimator in linear model with autocorrelated errors," *Statistical Papers*, vol. 56, no. 1, pp. 217–230, 2015.

[27] A. Hoerl, R. Kennard, and K. Baldwin, "Ridge regression: some simulations," *Communication in Statistics*, vol. 4, pp. 105–123, 1975.

[28] B. M. Kibria, "Performance of some new ridge regression estimators," *Communications in Statistics. Simulation and Computation*, vol. 32, no. 2, pp. 419–435, 2003.

[29] G. C. McDonald and D. I. Galarneau, "A monte carlo evaluation of some ridge-type estimators," *Journal of the American Statistical Association*, vol. 70, no. 350, pp. 407–416, 1975.

[30] D. G. Gibbons, "A simulation study of some ridge estimators," *Journal of the American Statistical Association*, vol. 76, no. 373, pp. 131–139, 1981.

[31] G. Judge, W. Griffiths, R. Hill, H. Lütkepohl, and T. Lee, *The Theory and Practice of Econometrics*, John Wiley & Sons, New York, NY, USA, 1985.

[32] R. A. Johnson and D. W. Wichern, *Applied Multivariate Statistical Analysis*, Pearson-Prentice Hall, New York, NY, USA, 2007.

[33] A. Hald, *Statistical Theory with Engineering Applications*, John Wiley & Sons, New York, NY, USA, 1952.

[34] D. N. Gujarati, *Basic Econometrics*, Mc-Graw Hill, New York, NY, USA, 2002.

[35] K. Ohtani, "Inadmissibility of the iterative Stein-rule estimator of the disturbance variance in a linear regression," *Economics Letters*, vol. 24, no. 1, pp. 51–55, 1987.

[36] M. Dube and S. Chandra, "A note on inadmissibility of the iterative stein-rule estimator of the disturbance variance," *Journal of*

the Indian Society of Agricultural Statistics, vol. 61, pp. 341–343, 2007.

[37] D. Ünal, "The effects of the proxy information on the iterative Stein-rule estimator of the disturbance variance," *Statistical Papers*, vol. 51, no. 2, pp. 477–484, 2010.

[38] H. woods, H. H. Steinour, and H. R. Starke, "Effect of composition of portland cement on heat evolved during hardening," *Industrial & Engineering Chemistry*, vol. 24, no. 11, pp. 1207–1214, 1932.

A Fractional-Order Model for HIV Dynamics in a Two-Sex Population

Fatmawati, Endrik Mifta Shaiful, and Mohammad Imam Utoyo

Department of Mathematics, Faculty of Science and Technology, Universitas Airlangga, Surabaya 60115, Indonesia

Correspondence should be addressed to Fatmawati; fatma47unair@gmail.com

Academic Editor: Shyam L. Kalla

Human Immunodeficiency Virus (HIV) is a virus that attacks or infects cells in the immune system that causes immune decline. Acquired Immunodeficiency Syndrome (AIDS) is the most severe stage of HIV infection. AIDS is the rapidly spreading and becoming epidemic diseases in the world of almost complete influence across the country. A mathematical model approach of HIV/AIDS dynamic is needed to predict the spread of the diseases in the future. In this paper, we presented a fractional-order model of the spread of HIV and AIDS diseases which incorporates two-sex population. The fractional derivative order of the model is in the interval $(0, 1]$. We compute the basic reproduction number and prove the stability of the equilibriums of the model. The sensitivity analysis also is done to determine the important factor controlling the spread. Using the Adams-type predictor-corrector method, we then perform some numerical simulations for variation values of the order of the fractional derivative. Finally, the effects of various antiretroviral therapy (ART) treatments are studied and compared with numerical approach.

1. Introduction

Human Immunodeficiency Virus (HIV) is a virus that attacks or infects cells in the immune system that causes immune decline. Acquired Immunodeficiency Syndrome (AIDS) is the most severe stage of HIV infection, which can take from 2 to 15 years to develop depending on the individual. AIDS is defined by the development of certain cancers, infections, or other severe clinical manifestations. HIV can be transmitted via the exchange of a variety of body fluids from infected individuals, such as blood, breast milk, semen, and vaginal secretions. There were approximately 36.7 million people living with HIV at the end of 2016 with 1.0 million people died from HIV-related causes globally. In 2015, an estimated 44% of new infections occurred among key populations and their partners [1].

Until now, there is no cure for HIV infection. However, effective antiretroviral therapy (ART) can inhibit HIV progression in immune defects. Since 1996, ART has begun to be used by people living with HIV in the world because it can prevent death early [2]. The benefits of ART for people with HIV/AIDS are to improve quality of life, prevent mother-to-child transmission of HIV, prolong survival, and restore the immune system [3]. In 2016, 19.5 million people with HIV have been receiving ART globally [1].

Mathematical models are needed to understand the dynamics of epidemic infection [4–8]. At present many models have been proposed to describe the dynamics of HIV/AIDS infection [9–11]. For instance, authors in [9] formulated a mathematical model for the transmission dynamics of HIV/AIDS in a two-sex population considering counseling and antiretroviral therapy. Authors in [10] studied the impact of the optimal control on the treatment of HIV/AIDS incorporating use of condom, screening of unaware infective, and treatment of HIV individuals. In recent year, Yang et al. [11] formulated a two-group (female sex workers and senior male clients) compartmental model to study the impact of senior male clients on the transmission dynamics, the containment, and the elimination of the HIV.

Memory effect plays an important role in the spread of disease. The presence of memory effects on past events

will affect the spread of disease in the future so that the spread of disease in the future can be controlled. The distance of memory effect indicates the history of disease spread. Thus, memory effects on the spread of infectious diseases can be investigated using fractional derivatives. Fractional derivatives have been used in the literature to observe the effect of memory on a system dynamics by replacing the ordinary derivative order with the fractional derivative order [12–15]. Sardar et al. [13] formulated the dengue model with memory in the transmission process by using fractional differential operator and order of the fractional derivative as an index of memory. Huo et al. [12] analyzed the effects of vaccines on mathematical models of fractional order of HIV disease spread. They also performed a local stability analysis on the fractional-order framework of HIV disease spread and bifurcation behavior of the system. In 2017, Saeedian et al. [14] studied the evolution of the SIR epidemic model, considering memory effects. Using the fractional calculus technique, the authors in [14] show that the dynamics of such a system depend on the strength of memory effects, controlled by the order of fractional derivatives. In 2017, Pinto and Carvalho [15] derived a fractional-order model for the dynamics of the coinfection of HIV and TB in the presence of TB resistant strains.

In this paper, we proposed a fractional order of two-sex mathematical model for dynamic HIV transmission, as a generalization of an integer model, proposed by Kimbir et al. [9]. We also modified the basic model in [9] by distinguishing populations infected with HIV and infected with AIDS. By using fractional ordinary differential equation, we hope that the fractional-order model can accommodate the real phenomenon of the spread of HIV/AIDS. The structure of the paper is organized as follows. In Section 2, we introduce the description of the fractional order of the HIV/AIDS model. In Section 3, the stability analysis of the equilibriums of the model is proven. In Section 4, we carry out the sensitivity analysis of the reproduction number to the parameters in the model. Section 5 shows some numerical results for distinct values of the fractional order α. Finally, in Section 6, we give a brief conclusion.

2. Description of the Model

In this section we propose a mathematical model of two-sex HIV/AIDS transmission based on [9]. The model is constructed under the following assumptions:

(1) The total population is divided into two groups, namely, the population of males and females.

(2) The population of males is divided into three compartments: the susceptible males (S_m), the HIV infected males (I_m), and the AIDS infected males (A_m). The population of females is also divided into three compartments: the susceptible females (S_f), the HIV infected females (I_f), and the AIDS infected females (A_f). Moreover, the total population of males and females is given by $N = S_m + I_m + A_m + S_f + I_f + A_f$.

(3) The HIV transmission is by heterosexual contact only.

(4) Vertical transmission and age-structure are ignored.

(5) The population is homogeneous mixing.

(6) Male and female AIDS populations were isolated and then do not contribute to HIV infection.

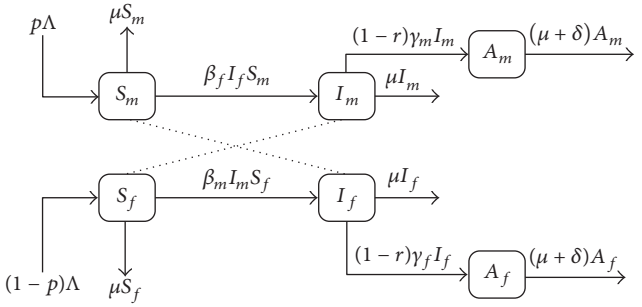

Figure 1: HIV/AIDS transmission diagram.

The transmission diagram of the model is shown in Figure 1.

The basic model is derived as follows:

$$\begin{aligned}
\frac{dS_m}{dt} &= p\Lambda - \beta_f I_f S_m - \mu S_m,\\
\frac{dI_m}{dt} &= \beta_f I_f S_m - (1-r)\,\gamma_m I_m - \mu I_m,\\
\frac{dA_m}{dt} &= (1-r)\,\gamma_m I_m - (\mu+\delta)\,A_m,\\
\frac{dS_f}{dt} &= (1-p)\,\Lambda - \beta_m I_m S_f - \mu S_f,\\
\frac{dI_f}{dt} &= \beta_m I_m S_f - (1-r)\,\gamma_f I_f - \mu I_f,\\
\frac{dA_f}{dt} &= (1-r)\,\gamma_f I_f - (\mu+\delta)\,A_f,
\end{aligned} \tag{1}$$

The description of the parameter for model (1) could be seen in Table 1. The biologically feasible region of model (1) is

$$\Omega = \left\{\left(S_m, I_m, A_m, S_f, I_f, A_f\right) \in \mathbb{R}_+^6 : 0 \le N \le \frac{\Lambda}{\mu}\right\}, \tag{2}$$

and all of the parameters used in model (1) are nonnegative.

The region Ω is positively invariant. In this region, model (1) is well-posed. So, if it is given an initial condition in the region, then the solution is defined for all time $t \ge 0$ and remains in the region.

Next, we consider a fractional-order model of system (1). The fractional model corresponding to system (1) is as follows:

$$\begin{aligned}
\frac{d^{\alpha}S_m}{dt^{\alpha}} &= p\Lambda - \beta_f I_f S_m - \mu S_m,\\
\frac{d^{\alpha}I_m}{dt^{\alpha}} &= \beta_f I_f S_m - (1-r)\,\gamma_m I_m - \mu I_m,\\
\frac{d^{\alpha}A_m}{dt^{\alpha}} &= (1-r)\,\gamma_m I_m - (\mu+\delta)\,A_m,\\
\frac{d^{\alpha}S_f}{dt^{\alpha}} &= (1-p)\,\Lambda - \beta_m I_m S_f - \mu S_f,\\
\frac{d^{\alpha}I_f}{dt^{\alpha}} &= \beta_m I_m S_f - (1-r)\,\gamma_f I_f - \mu I_f,\\
\frac{d^{\alpha}A_f}{dt^{\alpha}} &= (1-r)\,\gamma_f I_f - (\mu+\delta)\,A_f,
\end{aligned} \tag{3}$$

where $\alpha \in (0,1]$ is the order of the fractional derivative. Fractional derivative of model (3) is in the sense of Caputo. The Caputo approach is mostly used in real applications. The main advantages of Caputo approach are the initial values for fractional differential equations with the Caputo derivatives taking on the same form as for integer order differential equations [16]. The Caputo fractional derivative is defined as follows.

Definition 1 (see [16]). The Caputo fractional differential operator of order $\alpha > 0$, with $n-1 < \alpha < n$, $n \in \mathbb{N}$, is defined by

$$\begin{aligned}
\frac{d^{\alpha}f(t)}{dt^{\alpha}} &:= I^{n-\alpha}\frac{d^{n}f(t)}{dt^{n}}\\
&= \frac{1}{\Gamma(n-\alpha)}\int_0^t (t-s)^{(n-\alpha-1)}\, f^{(n)}(s)\,ds,
\end{aligned} \tag{4}$$

where $\Gamma(\cdot)$ is the gamma function.

3. Model Analysis

In this section, we study the stability of the equilibrium of the fractional-order model (3). We begin by computing the basic reproduction number (R_0) of model (3). The basic reproduction number is defined as the number of secondary cases of primary case during the infectious period due to the type of infection [17, 18].

Now, we recall the properties of the stability of the fractional-order systems. The stability theorem on fractional-order system is as follows.

Table 1: Parameters of model (1).

Description	Parameter
Recruitment rate	Λ
Proportion of the recruitment rate	p
Natural death rate	μ
Transmission rate by an infected male	β_m
Transmission rate by an infected female	β_f
Progression rate from male HIV infection to AIDS	γ_m
Progression rate from female HIV infection to AIDS	γ_f
AIDS disease induced death rate	δ
Proportion of the efficacy of ART treatment for HIV infection	r

Theorem 2 (see [19, 20]). *Consider the following autonomous nonlinear fractional-order system:*

$$\begin{aligned}
\frac{d^{\alpha}x}{dt^{\alpha}} &= f(x),\\
x(0) &= x_0,
\end{aligned} \tag{5}$$

with $0 < \alpha < 1$ and $x \in \mathbb{R}^n$. The equilibrium points of the above system are solutions to the equation $f(x) = 0$. An equilibrium is locally asymptotically stable if all eigenvalues (λ_j) of the Jacobian matrix $J = \partial f/\partial x$ evaluated at the equilibrium satisfy $|\arg(\lambda_j)| > \alpha\pi/2$.

Based on Theorem 2, the equilibria are obtained by setting the right-hand sides of the equations in model (3) to zero. The disease-free equilibrium of model (3) to the coordinate $(S_m, I_m, A_m, S_f, I_f, A_f)$ is given by $E_0 = (\Lambda p/\mu, 0, 0, \Lambda(1-p)/\mu, 0, 0)$.

Then, the basic reproduction number (R_0) is computed by using the next-generation method [21, 22]. For the next-generation matrix method [22], we take the infected compartments (I_m, I_f). The Jacobian matrices F and V for the new infection in the compartment and the transfer of individuals between the compartment respectively, evaluated at E_0, are given by

$$\begin{aligned}
F &= \begin{pmatrix} 0 & \dfrac{\beta_f \Lambda p}{\mu} \\ \dfrac{\beta_m \Lambda (1-p)}{\mu} & 0 \end{pmatrix},\\
V &= \begin{pmatrix} \dfrac{1}{(1-r)\,\gamma_m + \mu} & 0 \\ 0 & \dfrac{1}{(1-r)\,\gamma_f + \mu} \end{pmatrix}.
\end{aligned} \tag{6}$$

The basic reproduction number of model (3) is the spectral radius of the matrix FV^{-1} such that we have

$$R_0 = \frac{\Lambda}{\mu}\sqrt{\frac{\beta_m \beta_f p\,(1-p)}{\left((1-r)\,\gamma_m + \mu\right)\left((1-r)\,\gamma_f + \mu\right)}}. \tag{7}$$

The following theorem provides the local stability of the disease-free equilibrium.

Theorem 3. *The disease-free equilibrium E_0 is locally asymptotically stable if $R_0 < 1$.*

Proof. The Jacobian matrix of model (3) around the disease-free equilibrium, E_0, is given by

$$J = \begin{pmatrix} -\mu & 0 & 0 & 0 & \dfrac{-\beta_f p\Lambda}{\mu} & 0 \\ 0 & -(1-r)\,\gamma_m - \mu & 0 & 0 & \dfrac{\beta_f p\Lambda}{\mu} & 0 \\ 0 & (1-r)\,\gamma_m & -\mu-\delta & 0 & 0 & 0 \\ 0 & \dfrac{\beta_m \Lambda\,(p-1)}{\mu} & 0 & -\mu & 0 & 0 \\ 0 & -\dfrac{\beta_m \Lambda\,(p-1)}{\mu} & 0 & 0 & -(1-r)\,\gamma_f - \mu & 0 \\ 0 & 0 & 0 & 0 & (1-r)\,\gamma_f & -\mu-\delta \end{pmatrix}. \tag{8}$$

The eigenvalues of matrix J are $\lambda_1 = \lambda_2 = -\mu$ and $\lambda_3 = \lambda_4 = -(\mu+\delta)$ and the roots of quadratic equation $x^2 + a_1 x + a_2 = 0$, where $a_1 = 2(1-r)\mu(\gamma_m + \gamma_f)$ and $a_2 = [(1-r)^2\gamma_m\gamma_f + \mu(1-r)(\gamma_m+\gamma_f) + \mu^2](1-T_0)$, with $R_0 = \sqrt{T_0}$. Thus, we have $|\arg(\lambda_1)| = |\arg(\lambda_2)| = |\arg(\lambda_3)| = |\arg(\lambda_4)| = \pi > \alpha\pi/2$. Next, we check the roots of the quadratic equation $x^2 + a_1 x + a_2 = 0$. Authors in [23] show that the Routh-Hurwitz criteria, $a_1, a_2 > 0$, are necessary and sufficient for $|\arg(\lambda_i)| > \alpha\pi/2$. It is clear that all of the eigenvalues are negative ($|\arg(\lambda_j)| > \alpha\pi/2$, for $j = 1, 2, \ldots, 6$) if $T_0 < 1$ or equivalently $R_0 < 1$. Hence, the disease-free equilibrium E_0 is locally asymptotically stable for $\alpha \in (0, 1]$ if $R_0 < 1$. □

We continue with the computing of the endemic equilibrium (E_1) of model (3). The endemic equilibrium E_1 is given by

$$E_1 = \left(S_m^*, I_m^*, A_m^*, S_f^*, I_f^*, A_f^*\right), \tag{9}$$

where

$$S_m^* = \frac{p\Lambda}{\beta_f I_f^* + \mu},$$

$$I_m^* = \frac{\left[(1-r)\,\gamma_m + \mu\right]\left[(1-r)\,\gamma_f + \mu\right]\mu^2\,[T_0 - 1]}{\beta_m\left[(1-r)\,\gamma_m + \mu\right]\left[\beta_f \Lambda\,(1-p) + \left((1-r)\,\gamma_f + \mu\right)\mu\right]},$$

$$A_m^* = \frac{(1-r)\,\gamma_m I_m^*}{\mu+\delta},$$

$$S_f^* = \frac{(1-p)\,\Lambda}{\beta_m I_m^* + \mu},$$

$$I_f^* = \frac{\beta_m I_m^*\,(1-p)\,\Lambda}{\left[(1-r)\,\gamma_f + \mu\right]\left[\beta_m I_m^* + \mu\right]},$$

$$A_f^* = \frac{(1-r)\,\gamma_f I_f^*}{\mu+\delta}, \tag{10}$$

with $R_0 = \sqrt{T_0}$. The endemic equilibrium E_1 exists if $T_0 > 1$ or equivalently $R_0 > 1$.

The stability of the endemic equilibrium E_1 is difficult to prove analytically, because it involves a quartic equation which depend on the variables I_m and I_f. Numerical simulations show that the endemic equilibrium is locally asymptotically stable if $R_0 > 1$. This can be seen in Figures 2 and 3. Using three different initial conditions for the simulation, these orbits converge to the same point as time evolves.

4. Sensitivity Analysis

In this section we present the sensitivity analysis of the reproduction number R_0 to the parameters in model (3). The aim of this analysis was to measure the parameters that have the most effects on the reproduction number. We derived

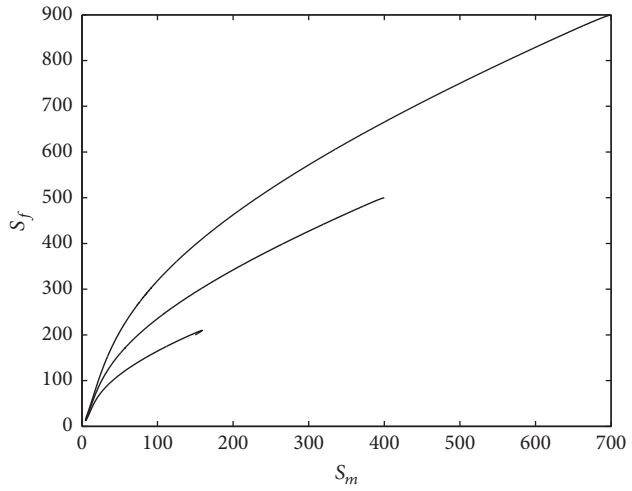

Figure 2: Phase portrait of model (3) in S_m-S_f plane for $\alpha = 0.8$.

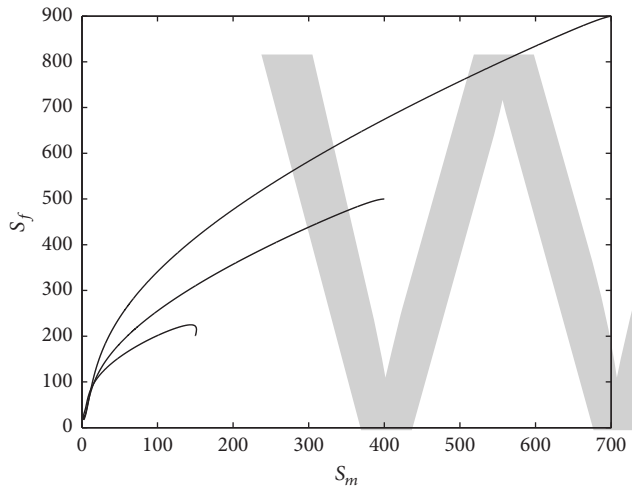

Figure 3: Phase portrait of model (3) in S_m-S_f plane for $\alpha = 0.9$.

analytically the sensitivity index of R_0 to each parameter following the approach in [24].

Definition 4 (see [24]). The normalized forward sensitivity index of a variable, R_0, that depends differentially on a parameter, l, is defined as

$$\Upsilon_l^{R_0} := \frac{\partial R_0}{\partial l} \times \frac{l}{R_0}. \tag{11}$$

Based on Definition 4, the sensitivity indices of R_0 with respect to each parameter such as $\Lambda, \mu, \beta_m, \beta_f, \gamma_m, \gamma_f$, and p can be computed in the same way as (11). For example, the sensitivity index of R_0 with respect to Λ is

$$\Upsilon_\Lambda^{R_0} := \frac{\partial R_0}{\partial \Lambda} \times \frac{\Lambda}{R_0} = 1. \tag{12}$$

Table 2: Parameter values for simulations.

Parameter	Value	Ref.
p	0.5	Assumed
Λ	20	[12]
β_m	2×10^{-3}	Assumed
β_f	5×10^{-3}	Assumed
μ	0.02	[12]
δ	0.125	[12]
γ_m	8×10^{-3}	Assumed
γ_f	9×10^{-3}	Assumed
r	0.5	Assumed

Table 3: Sensitivity indices to parameter for model (3).

Parameter	Sensitivity index
Λ	1
β_m	0.5
β_f	0.5
r	0.175
μ	−1.825
γ_f	−0.092
γ_m	−0.083
p	0

Thus, we compute the sensitivity indexes of the remaining parameters using the parameter values in the Table 2. The results are given in Table 3.

The sensitivity index can be analyzed as follows. The positive sensitivity index shows that an increase in the parameters will lead to increase in the basic reproduction number, while a negative sensitivity index means that an increase in the parameter will lead to a decrease in the basic reproduction number. For example, for $\Upsilon_{\beta_m}^{R_0} = 0.5$, increasing the value β_m by 10% increases the reproduction number R_0 by 5%. Thus, increasing natural death rate μ by 10% decreases R_0 by 18.25%.

We also perform sensitivity simulation to verify our sensitivity analysis. The parameter values used in the simulations are given in Table 2. In Figures 4 and 5, we can see that, for the parameter chosen with distinct values of β_f and β_m, respectively, R_0 increases monotonically with both β_m and β_f. This results indicate that increasing β_m and β_f will increase the basic reproduction number R_0.

5. Numerical Simulation

In this section, we conduct several numerical simulations of model (3). An Adams-type predictor-corrector method [25–27] is applied to solve the numerical solution of the fractional-order model (3). Parameters values used in these

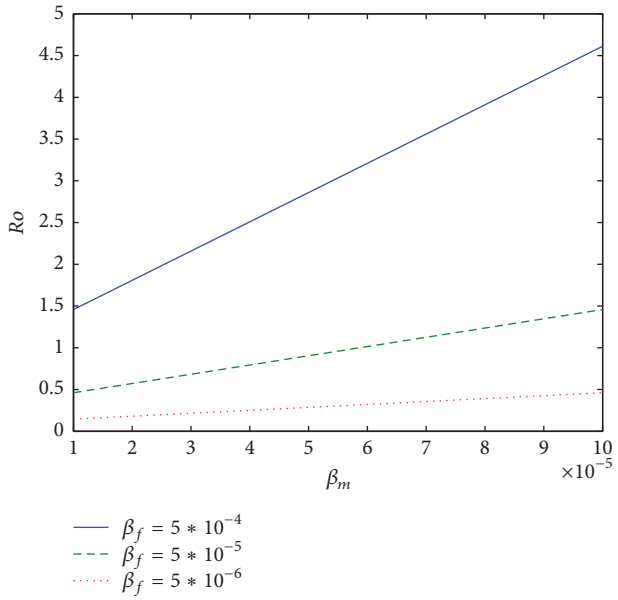

FIGURE 4: Sensitivity of R_0 with respect to β_m for different values of β_f.

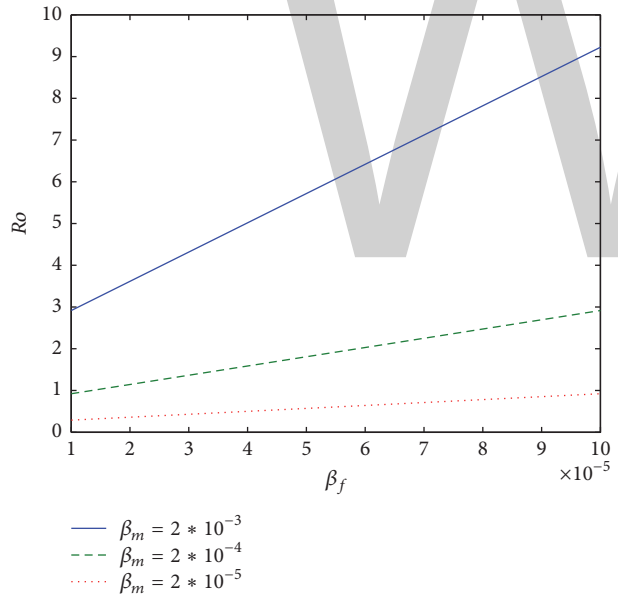

FIGURE 5: Sensitivity of R_0 with respect to β_f for different values of β_m.

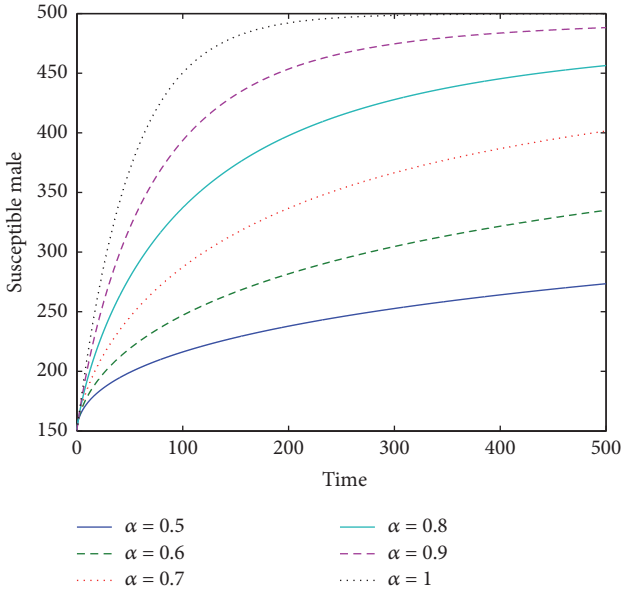

FIGURE 6: Dynamic of nonendemic S_m.

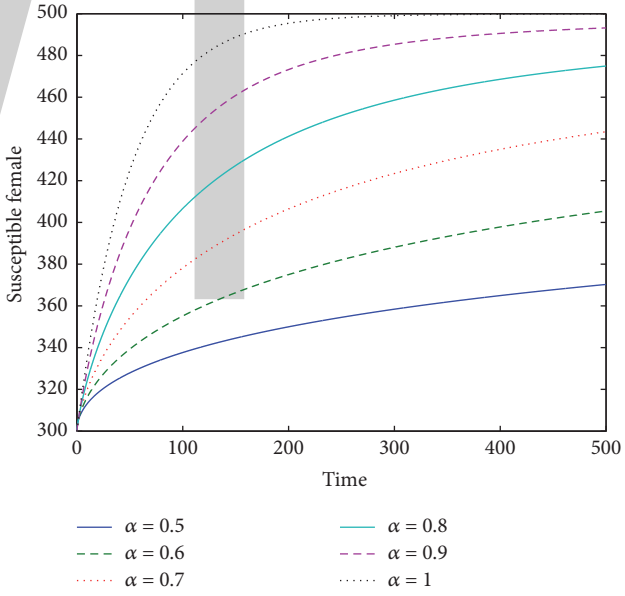

FIGURE 7: Dynamic of nonendemic S_f.

simulations could be seen in Table 2. The adopted initial conditions are $(S_m(0), I_m(0), A_m(0), S_f(0), I_f(0), A_f(0)) = (150, 10, 6, 300, 7, 2)$. Here, we take 500 days for the time horizon. The simulations are carried out with varying values of the order of the fractional derivative $\alpha \in [0.5, 1.0]$.

In Figures 6–11, we display the dynamic of the populations when $R_0 < 1$ and in Figures 12–17 when $R_0 > 1$. In each figure six different values of α are employed.

Now, we set $\beta_m = 2 \times 10^{-5}$ and $\beta_f = 5 \times 10^{-5}$ and the remaining of parameters as in Table 2 to simulate Figures 6–11. In this case, the value of R_0 is $R_0 = 0.6521 < 1$ which means that the infection will die out in the population. This condition is confirmed by simulation results in Figures

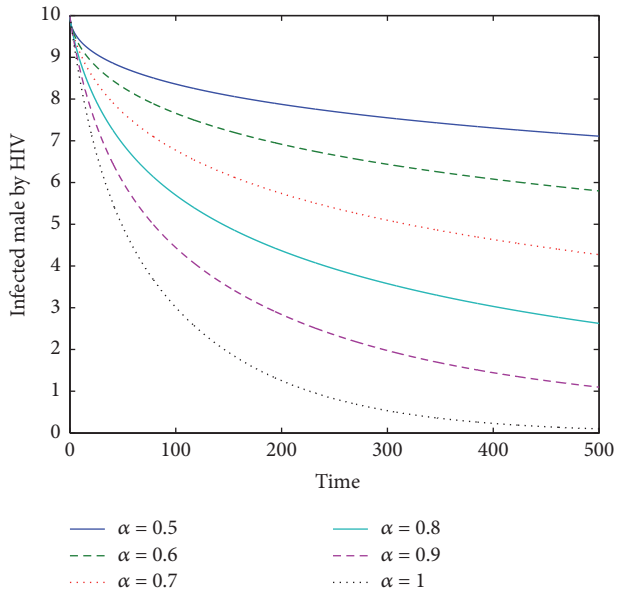

FIGURE 8: Dynamic of nonendemic I_m.

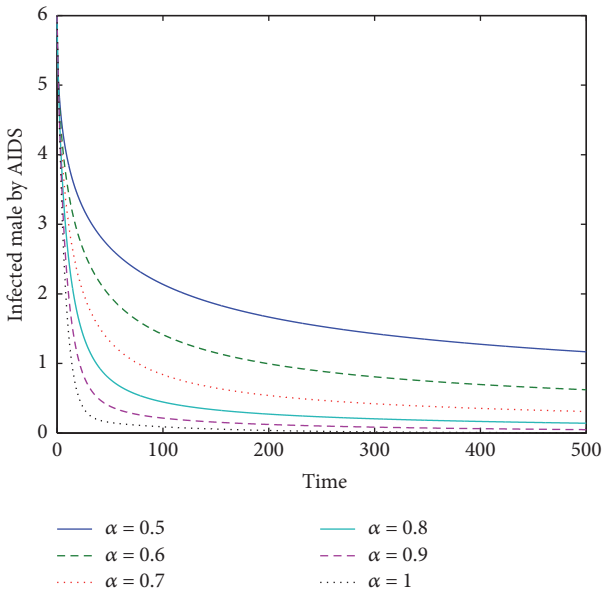

FIGURE 10: Dynamic of nonendemic A_m.

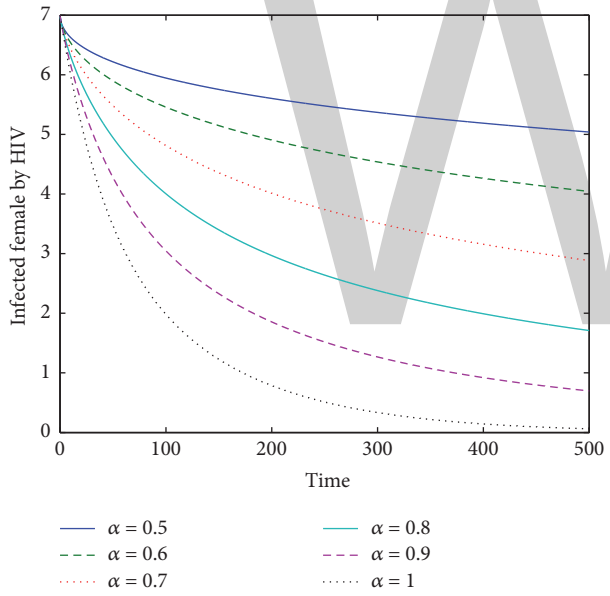

FIGURE 9: Dynamic of nonendemic I_f.

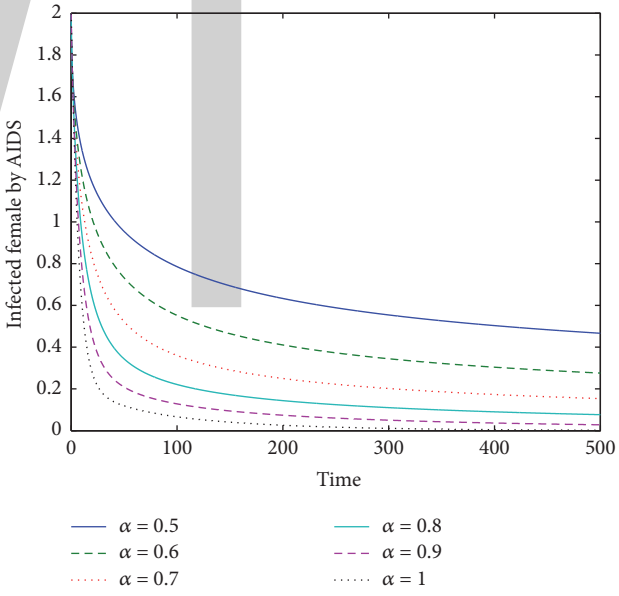

FIGURE 11: Dynamic of nonendemic A_f.

6 and 7, Figures 8 and 9, and Figures 10 and 11 for susceptible male and female populations, respectively, infected by HIV and infected by AIDS. These figures show that the solutions of model (3) are convergent to the disease-free equilibrium. Moreover, we observe that the solutions with higher order α have faster convergence speed compared to the smaller.

Next, we plot in Figures 12–17 the numerical simulations using the parameters as in Table 2. In this condition, the value of R_0 is $R_0 = 65.2051 > 1$ which means that the infection will persist in the population. In Figures 12 and 13, Figures 14 and 15, and Figures 16 and 17 the dynamics of the susceptible male and female populations, respectively, are seen, infected by HIV and infected by AIDS with different values of α. The figures show that the solutions of model (3) converge to the endemic equilibrium when $R_0 > 1$. Similar to the nonendemic condition, we see that as the order α increases, the convergence of solutions is faster for the endemic condition.

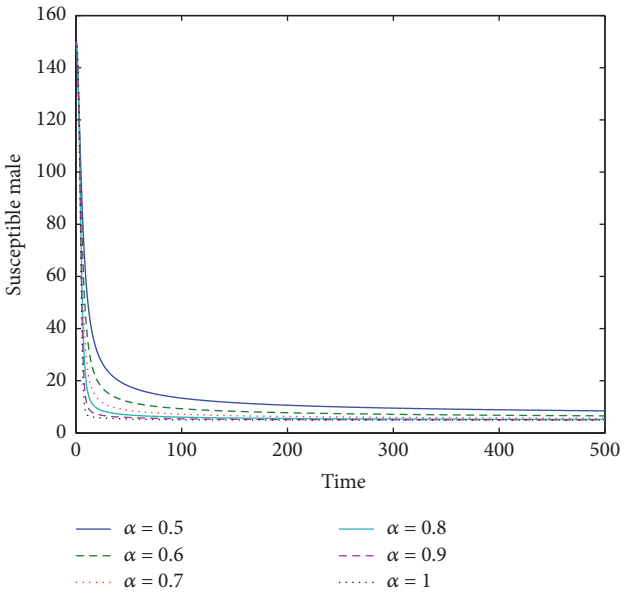

Figure 12: Dynamic of endemic S_m.

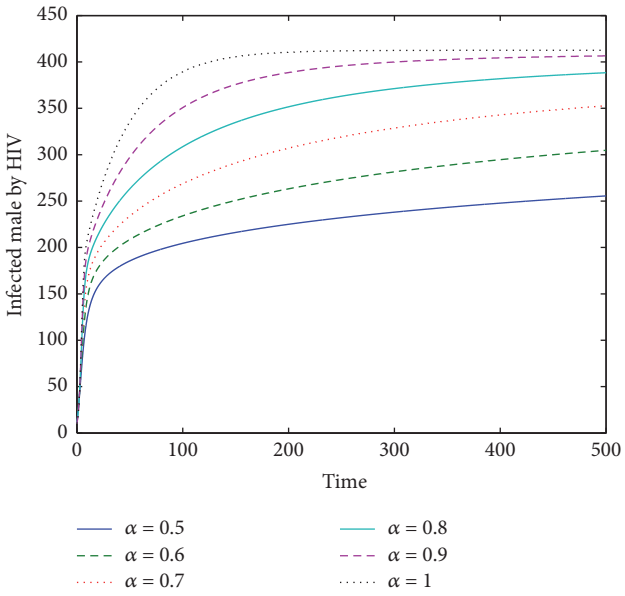

Figure 14: Dynamic of endemic I_m.

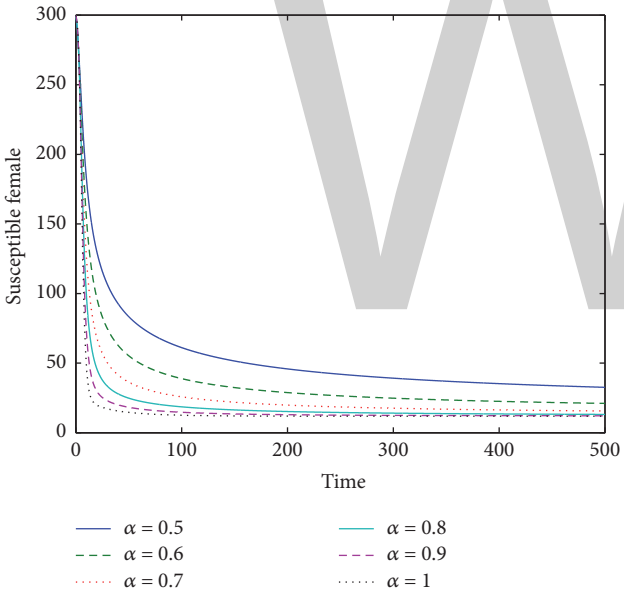

Figure 13: Dynamic of endemic S_f.

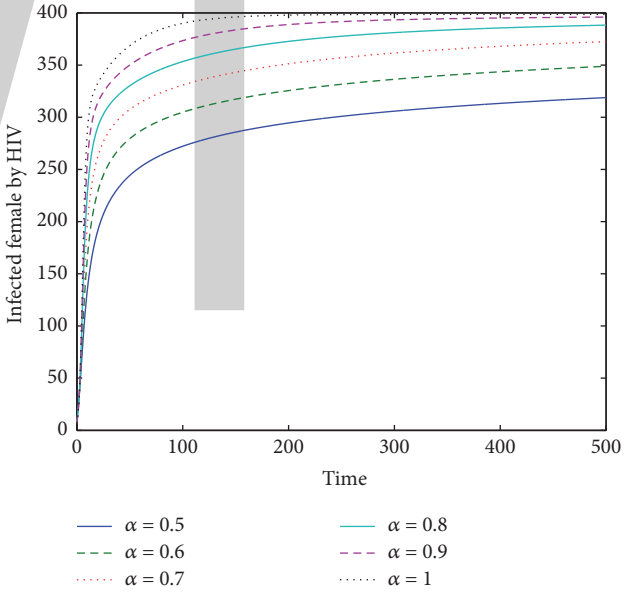

Figure 15: Dynamic of endemic I_f.

In Figures 18–23, we depict the dynamic of both male and female populations infected by AIDS for different values of the efficacy of ART treatment (r) for $\alpha = 1$, $\alpha = 0.7$, and $\alpha = 0.5$. For $\alpha = 1$, we observe that the AIDS infected both male and female populations decrease when the value of r is increase. On the contrary, the number of both AIDS infections increases when the efficacy of ART treatment, r, is smaller. The similar behavior is seen for $\alpha = 0.7$ and $\alpha = 0.5$. It is well known that the ART treatment could improve the quality of HIV infected both male and female patients.

6. Conclusion

In this paper, we have investigated a fractional order of two-sex mathematical model for dynamic HIV, as a generalization of an integer order model, proposed by Kimbir et al. [9]. The basic model in [9] is modified by distinguishing

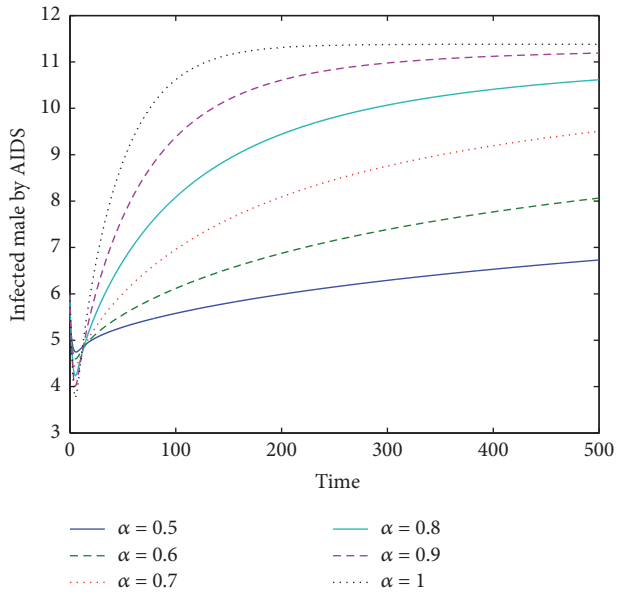

FIGURE 16: Dynamic of endemic A_m.

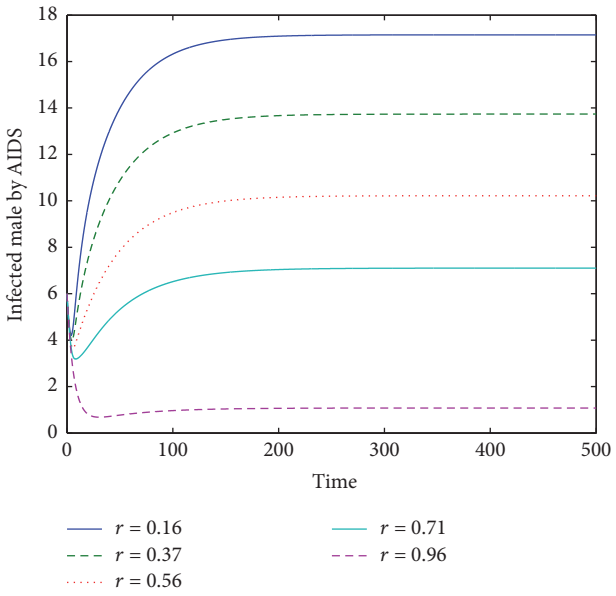

FIGURE 18: Dynamic of A_m with $\alpha = 1$ for various r.

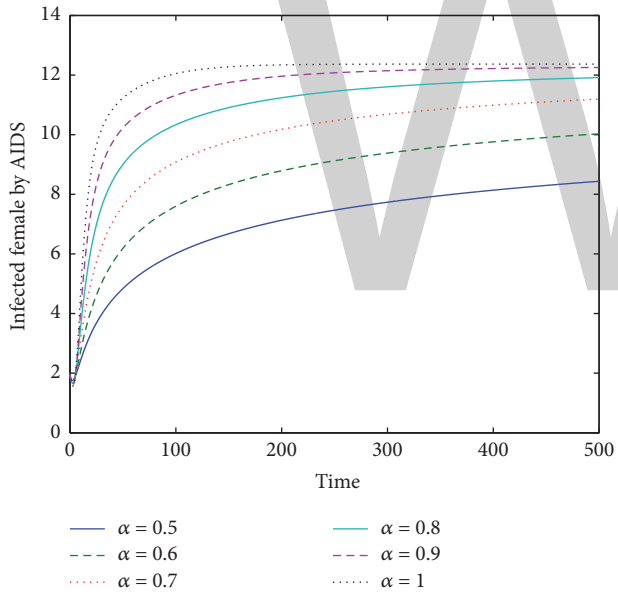

FIGURE 17: Dynamic of endemic A_f.

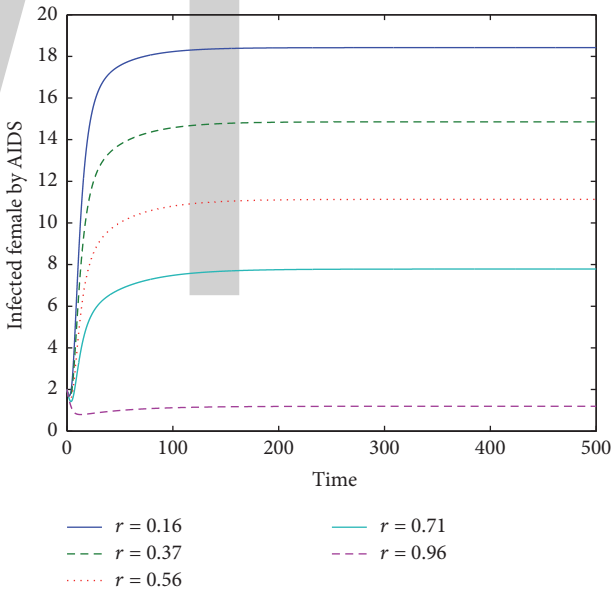

FIGURE 19: Dynamic of A_f with $\alpha = 1$ for various r.

populations infected with HIV and AIDS. We have computed the basic reproduction number (R_0) and proved the stability of equilibriums of the fractional-order model of the HIV infection. Based on the mathematical analysis, the disease-free equilibrium is locally asymptotically stable when $R_0 < 1$ that means the infection will die out in the population. Numerically, the endemic equilibrium tends to be locally asymptotically stable when $R_0 > 1$ which means that the infection will persist in the population. We also studied analytically and numerically the sensitivity analysis to measure the parameters that have high impact on R_0. Finally, we have carried out the numerical simulations for different values of the order (α) of the fractional derivative. The simulations results show that the solutions with higher order α have faster convergence compared to the smaller α. We also found that as the efficacy of ART treatment (r) increases there is a

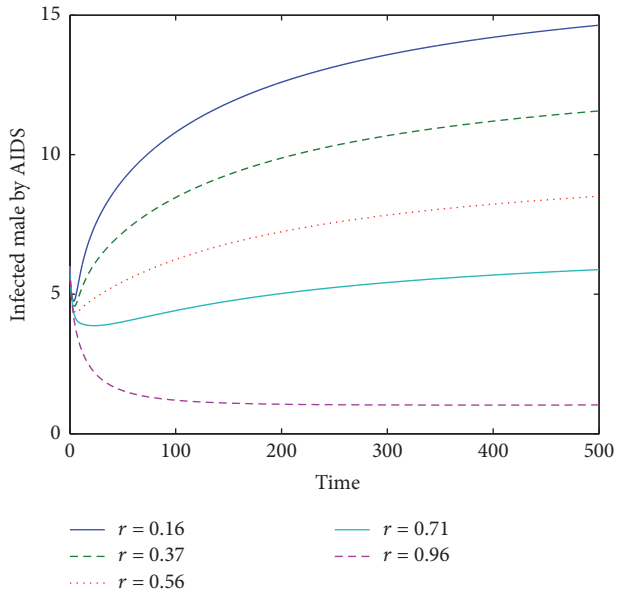

Figure 20: Dynamic of A_m with $\alpha = 0.7$ for various r.

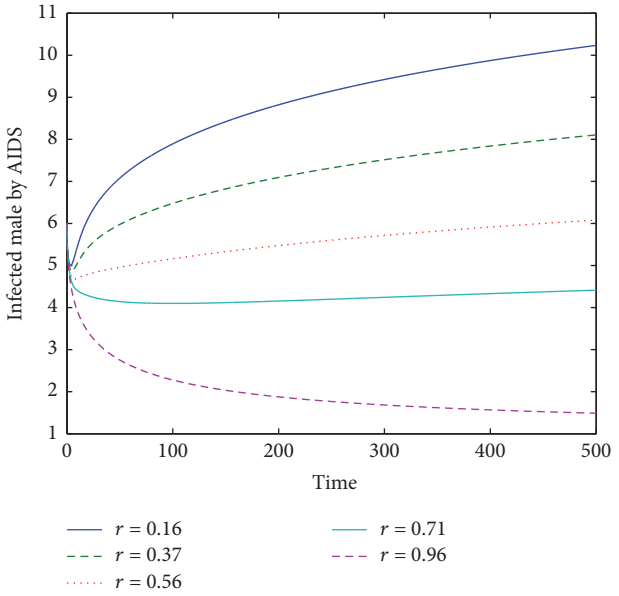

Figure 22: Dynamic of A_m with $\alpha = 0.5$ for various r.

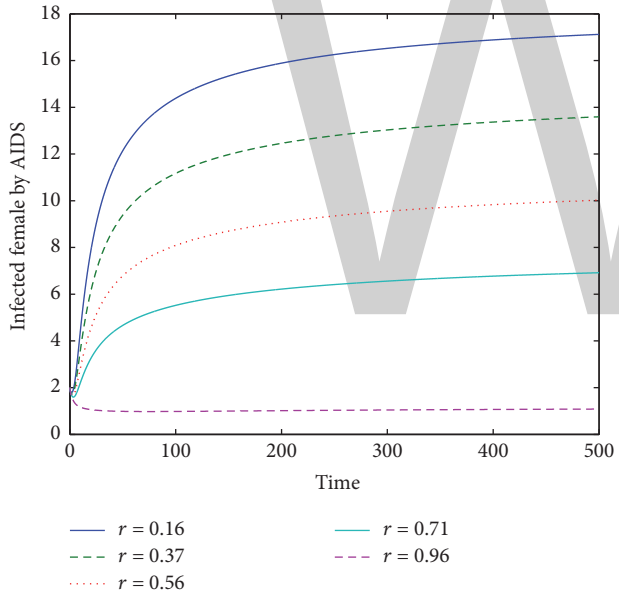

Figure 21: Dynamic of A_f with $\alpha = 0.7$ for various r.

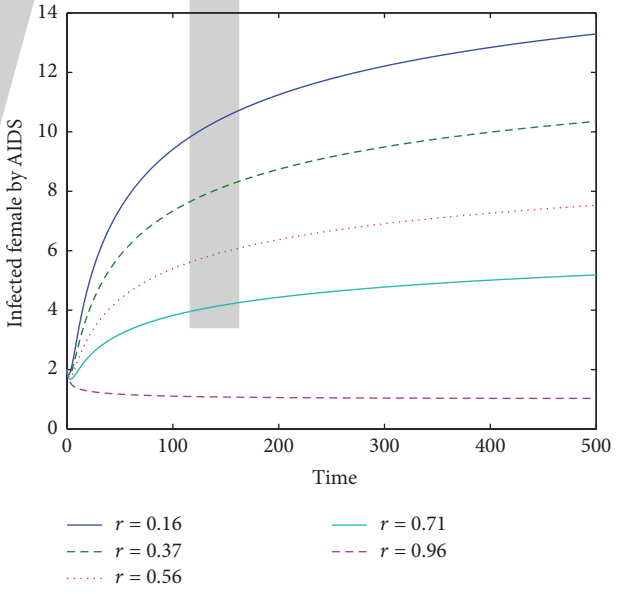

Figure 23: Dynamic of A_f with $\alpha = 0.5$ for various r.

corresponding decrease in the number of the AIDS infected both male and female populations for three values of α. These results indicate the effectiveness of the ART treatment to reduce the AIDS infected.

Conflicts of Interest

The authors declare that there are no conflicts of interest regarding the publication of this manuscript.

Acknowledgments

Part of this research is financially supported by the Hibah Riset Mandat, Universitas Airlangga, 2017, according to SK Rektor no. 569/UN3//2017.

References

[1] World Health Organization, *HIV/AIDS*, World Health Organization, Geneva, Switzerland, 2017, http://www.who.int/mediacentre/factsheets/fs360/en/.

[2] UNAIDS, "Fast Facts About HIV Treatment," 2009, http://data.unaids.org/pub/factsheet/2009/20090903_fastfacts_treatment_en.pdf.

[3] J. R. Durham and F. R. Lashley, *The Person with HIV/AIDS*, Springer, New York, NY, USA, 2010.

[4] F. B. Agusto and A. I. Adekunle, "Optimal control of a two-strain tuberculosis-HIV/AIDS co-infection model," *BioSystems*, vol. 119, no. 1, pp. 20–44, 2014.

[5] Fatmawati and H. Tasman, "An optimal control strategy to reduce the spread of malaria resistance," *Mathematical Biosciences*, vol. 262, pp. 73–79, 2015.

[6] Fatmawati and H. Tasman, "An optimal treatment control of TB-HIV coinfection," *International Journal of Mathematics and Mathematical Sciences*, vol. 2016, Article ID 8261208, 11 pages, 2016.

[7] Fatmawati and H. Tasman, "Optimal control of HIV resistance and tuberculosis co-infection using treatment intervention," *Asian Pacific Journal of Tropical Disease*, vol. 7, no. 6, pp. 366–373, 2017.

[8] T. Gotz, N. Altmeier, W. Bock, R. Rockenfeller, Sutimin, and K. P. Wijaya, "Modeling dengue data from Semarang, Indonesia," *Ecological Complexity*, vol. 30, pp. 57–62, 2017.

[9] R. A. Kimbir, M. J. I. Udoo, and T. Aboiyar, "A mathematical model for the transmission dynamics of HIV/AIDS in a two-sex population considering counseling and antiretroviral therapy (ART)," *Journal of Mathematical and Computational Science*, vol. 2, no. 6, pp. 1671–1684, 2012.

[10] K. O. Okosun, O. D. Makinde, and I. Takaidza, "Impact of optimal control on the treatment of HIV/AIDS and screening of unaware infectives," *Applied Mathematical Modelling*, vol. 37, no. 6, pp. 3802–3820, 2013.

[11] W. Yang, Z. Shu, J. Lam, and C. Sun, "Global dynamics of an HIV model incorporating senior male clients," *Applied Mathematics and Computation*, vol. 311, pp. 203–216, 2017.

[12] J. Huo, H. Zhao, and L. Zhu, "The effect of vaccines on backward bifurcation in a fractional order HIV model," *Nonlinear Analysis: Real World Applications*, vol. 26, pp. 289–305, 2015.

[13] T. Sardar, S. Rana, and J. Chattopadhyay, "A mathematical model of dengue transmission with memory," *Communications in Nonlinear Science and Numerical Simulation*, vol. 22, no. 1–3, pp. 511–525, 2015.

[14] M. Saeedian, M. Khalighi, N. Azimi-Tafreshi, G. R. Jafari, and M. Ausloos, "Memory effects on epidemic evolution: The susceptible-infected-recovered epidemic model," *Physical Review E: Statistical, Nonlinear, and Soft Matter Physics*, vol. 95, no. 2, Article ID 022409, 2017.

[15] C. M. A. Pinto and A. R. M. Carvalho, "The HIV/TB coinfection severity in the presence of TB multi-drug resistant strains," *Ecological Complexity*, vol. 32, pp. 1–20, 2017.

[16] I. Podlubny, *Fractional Differential Equations*, vol. 198 of *Mathematics in Science and Engineering*, Academic Press, San Diego, Calif, USA, 1999.

[17] O. Diekmann, J. A. Heesterbeek, and J. A. Metz, "On the definition and the computation of the basic reproduction ratio R0 in models for infectious diseases in heterogeneous populations," *Journal of Mathematical Biology*, vol. 28, no. 4, pp. 365–382, 1990.

[18] O. Diekmann and J. A. P. Heesterbeek, *Mathematical Epidemiology of Infectious Diseases, Model Building, Analysis and Interpretation*, John Wiley & Sons, 2000.

[19] K. Diethelm, *The Analysis of Fractional Differential Equations*, vol. 2004 of *Lecture Notes in Mathematics*, Springer, New York, NY, USA, 2010.

[20] D. Matignon, "Stability result on fractional differential equations with applications to control processing," in *Proceedings of the IMACS-SMC*, pp. 963–968, Lille, France, 1996.

[21] C. Castillo-Chavez, Z. Feng, and W. Huang, "On the computation of R0 and its role on global stability," in *Mathematical Approaches for Emerging and Reemerging Infectious Diseases: An Introduction*, C. Castillo-Chavez, S. Blower, P. van den Driessche, D. Kirschner, and A.-A. Yakubu, Eds., vol. 125, pp. 229–250, Springer, New York, NY, USA, 2002.

[22] P. van den Driessche and J. Watmough, "Reproduction numbers and sub-threshold endemic equilibria for compartmental models of disease transmission," *Mathematical Biosciences*, vol. 180, pp. 29–48, 2002.

[23] E. Ahmed, A. M. A. El-Sayed, and H. A. A. El-Saka, "On some Routh-Hurwitz conditions for fractional order differential equations and their applications in Lorenz, Rössler, Chua and Chen systems," *Physics Letters A*, vol. 358, no. 1, pp. 1–4, 2006.

[24] N. Chitnis, J. M. Hyman, and J. M. Cushing, "Determining important parameters in the spread of malaria through the sensitivity analysis of a mathematical model," *Bulletin of Mathematical Biology*, vol. 70, no. 5, pp. 1272–1296, 2008.

[25] K. Diethelm, N. J. Ford, and A. D. Freed, "A predictor-corrector approach for the numerical solution of fractional differential equations," *Nonlinear Dynamics*, vol. 29, no. 1–4, pp. 3–22, 2002.

[26] K. Diethelm, N. J. Ford, and A. D. Freed, "Detailed error analysis for a fractional Adams method," *Numerical Algorithms*, vol. 36, no. 1, pp. 31–52, 2004.

[27] R. Garrappa, "On linear stability of predictor-corrector algorithms for fractional differential equations," *International Journal of Computer Mathematics*, vol. 87, no. 10, pp. 2281–2290, 2010.

On the Characterization and Enumeration of Some Generalized Trapezoidal Numbers

Somphong Jitman and Chakrit Phongthai

Department of Mathematics, Faculty of Science, Silpakorn University, Nakhon Pathom 73000, Thailand

Correspondence should be addressed to Somphong Jitman; sjitman@gmail.com

Academic Editor: Susana Montes

A trapezoidal number, a sum of at least two consecutive positive integers, is a figurate number that can be represented by points rearranged in the plane as a trapezoid. Such numbers have been of interest and extensively studied. In this paper, a generalization of trapezoidal numbers has been introduced. For each positive integer m, a positive integer N is called an *m-trapezoidal number* if N can be written as an arithmetic series of at least 2 terms with common difference m. Properties of m-trapezoidal numbers have been studied together with their trapezoidal representations. In the special case where $m = 2$, the characterization and enumeration of such numbers have been given as well as illustrative examples. Precisely, for a fixed 2-trapezoidal number N, the ways and the number of ways to write N as an arithmetic series with common difference 2 have been determined. Some remarks on 3-trapezoidal numbers have been provided as well.

1. Introduction

A triangular number is a figurate number that can be represented by an equilateral triangular arrangement of points equally spaced. For each positive integer ℓ, the ℓth triangular number is the number of points composing a triangle with ℓ points on a side and is equal to the sum of the ℓ natural numbers of the form $\mathrm{Tri}(\ell) = 1 + 2 + 3 + \cdots + \ell$. The ℓth triangular number can be represented as points in an equilateral triangle as in Figure 1.

Triangular numbers have been studied since the ancient Greeks. The Pythagoreans revered the Tetractys which is Tri(4). Triangular numbers have applications to other areas of number theory, such as perfect numbers and binomial coefficients. They are also practically the simplest example of an arithmetic sequence. Therefore, the triangular numbers have fascinated people and cultures all over the world (see [1–3] and references therein).

A trapezoidal number (see [4], e.g.) is a generalization of a triangular number defined to be a sum of at least two consecutive positive integers. Precisely, a positive integer N is a *trapezoidal number* if

$$N = (k+1) + (k+2) + \cdots + (k+\ell) \tag{1}$$

for some integers $k \geq 0$ and $\ell \geq 2$. Trapezoidal numbers form an important class of figurate numbers that has extensively been studied (see [2–7]).

From the definition, it is not difficult to see that every trapezoidal number N can be represented by a rearrangement of N points in the plane as a trapezoid as in Figure 2. For convenience, denote by $T(\ell, k)$ the number of the form (1). The characterization and enumeration of trapezoidal numbers have been given in [4, 8]. The main results are summarized as follows.

Theorem 1 ([4, Proposition 1]). *Let N be a positive integer. Then N is a trapezoidal number if and only if N is not of the form 2^i for all $i \in \mathbb{N} \cup \{0\}$.*

Theorem 2 ([4, Proposition 2]). *Let $N = 2^r p_1^{r_1} p_2^{r_2} \cdots p_s^{r_s}$ be a positive integer such that $s \geq 1$ and $r \geq 0$ are integers, $p_1, p_2, \ldots, p_s$ are distinct odd primes, and $r_i \geq 1$ is an integer for all $i = 1, 2, \ldots, s$. Then N is a trapezoidal number and there are*

$$\tau\left(\frac{n}{2^r}\right) - 1 = (r_1 + 1)(r_2 + 1)\cdots(r_s + 1) - 1 \tag{2}$$

ways of writing N as a sum of at least two consecutive integers.

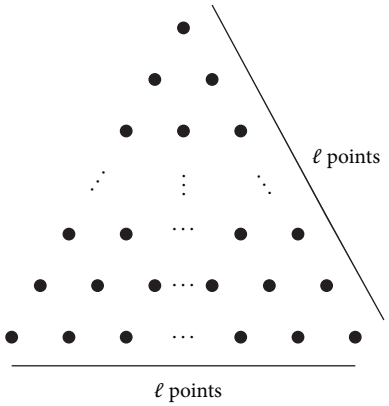

Figure 1: The ℓth triangular number.

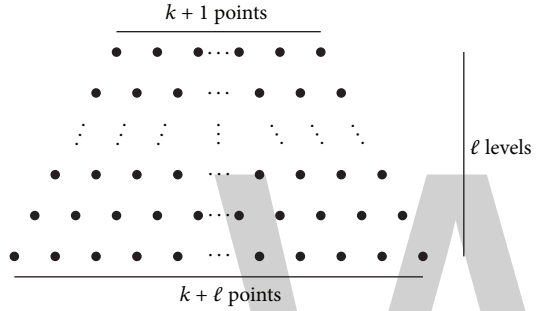

Figure 2: Trapezoidal number $T(\ell, k)$.

Some properties of nontrapezoidal numbers can be found in [9].

Triangular numbers and trapezoidal numbers have a closed connection (see Section 2 for more details) with a *rectangular number* which is defined to be

$$R(\ell, k) := \ell k, \tag{3}$$

where $\ell \geq 2$ and $k \geq 2$ are integers. A rectangular number can be represented as a rectangle as in Figure 3.

In this paper, we focus on a general concept of trapezoidal numbers. For each positive integer m, a positive integer N is called an *m-trapezoidal number* if N can be written as an arithmetic series of at least 2 terms with common difference m. It follows that an m-trapezoidal number can be represented as

$$\begin{aligned}(k+1) + (k+1+m) + (k+1+2m) + \cdots \\ + (k+1+m(\ell-1))\end{aligned} \tag{4}$$

for some integers $k \geq 0$ and $\ell \geq 2$. It is not difficult to see that a 1-trapezoidal number is a classical trapezoidal number. For convenience, denote by $T(\ell, k, m)$ the series in (4).

We note that an m-trapezoidal number is not uniquely determined by a triple (ℓ, k, m) (see Example 3). Every m-trapezoidal number can be represented by an arrangement of points in the plane as a trapezoid. Some examples are given as follows.

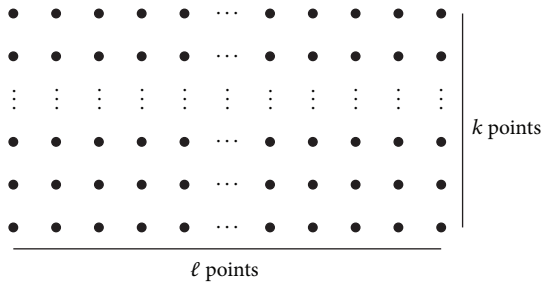

Figure 3: Rectangular number $R(\ell, k)$.

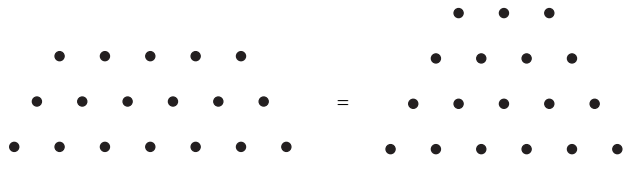

Figure 4: $T(3, 4, 1) = 18 = T(4, 3, 1)$.

Example 3. The positive integer 18 is a (1-)trapezoidal number represented in the forms of series

$$\begin{aligned}T(3,4,1) &= 5+6+7 = 18 = 3+4+5+6 \\ &= T(4,3,1).\end{aligned} \tag{5}$$

The above series can be represented as trapezoids of 18 points in the plane as in Figure 4.

Example 4. The numbers $T(3, 4, 2) = 5 + 7 + 9 = 21$ and $T(3, 4, 3) = 5 + 8 + 11 = 24$ are examples of 2-trapezoidal and 3-trapezoidal numbers, respectively. They can be represented as trapezoids in Figure 5.

In this paper, we focus on properties of m-trapezoidal numbers and their representations as trapezoids in the plane. The characterization and enumeration of m-trapezoidal numbers are studied in the special case where $m = 2$. The paper is organized as follows. In Section 2, general properties of m-trapezoidal numbers are discussed as well as links with other figurate numbers. In Section 3, the characterization and enumeration of 2-trapezoidal numbers have been given together with some illustrative examples. Remarks on 3-trapezoidal numbers have been provided in Section 4. Conclusion and open problems are given in Section 5.

2. Generalized Trapezoidal Numbers

In this section, we focus on general properties of m-trapezoidal numbers and links with other figurate numbers such as triangular numbers, trapezoidal number, and rectangular numbers.

First, we simplify the formula for an m-trapezoidal number.

Lemma 5. *Let $k \geq 0$, $m \geq 1$, and $l \geq 2$ be integers. Then*

$$T(\ell, k, m) = \frac{\ell(2(k+1) + m(\ell-1))}{2}. \tag{6}$$

(a) $T(3,4,2) = 21$ (b) $T(3,4,3) = 24$

FIGURE 5: $T(3,4,2) = 21$ and $T(3,4,3) = 24$.

Proof. From the definition, we have

$$\begin{aligned} T(\ell,k,m) &= (k+1)+(k+1)+\cdots+(k+1) \\ &\quad + m(1+2+\cdots+(\ell-1)) \\ &= \ell(k+1)+\frac{m(\ell-1)\ell}{2} \\ &= \frac{\ell(2(k+1)+m(\ell-1))}{2} \end{aligned} \tag{7}$$

as desired. □

From the formula in Lemma 5, the following properties can be deduced.

Corollary 6. *Let m be a positive integer. If m is even, then an m-trapezoidal number $T(\ell,k,m)$ is a rectangular number for all integers $k \geq 0$ and $\ell \geq 2$.*

Proof. Assume that m is even. Let $k \geq 0$ and $\ell \geq 2$ be integers. Then

$$\begin{aligned} T(\ell,k,m) &= \frac{\ell(2(k+1)+2a(\ell-1))}{2} \\ &= \ell(k+1+a(\ell-1)). \end{aligned} \tag{8}$$

Since $\ell \geq 2$ and $k+1+a(\ell-1) \geq 1+a \geq 2$, $T(\ell,k,m)$ is a rectangular number. □

Corollary 7. *Let m be a positive integer. If m is odd, then an m-trapezoidal number $T(\ell,k,m)$ is a rectangular number for all integers $k \geq 0$ and $\ell \geq 3$.*

Proof. Assume that m is odd. Let $k \geq 0$ and $\ell \geq 3$ be integers. We consider the following two cases.

Case 1 (ℓ is even). Then $\ell = 2a$ for some $a \in \mathbb{N} \setminus \{1\}$ and

$$\begin{aligned} T(\ell,k,m) &= \frac{\ell(2(k+1)+m(\ell-1))}{2} \\ &= \frac{(2a)(2(k+1)+m(2a-1))}{2} \\ &= a(2(k+1)+m(2a-1)). \end{aligned} \tag{9}$$

Since $a \geq 2$ and $(2(k+1)+m(2a-1)) \geq 5 \geq 2$, $T(\ell,k,m)$ is a rectangular number.

Case 2 (ℓ is odd). Then $\ell = 2b+1$ for some $b \in \mathbb{N}$ and

$$\begin{aligned} T(\ell,k,m) &= \frac{\ell(2(k+1)+m(\ell-1))}{2} \\ &= \frac{(2b+1)(2(k+1)+m(2b+1-1))}{2} \\ &= (2b+1)((k+1)+mb). \end{aligned} \tag{10}$$

Since $(2b+1) \geq 3 \geq 2$ and $((k+1)+mb) \geq 2$, $T(\ell,k,m)$ is a rectangular number.

From the two cases, $T(\ell,k,m)$ is rectangular for all $k \geq 0$ and $\ell \geq 3$. □

Trapezoidal numbers, m-trapezoidal numbers, rectangular numbers, and triangular numbers are linked via the following relations.

Theorem 8. *Let ℓ, k, m be integers such that $\ell \geq 2$, $m \geq 1$, and $k \geq 0$. Then*

$$T(\ell,k,m) = T(\ell,k,m-i) + (m-i)\,\mathrm{Tri}(\ell-1) \tag{11}$$

for all positive integers $i \leq m$.

Proof. Let i be a positive integer. Then

$$\begin{aligned} T(\ell,k,m) &= \frac{\ell(2(k+1)+m(\ell-1))}{2} \\ &= \frac{\ell(2(k+1)+i\ell-i+i+m\ell-m-i\ell)}{2} \\ &= \frac{\ell(2(k+1)+i(\ell+1))}{2} \\ &\quad + \frac{\ell(m\ell-m+i-i\ell)}{2} \\ &= \frac{\ell(2(k+1)+i(\ell+1))}{2} \\ &\quad + \frac{(m-i)(\ell-1)\ell}{2} \\ &= T(\ell,k,i) + (m-i)\,\mathrm{Tri}(\ell-1). \end{aligned} \tag{12}$$

Hence, the result follows. □

The next corollary follows immediately from Theorem 8.

Corollary 9. *Let ℓ, k, m be integers such that $\ell \geq 2, m \geq 1$, and $k \geq 0$. Then the following statements hold:*

(1) $T(\ell,k,m) = T(\ell,k,1) + (m-1)\mathrm{Tri}(\ell-1)$.

(2) $T(\ell,k,m) = T(\ell,k,m-1) + \mathrm{Tri}(\ell-1)$.

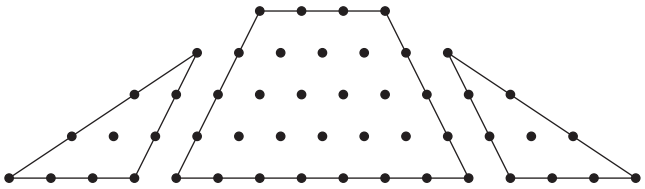

Figure 6: $T(5,3,3) = T(5,3,1) + 2\text{Tri}(4)$.

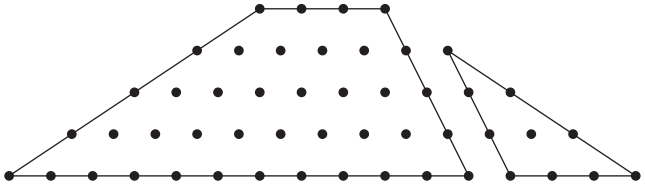

Figure 7: $T(5,3,3) = T(5,3,2) + \text{Tri}(4)$.

Illustrative examples of results in Corollary 9 are given as follows.

Example 10. Let $\ell = 5, \ell = 5, k = 3$ and $m = 3$. From Theorem 8, we have

$$\begin{aligned} T(5,3,3) &= 4 + 7 + 10 + 13 + 16 \\ &= (4 + 5 + 6 + 7 + 8) + 2(1 + 2 + 3 + 4) \\ &= T(5,3,1) + 2\text{Tri}(4), \\ T(5,3,3) &= 4 + 7 + 10 + 13 + 16 \\ &= (4 + 6 + 8 + 10 + 12) + (1 + 2 + 3 + 4) \\ &= T(5,3,2) + \text{Tri}(4). \end{aligned} \tag{13}$$

The above relations can be represented in the plane as in Figures 6 and 7.

Theorem 11. *Let m and N be positive integers. If N is an m-trapezoidal number such that $N \geq m + 4$, then N can be written as a sum of a rectangular number and an m-trapezoidal number.*

Proof. Assume that N is an m-trapezoidal number such that $N \geq m + 4$. Then

$$N = \frac{b(2(a+1) + m(b-1))}{2} = T(b,a,m) \tag{14}$$

for some integers $a \geq 1$ and $b \geq 2$.

Let $N_1 = (a+1)b$ and $N_2 = (b-1)(2m + m(b-2))/2 = T(b-1,a,m)$. Then N_1 is a rectangular number and N_2 is an m-trapezoidal number. It follows that

$$\begin{aligned} N_1 + N_2 &= (a+1)b + \frac{(b-1)(2m + m(b-2))}{2} \\ &= \frac{b(2(a+1) + (m)(b-1))}{2} = N. \end{aligned} \tag{15}$$

Hence, N is a sum of a rectangular number and an m-trapezoidal number. □

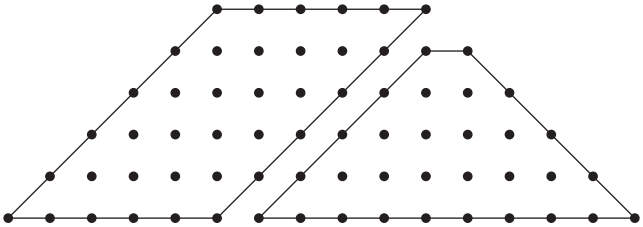

Figure 8: $T(6,5,2) = R(6,6) + T(5,1,2)$.

Example 12. Let $\ell = 6, k = 5$, and $m = 2$. Then

$$\begin{aligned} T(6,5,2) &= 6 + 8 + 10 + 12 + 14 + 16 \\ &= 6 \cdot 6 + (2 + 4 + 6 + 8 + 10) \\ &= R(6,6) + T(5,1,2) \end{aligned} \tag{16}$$

which can be represented in the plane as in Figure 8.

3. Characterization and Enumeration of 2-Trapezoidal Numbers

In this section, we focus on the special case where $m = 2$. The characterization and enumeration of 2-trapezoidal numbers are given together with some illustrative examples.

The characterization of 2-trapezoidal numbers is given in the next theorem which is totally different from the case of 1-trapezoidal numbers in Theorem 1.

Theorem 13. *Let $N \geq 2$ be an integer. Then N is a 2-trapezoidal number if and only if N is not a prime.*

Proof. Assume that N is a 2-trapezoidal number. By Corollary 6, N is a rectangular number. Hence, N is not a prime number.

Conversely, assume that N is not a prime number. Then there exist integers $1 < r \leq s < N$ such that $N = rs$. Choose $\ell = r$ and $k = s - r$. Then $\ell \geq 2, k \geq 0$, and

$$\begin{aligned} N = rs = \ell(k + \ell) &= \frac{\ell(2(k+1) + 2(\ell - 1))}{2} \\ &= T(\ell, k, 2). \end{aligned} \tag{17}$$

Hence, N is a 2-trapezoidal number as desired. □

From the proof of Theorem 13, a 2-trapezoidal number N can be represented as a series $T(\ell, k, 2)$ via the following steps:

(1) Determine the divisors r of N such that $1 < r \leq \sqrt{N}$.

(2) For each r, compute $s = N/r$.

(3) Write $T(\ell, k, 2)$, where $\ell = r$ and $k = s - r$.

Let us consider the following examples.

Example 14. Consider the 2-trapezoidal number $N = 54$. We have $54 = 2 \cdot 3^3$ which can be written as arithmetic series of at least 2 terms with common difference 2 as in Table 1.

Table 1: Trapezoidal representations of 54.

$\ell = r$	$s = N/r$	$k = s - r$	$T(\ell, k, 2)$
2	27	25	26 + 28
3	18	15	16 + 18 + 20
6	9	3	4 + 6 + 8 + 10 + 12 + 14

Table 2: Trapezoidal representations of 100.

$\ell = r$	$s = N/r$	$k = s - r$	$T(\ell, k, 2)$
2	50	48	49 + 51
4	25	21	22 + 24 + 26 + 28
5	20	15	16 + 18 + 20 + 22 + 24
10	10	0	1+3+5+7+9+11+13+15+17+19

Table 3: Trapezoidal representations of 175.

$\ell = r$	$s = N/r$	$k = s - r$	$T(\ell, k, 2)$
5	35	30	31 + 33 + 35 + 37 + 39
7	25	18	19 + 21 + 23 + 25 + 27 + 29 + 31

Example 15. Consider the 2-trapezoidal number $N = 100$. Then $100 = 2^2 \cdot 5^2$ which can be written as arithmetic series of at least 2 terms with common difference 2 as in Table 2.

Example 16. Consider the 2-trapezoidal number $N = 175$. Then $175 = 5^2 \cdot 7$ which can be written as arithmetic series of at least 2 terms with common difference 2 as in Table 3.

By the definition, every 2-trapezoidal number can be written as an arithmetic series with common difference 2. In the following theorem, we determine the number of ways to write a 2-trapezoidal number in terms of an arithmetic series of at least 2 terms with common difference 2.

Theorem 17. *Let N be a 2-trapezoidal number. Then the number of ways to write N as an arithmetic series of at least 2 terms with common difference 2 is*

$$\begin{cases} \dfrac{\tau(N) - 1}{2} & \text{if } N \text{ is a square,} \\ \dfrac{\tau(N)}{2} - 1 & \text{if } N \text{ is not a square,} \end{cases} \tag{18}$$

where $\tau(N)$ is the number of divisors of N.

Proof. From the proof of Theorem 13, it follows that $N = rs$ for some integers $1 < r \leq s$. Next, we consider the following two cases.

Case 1 (N is a square). In this case, we have $1 < r \leq s$. Then the number of ways to write N as an arithmetic series of at least 2 terms with common difference 2 is the number of divisors r of N such that $1 < r \leq \sqrt{N}$. Since N is a square, $N = p_1^{r_1} p_2^{r_2} \cdots p_s^{r_s}$ for some $s \geq 1$, $p_1, p_2, \ldots, p_s$ are distinct odd primes, and r_i is an even positive integer for all $i = 1, 2, \ldots, s$. Then the number of divisors of N is $\tau(N) = (r_1 + 1)(r_2 + 1) \cdots (r_s + 1)$ which is odd. Hence, the number of ways to write N as an arithmetic series of at least 2 terms with common difference 2 is $(\tau(N) - 1)/2 + 1 - 1 = (\tau(N) - 1)/2$.

Table 4: Number of representations of square 2-trapezoidal numbers.

N	$\dfrac{\tau(N) - 1}{2}$
$25 = 5^2$	$\dfrac{(2+1) - 1}{2} = 1$
$36 = 2^2 \cdot 3^2$	$\dfrac{(2+1)(2+1) - 1}{2} = 4$
$49 = 7^2$	$\dfrac{(2+1) - 1}{2} = 1$
$81 = 3^4$	$\dfrac{(4+1) - 1}{2} = 2$
$100 = 2^2 \cdot 5^2$	$\dfrac{(2+1)(2+1) - 1}{2} = 4$
$256 = 2^8$	$\dfrac{(8+1) - 1}{2} = 4$
$400 = 2^4 \cdot 5^2$	$\dfrac{(4+1)(2+1) - 1}{2} = 7$

Case 2 (N is not a square). In this case, we have $1 < r < s$. Then the number of ways to write N as an arithmetic series of at least 2 terms with common difference 2 is the number of divisors r of N such that $1 < r < \sqrt{N}$. Since N is not a square, $N = p_1^{r_1} p_2^{r_2} \cdots p_s^{r_s}$, where $s \geq 1$, $p_1, p_2, \ldots, p_s$ are distinct odd primes and r_i is a positive integer for all $i = 1, 2, \ldots, s$ such that r_j is odd for some $1 \leq j \leq s$. Then the number of divisors of N is $\tau(N) = (r_1 + 1)(r_2 + 1) \cdots (r_s + 1)$ which is even. Therefore, the number of ways to write N as an arithmetic series of at least 2 terms with common difference 2 is $\tau(N)/2 - 1$.

From the two cases, the result follows. □

The next corollary is a direct consequence of Theorem 17.

Corollary 18. *Let N be a 2-trapezoidal number. Then N has a unique representation as an arithmetic series of at least 2 terms with common difference 2 if and only one of the following statements holds:*

(1) *N is a product of two distinct primes.*

(2) *N is the square of a prime.*

(3) *N is the cube of a prime.*

Some illustrative examples of the number of ways to write a 2-trapezoidal number N as an arithmetic series of at least 2 terms with common difference 2 are shown in Tables 4 and 5.

4. Some Properties of 3-Trapezoidal Numbers

In this section, we focus on properties of 3-trapezoidal numbers. A necessary condition for a positive integer to be a 3-trapezoidal number is given. However, this condition is not sufficient.

Theorem 19. *Let N be a positive integer. If N is a 3-trapezoidal number, then N is not in the form of 2^i for all $i \in \mathbb{N} \cup \{0\}$.*

Table 5: Number of representations of nonsquare 2-trapezoidal numbers.

N	$\frac{\tau(N)}{2} - 1$
$10 = 2 \cdot 5$	$\frac{(1+1)(1+1)}{2} - 1 = 2 - 1 = 1$
$24 = 2^3 \cdot 3$	$\frac{(3+1)(1+1)}{2} - 1 = 3$
$27 = 3^3$	$\frac{(3+1)}{2} - 1 = 1$
$42 = 2 \cdot 3 \cdot 7$	$\frac{(1+1)(1+1)(1+1)}{2} - 1 = 4 - 1 = 3$
$54 = 2 \cdot 3^3$	$\frac{(1+1)(3+1)}{2} - 1 = 4 - 1 = 3$

Proof. Assume that N is a 3-trapezoidal number. Then

$$N = \frac{\ell\,(2\,(k+1) + 3\,(\ell-1))}{2} \tag{19}$$

for some $\ell \geq 2$ and $k \geq 0$. We consider the following two cases.

Case 1 (ℓ is odd). It follows that $3(\ell-1)$ is even and $(2(k+1)+3(\ell-1))/2 \in \mathbb{N}$. It follows that $\ell \geq 3$ is odd and $\ell \mid N$. Hence, $N \neq 2^i$ for all $i \in \mathbb{N} \cup \{0\}$.

Case 2 (ℓ is even). We have that $3(\ell-1)$ is odd and $2(k+1)+3(\ell-1)$ is odd. Since $\ell/2 \in \mathbb{N}$, it follows that $(2(k+1)+3(\ell-1)) \mid N$ and $2(k+1)+3(\ell-1) \geq 5$. Hence, $N \neq 2^i$ for all $i \in \mathbb{N} \cup \{0\}$.

Altogether, we have that $N \neq 2^i$ for all $i \in \mathbb{N} \cup \{0\}$ as desired. □

We note that the necessary condition given in Theorem 19 is not sufficient. It is not difficult to see that 6 is not of the form 2^i for all $i \in \mathbb{N} \cup \{0\}$ but 6 is not a 3-trapezoidal number.

5. Conclusion and Remarks

A general concept of trapezoidal numbers has been introduced. Some properties of m-trapezoidal numbers have been determined as well as links with other figurate numbers. Complete characterization and enumeration of 2-trapezoidal numbers are given. A necessary condition of a positive integer to be a 3-trapezoidal number is determined. However, the given condition is not sufficient.

In general, it is interesting to study the characterization and enumeration of m-trapezoidal numbers with $m \geq 3$.

Conflicts of Interest

The authors declare that there are no conflicts of interest regarding the publication of this paper.

Acknowledgments

This research was supported by the Thailand Research Fund and the Office of Higher Education Commission of Thailand under Research Grant MRG6080012.

References

[1] S. Asadulla, "Thirty-nine [thirty] perfect numbers and their divisors," *International Journal of Mathematics and Mathematical Sciences*, vol. 9, no. 1, pp. 205-206, 1986.

[2] P. J. Berana, J. Montalbo, and D. Magpantay, "On triangular and trapezoidal numbers," *Asia Pacific Journal of Multidisciplinary Research*, vol. 3, pp. 76–81, 2015.

[3] T. Verhoeff, "Rectangular and trapezoidal arrangements," *Journal of Integer Sequences*, vol. 2, Article 99.1.6 (HTML document) pages, 1999.

[4] C. Gamer, D. W. Roeder, and J. J. Watkins, "Trapezoidal Numbers," *Mathematics Magazine*, vol. 58, no. 2, pp. 108–110, 1985.

[5] C. Feinberg-McBrian, "The case of trapezoidal numbers," *Mathematics Teacher*, vol. 89, pp. 16–24, 1996.

[6] P. W. Haggard and K. L. Morales, "Discovering relationships and patterns by exploring trapezoidal numbers," *International Journal of Mathematical Education in Science and Technology*, vol. 24, no. 1, pp. 85–90, 1993.

[7] J. Smith, "Trapezoidal numbers," *Mathematics in School*, vol. 5, p. 42, 1997.

[8] R. Guy, "Sums of consecutive integers," *The Fibonacci Quarterly. Official Organ of the Fibonacci Association*, vol. 20, no. 1, pp. 36–38, 1982.

[9] C. Jones and N. Lord, "Characterising non-trapezoidal numbers," *The Mathematical Gazette*, vol. 83, no. 497, pp. 262-263, 1999.

A Joint Representation of Rényi's and Tsalli's Entropy with Application in Coding Theory

Litegebe Wondie and Satish Kumar

Department of Mathematics, College of Natural and Computational Science, University of Gondar, Gondar, Ethiopia

Correspondence should be addressed to Satish Kumar; drsatish74@rediffmail.com

Academic Editor: Hans Engler

We introduce a quantity which is called Rényi's-Tsalli's entropy of order ξ and discussed some of its major properties with Shannon and other entropies in the literature. Further, we give its application in coding theory and a coding theorem analogous to the ordinary coding theorem for a noiseless channel is proved. The theorem states that the proposed entropy is the lower bound of mean code word length.

1. Introduction

Let $\Delta_n = \{A = (a_1, a_2, \ldots, a_n) : a_i \geq 0,\ i = 1, 2, \ldots, n;\ \sum_{i=1}^{n} a_i = 1\}$, $n \geq 2$, be set of n-complete probability distributions. For any probability distribution $A = (a_1, a_2, \ldots, a_n) \in \Delta_n$, Shannon [1] defined an entropy given as

$$H(A) = -\sum_{i=1}^{n} (a_i) \log (a_i), \tag{1}$$

where the convention $0 \log(0) = 0$ is adopted (see Shannon [1]). Throughout this paper, logarithms are taken to the base $D(D > 1)$. A number of parametric generalizations of Shannon entropy are proposed by many authors in literature which produces (1) for specific values of parameters. The presence of parameters makes an entropy more flexible from application point of view. One of the first generalizations of (1) was proposed by Rényi [2] as

$$H_{Re}(A; \xi) = \frac{1}{1-\xi} \log \left(\sum_{i=1}^{n} a_i^{\xi} \right); \quad \xi > 0 (\neq 1). \tag{2}$$

Another well-known entropy was proposed by Havrda and Charvát [3]

$$H_{hc}(A; \xi) = \left(2^{1-\xi} - 1\right)^{-1} \left(\sum_{i=1}^{n} a_i^{\xi} - 1 \right); \quad \xi > 0 (\neq 1). \tag{3}$$

Independently, Tsalli [4] proposed another parametric generalization of the Shannon entropy as

$$H_T(A; \xi) = \frac{1}{1-\xi} \left(\sum_{i=1}^{n} a_i^{\xi} - 1 \right); \quad \xi > 0 (\neq 1). \tag{4}$$

Equations (3) and (4) essentially have the same expression except the normalized factor. The Havrda and Charvát entropy is normalized to 1. That is, if $A = (1/2, 1/2)$ then $H_{hc}(A; \xi) = 1$ whereas Tsalli's entropy is not normalized. Both the entropies yield the same result and we call these entropies as Tsalli-Havrda-Charvát entropy. Equations (2), (3), and (4) reduce to (1) when $\xi \to 1$.

N. R. Pal and S. K. Pal [5, 6] have proposed an exponential entropy as

$$H_{pp}(A) = \sum_{i=1}^{n} a_i \left(e^{1-a_i} - 1 \right). \tag{5}$$

These authors claim that the exponential entropy has some advantage over Shannon's entropy, especially within context of image processing. One such claim is that the exponential entropy has a fixed upper bound such as that for uniform distribution $(1/n, 1/n, \ldots, 1/n)$ and for the entropy in (5).

$$\lim_{n \to \infty} H_{pp} \left(\frac{1}{n}, \frac{1}{n}, \ldots, \frac{1}{n} \right) = e - 1, \tag{6}$$

as compared to infinite limit (as $n \to \infty$) for the entropies in (1) and (2) and also for that in (3) when $\xi \in (0,1)$. Equation (5) was further generalized by Kvalseth [7] introducing a parameter as

$$H_K(A;\xi) = \frac{1}{\xi}\sum_{i=1}^{n} a_i\left(e^{1-a_i^{\xi}} - 1\right); \quad \xi \in \mathbb{R}. \tag{7}$$

In this paper, we introduce and study a new information measure which is called Rényi's-Tsalli's entropy of order ξ and a new mean code word length and discuss the relation with each other. In Section 2, Rényi's and Tsalli's entropy is introduced and also some of its major properties are discussed. In Section 3, the application of proposed information measure in coding theory is given and it is proved that the proposed information measure is the lower bound of mean code word length.

Now, in the next section, we propose a new parametric information measure.

2. A New Generalized Information Measure

However, in literature of information theory, there exists various generalizations of Shannon entropy; we introduce a new information measure as

$$H^{\xi}(A) = \begin{cases} \dfrac{1}{\xi^{-1} - \xi}\left[\log\left(\sum_{i=1}^{n} a_i^{\xi}\right) + \sum_{i=1}^{n} a_i^{\xi} - 1\right], & \xi > 0\ (\neq 1); \\ -\sum_{i=1}^{n}(a_i)\log(a_i), & \xi = 1. \end{cases} \tag{8}$$

Second case in (8) is a well-known Shannon entropy.

The quantity (8) introduced in the present section is a joint representation of Rényi's and Tsalli's entropy of order ξ. Such a name will be justified, if it shares some major properties with Shannon entropy and other entropies in the literature. We study some such properties in the next theorem.

2.1. Properties of Proposed Entropy

Theorem 1. *The parametric entropy* $H^{\xi}(A), \{A = (a_1, a_2, \ldots, a_n),\ 0 < a_i \le 1, \sum_{i=1}^{n} a_i = 1\}$ *has the following properties.*

(1) Symmetry. $H^{\xi}(a_1, a_2, \ldots, a_n)$ *is a symmetric function of* $(a_1, a_2, \ldots, a_n)$.

(2) Nonnegative. $H^{\xi}(A) \ge 0$ *for all* $\xi > 0 (\neq 1)$.

(3) Expansible

$$H^{\xi}(a_1, a_2, \ldots, a_n; 0) = H^{\xi}(a_1, a_2, \ldots, a_n). \tag{9}$$

(4) Decisive

$$H^{\xi}(0,1) = H^{\xi}(1,0) = 0. \tag{10}$$

(5) Maximality

$$H^{\xi}(a_1, a_2, \ldots, a_n) \le H^{\xi}\left(\frac{1}{n}, \frac{1}{n}, \ldots, \frac{1}{n}\right) = \frac{1}{\xi^{-1} - \xi}\left[\log\left(n^{1-\xi}\right) + n^{1-\xi} - 1\right]. \tag{11}$$

(6) Concavity. The entropy $H^{\xi}(A)$ *is a concave function for* $0 < \xi < 1$ *of the probability distribution* $A = (a_1, a_2, \ldots, a_n)$, $a_i \ge 0$; $\sum_{i=1}^{n} a_i = 1$.

(7) Continuity. $H^{\xi}(a_1, a_2, \ldots, a_n)$ *is continuous in the region* $a_i \ge 0$ *for all* $i = 1, 2, \ldots, n$ *and* $\xi > 0 (\neq 1)$.

Proof. The properties (1), (3), (4), and (5) follow immediately from the definition. For property (7), we know that

$$\log\left(\sum_{i=1}^{n} a_i^{\xi}\right) + \sum_{i=1}^{n} a_i^{\xi} - 1 \tag{12}$$

is continuous in the region $a_i \ge 0$ for all $\xi > 0$. Thus, $H^{\xi}(A)$, is also continuous in the region $a_i \ge 0$ and $\xi > 0 (\neq 1)$ and $i = 1, 2, \ldots, n$.

Property (2)

Case 1 $(0 < \xi < 1)$

$$\sum_{i=1}^{n} a_i^{\xi} \ge 1. \tag{13}$$

From (13), we get

$$\log\left(\sum_{i=1}^{n} a_i^{\xi}\right) + \sum_{i=1}^{n} a_i^{\xi} - 1 \ge 0, \tag{14}$$

since $0 < \xi < 1 \Rightarrow \xi^{-1} - \xi > 0$.

Therefore, we get

$$\frac{1}{\xi^{-1} - \xi}\left[\log\left(\sum_{i=1}^{n} a_i^{\xi}\right) + \sum_{i=1}^{n} a_i^{\xi} - 1\right] \ge 0; \tag{15}$$

that is, $H^{\xi}(A) \ge 0$.

Therefore, we conclude that $H^{\xi}(A) \ge 0$ for all $0 < \xi < 1$.

Case 2 $(1 < \xi < \infty)$. The proof is on the same lines as in Case 1. (Note that inequality in (14) will get reversed for $1 < \xi < \infty$.)

Property (6). Now, we prove that $H^{\xi}(A)$ is a concave function of $A \in \Delta_n$.

Differentiating (8) twice with respect to a_i, we get

$$\frac{\partial^2 H^{\xi}(A)}{\partial a_i^2} = \frac{\xi}{\xi^{-1}-\xi}\left(\frac{(\xi-1)\sum_{i=1}^{n}\left(a_i^{\xi}\right)\sum_{i=1}^{n}\left(a_i^{\xi-2}\right)\left(\sum_{i=1}^{n}a_i^{\xi}+1\right)-\xi\left(\sum_{i=1}^{n}a_i^{\xi-1}\right)^2}{\left(\sum_{i=1}^{n}a_i^{\xi}\right)^2}\right). \tag{16}$$

Now, for $0<\xi<1$,

$$\begin{aligned}&(\xi-1)\sum_{i=1}^{n}\left(a_i^{\xi}\right)\sum_{i=1}^{n}\left(a_i^{\xi-2}\right)\left(\sum_{i=1}^{n}a_i^{\xi}+1\right)-\xi\left(\sum_{i=1}^{n}a_i^{\xi-1}\right)^2\\ &\quad<0,\\ &\frac{\xi}{\xi^{-1}-\xi}>0.\end{aligned} \tag{17}$$

This implies that $H^{\xi}(A)$ is a concave function of $A\in\Delta_n$. □

3. A Measure of Length

Let a finite set of n input symbols $X=(x_1,x_2,\ldots,x_n)$ be encoded using alphabet of D symbols; then it has been shown by Feinstein [8] that there is a uniquely decipherable code with lengths $N_1,N_2,\ldots,N_n$ if and only if Kraft's inequality holds; that is,

$$\sum_{i=1}^{n}D^{-N_i}\le 1, \tag{18}$$

where D is the size of code alphabet. Furthermore, if

$$L=\sum_{i=1}^{n}N_i a_i \tag{19}$$

is the average code word length, then for a code satisfying (18), the inequality

$$L\ge H(A) \tag{20}$$

is also fulfilled and the equality $L=H(A)$ holds if and only if

$$\begin{aligned}&N_i=-\log_D\left(a_i\right);\quad \forall i=1,2,\ldots,n,\\ &\sum_{i=1}^{n}D^{-N_i}=1.\end{aligned} \tag{21}$$

If $L<H(A)$, then by being suitably encoded into words of long sequences, the average length can be made arbitrarily close to $H(A)$ (see Feinstein [8]). This is Shannon's noiseless coding theorem. By considering Rényi's entropy [2], a coding theorem analogous to the above noiseless coding theorem has been established by Campbell [9] and the authors obtained bounds for it in terms of $H_{Re}(A;\xi)$.

Kieffer [10] defined class rules and showed $H_{Re}(A;\xi)$ is the best decision rule for deciding which of the two sources can be coded with expected cost of sequence of length N when $N\to\infty$, where the cost of encoding a sequence is assumed to be a function of length only. Further, in Jelinek [11], it is shown that coding with respect to Campbell's mean length is useful in minimizing the problem of buffer overflow which occurs when the source symbol is produced at a fixed rate and the code words are stored temporarily in a finite buffer.

There are many different codes whose lengths satisfy the constraints (18). To compare different codes and pick out an optimum code it is customary to examine the mean length, $\sum_{i=1}^{n}N_i a_i$, and to minimize this quantity. This is a good procedure if the cost of using a sequence of length N_i is directly proportional to N_i. However, there may be occasions when the cost is more nearly an exponential function of N_i. This could be the case, for example, if the cost of encoding and decoding equipment was an important factor. Thus, in some circumstances, it might be more appropriate to choose a code which minimizes the quantity

$$\begin{aligned}C=&\left[\xi\log_D\left(\sum_{i=1}^{n}a_i D^{-N_i((\xi-1)/\xi)}\right)\right.\\ &\left.+\left(\sum_{i=1}^{n}a_i D^{-N_i(\xi-1)/\xi}\right)^{\xi}-1\right];\quad \xi>0\,(\neq 1),\end{aligned} \tag{22}$$

where ξ is a parameter related to the cost. For reasons which will become evident later we prefer to minimize a monotonic function of C. Clearly, this will minimize C.

In order to make the result of this paper more directly comparable with the usual coding theorem we introduce a quantity which resembles the mean length. Let a code length of order ξ be defined by

$$\begin{aligned}L^{\xi}(A)=&\frac{1}{\xi^{-1}-\xi}\left[\xi\log_D\left(\sum_{i=1}^{n}a_i D^{-N_i((\xi-1)/\xi)}\right)\right.\\ &\left.+\left(\sum_{i=1}^{n}a_i D^{-N_i(\xi-1)/\xi}\right)^{\xi}-1\right],\quad \xi>0\,(\neq 1).\end{aligned} \tag{23}$$

Remark 2. If $\xi=1$, then (23) becomes the well-known result studied by Shannon.

Remark 3. If all N_i are the same, say, $N_i=N$, then (23) becomes

$$L^{\xi}(P)=\frac{1}{\xi^{-1}-\xi}\left[N(1-\xi)+1-D^{N(1-\xi)}\right];\quad \xi>0\,(\neq 1). \tag{24}$$

This is reasonable property for any measure of length to possess.

Table 1: $\xi > 0 (\neq 1)$ (taking $\xi = 0.5$). Relation between the entropy $H^{\xi}(A)$ and the average code word length $L^{\xi}(A)$. N_i denote the lengths of Huffman code words, $\eta = H^{\xi}(A)/L^{\xi}(A)$ is the efficiency code, and $\nu = 1 - \eta$ is the redundancy of the code.

Relation between $H^{\xi}(A)$ and $L^{\xi}(A)$							
Length of Huffman code words (N_i)	Huffman code words	a_i	ξ	$H^{\xi}(A)$	$L^{\xi}(A)$	Efficiency code $\eta = \frac{H^{\xi}(A)}{L^{\xi}(A)}$	Redundancy code $\nu = 1 - \eta$
2	00	0.3	0.5	1.7228	1.8707	0.9209	0.0791
2	10	.25					
2	11	0.2					
3	011	0.1					
4	0100	0.1					
4	0101	.05					

In the following theorem, we give a lower bound for $L^{\xi}(A)$ in terms of $H^{\xi}(A)$.

Theorem 4. *If $N_1, N_2, \ldots, N_n$, denote the length of a uniquely decipherable code satisfying (18); then*

$$L^{\xi}(A) \geq H^{\xi}(A). \tag{25}$$

Proof. By Hölder's inequality,

$$\left[\sum_{i=1}^{n} x_i^p\right]^{1/p} \left[\sum_{i=1}^{n} y_i^q\right]^{1/q} \leq \sum_{i=1}^{n} x_i y_i, \tag{26}$$

for all $x_i, y_i > 0$, $i = 1, 2, \ldots, n$, and $1/p + 1/q = 1$; $p < 1 (\neq 0)$; $q < 0$; or $q < 1 (\neq 0)$; $p < 0$; equality holds if and only if, for some c, $x_i^p = cy_i^q$. Note that the direction of Hölder's inequality is reverse of the usual one for $p < 1$. (Beckenbach and Bellman [12], see p. 19). Making the substitutions, $p = (\xi - 1)/\xi$; $q = 1 - \xi$; $x_i = a_i^{\xi/(\xi-1)} D^{-N_i}$; $y_i = a_i^{\xi/(1-\xi)}$, in (26) and simplifying using (18). The following cases arise.

Case 1 (*when* $\xi > 1$)

$$\left[\sum_{i=1}^{n} a_i D^{-N_i((\xi-1)/\xi)}\right] \leq \left[\sum_{i=1}^{n} a_i^{\xi}\right]^{1/\xi}. \tag{27}$$

From (27), we get

$$\xi \log_D \left(\sum_{i=1}^{n} a_i D^{-N_i((\xi-1)/\xi)}\right) + \left(\sum_{i=1}^{n} a_i D^{-N_i((\xi-1)/\xi)}\right)^{\xi} - 1 \leq \log_D \left(\sum_{i=1}^{n} a_i^{\xi}\right) + \left(\sum_{i=1}^{n} a_i^{\xi}\right) - 1. \tag{28}$$

Also,

$$\xi^{-1} - \xi < 0 \quad \text{for } \xi > 1. \tag{29}$$

Thus, from (28) and (29), we may conclude that $H^{\xi}(A) \leq L^{\xi}(A)$.

Case 2 (*when* $0 < \xi < 1$)

$$\left[\sum_{i=1}^{n} a_i D^{-N_i((\xi-1)/\xi)}\right] \geq \left[\sum_{i=1}^{n} a_i^{\xi}\right]^{1/\xi}. \tag{30}$$

From (30), we get

$$\xi \log_D \left(\sum_{i=1}^{n} a_i D^{-N_i((\xi-1)/\xi)}\right) + \left(\sum_{i=1}^{n} a_i D^{-N_i((\xi-1)/\xi)}\right)^{\xi} - 1 \geq \log_D \left(\sum_{i=1}^{n} a_i^{\xi}\right) + \left(\sum_{i=1}^{n} a_i^{\xi}\right) - 1. \tag{31}$$

Also,

$$\xi^{-1} - \xi > 0 \quad \text{for } 0 < \xi < 1. \tag{32}$$

From (31) and (32), we get

$$H^{\xi}(A) \leq L^{\xi}(A). \tag{33}$$

Case 3. It is clear that the equality in (25) is valid if $N_i = -\log_D(a_i^{\xi} / \sum_{i=1}^{n} a_i^{\xi})$. The necessity of this condition for equality in (25) follows from the condition for equality in Hölder's inequality: in the case of reverse Hölder's equality given above, equality holds if and only if for some c,

$$x_i^p = cy_i^q, \quad i = 1, 2, \ldots, n. \tag{34}$$

Plugging this condition into our situation, with the x_i, y_i and p, q as specified, and using the fact that $\sum_{i=1}^{n} a_i = 1$, the necessity is true one. This proves the theorem. □

Remark 5. Huffman [13] introduced a measure for designing a variable length source code which achieves performance close to Shannon's entropy bound. For individual code word lengths N_i, the average length $\overline{L} = \sum_{i=1}^{n} a_i N_i$ of Huffman code is always within one unit of Shannon's measure of entropy; that is, $H(A) \leq \overline{L} < H(A)+1$, where $H(A) = -\sum_{i=1}^{n} a_i \log_2(a_i)$ is the Shannon's measure of entropy. Huffman coding scheme can also be applied to code word length $L^{\xi}(A)$ for code word length N_i; the average length $L^{\xi}(A)$ of Huffman code satisfies

$$L^{\xi}(A) \geq H^{\xi}(A). \tag{35}$$

In Table 1, we have developed the relation between the entropy $H^{\xi}(A)$ and average code word length $L^{\xi}(A)$.

Table 2: Computed values $L^{\xi}(A)$ with respect to ξ ($\xi < 1$).

ξ	.1	.2	.3	.4	.5	.6	.7	.8	.9
$L^{\xi}(A)$	1.25	1.67	1.78	1.82	1.87	1.92	1.96	1.99	2.01

Table 3: Computed values $L^{\xi}(A)$ with respect to ξ ($\xi > 1$).

ξ	10	20	30	40	50	60	70	80	90	100
$L^{\xi}(A)$	2.1618	2.2037	2.2199	2.2285	2.2337	2.2373	2.2399	2.2418	2.2433	2.2446

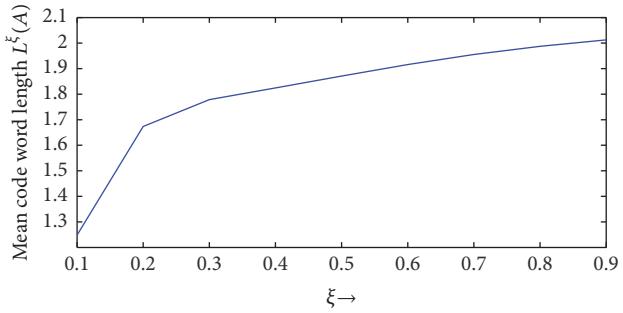

Figure 1: Monotonic behaviour of mean code word length $L^{\xi}(A)$ ($\xi < 1$).

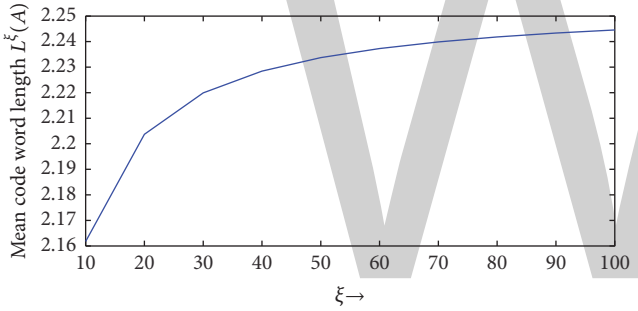

Figure 2: Monotonic behaviour of mean code word length $L^{\xi}(A)$ ($\xi > 1$).

From the Table 1, we can observe that average code word length $L^{\xi}(A)$ exceeds the entropy $H^{\xi}(A)$.

4. Monotonic Behaviour of Mean Code Word Length

In this section, we study the monotonic behaviour of mean code word length (23) with respect to parameter ξ. Let $P = (0.3, 0.25, 0.2, 0.1, 0.1, 0.05)$ be the set of probabilities. For different values of ξ, the calculated values of $L^{\xi}(A)$ are displayed in Tables 2 and 3.

Graphical representation of monotonic behaviour of $L^{\xi}(A)$ for ($\xi < 1$) is shown in Figure 1.

Graphical representation of monotonic behaviour of $L^{\xi}(A)$ for ($\xi > 1$) is shown in Figure 2.

Figures 1 and 2 explain the monotonic behaviour of $L^{\xi}(A)$ for $\xi < 1$ and $\xi > 1$, respectively. From the figures, it is clear that $L^{\xi}(A)$ is monotonically increasing for $\xi < 1$ as well as $\xi > 1$.

Conflicts of Interest

The authors declare that there are no conflicts of interest regarding the publication of this paper.

References

[1] C. E. Shannon, "A mathematical theory of communication," *Bell System Technical Journal*, vol. 27, no. 4, pp. 623–656, 1948.

[2] A. Rényi, "On measures of entropy and information," in *Proceedings of the 4th Berkeley Symposium on Mathematical Statistics and Probability*, pp. 547–561, University of California Press, 1961.

[3] J. Havrda and F. S. Charvát, "Quantification method of classification processes. Concept of structural α-entropy," *Kybernetika*, vol. 3, pp. 30–35, 1967.

[4] C. Tsallis, "Possible generalization of Boltzmann-Gibbs statistics," *Journal of Statistical Physics*, vol. 52, no. 1-2, pp. 479–487, 1988.

[5] N. R. Pal and S. K. Pal, "Object-background segmentation using new definitions of entropy," *IEE Proceedings Part E Computers and Digital Techniques*, vol. 136, no. 4, pp. 284–295, 1989.

[6] N. R. Pal and S. K. Pal, "Entropy: a new definition and its applications," *The Institute of Electrical and Electronics Engineers Systems, Man, and Cybernetics Society*, vol. 21, no. 5, pp. 1260–1270, 1991.

[7] T. O. Kvalseth, "On exponential entropies," in *Proceedings of the IEEE International Conference on Systems, Man And Cybernatics*, vol. 4, pp. 2822–2826, 2000.

[8] A. Feinstein, *Foundations of Information Theory*, McGraw-Hill, New York, NY, USA, 1956.

[9] L. L. Campbell, "A coding theorem and Rényi's entropy," *Information and Control*, vol. 8, no. 4, pp. 423–429, 1965.

[10] J. C. Kieffer, "Variable-length source coding with a cost depending only on the code word length," *Information and Control*, vol. 41, no. 2, pp. 136–146, 1979.

[11] F. Jelinek, "Buffer overflow in variable length coding of fixed rate sources," *IEEE Transactions on Information Theory*, vol. 14, no. 3, pp. 490–501, 1968.

[12] E. F. Beckenbach and R. Bellman, *Inequalities*, Springer, New York, NY, USA, 1961.

[13] D. A. Huffman, "A method for the construction of minimum-redundancy codes," *Proceedings of the IRE*, vol. 40, no. 9, pp. 1098–1101, 1952.

15

New Results on the (Super) Edge-Magic Deficiency of Chain Graphs

Ngurah Anak Agung Gede[1] and Adiwijaya[2]

[1]*Department of Civil Engineering, Universitas Merdeka Malang, Jl. Taman Agung No. 1, Malang 65146, Indonesia*
[2]*School of Computing, Telkom University, Jl. Telekomunikasi No. 1, Bandung 40257, Indonesia*

Correspondence should be addressed to Adiwijaya; kang.adiwijaya@gmail.com

Academic Editor: Dalibor Froncek

Let G be a graph of order v and size e. An *edge-magic labeling* of G is a bijection $f : V(G) \cup E(G) \to \{1, 2, 3, \ldots, v + e\}$ such that $f(x) + f(xy) + f(y)$ is a constant for every edge $xy \in E(G)$. An edge-magic labeling f of G with $f(V(G)) = \{1, 2, 3, \ldots, v\}$ is called a *super edge-magic labeling*. Furthermore, the *edge-magic deficiency* of a graph G, $\mu(G)$, is defined as the smallest nonnegative integer n such that $G \cup nK_1$ has an edge-magic labeling. Similarly, the *super edge-magic deficiency* of a graph G, $\mu_s(G)$, is either the smallest nonnegative integer n such that $G \cup nK_1$ has a super edge-magic labeling or $+\infty$ if there exists no such integer n. In this paper, we investigate the (super) edge-magic deficiency of chain graphs. Referring to these, we propose some open problems.

1. Introduction

Let G be a finite and simple graph, where $V(G)$ and $E(G)$ are its vertex set and edge set, respectively. Let $v = |V(G)|$ and $e = |E(G)|$ be the number of the vertices and edges, respectively. In [1], Kotzig and Rosa introduced the concepts of edge-magic labeling and edge-magic graph as follows: an *edge-magic labeling* of a graph G is a bijection $f : V(G) \cup E(G) \to \{1, 2, 3, \ldots, v + e\}$ such that $f(x) + f(xy) + f(y)$ is a constant, called the *magic constant* of f, for every edge xy of G. A graph that admits an edge-magic labeling is called an *edge-magic graph*. A *super edge-magic labeling* of a graph G is an edge-magic labeling f of G with the extra property that $f(V(G)) = \{1, 2, 3, \ldots, e\}$. A *super edge-magic graph* is a graph that admits a super edge-magic labeling. These concepts were introduced by Enomoto et al. [2] in 1998.

In [1], Kotzig and Rosa introduced the concept of edge-magic deficiency of a graph. They define the *edge-magic deficiency* of a graph G, $\mu(G)$, as the smallest nonnegative integer n such that $G \cup nK_1$ is an edge-magic graph. Motivated by Kotzig and Rosa's concept of edge-magic deficiency, Figueroa-Centeno et al. [3] introduced the concept of super edge-magic deficiency of a graph. The *super edge-magic deficiency* of a graph G, $\mu_s(G)$, is defined as the smallest nonnegative integer n such that $G \cup nK_1$ is a super edge-magic graph or $+\infty$ if there exists no such n.

A *chain graph* is a graph with blocks $B_1, B_2, \ldots, B_k$ such that, for every i, B_i and B_{i+1} have a common vertex in such a way that the block-cut-vertex graph is a path. We will denote the chain graph with k blocks $B_1, B_2, \ldots, B_k$ by $C[B_1, B_2, \ldots, B_k]$. If $B_1 = \cdots = B_t = B$, we will write $C[B_1, B_2, \ldots, B_k]$ as $C[B^{(t)}, B_{t+1}, \ldots, B_k]$. If, for every i, $B_i = H$ for a given graph H, then $C[B_1, B_2, \ldots, B_k]$ is denoted by kH-path. Suppose that $c_1, c_2, \ldots, c_{k-1}$ are the consecutive cut vertices of $C[B_1, B_2, \ldots, B_k]$. The *string* of $C[B_1, B_2, \ldots, B_k]$ is $(k-2)$-tuple $(d_1, d_2, \ldots, d_{k-2})$, where d_i is the distance between c_i and c_{i+1}, $1 \le i \le k-2$. We will write $(d_1, d_2, \ldots, d_{k-2})$ as $(d^{(t)}, d_{t+1}, \ldots, d_{k-2})$, if $d_1 = \cdots = d_t = d$.

For any integer $m \ge 2$, let $L_m = P_m \times P_2$. Let TL_m and DL_m be the graphs obtained from the ladder L_m by adding a single diagonal and two diagonals in each rectangle of L_m, respectively. Thus, $|V(\mathrm{TL}_m)| = |V(\mathrm{DL}_m)| = 2m$, $|E(\mathrm{TL}_m)| = 4m - 3$, and $|E(\mathrm{DL}_m)| = 5m - 4$. TL_m and DL_m are called triangle ladder and diagonal ladder, respectively.

Recently, the author studied the (super) edge-magic deficiency of $k\mathrm{DL}_m$-path, $C[K_4^{(k)}, \mathrm{DL}_m, K_4^{(n)}]$, and kC_4-path with some strings. Other results on the (super) edge-magic

deficiency of chain graphs can be seen in [4]. The latest developments in this area can be found in the survey of graph labelings by Gallian [5]. In this paper, we further investigate the (super) edge-magic deficiency of chain graphs whose blocks are combination of TL_m and DL_m and K_4 and TL_m, as well as the combination of C_4 and L_m. Additionally, we propose some open problems related to the (super) edge-magic deficiency of these graphs. To present our results, we use the following lemmas.

Lemma 1 (see [6]). *A graph G is a super edge-magic graph if and only if there exists a bijective function $f : V(G) \to \{1, 2, \ldots, v\}$ such that the set $S = \{f(x) + f(y) : xy \in E(G)\}$ consists of e consecutive integers.*

Lemma 2 (see [2]). *If G is a super edge-magic graph, then $e \leq 2v - 3$.*

2. Main Results

For $k \geq 3$, let $G = C[B_1, B_2, \ldots, B_k]$, where $B_j = TL_m$ when j is odd and $B_j = DL_m$ when j is even. Thus G is a chain graph with $|V(G)| = (2m-1)k+1$ and $|E(G)| = (1/2)(k+1)(4m-3)+(1/2)(k-1)(5m-4)$ when k is odd, or $|E(G)| = (k/2)(4m-3)+(k/2)(5m-4)$ when k is even. By Lemma 2, it can be checked that G is not super edge-magic when $m \geq 3$ and k is even and when $m \geq 4$ and k is odd. As we can see later, when $m = 3$ and k is odd, G is super edge-magic. Next, we investigate the super edge-magic deficiency of G. Our first result gives its lower bound. This result is a direct consequence of Lemma 2, so we state the result without proof.

Lemma 3. *Let $k \geq 3$ be an integer. For any integer $m \geq 3$,*

$$\mu_s(G) \geq \begin{cases} \left\lfloor \frac{1}{4}k(m-3) \right\rfloor + 1, & \text{if } k \text{ is even,} \\ \left\lfloor \frac{1}{4}(k(m-3) - (m-1)) \right\rfloor + 1, & \text{if } k \text{ is odd.} \end{cases} \quad (1)$$

Notice that the lower bound presented in Lemma 3 is sharp. We found that when m is odd, the chain graph G with particular string has the super edge-magic deficiency equal to its lower bound as we state in Theorem 4. First, we define vertex and edge sets of B_j as follows.

$V(B_j) = \{u_j^i, v_j^i : 1 \leq i \leq m\}$, for $1 \leq j \leq k$. $E(B_j) = \{u_j^i u_j^{i+1}, v_j^i v_j^{i+1} : 1 \leq i \leq m-1\} \cup \{e_j^i$: where e_j^i is either $u_j^i v_j^{i+1}$ or $v_j^i u_j^{i+1}, 1 \leq i \leq m-1\} \cup \{u_j^i v_j^i : 1 \leq i \leq m\}$, for $1 \leq j \leq k$, when j is odd, and $E(B_j) = \{u_j^i u_j^{i+1}, v_j^i v_j^{i+1}, u_j^i v_j^{i+1}, v_j^i u_j^{i+1} : 1 \leq i \leq m-1\} \cup \{u_j^i v_j^i : 1 \leq i \leq m\}$, for $1 \leq j \leq k$, when j is even.

Theorem 4. *Let $k \geq 3$ be an integer and $G = C[B_1, B_2, \ldots, B_k]$ with string $(m-1, d_1, m-1, d_2, m-1, \ldots, d_{(1/2)(k-3)}, m-1)$ when k is odd or $(m-1, d_1, m-1, d_2, \ldots, m-1, d_{(1/2)(k-2)})$ when k is even, where $d_1, d_2, \ldots, d_{\lfloor (1/2)(k-2) \rfloor} \in \{m-1, m\}$. For any odd integer $m \geq 3$,*

$$\mu_s(G) = \begin{cases} \frac{1}{4}k(m-3) + 1, & \text{if } k \text{ is even,} \\ \frac{1}{4}(k-1)(m-3), & \text{if } k \text{ is odd.} \end{cases} \quad (2)$$

Proof. First, we define G as a graph with vertex set $V(G) = \bigcup_{j=1}^{k} V(B_j)$, where $u_j^m = v_{j+1}^1$, $1 \leq j \leq k-1$, and edge set $E(G) = \bigcup_{j=1}^{k} E(B_j)$. Under this definition, $u_j^m = v_{j+1}^1$, $1 \leq j \leq k-1$, are the cut vertices of G.

Next, for $1 \leq i \leq m$ and $1 \leq j \leq k$, define the labeling $f : V(G) \cup \alpha K_1 \to \{1, 2, 3, \ldots, (2m-1)k + 1 + \alpha\}$, where $\alpha = (1/4)k(m-3)+1$ when k is even or $\alpha = (1/4)(k-1)(m-3)$ when k is odd, as follows:

$$f(x) = \begin{cases} \frac{1}{4}(j-1)(9m-7) + 2i - 1, & \text{if } x = u_j^i,\ j \text{ is odd,} \\ \frac{1}{4}(j-1)(9m-7) + 2i, & \text{if } x = v_j^i,\ j \text{ is odd,} \\ \beta + \frac{1}{2}(5i-3), & \text{if } x = u_j^i,\ i \text{ is odd},\ j \text{ is even,} \\ \beta + \frac{1}{2}(5i-4), & \text{if } x = u_j^i,\ i \text{ is even},\ j \text{ is even,} \\ \beta + \frac{1}{2}(5i-7), & \text{if } x = v_j^i,\ i \text{ is odd},\ j \text{ is even,} \\ \beta + \frac{1}{2}(5i-6), & \text{if } x = v_j^i,\ i \text{ is even},\ j \text{ is even,} \end{cases} \quad (3)$$

where $\beta = (1/4)(j-2)(9m-7) + 2m$.

Under the vertex labeling f, it can be checked that no labels are repeated, $f(u_j^m) = f(v_{j+1}^1)$, $1 \leq j \leq k-1$, $\{f(x) + f(y) : xy \in E(G)\}$ is a set of $|E(G)|$ consecutive integers, and the largest vertex label used is $(1/4)(k-2)(9m-7)+(1/2)(9m-3)$ when k is even or $(1/4)(k-1)(9m-7)+2m$ when k is odd. Also, it can be checked that $f(u_j^i) + f(v_j^{i+1}) = f(v_j^i) + f(u_j^{i+1})$ when j is odd.

Next, label the isolated vertices in the following way.

Case k Is Odd. In this case, we denote the isolated vertices with $\{z_{2j-1}^l \mid 1 \leq l \leq (1/2)(m-3), 1 \leq j \leq (1/2)(k-1)\}$ and set $f(z_{2j-1}^l) = f(v_{2j-1}^m) + 5l$.

Case k Is Even. In this case, we denote the isolated vertices with $\{z_{2j-1}^l \mid 1 \leq l \leq (1/2)(m-3), 1 \leq j \leq k/2\} \cup \{z_0\}$ and set $f(z_{2j-1}^l) = f(v_{2j-1}^m) + 5l$ and $f(z_0) = f(v_k^m) + 1$.

By Lemma 1, f can be extended to a super edge-magic labeling of $G \cup \alpha K_1$ with the magic constant $(k/4)(27m-21)+5$ when k is even or $(1/4)(k-1)(27m-21) + 6m$ when k is odd. Based on these facts and Lemma 3, we have the desired result. □

An example of the labeling defined in the proof of Theorem 4 is shown in Figure 1(a).

Notice that when $m = 3$ and k is odd, $\mu_s(G) = 0$. In other words, the chain graph G with string $(2, d_1, 2, d_2, 2, \ldots, d_{(1/2)(k-3)}, 2)$, where $d_i \in \{2, 3\}$, is super edge-magic

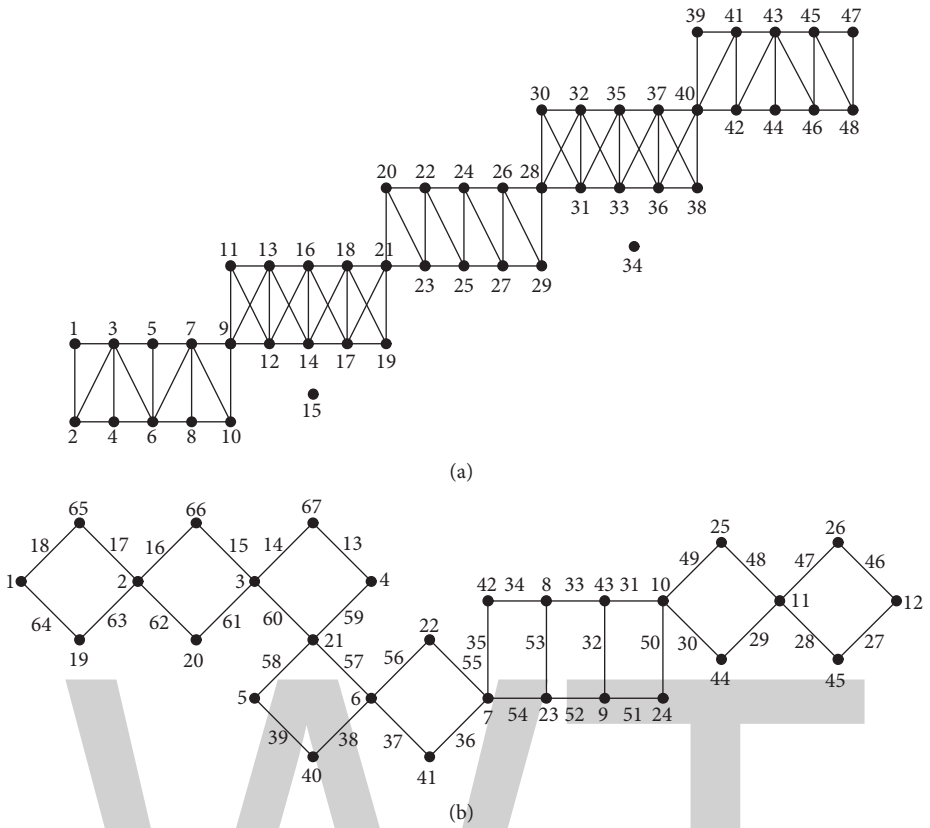

FIGURE 1: (a) Vertex labeling of $C[\mathrm{TL}_5, \mathrm{DL}_5, \mathrm{TL}_5, \mathrm{DL}_5, \mathrm{TL}_5] \cup 2K_1$ with string (4, 5, 4). (b) Vertex and edge labelings of $c[C_4^{(3+2)}, L_4, C_4^{(2)}]$ with string $(2, 1^{(2)}, 2, 4, 2)$.

when $m = 3$ and k is odd. Based on this fact and previous results, we propose the following open problems.

Open Problem 1. Let $k \geq 3$ be an integer. For $m = 2$, decide if there exists a super edge-magic labeling of G. Further, for any even integer $m \geq 2$, find the super edge-magic deficiency of G.

Next, we investigate the super edge-magic deficiency of the chain graph $H = C[K_4^{(p)}, \mathrm{TL}_m, K_4^{(q)}]$ with string $(1^{(p-1)}, d, 1^{(q-1)})$, where $d \in \{m-1, m\}$. H is a graph of order $3(p+q)+2m$ and size $6(p+q)+4m-3$. We define the vertex and edge sets of H as follows: $V(H) = \{a_i, b_i : 1 \leq i \leq p\} \cup \{c_i : 1 \leq i \leq p+1\} \cup \{u_j, v_j : 1 \leq j \leq m\} \cup \{x_t, y_t : 1 \leq t \leq q\} \cup \{z_t : 1 \leq t \leq q+1\}$, where $c_{p+1} = u_1$ and $v_m = z_1$, and $E(H) = \{a_i b_i, a_i c_i, a_i c_{i+1}, b_i c_i, b_i c_{i+1}, c_i c_{i+1} : 1 \leq i \leq p\} \cup \{u_j v_j \mid 1 \leq j \leq m\} \cup \{u_j u_{j+1}, v_j v_{j+1} : 1 \leq j \leq m-1\} \cup \{e_j : e_j \text{ is either } u_j v_{j+1} \text{ or } v_j u_{j+1}, 1 \leq j \leq m-1\} \cup \{x_t y_t, x_t z_t, x_t z_{t+1}, y_t z_t, y_t z_{t+1}, z_t z_{t+1} : 1 \leq t \leq q\}$. Hence, the cut vertices of H are c_i, $2 \leq i \leq p+1$, and z_t, $1 \leq t \leq q$. Notice that H has string $(1^{(p-1)}, m-1, 1^{(q-1)})$, if at least one of e_j is $u_j v_{j+1}$, and its string is $(1^{(p-1)}, m, 1^{(q-1)})$, if $e_j = v_j u_{j+i}$ for every $1 \leq j \leq m-1$.

Theorem 5. *For any integers $p, q \geq 1$ and $m \geq 2$, $\mu_s(H) = 0$.*

Proof. Define a bijective function $g : V(H) \to \{1, 2, 3, \ldots, 3(p+q)+2m\}$ as follows:

$$g(x) = \begin{cases} 3i-2, & \text{if } x = a_i,\ 1 \leq i \leq p, \\ 3i, & \text{if } x = b_i,\ 1 \leq i \leq p, \\ 3i-1, & \text{if } x = c_i,\ 1 \leq i \leq p+1, \\ 3p+2j, & \text{if } x = u_j,\ 1 \leq j \leq m, \\ 3p+2j-1, & \text{if } x = v_j,\ 1 \leq j \leq m, \\ 3p+2m+3t-2, & \text{if } x = x_t,\ 1 \leq t \leq q, \\ 3p+2m+3t, & \text{if } x = y_t,\ 1 \leq t \leq q, \\ 3p+2m+3t-4, & \text{if } x = z_t,\ 1 \leq t \leq q+1. \end{cases} \quad (4)$$

Under the labeling g, it can be checked that $g(c_{p+1}) = g(u_1)$ and $g(v_m) = g(z_1)$. Also, it can be checked that $g(u_j) + g(v_{j+1}) = g(v_j) + g(u_{j+1})$, $1 \leq j \leq m-1$, and $\{g(x) + g(y) \mid xy \in E(H)\} = \{3, 4, 5, \ldots, 6(p+q)+4m-1\}$. By Lemma 1, g can be extended to a super edge-magic labeling of H with the magic constant $9(p+q)+6m$. Hence, $\mu_s(H) = 0$. □

Open Problem 2. For any integers $p, q \geq 1$ and $m \geq 2$, find the super edge-magic deficiency of $C[K_4^{(p)}, \mathrm{TL}_m, K_4^{(q)}]$ with string $(1^{(p-1)}, d, 1^{(q-1)})$, where $d \in \{1, 2, 3, \ldots, m-2\}$.

Next, we study the edge-magic deficiency of ladder L_m and chain graphs whose blocks are combination of C_4 and L_m with some strings. In [6], Figueroa-Centeno et al. proved that the ladder L_m is super edge-magic for any odd m and suspected that L_m is super edge-magic for any even $m > 2$. Here, we can prove that L_m is edge-magic for any $m \geq 2$ by showing its edge-magic deficiency is zero. The result is presented in Theorem 6.

Theorem 6. *For any integer $m \geq 2$, $\mu(L_m) = 0$.*

Proof. Let $V(L_m) = \{u_i, v_i : 1 \leq i \leq m\}$ and $E(G) = \{u_iu_{i+1}, v_iv_{i+1}: 1 \leq i \leq m-1\} \cup \{u_iv_i : 1 \leq i \leq m\}$ be the vertex set and edge set, respectively, of L_m. It is easy to verify that the labeling $h : V(L_m) \cup E(L_m) \to \{1, 2, 3, \ldots, 5m-2\}$ is a bijection and, for every $xy \in E(L_m)$, $h(x)+h(xy)+h(y) = 6m$.

$$h(x) = \begin{cases} i, & \text{if } x = u_i,\ i \text{ is odd},\\ 3m + \frac{1}{2}(i-2), & \text{if } x = u_i,\ i \text{ is even},\\ m + \frac{1}{2}(i+1), & \text{if } x = v_i,\ i \text{ is odd},\\ i, & \text{if } x = v_i,\ i \text{ is even},\\ 3m - \frac{1}{2}(3i-1), & \text{if } x = u_iu_{i+1},\ i \text{ is odd},\\ 3m - \frac{3}{2}i, & \text{if } x = u_iu_{i+1},\ i \text{ is even},\\ 5m - \frac{3}{2}(i+1), & \text{if } x = v_iv_{i+1},\ i \text{ is odd},\\ 5m - \frac{1}{2}(3i+2), & \text{if } x = v_iv_{i+1},\ i \text{ is even},\\ 5m - \frac{1}{2}(3i+1), & \text{if } x = u_iv_i,\ i \text{ is odd},\\ 3m - \frac{1}{2}(3i-2), & \text{if } x = u_iv_i,\ i \text{ is even}. \end{cases} \quad (5)$$

Thus, $\mu(L_m) = 0$ for every $m \geq 2$. □

Theorem 7. *Let p and $q \geq 1$ be integers.*

(a) *If $m \geq 2$ is an even integer and $F_1 = C[C_4^{(p)}, L_m, c_4^{(q)}]$ with string $(2^{(p-1)}, m, 2^{(q-1)})$, then $\mu(F_1) = 0$.*

(b) *If $m \geq 3$ is an odd integer and $F_2 = C[C_4^{(p)}, L_m, c_4^{(q)}]$ with string $(2^{(p-1)}, m-1, 2^{(q-1)})$, then $\mu(F_2) = 0$.*

Proof. (a) First, we introduce a constant λ as follows: $\lambda = 1$, if m is odd and $\lambda = 2$, if m is even. Next, we define F_1 as a graph with $V(F_1) = \{a_i, b_i: 1 \leq i \leq p\} \cup \{c_i: 1 \leq i \leq p+1\} \cup \{u_j, v_j: 1 \leq j \leq m\} \cup \{x_t, y_t: 1 \leq t \leq q\} \cup \{z_t: 1 \leq t \leq q+1\}$, where $c_{p+1} = v_1$ and $u_m = z_1$, and $E(H) = \{c_ia_i, c_ib_i, a_ic_{i+1}, b_ic_{i+1}: 1 \leq i \leq p\} \cup \{u_jv_j \mid 1 \leq j \leq m\} \cup \{u_ju_{j+1}, v_jv_{j+1}: 1 \leq j \leq m-1\} \cup \{z_tx_t, z_ty_t, x_tz_{t+1}, y_tz_{t+1}: 1 \leq t \leq q\}$. The cut vertices of F_1 are c_i, $2 \leq i \leq p+1$, and z_t, $1 \leq t \leq q$.

Next, define a bijection $f_1 : V(F_1) \cup E(F_1) \to \{1, 2, 3, \ldots, 7(p+q)+5m-2\}$ as follows:

$$f_1(x) = \begin{cases} 4(p+q)+3m+i-1, & \text{if } x = a_i,\ 1 \leq i \leq p,\\ p+q+m+i, & \text{if } x = b_i,\ 1 \leq i \leq p,\\ i, & \text{if } x = c_i,\ 1 \leq i \leq p+1,\\ 5p+4q+3m+\frac{1}{2}(j-1), & \text{if } x = u_j,\ j \text{ is odd},\\ p+j, & \text{if } x = u_j,\ j \text{ is even},\\ p+j, & \text{if } x = v_j,\ j \text{ is odd},\\ 2p+q+m+\frac{j}{2}, & \text{if } x = v_j,\ j \text{ is even},\\ 5p+4q+\gamma_1+t, & \text{if } x = x_t,\ 1 \leq t \leq q,\\ 2p+q+\gamma_2+t, & \text{if } x = y_t,\ 1 \leq t \leq q,\\ p+m+t-1, & \text{if } x = z_t,\ 1 \leq t \leq q+1,\\ 4(p+q)+3m+1-2i, & \text{if } x = c_ia_i,\ 1 \leq i \leq p,\\ 7(p+q)+5m-2i, & \text{if } x = c_ib_i,\ 1 \leq i \leq p,\\ 4(p+q)+3m-2i, & \text{if } x = a_ic_{i+1},\ 1 \leq i \leq p,\\ 7(p+q)+5m-1-2i, & \text{if } x = b_ic_{i+1},\ 1 \leq i \leq p,\\ 2p+4q+3m-\frac{1}{2}(3j+1), & \text{if } x = u_ju_{j+1},\ j \text{ is odd},\\ 2p+4q+3m-\frac{1}{2}(3j), & \text{if } x = u_ju_{j+1},\ j \text{ is even},\\ 5p+7q+5m-\frac{1}{2}(3j+1), & \text{if } x = v_jv_{j+1},\ j \text{ is odd},\\ 5p+7q+5m-\frac{1}{2}(3j+2), & \text{if } x = v_jv_{j+1},\ j \text{ is even},\\ 2p+4q+3m-\frac{1}{2}(3i-1), & \text{if } x = u_jv_j,\ j \text{ is odd},\\ 5p+7q+5m-\frac{3}{2}j, & \text{if } x = u_jv_j,\ j \text{ is even},\\ 2p+4q+\gamma_3-2t & \text{if } x = z_tx_t,\ 1 \leq t \leq q,\\ 5p+7q+\gamma_4-2t, & \text{if } x = z_ty_t,\ 1 \leq t \leq q,\\ 2p+4q+\gamma_5-2t, & \text{if } x = x_tz_{t+1},\ 1 \leq t \leq q,\\ 5p+7q+\gamma_6-2t, & \text{if } x = y_tz_{t+1},\ 1 \leq t \leq q, \end{cases} \quad (6)$$

where $\gamma_1 = (1/2)(\lambda-1)(7m-2) - (1/2)(\lambda-2)(7m-1)$, $\gamma_2 = (1/2)(\lambda-1)(3m) - (1/2)(\lambda-2)(3m-1)$, $\gamma_3 = (1/2)(\lambda-1)(3m+4) - (1/2)(\lambda-2)(3m+3)$, $\gamma_4 = (1/2)(\lambda-1)(7m+2) - (1/2)(\lambda-2)(7m+3)$, $\gamma_5 = (1/2)(\lambda-1)(3m+2) - (1/2)(\lambda-2)(3m+1)$, and $\gamma_6 = (1/2)(\lambda-1)(7m) - (1/2)(\lambda-2)(7m+1)$. It is easy to verify that, for every edge $xy \in E(F_1)$, $f(x) + f(xy) + f(y) = 8(p+q) + 6m$.

(b) We define F_2 as graph with $V(F_2) = V(F_1)$, where $c_{p+1} = v_1$ and $v_m = z_1$, and $E(F_2) = E(F_1)$. Under this definition, the cut vertices of F_2 are c_i, $2 \leq i \leq p+1$, and z_t, $1 \leq t \leq q$. Next, we define a bijection $f_2 : V(F_2) \cup E(F_2) \to \{1, 2, 3, \ldots, 7(p+q)+5m-2\}$, where $f_2(x) = f_1(x)$ for all $x \in V(F_2) \cup E(F_2)$. It can be checked that f_2 is an edge-magic labeling of F_2 with the magic constant $8(p+q)+6m$. □

Open Problem 3. Let p and $q \geq 1$ be integers.

(a) If $m \geq 3$ is an odd integer, find the super edge-magic deficiency of $C[C_4^{(p)}, L_m, c_4^{(q)}]$ with string $(2^{(p-1)}, m, 2^{(q-1)})$.

(b) If $m \geq 2$ is an even integer, find the super edge-magic deficiency of $C[C_4^{(p)}, L_m, c_4^{(q)}]$ with string $(2^{(p-1)}, m-1, 2^{(q-1)})$.

Theorem 8. *Let $p, q \geq 2$ and $r \geq 1$ be integers.*

(a) *If $m \geq 2$ is an even integer and $H_1 = C[C_4^{(p+q)}, L_m, c_4^{(r)}]$ with string $(2^{(p-2)}, 1^{(2)}, 2^{(q-1)}, m, 2^{(r-1)})$, then $\mu(H_1) = 0$.*

(b) *If $m \geq 3$ is an odd integer and $H_2 = C[C_4^{(p+q)}, L_m, c_4^{(r)}]$ with string $(2^{(p-2)}, 1^{(2)}, 2^{(q-1)}, m-1, 2^{(r-1)})$, then $\mu(H_2) = 0$.*

Proof. (a) First, we define H_1 as a graph with $V(H_1) = \{a_i: 1 \leq i \leq 2p\} \cup \{b_i: 1 \leq i \leq p+1\} \cup \{u_j: 1 \leq j \leq 2q\} \cup \{v_j: 1 \leq j \leq q+1\} \cup \{w_s: 1 \leq s \leq 2m\} \cup \{x_t: 1 \leq t \leq 2r\} \cup \{y_t: 1 \leq t \leq r+1\}$, where $a_{2p} = u_1$, $v_{q+1} = w_1$, and $w_{2m} = y_1$, and $E(H_1) = \{b_i a_i, b_i a_{p+i}, a_i b_{i+1}, a_{p+i} b_{i+1}: 1 \leq i \leq p\} \cup \{v_j u_j, v_j u_{q+j}, u_j v_{j+1}, u_{q+j} v_{j+1} \mid 1 \leq j \leq q\} \cup \{w_s w_{s+1}, w_{m+s} w_{m+s+1}: 1 \leq s \leq m-1\} \cup \{w_s w_{m+s}: 1 \leq s \leq m\} \cup \{y_t x_t, y_t x_{r+t}, x_t y_{t+1}, x_{r+t} y_{t+1}: 1 \leq t \leq r\}$.

Next, define a bijection $g_1 : V(H_1) \cup E(H_1) \to \{1, 2, 3, \ldots, 7(p+q+r) + 5m - 2\}$ as follows:

$$g_1(z) = \begin{cases} 6p + 7(q+r) + 5m + i - 2, & \text{if } z = a_i,\ 1 \leq i \leq p, \\ 3p + q + r + m + 1 + i, & \text{if } z = a_{p+i},\ 1 \leq i \leq p, \\ i, & \text{if } z = b_i,\ 1 \leq i \leq p+1, \\ 4p + q + r + m + j, & \text{if } z = u_j,\ 1 \leq j \leq q, \\ 4(p+q+r) + 3m + j - 1, & \text{if } z = u_{q+j},\ 1 \leq j \leq q, \\ p + 1 + j, & \text{if } z = v_j,\ 1 \leq j \leq q+1, \\ p + q + 1 + s, & \text{if } z = w_s,\ s \text{ is odd}, \\ 4p + 2q + r + m + \frac{1}{2}s, & \text{if } z = w_s,\ s \text{ is even}, \\ 4p + 5q + 4r + 3m + \frac{1}{2}(s-1), & \text{if } z = w_{m+s},\ s \text{ is odd}, \\ p + q + 1 + s, & \text{if } z = w_{m+s},\ s \text{ is even}, \\ 4p + 2q + r + \gamma_2 + t, & \text{if } z = x_t,\ 1 \leq t \leq r, \\ 4p + 5q + 4r + \gamma_1 + t, & \text{if } z = x_{r+t},\ 1 \leq t \leq r, \\ p + q + m + t, & \text{if } z = y_t,\ 1 \leq t \leq r+1, \\ 3p + q + r + m + 3 - 2i, & \text{if } z = b_i a_i,\ 1 \leq i \leq p, \\ 6p + 7(q+r) + 5m - 2i, & \text{if } z = b_i a_{p+i},\ 1 \leq i \leq p, \\ 3p + q + r + m + 2 - 2i, & \text{if } z = a_i b_{i+1},\ 1 \leq i \leq p, \\ 6p + 7(q+r) + 5m - 2i - 1, & \text{if } z = a_{p+i} b_{i+1},\ 1 \leq i \leq p, \\ 4p + 7(q+r) + 5m - 2j, & \text{if } z = v_j u_j,\ 1 \leq j \leq q, \\ 4(p+q+r) + 3m + 1 - 2j, & \text{if } z = v_j u_{q+j},\ 1 \leq j \leq q, \\ 4p + 7(q+r) + 5m - 2j - 1, & \text{if } z = u_j v_{j+1},\ 1 \leq j \leq q, \\ 4(p+q+r) + 3m - 2j, & \text{if } z = u_{q+j} v_{j+1},\ 1 \leq j \leq q, \\ 4p + 5q + 7r + 5m - \frac{1}{2}(3s+1), & \text{if } z = w_s w_{s+1},\ s \text{ is odd}, \\ 4p + 5q + 7r + 5m - \frac{1}{2}(3s+2), & \text{if } z = w_s w_{s+1},\ s \text{ is even}, \\ 4p + 2q + 4r + 3m - \frac{1}{2}(3s+1), & \text{if } z = w_{m+s} w_{m+s+1},\ s \text{ is odd}, \\ 4p + 2q + 4r + 3m - \frac{1}{2}(3s), & \text{if } z = w_{m+s} w_{m+s+1},\ s \text{ is even}, \\ 4p + 2q + 4r + 3m - \frac{1}{2}(3s-1), & \text{if } z = w_s w_{m+s},\ s \text{ is odd}, \\ 4p + 5q + 7r + 5m - \frac{3}{2}s, & \text{if } z = w_s w_{m+s},\ s \text{ is even}, \\ 4p + 5q + 7r + \gamma_4 - 2t, & \text{if } z = y_t x_t,\ 1 \leq t \leq r, \\ 4p + 2q + 4r + \gamma_3 - 2t, & \text{if } z = y_t x_{r+t},\ 1 \leq t \leq r, \\ 4p + 5q + 7r + \gamma_6 - 2t, & \text{if } z = x_t y_{t+1},\ 1 \leq t \leq r, \\ 4p + 2q + 4r + \gamma_5 - 2t, & \text{if } z = x_{r+t} y_{t+1},\ 1 \leq t \leq r, \end{cases} \tag{7}$$

where $\gamma_1, \gamma_2, \gamma_3, \gamma_4, \gamma_5, \gamma_6$, and λ are defined as in the proof of Theorem 7. It can be checked that, for every edge $xy \in E(H_1)$, $g_1(x)+g_1(xy)+g_1(y) = 9p+8(q+r)+6m+1$. Hence $\mu(H_1) = 0$.

An illustration of the labeling defined in the proof of Theorem 8 is given in Figure 1(b).

(b) We define H_2 as graph with $V(H_2) = V(H_1)$, where $a_{2p} = u_1$, $v_{q+1} = w_1$, and $w_m = y_1$, and $E(H_2) = E(H_1)$. It can be checked that $g_2 : V(H_2) \cup E(H_2) \to \{1, 2, 3, \ldots, 7(p+q+r)+5m-2\}$ defined by $g_2(x) = g_1(x)$, for all $x \in V(H_2) \cup E(H_2)$, is an edge-magic labeling of H_2 with the magic constant $9p + 8(q + r) + 6m + 1$. □

Open Problem 4. Let $p, q \geq 2$ and $r \geq 1$ be integers.

(a) If $m \geq 3$ is an odd integer, find the edge-magic deficiency of $C[C_4^{(p)}, c_4^{(q)}, L_m, c_4^{(r)}]$ with string $(2^{(p-2)}, 1^{(2)}, 2^{(q-1)}, m, 2^{(r-1)})$.

(b) If $m \geq 2$ is an even integer, find the edge-magic deficiency of $C[C_4^{(p)}, c_4^{(q)}, L_m, c_4^{(r)}]$ with string $(2^{(p-2)}, 1^{(2)}, 2^{(q-1)}, m-1, 2^{(r-1)})$.

Conflicts of Interest

The authors declare that there are no conflicts of interest regarding the publication of this paper.

Acknowledgments

The first author has been supported by "Hibah Kompetensi 2016" (018/SP2H/P/K7/KM/2016) from the Directorate General of Higher Education, Indonesia.

References

[1] A. Kotzig and A. Rosa, "Magic valuations of finite graphs," *Canadian Mathematical Bulletin*, vol. 13, pp. 451–461, 1970.

[2] H. Enomoto, A. S. Llado, T. Nakamigawa, and G. Ringel, "Super edge-magic graphs," *SUT Journal of Mathematics*, vol. 34, no. 2, pp. 105–109, 1998.

[3] R. M. Figueroa-Centeno, R. Ichishima, and F. A. Muntaner-Batle, "On the super edge-magic deficiency of graphs," *Electronic Notes in Discrete Mathematics*, vol. 11, pp. 299–314, 2002.

[4] A. A. Ngurah, E. T. Baskoro, and R. Simanjuntak, "On super edge-magic deficiency of graphs," *Australasian Journal of Combinatorics*, vol. 40, pp. 3–14, 2008.

[5] J. A. Gallian, "A dinamic survey of graph labelings," *Electron. J. Combin*, vol. 16, 2015, DS6.

[6] R. M. Figueroa-Centeno, R. Ichishima, and F. A. Muntaner-Batle, "The place of super edge-magic labelings among other classes of labelings," *Discrete Mathematics*, vol. 231, no. 1-3, pp. 153–168, 2001.

16

A Geometric Derivation of the Irwin-Hall Distribution

James E. Marengo, David L. Farnsworth, and Lucas Stefanic

School of Mathematical Sciences, Rochester Institute of Technology, Rochester, NY 14623, USA

Correspondence should be addressed to David L. Farnsworth; dlfsma@rit.edu

Academic Editor: Shyam L. Kalla

The Irwin-Hall distribution is the distribution of the sum of a finite number of independent identically distributed uniform random variables on the unit interval. Many applications arise since round-off errors have a transformed Irwin-Hall distribution and the distribution supplies spline approximations to normal distributions. We review some of the distribution's history. The present derivation is very transparent, since it is geometric and explicitly uses the inclusion-exclusion principle. In certain special cases, the derivation can be extended to linear combinations of independent uniform random variables on other intervals of finite length. The derivation adds to the literature about methodologies for finding distributions of sums of random variables, especially distributions that have domains with boundaries so that the inclusion-exclusion principle might be employed.

1. Introduction

The simple continuous uniform or rectangular distribution Uniform$(0,1)$ with probability density function (PDF) $f(x) = 1$ for $0 < x < 1$ and $f(x) = 0$ otherwise is very important. Two applications arise in numerical simulation and Bayesian analysis of proportions. If F is the cumulative distribution function (CDF) of the continuous random variable X, then the random variable $Y = F(X)$ has a Uniform$(0,1)$ distribution. The random variable X can be simulated by first simulating Y and then letting $X = F^{-1}(Y)$. This is called the *inversion method* ([1, page 295], [2, pages 194–196]). The transformation is called the *probability integral transformation* ([3], [4, pages 203-204]). The uniform distribution is a Bayesian *noninformative prior distribution* for the distribution of a random variable defined on the unit interval, such as a beta distribution for a proportion ([2, page 33], [5, pages 82–90]). For other applications and generalizations of the uniform distribution, see [6–8].

The present goal is to derive the CDF and the PDF of the sum $T = \sum_{i=1}^{n} X_i$, where X_i are independent identically distributed Uniform$(0,1)$ random variables for $i = 1, 2, \ldots, n$. The CDF and PDF are

$$F(t) = \sum_{i=0}^{n} \left[(-1)^i \binom{n}{i} \frac{(t-i)^n}{n!} s_i(t) \right], \tag{1}$$

$$f(t) = \sum_{i=0}^{n} \left[(-1)^i \binom{n}{i} \frac{(t-i)^{n-1}}{(n-1)!} s_i(t) \right], \tag{2}$$

respectively, where $s_a(t)$ is the unit step function

$$s_a(t) = \begin{cases} 0 & t < a \\ 1 & a \le t. \end{cases} \tag{3}$$

The derivation in Section 2 is geometric and explicitly uses the inclusion-exclusion principle.

Derivations of the distribution, which more recently acquired its name Irwin-Hall, go back to Lagrange and Laplace in the latter 18th century and the early 19th century. Lagrange used generating functions based on a^x to obtain the distribution of T ([9, pages 603–612], [10, page 283]). Those generating functions are a predecessor of characteristic functions [10, page 286]. Laplace often revisited the problem of finding the distribution of T and employed many methods ([9, pages 714-715], [10, pages 286–301]). The distribution is described in [1, pages 296–300], where it is called the *Irwin-Hall distribution*.

Some derivations employ characteristic functions in a variety of ways, since the characteristic function of a sum of independent random variables is the product of each summand's characteristic function and the inverse transform

is not intractable ([11, pages 188-189], [12–14], [15, pages 362-363], [16, 17]). Others utilize the convolution integral for sums and mathematical induction ([4, page 225], [11, pages 190-191 and 244–246], [18]). The distribution of the sum of uniform random variables that may have differing domains is found in [18–21]. Sums of dependent uniform random variables are examined in [22, 23].

Direct integration techniques can be used to obtain the distribution of a linear combination of Uniform(0, 1) random variables ([15, pages 358–360], [24, 25]). Similar techniques are used in [26] for uniform distributions whose domains are intervals with zero as their left endpoints. The distribution of the mean is obtained when all the constants are $1/n$. In this case, the distribution is called the *Bates distribution* ([1, page 297], [27]), which can also be found by a simple transformation of the Irwin-Hall distribution ([15, page 359], [25, page 241]). Using moment generating functions, instead of characteristic functions, Gray and Odell [28] found the distribution of any linear combination of uniform random variables with different domains allowed. In Section 3, the present method or style of proof is extended to those cases giving the same distributions.

Because T is a sum, the Irwin-Hall distribution approximates a normal distribution with a spline, since the Irwin-Hall distribution in (2) is composed of polynomials. The support of T is the interval $[0, n]$; the mean, mode, and median of T are $n/2$; and its variance is $n/12$. By symmetry, all odd central moments are zero, including skewness. The kurtosis is $3 - 6/(5n)$ [1, page 300]. This is the measure of kurtosis that is 3 for a normal distribution, so Irwin-Hall distributions are platykurtic, and the kurtosis is close to 3 for large n. According to the Central Limit Theorem,

$$Z = \frac{T - n/2}{\sqrt{n/12}} \xrightarrow{D} \text{Normal}(0, 1) \text{ as } n \longrightarrow \infty \tag{4}$$

([4, pages 280–283], [11, pages 213–218 and 245], [29, pages 220–222]). Figure 1 contains a normal distribution with mean $n/2 = 3/2$ and variance $n/12 = 3/12 = 1/4$ and its approximating Irwin-Hall distribution with $n = 3$. The approximation is very good even for this small value of n [30]. The uniform error bound for the normal(0, 1) CDF $\Phi(z)$ is

$$|F(z) - \Phi(z)| \leq \frac{\sqrt{3}}{20\sqrt{n}} \tag{5}$$

([31], [32, page 51]). Approximations with spline fitting can be useful with or without complete information about the distributional shape [33, 34].

Since round-off errors for random variables that are rounded to the nearest integer are distributed Uniform(−1/2, 1/2), the sum of round-off errors is a linearly transformed Irwin-Hall distribution [12]. For large n, the sum of round-off errors is easily described with a normal distribution [29, page 222]. For small n, the Irwin-Hall distribution is also appropriate and not too complicated.

Lee et al. [35] use the Irwin-Hall distribution to examine the efficacy of goodness-of-fit tests. Heinrich et al. [36] adapt the Irwin-Hall distribution in consideration of the accumulated accuracy of round-off errors. Inequalities for linear combinations of independent random variables whose domains have an upper bound are given in [37].

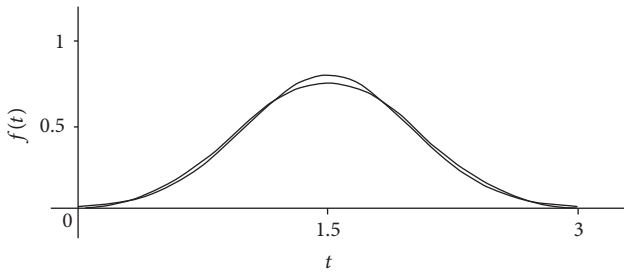

Figure 1: Irwin-Hall distribution with $n = 3$ and the matching normal distribution with mean 3/2 and variance 1/4.

2. Derivation of the Irwin-Hall Distribution

Theorem 1. *Let X_i for $i = 1, 2, \ldots, n$ be independent random variables, each having the continuous uniform distribution on the unit interval, and let $T = \sum_{i=1}^{n} X_i$. Then, the CDF and PDF of T are given by (1) and (2), respectively.*

Proof. For $m \in \{0, 1, 2, \ldots, n-1\}$ and $t \in [m, m+1)$, let

$$\begin{aligned} A_n(t) &= \left\{ (x_1, x_2, \ldots, x_n) : x_i \geq 0 \text{ for } i \right. \\ &\quad \left. \in \{1, 2, \ldots, n\}, \sum_{i=1}^{n} x_i \leq t \right\}, \\ B_j(t) &= \left\{ (x_1, x_2, \ldots, x_n) \in A_n(t) : x_j > 1 \right\}, \\ C_n &= \left\{ (x_1, x_2, \ldots, x_n) : 0 \leq x_i \leq 1 \right\}, \end{aligned} \tag{6}$$

which is the n-dimensional unit cube. The set complement of C_n with respect to $\mathfrak{R}^n$ is denoted by C_n'.

The hypervolume of the n-dimensional solid $A_n(t)$ has value

$$\text{Vol}\left(A_n(t)\right) = \frac{t^n}{n!} \tag{7}$$

[38], since the solid is a standard orthogonal simplex from the corner of an n-cube. Similarly, if $k \in \{1, 2, \ldots, m\}$, then the hypervolume of $\bigcap_{j=1}^{k} B_j(t)$ is

$$\text{Vol}\left(\bigcap_{j=1}^{k} B_j(t)\right) = \frac{(t-k)^n}{n!}. \tag{8}$$

For $k \in \{m+1, m+2, \ldots, n\}$,

$$\begin{aligned} \bigcap_{j=1}^{k} B_j(t) &= \varphi, \\ \text{Vol}\left(\bigcap_{j=1}^{k} B_j(t)\right) &= 0, \end{aligned} \tag{9}$$

since the sum of nonnegative coordinates exceeds the number of coordinates which are greater than 1.

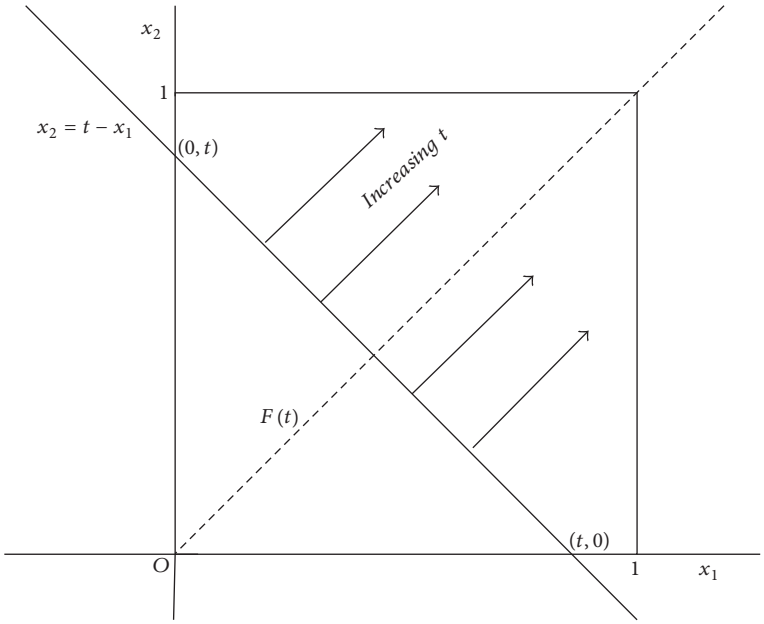

FIGURE 2: The CDF $F(t)$ increases as t increases.

By the inclusion-exclusion principle,

$$F(t) = P(T \le t) = \mathrm{Vol}\left(A_n(t) \cap C_n\right) = \mathrm{Vol}\left(A_n(t)\right) - \mathrm{Vol}\left(A_n(t) \cap C_n'\right) = \mathrm{Vol}\left(A_n(t)\right) - \mathrm{Vol}\left(\bigcup_{j=1}^{n} B_j(t)\right) = \frac{t^n}{n!} - \sum_{k=1}^{m} (-1)^{k-1} \cdot \sum_{1 \le j_1 < j_2 < \cdots < j_k \le n} \mathrm{Vol}\left(B_{j_1}(t) \cap B_{j_2}(t) \cap \cdots \cap B_{j_k}(t)\right) = \frac{t^n}{n!} - \sum_{k=1}^{m} (-1)^{k-1} \cdot \binom{n}{k} \mathrm{Vol}\left(B_1(t) \cap B_2(t) \cap \cdots \cap B_k(t)\right) = \frac{t^n}{n!} - \sum_{k=1}^{m} (-1)^{k-1} \binom{n}{k} \frac{(t-k)^n}{n!} = \sum_{k=0}^{m} (-1)^k \binom{n}{k} \cdot \frac{(t-k)^n}{n!}. \quad (10)$$

In (1), $F(n)$ is the Stirling number of the second kind with both parameters equal to n and has numerical value 1 [39, pages 38-39]. If $t \ge n$, then $C_n \subset A_n(t)$, so $F(t) = 1$ in this case. Since F is a polynomial, $\sum_{k=0}^{n} (-1)^k \binom{n}{k} ((t-k)^n/n!) = 1$ for all real-valued t. Introducing the unit step function gives (1), and differentiation with respect to t gives (2). □

3. Discussion and a Generalization

Figures 2 and 3 reveal the structure of the CDF

$$F(t) = \frac{1}{2} t^2 s_0(t) - (t-1)^2 s_1(t) + \frac{1}{2} (t-2)^2 s_2(t) \quad (11)$$

for $n = 2$. Figure 2 demonstrates how the hyperplane (line), which is the line of a constant sum of the values of the random variables and is perpendicular to the n-cube's (square's) main diagonal, accrues volume (area) below it. Figure 3 illustrates the regions that are included and excluded for various positions of the hyperplane (line) and how vertices are meet in sets. For $n = 2$, the binomial coefficients, which provide the counts of the vertices, are 1 for $(0, 0)$, 2 for $(1, 0)$ and $(0, 1)$, and 1 for $(1, 1)$, as seen in Figures 2 and 3. In (11), the first term is the area of the large triangle in Figures 3(a), 3(b), and 3(c); the second term is the sum of the areas of the two hatched triangles in Figure 3(b), where exactly one of $\{x_1, x_2\}$ is greater than 1, and in Figure 3(c); and the third term is the area of the crosshatched triangle in Figure 3(c), where both x_1 and x_2 are greater than 1.

Figure 4 shows the same geometric interpretation for $n = 3$. In its CDF

$$F(t) = \frac{1}{6} t^3 s_0(t) - \frac{1}{2} (t-1)^3 s_1(t) + \frac{1}{2} (t-2)^3 s_2(t) - \frac{1}{6} (t-3)^3 s_3(t), \quad (12)$$

the first term is the volume using (7) of the large orthogonal simplex in Figures 4(a), 4(b), and 4(c) with edges of length t. The second term is the sum of the volumes using (8) of the three orthogonal simplexes, where exactly one of $\{x_1, x_2, x_3\}$ is greater than 1. In Figure 4(b), the vertices P_1, P_2, P_3, and P_4 of the simplex with $x_1 > 1$ are labeled. Their coordinates are $P_1 : (t, 0, 0)$, $P_2 : (1, 0, t-1)$, $P_3 : (1, t-1, 0)$, and $P_4 : (1, 0, 0)$. The lengths of the edges P_1P_4, P_2P_4, and P_3P_4 are $t - 1$. The third term of (12) is the sum of the three volumes using (8), where exactly two of $\{x_1, x_2, x_3\}$ are greater than 1. In Figure 4(c), the vertices are labeled P_3, P_5, P_6, and P_7 in the region where both x_1 and x_2 are greater than 1. Their

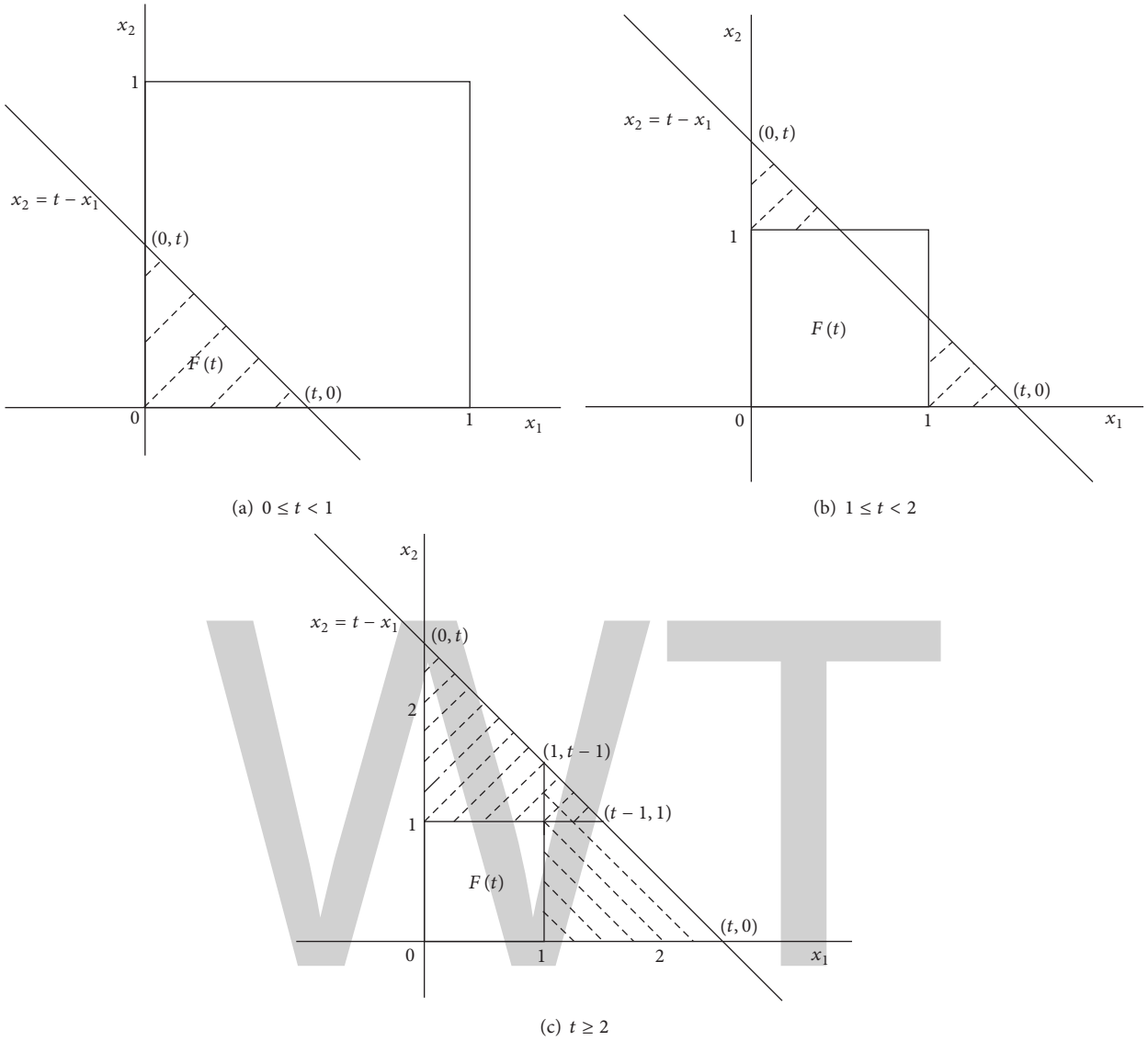

Figure 3: Computing the CDF for $n = 2$ for increasing values of t.

coordinates are $P_3 : (1, t-1, 0)$, $P_5 : (t-1, 1, 0)$, $P_6 : (1, 1, t-2)$, and $P_7 : (1, 1, 0)$. The lengths of the edges P_3P_7, P_5P_7, and P_6P_7 are $t - 2$. The fourth term is the region that is shared by all the other regions, analogous to the crosshatched region in Figure 3(c).

In the same way, for any n, the terms are the n-volumes of orthogonal n-simplexes, whose multiplicity is counted by binomial coefficients determined by the number of vertices of the n-cube in sets as the "moving" $n - 1$-dimensional hyperplane "passes" them as t increases. The hyperplane is perpendicular to the diagonal line $x_1 = x_2 = x_3 = \cdots = x_n$. The volumes of the simplexes are computed using (7) and (8).

The Website [40] has a free simulator for T, where selecting n yields the PDF (2). Other calculators are at [41, 42].

The method of proof in Section 2 can be extended to linear combinations of uniform random variables on different intervals. Suppose that $X_1, X_2, \ldots, X_n$ are independent, that X_k is uniformly distributed on the interval $[a_k, b_k]$, and that $c_1, c_2, \ldots, c_n$ are real constants. Also,

$$P\left(\sum_{k=1}^{n} c_k X_k \le t\right) = P\left(\sum_{k=1}^{n} d_k Y_k \le t'\right), \tag{13}$$

where

$$\begin{aligned} Y_k &= \frac{X_k - a_k}{b_k - a_k}, \\ d_k &= c_k\left(b_k - a_k\right), \\ t' &= \sum_{k=1}^{n} a_k c_k. \end{aligned} \tag{14}$$

Then, $Y_1, Y_2, \ldots, Y_n$ are independent uniform random variables on $[0, 1]$, and $P(\sum_{k=1}^{n} c_k X_k \le t)$ can be interpreted as

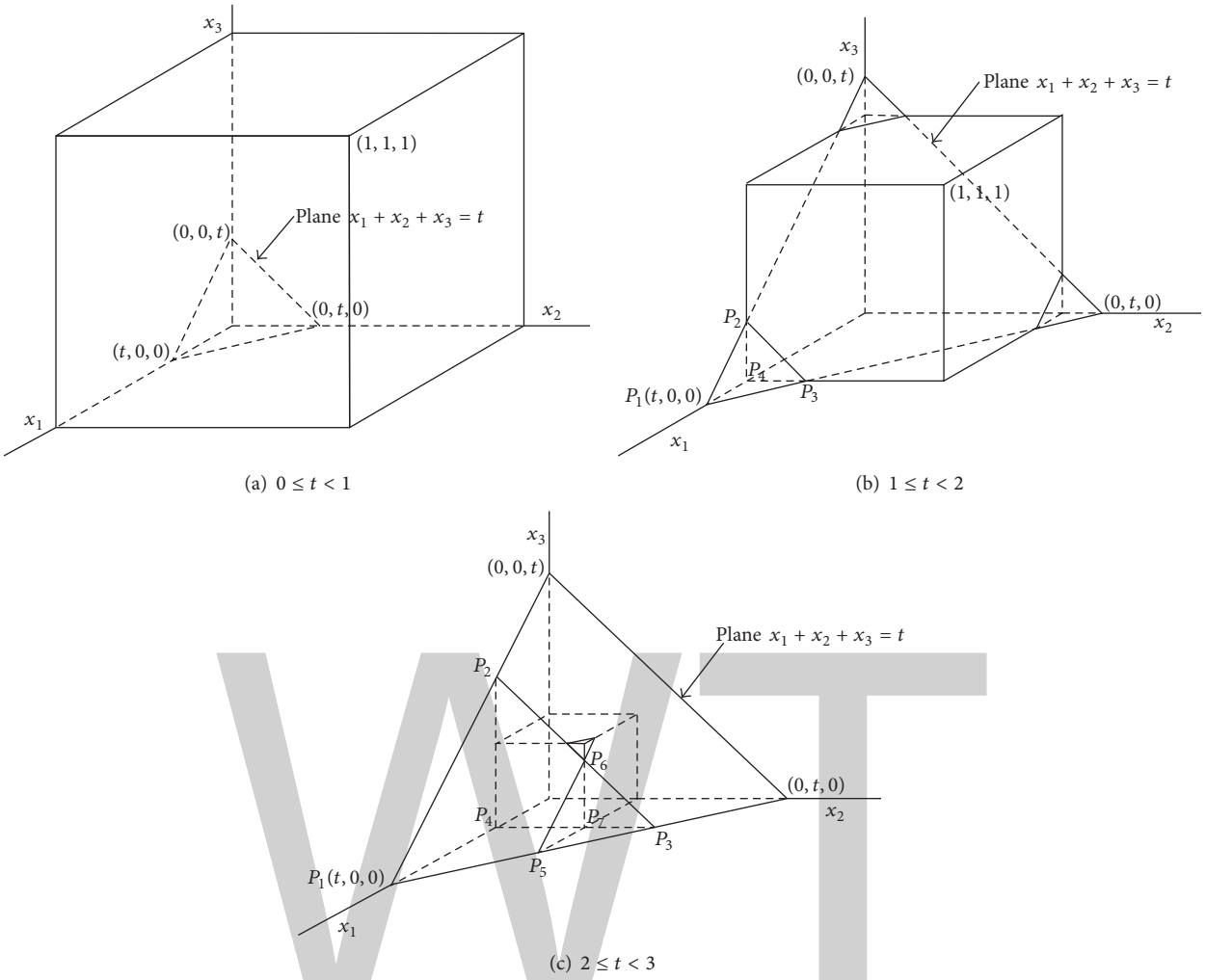

Figure 4: Computing the CDF for $n = 3$ for increasing values of t.

the hypervolume of the solid that consists of all points that lie inside the unit hypercube $[0, 1]^n$ and on one side of the hyperplane $\sum_{k=1}^{n} d_k Y_k = t'$. Now, proceed by inclusion-exclusion as in Section 2. In general, the formula for $P(\sum_{k=1}^{n} c_k X_k \le t)$ is complicated because of the lack of symmetry that is caused by the presence of $d_1, d_2, \ldots, d_n$. This increases the number cases and removes the congruence of the solids of each size whose hypervolumes need to be added or subtracted at each stage of the inclusion-exclusion process. Nevertheless, the correct distribution is obtained in this manner. A special case in which these problems disappear is $d_1 = d_2 = \cdots = d_n = d$, so that

$$P\left(\sum_{k=1}^{n} c_k X_k \le t\right) = \begin{cases} F\left(\dfrac{t'}{d}\right) & \text{for } d > 0 \\ 1 - F\left(\dfrac{t'}{d}\right) & \text{for } d < 0, \end{cases} \tag{15}$$

where F is given in (1).

Conflicts of Interest

The authors declare that there are no conflicts of interest regarding the publication of this article.

References

[1] N. L. Johnson, S. Kotz, and N. Balakrishnan, *Continuous Univariate Distributions*, vol. 2, John Wiley & Sons, New York, NY, USA, 2nd edition, 1995.

[2] K. R. Koch, *Introduction to Bayesian Statistics*, Springer, Berlin, Germany, 2nd edition, 2010.

[3] C. P. Quesenberry, "Probability integral transformations," in *Encyclopedia of Statistical Sciences*, S. Kotz, N. L. Johnson, and C. B. Read, Eds., vol. 7, pp. 225–231, Wiley, New York, NY, USA, 1986.

[4] V. K. Rohatgi, *An Introduction to Probability Theory and Mathematical Statistics*, John Wiley & Sons, New York, NY, USA, 1976.

[5] J. O. Berger, *Statistical Decision Theory and Bayesian Analysis*, Springer Series in Statistics, Springer, New York, NY, USA, 2nd edition, 1985.

[6] P. C. Silva, J. O. Cerdeira, M. J. Martins, and T. Monteiro-Henriques, "Data depth for the uniform distribution," *Environmental and Ecological Statistics*, vol. 21, no. 1, pp. 27–39, 2014.

[7] K. Jayakumar and K. K. Sankaran, "On a generalization of uniform distribution and its properties," *Statistica*, vol. 76, no. 1, pp. 83–91, 2016.

[8] C. P. Dettmann and M. K. Roychowdhury, "Quantization for uniform distributions on equilateral triangles," *Real Analysis Exchange*, vol. 42, no. 1, pp. 149–166, 2017.

[9] E. S. Pearson, *The History of Statistics in the 17th and 18th Centuries, Against the Changing Background of Intellectual, Scientific and Religious Thought, Lectures by Karl Pearson given at University College London during the Academic Sessions*, Macmillan, New York, NY, USA, 1978.

[10] O. B. Sheynin, "Finite random sums (a historical essay)," *Archive for History of Exact Sciences*, vol. 9, no. 4-5, pp. 275–305, 1972/1973.

[11] H. Cramer, *Mathematical Methods of Statistics*, Princeton, Princeton, NJ, USA, 1946.

[12] S. K. Mitra and S. N. Banerjee, "On the probability distribution of round-off errors propagated in tabular differences," *The Australian Computer Society. The Australian Computer Journal*, vol. 3, no. 2, pp. 60–68, 1971.

[13] J. O. Irwin, "On the frequency distribution of the means of samples from a population having any law of frequency with finite moments, with special reference to Pearson's Type II," *Biometrika*, vol. 19, no. 3/4, pp. 225–239, 1927.

[14] A. N. Lowan and J. Laderman, "On the distribution of errors in Nth tabular differences," *The Annals of Mathematical Statistics*, vol. 10, no. 4, pp. 360–364, 1939.

[15] A. Stuart and J. K. Ord, *Kendall's Advanced Theory of Statistics*, vol. 1, Oxford, New York, NY, USA, 5th edition, 1987.

[16] V. M. Kruglov, "On one identity for distribution of sums of independent random variables," *Theory of Probability and its Applications*, vol. 58, no. 2, pp. 329–331, 2014.

[17] H. Potuschak and W. G. Müller, "More on the distribution of the sum of uniform random variables," *Statistical Papers*, vol. 50, no. 1, pp. 177–183, 2009.

[18] E. G. Olds, "A note on the convolution of uniform distributions," *Annals of Mathematical Statistics*, vol. 23, no. 2, pp. 282–285, 1952.

[19] S. K. Mitra, "On the probability distribution of the sum of uniformly distributed random variables," *SIAM Journal on Applied Mathematics*, vol. 20, no. 2, pp. 195–198, 1971.

[20] D. M. Bradley and R. C. Gupta, "On the distribution of the sum of *n* non-identically distributed uniform random variables," *Annals of the Institute of Statistical Mathematics*, vol. 54, no. 3, pp. 689–700, 2002.

[21] S. M. Sadooghi-Alvandi, A. R. Nematollahi, and R. Habibi, "On the distribution of the sum of independent uniform random variables," *Statistical Papers*, vol. 50, no. 1, pp. 171–175, 2009.

[22] H. Murakami, "A saddlepoint approximation to the distribution of the sum of independent non-identically uniform random variables," *Statistica Neerlandica. Journal of the Netherlands Society for Statistics and Operations Research*, vol. 68, no. 4, pp. 267–275, 2014.

[23] G. S. Lo, H. Sangare, and C. . Ndiaye, "A review on asymptotic normality of sums of associated random variables," *Afrika Statistika*, vol. 11, no. 1, pp. 855–867, 2016.

[24] D. L. Barrow and P. W. Smith, "Classroom Notes: spline notation applied to a volume problem," *American Mathematical Monthly*, vol. 86, no. 1, pp. 50-51, 1979.

[25] P. Hall, "The distribution of means for samples of size *N* drawn from a population in which the variate takes values between 0 and 1, all such values being equally probable," *Biometrika*, vol. 19, no. 3/4, pp. 240–245, 1927.

[26] S. A. Roach, "The frequency distribution of the sample mean where each member of the sample is drawn from a different rectangular distribution," *Biometrika*, vol. 50, pp. 508–513, 1963.

[27] G. E. Bates, "Joint distributions of time intervals for the occurrence of successive accidents in a generalized Polya scheme," *Annals of Mathematical Statistics*, vol. 26, no. 4, pp. 705–720, 1955.

[28] H. L. Gray and P. L. Odell, "On sums and products of rectangular variates," *Biometrika*, vol. 53, no. 3-4, pp. 615–617, 1966.

[29] R. V. Hogg, J. W. McKean, and A. T. Craig, *Introduction to Mathematical Statistics*, Pearson-Prentice Hall, Upper Saddle River, NJ, USA, 6th edition, 2005.

[30] J. P. Hoyt, "The teacher's corner: a simple approximation to the standard normal probability density function," *American Statistician*, vol. 22, no. 2, pp. 25-26, 1968.

[31] G. Allasia, "Approximation of the normal distribution function by means of a spline function," *Statistica*, vol. 41, no. 2, pp. 325–332, 1981.

[32] J. K. Patel and C. B. Read, *Handbook of the Normal Distribution*, Statistics: Textbooks and Monographs, Marcel Dekker, New York, NY, USA, 2nd edition, 1982.

[33] M. S. Muminov and K. Soatov, "A note on spline estimator of unknown probability density function," *Open Journal of Statistics*, vol. 1, no. 3, pp. 157–160, 2011.

[34] M. S. Muminov and K. S. Soatov, "On the approximation of maximum deviation spline estimation of the probability density Gaussian process," *Open Journal of Statistics*, vol. 5, no. 4, pp. 334–339, 2015.

[35] C. Lee, S. Kim, and J. Jeong, "A view on the validity of central limit theorem: an empirical study using random samples from uniform distribution," *Communications for Statistical Applications and Methods*, vol. 21, no. 6, pp. 539–559, 2014.

[36] L. Heinrich, F. Pukelsheim, and V. Wachtel, "The variance of the discrepancy distribution of rounding procedures, and sums of uniform random variables," *Metrika. International Journal for Theoretical and Applied Statistics*, vol. 80, no. 3, pp. 363–375, 2017.

[37] E. Rio, "Exponential inequalities for weighted sums of bounded random variables," *Electronic Communications in Probability*, vol. 20, no. 77, pp. 1–10, 2015.

[38] P. Stein, "Classroom Notes: a note on the volume of a simplex," *American Mathematical Monthly*, vol. 73, no. 3, pp. 299–301, 1966.

[39] C. L. Liu, *Introduction to Combinatorial Mathematics*, McGraw-Hill, New York, NY, USA, 1968.

[40] 2017, http://www.math.uah.edu/stat/special/IrwinHall.html.

[41] 2017, http://www.distributome.org/V3/calc/IrwinHallCalculator.html.

[42] 2017, http://randomservices.org/distributions/IrwinHall/Calculator.html.

Mathematical Model for Hepatocytic-Erythrocytic Dynamics of Malaria

Titus Okello Orwa, Rachel Waema Mbogo, and Livingstone Serwadda Luboobi

Institute of Mathematical Sciences, Strathmore University, P.O. Box 59857-00200, Nairobi, Kenya

Correspondence should be addressed to Titus Okello Orwa; torwa@strathmore.edu

Academic Editor: Niansheng Tang

Human malaria remains a major killer disease worldwide, with nearly half (3.2 billion) of the world's population at risk of malaria infection. The infectious protozoan disease is endemic in tropical and subtropical regions, with an estimated 212 million new cases and 429,000 malaria-related deaths in 2015. An in-host mathematical model of *Plasmodium falciparum* malaria that describes the dynamics and interactions of malaria parasites with the host's liver cells (hepatocytic stage), the red blood cells (erythrocytic stage), and macrophages is reformulated. By a theoretical analysis, an in-host basic reproduction number R_0 is derived. The disease-free equilibrium is shown to be locally and globally asymptotically stable. Sensitivity analysis reveals that the erythrocyte invasion rate β_r, the average number of merozoites released per bursting infected erythrocyte K, and the proportion of merozoites that cause secondary invasions at the blood phase ζ are the most influential parameters in determining the malaria infection outcomes. Numerical results show that macrophages have a considerable impact in clearing infected red blood cells through phagocytosis. Moreover, the density of infected erythrocytes and hence the severity of malaria are shown to increase with increasing density of merozoites in the blood. Concurrent use of antimalarial drugs and a potential erythrocyte invasion-avoidance vaccine would minimize the density of infected erythrocytes and hence malaria disease severity.

1. Introduction

Human malaria remains a major killer disease worldwide, with nearly half (3.2 billion) of the world's population at risk of malaria infection [1]. The infectious disease is endemic in tropical and subtropical regions, with an estimated 212 million new cases (uncertainty range: 148–304 million) and 429,000 malaria-related deaths (range: 235,000–639,000) in 2015 [2]. 92% of the deaths and 90% of the cases occurred in sub-Saharan Africa. 70% of the reported deaths occurred among children below the age of five. Despite existing vector control measures and tremendous progress in the development of antimalarial therapy accompanied with worldwide decline in incidence rate (fell by 21% in 2015) and mortality rate (fell by 29% in 2015), malaria remains one of the greatest global health challenges to date [2].

The protozoan disease is caused by parasites of the genus *Plasmodium* which are transmitted to humans by the bite of female *Anopheles* mosquito. *Plasmodium falciparum*, which is predominant in sub-Saharan Africa, New Guinea, and Haiti [3], is the major cause of malaria infections. The other *Plasmodium* species that cause malaria are *P. vivax*, *P. ovale*, *P. malariae*, and *P. knowlesi* [4]. *P. vivax* and *P. ovale* can hide in the liver for prolonged periods as hypnozoites, causing relapsing malaria months or even years after the initial infection [5]. *P. vivax* has the greatest geographical range of the disease and hence is the main contributor to worldwide malaria morbidity [3]. Our study focuses on the dynamics of *Plasmodium falciparum* in the human host.

During their obligatory blood meals, infected female *Anopheles* mosquitoes inject sporozoites belonging to *Plasmodium falciparum* species into the human dermis [6]. The motile sporozoites travel through the blood vessels and enter the host's liver. Hepatocyte invasion is accompanied by the formation of parasitophorous vacuole (PV) around the sporozoite [7]. They form preerythrocytic schizonts and multiply by schizogony, culminating in the production of 8–24 first generation merozoites that are released into the

blood when the liver schizonts burst open [8]. The released merozoites invade susceptible erythrocytes and undergo another phase of schizogony, which is relatively faster compared to that at the exoerythrocytic stage [9].

Within a period of two days, the infected red blood cells rupture to release about 16 daughter merozoites [10]. Most of the released merozoites quickly invade susceptible erythrocytes, leading to another cycle of infections. The waves of bursting erythrocytes and the invasion of fresh erythrocytes by the newly released merozoites increase parasitemia and produce malaria's characteristic symptoms [11]. In the absence of adequate protective immune response or antimalarial therapy, the host is likely to suffer severe anaemia or even die [12]. The rest of the daughter merozoites develop into sexual forms called gametocytes [10]. These gametocytes are later taken up by other female *Anopheles* mosquitoes during feeding [13]. This marks the beginning of the sporogenic cycle that occurs within the mosquito vector.

The presence of the malaria parasites in the human body elicits response from numerous immune cells. The innate immune system and the adaptive immune system form the first and the second lines of defence, respectively [14]. Adaptive immune system further provides protection against future exposures to malaria pathogens. Innate immune cells such as the *Plasmodium falciparum* DNA, natural killer cells (NK cells), dendritic cells (DCs), macrophages, natural killer T (NKT) cells, and T cells are involved in the clearance of circulating parasites, infected erythrocytes, and infected hepatocytes [14]. Subject to parasite strain, the DCs and NK cells may prompt or restrain inflammatory responses [15]. The NKT cells also help regulate DCs and T cell responses to *Plasmodium* [14]. Moreover, studies in [16] have demonstrated that malaria infection induces activation of Toll-like receptors (TLRs): TLR1, TLR2, TLR4 (which are located on the cell surface), and TLR9 which is not expressed on the cell surface. TLR2 and TLR9 are also activated by malarial glycosylphosphatidylinositol (GPI) anchors and parasite-derived DNA bound to hemozoin [16].

Unlike the NK cells, the macrophages have been shown to effectively phagocytose malaria-infected red blood cells during the erythrocytic phase [17]. A part from its ability to wholly ingest infected red blood cells, the macrophages can also selectively extract malaria parasites from recently infected erythrocytes [18]. The parasite-extraction capability of macrophage therefore leaves the surviving erythrocytes to continue circulating like the other healthy red blood cells.

The rest of the paper is organized as follows: in Section 2, we formulate the in-host malaria model and state the invariant region in which the model is defined. In Section 3, we compute and describe the model in-host reproduction number. The results on model equilibrium points (disease-free equilibrium and endemic equilibrium points) and the stability of the disease-free equilibrium point are also considered in Section 3. Section 4 is devoted to numerical solution of the in-host model under different conditions of the threshold parameter (in-host reproduction number). Parameter sensitivity analysis and the effects of parameter variation on different populations are investigated in Section 4. A conclusion and discussion complete the paper in Section 5.

2. In-Host Malaria Model

Several studies on mathematical modelling of in-host malaria and its dynamics within the human host have been done. Nearly all the earlier mathematical models (see, e.g., [25–27]) focused on improving *Plasmodium falciparum* control while focusing on the blood stage of parasite development. These models have been found to be useful in explaining in-host observations by means of biologically plausible assumptions such as parasite diversity, predicting the impact of interventions or the use of antimalarials [28], and estimating hidden parameter values [29]. Although the models in [19, 21, 23, 30] have considered the impact of immune response and treatment, the modelling is only limited to the blood stage of *Plasmodium falciparum* development. In [20, 22, 31], the liver stage is incorporated in the malaria model. However, the contribution of immune system is ignored in [20, 31]. Moreover, all the immune cells are assumed to play an active role during malaria infection in [22]. This may not be entirely true. The specific impacts of immune responses to malaria infection are well discussed in [32–36].

In the following sections, we extended the model in [21] by incorporating the liver stage of parasite development. The reformulated in-host malaria model focuses on the erythrocytic and hepatocytic stages and describes the dynamics of interactions between the malaria parasites, the liver hepatocytes, the red blood cells, and the macrophages (immune system cells). Unlike the work in [20, 22], we ignored the vector stage of parasite development and assumed a twofold process in the generation of hepatocytes: from the bone marrow and from self-replication of the existing hepatocytes. Again, we have assumed that the generation of macrophages and the susceptible red blood cells from the bone marrow increase with increasing density of the infected erythrocytes. However, whatever density of the infected erythrocytes, there is a limit on the rate at which cells can be released from the bone marrow.

2.1. Model Formulation. The hepatocytic-erythrocytic malaria model describes the dynamics of *Plasmodium falciparum* parasite during the hepatocytic and erythrocytic stages and their interactions with the host's red blood cells, liver hepatocytes, and the macrophages. The compartmental model assumes seven interacting populations of sporozoites $S(t)$, susceptible hepatocytes $H(t)$, infected hepatocytes $H_X(t)$, susceptible red blood cells (RBCs) $R(t)$, infected red blood cells (IRBCs) $R_X(t)$, merozoites $M(t)$, and macrophages $Z(t)$ at any time t. The dynamics of malaria parasites and host-cell populations in each compartment are described as follows.

Sporozoites (S). The female *Anopheles* mosquito is assumed to inject sporozoites into the human system during blood meal at a constant rate Λ. The sporozoites molt through the blood stream and reach the liver in about 2 hours, where they invade the hepatocytes at the rate β_s. We assume that the sporozoites can die naturally at a rate δ_s.

Susceptible Hepatocytes (H). We consider the bone marrow and self-replication as the main sources of the liver hepatocytes. The recruitment of hepatocytes from the bone marrow is assumed to occur at a constant rate λ_h. Just like during liver transplant [37], we argue that, during severe malaria infections, the rate of generation of healthy hepatocytes is likely to increase tremendously and in proportion to the concentrations of the infected liver cells [38]. This additional increase is represented by the term $\rho_1 H_X/(\kappa_1 + H_X) = \psi_1(H_X)$, where H_X and ρ_1, respectively, represent the concentration of infected hepatocytes and their rates of generation. The parameter κ_1 represents the number/concentration of the infected hepatocytes at which the recruitment of the healthy hepatocytes is a half of the maximum rate. Owing to invasion by sporozoites at the rate β_s, susceptible hepatocytes get infected and progress to subpopulation H_X. In addition, hepatocytes in compartment H are assumed to have a natural life expectancy and may hence die naturally at the rate μ_1.

Infected Hepatocytes (H_X). Infected hepatocytes mature into liver-stage schizonts. These schizonts burst open releasing 2000–40000 uninucleate merozoites into the blood stream [39]. The term $N\mu_2 H_X$ represents the total population of merozoites released upon bursting of infected hepatocytes. The parameter μ_2 represents the death rate of the infected hepatocytes.

Susceptible Red Blood Cells (R). Similar to malaria models in [21, 23, 30], we have assumed that the susceptible RBCs get recruited at a constant rate λ_r from the bone marrow. We further assume that, during infection, the erythrocyte production is accelerated owing to the presence of IRBCs at the rate ρ_2. This increase is denoted by the term $\rho_2 R_X/(\kappa_2 + R_X) = \psi_2(R_X)$, where κ_2 represents number/concentration of the infected red blood cells at which the recruitment of susceptible red blood cells is a half of the maximum rate. The particular mechanisms involved in this accelerated process are, however, still poorly understood [40]. The susceptible RBCs get infected by merozoites at a rate proportional to the contact rate of their density, $\beta_r MR$. The positive constant β_r describes the rate of successful invasion by a malaria merozoite. The susceptible RBCs die naturally at a rate μ_3.

Infected Red Blood Cells (R_X). Upon invasion by merozoites, the healthy RBCs get infected, leading to the formation of infected red blood cells R_X. Although the RBCs die at a constant rate μ_4, they can similarly be killed through phagocytosis by the macrophages at the rate η. At maturity, the IRBCs burst open, releasing free merozoites into the blood system, causing secondary invasion and disease progression.

Merozoites (M). After 2–15 days, the infected hepatocytes burst open and release merozoites into the blood system. This is represented by the term $N\mu_2 H_X$, where N is the average number of merozoites released per bursting infected hepatocytes. An average of K merozoites is released per each bursting IRBC. These free parasites suffer a natural death at a rate δ_m and invade susceptible RBCs at a rate β_r. Within the red blood cells, the merozoites mature either into uninucleate

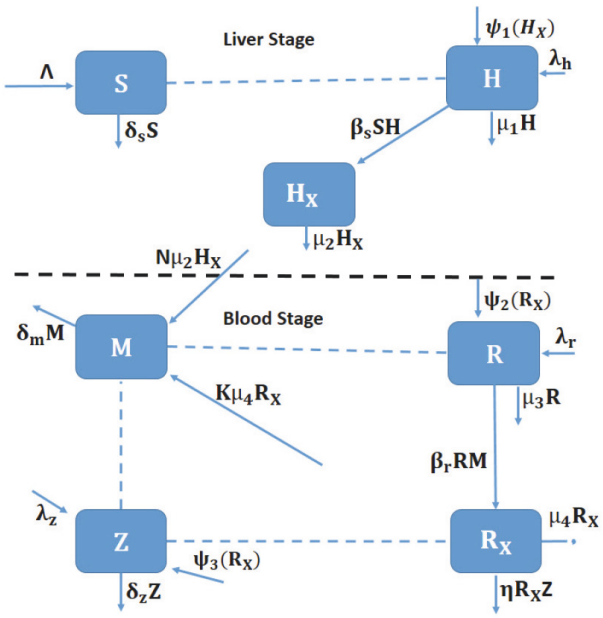

FIGURE 1: Schematic diagram for hepatocytic-erythrocytic and malaria parasite dynamics. The dotted lines without arrows indicate cell-parasite interaction and the solid lines show progression from one compartment to another.

gametocyte or into erythrocytic stage schizont containing 10–36 merozoites [39]. After about 48–72 hours, the erythrocytic stage schizont ruptures, releasing more merozoites into blood stream to cause further invasion of healthy RBCs. We assume that a proportion ζ of the merozoites contribute to secondary invasion of the susceptible RBCs. The rest of the merozoites $(1 - \zeta)$ transform into gametocytes that are later picked up by female *Anopheles* mosquitoes during feeding.

Macrophages (Z). Owing to their effectiveness in elimination of infected erythrocytes and infective malaria parasites, we have considered the innate macrophage cells as the main part of the immune response in malaria infection. Consequently, we have assumed that the macrophage cells are recruited at a constant rate λ_z from the bone marrow. Moreover, they proliferate at a rate ρ_3 in the sites of infection in proportion to the density of IRBCs. This is represented by the term $\rho_3 R_X/(\kappa_3 + R_X) = \psi_3(R_X)$, where κ_3 denotes the number/concentration of the infected red blood cells at which the recruitment of the macrophages is a half of the maximum rate. We further assume that they can die naturally at a constant rate δ_z.

The variables and parameters that describe in-host malaria dynamics are as in Tables 1 and 2, respectively.

The above transmission dynamics of malaria are summarised in the compartmental diagram in Figure 1.

From the above description of the in-host dynamics of malaria and the representation in Figure 1, we derive the following system of ordinary differential equations:

$$\frac{dH}{dt} = \lambda_h + \frac{\rho_1 H_X}{\kappa_1 + H_X} - \mu_1 H - \beta_s SH,$$

Table 1: Symbols and definition of state variables considered in the model.

Variable	Description
$H(t)$	The population of susceptible hepatocytes at time t
$H_X(t)$	The population of infected hepatocytes at time t
$R(t)$	The population of susceptible red blood cells (erythrocytes) at time t
$R_X(t)$	The population of infected red blood cells at time t
$Z(t)$	The density of macrophages in the human body at time t
$S(t)$	The population of sporozoites at time t
$M(t)$	The population of merozoites at time t

Table 2: Symbols and description of parameters used in the model.

Parameter	Description
Λ	The total rate of injection of sporozoites into liver due to mosquito bites
δ_s	The death rate of sporozoites
λ_h	Recruitment rate of susceptible hepatocytes from the bone marrow
μ_1	Natural death rate of susceptible hepatocytes
β_s	The invasion rate of hepatocytes by sporozoites
μ_2	Death rate of infected hepatocytes
λ_r	Recruitment rate of susceptible RBCs by the bone marrow
μ_3	The natural death rate of RBCs
β_r	The invasion rate of RBCs by merozoites
μ_4	Death rates of IRBCs
δ_m	The death rate of merozoites
λ_z	Recruitment rate of macrophages from the bone marrow
δ_z	The death rate of a macrophage
η	Elimination rate of IRBCs by macrophages
ρ_1	Production rate of hepatocytes due to presence of infected hepatocytes
ρ_2	Production rate of RBCs due to presence of IRBCs
ρ_3	Immunogenicity of IRBCs
κ_1	Number of H_X at which the recruitment of H is a half of the maximum rate
κ_2	Number of R_X at which the recruitment of R is a half of the maximum rate
κ_3	Number of R_X at which the recruitment of Z is a half of the maximum rate
ζ	The proportion of the merozoites that cause secondary infections
K	The average number of merozoites released per bursting IRBCs
N	The average number of merozoites released per bursting infected hepatocytes

$$\begin{aligned}
\frac{dH_X}{dt} &= \beta_s SH - \mu_2 H_X,\\
\frac{dR}{dt} &= \lambda_r + \frac{\rho_2 R_X}{\kappa_2 + R_X} - \mu_3 R - \beta_r RM,\\
\frac{dR_X}{dt} &= \beta_r RM - \mu_4 R_X - \eta R_X Z,\\
\frac{dZ}{dt} &= \lambda_z + \frac{\rho_3 R_X}{\kappa_3 + R_X} - \delta_z Z,\\
\frac{dS}{dt} &= \Lambda - \delta_s S - \beta_s SH,\\
\frac{dM}{dt} &= N\mu_2 H_X + K\zeta\mu_4 R_X - \delta_m M - \beta_r RM,
\end{aligned} \tag{1}$$

where $H(0) \geq 0$, $H_X(0) \geq 0$, $R(0) \geq 0$, $R_X(0) \geq 0$, $Z(0) \geq 0$, $S(0) \geq 0$, and $M(0) \geq 0$.

3. Model Analysis

3.1. Basic Properties. In this section, we study whether the formulated model (1) is biologically and mathematically meaningful. We establish model equilibrium points and investigate their stability properties.

3.1.1. Well-Posedness of the Model. For the in-host malaria model (1) to be mathematically and biologically meaningful, we need to prove that all the solutions of model system (1) with nonnegative initial conditions would remain nonnegative for all time $t \geq 0$. Positivity in the model is shown by proving the following theorem.

Theorem 1. *Let the parameters in model (1) be positive constants. A nonnegative solution* $(H(t), H_X(t), R(t), R_X(t), Z(t), S(t), M(t))$ *exists for all the state variables with nonnegative initial conditions* $\{H(0) = H_0 \geq 0, H_X(0) = H_{X0} \geq 0, R(0) = R_0 \geq 0, R_X(0) = R_{X0} \geq 0, Z(0) = Z_0 \geq 0, S(0) = S_0 \geq 0, M(0) = M_0 \geq 0\} \forall t \geq 0$.

Proof. Considering the first equation in system (1), let $\psi_1(t) = \rho_1 H_X/(\kappa_1 + H_X)$, so that

$$\begin{aligned} \frac{\mathrm{d}H}{\mathrm{d}t} &= \lambda_h + \varphi(t) - \mu_1 H - \beta_s S H, \\ \frac{\mathrm{d}H}{\mathrm{d}t} &\geq -(\mu_1 + \beta_s S) H, \end{aligned} \tag{2}$$

which yields

$$H(t) \geq H(0) \exp\left\{-\left(\int_0^t \beta_s S(s)\, ds + \mu_1 t\right)\right\} > 0. \tag{3}$$

In a similar fashion, this procedure can be applied to all the remaining six equations in model system (1), so that we have the following solutions:

$$\begin{aligned} H_X(t) &\geq H_X(0) \exp\{-\mu_2 t\} > 0, \\ R(t) &\geq R(0) \exp\left\{-\left(\int_0^t \beta_r M(s)\, ds + \mu_3 t\right)\right\} > 0, \\ R_X(t) &\geq R_X(0) \exp\left\{-\left(\int_0^t \eta Z(s)\, ds + \mu_4 t\right)\right\} > 0, \\ Z(t) &\geq Z(0) \exp\{-\delta_z t\} > 0, \\ S(t) &\geq S(0) \exp\left\{-\left(\int_0^t \beta_s H(s)\, ds + \delta_s t\right)\right\} > 0, \\ M(t) &\geq M(0) \exp\left\{-\left(\int_0^t \beta_r R(s)\, ds + \delta_m t\right)\right\} > 0. \end{aligned} \tag{4}$$

Therefore, state variables $(H, H_X, R, R_X, Z, S, M)$ of model system (1) are nonnegative for all time $t > 0$. □

3.1.2. Invariant Region. Let $N_H(t)$ represent the total hepatocyte population, so that $N_H(t) = H(t) + H_X(t)$.

On substituting the derivatives in system (1) and simplifying, we have

$$\frac{dN_H}{dt} \leq \lambda_h + \psi_1(t) - \mu_h N_H, \tag{5}$$

where $\psi_1(t) = \rho_1 H_X/(\kappa_1 + H_X)$ and $\mu_h = \min\{\mu_1, \mu_2\}$.

Using integrating factor $e^{\mu_h t}$,

$$N_H(t) \leq \frac{\lambda_h}{\mu_h} + e^{-\mu_h t} \int_0^t \psi_1(\tau)\, e^{\mu_h \tau} d\tau + c_1 e^{-\mu_h t}, \tag{6}$$

where c_1 is a constant of integration. By applying the initial condition $N_H(0) = N_{H0} > 0$ in (6), we obtain

$$c_1 = \left(N_H(0) - \frac{\lambda_h}{\mu_h}\right) - \int_0^t \psi_1(\tau)\, e^{-\mu_h \tau} d\tau. \tag{7}$$

Substituting the value of c_1 into $N_H(t)$ in (6) and simplifying, we get

$$N_H(t) \leq \frac{\lambda_h}{\mu_h} + e^{-\mu_h t}\left(N_H(0) - \frac{\lambda_h}{\mu_h}\right). \tag{8}$$

There are two possible cases in analyzing the behaviour of $N_H(t)$ in (8). In the first case, we consider $N_H(0) > \lambda_h/\mu_h$ so that, at time $t = 0$, the right-hand side (RHS) of (8) experiences the largest possible value of $N_H(0)$. That is, $N_H(t) \leq N_H(0)$ for all time $t > 0$.

In the second case, we consider $N_H(0) < \lambda_h/\mu_h$, so that the largest possible value of the RHS of (8) approaches λ_h/μ_h as time t goes to infinity. Thus, $N_H(t) \leq \lambda_h/\mu_h$, $\forall t > 0$. From these two cases, we conclude that $N_H(t) \leq \max\{N_H(0), \lambda_h/\mu_h\}$ for all time $t > 0$.

Using the above approach, let the total red blood cells population be $N_R(t)$, so that $N_R(t) = R(t) + R_X(t)$. From the model equations in system (1), we have

$$\frac{dN_R}{dt} \leq \lambda_r + \psi_2(t) - \mu_r N_R(t), \tag{9}$$

where $\psi_2(t) = \rho_2 R_X/(\kappa_2 + R_X)$ and $\mu_r = \min\{\mu_3, \mu_4\}$. Upon solving for N_R in (9), we have $N_R(t) \leq \max\{N_R(0), \lambda_r/\mu_r\}$, $\forall t > 0$.

For the macrophage compartment $Z(t)$, we have

$$\frac{\mathrm{d}Z}{\mathrm{d}t} = \lambda_z + \psi_3(t) - \delta_z Z, \quad \text{for } \psi_3(t) = \frac{\rho_3 R_X}{\kappa_3 + R_X}. \tag{10}$$

By integration, the solution of (10) is presented as

$$Z(t) \leq \frac{\lambda_z}{\delta_z} + e^{-\delta_z t}\left(Z(0) - \frac{\lambda_z}{\delta_z}\right). \tag{11}$$

By inspection, $Z(t) \leq \max\{Z(0), \lambda_z/\delta_z\}$ for all time $t > 0$.

Finally, let $N_P(t)$ represent the total population of malaria parasites at any time t. That is, $N_P(t) = S(t) + M(t)$ and, from system (1),

$$\begin{aligned} \frac{\mathrm{d}N_P}{\mathrm{d}t} &= \Lambda - \delta_s S - \beta_s S H + N\mu_2 H_X + K\zeta\mu_4 R_X \\ &\quad - \delta_m M, \leq \Lambda + (K\zeta\mu_4 R_X + N\mu_2 H_X) - \delta_p N_p, \\ &\quad \text{where } \delta_p = \min\{\delta_s, \delta_m\}. \end{aligned} \tag{12}$$

Let $(K\zeta\mu_4 R_X + N\mu_2 H_X) = \psi_4(t)$, so that on solving for $N_P(t)$ we get

$$N_p(t) \leq \frac{\Lambda}{\delta_p} + e^{-\delta_p t}\left(N_p(0) - \frac{\Lambda}{\delta_p}\right) \tag{13}$$

Clearly, the malaria parasite populations $S(t)$ and $M(t)$ are bounded above. That is,

$N_P(t) \leq \max\{N_P(0), \Lambda/\delta_p\}$ for all time $t > 0$.

Based on this discussion, we have shown the existence of a bounded positive invariant region for our model system (1). Let us denote this region as $\Omega \in \mathbb{R}_+^7$, where

$$\begin{aligned}\Omega = \Bigg\{ & \left(H, H_X, R, R_X, Z, S, M\right) \in \mathbb{R}_+^7 : N_P(t) \\ & \leq \max\left\{N_P(0), \frac{\Lambda}{\delta_p}\right\}, N_H(t) \\ & \leq \max\left\{N_H(0), \frac{\lambda_h}{\mu_h}\right\}, N_R(t) \\ & \leq \max\left\{N_R(0), \frac{\lambda_r}{\mu_r}\right\}, Z(t) \leq \max\left\{Z(0), \frac{\lambda_z}{\delta_z}\right\}\Bigg\}.\end{aligned} \tag{14}$$

Moreover, any solution of our system (1) which commences in Ω at any time $t \geq 0$ will always remain confined in that region. We therefore deduce that the region Ω is positively invariant and attracting with respect to malaria model (1). Our in-host malaria model (1) is hence well posed mathematically and biologically.

3.1.3. Disease-Free Equilibrium Point. The disease-free equilibrium point, $\mathscr{E}_0$, is the state in which the human host is free of malaria infection. At $\mathscr{E}_0$, the sporozoite recruitment rate, $\Lambda = 0$, and parasite and host-infected compartments have zero values; that is, $S^* = M^* = R_X^* = H_X^* = 0$. Therefore,

$$\begin{aligned}\mathscr{E}_0 &= \left(H^*, H_X^*, R^*, R_X^*, Z^*, S^*, M^*\right) \\ &= \left(\frac{\lambda_h}{\mu_1}, 0, \frac{\lambda_r}{\mu_3}, 0, \frac{\lambda_z}{\delta_z}, 0, 0\right).\end{aligned} \tag{15}$$

3.1.4. In-Host Basic Reproduction Number. The in-host reproduction number of model (1) denoted by R_0 is computed using the technique of the next-generation matrix approach described in [41]. We consider H_X, R_X, S, and M as the parasite infested compartments. Adopting the notations in [41], we generate a nonnegative matrix F of new infections and a nonsingular matrix V, showing the transfer of infections from one compartment to the other as follows:

$$F = \begin{pmatrix} 0 & 0 & \dfrac{\beta_s \lambda_h}{\mu_1} & 0 \\ 0 & 0 & 0 & \dfrac{\beta_r \lambda_r}{\mu_3} \\ 0 & 0 & 0 & 0 \\ 0 & 0 & 0 & 0 \end{pmatrix} \tag{16}$$

and

$$V = \begin{pmatrix} \mu_2 & 0 & 0 & 0 \\ 0 & \mu_4 + \dfrac{\eta\lambda_z}{\delta_z} & 0 & 0 \\ 0 & 0 & \delta_s + \dfrac{\beta_s\lambda_h}{\mu_1} & 0 \\ -N\mu_2 & -K\zeta\mu_4 & 0 & \delta_m + \dfrac{\beta_r\lambda_r}{\mu_3} \end{pmatrix}. \tag{17}$$

The inverse of matrix V is hence given by

$$V^{-1} = \begin{pmatrix} \dfrac{1}{\mu_2} & 0 & 0 & 0 \\ 0 & \dfrac{\delta_z}{\eta\lambda_z + \delta_z\mu_4} & 0 & 0 \\ 0 & 0 & \dfrac{1}{\delta_s + \beta_s\lambda_h/\mu_1} & 0 \\ \dfrac{N\mu_3}{\beta_r\lambda_r + \delta_m\mu_3} & \dfrac{K\zeta\delta_z\mu_3\mu_4}{(\beta_r\lambda_r + \delta_m\mu_3)(\eta\lambda_z + \delta_z\mu_4)} & 0 & \dfrac{1}{\delta_m + \beta_r\lambda_r/\mu_3} \end{pmatrix}. \tag{18}$$

The next-generation matrix G, which is the product of matrices F and V^{-1}, works out to be

$$G = \begin{pmatrix} 0 & 0 & \dfrac{\beta_s\lambda_h}{\beta_s\lambda_h + \delta_s\mu_1} & 0 \\ \dfrac{N\beta_r\lambda_r}{\beta_r\lambda_r + \delta_m\mu_3} & \dfrac{K\zeta\beta_r\delta_z\lambda_r\mu_4}{(\beta_r\lambda_r + \delta_m\mu_3)(\eta\lambda_z + \delta_z\mu_4)} & 0 & \dfrac{\beta_r\lambda_r}{\beta_r\lambda_r + \delta_m\mu_3} \\ 0 & 0 & 0 & 0 \\ 0 & 0 & 0 & 0 \end{pmatrix}. \tag{19}$$

The in-host basic reproduction number R_0 is the spectral radius of the next-generation matrix G. It can clearly be seen that three of the four eigenvalues of matrix G in (19) have zero values; that is, $\lambda_1 = \lambda_2 = \lambda_3 = 0$. The fourth and largest nonnegative eigenvalue λ_4 becomes the in-host model reproduction number. We therefore have

$$R_0 = \frac{K\beta_r\lambda_r}{(\beta_r\lambda_r + \delta_m\mu_3)} \cdot \frac{\zeta\delta_z\mu_4}{(\eta\lambda_z + \delta_z\mu_4)}. \tag{20}$$

The terms in model R_0 can be interpreted as follows:

(1) The term $K\beta_r\lambda_r/(\beta_r\lambda_r + \delta_m\mu_3)$ represents the expected number of infectious merozoite parasites resulting from bursting blood schizonts at the blood stage of malaria infection.

(2) The second term $\zeta\delta_z\mu_4/(\eta\lambda_z + \delta_z\mu_4)$ represents the expected proportion of merozoites that participate in the cycle of erythrocytic schizogony.

(3) Observe that the terms $(\beta_r\lambda_r)/(\beta_r\lambda_r + \delta_m\mu_3) < 1$ and $(\delta_z\mu_4)/(\eta\lambda_z + \delta_z\mu_4) < 1$. So our $R_0 \leq K\zeta$. This implies that the number of secondary infections during malaria infections is largely influenced by the average number of merozoites released K, from a bursting blood schizont, most of which are responsible for secondary infections at the blood stage.

Despite the inclusion of the liver stage dynamics, it is interesting to observe that the above in-host reproduction number and hence the disease progression are heavily driven by the dynamics at the erythrocytic stage.

In the sections that follow, we shall establish both the local stability and global stability of disease-free equilibrium point (15) of model system (1).

3.1.5. Local Stability of the Disease-Free Equilibrium Point, $\mathscr{E}_0$. The Jacobian matrix of model system (1) evaluated at the disease-free equilibrium $\mathscr{E}_0$ is given by

$$J_1(\mathscr{E}_0) = \begin{pmatrix} -\mu_1 & \frac{\rho_1}{\kappa_1} & 0 & 0 & 0 & -\frac{\beta_s\lambda_h}{\mu_1} & 0 \\ 0 & -\mu_2 & 0 & 0 & 0 & \frac{\beta_s\lambda_h}{\mu_1} & 0 \\ 0 & 0 & -\mu_3 & \frac{\rho_2}{\kappa_2} & 0 & 0 & -\frac{\beta_r\lambda_r}{\mu_3} \\ 0 & 0 & 0 & -\frac{\eta\lambda_z}{\delta_z} - \mu_4 & 0 & 0 & \frac{\beta_r\lambda_r}{\mu_3} \\ 0 & 0 & 0 & \frac{\rho_3}{\kappa_3} & -\delta_z & 0 & 0 \\ 0 & 0 & 0 & 0 & 0 & -\frac{\beta_s\lambda_h}{\mu_1} - \delta_s & 0 \\ 0 & N\mu_2 & 0 & K\zeta\mu_4 & 0 & 0 & -\frac{\beta_r\lambda_r}{\mu_3} - \delta_m \end{pmatrix}. \tag{21}$$

It is clear from the first, third, and fifth columns of matrix (21) that the Jacobian matrix has negative eigenvalues $\lambda_1 = -\mu_1, \lambda_2 = -\mu_3$, and $\lambda_3 = -\delta_z$. Upon deleting the first, third, and fifth rows and columns, matrix (21) is reduced to the following 4×4 matrix:

$$J_2(\mathscr{E}_0) = \begin{pmatrix} -\mu_2 & 0 & \frac{\beta_s\lambda_h}{\mu_1} & 0 \\ 0 & -\frac{\eta\lambda_z}{\delta_z} - \mu_4 & 0 & \frac{\beta_r\lambda_r}{\mu_3} \\ 0 & 0 & -\frac{\beta_s\lambda_h}{\mu_1} - \delta_s & 0 \\ N\mu_2 & K\zeta\mu_4 & 0 & -\frac{\beta_r\lambda_r}{\mu_3} - \delta_m \end{pmatrix}. \tag{22}$$

From row three in (22), $\lambda_4 = -\beta_s\lambda_h/\mu_1 - \delta_s$. We further reduce matrix (22) by deleting row three and column three. So,

$$J_3(\mathscr{E}_0) = \begin{pmatrix} -\mu_2 & 0 & 0 \\ 0 & -\frac{\eta\lambda_z}{\delta_z} - \mu_4 & \frac{\beta_r\lambda_r}{\mu_3} \\ N\mu_2 & K\zeta\mu_4 & -\frac{\beta_r\lambda_r}{\mu_3} - \delta_m \end{pmatrix}. \tag{23}$$

Note from row one of (23) that the fifth eigenvalue $\lambda_5 = -\mu_2 < 0$.

The remaining two eigenvalues can be obtained by reducing matrix (23) into the following 2×2 matrix:

$$J_6(\mathscr{E}_0) = \begin{pmatrix} -\frac{\eta\lambda_z}{\delta_z} - \mu_4 & \frac{\beta_r\lambda_r}{\mu_3} \\ K\zeta\mu_4 & -\frac{\beta_r\lambda_r}{\mu_3} - \delta_m \end{pmatrix}. \tag{24}$$

Using the variable λ, the characteristic polynomial associated with matrix (24) is

$$p(\lambda) = \lambda^2 + A\lambda + B, \tag{25}$$

where

$$A = \delta_m + \frac{\eta\lambda_z}{\delta_z} + \frac{\beta_r\lambda_r}{\mu_3} + \mu_4 \text{ and} \tag{26}$$

$$B = \frac{\eta\delta_m\lambda_z}{\delta_z} + \frac{\eta\beta_r\lambda_r\lambda_z}{\delta_z\mu_3} + \delta_m\mu_4 + \frac{\beta_r\lambda_r\mu_4}{\mu_3} - \frac{K\zeta\beta_r\lambda_r\mu_4}{\mu_3}. \tag{27}$$

The characteristic polynomial (25) has negative roots (eigenvalues) if $A > 0$ and $B > 0$. The coefficient A in (26) is clearly positive. We now need to show that B in (27) is strictly positive if $R_0 < 1$. This is done by expressing the coefficient term B in terms of model R_0 as follows:

$$\begin{aligned} B &= \frac{1}{\delta_z\mu_3}\left[\left(\mu_4\delta_z + \eta\lambda_z\right)\left(\beta_r\lambda_r + \delta_m\mu_3\right) - K\zeta\beta_r\delta_z\lambda_r\mu_4\right], \\ &= \frac{1}{\delta_z\mu_3}\left[\left(\mu_4\delta_z + \eta\lambda_z\right)\left(\beta_r\lambda_r + \delta_m\mu_3\right) \cdot \left[1 - \frac{K\zeta\beta_r\delta_z\lambda_r\mu_4}{\left(\mu_4\delta_z + \eta\lambda_z\right)\left(\beta_r\lambda_r + \delta_m\mu_3\right)}\right]\right], \\ &= \frac{\left(\mu_4\delta_z + \eta\lambda_z\right)\left(\beta_r\lambda_r + \delta_m\mu_3\right)}{\delta_z\mu_3}\left[1 - R_0\right]. \end{aligned} \tag{28}$$

It can clearly be seen from (28) that the coefficient B is positive if and only if $R_0 < 1$. We have thus established the following result.

Theorem 2. *The disease-free equilibrium $\mathscr{E}_0$ is locally asymptotically stable in Ω if $R_0 < 1$. If $R_0 > 1$, then $\mathscr{E}_0$ is unstable.*

Biologically, Theorem 2 implies that malaria infection can be eliminated from the human host when $R_0 < 1$. To ensure that elimination of malaria is independent of the initial sizes of the subpopulations, it is necessary to show that $\mathscr{E}_0$ is globally asymptotically stable in Ω, where the model is mathematically and biologically sensible.

3.1.6. Global Asymptotic Stability of the Disease-Free Equilibrium. Using the results obtained in [42], we show that the malaria-free equilibrium state $\mathscr{E}_0$ is globally asymptotically stable when $R_0 < 1$. We begin by rewriting the model system (1) in pseudotriangular form as follows:

$$\begin{aligned} \dot{X}_1 &= A_1(X)\left(X_1 - X_1^*\right) + A_2(X)X_2, \\ \dot{X}_2 &= A_3(X)X_2, \end{aligned} \tag{29}$$

where X_1 is the vector representing the state of different compartment of liver and blood cells that are not infected and do not transmit malaria infections. X_2 represents the states of malaria parasites and host's cells that are responsible for disease transmission. Hence,

$$\begin{aligned} X &= \left(X_1, X_2\right), \\ X_1 &= \left(H, R, Z\right), \\ X_2 &= \left(H_X, R_X, S, M\right) \text{ and} \\ X_1^* &= \left(\frac{\lambda_h}{\mu_1}, \frac{\lambda_r}{\mu_3}, \frac{\lambda_z}{\delta_z}\right). \end{aligned} \tag{30}$$

From the subsystem X_1, we have

$$\begin{aligned} A_1(X) &= \begin{pmatrix} -\mu_1 & 0 & 0 \\ 0 & -\mu_3 & 0 \\ 0 & 0 & -\delta_z \end{pmatrix} \text{ and} \\ A_2(X) &= \begin{pmatrix} \frac{\rho_1}{\kappa_1} & 0 & -\frac{\lambda_h}{\mu_1}\beta_s & 0 \\ 0 & \frac{\rho_2}{\kappa_2} & 0 & -\frac{\lambda_r}{\mu_3}\beta_r \\ 0 & \frac{\rho_3}{\kappa_3} & 0 & 0 \end{pmatrix}. \end{aligned} \tag{31}$$

A direct computation indicates that the eigenvalue of matrix $A_1(X)$ is real and negative. This shows that the system $\dot{X}_1 = A_1(X)(X_1 - X_1^*) + A_2(X)X_2$ is globally asymptotically stable at the disease-free equilibrium, $\mathscr{E}_0$. Similarly, the subsystem X_2 gives rise to the following matrix $A_3(X)$:

$$A_3(X) = \begin{pmatrix} -\mu_2 & 0 & \beta_s\frac{\lambda_h}{\mu_1} & 0 \\ 0 & -\left(\eta\frac{\lambda_z}{\delta_z} + \mu_4\right) & 0 & \beta_r\frac{\lambda_r}{\mu_3} \\ 0 & 0 & -\left(\beta_s\frac{\lambda_h}{\mu_1} + \delta_s\right) & 0 \\ N\mu_2 & K\zeta\mu_4 & 0 & -\left(\beta_r\frac{\lambda_r}{\mu_3} + \delta_m\right) \end{pmatrix}. \tag{32}$$

It can clearly be seen that $A_3(X)$ is a Metzler matrix: all the off-diagonal elements of $A_3(X)$ are nonnegative.

In order to establish the global stability of the disease-free equilibrium, we need to show that the matrix $A_3(X)$

is Metzler stable by providing a proof of the following lemma.

Lemma 3. *Let M be a square Metzler matrix that is block decomposed:*

$$M = \begin{pmatrix} A & B \\ C & D \end{pmatrix}, \tag{33}$$

where A and D are square matrices. The matrix M is Metzler stable if and only if A and $D - CA^{-1}B$ are Metzler stable.

In our case, matrix M is represented by matrix A_3 in (32), so that

$$\begin{aligned} A &= \begin{pmatrix} -\mu_2 & 0 \\ 0 & -\left(\eta\frac{\lambda_z}{\delta_z} + \mu_4\right) \end{pmatrix}, \\ B &= \begin{pmatrix} \beta_s\frac{\lambda_h}{\mu_1} & 0 \\ 0 & \beta_r\frac{\lambda_r}{\mu_3} \end{pmatrix}, \\ C &= \begin{pmatrix} 0 & 0 \\ N\mu_2 & K\zeta\mu_4 \end{pmatrix} \text{ and} \\ D &= \begin{pmatrix} -\left(\beta_s\frac{\lambda_h}{\mu_1} + \delta_s\right) & 0 \\ 0 & -\left(\beta_r\frac{\lambda_r}{\mu_3} + \delta_m\right) \end{pmatrix}. \end{aligned} \tag{34}$$

Upon computation in Mathematica software, we obtain

$$D - CA^{-1}B = \begin{pmatrix} -\omega_1 & 0 \\ \omega_2 & -\omega_3 \end{pmatrix}, \tag{35}$$

where $\omega_1 = \delta_s + \beta_s(\lambda_h/\mu_1)$, $\omega_2 = N\beta_s\lambda_h/\mu_1$, and $\omega_3 = \delta_m + \beta_r\lambda_r(\eta\lambda_h + (1 - K\zeta)\delta_z\mu_4)/\mu_3(\eta\lambda_z + \delta_z\mu_4)$.

For the matrix $D - CA^{-1}B$ to be Metzler stable, ω_3 should be strictly nonnegative. Therefore, the expression in the numerator

$$\beta_r\lambda_r\left(\eta\lambda_h + (1 - K\zeta)\,\delta_z\mu_4\right) \geq 0. \tag{36}$$

Upon simplification of (36),

$$K\zeta\beta_r\lambda_r\delta_z\mu_4 \leq \beta_r\lambda_r\left(\eta\lambda_h + \delta_z\mu_4\right), \tag{37}$$

$$\left(\frac{\beta_r\lambda_r + \delta_m\mu_3}{\beta_r\lambda_r}\right)\left(\frac{K\zeta\beta_r\lambda_r\delta_z\mu_4}{(\beta_r\lambda_r + \delta_m\mu_3)(\eta\lambda_z + \delta_z\mu_4)}\right) \leq 1, \tag{38}$$

$$\left(\frac{\beta_r\lambda_r + \delta_m\mu_3}{\beta_r\lambda_r}\right)R_0 \leq 1 \tag{39}$$

$$R_0 \leq \frac{\beta_r\lambda_r}{\beta_r\lambda_r + \delta_m\mu_3} < 1. \tag{40}$$

Clearly, matrix A in (34) is Metzler stable. However, the matrix $D - CA^{-1}B$ is Metzler stable if and only if $R_0 < 1$. From Lemma 3, we deduce the following theorem.

Theorem 4. *The malaria-free equilibrium $\mathscr{E}_0$ of model system (1) is globally asymptotically stable if the threshold quantity $R_0 < 1$.*

The above result is quite significant in malaria control. The global stability of the disease-free status would be guaranteed if and only if the in-host basic reproduction number R_0 is less than one. Malaria intervention should therefore focus on eliminating infected erythrocytes and/or malaria merozoites that are responsible for erythropoiesis cycle and invasions at the blood stage.

3.2. The Endemic Equilibrium Analysis. When $R_0 > 1$, the stability of the disease-free equilibrium (15) is violated. A different equilibrium state termed the endemic equilibrium is achieved. Equating to zero the RHS of system (1) and solving for the state variables R, H, Z, S, and M in terms of the infected states H_X and R_X, we obtain the endemic state $\mathscr{E}_1 = (H^*, H_X^*, R^*, R_X^*, Z^*, S^*, \mathrm{M}^*)$, where

$$\begin{aligned} H^* &= \frac{1}{\mu_1}\left\{\lambda_h + \frac{\rho_1 H_X^*}{\kappa_1 + H_X^*} - \mu_2 H_X^*\right\}, \\ S^* &= \frac{\mu_1\mu_2 H_X^*}{\beta_s\left(\lambda_h + \rho_1 H_X^*/\left(\kappa_1 + H_X^*\right) - \mu_2 H_X^*\right)}, \end{aligned} \tag{41}$$

$$\begin{aligned} R^* &= \frac{1}{\mu_3}\left\{\lambda_r + \frac{\rho_2 R_X^*}{\kappa_2 + R_X^*} - \mu_4 R_X^*\right\}, \\ M^* &= \mu_3\left(R_X^*\mu_4 + \frac{\eta R_X^*\left(\rho_3 R_X^*/\left(\kappa_3 + R_X^*\right) + \lambda_z\right)}{\mu_1}\right) \end{aligned} \tag{42}$$

$$Z^* = \frac{1}{\delta_z}\left\{\lambda_z + \frac{\rho_3 R_X^*}{\kappa_3 + R_X^*}\right\} \tag{43}$$

Substituting (41) into the 2^{nd} equation in (1) and simplifying, we obtain the following cubic equation:

$$\alpha_3 H_X^{*3} + \alpha_2 H_X^{*2} + \alpha_1 H_X^* + \alpha_0 = 0, \tag{44}$$

where

$$\begin{aligned} \alpha_3 &= \mu_2^2\beta_s > 0, \\ \alpha_2 &= \mu_2\left(\mu_1\left(-\delta_s\right) - \beta_s\left(\lambda_h - \kappa_1\mu_2 + \Lambda + \rho_1\right)\right), \\ \alpha_1 &= \beta_s\left(\lambda_h\left(\Lambda - \kappa_1\mu_2\right) + \Lambda\left(\rho_1 - \kappa_1\mu_2\right)\right) \\ &\quad - \kappa_1\mu_1\mu_2\delta_s, \text{ and} \\ \alpha_0 &= \kappa_1\Lambda\lambda_h\beta_s > 0. \end{aligned} \tag{45}$$

The number and nature of the roots of (44) are determined by the following discriminant:

$$\begin{aligned} \Delta = {} & 18\alpha_3\alpha_2\alpha_1\alpha_0 - 4{\alpha_2}^3\alpha_0 + {\alpha_2}^2{\alpha_1}^2 - 4\alpha_3{\alpha_1}^3 \\ & - 27{\alpha_3}^2{\alpha_0}^2. \end{aligned} \tag{46}$$

So

(i) if $\Delta = 0$, then (44) has multiple real roots and only one endemic equilibrium would exist,

(ii) if $\Delta < 0$, then (44) has 1 real root and a complex conjugate root and hence only one endemic equilibrium,

(iii) if $\Delta > 0$, then (44) has 3 distinct real roots and so there is more than one endemic equilibrium when $R_0 > 1$ for model system (1).

Analysis under (46) implies that, in the absence of external interventions in the form of antimalarial treatment, there will always be some infected hepatocytes during malaria infection. We then evaluate the possible values of the state variable R_X at equilibrium by substituting expressions in (42) and (43) into the 4^{th} equation in (1). After simplification in Mathematica software, we obtain the following cubic equation:

$$R_X^* \left(\theta_3 R_X^{*3} + \theta_2 R_X^{*2} + \theta_1 R_X^* + \theta_0\right) = 0, \tag{47}$$

where

$$\begin{aligned}
\theta_3 &= -\mu_4\beta_r\left(\mu_1\mu_4 + \eta\left(\rho_3 + \lambda_z\right)\right) < 0,\\
\theta_2 &= \eta\rho_3\left(\beta_r\left(-\kappa_2\mu_4 + \rho_2 + \lambda_r\right) - 1\right) + \left(\mu_1\mu_4 + \eta\lambda_z\right)\\
&\quad \cdot \left(\beta_r\left(-\left(\kappa_2 + \kappa_3\right)\mu_4 + \rho_2 + \lambda_r\right) - 1\right),\\
\theta_1 &= \eta\kappa_2\rho_3\left(\beta_r\lambda_r - 1\right) - \left(\mu_1\mu_4 + \eta\lambda_z\right)\left(\kappa_3\right.\\
&\quad \left. + \kappa_2\left(\beta_r\left(\kappa_3\mu_4 - \lambda_r\right) + 1\right) + \kappa_3\left(-\beta_r\right)\left(\rho_2 + \lambda_r\right)\right),\\
\theta_0 &= \kappa_2\kappa_3\left(\beta_r\lambda_r - 1\right)\left(\mu_1\mu_4 + \eta\lambda_z\right).
\end{aligned} \tag{48}$$

Clearly, $R_X^* = 0$ or

$$\theta_3 R_X^{*3} + \theta_2 R_X^{*2} + \theta_1 R_X^* + \theta_0 = 0. \tag{49}$$

The state $R_X^* = 0$ corresponds to a scenario in which there are no parasite-infected red blood cells. This could signify the liver stage of parasite development so that an endemic state $(H^{**}, H_X^{**}, R^{**}, 0, 0, S^{**}, 0)$ exists. Alternatively, $R_X^* = 0$ could correspond to the disease-free equilibrium point (15) for system (1).

The roots of the cubic equation (49) are given as

$$\begin{aligned}
R_{X1}^* &= -\frac{\kappa_3\left(\mu_1\mu_4 + \eta\lambda_z\right)}{\eta\rho_3 + \mu_1\mu_4 + \eta\lambda_z} < 0,\\
R_{X2,3}^* &= \frac{\left(\beta_r\lambda_r - \kappa_2\mu_4\beta_r + \rho_2\beta_r - 1\right) \pm \sqrt{\Theta}}{2\mu_4\beta_r},
\end{aligned} \tag{50}$$

where

$$\begin{aligned}
\Theta &= 4\mu_4\beta_r\left(\kappa_2\beta_r\lambda_r - \kappa_2\right)\\
&\quad + \left(\beta_r\lambda_r - \kappa_2\mu_4\beta_r + \rho_2\beta_r - 1\right)^2.
\end{aligned} \tag{51}$$

The root $R_{X1}^* < 0$ should be ignored, since all the model state variables are nonnegative for all time $t \geq 0$. This leaves $R_{X2,3}^*$ as the only two possible roots of (49).

From the above discussion, model (1) could experience a single endemic state or multiple endemic states subject to the roots of (44) and (47). If $R_{X2,3}^*$ are real and positive, then one or two endemic equilibrium points are possible for model (1). It is thus evident that the explicit form of the endemic equilibrium state for model (1) is cumbersome. We shall therefore show its existence numerically based on a certain choice of parameter values in Section 4. Note that case (iii) of (46) indicates the possibility of having multiple endemic equilibria and hence the likelihood of experiencing a backward bifurcation phenomenon. This will be investigated in another research paper.

4. Numerical Simulations and Discussions

In this section, we provide some numerical simulations to illustrate the behaviour of model system (1). We carry out model sensitivity analysis and investigate parameter influence on the dynamics of red blood cells, macrophages, and malaria parasites under different conditions on the in-host reproduction number, R_0.

4.1. Sensitivity Analysis. In epidemic modelling, sensitivity analysis is performed to investigate model parameters with significant influence on R_0 and hence on the transmission and the spread of the disease under study [43]. Following [44], the normalised forward-sensitivity index of a variable, $\triangle$, which depends differentially on a parameter, α, is defined as

$$\Upsilon_\alpha^{\triangle} = \frac{\partial\triangle}{\partial\alpha} \times \frac{\alpha}{\triangle}. \tag{52}$$

Using the formulation in (52) and the parameter values in Table 3, the local sensitivity indices (SI) of R_0 (see (20)) relative to the model parameters are calculated in Mathematica software and the results summarised in Table 4. Note that, due to limited data on in-host dynamics, all the parameter values used in evaluating the sensitivity indices are obtained from indicated past literature.

A positive sign on the SI indicates that an increase (decrease) in the value of such a parameter increases (decreases) the value of R_0 and hence the growth of malaria infection. On the other hand, a negative sign is indicative of a parameter that negatively affects R_0. In order to eliminate in-host malaria infection, the in-host reproduction number should be less than one, that is, $R_0 < 1$.

The average number of merozoites released per bursting infected erythrocyte K and the proportion of merozoites that cause secondary invasions at the blood phase ζ are the most sensitive parameters in determining the disease outcomes. They have the highest sensitivity indices of +1.0000. For instance, a 10% increase (decrease) ζ or K generates a 10% increase (decrease) on R_0 and hence malaria infection severity.

The parameters λ_z, η, μ_4, and δ_z occupy the second rank in influencing the model outcomes. An increase in the parameters μ_4 and δ_z is likely to increase the model R_0. On the other hand, an increase in λ_z and η has a direct negative influence on R_0. Macrophages are highly

Table 3: Parameter values used in the numerical simulation and demonstration of the existence of endemic equilibrium point. See Table 2 for detailed parameter descriptions.

Symbol	Interpretation	Value	Source
δ_z	Death rate of macrophages	0.05/day	[19]
δ_s	Death rate of sporozoites	1.2×10^{-11} /day	[20]
η	Elimination rate of IRBCs by macrophages	$10^{-10} cells\mu l^{-1}//day$	[19]
λ_h	Recruitment rate of H	$2.5 \times 10^8 cells/\mu l^{-1}/day$	[21]
ρ_1	Production rate of H due to H_X	$2.5 \times 10^{-5}/day$	[19]
μ_1	Death rate of H	0.029 /day	[20]
Λ	Rate of injection of sporozoites	20 sporozoites/day	[20]
ρ_2	Production rate of RBCs due to IRBCs	$2.5 \times 10^{-5}/day$	[19]
β_s	Hepatocyte invasion rate	$1.0 \times 10^{-6}/sporozoites/day$	[20]
ρ_3	Immunogenicity of IRBCs	$2.5 \times 10^{-5}/day$	[19]
μ_2	Death rate of infected hepatocytes	0.02/day	[20]
κ_1	Inhibition rate	$1\, cells/\mu l^{-1}$	[22]
λ_r	Recruitment rate of RBCs	$2.5 \times 10^8 cells/\mu l^{-1}/day$	[23]
ζ	Merozoites that cause secondary infections	0.726 (unitless)	[24]
μ_3	Death rate of healthy RBCs	0.0083/day	[23]
κ_2	Inhibition rate	$1\, cells/\mu l^{-1}$	[22]
β_r	Invasion rate of RBCs	$2.0 \times 10^{-9}/merozoites/day$	[23]
N	Merozoites per liver schizont	10000/day	[21]
μ_4	Death rate of infected RBCs	0.025/day	[19]
κ_3	Inhibition rate	$1\, cells/\mu l^{-1}$	[22]
δ_m	Death rate of merozoites	48/day	[23]
K	Merozoites per blood schizont	16	[21]
λ_z	Recruitment rate of macrophages	$30/\mu l^{-1}/day$	[19]

Table 4: Sensitivity indices of R_0 relative to the model parameters.

Parameter	SI	Parameter	SI
K	+1.0000	ζ	+1.0000
β_r	+0.920422	μ_3	-0.920422
λ_r	+0.920422	λ_z	-0.998585
μ_4	+0.998585	η	-0.998585
δ_z	+0.998585	δ_m	-0.920422

instrumental in malaria parasite clearance and should be preserved.

The rate of generation of macrophages from the bone marrow, λ_z, together with the rate of phagocytosis of infected red blood cells, η, is likely to decrease, proportionally, the disease progression when they are increased. With increased λ_z, there would be more macrophages to phagocytose and clear the rapidly growing density of blood schizonts. This would negatively affect the erythrocytic schizogony. Decreased clearance rate by macrophages would only guarantee successful multiplication of the merozoites through the erythrocytic schizogonic cycle. The subsequent result is increased concentration of merozoites in the host blood and disease progression to even deadly levels.

The parameters β_r and λ_r increase (or decrease) R_0 when they are increased (or decreased). Epidemiologically, an improved erythrocyte invasion rate, β_r, is likely to generate even more new blood schizonts. This increases parasitemia in the host. A 10% increase (decrease) in β_r would increase (decrease) the threshold parameter R_0 by about +9.2%.

Any therapeutic effort that clears the blood schizonts and the infectious merozoites at the blood stage would definitely guarantee immense reduction in model R_0. Therefore, an increase in the death rate of the infected red blood cells and that of the merozoites is likely to decrease significantly the in-host reproduction number R_0. This can be achieved through the use of effective antimalarials such as the use of artemisinin based combination therapy (ACT) in malaria treatment. Moreover, effective vaccines at the erythrocytic stage could greatly help minimize erythrocyte infection rate β_r.

Since the local sensitivity indices are relatively close, we carry out further investigation on parameter influence on disease progression by generating the partial rank correlation coefficients (PRCCs) for each parameter value in model R_0 in the following section.

4.1.1. Global Sensitivity Analysis. A global sensitivity analysis (GSA) is performed to examine the response of an epidemic model to parameter variation within a wider range of parameter space [45]. Applying the approach in [45], the PRCCs between the in-host basic reproduction number R_0 and each of the parameters in Table 2 are derived. Using 1000 simulations per run of the Latin Hypercube Sampling (LHS) scheme [46], the established PRCCs are derived and presented in Figure 2.

Unlike the results in Table 4, the model parameter with the highest influence on R_0 according to the PRCCs results shown in Figure 2 is the rate of invasion of red blood cells by merozoites, β_r. This is followed closely by the recruitment rate of susceptible red blood cells λ_r from the bone marrow. The second set of parameters that also increase (decrease) model R_0 when they are increased (decreased) are ζ, K, μ_3, and δ_z, respectively.

The merozoites' death rate δ_m, the death rate of IRBCs μ_4, and the rate of elimination of IRBCs by macrophages η are shown to have the highest negative influence on disease progression. Although an increase in μ_4 was shown to decrease disease progression in Table 4, the results from global sensitivity analysis are contradictory. An increase in the death rate of parasitized erythrocytes μ_4 decreases parasitemia and hence disease progression.

Based on these results of sensitivity analysis, we make the following remarks: (1) results of global sensitivity analysis are robust and a lot more realistic for implementation, (2) malaria control should target elimination of merozoites and infected red blood cells, (3) an effective and efficient malaria vaccine that deactivates infectious merozoites could be helpful in limiting erythrocyte invasion rate, and (4) a vaccine that is protective of susceptible erythrocytes could further ensure reduced density of second and future generation of merozoites that are responsible for disease progression.

4.2. Numerical Results. Model system (1) is solved numerically using the package scipy.integrate.odeint in Python language. The simulations are performed to illustrate the possible dynamics of the red blood cells, the malaria parasite, and macrophages. For purposes of these simulations, the initial conditions of the variables are hereby assumed. We note that different dynamics could be achieved for a different set of initial conditions.

For $R_0 < 1$ (see Figure 3), the density of susceptible hepatocyte initially declines as the density of infected hepatocytes rises due to invasion from sporozoites. The host's immune system responds to sporozoite invasion by increasing hepatocyte density that levels off at the disease-free equilibrium point $\mathscr{E}_0$ (see Figure 3(a)). As the sporozoites decline to near zero (see Figure 3(b)), infected hepatocytes decline and stabilize at $\mathscr{E}_0$ in (15).

At the blood stage, the rising density of infected erythrocytes declines in a similar fashion to that of the infective merozoites when $R_0 < 1$ (see Figure 3(c)). The densities of the infected erythrocytes and merozoites approach $\mathscr{E}_0$ asymptotically. On the other hand, we observe that the density of susceptible red blood cells initially diminishes due to infection by merozoites and later rises before it plateaus as shown in Figure 3(c).

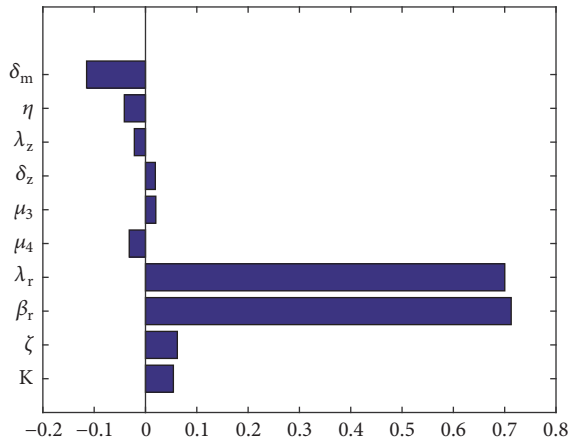

Figure 2: Tornado plots of PRCCs of parameters that influence model R_0 generated using parameter values in Table 3. Parameters with $PRCC > 0$ and $PRCC < 0$ increase and decrease model R_0, respectively.

When $R_0 > 1$, a sharp fall in the density of susceptible hepatocytes in the liver is observed (see Figure 4(a)). This is due to rapid invasion of hepatocytes by the sporozoites. An invasion on susceptible hepatocyte generates a corresponding steady rise in the density of infected hepatocytes (see Figure 4(b)). Owing to natural intervention by the immune system cells, the respective decline and rising levels of susceptible and infected hepatocytes level off and remain relatively constant after the third month. More liver cells are generated to replace infected ones. Figure 4(c) indicates a steady decline in sporozoite density at the liver stage during infections. Invaded hepatocytes burst open to produce merozoites instead of sporozoites and hence the steady decline in sporozoite levels.

Malaria infection dynamics are most rapid in the first 2 weeks within the host liver as illustrated in Figures 4(a), 4(b), and 4(c). This is similar to results in [22, 31]. In the absence of clinical intervention, some of the sporozoites may remain dormant in the human liver and could cause future malaria infections. As the liver schizonts release merozoites into host's blood stream, a rapid decline in the density of red blood cells is observed (see Figure 5(a)). However, the density of infected erythrocytes is noted to rise with equal proportion as shown in Figure 5(b).

An early sharp rise in the density of merozoites in the first one week of the blood stage is noted in Figure 5(c). The density remains high for several weeks and does not decline for the entire infection period of one month. A second-generation merozoite invades other sets of healthy erythrocytes within minutes, leading to an exponential growth in the density of blood schizonts and hence merozoites in the human blood. Without therapeutic intervention, the density of merozoites stabilizes several weeks after infection at the endemic equilibrium point. This is consistent with the findings in [19, 20, 23].

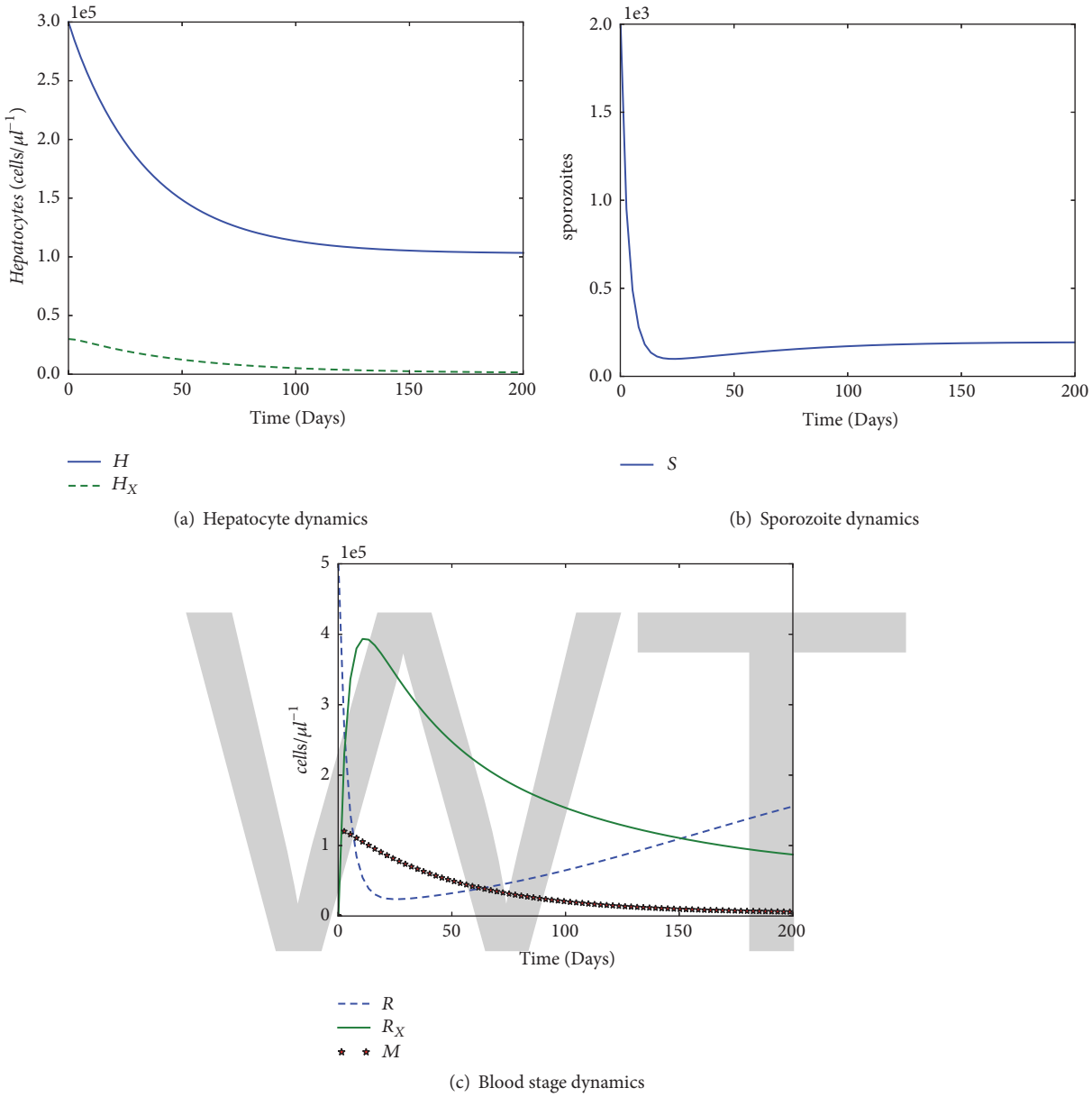

(a) Hepatocyte dynamics

(b) Sporozoite dynamics

(c) Blood stage dynamics

FIGURE 3: Graphs showing the simulation of in-host malaria model (1) when the model $R_0 = 0.22866 < 1$. Figures (a) and (b) show model dynamics at the liver stage. The chosen initial conditions are $H0 = 300000$, $H_X0 = 20000$, $R0 = 500000$, $R_X0 = 50$, $Z0 = 300000$, $S0 = 2000$, and $M = 70$. Used parameter values are given in Table 3.

The invasion of healthy erythrocytes prompts an immune response from host's macrophages. These macrophages phagocyte on the generated blood schizonts. At the onset of erythrocytic infection, several macrophages are generated. The rise in the density of macrophages is proportional to that of infected erythrocytes as shown in Figure 5(d). This rising density is shown to level off after about 16 days at the endemic equilibrium point. It remains high throughout the infection period.

From these discussions, we make the following observations: (1) if $R_0 < 1$, low level malaria infection can easily be contained by the host's defence mechanism and loss of life is less likely; (2) therapeutically, $R_0 < 1$ may be achieved through quick interventions targeting the blood schizonts and the merozoites responsible for secondary infections during the erythrocytic cycle; (3) Figures 4 and 5 prove the existence of malaria endemic equilibrium point.

Hematological parameters such as the density of healthy and infected erythrocytes in malaria hosts have considerable influence on malaria infection and possible impacts [47]. According to WHO [48], hyperparasitemia causes drastic reduction in concentrations of erythrocytes, leading to anaemia among malaria patients. The impacts of increasing the model parameters δ_m and β_r on healthy and infected red blood cells are as shown in Figures 6 and 7, respectively.

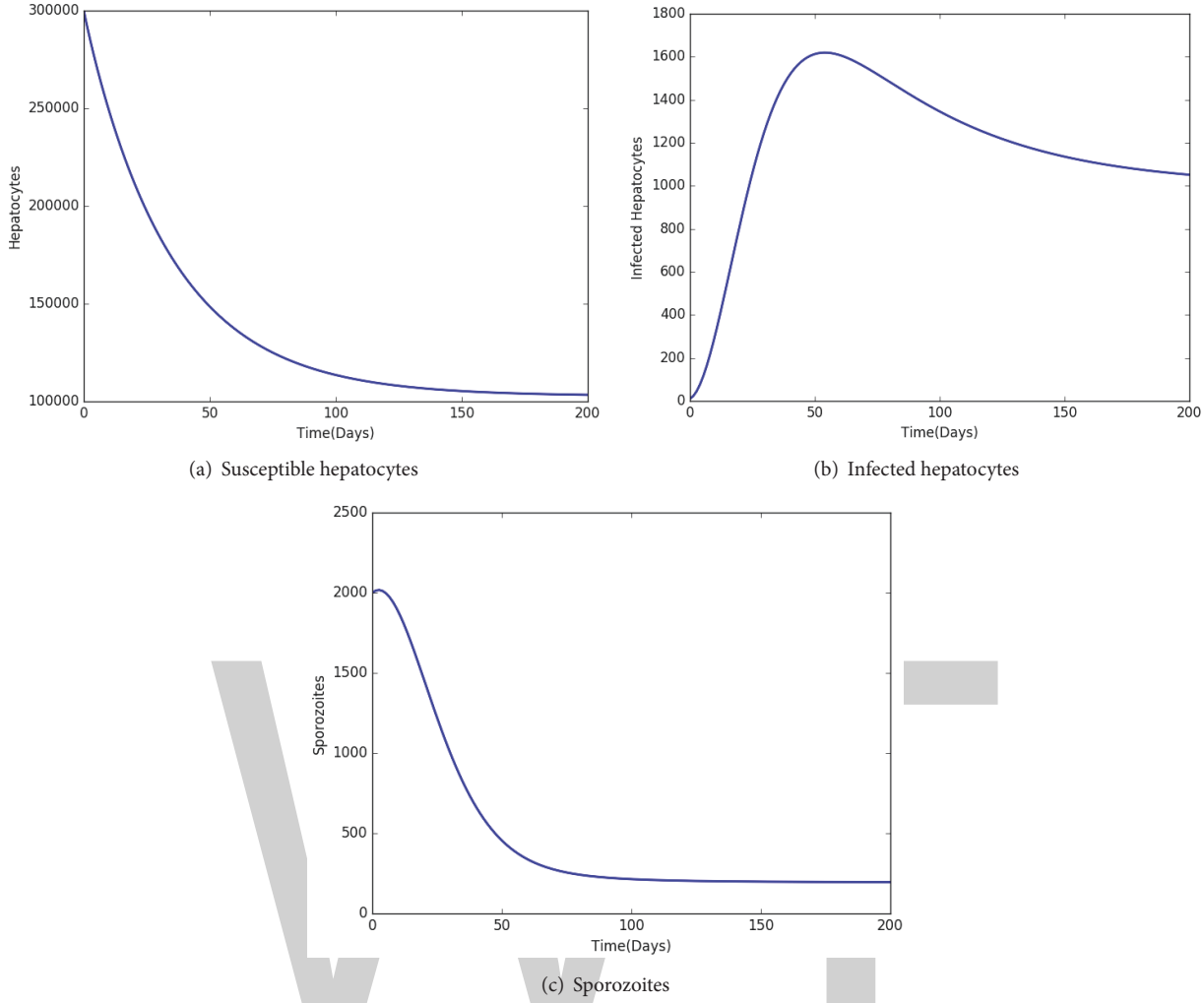

(a) Susceptible hepatocytes

(b) Infected hepatocytes

(c) Sporozoites

FIGURE 4: Graphs showing population dynamics of the liver hepatocytes and malaria sporozoites when $R_0 = 1.58690 > 1$. Used parameter values can be found in Table 3 with the chosen initial conditions described by $H0 = 300000$, $H_X0 = 10$, $R0 = 500000$, $R_X0 = 10$, $Z0 = 10$, $S0 = 2000$, and $M = 20$.

Observe that increased death rate of malaria merozoites δ_m decreases and increases the concentration of parasitized red blood cells and healthy red blood cells, respectively (see Figures 6(a) and 6(b)). Malaria control should thus target the infectious merozoites at the blood stage.

Results in Figure 7(a) indicate that an improved invasion rate by merozoites on susceptible red blood cells causes more loss in healthy erythrocytes. The reverse effect is observed in Figure 7(b), where an increase in the rate of infection of healthy erythrocytes produces a corresponding increase in the density of IRBCs. A keen look at Figure 7(b) reveals that the infected red blood cells begin to appear after about 10–15 days of initial infection. This is consistent with the incubation period of *Plasmodium falciparum* malaria [49].

The severity of malaria infection can easily increase if the density or production of macrophages is compromised [19]. Figure 8(b) shows a near direct relationship on the density of infected red blood cells R_X and the death rate of the macrophages δ_z. An increase in the death of macrophages would propel erythrocytic schizogony and hence increased merozoite numbers in the human blood. A high merozoite density increases the severity of malaria infection. This result is quite vital in malaria intervention, especially with respect to malaria patients who may be suffering from other infections that are deleterious to immune cells. Diseases such as HIV/AIDS greatly weaken the immune system of the patient as crucial immune cells such as macrophages are destroyed. Macrophages are important target cells for HIV-1 virus [50]. During malaria infections, such patients often suffer from severe malaria and should seek immediate medical attention.

Like the senescent red blood cells, aberrant infected erythrocytes formed during malaria infection are eliminated phagocytically by the host's macrophage cells in the red pulp of the spleen [51]. The phagocytic potential of the spleen is vital at the erythrocytic cycle. The higher the phagocytic behaviour of the macrophage, the lower the density of parasitized erythrocytes (see Figure 8(a)). The severity of

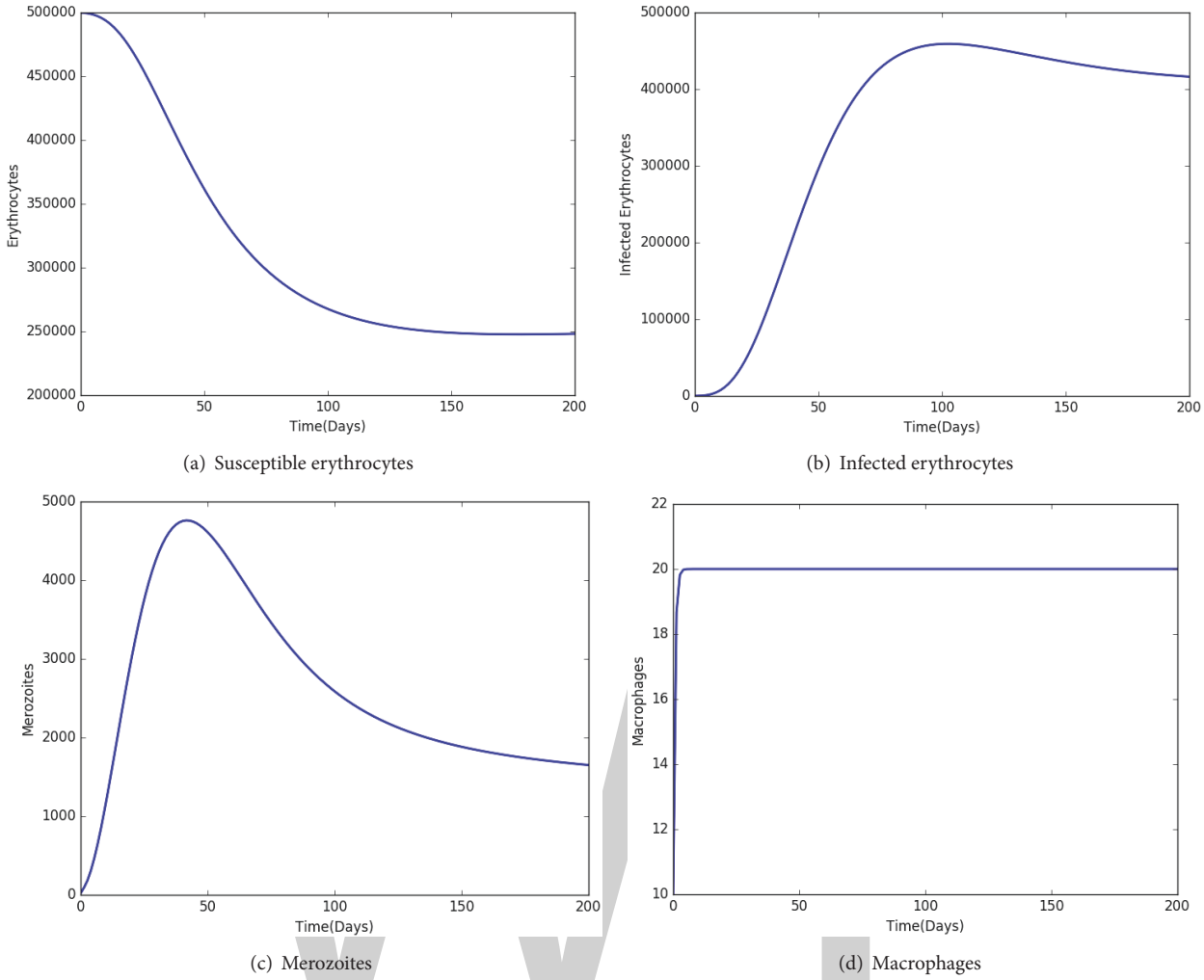

(a) Susceptible erythrocytes

(b) Infected erythrocytes

(c) Merozoites

(d) Macrophages

FIGURE 5: Graphs showing population dynamics of red blood cells, macrophages, and malaria merozoites when $R_0 = 1.58690 > 1$. Simulation parameter values are available in Table 3.

malaria infection increases with decreasing ability of the host's phagocytic merozoites to clear infected red blood cells from circulation during the erythrocytic cycle.

5. Conclusion and Discussion

In this paper, a mathematical model of in-host malaria infection in [21] is extended to include the liver stage of parasite development. Unlike the models in [19, 23, 30], we considered the macrophages as the most effective innate immune cells in eliminating malaria parasites from the human blood circulation. In addition, the liver hepatocytes are assumed to be generated from the bone marrow and through a process of self-regeneration from existing hepatocytes.

We proved that the formulated model is biologically and mathematically well posed in an invariant region Ω. The malaria-free equilibrium is shown to be locally asymptotically stable when the in-host reproduction number is less than unity. The global stability of the malaria-free state is only guaranteed if the threshold quantity R_0 is less than unity.

Our numerical results show that intervention during malaria infection should focus on minimizing merozoite invasion rate on healthy erythrocytes and the density of merozoites in circulation, which are responsible for secondary invasion at the blood stage. In the absence of malaria treatment, the immune cells (macrophages) are shown to be vital in eliminating infected red blood cells at the blood stage. The higher the rate of phagocytosis of infected erythrocytes by macrophages, the lower the density of infected red blood cells and hence malaria parasitemia. Patients suffering from such infections as HIV/AIDS and TB that have deleterious effect on the protective immune cells should seek immediate medical treatment when infected with malaria. Their compromised immune system exposes them to severe malaria attacks and possible untimely death.

For quick and timely reduction of parasitemia, an increased merozoite death rate using antimalarial drugs such as ACT would be necessary. This would further ensure reduced density of infected red blood cells and hence future generation merozoites. By killing a single blood schizont,

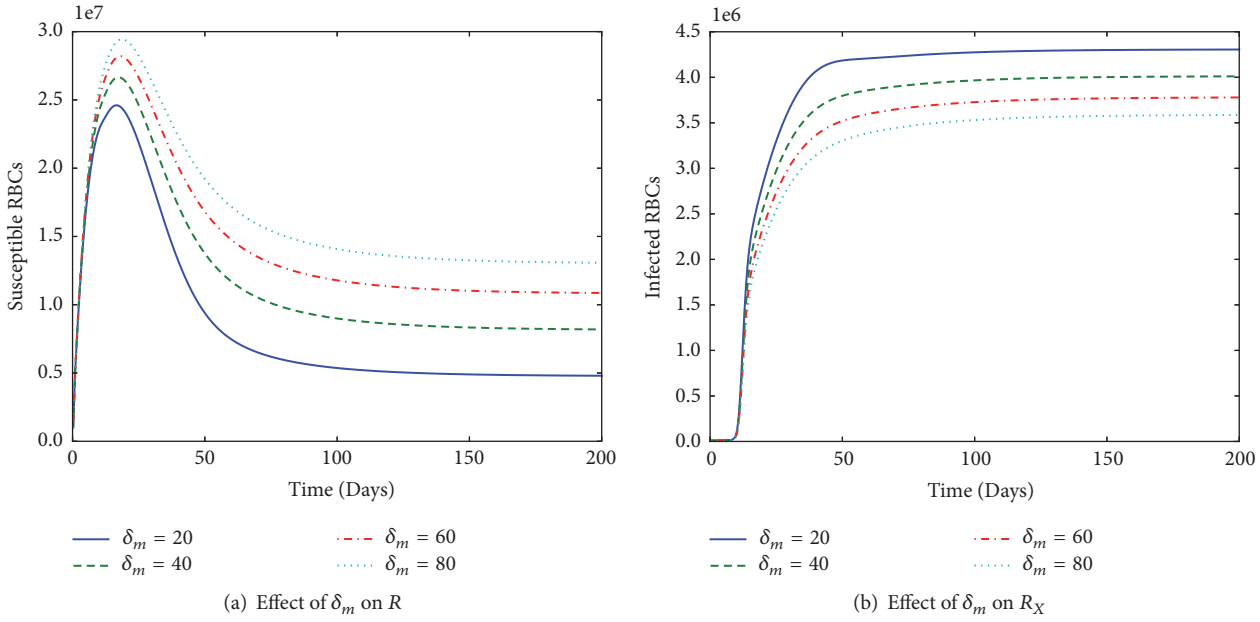

(a) Effect of δ_m on R (b) Effect of δ_m on R_X

FIGURE 6: Graphs showing the behaviour of (a) susceptible RBCs and (b) infected RBCs. They were obtained by varying the death rate of merozoites δ_m from 20 to 80 in steps of 20, while keeping the other parameters (see Table 3) constant.

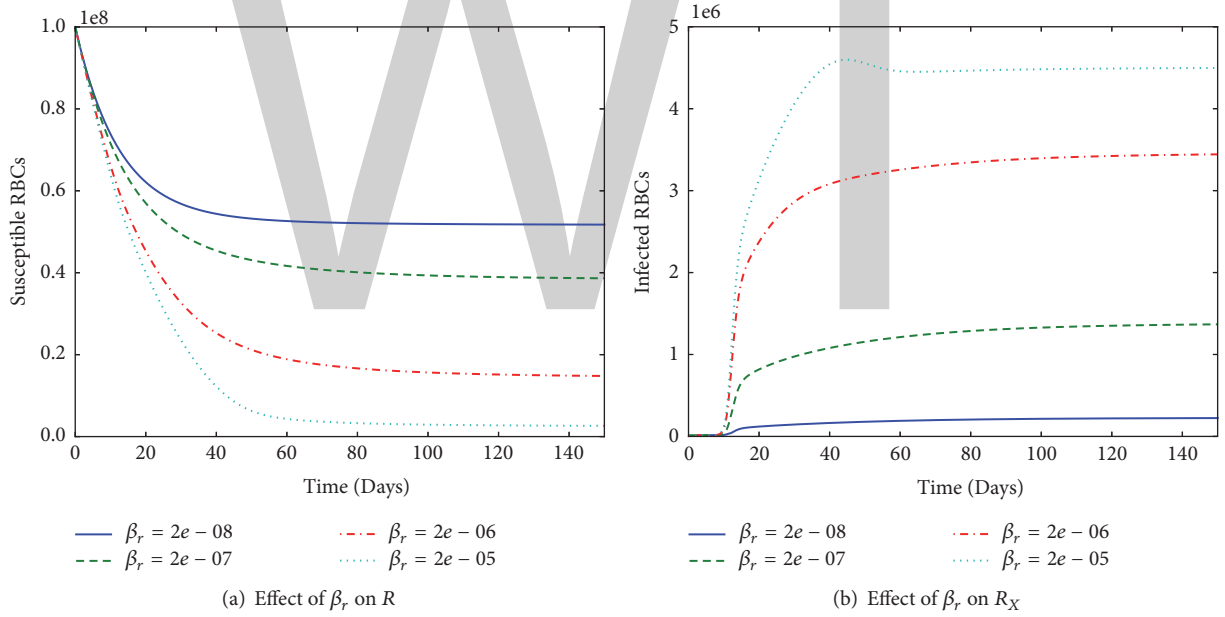

(a) Effect of β_r on R (b) Effect of β_r on R_X

FIGURE 7: Graphs showing the behaviour of (a) susceptible RBCs and (b) infected RBCs. They were obtained by varying the merozoite invasion rate β_r from 2×10^{-8} to 2×10^{-5} in steps of 10^{-1}, while keeping the other parameters in Table 3 constant.

we are likely to avoid the production of sixteen merozoites at maturity. Moreover, an appropriate vaccine that targets erythrocyte invasion process may equally guarantee minimal erythropoiesis. The erythrocyte invasion-avoidance vaccine would minimize the density of infected erythrocytes and hence malaria disease severity. This intervention could help terminate the erythrocytic schizont, leading to minimal parasite transmission to mosquito vector for further development and sexual reproduction.

In this study, drug resistance was not analyzed; this can be considered as a potential area for future investigation.

Conflicts of Interest

The authors declare that there are no conflicts of interest regarding the publication of this article.

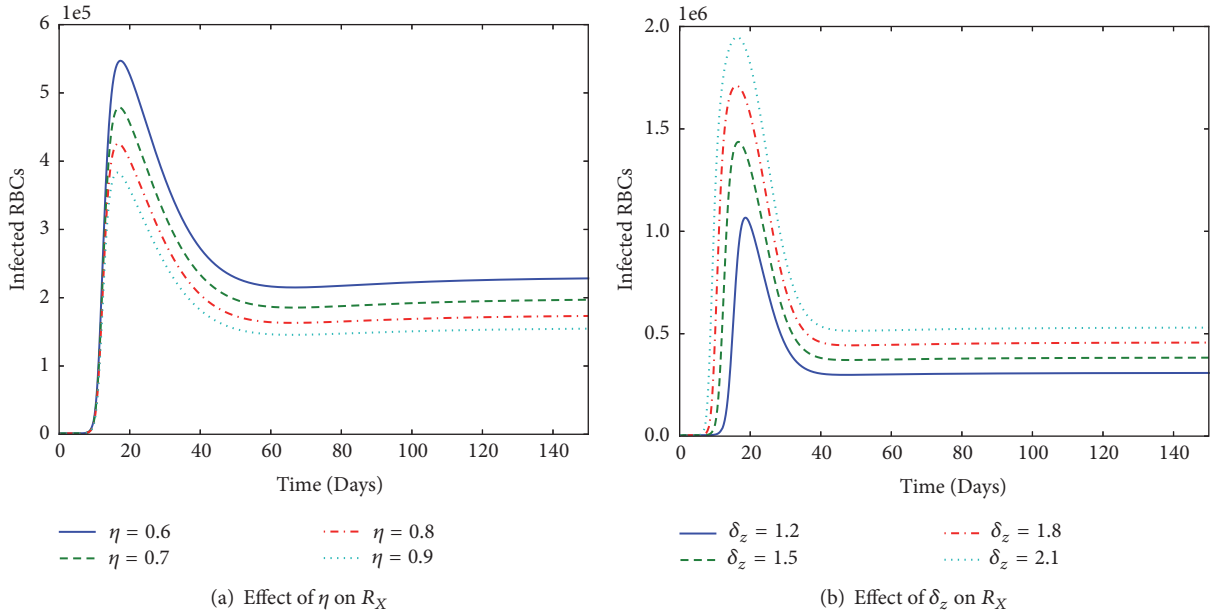

(a) Effect of η on R_X (b) Effect of δ_z on R_X

FIGURE 8: Graphs showing the effect of varying the rate of phagocytosis of IRBCs by macrophages, η (in (a)), and the effect of increased decay rate of macrophages, δ_z (in (b)), on the behaviour of infected erythrocytes R_X. All parameter values are in Table 3.

Acknowledgments

The authors acknowledge with gratitude the support from the Institute of Mathematical Sciences, Strathmore University, and the National Research Fund (NRF), Kenya, for the production of this manuscript.

References

[1] WHO, *Global Health Observatory (GHO) data: Malaria*, 2017, http://www.who.int/gho/malaria/en/.

[2] WHO, "Fact sheet: World malaria report 2016," http://www.who.int/malaria/media/world-malaria-report-2016/en/.

[3] WHO, "Fact sheet: Malaria," http://www.who.int/mediacentre/factsheets/fs094/en/.

[4] WHO., "Achieving the malaria MDG target: Reversing the incidence of malaria 2000-2015," http://www.who.int/malaria/publications/atoz/9789241509442/en/.

[5] K. Mendis, B. J. Sina, P. Marchesini, and R. Carter, "The neglected burden of *Plasmodium vivax* malaria," *The American Journal of Tropical Medicine and Hygiene*, vol. 64, no. 1-2, supplement, pp. 97–106, 2001.

[6] N. T. Bailey, *The biomathematics of malaria*, Charles Griffin, 1982.

[7] M. M. Mota, G. Pradel, J. P. Vanderberg et al., "Migration of Plasmodium sporozoites through cells before infection," *Science*, vol. 291, no. 5501, pp. 141–144, 2001.

[8] A. M. Vaughan, A. S. I. Aly, and S. H. I. Kappe, "Malaria Parasite Pre-Erythrocytic Stage Infection: Gliding and Hiding," *Cell Host & Microbe*, vol. 4, no. 3, pp. 209–218, 2008.

[9] M. F. Good, H. Xu, M. Wykes, and C. R. Engwerda, "Development and regulation of cell-mediated immune responses to the blood stages of malaria: implications for vaccine research," *Annual Review of Immunology*, vol. 23, pp. 69–99, 2005.

[10] H. H. Diebner, M. Eichner, L. Molineaux, W. E. Collins, G. M. Jeffery, and K. Dietz, "Modelling the transition of asexual blood stages of Plasmodium falciparum to gametocytes," *Journal of Theoretical Biology*, vol. 202, no. 2, pp. 113–127, 2000.

[11] C. Chiyaka, "Using mathematics to understand malaria infection during erythrocytic stages," *NuSpace Institutional Repository*, 2010.

[12] S. H. I. Kappe, K. Kaiser, and K. Matuschewski, "The Plasmodium sporozoite journey: A rite of passage," *Trends in Parasitology*, vol. 19, no. 3, pp. 135–143, 2003.

[13] L. H. Miller, D. I. Baruch, K. Marsh, and O. K. Doumbo, "The pathogenic basis of malaria," *Nature*, vol. 415, no. 6872, pp. 673–679, 2002.

[14] A. D. Augustine, B. F. Hall, W. W. Leitner, A. X. Mo, T. M. Wali, and A. S. Fauci, "NIAID workshop on immunity to malaria: Addressing immunological challenges," *Nature Immunology*, vol. 10, no. 7, pp. 673–678, 2009.

[15] Q. Chen, A. Amaladoss, W. Ye et al., "Human natural killer cells control Plasmodium falciparum infection by eliminating infected red blood cells," *Proceedings of the National Acadamy of Sciences of the United States of America*, vol. 111, no. 4, pp. 1479–1484, 2014.

[16] B. S. Franklin, P. Parroche, M. A. Ataíde et al., "Malaria primes the innate immune response due to interferon-γ induced enhancement of toll-like receptor expression and function," *Proceedings of the National Acadamy of Sciences of the United States of America*, vol. 106, no. 14, pp. 5789–5794, 2009.

[17] D. Z. de Back, E. B. Kostova, M. van Kraaij, T. K. van den Berg, and R. van Bruggen, "Of macrophages and red blood cells; A complex love story," *Frontiers in Physiology*, vol. 5, article 9, 2014.

[18] K. Chotivanich, R. Udomsangpetch, R. McGready et al., "Central role of the spleen in malaria parasite clearance," *The Journal of Infectious Diseases*, vol. 185, no. 10, pp. 1538–1541, 2002.

[19] C. Chiyaka, W. Garira, and S. Dube, "Modelling immune response and drug therapy in human malaria infection," *Computational and Mathematical Methods in Medicine. An Interdisciplinary Journal of Mathematical, Theoretical and Clinical Aspects of Medicine*, vol. 9, no. 2, pp. 143–163, 2008.

[20] M. A. Selemani, L. S. Luboobi, and Y. Nkansah-Gyekye, "On stability of the in-human host and in-mosquito dynamics of malaria parasite," *Asian Journal of Mathematics and Applications*, 2016.

[21] J. Tumwiine, J. Y. Mugisha, and L. S. Luboobi, "On global stability of the intra-host dynamics of malaria and the immune system," *Journal of Mathematical Analysis and Applications*, vol. 341, no. 2, pp. 855–869, 2008.

[22] M. A. Selemani, L. S. Luboobi, and Y. Nkansah-Gyekye, "The in-human host and in-mosquito dynamics of malaria parasites with immune responses," *New Trends in Mathematical Sciences*, vol. 5, no. 3, pp. 182–207, 2017.

[23] Y. Li, S. Ruan, and D. Xiao, "The within-host dynamics of malaria infection with immune response," *Mathematical Biosciences and Engineering*, vol. 8, no. 4, pp. 999–1018, 2011.

[24] A. M. Talman, O. Domarle, F. E. McKenzie, F. Ariey, and V. Robert, "Gametocytogenesis: the puberty of *Plasmodium falciparum*," *Malaria Journal*, vol. 3, article 24, 2004.

[25] R. M. Anderson, R. M. May, and S. Gupta, "Non-linear phenomena in host-parasite interactions," *Parasitology*, vol. 99, pp. S59–S79, 1989.

[26] B. Hellriegel, "Modelling the immune response to malaria with ecological concepts: Short-term behaviour against long-term equilibrium," *Proceedings of the Royal Society B Biological Science*, vol. 250, no. 1329, pp. 249–256, 1992.

[27] J. Swinton, "The dynamics of blood-stage malaria: Modelling strain specific and strain transcending immunity. Models for Infectious Human Diseases," in *Their Structure and Relation to Data*, V. Isham and and G. Medley, Eds., pp. 210–212, Cambridge University Press, Cambridge, UK, 1996.

[28] A. M. Dondorp, S. Yeung, L. White et al., "Artemisinin resistance: current status and scenarios for containment," *Nature Reviews Microbiology*, vol. 8, no. 4, pp. 272–280, 2010.

[29] N. J. White, "Antimalarial drug resistance," *The Journal of Clinical Investigation*, vol. 113, no. 8, pp. 1084–1092, 2004.

[30] J. Tumwiine, S. D. Hove-Musekwa, and F. Nyabadza, "A Mathematical Model for the Transmission and Spread of Drug Sensitive and Resistant Malaria Strains within a Human Population," *ISRN biomathematics*, vol. 2014, Article ID 636973, pp. 1–12, 2014.

[31] Z. Tabo, L. S. Luboobi, and J. Ssebuliba, "Mathematical modelling of the in-host dynamics of malaria and the effects of treatment," *Journal of Mathematics and Computer Science*, vol. 17, no. 1, pp. 1–21, 2017.

[32] C. A. W. Bate, J. Taverne, and J. H. L. Playfair, "Malarial parasites induce TNF production by macrophages," *The Journal of Immunology*, vol. 64, no. 2, pp. 227–231, 1988.

[33] M. M. Elloso, H. C. Van Der Heyde, J. A. Vande Waa, D. D. Manning, and W. P. Weidanz, "Inhibition of Plasmodium falciparum in vitro by human $\gamma\delta$ T cells," *The Journal of Immunology*, vol. 153, no. 3, pp. 1187–1194, 1994.

[34] V. V. Ganusov, C. T. Bergstrom, and R. Antia, "Within-host population dynamics and the evolution of microparasites in a heterogeneous host population," *Evolution*, vol. 56, no. 2, pp. 213–223, 2002.

[35] I. M. Rouzine and F. E. McKenzie, "Link between immune response and parasite synchronization in malaria," *Proceedings of the National Acadamy of Sciences of the United States of America*, vol. 100, no. 6, pp. 3473–3478, 2003.

[36] N. J. White et al., "Malaria pathophysiology," *Malaria, parasite biology, pathogenesis and protection*, pp. 371–385, 1998.

[37] N. Fausto, J. S. Campbell, and K. J. Riehle, "Liver regeneration," *Hepatology*, vol. 43, no. 2, pp. S45–S53, 2006.

[38] N. Fausto, "Liver regeneration and repair: hepatocytes, progenitor cells, and stem cells," *Hepatology*, vol. 39, no. 6, pp. 1477–1487, 2004.

[39] J. Crutcher and S. Hoffman, *Malaria. Medical Microbiology*, University of Texas Medical Branch at Galveston, 4th edition, 1996.

[40] S. N. Wickramasinghe and S. H. Abdalla, "Blood and bone marrow changes in malaria," *Baillieres Best Practice and Research in Clinical Haematology*, vol. 13, no. 2, pp. 277–299, 2000.

[41] P. van den Driessche and J. Watmough, "Reproduction numbers and sub-threshold endemic equilibria for compartmental models of disease transmission," *Mathematical Biosciences*, vol. 180, pp. 29–48, 2002.

[42] J. C. Kamgang and G. Sallet, "Global asymptotic stability for the disease free equilibrium for epidemiological models," *Comptes Rendus Mathématique. Académie des Sciences. Paris*, vol. 341, no. 7, pp. 433–438, 2005.

[43] N. Chitnis, J. M. Hyman, and J. M. Cushing, "Determining important parameters in the spread of malaria through the sensitivity analysis of a mathematical model," *Bulletin of Mathematical Biology*, vol. 70, no. 5, pp. 1272–1296, 2008.

[44] L. Arriola and J. Hyman, "Lecture notes, forward and adjoint sensitivity analysis: with applications in dynamical systems," *Linear Algebra and Optimisation Mathematical and Theoretical Biology Institute*, 2005.

[45] J. Wu, R. Dhingra, M. Gambhir, and J. V. Remais, "Sensitivity analysis of infectious disease models: Methods, advances and their application," *Journal of the Royal Society Interface*, vol. 10, no. 86, article 1018, 2013.

[46] M. Stein, "Large sample properties of simulations using Latin hypercube sampling," *Technometrics. A Journal of Statistics for the Physical, Chemical and Engineering Sciences*, vol. 29, no. 2, pp. 143–151, 1987.

[47] L. M. Erhart, K. Yingyuen, N. Chuanak et al., "Hematologic and clinical indices of malaria in a semi-immune population of Western Thailand," *The American Journal of Tropical Medicine and Hygiene*, vol. 70, no. 1, pp. 8–14, 2004.

[48] WHO, "Severe and complicated malaria," *Transactions of the Royal Society of Tropical Medicine and Hygiene*, vol. 84, pp. 1–65, 1990.

[49] W. E. Collins and G. M. Jeffery, "Plasmodium malariae: Parasite and disease," *Clinical Microbiology Reviews*, vol. 20, no. 4, pp. 579–592, 2007.

[50] T. Shiri, W. Garira, and S. D. Musekwa, "A two-strain HIV-1 mathematical model to assess the effects of chemotherapy on disease parameters," *Mathematical Biosciences and Engineering*, vol. 2, no. 4, pp. 811–832, 2005.

[51] J. Krücken, L. I. Mehnert, M. A. Dkhil et al., "Massive destruction of malaria-parasitized red blood cells despite spleen closure," *Infection and Immunity*, vol. 73, no. 10, pp. 6390–6398, 2005.

On Super Mean Labeling for Total Graph of Path and Cycle

Nur Inayah,[1] **I. Wayan Sudarsana**,[2] **Selvy Musdalifah**,[2] **and Nurhasanah Daeng Mangesa**[2]

[1]*Mathematics Department, Faculty of Sciences and Technology, State Islamic University of Syarif Hidayatullah, Jakarta, Indonesia*
[2]*Combinatorial and Applied Mathematics Research Group (CAMRG), Department of Mathematics, Faculty of Mathematics and Natural Sciences, Tadulako University, Palu, Indonesia*

Correspondence should be addressed to Nur Inayah; nur.inayah@uinjkt.ac.id

Academic Editor: Dalibor Froncek

Let $G(V, E)$ be a graph with the vertex set V and the edge set E, respectively. By a graph $G = (V, E)$ we mean a finite undirected graph with neither loops nor multiple edges. The number of vertices of G is called order of G and it is denoted by p. Let G be a (p, q) graph. A super mean graph on G is an injection $f : V \to \{1, 2, 3 \ldots, p + q\}$ such that, for each edge $e = uv$ in E labeled by $f^*(e) = \lceil (f(u) + f(v))/2 \rceil$, the set $f(V) \cup \{f^*(e) : e \in E\}$ forms $\{1, 2, 3, \ldots, p + q\}$. A graph which admits super mean labeling is called super mean graph. The *total graph* $T(G)$ *of* G is the graph with the vertex set $V \cup E$ and two vertices are adjacent whenever they are either adjacent or incident in G. We have showed that graphs $T(P_n)$ and $T(C_n)$ are super mean, where P_n is a path on n vertices and C_n is a cycle on n vertices.

1. Introduction and Preliminary Results

Let $G(V, E)$ be a graph with the vertex set V and the edge set E, respectively. By a graph $G = (V, E)$ we mean a finite undirected, graph with neither loops nor multiple edges. The number of vertices of G is called order of G and it is denoted by p. The number of edges of G is called size of G and it is denoted by q. A (p, q) graph G is a graph with p vertices and q edges. Terms and notations not defined here are used in the sense of Harary [1].

In 2003, Somasundaram and Ponraj [2] have introduced the notion of mean labelings of graphs. Let G be a (p, q) graph. A graph G is called a mean graph if there is an injective function f from the vertices of G to $\{0, 1, 2, \cdots, q\}$ such that when each edge $e = uv$ is labeled with $f^*(e) = (f(u) + f(v) + 1)/2$ if $f(u) + f(v)$ is even and $f^*(e) = (f(u) + f(v) + 1)/2$ if $f(u) + f(v)$ is odd, then the resulting edge labels are distinct. Furthermore, the concept of super mean labeling was introduced by Ponraj and Ramya [3]. Let $f : V \to \{1, 2, 3, \cdots, p+q\}$ be an injection on G. For each edge $e = uv$ and an integer $m \geq 2$, the induced Smarandachely edge m*–labeling* f^* is defined by $f^*(e = uv) = \lceil (f(u)+f(v))/m \rceil$. Then f is called a Smarandachely super m *– mean* labeling if $f(V) \cup \{f^*(e) : e \in E\} = \{1, 2, 3, \cdots, p + q\}$. A graph that admits a Smarandachely super mean m *– labeling* is called Smarandachely super m *– mean* graph. Particularly, if $m = 2$, we know that

$$f^*(e = uv) = \begin{cases} \dfrac{f(u) + f(v)}{2}, & \text{if } f(u) + f(v) \text{ is even;} \\ \dfrac{f(u) + f(v) + 1}{2}, & \text{if } f(u) + f(v) \text{ is odd.} \end{cases} \quad (1)$$

Such a labeling f is called a super mean labeling of G if $f(V) \cup \{f^*(e) : e \in E\} = \{1, 2, 3, \cdots, p + q\}$. A graph that admits a super mean labeling is called a super mean graph. Further discussions of mean and super mean labelings for some families of graph are provided in [4–10] and Gallian [11].

The *total graph* $T(G)$ of G is the graph with the vertex set $V \cup E$ and two vertices are adjacent whenever they are either adjacent or incident in G. For instance, when $G = P_n$, total graph of path $T(P_n)$ is provided in Figure 1. Since the problem on super mean labeling for total graph of path and cycle are still open, the new our contributions are stated in the following sections.

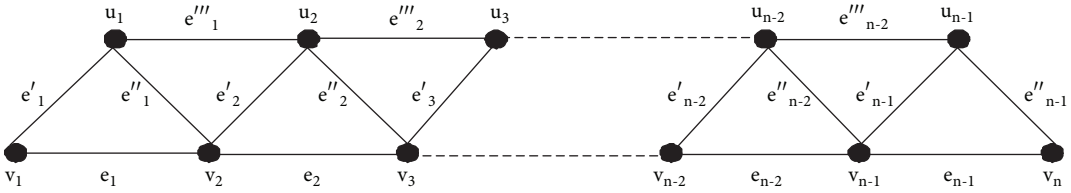

Figure 1: The total graph of path on n vertices.

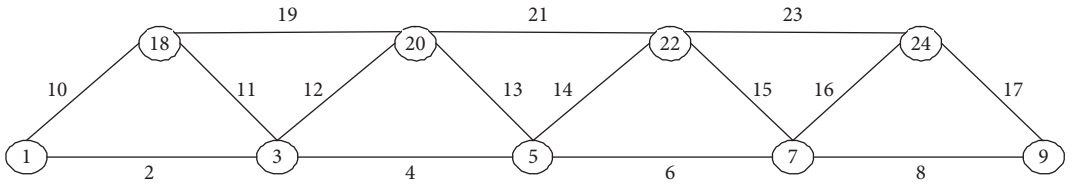

Figure 2: The super mean labeling for total graph of path on 5 vertices, $T(P_5)$.

2. On Super Mean Labeling for Total Graph of Path

The theorem proposed in this section deals with the super mean labeling for total graph of path on n vertices, $T(P_n)$.

Theorem 1. *The total graph of path on n vertices, $T(P_n)$, is a super mean graph for all $n \geq 3$.*

Proof. Let $V(T(P_n)) = \{v_i : 1 \leq i \leq n\} \cup \{u_i : 1 \leq i \leq n-1\}$ and $E(T(P_n)) = \{e_i, e_i', e_i'' : 1 \leq i \leq n-1\} \cup \{e_i''' : 1 \leq i \leq n-2\}$ with $e_i = v_i v_{i+1}$, $e_i' = v_i u_i$, $e_i'' = v_{i+1} u_i$ for $1 \leq i \leq n-1$, and $e_i''' = u_i u_{i+1}$ for $1 \leq i \leq n-2$. Immediately, we have that the cardinality of the vertex set and the edge set of $T(P_n)$ are $p = 2n-1$ and $q = 4n-5$, respectively, and so $p+q = 6n-6$. Define an injection $f : V(T(P_n)) \to \{1, 2, \ldots, 6n-6\}$ for $n \geq 3$ as follows. $f(v_i) = 2i-1$ for $i = 1, 2, \ldots, n$. $f(u_i) = 2i+4n-4$ for $i = 1, 2, \ldots, n-1$. □

And so we have

$$\begin{aligned} f^*(e_i) &= 2i \quad \text{for } i = 1, 2, \ldots, n-1. \\ f^*(e_i') &= 2n + 2i - 2 \quad \text{for } i = 1, 2, \ldots, n-1. \\ f^*(e_i'') &= 2n + 2i - 1 \quad \text{for } i = 1, 2, \ldots, n-1. \\ f^*(e_i''') &= 4n + 2i - 3 \quad \text{for } i = 1, 2, \ldots, n-2. \end{aligned} \tag{2}$$

Next, we consider the following sets:

$$\begin{aligned} A_1 &= \{f(v_i) = 2i-1 : i = 1, 2, \ldots, n\}; \\ A_2 &= \{f(u_i) = 4n + 2i - 4 : i = 1, 2, \ldots, n-1\}; \\ A_3 &= \{f^*(e_i) = 2i : i = 1, 2, \ldots, n-1\}; \\ A_4 &= \{f^*(e_i') = 2n + 2i - 2 : i = 1, 2, \ldots, n-1\}; \\ A_5 &= \{f^*(e_i'') = 2n + 2i - 1 : i = 1, 2, \ldots, n-1\}; \\ A_6 &= \{f^*(e_i''') = 4n + 2i - 3 : i = 1, 2, \ldots, n-2\}. \end{aligned} \tag{3}$$

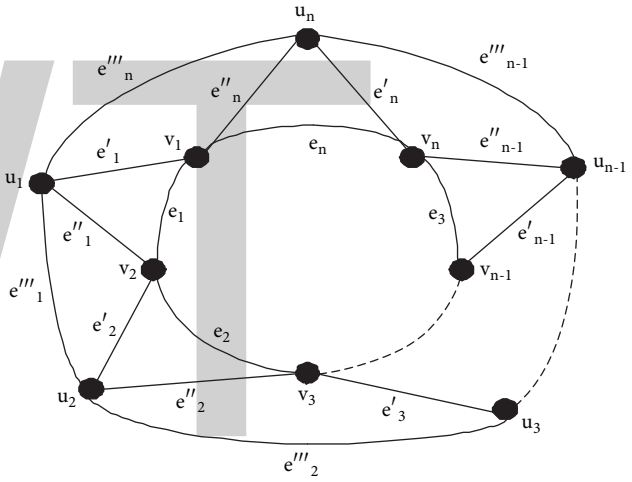

Figure 3: The total graph of cycle on n vertices, $T(C_n)$.

It can be verified that $f(V(T(P_n))) \cup f^*(E(T(P_n))) = \bigcup_{i=1}^{6} A_i = \{1, 2, 3, \ldots, 6n-6\}$ and so f is a super mean labeling of $T(P_n)$. Hence, $T(P_n)$ is a super mean graph. For a simple example, the super mean labeling for total graph of path on five vertices is provided in Figure 2.

3. On Super Mean Labeling for Total Graph of Cycle

The theorem proposed in this section deals with the super mean labeling for total graph of cycle on n vertices, $T(C_n)$. For illustration, total graph of cycle on n vertices is provided in Figure 3.

Theorem 2. *The total graph of cycle on n vertices, $T(C_n)$, is a super mean graph if either n is odd and $n \geq 3$ or n is even and $n \geq 6$.*

Proof. Let $V(T(C_n)) = \{v_i, u_i : 1 \le i \le n\}$ and $E(T(C_n)) = \{e_i, e_i', e_i'', e_i''' : 1 \le i \le n\}$, where

$$e_i = \begin{cases} v_i v_{i+1}, & 1 \le i \le n-1; \\ v_1 v_i, & i = n. \end{cases}$$

$$e_i' = v_i u_i \quad \text{for } 1 \le i \le n$$

$$e_i'' = \begin{cases} v_{i+1} u_i, & 1 \le i \le n-1; \\ v_1 u_i, & i = n. \end{cases} \tag{4}$$

$$e_i''' = \begin{cases} u_i u_{i+1}, & 1 \le i \le n-1; \\ u_1 u_i, & i = n. \end{cases}$$

Immediately, we have that the cardinality of the vertex set and the edge set of $T(C_n)$ are $p = 2n$ and $q = 4n$, respectively, and so $p + q = 6n$. □

Define an injection $f : V(T(C_n)) \to \{1, 2, \ldots, 6n\}$ for odd $n \ge 3$ as follows:

$$f(v_i) = \begin{cases} 2i - 1 & i = 1, 2, 3, \ldots, \left\lceil \frac{n}{2} \right\rceil; \\ 2i & i = \left\lceil \frac{n}{2} \right\rceil + 1, \left\lceil \frac{n}{2} \right\rceil + 2, \ldots, n. \end{cases}$$

$$f(u_i) = \begin{cases} 4n + 2i - 1, & i = 1, 2, 3, \ldots, \left\lceil \frac{n}{2} \right\rceil; \\ 4n + 2i, & i = \left\lceil \frac{n}{2} \right\rceil + 1, \left\lceil \frac{n}{2} \right\rceil + 2, \ldots, n. \end{cases} \tag{5}$$

And so we have

$$f^*(e_i) = \begin{cases} 2i, & i = 1, 2, 3, \ldots, \left\lceil \frac{n}{2} \right\rceil - 1; \\ n + 2, & i = \left\lceil \frac{n}{2} \right\rceil; \\ 2i + 1, & i = \left\lceil \frac{n}{2} \right\rceil + 1, \left\lceil \frac{n}{2} \right\rceil + 2, \ldots, n - 1; \\ n + 1, & i = n. \end{cases}$$

$$f(e_i') = \begin{cases} 2n + 2i - 1, & i = 1, 2, 3, \ldots, \left\lceil \frac{n}{2} \right\rceil; \\ 2n + 2i, & i = \left\lceil \frac{n}{2} \right\rceil + 1, \left\lceil \frac{n}{2} \right\rceil + 2, \ldots, n. \end{cases}$$

$$f^*(e_i'') = \begin{cases} 2n + 2i, & i = 1, 2, 3, \ldots, \left\lceil \frac{n}{2} \right\rceil - 1; \\ 3n + 2, & i = \left\lceil \frac{n}{2} \right\rceil; \\ 2n + 2i + 1, & i = \left\lceil \frac{n}{2} \right\rceil + 1, \left\lceil \frac{n}{2} \right\rceil + 2, \ldots, n - 1; \\ 3n + 1, & i = n. \end{cases} \tag{6}$$

$$f^*(e_i''') = \begin{cases} 4n + 2i, & i = 1, 2, 3, \ldots, \left\lceil \frac{n}{2} \right\rceil - 1; \\ 5n + 2, & i = \left\lceil \frac{n}{2} \right\rceil; \\ 4n + 2i + 1, & i = \left\lceil \frac{n}{2} \right\rceil + 1, \left\lceil \frac{n}{2} \right\rceil + 2, \ldots, n - 1; \\ 5n + 1, & i = n. \end{cases}$$

Next, we consider the following sets:

$$A_1 = \left\{ f(v_i) = 2i - 1 : i = 1, 2, \ldots, \left\lceil \frac{n}{2} \right\rceil \right\};$$

$$A_2 = \left\{ f(v_i) = 2i : i = \left\lceil \frac{n}{2} \right\rceil + 1, \left\lceil \frac{n}{2} \right\rceil + 2, \ldots, n \right\};$$

$$A_3 = \left\{ f(u_i) = 4n + 2i - 1 : i = 1, 2, \ldots, \left\lceil \frac{n}{2} \right\rceil \right\};$$

$$A_4 = \left\{ f(u_i) = 4n + 2i : i = \left\lceil \frac{n}{2} \right\rceil + 1, \left\lceil \frac{n}{2} \right\rceil + 2, \ldots, n \right\};$$

$$A_5 = \left\{ f^*(e_i) = 2i : i = 1, 2, \ldots, \left\lceil \frac{n}{2} \right\rceil - 1 \right\};$$

$$A_6 = \left\{ f^*(e_i) = n + 2 : i = \left\lceil \frac{n}{2} \right\rceil \right\};$$

$$A_7 = \left\{ f^*(e_i) = 2i + 1 : i = \left\lceil \frac{n}{2} \right\rceil + 1, \left\lceil \frac{n}{2} \right\rceil + 2, \ldots, n - 1 \right\};$$

$$A_8 = \{ f(e_i) = n + 1 : i = n \};$$

$$A_9 = \left\{ f^*(e_i') = 2n + 2i - 1 : i = 1, 2, \ldots, \left\lceil \frac{n}{2} \right\rceil \right\};$$

$$A_{10} = \left\{ f^*(e_i') = 2n + 2i : i = \left\lceil \frac{n}{2} \right\rceil + 1, \left\lceil \frac{n}{2} \right\rceil + 2, \ldots, n \right\}; \tag{7}$$

$$A_{11} = \left\{ f^*(e_i'') = 2n + 2i : i = 1, 2, \ldots, \left\lceil \frac{n}{2} \right\rceil - 1 \right\};$$

$$A_{12} = \left\{ f^*(e_i'') = 3n + 2 : i = \left\lceil \frac{n}{2} \right\rceil \right\};$$

$$A_{13} = \left\{ f^*(e_i'') = 2n + 2i + 1 : i = \left\lceil \frac{n}{2} \right\rceil + 1, \left\lceil \frac{n}{2} \right\rceil + 2, \ldots, n - 1 \right\};$$

$$A_{14} = \left\{ f^*(e_i'') = 3n + 1 : i = n \right\};$$

$$A_{15} = \left\{ f^*(e_i''') = 4n + 2i : i = 1, 2, \ldots, \left\lceil \frac{n}{2} \right\rceil - 1 \right\};$$

$$A_{16} = \left\{ f^*(e_i''') = 5n + 2 : i = \left\lceil \frac{n}{2} \right\rceil \right\};$$

$$A_{17} = \left\{ f^*(e_i''') = 4n + 2i + 1 : i = \left\lceil \frac{n}{2} \right\rceil + 1, \left\lceil \frac{n}{2} \right\rceil + 2, \ldots, n - 1 \right\};$$

$$A_{18} = \left\{ f^*(e_i''') = 5n + 1 : i = n \right\}.$$

It can be verified that $f(V(T(C_n))) \cup f^*(E(T(C_n))) = \bigcup_{i=1}^{18} A_i = \{1, 2, 3, \ldots, 6n\}$ and so f is a super mean labeling of $T(C_n)$. Hence $T(C_n)$ is a super mean graph for odd $n \ge 3$.

Now define an injection $f_1 : V(T(C_n)) \to \{1, 2, 3, \ldots, 6n\}$ for even $n \geq 6$ as follows:

$$f_1(v_i) = \begin{cases} 1, & i = 1; \\ 3i - 3, & i = 2, 3; \\ 4i - 7, & i = 4, 5, 6, \ldots \frac{n}{2} + 1; \\ 4n - 4i + 8, & i = \frac{n}{2} + 2, \frac{n}{3} + 3, \ldots, n - 1 \\ 7, & i = n \end{cases}$$

$$f_1(u_i) = \begin{cases} 4n + 1, & i = 1; \\ 4n + 3i - 3, & i = 2, 3; \\ 4n + 4i - 7, & i = 4, 5, 6, \ldots \frac{n}{2} + 1; \\ 8n - 4i + 8, & i = \frac{n}{2} + 2, \frac{n}{3} + 3, \ldots, n - 1 \\ 4n + 7, & i = n \end{cases} \tag{8}$$

and so we have

$$f_1^*(e_i) = \begin{cases} 2, & i = 1; \\ 3i - 1, & i = 2, 3; \\ 4i - 5, & i = 4, 5, 6, \ldots \frac{n}{2} + 1; \\ 4n - 4i + 6, & i = \frac{n}{2} + 2, \frac{n}{3} + 3, \ldots, n - 1 \\ 4, & i = n \end{cases}$$

$$f_1^*(e_i') = \begin{cases} 2n + 1, & i = 1; \\ 2n + 3i - 3, & i = 2, 3; \\ 2n + 4i - 7, & i = 4, 5, 6, \ldots \frac{n}{2} + 1; \\ 6n - 4i + 8, & i = \frac{n}{2} + 2, \frac{n}{3} + 3, \ldots, n - 1 \\ 2n + 7, & i = n \end{cases} \tag{9}$$

$$f_1^*(e_i'') = \begin{cases} 2n + 2, & i = 1; \\ 2n + 3i - 1, & i = 2, 3; \\ 2n + 4i - 5, & i = 4, 5, 6, \ldots \frac{n}{2} + 1; \\ 6n - 4i + 6, & i = \frac{n}{2} + 2, \frac{n}{3} + 3, \ldots, n - 1 \\ 2n + 4, & i = n \end{cases}$$

$$f_1^*(e_i''') = \begin{cases} 4n + 2, & i = 1; \\ 4n + 3i - 1, & i = 2, 3; \\ 4n + 4i - 5, & i = 4, 5, 6, \ldots \frac{n}{2} + 1; \\ 8n - 4i + 6, & i = \frac{n}{2} + 2, \frac{n}{3} + 3, \ldots, n - 1 \\ 4n + 4, & i = n \end{cases}$$

It can be verified that $f_1(V(T(C_n))) \cup f_1^*(E(T(C_n))) = \{1, 2, 3, \ldots, 6n\}$ and so f_1 is a super mean labeling of $T(C_n)$. Hence $T(C_n)$ is a super mean graph for even $n \geq 6$. For illustration, a super mean labeling for total graph of cycle on8 vertices is provided in Figure 4.

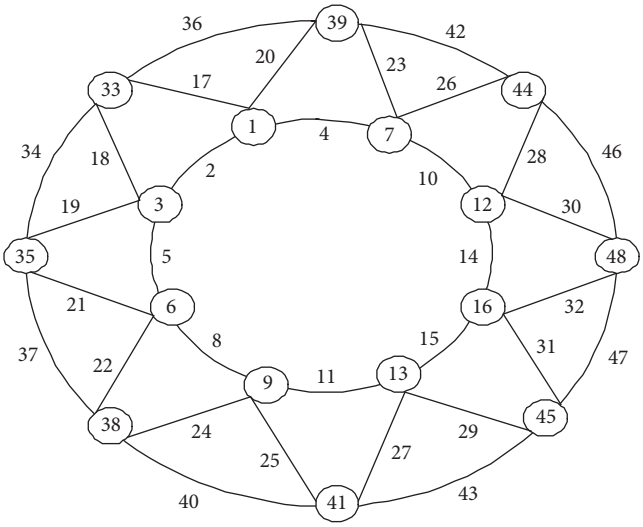

Figure 4: The super mean labeling for total graph of cycle on 8 vertices, $T(C_8)$.

4. The Duality of Super Mean Labeling

Let G be a (p, q) graph. Given any Smarandachely super 2 – *mean* labeling λ on graph G, the labeling λ_1 defined by

$$\begin{aligned} \lambda_1(x) &= p + q + 1 - \lambda(x), \quad \text{for any vertex } x, \\ \lambda_1^*(xy) &= p + q + 1 - \lambda^*(xy), \quad \text{for any edges } xy \end{aligned} \tag{10}$$

is also a Smarandachely super 2 – *mean* labeling of G.

For the proof, since λ is an injection then it is follows that λ_1 is also an injection on G. Hence it can be verified that the set $\lambda_1(V) \cup \{\lambda^* 1(e) : e \in E\}$ forms $\{1, 2, 3, \cdots, p+q\}$ and so the injection λ_1 is also a Smarandachely super 2 – *mean* labeling on graph G. Furthermore we call that the labeling λ_1 is a *dual* super mean labeling of λ.

By using the duality property above, Theorems 1 and 2, we have the following corollary.

Corollary 3. *Let $T(P_n)$ and $T(C_n)$ be the total graph of path and cycle with n vertices, respectively.*

(i) *For all $n \geq 3$, if $\lambda(v_i) = 6n - 2i - 4$ for $1 \leq i \leq n$ and $\lambda(u_i) = 2n - 2i - 1$ for $1 \leq i \leq n - 1$ then λ is a super mean labeling for $T(P_n)$.*

(ii) *For odd $n \geq 3$ if*

$$\lambda(v_i) = \begin{cases} 6n - 2i + 2, & i = 1, 2, 3, \ldots, \left\lceil \frac{n}{2} \right\rceil; \\ 6n - 2i + 1 & i = \left\lceil \frac{n}{2} \right\rceil + 1, \left\lceil \frac{n}{2} \right\rceil + 2, \ldots, n, \end{cases}$$

$$\lambda(u_i) = \begin{cases} 2n - 2i + 2, & i = 1, 2, 3, \ldots, \left\lceil \frac{n}{2} \right\rceil; \\ 2n - 2i + 1 & i = \left\lceil \frac{n}{2} \right\rceil + 1, \left\lceil \frac{n}{2} \right\rceil + 2, \ldots, n \end{cases} \tag{11}$$

then λ is a super mean labeling for $T(C_n)$.

(iii) *For even* $n \geq 6$, *if*

$$\lambda_1(v_i) = \begin{cases} 6n, & i = 1; \\ 6n - 3i + 4, & i = 2, 3; \\ 6n - 4i + 8, & i = 4, 5, 6, \ldots \frac{n}{2} + 1; \\ 2n + 4i - 7, & i = \frac{n}{2} + 2, \frac{n}{3} + 3, \ldots, n - 1 \\ 6n - 6, & i = n, \end{cases}$$

$$\lambda_1(u_i) = \begin{cases} 2n, & i = 1; \\ 2n - 3i + 4, & i = 2, 3; \\ 2n - 4i + 8, & i = 4, 5, 6, \ldots \frac{n}{2} + 1; \\ 2n - 4i - 7, & i = \frac{n}{2} + 2, \frac{n}{3} + 3, \ldots, n - 1 \\ 2n - 6, & i = n \end{cases} \quad (12)$$

then λ_1 *is a super mean labeling for* $T(C_n)$.

5. Summary and Remarks

Here we propose new results corresponding to super mean labeling for total graph of path and cycle. This work is an effort to relate Smarandachely super m – *mean* labeling and its dual for $m \geq 2$. All results reported here are in total graph of path and cycle, $T(P_n)$ and $T(C_n)$. In future, it is not only possible to investigate some more results corresponding to other graph families but also Smarandachely super m-mean labeling in general as well.

Disclosure

An earlier version of this paper was presented as an abstract at Distace in Graph 2016.

Conflicts of Interest

The authors declare that they have no conflicts of interest.

Acknowledgments

The authors would like to express their very great appreciation to Dr. I Wayan Sudarsana, Mrs. Selvy Musdalifah, and Mrs. Nurhasanah Daeng Mangesa for their valuable and constructive suggestion during the conducting of this research work. Their willingness to give their time so generously has been very much appreciated.

References

[1] F. Harary, "Recent results on generalized Ramsey theory for graphs," in *Graph Theory and Applications*, vol. 303 of *Lecture Notes in Mathematics*, pp. 125–138, Springer Berlin Heidelberg, Berlin, Heidelberg, 1972.

[2] S. Somasundaram and R. Ponraj, "Mean labelings of graphs," *National Academy of Science Letters*, vol. 26, no. 7-8, pp. 210–213, 2003.

[3] R. Ponraj and D. Ramya, "On super mean graphs of order," *Bulletin of Pure & Applied Sciences*, vol. 25, no. 1, pp. 143–148, 2006.

[4] S. Somasundaram and R. Ponraj, "Non-existence of mean labeling for a wheel," *Bulletin of Pure & Applied Sciences-Mathematics and Statistics*, vol. 22E, pp. 103–111, 2003.

[5] S. Somasundaram and R. Ponraj, "Some results on mean graphs," *Pure and Applied Mathematics Journal*, vol. 58, pp. 29–35, 2003.

[6] P. Jeyanthi and D. Ramya, "Super mean labeling of some classes of graphs," *International Journal of Mathematical Combinatorics*, vol. 1, pp. 83–91, 2012.

[7] P. Jeyanthi, D. Ramya, and P. Thangavelu, "On super mean graphs," *AKCE International Journal of Graphs and Combinatorics*, vol. 6, no. 1, pp. 103–112, 2009.

[8] P. Jeyanthi, D. Ramya, and P. Thangavelu, "On super mean labeling of some graphs," *SUT Journal of Mathematics*, vol. 46, no. 1, pp. 53–66, 2010.

[9] P. Jeyanthi and D. Ramya, "Super mean graphs," *Utilitas Mathematica*, vol. 96, pp. 101–109, 2015.

[10] D. Ramya, R. Ponraj, and P. Jeyanthi, "Super mean labeling of graphs," *Ars Combinatoria*, vol. 112, pp. 65–72, 2013.

[11] J. A. Gallian, "A dynamic survey of graph labellings," *The Electronic Journal of Combinatorics*, 2016.

Stability Analysis of a Fractional Order Modified Leslie-Gower Model with Additive Allee Effect

Agus Suryanto, Isnani Darti, and Syaiful Anam

Department of Mathematics, Brawijaya University, Jl. Veteran, Malang 65145, Indonesia

Correspondence should be addressed to Agus Suryanto; suryanto@ub.ac.id

Academic Editor: Shyam L. Kalla

We analyze the dynamics of a fractional order modified Leslie-Gower model with Beddington-DeAngelis functional response and additive Allee effect by means of local stability. In this respect, all possible equilibria and their existence conditions are determined and their stability properties are established. We also construct nonstandard numerical schemes based on Grünwald-Letnikov approximation. The constructed scheme is explicit and maintains the positivity of solutions. Using this scheme, we perform some numerical simulations to illustrate the dynamical behavior of the model. It is noticed that the nonstandard Grünwald-Letnikov scheme preserves the dynamical properties of the continuous model, while the classical scheme may fail to maintain those dynamical properties.

1. Introduction

The dynamical interaction of predator and prey is one of important subjects in ecological science. In recent years, one of the most important species interactions is predator-prey model [1]. One of well-known mathematical models which describe the dynamics of prey-predator interaction is the modified Leslie-Gower model proposed by Aziz-Alaoui and Okiye [2]. In this model, the growth rate of predator is in the form of logistics-type where its carrying capacity is proportional to the prey number and environment protection for predator. One of important parameters describing the prey-predator interaction is the functional response which describes the predator's rate of prey consumption per capita. Aziz-Alaoui and Okiye [2] and Yu [3] have considered a modified Leslie-Gower model with Holling type II functional response, while Yu [4] considered the same model but with Beddington-DeAngelis functional response. In the normalized variables, the modified Leslie-Gower equation with Beddington-DeAngelis functional response can be written as

$$\begin{aligned}\frac{dN}{dt} &= N(1-N) - \frac{\omega NP}{a+bN+cP}\\ \frac{dP}{dt} &= sP\left(1-\frac{P}{N+k}\right),\end{aligned} \tag{1}$$

where $N = N(t)$ and $P = P(t)$ denote population densities of prey and predator at time t, respectively. The pa rameters ω, a, b, c, s, and k are positive constants.

One of other factors that influence the interaction of predator and prey is Allee effect, referring to a decrease in per capita fertility rate at low population densities. Allee effect may occur under several mechanisms, such as difficulties in finding mates when population density is low or social dysfunction at small population sizes. When such a mechanism operates, the per capita fertility rate of the species increases with density; that is, positive interaction among species occurs [5–8]. Recently Indrajaya et al. [9] investigate a modified Leslie-Gower equation with Beddington-DeAngelis functional response and additive (both weak and strong) Allee effect on prey

$$\begin{aligned}\frac{dN}{dt} &= N\left(1-N-\frac{m}{N+h}\right) - \frac{\omega NP}{a+bN+cP}\\ \frac{dP}{dt} &= sP\left(1-\frac{P}{N+k}\right),\end{aligned} \tag{2}$$

with initial conditions $N(0) > 0$ and $P(0) > 0$. The criteria of the Allee effect are as follows [7, 8]:

(i) If $0 < m < h$, then the Allee effect is weak.

(ii) If $m > h$, then the Allee effect is strong.

It is shown in system (2) that the growth rates of both prey and predator depend only on the current state. In many situations, the growth rate is also dependent on the history of variable or its memory. With the rapid development of fractional calculus, fractional differential equations have been implemented in various fields including biological system. This is due the fact that fractional differential equations are naturally related to the real life phenomena with memory which exists in most of biological system [10–16]. To describe such memory effect, we first recall the definition of fractional integral operator as well as fractional differential operator.

Definition 1 (see [17]). The Riemann-Liouville α-order fractional integral operator of any function $u \in L_1[0,a]$, $x \in [0,a]$ is defined by

$$J^{\alpha}u(x) = \frac{1}{\Gamma(\alpha)}\int_0^a (x-t)^{\alpha-1}u(t)\,dt, \tag{3}$$

where $\Gamma(\cdot)$ is the Euler Gamma function.

Definition 2 (see [17]). Let m be an integer which satisfies $m-1 < \alpha < m$. The Riemann-Liouville α-order fractional derivative of function $u \in L_1[0,a]$ is defined as

$$\begin{aligned} D_{RL}^{\alpha}u(x) &:= \frac{d^m}{dx^m}J^{m-\alpha}u(x) \\ &= \frac{1}{\Gamma(m-\alpha)}\frac{d^m}{dx^m}\int_0^a (x-t)^{m-\alpha-1}u(t)\,dt, \end{aligned} \tag{4}$$

where d^m/dx^m is the common m-order derivative.

The Riemann-Liouville fractional derivative is historically the first concept of fractional derivative and theoretically well established. However, in the case of Riemann-Liouville fractional differential equation, the initial value is usually given in the form of fractional derivative, which is not practical. Consequently, one applies the Caputo fractional derivative which is defined as follows.

Definition 3 (see [17]). The Caputo fractional differential operator of order $\alpha > 0$, with $m-1 < \alpha < m$, $m \in N$, is defined by

$$\begin{aligned} D_C^{\alpha}u(x) &:= J^{m-\alpha}u^{(m)}(x) \\ &= \frac{1}{\Gamma(m-\alpha)}\int_0^a (x-t)^{m-\alpha-1}u^{(m)}(t)\,dt. \end{aligned} \tag{5}$$

For simplicity, the Caputo fractional derivative of function $u(t)$ of order α is denoted by $d^{\alpha}u(t)/dt^{\alpha}$.

From Definition 3, we see the α-order fractional derivative at time t is not defined locally; it relies on the total effects of the commonly used m-order integer derivative on the interval $[0,t]$. So it can be used to describe the variation of a system in which the instantaneous change rate depends on the past state, which is called the "memory effect" in a visualized manner [18].

In this paper we reconsider system (2). By assuming that the growth rates of both prey and predator at time t do not only depend instantaneously on the current state but also depend on the past state, we replace the first order derivatives in system (2) with the fractional order Caputo type derivatives:

$$\begin{aligned} \frac{d^{\alpha}N}{dt^{\alpha}} &= N\left(1-N-\frac{m}{N+h}\right)-\frac{\omega NP}{a+bN+cP} \\ \frac{d^{\alpha}P}{dt^{\alpha}} &= sP\left(1-\frac{P}{N+k}\right), \end{aligned} \tag{6}$$

where $0 < \alpha < 1$. Hence we have a system of fractional differential equation. In the following we discuss the dynamical properties of system (6). To study the stability of equilibrium points, we apply the following stability theorem.

Theorem 4 (see [19]). *Consider the following autonomous nonlinear fractional order system:*

$$\frac{d^{\alpha}\vec{u}(t)}{dt^{\alpha}} = \vec{f}(\vec{u}(t)); \quad \vec{u}(0) = \vec{u}_0; \ 0 < \alpha < 1. \tag{7}$$

The equilibrium points of the above system are solutions to the equation $\vec{f}(\vec{u}(t)) = 0$. An equilibrium point $\vec{u}^*$ is locally asymptotically stable if all eigenvalues (λ_j) of the Jacobian matrix $J = \partial\vec{f}/\partial\vec{u}$ evaluated at equilibrium $\vec{u}^*$ satisfy $|\arg(\lambda_j)| > \alpha\pi/2$.

2. Equilibria and Their Stability

Based on Theorem 4, equilibria of model (6) can be determined by solving the following system:

$$\begin{aligned} N\left(1-N-\frac{m}{N+h}\right)-\frac{\omega NP}{a+bN+cP} &= 0 \\ sP\left(1-\frac{P}{N+k}\right) &= 0. \end{aligned} \tag{8}$$

System (8) has been solved by Indrajaya et al. [9], and the obtained equilibria are as follows:

(1) The equilibria of system (6) for the weak Allee effect case are

(a) trivial equilibrium $E_{w0} = (0,0)$, that is, the extinction of both prey and predator point,

(b) two axial equilibria, that is, the prey extinction point $E_{w1} = (0,k)$ and the predator extinction point $E_{w2} = (N_{w2},0)$ where

$$N_{w2} = \frac{1}{2}\left(1-h+\sqrt{(1-h)^2+4(h-m)}\right), \tag{9}$$

(c) positive or coexistence equilibrium $E_w^* = (N_w^*, P_w^* = N_w^* + k)$, where N_w^* are all possible real positive solutions of cubic equation

$$N^3 + 3\eta_1 N^2 + 3\eta_2 N + \eta_3 = 0, \tag{10}$$

where

$$\eta_1 = -\frac{(b+c)(1-h)-(a+ck)-\omega}{3(b+c)},$$
$$\eta_2 = -\frac{(a+ck)(1-h)+(b+c)(h-m)-\omega(h+k)}{3(b+c)}, \quad (11)$$
$$\eta_3 = -\frac{(a+ck)(h-m)-h\omega k}{(b+c)}.$$

(2) The equilibria of system (6) for the strong Allee effect case are

(a) trivial equilibrium $E_{s0} = (0,0)$, that is, the extinction of both prey and predator point,

(b) three axial equilibria that are the prey extinction point $E_{w1} = (0,k)$ and two predator extinction points: $E_{s2} = (N_{s2}, 0)$ and $E_{s3} = (N_{s3}, 0)$, where

$$N_{s2} = \frac{1}{2}\left(1-h+\sqrt{(1-h)^2+4(h-m)}\right),$$
$$N_{s3} = \frac{1}{2}\left(1-h-\sqrt{(1-h)^2+4(h-m)}\right), \quad (12)$$

(c) positive or coexistence equilibrium point $E_s^* = (N_s^*, P_s^* = N_s^* + k)$, where N_s^* are also all possible real positive solutions of cubic equation (10).

Using transformation $z = N^* + \eta_1$, (10) can be reduced to

$$h(z) = z^3 + 3pz + q = 0, \quad (13)$$

where $p = \eta_2 - \eta_1^2$ and $q = \eta_3 - 3\eta_1\eta_2 + 2\eta_1$. Implementing Cardan's method as performed by Cai et al. [7], we obtain the existence of the positive equilibria as follows.

Lemma 5 (existence of positive equilibria). *Let (N^*, P^*) be the interior equilibrium of model (6) for both weak and strong Allee effects where N^* is a real positive solution of (10). Then the following statements hold:*

(a) *If $q < 0$, then (13) has a single positive root z_1. As a result, model (6) has a unique positive equilibrium point, that is, $E^* = (N^*, N^* + k) = (z_1 - \eta_1, z_1 - \eta_1 + k)$, with $z_1 > \eta_1$.*

(b) *Suppose that $q > 0$ and $p < 0$, then*

(b1) *If $q^2 + 4p^3 = 0$, then (13) has a positive root of multiplicity two. Thus, model (6) has a unique positive equilibrium point, that is, $E^* = (N^*, N^* + k) = (\sqrt{-p}, \sqrt{-p} + k)$.*

(b2) *If $q^2 + 4p^3 < 0$, then (13) has two positive roots z_1 and z_2. Thus, model (6) has two positive equilibrium points, namely, $E_1^* = (N_1^*, N_1^* + k) = (z_1 - \eta_1, z_1 - \eta_1 + k)$ and $E_2^* = (N_2^*, N_2^* + k) = (z_2 - \eta_1, z_2 - \eta_1 + k)$, with $E_1^* = (N_1^*, N_1^* + k)$ $z_{1,2} > \eta_1$.*

(c) *If $q = 0$ and $p < 0$, then (13) has a unique positive root $z_1 = \sqrt{-3p}$. As a result, model (6) has a unique positive equilibrium point, that is, $E^* = (N^*, N^* + k) = (\sqrt{-3p}, \sqrt{-3p} + k)$ with $q|_{m=0} = 0$.*

Moreover, algebraic computations show that if (13) has two positive roots, then they are

$$z_1 = \frac{\left(-4q + 4\sqrt{4p^3+q^2}\right)^{2/3} - 4p}{2\left(-4q + 4\sqrt{4p^3+q^2}\right)^{2/3}},$$
$$z_2 = -\frac{z_1}{2} + \frac{\sqrt{z_1^3 + 4q}}{2\sqrt{z_1}}. \quad (14)$$

If (13) has a positive root, then it must be

$$z_1 = \frac{\left(-4q + 4\sqrt{4p^3+q^2}\right)^{2/3} - 4p}{2\left(-4q + 4\sqrt{4p^3+q^2}\right)^{2/3}}. \quad (15)$$

To check the local stability of each equilibrium point, we linearize system (6) around the equilibrium and verify all eigenvalues of the Jacobian matrix evaluated at the equilibrium. The stability properties of trivial and axial equilibrium points for the case of weak and strong Allee effect are, respectively, stated in Theorems 6 and 7.

Theorem 6. *Stability of trivial and axial equilibrium for weak Allee effect ($0 < m < h$):*

(i) *the trivial equilibrium $E_{w0} = (0,0)$ and the axial equilibrium $E_{w2} = (N_{w2}, 0)$ are always unstable;*

(ii) *the axial equilibrium $E_{w1} = (0,k)$ is asymptotically stable if $h - m < h\omega k/(a + ck)$.*

Proof. (i) The Jacobian matrix at E_{w0} is $J(E_{w0}) = \begin{pmatrix} 1-m/h & 0 \\ 0 & s \end{pmatrix}$, and the eigenvalues are $\lambda_1 = 1 - m/h > 0$ and $\lambda_1 = s > 0$. It is clear that $\arg(\lambda_{1,2}) = 0 < \alpha\pi/2, \alpha > 0$. Hence E_{w0} is unstable. The Jacobian matrix at E_{w2} is $J(E_{w2}) = \begin{pmatrix} 1-2N_{w2}^* - mh/(2N_{w2}^*+h)^2 & -\omega N_{w2}^*/(a+bN_{w2}^*) \\ 0 & s \end{pmatrix}$ where one of its eigenvalues is $\lambda = s > 0$ and therefore E_{w2} is unstable because $\arg(\lambda) = 0 < \alpha\pi/2, \alpha > 0$.

(ii) The Jacobian matrix at E_{w1} is $J(E_{w1}) = \begin{pmatrix} 1-m/h-\omega k/(a+ck) & 0 \\ 0 & -s \end{pmatrix}$. The eigenvalues of $J(E_{w1})$ are $\lambda_1 = -s < 0$ and $\lambda_2 = 1 - m/h - \omega k/(a + ck)$. Thus $\arg(\lambda_1) = \pi > \alpha\pi/2$ and $\arg(\lambda_2) = \pi > \alpha\pi/2$ whenever $h - m < h\omega k/(a + ck)$. This proves part (ii). □

Using the same argument as in the proof of Theorem 6, we obtain the following stability properties of equilibria for the case of strong Allee effect.

Theorem 7. *Stability of trivial and axial equilibrium for strong Allee effect ($m > h$):*

(i) *the trivial equilibrium $E_{s0} = (0,0)$; the axial equilibria: $E_{s2} = (N_{s2}, 0)$ and $E_{s3} = (N_{s3}, 0)$ are always unstable;*

(ii) *the axial equilibrium* $E_{s1} = (0, k)$ *is always asymptotically stable.*

The stability properties of positive (coexistence) equilibrium for the case of weak and strong Allee effect are stated in Theorems 8 and 9.

Theorem 8. *Stability of coexistence equilibrium for weak Allee effect* $(0 < m < h)$*:*

suppose $J(E_w^*)$ *is the Jacobian matrix at coexistence equilibrium* E_w^**. Equilibrium* E_w^* *is asymptotically stable if one of the following mutually exclusive conditions holds:*

(i) $\text{Trace}(J(E_w^*)) < 0$; $\text{Det}(J(E_w^*)) > 0$ *and* $\Delta = \text{Trace}^2(J(E_w^*)) - 4\text{Det}(J(E_w^*)) \geq 0$.

(ii) $\text{Det}(J(E_w^*)) > 0$, $\Delta < 0$ *and*

$$\frac{\sqrt{|\Delta|}}{\text{Trace}\left(J\left(E_w^*\right)\right)} > \tan\left(\frac{\alpha\pi}{2}\right). \tag{16}$$

Proof. The characteristics equation of $J(E_w^*)$ is given by

$$\lambda^2 - \text{Trace}\left(J\left(E_w^*\right)\right)\lambda + \text{Det}\left(J\left(E_w^*\right)\right) = 0. \tag{17}$$

(i) If $\text{Trace}(J(E_w^*)) < 0$; $\text{Det}(J(E_w^*)) > 0$; and $\Delta \geq 0$ then $\lambda_{1,2} < 0$; hence $\arg(\lambda_{1,2}) = \pi > \alpha\pi/2$ and the result follows.

(ii) If λ is an eigenvalue of $J(E_w^*)$ and $\Delta < 0$, then $\overline{\lambda}$ is also an eigenvalue. Using $\sqrt{|\Delta|}/\text{Trace}(J(E_w^*)) > \tan(\alpha\pi/2)$, we have that $|(\lambda - \overline{\lambda})/(\lambda + \overline{\lambda})| = |\text{Im}(\lambda)/\text{Re}(\lambda)| = |\arg(\lambda)| > \tan(\alpha\pi/2)$. Therefore the stability of E_w^* follows. □

Similarly we have Theorem 9 for the stability of coexistence equilibrium for strong Allee effect case.

Theorem 9. *Stability of coexistence equilibrium for strong Allee effect* $(m > h)$*:*

suppose $J(E_s^*)$ *is the Jacobian matrix evaluated at the coexistence equilibrium* E_s^**. Equilibrium* E_s^* *is asymptotically stable if one of the following mutually exclusive conditions holds:*

(i) $\text{Trace}(J(E_s^*)) < 0$; $\text{Det}(J(E_s^*)) > 0$; *and*

$$\Delta = \text{Trace}^2\left(J\left(E_s^*\right)\right) - 4\text{Det}\left(J\left(E_s^*\right)\right) \geq 0. \tag{18}$$

(ii) $\text{Det}(J(E_s^*)) > 0$, $\Delta < 0$, *and*

$$\frac{\sqrt{|\Delta|}}{\text{Trace}\left(J\left(E_s^*\right)\right)} > \tan\left(\frac{\alpha\pi}{2}\right). \tag{19}$$

Based on the above theorems it can be seen that the stability properties of both trivial and axial equilibrium points are not dependent on α (order of fractional derivative). But α may influence significantly the stability of coexistence equilibrium point. Coexistence point can be asymptotically stable although the eigenvalue of Jacobian matrix has positive real part, provided that conditions of Theorem 8(ii) or Theorem 9(ii) are met. This is in contrast to the coexistence equilibrium point of the integer-order model (2) where coexistence point is asymptotically stable only if all real parts of the eigenvalues of the Jacobian matrix are negative [9].

3. Numerical Simulations

To solve system (6), we implement a nonstandard Grünwald-Letnikov scheme which is a combination of the Grünwald-Letnikov approximation [20] and the nonstandard finite difference (NSFD) method [21, 22]. According to [20], the explicit (or implicit) Grünwald-Letnikov (GL) approximation for a fractional differential equation with initial value

$$\frac{d^\alpha y(t)}{dt^\alpha} = f\left(y(t)\right), \quad y(0) = y_0 \ \ (0 < \alpha < 1) \tag{20}$$

is given by

$$y\left(t_{n+1}\right) - \sum_{\nu=1}^{n+1} c_\nu^\alpha y\left(t_{n+1-\nu}\right) - r_{n+1}^\alpha y_0 = \Delta t^\alpha f\left(y_n\right) \left(\text{or} = \Delta t^\alpha f\left(y_{n+1}\right)\right), \tag{21}$$

where $c_\nu^\alpha = (1 - (\alpha + 1)/\nu)c_{\nu-1}^\alpha$; $c_1^\alpha = \alpha$; and $r_{n+1}^\alpha = \Delta t^\alpha r_0^\alpha(t_{n+1}) = (n+1)^{-\alpha}/\Gamma(1-\alpha)$. Here, Δt represents the time step of numerical integration. The Grünwald-Letnikov approximation is proceeding iteratively but the sum in the scheme becomes longer and longer which represents the memory effects. Scherer et al. [20] have shown that the coefficient c_ν^α is positive and satisfies $0 < c_{n+1}^\alpha < c_n^\alpha < \cdots < c_1^\alpha = \alpha$ for $n \geq 1$. Observe that in the standard Grünwald-Letnikov approximation (21), the right hand side of (20) is approximated locally. We implement a nonstandard method which is adopted from the NSFD method [23]. A numerical scheme for an initial value problem

$$\frac{d\vec{u}}{dt} = \vec{f}(t, \vec{u}); \quad \vec{u}(0) = \vec{u}_0 \tag{22}$$

is called a NSFD method if at least one of the following conditions is satisfied [21, 22]:

(i) The left hand side is approximated by the generalization of forward difference scheme

$$\frac{d\vec{u}_n}{dt} \approx \frac{\vec{u}_{n+1} - \vec{u}_n}{\psi(\Delta t)}. \tag{23}$$

The nonnegative denominator function has to satisfy $\psi(\Delta t) = \Delta t + O(\Delta t^2)$.

(ii) The approximation of $f(t, \vec{u})$ is nonlocal.

By implementing the Grünwald-Letnikov approximation for the fractional derivative and the nonlocal approximation

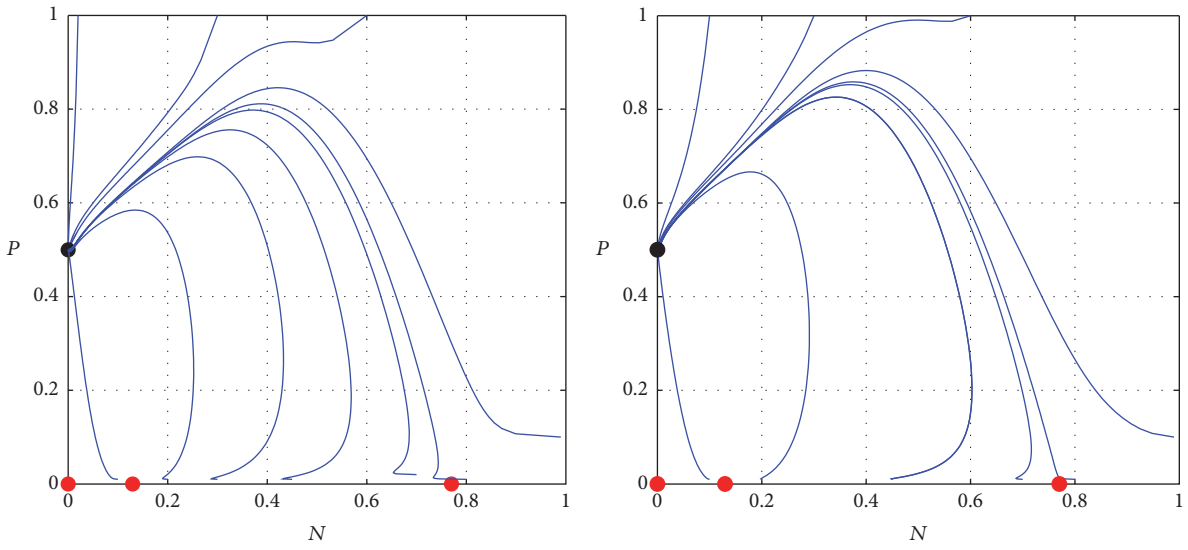

(a) $\alpha = 0.80$ (b) $\alpha = 0.95$

FIGURE 1: Phase portrait of system (6). The values of parameters are $s = 1$, $k = 0.5$, $m = 0.2$, $h = 0.1$, $\omega = 0.7$, $a = 1$, $b = 0.5$, $c = 0.05$, and $\Delta t = 0.1$.

for the right hand side of system (6) we get the following scheme:

$$N_{n+1} = \frac{r_{n+1}^{\alpha} N_0 + \sum_{j=1}^{n+1} c_j^{\alpha} N_{n+1-j} + \Delta t^{\alpha} N_n}{1 + \Delta t^{\alpha} \left(N_n + m/\left(N_n + h\right) + \omega P_n/\left(a + bN_n + cP_n\right)\right)} \quad (24)$$

$$P_{n+1} = \frac{r_{n+1}^{\alpha} P_0 + \sum_{j=1}^{n+1} c_j^{\alpha} P_{n+1-j} + \Delta t^{\alpha} s P_n}{1 + \Delta t^{\alpha} s P_n/\left(N_n + k\right)}.$$

Observe that scheme (24) is explicit and hence it is simple and easy to be implemented. Besides that, the nonstandard Grünwald-Letnikov scheme (24) also maintains the positivity solutions.

To verify our stability analysis as well as the effectiveness our numerical scheme, we perform some numerical simulations. First we use hypothetic values of parameters $s = 1$, $k = 0.5$, $m = 0.2$, $h = 0.1$, $\omega = 0.7$, $a = 1$, $b = 0.5$, $c = 0.05$, and $\Delta t = 0.1$. Model (6) with these parameters has four equilibrium points: $(0, 0)$, $(0.1298, 0)$, $(0.7701, 0)$, and $(0, 0.5)$. According to Theorem 7, only axial equilibrium $(0, 0.5)$ is stable for any order of fractional derivative (α), where $0 < \alpha < 1$. This stability behavior is confirmed by our numerical solutions; see Figures 1 and 2. This shows that strong Allee effect may lead to an extinction of prey population. It is shown in Figure 2 that our numerical solutions for $\alpha = 0.5, 0.6, 0.7, 0.8, 0.9, 1.0$ are convergent to the axial equilibrium $(0, 0.5)$, indicating that equilibrium $(0, 0.5)$ is stable asymptotically for any order of fractional derivative. Detail observation shows that as the order of fractional derivative increases the convergence of solution is faster and the solution of system (6) closes to the integer-order model (2).

Next, we set $s = 0.02$ and $h = 0.3$ and keep the rest of parameters as in Figure 1. This weak Allee case has a trivial equilibrium $(0, 0)$; two axial equilibria: $(0.8217, 0)$ and $(0, 0.5)$; and two interior points: $E_{w1}^* = (0.0128, 0.5128)$ and $E_{w2}^* = (0.1373, 0.6373)$. Theorems 7 and 9 state that axial equilibrium $(0, 0.5)$ is locally stable for $0 < \alpha < 1$ and interior point $E_{w2}^* = (0.1373, 0.6373)$ is locally stable if $\alpha < \alpha^* = 0.886$, and other equilibria are always unstable. Such behavior is in accordance with our numerical results depicted in Figures 3(a) and 3(b). It is clearly seen in Figure 3(a) that $\alpha = 0.8$ produces bistable dynamic where depending on the initial values, solutions may be convergent to the extinction of prey point $(0, 0.5)$ or to interior point. In other words, the solution of system (6) is highly sensitive to the initial conditions. An initially relatively small prey will converge to the prey extinction point. On the other hand, if the prey is initially relatively large then prey and predator will coexist. If we increase the order of derivative such that $\alpha = 0.95$, the axial equilibrium $(0, 0.5)$ is still locally stable but the interior point becomes unstable; see Figure 3(b). In latter case, there exists a stable limit cycle which shows that both prey and predator are fluctuating around the interior point. However, the appearance of limit cycle may be suppressed by increasing the coefficient of predator interference. For example we plot in Figure 4(a) the numerical solution using the same parameters as in Figure 3(b) but with $c = 0.1$. We see that the interior point is now stable while the axial equilibrium point $(0, 0.5)$ is unstable. It can be said that relatively large predator interference can stabilize the interior point. On the other hand, strong Allee effect can destabilize or even remove the interior equilibrium and can cause the extinction of prey population. For example, we show numerical simulation using parameters the same as in Figure 3(b) except $m = 0.3$. This simulation shows that all initial values converge to the

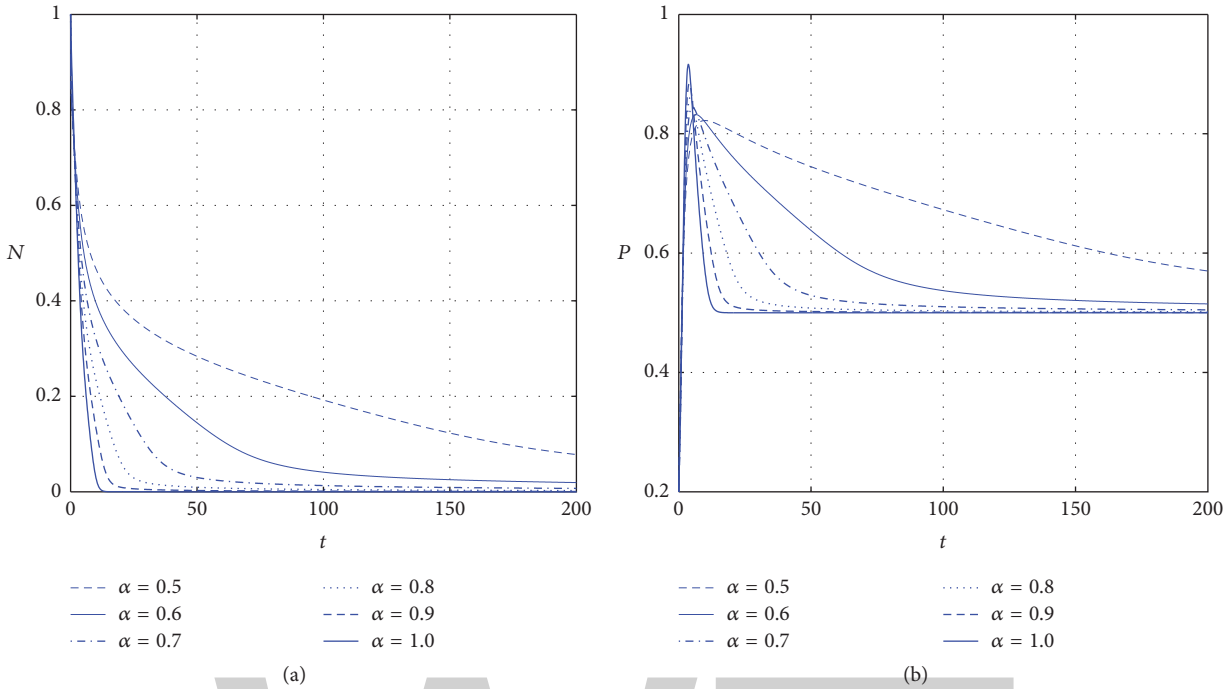

FIGURE 2: Solutions of system (6) with initial value (1, 0.2) and parameter values: $s = 1$, $k = 0.5$, $m = 0.2$, $h = 0.1$, $\omega = 0.7$, $a = 1$, $b = 0.5$, $c = 0.05$, and $\Delta t = 0.1$, for various values of α. All numerical solutions are convergent to axial equilibrium (0, 0.5). Solution of system (6) with larger order of fractional derivative (α) has faster convergence compared to that with smaller α.

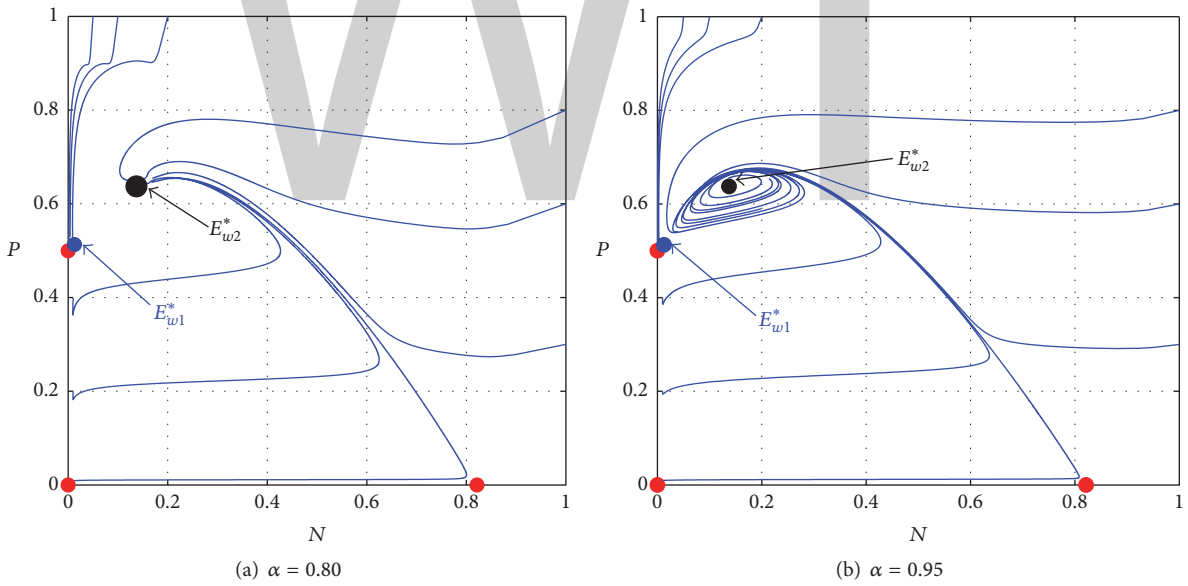

FIGURE 3: Phase portrait of system (6). The values of parameters are $s = 0.02$, $k = 0.5$, $m = 0.2$, $h = 0.3$, $\omega = 0.7$, $a = 1$, $b = 0.5$, $c = 0.05$, and $\Delta t = 0.1$.

axial equilibrium $(0, 0.5)$ which shows the extinction of prey population but predator species can still survive in the habitat because there is an enough environmental protection; see Figure 4(b).

Finally, we compare our numerical results obtained by the NSGL scheme to those obtained by the standard GL scheme using parameters $s = 0.02$, $k = 0.5, m = 0.2$, $h = 0.3$, $\omega = 0.7$, $a = 1$, $b = 0.5$, $c = 0.1$, and $\alpha = 0.95$; see Figure 5. We see that both NSGL and GL schemes using $\Delta t = 0.005$ produce solutions where their difference cannot be observed in the scale of Figure 5. Using $\Delta t = 0.01$, the numerical solutions of both NSGL and GL schemes are in excellent agreement with those of both schemes using $\Delta t = 0.005$. If we take time step $\Delta t = 0.1$, both schemes have comparable

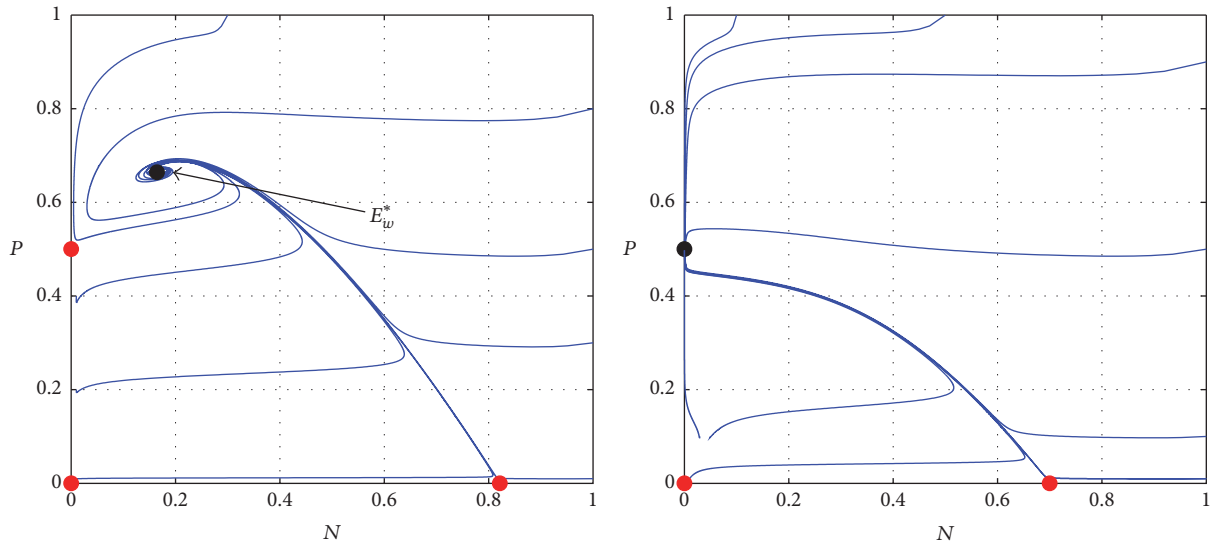

FIGURE 4: Phase portrait of system (6). The values of parameters are $s = 0.02, k = 0.5, h = 0.3, \omega = 0.7, a = 1, b = 0.5, \alpha = 0.95$, and $\Delta t = 0.1$.

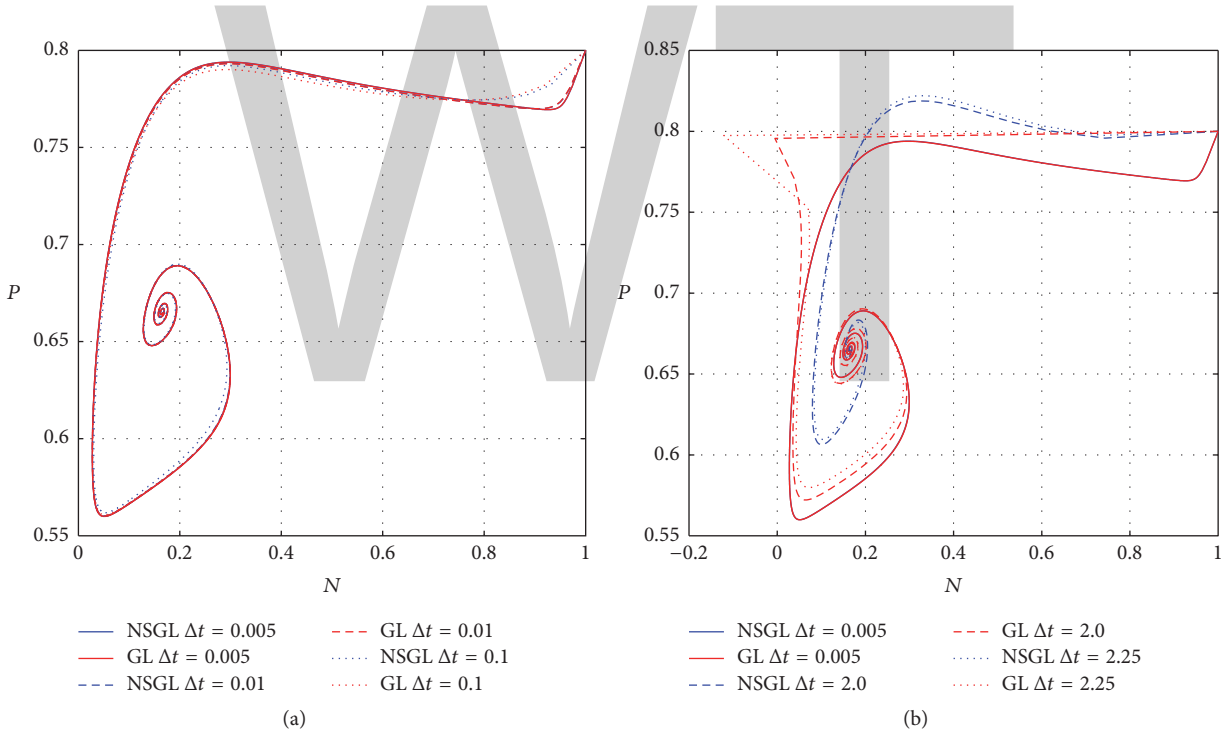

FIGURE 5: Phase portrait of system (6) calculated using nonstandard (NSGL) and standard (GL) schemes. The values of parameters are $s = 0.02, k = 0.5, m = 0.2, h = 0.3, \omega = 0.7, a = 1, b = 0.5, c = 0.1$, and $\alpha = 0.95$.

solutions which are initially distorted from solutions with much smaller time step; see Figure 5(a). In Figure 5(b), we plot solutions using relatively large time step ($\Delta t = 2.0$ and $\Delta t = 2.25$). Although the NSGL scheme has solutions which are quantitatively different from solution with $\Delta t = 0.005$, nevertheless those solutions still have the same behavior as before; that is, they are always positive and convergent to the correct equilibrium point. However, the GL scheme in this case gives unrealistic negative value for prey population. If the time step is further increased, the GL scheme will be unstable and leads to blowing up solutions.

4. Conclusion

The dynamic of a fractional order modified Leslie-Gower model with Beddington-DeAngelis functional response and

additive Allee effect has been analyzed. Our model has four types of equilibria that are the trivial (extinction of both prey and predator) equilibrium, two axial equilibria (the prey extinction point and the predator extinction point), and the interior (coexistence) point. The trivial and the predator extinction for both weak and strong Allee effects are always unstable. For the case of weak Allee effect, the prey extinction is conditionally stable while for that of strong Allee effect, the prey extinction is always stable. Our analysis also shows that the interior point for both weak and Allee effects is conditionally stable. The order of fractional derivative may influence the stability of interior point. Here, when the order α is larger than critical order α^*, then the interior point may be destabilized. These dynamical properties are confirmed by our NSGL schemes which shows the effectiveness of NSGL scheme. It is also shown that the NSGL scheme preserves the positivity of numerical solutions. Furthermore, our numerical results show that the NSGL scheme produces numerical solutions which satisfy the dynamical behavior of our model. However, the standard GL scheme may fail to preserve such properties; for example, it can produce nonrealistic negative solutions.

Conflicts of Interest

The authors declare that there are no conflicts of interest regarding the publication of this paper.

Acknowledgments

This work was supported by the Directorate of Research and Community Service, The Directorate General of Strengthening Research and Development, and the Ministry of Research, Technology and Higher Education (Brawijaya University), Indonesia, Contract no. 137/SP2H/LT/DRPM/III/2016 dated March 10, 2016, and Contract no. 460.18/UN10.C10/PN/2017 dated April 18, 2017.

References

[1] A. A. Berryman, "The origins and evolution of predator-prey theory," *Ecology*, vol. 73, no. 5, pp. 1530–1535, 1992.

[2] M. A. Aziz-Alaoui and M. D. Okiye, "Boundedness and global stability for a predator-prey model with modified leslie-gower and holling-type II schemes," *Applied Mathematics Letter*, vol. 16, no. 7, pp. 1069–1075, 2003.

[3] S. Yu, "Global asymptotic stability of a predator-prey model with modified Leslie-Gower and Holling-type II schemes," *Discrete Dynamics in Nature and Society*, vol. 2012, Article ID 208167, 2012.

[4] S. Yu, "Global stability of a modified Leslie-Gower model with Beddington-DeAngelis functional response," *Advances in Difference Equations*, 2014:84, 14 pages, 2014.

[5] B. Sahoo, "Role of additional food in eco-epidemiological system with disease in the prey," *Applied Mathematics and Computation*, vol. 259, pp. 61–79, 2015.

[6] P. J. Pal and P. K. Mandal, "Bifurcation analysis of a modified Leslie-Gower predator-prey model with Beddington-DeAngelis functional response and strong ALLee effect," *Mathematics and Computers in Simulation*, vol. 97, pp. 123–146, 2014.

[7] Y. Cai, C. Zhao, W. Wang, and J. Wang, "Dynamics of a Leslie-Gower predator-prey model with additive Allee effect," *Applied Mathematical Modelling. Simulation and Computation for Engineering and Environmental Systems*, vol. 39, no. 7, pp. 2092–2106, 2015.

[8] M.-H. Wang and M. Kot, "Speeds of invasion in a model with strong or weak Allee effects," *Mathematical Biosciences*, vol. 171, no. 1, pp. 83–97, 2001.

[9] D. Indrajaya, A. Suryanto, and A. R. Alghofari, "Dynamics of modified Leslie-Gower predator-prey model with Beddington-DeAngelis functional response and additive Allee effect," *International Journal of Ecology and Development*, vol. 31, no. 3, pp. 60–71, 2016.

[10] E. Ahmed, A. M. El-Sayed, and H. A. El-Saka, "Equilibrium points, stability and numerical solutions of fractional-order predator-prey and rabies models," *Journal of Mathematical Analysis and Applications*, vol. 325, no. 1, pp. 542–553, 2007.

[11] S. Das and P. K. Gupta, "A mathematical model on fractional Lotka-Volterra equations," *Journal of Theoretical Biology*, vol. 277, pp. 1–6, 2011.

[12] Y. Ding, Z. Wang, and H. Ye, "Optimal control of a fractional-order HIV-immune system with memory," *IEEE Transactions on Control Systems Technology*, vol. 20, no. 3, pp. 763–769, 2012.

[13] F. A. Rihan, "Numerical modeling of fractional-order biological systems," *Abstract and Applied Analysis*, vol. 2013, Article ID 816803, 2013.

[14] M. Javidi and N. Nyamoradi, "Dynamic analysis of a fractional order prey-predator interaction with harvesting," *Applied Mathematical Modelling. Simulation and Computation for Engineering and Environmental Systems*, vol. 37, no. 20-21, pp. 8946–8956, 2013.

[15] F. A. Rihan, D. Baleanu, S. Lakshmanan, and R. Rakkiyappan, "On fractional SIRC model with *Salmonella* bacterial infection," *Abstract and Applied Analysis*, Article ID 136263, Art. ID 136263, 9 pages, 2014.

[16] A. E. Matouk, A. A. Elsadany, E. Ahmed, and H. N. Agiza, "Dynamical behavior of fractional-order Hastings-Powell food chain model and its discretization," *Communications in Nonlinear Science and Numerical Simulation*, vol. 27, no. 1-3, pp. 153–167, 2015.

[17] I. Podlubny, *Fractional Differential Equations*, vol. 198 of *Mathematics in Science and Engineering*, Academic Press, San Diego, Calif, USA, 1999.

[18] Y. S. Mishura, *Stochastic Calculus for Fractional Brownian Motion and Related Processes*, vol. 1929 of *Lecture Notes in Mathematics*, Springer, Berlin, Germany, 2008.

[19] D. Matignon, "Stability results for fractional differential equations with applications to control processing," in *Computational Engineering in Systems Applications*, pp. 963–968, Lille, France, 1996.

[20] R. Scherer, S. L. Kalla, Y. Tang, and J. Huang, "The Grnwald-Letnikov method for fractional differential equations," *Computers and Mathematics with Applications*, vol. 62, no. 3, pp. 902–917, 2011.

[21] R. E. Mickens, "Nonstandard finite difference schemes," in *Applications of nonstandard finite difference schemes (Atlanta, GA, 1999)*, pp. 1–54, World Sci. Publ., River Edge, NJ, 2000.

[22] R. E. Mickens, *Application of Nonstandard Finite Difference Schemes*, World Scientific Publishing Co Pte. Ltd, Singapore, 2000.

[23] A. J. Arenas, G. González-Parra, and B. M. Chen-Charpentier, "Construction of nonstandard finite difference schemes for the SI and SIR epidemic models of fractional order," *Mathematics and Computers in Simulation*, vol. 121, pp. 48–63, 2016.

The Agreement between the Generalized p Value and Bayesian Evidence in the One-Sided Testing Problem

Yuliang Yin and Bingbing Wang

School of Economics, Beijing Technology and Business University, Beijing 100048, China

Correspondence should be addressed to Yuliang Yin; imyyl@163.com

Academic Editor: Shey-Huei Sheu

In the problem of testing one-sided hypotheses, a frequentist may measure evidence against the null hypothesis by the p value, while a Bayesian may measure it by the posterior probability that the null hypothesis is true. In this paper, we consider the relationship between the generalized p value and the Bayesian evidence in testing one-sided hypotheses in the presence of nuisance parameters. The sufficient conditions for the agreement between these two kinds of evidence are given. Some examples are provided to show the agreement of Bayesian and frequentist evidence in many classical testing problems. This is an illustration of reconcilability of evidence in a general framework where the nuisance parameters are present.

1. Introduction

In testing a statistical hypothesis H_0, Lindley [1] illustrated the possible discrepancy between the Bayesian and frequentist evidence. The relationship between these two kinds of evidence is then extensively studied in the literature. Some important references on this topic include Bartlett [2], Edwards et al. [3], Pratt [4], Dickey [5], Shafer [6], Berger and Delampady [7], Berger and Sellke [8], Meng [9], and Micheas and Dey [10].

For the one-sided testing problem

$$H_0\colon \theta \le \theta_0 \quad \text{versus } H_1\colon \theta > \theta_0, \tag{1}$$

the Bayesian evidence is typically given by the posterior probability of H_0 and the frequentist evidence is given by the p value. For the situation of testing a location parameter, Casella and Berger [11] considered testing hypotheses (1) based on observing $X = x$, where X has a location density $f(x-\theta)$. Under the assumptions that $f(\cdot)$ is symmetric about zero and that $f(x-\theta)$ has monotone likelihood ratio, it is showed that the lower bound of the posterior probability of H_0 is equal to the corresponding p value for many classes of prior distributions.

This means that the Bayesian and frequentist evidence are reconcilable in the situation of testing one-sided hypotheses of a location parameter. However, this is not a very general result on the agreement between the Bayesian and frequentist evidence which can cover more testing situations. The relationship of evidence in testing a scale parameter or other parameters is not considered. More generally, it does not consider the situation where nuisance parameters are present. However, the presence of nuisance parameters is very common in practice. For example, we are frequently confronted with the problem of testing a location parameter in the presence of an unknown scale parameter.

In the presence of nuisance parameters, Yin [12] derived the equality of the generalized p value and Bayesian posterior probability of the null hypothesis in the one-sided testing problem under the exponential distribution. However, this is also a result of agreement of evidence in quite specific situation. In this paper, we focus on the one-sided testing problem and study the relationship between the Bayesian and frequentist evidence in a more general setting where the presence of nuisance parameters is allowed. The sufficient conditions for the equivalence between the Bayesian and frequentist evidence are, respectively, given for the one sample and two (or more) samples testing situations.

This paper is organized as follows. In Section 2, we give the main results on the agreement between the Bayesian and frequentist evidence in the one-sided testing problem. Section 3 illustrates the proposed method by applying it to several classical examples of testing one-sided hypotheses. Conclusions are stated in Section 4.

2. Agreement of Evidence

In the presence of nuisance parameters, we consider testing one-sided hypotheses in (1) based on a random sample $X = (X_1, X_2, \ldots, X_n)$. However, the classical p value is typically not available when nuisance parameters are present. Tsui and Weerahandi [13] introduced the concept of the generalized p value which appears to be useful in situations where conventional frequentist approaches do not provide appropriate measure of evidence.

Let $X = (X_1, X_2, \ldots, X_n)$ be a random sample distributed with distribution function $F(x; \zeta)$, where $\zeta = (\theta, \delta)$ is an unknown vector in parameter space Ω, $\theta \in \Theta$ is a real-valued parameter of interest, and $\delta \in \Delta$ is the nuisance parameter. Assume that $x \in \chi$ is the observed value of X.

Definition 1. Let $T = T(X; x, \zeta)$ be a function of X, x, and $\zeta = (\theta, \delta)$. T is said to be a generalized test variable if it has the following three properties:

(a) $t = T(x; x, \zeta)$ does not depend on unknown parameters.

(b) When θ is specified, T has a probability distribution that is free of nuisance parameters.

(c) For fixed x and δ, $P(T(X; x, \zeta) \geq T(x; x, \zeta) \mid \theta)$ is nondecreasing in θ for any given $t = T(x; x, \zeta)$.

According to properties (a)–(c) of Definition 1, the larger observed values $T(x; x, \zeta)$ of $T(X; x, \zeta)$ can be considered as extreme values of the distribution under the null hypothesis H_0, so they suggest stronger evidence against H_0.

Definition 2. Based on a generalized test variable $T = T(X; x, \zeta)$, the generalized p value for testing the one-sided hypotheses (1) is defined as

$$\begin{aligned} p(x) &= \sup_{\theta \leq \theta_0} P(T(X; x, \zeta) \geq T(x; x, \zeta) \mid \theta) \\ &= P(T(X; x, \zeta) \geq T(x; x, \zeta) \mid \theta = \theta_0). \end{aligned} \tag{2}$$

Many researches have been carried out to construct the generalized p value for many specific examples including the well-known Behrens-Fisher problem. Hannig et al. [14] provided a general method for constructing the generalized p value under the framework of fiducial inference.

Definition 3. Suppose that there is a random variable E with known distribution on space Ξ and that $h(\zeta, e)$ is a function from $\Omega \times \Xi$ to χ such that

$$X = h(\zeta, E) \tag{3}$$

for every $\zeta \in \Omega$. Furthermore, assume that for any observation $x \in \chi$ of X and $e \in \Xi$ of E, the equation $x = h(\zeta, e)$ has a unique solution in Ω which is denoted by $\zeta_x(e)$. Then

(a) the distribution of $\zeta_x(E)$ is called the fiducial distribution of ζ with respect to x;

(b) the distribution of $\theta(\zeta_x(E))$ is called the (marginal) fiducial distribution of $\theta = \theta(\zeta)$ with respect to x.

By Definition 3, the fiducial distribution of $\theta = \theta(\zeta)$ is

$$F_x(\theta) = P(\theta(\zeta_x(E)) \leq \theta). \tag{4}$$

Hannig et al. established that if the conditions in Definition 3 hold and if the equation $x = h(\zeta, e)$ has a unique solution in Ξ for any ζ and x, the generalized p value for testing the one-sided hypotheses (1) is just equal to the fiducial p value, $p = F_x(\theta_0)$.

For one-sided hypothesis testing problem (1) and in the presence of nuisance parameters, we now give the conditions for the agreement between the frequentist evidence, the generalized p value, and the Bayesian evidence, the posterior probability that H_0 is true.

Theorem 4. *Let $X_1, X_2, \ldots, X_n$ be independently distributed with $F(x; \xi)$, where $\xi = (\mu, \sigma)$. Suppose that there exit two statistics T_1 and T_2 which satisfy*

$$(T_1, T_2) = (\mu + \sigma E_1, \sigma E_2), \tag{5}$$

where E_1 and E_2 are two independent random variables with a known joint probability density $g(e_1, e_2)$, and suppose that the prior distribution of (μ, σ) is $\pi(\mu, \sigma) = 1/\sigma$.

(i) *The fiducial distribution of (μ, σ) is equivalent to its posterior distribution.*

(ii) *For the one-sided testing problem of form (1), where $\theta = \theta(\mu, \sigma)$ is the parameter of interest, the generalized p value is equivalent to the posterior probability of H_0.*

Proof. (i) On the one hand, since $(T_1, T_2) = (\mu + \sigma E_1, \sigma E_2)$, we can obtain the functional model as

$$\begin{aligned} T_1 &= \mu + \sigma E_1, \\ T_2 &= \sigma E_2, \end{aligned} \tag{6}$$

based on which we have

$$\begin{aligned} \mu &= T_1 - T_2 \frac{E_1}{E_2}, \\ \sigma &= \frac{T_2}{E_2}. \end{aligned} \tag{7}$$

Since (E_1, E_2) has a density $g(e_1, e_2)$, it can be obtained that the fiducial distribution of (μ, σ) is

$$f_{t_1, t_2}(\mu, \sigma) = \frac{t_2}{\sigma^3} g\left(\frac{t_1 - \mu}{\sigma}, \frac{t_2}{\sigma}\right). \tag{8}$$

On the other hand, the density of (T_1, T_2) can be obtained as

$$f(t_1, t_2 \mid \mu, \sigma) = \frac{1}{\sigma^2} g\left(\frac{t_1 - \mu}{\sigma}, \frac{t_2}{\sigma}\right). \tag{9}$$

If the prior distribution for (μ, σ) is $\pi(\mu, \sigma) = 1/\sigma$, the posterior distribution of (μ, σ) is

$$\begin{aligned} & f(\mu, \sigma \mid t_1, t_2) \\ &= \frac{\left(1/\sigma^3\right) g\left(\left(t_1 - \mu\right)/\sigma, t_2/\sigma\right)}{\iint \left(1/\sigma^3\right) g\left(\left(t_1 - \mu\right)/\sigma, t_2/\sigma\right) d\mu\, d\sigma} \\ &= \frac{t_2}{\sigma^3} g\left(\frac{t_1 - \mu}{\sigma}, \frac{t_2}{\sigma}\right). \end{aligned} \tag{10}$$

By (8) and (10) we know that the fiducial distribution of (μ, σ) is equivalent to its posterior distribution.

(ii) On the one hand, we know by (i) that the posterior probability of H_0 is equivalent to the corresponding fiducial p value $F_x(\theta_0)$, where $F_x(\theta)$ denotes the fiducial distribution of θ. On the other hand, under the assumptions of the theorem it is obvious that the conditions of Definition 3 are satisfied and $(t_1, t_2) = (\mu + \sigma e_1, \sigma e_2)$ has unique solution in the space of (E_1, E_2) for any given (t_1, t_2) and (μ, σ), so that the generalized p value is equivalent to the fiducial p value $F_x(\theta_0)$. This completes the proof. □

For the two-sample testing situation, we also have the result on the agreement between the Bayesian and frequentist evidence which we summarize as Theorem 5.

Theorem 5. *Let $X_1, X_2, \ldots, X_m$ and $Y_1, Y_2, \ldots, Y_n$ be independently distributed with $F(x; \xi_1)$ and $G(y; \xi_2)$, respectively, where $\xi_1 = (\mu_1, \sigma_1)$ and $\xi_2 = (\mu_2, \sigma_2)$. Suppose that there exit four statistics T_{11}, T_{12}, T_{21}, and T_{22} which satisfy*

$$\begin{aligned} & \left(T_{11}, T_{12}, T_{21}, T_{22}\right) \\ &= \left(\mu_1 + \sigma_1 E_{11}, \sigma_1 E_{12}, \mu_2 + \sigma_2 E_{21}, \sigma_2 E_{22}\right), \end{aligned} \tag{11}$$

where E_{11}, E_{12}, E_{21}, and E_{22} are four independent random variables with a known joint probability density $g(e_{11}, e_{12}, e_{21}, e_{22})$, and suppose that the prior distribution of $(\mu_1, \sigma_1, \mu_2, \sigma_2)$ is $\pi(\mu_1, \sigma_1, \mu_2, \sigma_2) = 1/(\sigma_1 \sigma_2)$.

(i) *The fiducial distribution of $(\mu_1, \sigma_1, \mu_2, \sigma_2)$ is equivalent to its posterior distribution.*

(ii) *For the one-sided testing problem of form (1), where $\theta = \theta(\mu_1, \sigma_1, \mu_2, \sigma_2)$ is the parameter of interest, the generalized p value is equivalent to the posterior probability of H_0.*

Proof. (i) By the assumptions that

$$\begin{aligned} & \left(T_{11}, T_{12}, T_{21}, T_{22}\right) \\ &= \left(\mu_1 + \sigma_1 E_{11}, \sigma_1 E_{12}, \mu_2 + \sigma_2 E_{21}, \sigma_2 E_{22}\right), \end{aligned} \tag{12}$$

the functional model can be obtained as

$$\begin{aligned} T_{11} &= \mu_1 + \sigma_1 E_{11}, \\ T_{12} &= \sigma_1 E_{12}, \\ T_{21} &= \mu_2 + \sigma_2 E_{21}, \\ T_{22} &= \sigma_2 E_{22}. \end{aligned} \tag{13}$$

Consequently, we have

$$\begin{aligned} \mu_1 &= T_{11} - T_{12} \frac{E_{11}}{E_{12}}, \\ \sigma_1 &= \frac{T_{12}}{E_{12}}, \\ \mu_2 &= T_{21} - T_{22} \frac{E_{21}}{E_{22}}, \\ \sigma_2 &= \frac{T_{22}}{E_{22}}. \end{aligned} \tag{14}$$

Since $(E_{11}, E_{12}, E_{21}, E_{22})$ has a density $g(e_{11}, e_{12}, e_{21}, e_{22})$, we can obtain the fiducial distribution of $(\mu_1, \sigma_1, \mu_2, \sigma_2)$ as

$$\begin{aligned} & f_{t_{11}, t_{12}, t_{21}, t_{22}}(\mu_1, \sigma_1, \mu_2, \sigma_2) \\ &= \frac{t_{12} t_{22}}{\sigma_1^3 \sigma_2^3} g\left(\frac{t_{11} - \mu_1}{\sigma_1}, \frac{t_{12}}{\sigma_1}, \frac{t_{21} - \mu_2}{\sigma_2}, \frac{t_{22}}{\sigma_2}\right). \end{aligned} \tag{15}$$

On the other hand, the density of $(T_{11}, T_{12}, T_{21}, T_{22})$ is

$$\begin{aligned} & f(t_{11}, t_{12}, t_{21}, t_{22} \mid \mu_1, \sigma_1, \mu_2, \sigma_2) \\ &= \frac{1}{\sigma_1^2 \sigma_2^2} g\left(\frac{t_{11} - \mu_1}{\sigma_1}, \frac{t_{12}}{\sigma_1}, \frac{t_{21} - \mu_2}{\sigma_2}, \frac{t_{22}}{\sigma_2}\right). \end{aligned} \tag{16}$$

Consequently, the posterior distribution of $(\mu_1, \sigma_1, \mu_2, \sigma_2)$ under the prior $\pi(\mu_1, \sigma_1, \mu_2, \sigma_2) = 1/(\sigma_1 \sigma_2)$ is

$$\begin{aligned} f(\mu_1, \sigma_1, \mu_2, \sigma_2 \mid t_{11}, t_{12}, t_{21}, t_{22}) &= \frac{\left(1/\sigma_1^3 \sigma_2^3\right) g\left(\left(t_{11} - \mu_1\right)/\sigma_1, t_{12}/\sigma_1, \left(t_{21} - \mu_2\right)/\sigma_2, t_{22}/\sigma_2\right)}{\iiiint \left(1/\sigma_1^3 \sigma_2^3\right) g\left(\left(t_{11} - \mu_1\right)/\sigma_1, t_{12}/\sigma_1, \left(t_{21} - \mu_2\right)/\sigma_2, t_{22}/\sigma_2\right) d\mu_1 d\mu_2 d\sigma_1 d\sigma_2} \\ &= \frac{t_{12} t_{22}}{\sigma_1^3 \sigma_2^3} g\left(\frac{t_{11} - \mu_1}{\sigma_1}, \frac{t_{12}}{\sigma_1}, \frac{t_{21} - \mu_2}{\sigma_2}, \frac{t_{22}}{\sigma_2}\right). \end{aligned} \tag{17}$$

By (15) and (17), it is obtained that the fiducial distribution of (μ, σ) is equivalent to its posterior distribution.

(ii) The proof is by analogy with that of (ii) of Theorem 4. □

Note that the result on the agreement between the Bayesian and frequentist evidence in the two samples situation of Theorem 5 can be easily extended to the general situation of n ($n \geq 2$) samples.

3. Examples

3.1. Normal Distribution. The problem of testing parameters of a normal distribution has its wide applicability. Let $X_1, X_2, \ldots, X_n$ be independently distributed according to the normal distribution $N(\mu, \sigma^2)$, where both μ and σ^2 are unknown. Let

$$T_1 = \overline{X} = \frac{\sum_{i=1}^{n} X_i}{n},$$
$$T_2^2 = S^2 = \frac{\sum_{i=1}^{n} \left(X_i - \overline{X}\right)^2}{n-1}. \tag{18}$$

We know that $\sqrt{n}(T_1 - \mu)/\sigma$ and $(n-1)T_2^2/\sigma^2$ are independently distributed with $N(0,1)$ and $\chi^2(n-1)$. Let

$$E_1 \sim N(0,1),$$
$$E_2^2 \sim \chi^2(n-1) \tag{19}$$

be independent. We have

$$(T_1, T_2) = \left(\mu + \frac{\sigma E_1}{\sqrt{n}}, \frac{\sigma E_2}{\sqrt{n-1}}\right). \tag{20}$$

By Theorem 4 we know that if the noninformative prior distribution for $\pi(\mu, \sigma) = 1/\sigma$ is used, then for any parameter $\theta = \theta(\mu, \sigma)$ of interest in the problem of testing hypotheses in (1) the generalized p value is equivalent to the posterior probability that the null hypothesis is true.

The problem of comparing the parameters of two normal distributions arises in comparing two treatments, products, and so forth. We now consider the two-sample testing situation. Let $X_1, X_2, \ldots, X_m$ and $Y_1, Y_2, \ldots, Y_n$ be independently distributed with the normal distributions $N(\mu_1, \sigma_1^2)$ and $N(\mu_2, \sigma_2^2)$, respectively. Let

$$T_{11} = \overline{X} = \frac{\sum_{i=1}^{m} X_i}{m},$$
$$T_{12}^2 = S_1^2 = \frac{\sum_{i=1}^{m} \left(X_i - \overline{X}\right)^2}{m-1},$$
$$T_{21} = \overline{Y} = \frac{\sum_{i=1}^{n} Y_i}{n},$$
$$T_{22}^2 = S_2^2 = \frac{\sum_{i=1}^{n} \left(Y_i - \overline{Y}\right)^2}{n-1}, \tag{21}$$

and let

$$E_{11} \sim N(0,1),$$
$$E_{12}^2 \sim \chi^2(m-1),$$

Table 1: Fiducial (or posterior) distributions for some important parameters of interest under the normal distribution.

Parameter	Fiducial (or posterior) distribution
$c_1\mu + c_2\sigma$	$c_1\left(\overline{x} - \frac{\sqrt{n-1}sZ}{\sqrt{n}\sqrt{\chi^2_{n-1}}}\right) + c_2\frac{\sqrt{n-1}s}{\sqrt{\chi^2_{n-1}}}$
$\mu_1 - \mu_2$	$\overline{x} - \overline{y} - \left(\frac{\sqrt{m-1}s_1 Z}{\sqrt{m}\sqrt{\chi^2_{m-1}}} - \frac{\sqrt{n-1}s_2 Z}{\sqrt{n}\sqrt{\chi^2_{n-1}}}\right)$
$\frac{\sigma_1}{\sigma_2}$	$\frac{s_1^2}{s_2^2}F_{n-1,m-1}$

$$E_{21} \sim N(0,1),$$
$$E_{22}^2 \sim \chi^2(n-1), \tag{22}$$

which are independent. We then have that $(T_{11}, T_{12}, T_{21}, T_{22})$ are sufficient statistics and

$$(T_{11}, T_{12}, T_{21}, T_{22}) = \left(\mu_1 + \frac{\sigma_1 E_{11}}{\sqrt{m}}, \frac{\sigma_1 E_{12}}{\sqrt{m-1}}, \mu_2 + \frac{\sigma_2 E_{21}}{\sqrt{n}}, \frac{\sigma_2 E_{22}}{\sqrt{n-1}}\right). \tag{23}$$

By applying Theorem 5, it is obtained that if we use the noninformative prior $\pi(\mu_1, \sigma_1, \mu_2, \sigma_2) = 1/(\sigma_1\sigma_2)$, then for any parameter $\theta = \theta(\mu_1, \sigma_1, \mu_2, \sigma_2)$ in testing hypotheses (1), the generalized p value is equivalent to the posterior probability of the null hypothesis being true.

The fiducial (or posterior) distributions for some important parameters of interest are listed in Table 1, based on which we can give the generalized p value which is also the posterior probability of the null hypothesis for testing hypotheses of form (1). In Table 1, Z is a standard normal random variable, χ^2_{m-1} and χ^2_{n-1} are chi-squared random variables with the indicated degrees of freedom, $F_{n-1,m-1}$ is F-variable with the indicated degrees of freedom, and c_1 and c_2 are two constants.

From Table 1 we observe that if $c_1 = 1$ and $c_2 = 0$, the distribution reduces to the fiducial (or posterior) distribution of a normal mean. If $c_1 = 0$ and $c_2 = 1$, the distribution reduces to the fiducial (or posterior) distribution of a normal standard variance. If $c_1 = 1$ and $c_2 = z_p$, the distribution then reduces to the fiducial (or posterior) distribution of the p-quantile, where z_p is the p-quantile of the standard normal distribution.

In addition, by Theorem 4, an immediate agreement of evidence can be obtained in testing H_0: $\theta = \mu/\sigma \leq \theta_0$, which is the hypothesis about the mean expressed in σ-unit, and in testing H_0: $\theta = P(X \leq x_0) \leq \theta_0$, which is the hypothesis about the distribution function of the normal variable with mean μ and variance σ^2 at a fixed value x_0. The generalized p value which is equivalent to the posterior probability of H_0 can be easily obtained according to Table 1 since these two null hypotheses can be equivalently expressed as H_0': $\mu - \theta_0\sigma \leq 0$ and H_0': $-\mu - \Phi^{-1}(\theta_0)\sigma \leq -x_0$, respectively.

3.2. Two-Parameter Exponential Distribution. We first consider the relationship between the Bayesian and frequentist evidence for testing one-sided hypotheses in the one-sample situation. Let $X_1, X_2, \ldots, X_n$ be independently distributed according to the two-parameter exponential population $E(\mu, \sigma)$, where both μ and σ are unknown. Suppose that the observations are type II censored data $X_{(1)} < X_{(2)} < \cdots < X_{(k)}$, $k < n$.

We know that

$$T_1 = X_{(1)},$$
$$T_2 = \sum_{i=1}^{k} X_{(i)} + (n-k)\, X_{(k)} - nX_{(1)} \tag{24}$$

are jointly sufficient statistics for (μ, σ) and

$$\frac{2n\left(X_{(1)} - \mu\right)}{\sigma}, \quad \frac{2\left(\sum_{i=1}^{k} X_{(i)} + (n-k)\, X_{(k)} - nX_{(1)}\right)}{\sigma} \tag{25}$$

are independently distributed with $\chi^2(2)$ and $\chi^2(2k-2)$. Let

$$E_1 \sim \chi^2(2), \quad E_2 \sim \chi^2(2k-2) \tag{26}$$

be independent. We have

$$\left(T_1, T_2\right) = \left(\mu + \frac{\sigma E_1}{2n}, \frac{\sigma E_2}{2}\right). \tag{27}$$

If the prior distribution of (μ, σ) is $\pi(\mu, \sigma) = 1/\sigma$, then according to Theorem 4, for each parameter $\theta = \theta(\mu, \sigma)$ of interest in testing hypotheses (1) under a two-parameter exponential distribution, the generalized p value is equivalent to the corresponding posterior probability of the null hypothesis.

The problem of comparing parameters of two exponential distributions arises in many theoretical and applied contexts. A case in point is the problem of lifetime testing in the theory of reliability. We then begin to consider the relationship between the Bayesian and frequentist evidence in a two-population context.

Let $X_1, X_2, \ldots, X_m$ and $Y_1, Y_2, \ldots, Y_n$ be independently distributed with the two-parameter exponential distributions $E(\mu_1, \sigma_1)$ and $E(\mu_2, \sigma_2)$, respectively, where all the parameters are unknown. The observations are type II censored data $X_{(1)} < X_{(2)} < \cdots < X_{(k)}$, $k < m$, and $Y_{(1)} < Y_{(2)} < \cdots < Y_{(l)}$, $l < n$. The prior distribution in the situation of two populations is $\pi(\mu_1, \sigma_1, \mu_2, \sigma_2) = 1/(\sigma_1 \sigma_2)$.

If we denote

$$T_{11} = X_{(1)},$$
$$T_{12} = \sum_{i=1}^{k} X_{(i)} + (m-k)\, X_{(k)} - mX_{(1)},$$
$$T_{21} = Y_{(1)},$$
$$T_{22} = \sum_{i=1}^{l} Y_{(i)} + (n-l)\, Y_{(l)} - nY_{(1)} \tag{28}$$

and if

$$E_{11} \sim \chi^2(2), \quad E_{12} \sim \chi^2(2k-2), \quad E_{21} \sim \chi^2(2), \quad E_{22} \sim \chi^2(2l-2), \tag{29}$$

which are independent, then we have that $(T_{11}, T_{12}, T_{21}, T_{22})$ are sufficient statistics and

$$\left(T_{11}, T_{12}, T_{21}, T_{22}\right) = \left(\mu_1 + \frac{\sigma_1 E_{11}}{2m}, \frac{\sigma_1 E_{12}}{2}, \mu_2 + \frac{\sigma_2 E_{21}}{2n}, \frac{\sigma_2 E_{22}}{2}\right). \tag{30}$$

By Theorem 5, for any parameter $\theta = \theta(\mu_1, \sigma_1, \mu_2, \sigma_2)$ of interest in one-sided testing problem (1), the equivalence between the generalized p value and the posterior probability of the null hypothesis being true can be obtained.

Table 2 lists the fiducial (or posterior) distributions for some important parameters of interest under the two-parameter exponential distribution. The generalized p value which is also the posterior probability of the null hypothesis for testing one-sided hypotheses (1) can be easily obtained according to the corresponding distribution in Table 2, where χ^2_2, χ^2_{2k-2}, and χ^2_{2l-2} are chi-squared random variables with the indicated degrees of freedom, $F_{2l-2,2k-2}$ is a F-variable with the indicated degrees of freedom, and c_1 and c_2 are two constants.

Note from Table 2 that if $c_1 = 1$ and $c_2 = 0$, the distribution reduces to the fiducial (or posterior) distribution for testing the location parameter μ. If $c_1 = 0$ and $c_2 = 1$, the distribution reduces to the fiducial (or posterior) distribution for testing the scale parameter σ.

In the theory of reliability, a parameter of particular interest under a two-parameter exponential distribution is often a quantile of the form $\mu + b\sigma$, where b is a known and fixed constant. The agreement between the generalized p value and the Bayesian evidence for testing this quantile can be obtained by Theorem 5 and the evidence can be given easily according to Table 2.

Moreover, the agreement between the Bayesian and frequentist evidence for testing the reliability function $\theta = P(X \geq x_0) = \exp\{-(x_0 - \mu)/\sigma\}$, where x_0 is a fixed value, can be obtained by Theorem 5. Since the hypothesis H_0: $\exp\{-(x_0 - \mu)/\sigma\} \leq \theta_0$ can be equivalently expressed as H_0': $\mu - \ln^{\theta_0}\sigma \leq x_0$, the generalized p value which is equivalent to the posterior probability of the null hypothesis can be obtained easily according to Table 2.

Table 2: Fiducial (or posterior) distribution for some important parameters of interest under the two-parameter exponential distribution.

Parameter	Fiducial (or posterior) distribution
$c_1\mu + c_2\sigma$	$c_1 x_{(1)} - \frac{c_1\left[\sum_{i=1}^{k} x_{(i)} + (n-k)\,x_{(k)} - nx_{(1)}\right]\chi_2^2}{n\chi_{2k-2}^2} + \frac{2c_2\left[\sum_{i=1}^{k} x_{(i)} + (n-k)\,x_{(k)} - nx_{(1)}\right]}{\chi_{2k-2}^2}$
$\mu_1 - \mu_2$	$x_{(1)} - y_{(1)} + \frac{\sum_{i=1}^{l} y_{(i)} + (n-l)\,y_{(l)} - ny_{(1)}}{n}\frac{\chi_2^2}{\chi_{2l-2}^2} - \frac{\sum_{i=1}^{k} x_{(i)} + (m-k)\,x_{(k)} - mx_{(1)}}{m}\frac{\chi_2^2}{\chi_{2k-2}^2}$
$\frac{\sigma_1}{\sigma_2}$	$\frac{(l-1)\left[\sum_{i=1}^{k} x_{(i)} + (m-k)\,x_{(k)} - mx_{(1)}\right]}{(k-1)\left[\sum_{i=1}^{l} y_{(i)} + (n-l)\,y_{(l)} - ny_{(1)}\right]}F_{2l-2,2k-2}$

3.3. Weibull Distribution. In the theory of survival analysis and the theory of reliability, one of the most important distributions is the Weibull distribution $W(\tau,\eta)$ whose density is

$$f(x) = \frac{\tau x^{\tau-1}}{\eta^{\tau}} e^{-x^{\tau}/\eta^{\tau}}, \quad x > 0, \tag{31}$$

where $\tau > 0$ and $\eta > 0$.

Suppose that $X \sim W(\tau,\eta)$ and let $Y = \ln X$, then the density of Y is

$$f(y) = \frac{1}{\sigma} e^{(y-\mu)/\sigma} e^{-e^{(y-\mu)/\sigma}}, \tag{32}$$

where $\mu = \ln\eta$ and $\sigma = 1/\tau$. We know that (32) is the density of the extreme value distribution which is denoted by $\mathrm{EV}(\mu,\sigma)$. It can be verified that $E(Y) = \mu - r\sigma$ and $\mathrm{Var}(Y) = \pi^2\sigma^2/6$, where r is the Euler constant.

Note that it is more convenient to make inferences on the parameters of a Weibull distribution under (32) since it is a location-scale family. Let $X_1, X_2, \ldots, X_n$ be independently distributed according to the Weibull distribution $W(\tau,\eta)$ and let $Y_i = \ln X_i$, $i = 1,2,\ldots,n$. Then $Y_1, Y_2, \ldots, Y_n$ are independently distributed according to the density (32). Let

$$\begin{aligned} T_1 &= \overline{Y} = \frac{\sum_{i=1}^{n} Y_i}{n} = \frac{\ln\prod_{i=1}^{n} X_i}{n}, \\ T_2^2 &= S^2 = \frac{\sum_{i=1}^{n}\left(Y_i - \overline{Y}\right)^2}{n-1}, \end{aligned} \tag{33}$$

and let

$$\begin{aligned} E_1 &= \frac{\sqrt{6}\left[T_1 - (\mu - r\sigma)\right]}{\pi\sigma}, \\ E_2 &= \frac{\sqrt{6}T_2}{\pi\sigma}, \end{aligned} \tag{34}$$

and then we have

$$(T_1, T_2) = \left(\mu + \sigma\left(\frac{\pi E_1}{\sqrt{6}} + r\right), \sigma\frac{\pi E_2}{\sqrt{6}}\right). \tag{35}$$

If the prior distribution for (μ,σ) is $\pi(\mu,\sigma) = 1/\sigma$, then according to Theorem 4, we can obtain the equivalence between the generalized p value and the posterior probability of the null hypothesis for the problem of testing hypotheses about $\theta = \theta(\mu,\sigma) = \theta^*(\tau,\eta)$. But we have to note that (T_1, T_2) is not sufficient for (μ,σ) in this situation and therefore may lead to some loss of information about the parameters which is contained in the sample.

Now we consider the two-sample situation. Let $X_{11}, X_{12}, \ldots, X_{1m}$ and $X_{21}, X_{22}, \ldots, X_{2n}$ be independently distributed with the Weibull distributions $W(\tau_1,\eta_1)$ and $W(\tau_2,\eta_2)$, respectively. Let $Y_{1i} = \ln X_{1i}$, $i = 1,2,\ldots,m$, and $Y_{2j} = \ln X_{2j}$, $j = 1,2,\ldots,n$. Then $Y_{11}, Y_{12}, \ldots, Y_{1m}$ and $Y_{21}, Y_{22}, \ldots, Y_{2n}$ are independently distributed with the extreme value distributions $\mathrm{EV}(\mu_1,\sigma_1)$ and $\mathrm{EV}(\mu_2,\sigma_2)$, respectively, where $\mu_i = \ln\eta_i$, $i = 1,2$, and $\sigma_j = 1/\tau_j$, $j = 1,2$. Now let

$$\begin{aligned} T_{11} &= \overline{Y_1} = \frac{\sum_{i=1}^{m} Y_{1i}}{m} = \frac{\ln\prod_{i=1}^{m} X_{1i}}{m}, \\ T_{12}^2 &= S_1^2 = \frac{\sum_{i=1}^{m}\left(Y_{1i} - \overline{Y_1}\right)^2}{m-1}, \\ T_{21} &= \overline{Y_2} = \frac{\sum_{i=1}^{n} Y_{2i}}{n} = \frac{\ln\prod_{i=1}^{n} X_{2i}}{n}, \\ T_{22}^2 &= S_2^2 = \frac{\sum_{i=1}^{n}\left(Y_{2i} - \overline{Y_2}\right)^2}{n-1}, \end{aligned} \tag{36}$$

and let

$$\begin{aligned} E_{11} &= \frac{\sqrt{6}\left[T_{11} - (\mu_1 - r\sigma_1)\right]}{\pi\sigma_1}, \\ E_{12} &= \frac{\sqrt{6}T_{12}}{\pi\sigma_1}, \\ E_{21} &= \frac{\sqrt{6}\left[T_{21} - (\mu_2 - r\sigma_2)\right]}{\pi\sigma_2}, \\ E_{22} &= \frac{\sqrt{6}T_{22}}{\pi\sigma_2}, \end{aligned} \tag{37}$$

and then we have

$$(T_{11}, T_{12}, T_{21}, T_{22}) = \left(\mu_1 + \sigma_1\left(\frac{\pi E_{11}}{\sqrt{6}} + r\right), \sigma_1\frac{\pi E_{12}}{\sqrt{6}}, \mu_2 + \sigma_2\left(\frac{\pi E_{21}}{\sqrt{6}} + r\right), \sigma_2\frac{\pi E_{22}}{\sqrt{6}}\right). \quad (38)$$

Consequently, we can obtain the equivalence between the Bayesian and frequentist evidence in testing one-sided hypotheses about $\theta = \theta(\mu_1, \sigma_1, \mu_2, \sigma_2) = \theta^*(\tau_1, \eta_1, \tau_2, \eta_2)$ of interest by Theorem 5 given that the prior distribution for $(\mu_1, \sigma_1, \mu_2, \sigma_2)$ is $\pi(\mu_1, \sigma_1, \mu_2, \sigma_2) = 1/(\sigma_1\sigma_2)$.

4. Conclusions

For the one-sided testing problem, we give the sufficient conditions for the equivalence between the generalized p value and the posterior probability that the null hypothesis is true. By applying the proposed method to some specific examples we show the agreement between the Bayesian and frequentist evidence in many classical testing situations. This is an illustration of reconcilability of the Bayesian and frequentist evidence in the one-sided testing problems under a quite general framework where the presence of nuisance parameters is allowed.

For the testing problems we have considered in this paper, the posterior distribution of the parameter of interest is equivalent to the corresponding fiducial distribution, which is basically the main reason for the equivalence between the generalized p value and the posterior probability of the null hypothesis. In the problem of testing a normal standard variance, we have that

$$\sigma \mid x \sim \sqrt{n-1}s\left(\chi^2_{n-1}\right)^{-1/2}, \quad (39)$$

where χ^2_{n-1} is a chi-squared random variable with $n-1$ degrees of freedom. This means that we can give a constructive form of the posterior distribution for a parameter of interest since we have a general method of formulating a fiducial distribution. This kind of constructive form of distributions may bring us significant convenience in computation and simulation. If the conditions for the agreement of evidence hold for a certain distribution or a family of distributions, the corresponding fiducial (or posterior) distribution table like Table 1 or Table 2 can be given for the convenience of use in theory and practice.

Competing Interests

The authors declare that they have no competing interests.

References

[1] D. V. Lindley, "A statistical paradox," *Biometrika*, vol. 44, pp. 187–192, 1957.

[2] M. S. Bartlett, "A comment on D. V. Lindley's statistical paradox," *Biometrika*, vol. 44, no. 3-4, pp. 533–534, 1957.

[3] W. Edwards, H. Lindman, and L. J. Savage, "Bayesian statistical inference for psychological research," *Psychological Review*, vol. 70, pp. 193–242, 1963.

[4] J. W. Pratt, "Bayesian interpretation of standard inference statements (with discussion)," *Journal of the Royal Statistical Society, Series B*, vol. 27, pp. 169–203, 1965.

[5] J. M. Dickey, "Is the tail area useful as an approximate Bayes factor?" *Journal of the American Statistical Association*, vol. 72, no. 357, pp. 138–142, 1977.

[6] G. Shafer, "Lindley's paradox," *Journal of the American Statistical Association*, vol. 77, no. 378, pp. 325–351, 1982.

[7] J. O. Berger and M. Delampady, "Testing precise hypotheses (with discussion)," *Statistical Science*, vol. 2, pp. 317–352, 1987.

[8] J. O. Berger and T. Sellke, "Testing a point null hypothesis: the irreconcilability of p-values and evidence," *Journal of the American Statistical Association*, vol. 82, no. 397, pp. 112–122, 1987.

[9] X.-L. Meng, "Posterior predictive p-values," *The Annals of Statistics*, vol. 22, no. 3, pp. 1142–1160, 1994.

[10] A. C. Micheas and D. K. Dey, "Reconciling Bayesian and frequentist evidence in the one-sided scale parameter testing problem," *Communications in Statistics—Theory and Methods*, vol. 36, no. 6, pp. 1123–1138, 2007.

[11] G. Casella and R. L. Berger, "Reconciling Bayesian and frequentist evidence in the one-sided testing problem," *The Journal of the American Statistical Association*, vol. 82, no. 397, pp. 106–111, 1987.

[12] Y. Yin, "Generalized p-values and Bayesian evidence in the one-sided testing problems under exponential distributions," *Statistica Neerlandica*, vol. 65, no. 3, pp. 319–336, 2011.

[13] K.-W. Tsui and S. Weerahandi, "Generalized p -values in significance testing of hypotheses in the presence of nuisance parameters," *Journal of the American Statistical Association*, vol. 84, no. 406, pp. 602–607, 1989.

[14] J. Hannig, H. Iyer, and P. Patterson, "Fiducial generalized confidence intervals," *Journal of the American Statistical Association*, vol. 101, no. 473, pp. 254–269, 2006.

Calculation of Precise Constants in a Probability Model of Zipf's Law Generation and Asymptotics of Sums of Multinomial Coefficients

Vladimir Bochkarev and Eduard Lerner

Kazan (Volga Region) Federal University, 18 St. Kremlevskaya, Kazan 420008, Russia

Correspondence should be addressed to Eduard Lerner; eduard.lerner@gmail.com

Academic Editor: Niansheng Tang

Let $\omega_0, \omega_1, \ldots, \omega_n$ be a full set of outcomes (symbols) and let positive p_i, $i = 0, \ldots, n$, be their probabilities ($\sum_{i=0}^{n} p_i = 1$). Let us treat ω_0 as a stop symbol; it can occur in sequences of symbols (we call them words) only once, at the very end. The probability of a word is defined as the product of probabilities of its symbols. We consider the list of all possible words sorted in the nonincreasing order of their probabilities. Let $p(r)$ be the probability of the rth word in this list. We prove that if at least one of the ratios $\log p_i / \log p_j$, $i, j \in \{1, \ldots, n\}$, is irrational, then the limit $\lim_{r\to\infty} p(r)/r^{-1/\gamma}$ exists and differs from zero; here γ is the root of the equation $\sum_{i=1}^{n} p_i^{\gamma} = 1$. The limit constant can be expressed (rather easily) in terms of the entropy of the distribution $(p_1^{\gamma}, \ldots, p_n^{\gamma})$.

1. Introduction: The Statement of the Main Theorem

1.1. Brief Literature Overview. The wide presence of power laws in real networks, biology, economics, and linguistics can be explained in the framework of various mathematical models (see, e.g., [1, 2]). According to Zipf's law [3], in a list of word forms ordered by the frequency of occurrence, the frequency of the rth word form obeys a power function of r (the value r is called the rank of the word form). One can easily explain this law with the help of the so-called monkey model.

Recall that the word forms "the"; "of"; and "and" are used most frequently in English texts. According to Zipf's law, the word "the" is used in the texts twice as much as "of" and three times as much as "and"; in other words the word form occurrence frequency obeys the power function of rank r (the position number of the word form in an ordered frequency list) whose exponent is approximately -1. It should be noted that further surveys showed that Zipf's law is roughly realised only for the most frequent words. At present, the researches try to describe the main part of the lexicon using the power law with an exponent $-\alpha$, where $\alpha > 1$. Zipf explained his law on the basis of the principle of least effort. In accordance with this principle, the authors aim to minimise the length of the text, which is required to convey their thoughts, even if this introduces ambiguities. On the other hand, readers want to minimize the effort required to understand the text [4].

Another explanation of Zipf's law was suggested by Mandelbrot who slightly modified the law by introducing translation constant [5] into the argument of the power function. The important thing for our case is that later he hypothesized the existence of more simple explanation of the Zipf law associated with a simple probability model when all symbols in the text (including white-space) appear independently of each other with certain probability. Moreover, he analysed the Markovian dependence between these symbols and wrote out the correct (in a typical case) formula on the basis of special cases to determine the parameter α by the transition probabilities matrix in the Markov model [6].

First, we will consider the model thoroughly described by Miller [7] and Li [8] for a special case of Mandelbrot's experiment in which the monkey types the keys with uniform probability. To learn some other important references on the monkey model, we recommend to read the recent article by Richard Perline and Ron Perline [9] (see also references in the next subsection).

1.2. Statement of the Main Theorem and Its Connection with Other Results. Assume that a monkey types any of 26 Latin letters or the space on a keyboard with the same probability of 1/27. We understand a word as a sequence of symbols typed by the monkey before the space. Let us sort the list of possible words with respect to probabilities of their occurrence (the empty word, whose probability equals 1/27, will go first in this list followed by 26 one-letter words whose probabilities equal $1/27^2$ and then by 26^2 possible two-letters words and so on). We can prove (see [7, 8]) that the probability $p(r)$ of a word with the rank of r satisfies the inequality

$$c_1 r^{-\alpha} < p(r) < c_2 r^{-\alpha}, \tag{1}$$

where $\alpha = \log 27/\log 26$ and $c_1, c_2 > 0$ (here and below we use the symbol log if the base of the logarithm is not significant; but for the natural logarithm we use the symbol ln).

Relatively recently inequality (1) was generalized to the case of nonequiprobable letters. Let p_0 be the probability that the monkey types the space, let p_i, $i = 1, \ldots, n$, denote probabilities of choosing the ith letter from the set of n letters ($p_i > 0$, $\sum_{i=0}^{n} p_i = 1$), and let $p(r)$ be, as above, the probability of a word with a rank of r. Then, as is proved in [10, 11], the following inequality analogous to (1) takes place; namely, $\exists c_1, c_2 : 0 < c_1 < c_2$, such that

$$c_1 r^{-\alpha} < p(r) < c_2 r^{-\alpha}, \quad \text{where } \alpha = \frac{1}{\gamma} \tag{2}$$

and γ is the root of the equation $\sum_{i=1}^{n} p_i^{\gamma} = 1$ (evidently, $0 < \gamma < 1$). Note that inequality (2) is equivalent to the boundedness of the difference $-\log p(r) - \alpha \log r$.

In the case when the probability of each letter is not fixed but depends on the previous one, words represent trajectories of a Markov chain with the absorbing state ω_0 and transient states $\omega_1, \ldots, \omega_n$. Then the value $p(r)$ is the probability of the rth trajectory in the list of possible trajectories sorted in the nonincreasing order of probabilities. In this case, the asymptotic behavior of $p(r)$ does not necessarily have a power order. Namely, in this case one of the two alternatives takes place [12, 13]. The first variant is that there exists the limit

$$\lim_{r\to\infty} \frac{-\log p(r)}{r^{1/m}} = c, \quad c > 0, \tag{3}$$

where m is some positive integer constant value that depends on the structure of the transition probability matrix and the structure of states, where the initial distribution of the Markov chain is concentrated. The second variant is that independently of the initial distribution there exists the following nonzero limit (the so-called *weak* power law):

$$\lim_{r\to\infty} \frac{-\log p(r)}{\log r}. \tag{4}$$

This limit equals $1/\gamma$, where γ is now defined with the help of the substochastic matrix P of transition probabilities where the row and the column that correspond to the absorbing state ω_0 are deleted. Namely, raising all elements of the mentioned matrix to the power of γ would equate its spectral radius to 1.

These results were obtained independently in [12, 14] and later refined in [13]. Namely, as appeared, the first alternative means the subexponential order of the asymptotics; that is, in this case $\exists c_1, c_2 : 0 < c_1 < c_2$, such that

$$c_1 \exp\left(-cr^{-1/m}\right) < p(r) < c_2 \exp\left(-cr^{-1/m}\right). \tag{5}$$

The case of the second alternative is much more difficult. If the matrix P does not have the block-diagonal structure with coinciding powers such that raising elements of blocks to these powers makes the spectral radius equal 1, then one can replace the weak power law with a *strong* one. Namely, in this case the asymptotic behavior of $p(r)$ has the power order; that is, inequality (2) is valid (with "matrix" γ defined above). Therefore, inequality (2) takes place in a "typical" case of letter probabilities.

However, one more natural question still remains without an answer.

Inequality (2) means that the asymptotic form has a power *order* but does not imply the *exact* power asymptotics. In a general case, as follows from the first example given in this section, useful properties can be established neither when letters in words are Markov-dependent nor when they are independent. However, as we prove later in this paper, in a "typical" case, for words composed of independent letters, the asymptotic behavior of the function $p(r)$ is exact power. The following theorem is valid.

Theorem 1 (main). *Let at least one of the ratios* $\log p_i/\log p_j$, $i, j \in \{1, \ldots, n\}$, *be irrational and let* γ *be the root of the equation* $\sum_{i=1}^{n} p_i^{\gamma} = 1$. *Then the limit*

$$\lim_{r\to\infty} \frac{p(r)^{-\gamma}/p_0^{-\gamma}}{r} \tag{6}$$

exists and equals $H(\mathbf{p}^{\gamma})$, *where* $H(\mathbf{p}^{\gamma})$ *is the entropy of* $\mathbf{p}^{\gamma} = (p_1^{\gamma}, \ldots, p_n^{\gamma})$; *that is,* $H(\mathbf{p}^{\gamma}) = -\gamma \sum_{i=1}^{n} p_i^{\gamma} \ln p_i$.

Here and below we always write the function under consideration in the numerator and do the norming (defined analytically) function in the denominator of the fraction, whose limit is to be calculated. In intermediate calculations it may be more convenient to do the opposite, but since this results only in the trivial raising of the limit constant to the power of -1, we sacrifice the convenience of calculations for the clarity of statements of results. Evidently, the theorem asserts that under certain assumptions there exists the nonzero limit $p(r)/r^{-\alpha}$ (where $\alpha = 1/\gamma$) as $r \to \infty$. It is equal to $p_0 H(\mathbf{p}^{\gamma})^{-1/\gamma}$.

Let us describe the structure of the remaining part of the paper. In Section 2 we state the main theorem in terms of multinomial coefficients (of the Pascal pyramid). The proof of the theorem is reduced to the estimation of the limit behavior of the sum of these coefficients over some simplex. In Section 3 we prove an analog of this theorem with an integral in place of the sum. In this section we essentially use the Stirling formula which allows us to reduce calculations to the evaluation of a multivariate Gaussian integral. We establish an explicit formula for the determinant of the matrix

of the quadratic form that defines the integrand. Finally, in Section 4 we prove that the ratio of the integral to the sum tends to 1. Here we use the general properties of the Riemann integral and uniformly distributed sequences. In conclusion we discuss possible generalizations and unsolved problems.

2. Equivalent Statements of the Main Theorem and the Pascal Pyramid

Let us first note that if $p_0 \to 0$, then $\gamma \to 1$. Reducing the nominator of fraction (6) by $p_0^{-\gamma}$, we write the following statement in this case:

Theorem 2 (the case of $\gamma = 1$). *Let $p_i > 0$ be the probability of the symbol ω_i, $i = 1, \dots, n$, while $\sum_{i=1}^{n} p_i = 1$ (there is no stop symbol). Assume that at least one of the ratios $\log p_i / \log p_j$, $i, j \in \{1, \dots, n\}$, is irrational. Let us consider all possible finite words (including the empty one) and sort them in the nonincreasing order of probabilities (we equate the probability of the empty word to 1 and calculate the probability of any other word as the product of probabilities of its letters). Let $p(r)$ be the probability of the rth word in the list (the word with the rank of r). Then the limit $\lim_{r\to\infty} p(r)/r^{-1}$ exists and equals $H^{-1}(\mathbf{p})$, where $H(\mathbf{p})$ is the entropy of the vector $\mathbf{p} = (p_1, \dots, p_n)$; that is, $H(\mathbf{p}) = -\sum_{i=1}^{n} p_i \ln p_i$.*

In the statement of Theorem 2, as well as in Theorem 1, we use the bold font for the vector whose components are denoted by the same letter with the index ranging from 1 to n. In what follows we use the bold font for analogous denotations without mentioning this fact.

One can easily see that Theorem 2 is not just a particular case of Theorem 1, but these theorems are equivalent. Namely, the replacement of probabilities p_i^{γ} with new ones p_i turns the general case into the particular one. Therefore, in what follows we neglect p_0, assuming (without loss of generality) that $\sum_{i=1}^{n} p_i = 1$.

Fix some probability $q \in (0, 1]$ and denote by $Q(q)$ the rank of the last word whose probability is not less than q in the list of all words sorted in the nonincreasing order of their probabilities. Let us redefine the function $p(r)$ for noninteger r as $p(r) = p(\lfloor r \rfloor)$ (here $\lfloor \cdot \rfloor$ is the integer part of a number). Evidently, functions $q = p(r)$ and $r = Q(q)$ $(q \in (0, 1],\ r \geq 1)$ are inverse (more exactly, quasi-inverse); namely, the graph of one of the hyperbola-shaped, decreasing stepwise functions turns into another one when axes r and q switch roles (in the first case, q is the argument and r is the value and vice versa in the second case).

It can be clearly seen that $\lim_{r\to\infty} cp(r)/r^{-1} = 1$ is equivalent to

$$\frac{\lim_{q\to 0} c^{-1} Q(q)}{q^{-1}} = 1. \tag{7}$$

Therefore the equality in the assertion of Theorem 2 is equivalent to that

$$\frac{\lim_{q\to 0} Q(q)}{q^{-1}} = H^{-1}(\mathbf{p}). \tag{8}$$

Denote the logarithm of the denominator in the last fraction by $z = -\ln q$ (i.e., $q = e^{-z}$) and let $\widetilde{Q}(z) = Q(e^{-z})$. In view of considerations in the above paragraph the equality in the assertion of Theorem 2 is equivalent to that

$$\lim_{z\to\infty} \left(\ln \widetilde{Q}(z) - z\right) = -\ln H(\mathbf{p}). \tag{9}$$

Recall the proof of inequality (2) in [11]. It is reduced to the proof of the boundedness of the difference $\ln \widetilde{Q}(z) - z$ for the introduced function $\widetilde{Q}(z)$ with $z \geq 0$. Nonnegative values of z form the definition domain of the function $\widetilde{Q}(z)$ because $q \leq 1 \Leftrightarrow z \geq 0$. For convenience we redefine the function $\widetilde{Q}(z)$ by putting $\widetilde{Q}(z) = 0$ for $z < 0$.

Let $a_i = -\ln p_i$. Considering all possible variants of the last letters in words, whose quantity equals the value of the function $\widetilde{Q}$, we obtain the functional equation $\widetilde{Q}(z) = \widetilde{Q}(z - a_1) + \cdots + \widetilde{Q}(z - a_n) + \chi(z)$, where χ is the Heaviside step (i.e., the function that vanishes with negative values of the argument and equals 1 with nonnegative values). For $z \geq M = \max\{a_1, \dots, a_n\}$ we get the following recurrent correlation:

$$Q_n(z) = Q_n(z - a_1) + \cdots + Q_n(z - a_n), \tag{10}$$

where $Q_n(z) = \widetilde{Q}(z) + 1/(n-1)$.

The equality $\sum_{i=1}^{n} p_i = 1$ implies that the function $\mathrm{const} \exp z$ satisfies (10). Since the function $Q_n(z)$ takes a finite number of positive values within $[0, M]$ interval, there exist positive c_1 and c_2 such that

$$c_1 \exp z < Q_n(z) < c_2 \exp z \tag{11}$$

for all $0 \leq z \leq M$.

Replacing terms in the right-hand side of the recurrent correlation (10) with their lower (upper) bounds, we extend the solution set of inequality (11) to the domain $0 \leq z \leq M + m$, where $m = \min\{a_1, \dots, a_n\}$. Repeating this procedure several times, in a finite number of steps we prove that the inequality is valid for any arbitrarily large z. Performing the logarithmic transformation of the inequality, we conclude that $\ln Q_n(z) - z$ is bounded, and then so is the difference $\ln \widetilde{Q}(z) - z$.

Let us return to Theorem 2. As was mentioned above, Theorem 2 asserts (under certain assumptions) not only the boundedness of $\ln \widetilde{Q}(z) - z$ but also the validity of equality (9). Let us recall the combinatory sense of the function $\widetilde{Q}$; it is mentioned in [11]. Evidently, all words that contain k_1 letters of the 1st kind, k_2 letters of the 2nd kind, …, and k_n letters of the nth kind have one and the same probability of $\Pr(\mathbf{k}) = p_1^{k_1} \cdots p_n^{k_n}$ (i.e., $-\ln \Pr(\mathbf{k}) = \sum_{i=1}^{n} k_i a_i$); ranks of these words are consecutive. The quantity of such words is defined by the multinomial coefficient

$$M(\mathbf{k}) = \frac{(k_1 + \cdots + k_n)!}{k_1! \cdots k_n!}. \tag{12}$$

Considering the nonnegative part of the n-dimensional integer grid and associating the point $(k_1, \dots, k_n)$ with the number $M(k_1, \dots, k_n)$, we get one of the variants of the Pascal

pyramid. By the definition of the function $\widetilde{Q}$ the value $\widetilde{Q}(z)$ equals the sum of multinomial coefficients $M(\mathbf{k})$ over all integer vectors $\mathbf{k}$ that lie inside the n-dimensional simplex $S(z) = \{\mathbf{x} : \mathbf{x} \geq 0,\ \sum_{i=1}^{n} a_i x_i \leq z\}$:

$$\widetilde{Q}(z) = \sum_{\mathbf{k} \in S(z)} M(\mathbf{k}). \tag{13}$$

As a result, we obtain one more equivalent statement of the main theorem, which we are going to prove.

Theorem 3 (the multinomial statement). *Let a_i, $i = 1, \ldots, n$, be arbitrary positive numbers such that at least one of the ratios a_i/a_j, $i, j \in \{1, \ldots, n\}$, be irrational and $\sum_{i=1}^{n} p_i = 1$, where $p_i = \exp(-a_i)$. Let a function $\widetilde{Q}$ obey formula (13). Then*

$$\lim_{z \to \infty} \frac{\widetilde{Q}(z)}{\exp(z)} = H^{-1}(\mathbf{p}), \tag{14}$$

where $H(\mathbf{p}) = \sum_{i=1}^{n} a_i p_i$.

3. The Proof of an Analog of Theorem 3 with Integration instead of Summation

3.1. Reduction of the Integration to the Calculation of a Gaussian Integral. The function $M(k_1, \ldots, k_n)$ is defined for integer nonnegative vectors $\mathbf{k}$. Let us redefine it for noninteger vectors by replacing (in this case) $x!$ in Definition (12) with $\Gamma(x+1)$. In what follows we use the denotation $M(x_1, \ldots, x_n)$ (or $M(\mathbf{x})$) for the corresponding function which is continuous for nonnegative x_i. Further we consider this function and study its properties only for such (nonnegative) x_i.

In this section we prove the following theorem.

Theorem 4 (on the integral). *Let a_i, $i = 1, \ldots, n$, be arbitrary positive numbers such that $\sum_{i=1}^{n} p_i = 1$, where $p_i = \exp(-a_i)$. Let a function $f(z)$ obey the formula $f(z) = \int_{\mathbf{x} \in S(z)} M(\mathbf{x}) d\mathbf{x}$, where $d\mathbf{x} = \prod_{i=1}^{n} dx_i$. Then*

$$\lim_{z \to \infty} \frac{f(z)}{\exp(z)} = H^{-1}(\mathbf{p}). \tag{15}$$

Proof. Let us first recall some evident properties of the integrand. Note that the existence of the (Riemann) integral of $f(z)$ over the compact set $S(z)$ evidently follows from the continuity of $M(\mathbf{x})$ in the domain under consideration.

If all components of the vector $(x_1, \ldots, x_n)$, possibly, except one component x_i, equal zero, then by definition we have $M(x_1, \ldots, x_n) \equiv 1$. Let us prove that otherwise the function $M(x_1, \ldots, x_n)$ is strictly increasing in x_i. Since the gamma function is positive definite, it suffices to prove that in this case the partial derivative of $\ln M(x_1, \ldots, x_n)$ with respect to x_i is positive. It equals

$$(\ln \Gamma)'(x_1 + \cdots + x_n + 1) - (\ln \Gamma)'(x_i + 1). \tag{16}$$

The positiveness of this difference follows from the fact that the function $(\ln \Gamma)'$ is increasing; this property, in turn, follows from the logarithmic convexity of the gamma function (it is well known [15] that $(\ln \Gamma)''(x) = \sum_{i=0}^{\infty} 1/(i+x)^2 > 0$ with $x > 0$).

The proved assertion implies that the function $M(\mathbf{x})$ attains its maximum in the domain $S(z)$ at the boundary $\langle \mathbf{a}, \mathbf{x} \rangle = z$, where $\langle \mathbf{a}, \mathbf{x} \rangle = \sum_{i=1}^{n} a_i x_i$. Let us calculate the exact asymptotics of the maximal value of the function $M(\mathbf{x})$ in the domain $S(z)$ with $z \to \infty$. For the vector $\mathbf{x}$ we denote by x the sum of its components and parameterize $\mathbf{x}$ by the value x and ratios $q_i = x_i/x$:

$$x_i = q_i x, \quad q_i \geq 0,\ i = 1, \ldots, n, \qquad \sum_{i=1}^{n} q_i = 1. \tag{17}$$

Let us use one simplest corollary of the Stirling formula [15], namely, the fact that with a nonnegative argument the value of the difference $\ln \Gamma(x+1) - (x \ln(x) - x + \ln(x+1)/2)$ is bounded. We obtain that, with any $x > 0$,

$$\ln M(x_1, \ldots, x_n) = xH(\mathbf{q}) + O(\ln(x+1)), \tag{18}$$

where $H(\mathbf{q}) = -\sum_{i=1}^{n} q_i \ln q_i$ (this correlation is closely connected with the so-called entropy inequality for multinomial coefficients).

We seek for the maximum of this function with $z \to \infty$ under one additional condition (namely, the requirement that the maximum is attained at the boundary) $\langle \mathbf{a}, \mathbf{x} \rangle = z$, where $a_i = -\ln p_i$, $0 < p_i < 1$, and $\sum_{i=1}^{n} p_i = 1$. Since $a_i > 0$, we get $O(\ln(x+1)) = O(\ln z)$. Moreover, the condition $\langle \mathbf{a}, \mathbf{x} \rangle = z$ with mentioned x_i gives the correlation

$$x = zH(\mathbf{q}; \mathbf{p})^{-1}, \tag{19}$$

where $H(\mathbf{q}; \mathbf{p}) = \sum_{i=1}^{n} a_i q_i = -\sum_{i=1}^{n} q_i \ln p_i$. Substituting this expression in (18), we conclude that the maximum of $\ln M$ (accurate to $O(\ln z)$) is attained at a vector $\mathbf{q}$ such that the fraction $H(\mathbf{q})/H(\mathbf{q}; \mathbf{p})$ takes on the maximal value. Recall that the difference $H(\mathbf{q}; \mathbf{p}) - H(\mathbf{q})$ takes on only nonnegative values and is called the Kullback–Leibler distance (divergence) $D(\mathbf{q} \mid \mathbf{p})$ between distributions $\mathbf{q}$ and $\mathbf{p}$ (see [16]). The minimum of this difference is attained at only one value of $\mathbf{q} = \mathbf{p}$; evidently, an analogous assertion is also true for $H(\mathbf{q}; \mathbf{p})/H(\mathbf{q})$: if $\mathbf{q} \neq \mathbf{p}$

$$\frac{H(\mathbf{q})}{H(\mathbf{q}; \mathbf{p})} < 1. \tag{20}$$

Consequently, the maximum of the function $\ln M(\mathbf{x})$ in the domain $S(z)$ is attained (accurate to $O(\ln z)$) at the intersection of the hyperplane $\langle \mathbf{a}, \mathbf{x} \rangle = z$ with the straight line $x_i = p_i x$, $i = 1, \ldots, n$, where it equals $z + O(\ln z)$.

Let us now immediately prove Theorem 4. Note first that by using the L'Hopital rule we can reduce the proof to that of the formula obtained by differentiating $f(z)/\exp(z)$ numerator and denominator with respect to z and to the proof of the equality

$$\lim_{z \to \infty} \frac{\widehat{f}(z)}{\exp(z)} = H^{-1}(\mathbf{p}), \tag{21}$$

where $\widehat{f}(z) = \int_{\mathbf{x}\geq 0} M(\mathbf{x})\delta(z - \langle \mathbf{a}, \mathbf{x}\rangle)d\mathbf{x}$ and $\delta(\cdot)$ is the delta function.

Let ε be a real arbitrarily small positive value. Denote by Λ_ε the sector consisting of points $\mathbf{x}$, $x_i = q_i x$, and $\sum_i q_i = 1$, such that

$$p_i - \varepsilon < q_i < p_i + \varepsilon, \quad i = 1, \ldots, n. \tag{22}$$

With fixed z on the hyperplane $\langle \mathbf{a}, \mathbf{x}\rangle = z$ correlations (18) and (19) take the form

$$\ln M(\mathbf{x}) = \frac{zH(\mathbf{q})}{H(\mathbf{q};\mathbf{p})} + O(\ln(z)). \tag{23}$$

Let us now strengthen inequality (20); namely, let us prove that if for $\mathbf{q}$ correlations (22) are violated, then

$$\frac{H(\mathbf{q})}{H(\mathbf{q};\mathbf{p})} < 1 - C_1(\mathbf{p})\varepsilon^2, \tag{24}$$

where $C_1(\mathbf{p})$ is a positive constant independent of $\mathbf{q}$.

Since $H(\mathbf{q};\mathbf{p})$ is a convex combination of $-\ln p_i$, it evidently is bounded:

$$0 < \min_i(-\ln p_i) \leq H(\mathbf{q};\mathbf{p}) \leq \max_i(-\ln p_i). \tag{25}$$

Consequently, formula (24) is equivalent to the inequality

$$H(\mathbf{q};\mathbf{p}) - H(\mathbf{q}) = D(\mathbf{q} \mid \mathbf{p}) > C_2(\mathbf{p})\varepsilon^2. \tag{26}$$

The latter correlation follows from the well-known property of the Kullback-Leibler divergence

$$D(\mathbf{q} \mid \mathbf{p}) \geq \frac{1}{4}\left(\sum_{i=1}^{n} |p_i - q_i|\right)^2 \tag{27}$$

(see, e.g., lemma 3.6.10 in [16]).

The proved inequality (24) (in view of formula (23)) implies that outside the domain Λ_ε the function $M(\mathbf{x})$ is exponentially small in comparison to the maximal value inside the domain which equals $\exp(z)$. More precisely, with $x \notin \Lambda_\varepsilon$ and $\langle \mathbf{a}, \mathbf{x}\rangle = z$, we get

$$M(\mathbf{x}) < \exp\left\{\left(1 - C\varepsilon^2\right)z\right\} \quad \text{for some } C > 0. \tag{28}$$

Note that the condition of the exponential smallness in comparison to $\exp z$ remains valid, even if ε depends on z and tends to 0 as z increases, though not too fast. In what follows we assume that

$$\varepsilon = \varepsilon(z) = z^{-1/2+\delta}, \quad \text{where } \delta > 0 \text{ is sufficiently small.} \tag{29}$$

One can easily see that the same exponential upper bound as in (28) also takes place not only for M function but also for its integral over the domain whose volume grows according to a power law:

$$\int_{\mathbf{x}\notin\Lambda_{\varepsilon(z)},\mathbf{x}\geq 0} M(\mathbf{x})\,\delta(z - \langle \mathbf{a}, \mathbf{x}\rangle)\,d\mathbf{x} < \exp\left\{\left(1 - C\varepsilon^2\right)z\right\} \tag{30}$$

with $z \to \infty$. Therefore in limit (21) we can treat $\widehat{f}(z)$ as the integral

$$\int_{\mathbf{x}\in\Lambda_{\varepsilon(z)}} M(\mathbf{x})\,\delta(z - \langle \mathbf{a}, \mathbf{x}\rangle)\,d\mathbf{x}. \tag{31}$$

Let us define the asymptotics (18) of the function $M(\mathbf{x})$ in the domain $\Lambda_{\varepsilon(z)}$ more precisely. Let us use the standard Stirling formula, namely, the fact that with $x \to \infty$ it holds that $\ln\Gamma(x+1) = x\ln(x) - x + \ln(x)/2 + \ln(2\pi)/2 + R(x)$, where $0 < R(x) < 1/(12x)$. We obtain that, in the domain $\Lambda_{\varepsilon(z)}$,

$$M(\mathbf{x}) = \frac{1}{\sqrt{(2\pi)^{n-1}}} \cdot \exp\left\{xH(\mathbf{q}) + \frac{\ln(x)}{2} - \frac{\sum_{i=1}^{n}\ln(x_i)}{2} + O\left(\frac{1}{z}\right)\right\}. \tag{32}$$

Here, as usual, $x = \sum_{i=1}^{n} x_i$; $q_i = x_i/x$. Therefore, we conclude that when considering the asymptotics of function (31) we can treat $M(\mathbf{x})$ as follows:

$$\widetilde{M}(\mathbf{x}) = \frac{1}{\sqrt{(2\pi)^{n-1}}}\exp\left\{xH(\mathbf{q}) + \frac{\ln(x)}{2} - \frac{\sum_{i=1}^{n}\ln(x_i)}{2}\right\}. \tag{33}$$

In the latter formula we can write the exponent as

$$\{\} = x\ln x + \frac{\ln(x)}{2} - \sum_{i=1}^{n}\left(x_i \ln x_i + \frac{\ln(x_i)}{2}\right). \tag{34}$$

Let us write the Taylor expansion up to second-order terms near the maximum point in the plane $\langle \mathbf{a}, \mathbf{x}\rangle = z$, that is, near the point $\mathbf{x}' = \mathbf{p}z/H(\mathbf{p})$ (in what follows we denote by x_i' coordinates of the point $\mathbf{x}'$ and do by x' the sum of these coordinates which evidently equals $zH(\mathbf{p})^{-1}$).

First of all, note that

$$\widetilde{M}(\mathbf{x}') = \frac{1}{\sqrt{(2\pi x')^{n-1}\prod_{i=1}^{n} p_i}}\exp(z). \tag{35}$$

One can easily calculate second derivatives of expression (34):

$$\frac{\partial^2}{\partial x_i \partial x_j}\{\} = \begin{cases} x^{-1} - \left(2x^2\right)^{-1}, & \text{if } i \neq j, \\ x^{-1} - \left(2x^2\right)^{-1} - x_i^{-1} + \left(2x_i^2\right)^{-1}, & \text{else.} \end{cases} \tag{36}$$

(note that we do not use first derivatives in the Taylor expansion near the maximum point).

If $x \in \Lambda_\varepsilon$, then by formula (19) we have $x - x' = z(H(\mathbf{q};\mathbf{p})^{-1} - H(\mathbf{p})^{-1}) = zO(\varepsilon)$ (in the latter inequality we use the continuity of the function $H(\mathbf{q};\mathbf{p})^{-1}$). Consequently,

$$x_i - x_i' = xq_i - x'p_i = \left(x' + zO(\varepsilon)\right)\left(p_i + O(\varepsilon)\right) - x'p_i = zO(\varepsilon). \tag{37}$$

In particular, with chosen $\varepsilon = \varepsilon(z)$ we have $|x_i - x_i'| = O(z^{1/2+\delta})$. We obtain that, in the domain $\Lambda_{\varepsilon(z)}$,

$$\widetilde{M}(\mathbf{x}) = \frac{1}{\sqrt{(2\pi x')^{n-1}\prod_{i=1}^{n} p_i}} \exp(z) \times \exp\left\{ \frac{\sum_{i,j=1}^{n} (x_i - x_i')(x_j - x_j')}{2x'} - \frac{\sum_{i=1}^{n} (x_i - x_i')^2}{2p_i x'} + O\left(z^{-1/2+3\delta}\right) \right\}. \tag{38}$$

Here the term $O(z^{-1/2+3\delta})$ contains both the remainder of terms of the series whose order exceeds 2 and the value of $O(z^{-1+2\delta})$ added by some omitted second-order terms. With $z \to \infty$ we can neglect the term of $O(z^{-1/2+3\delta})$. Therefore, in integral (31) in place of $M(\mathbf{x})$ we should substitute the function $\widehat{M}(\mathbf{x})$ which differs from $\widetilde{M}(\mathbf{x})$ in the fact that its exponent does not contain the term of $O(z^{-1/2+3\delta})$.

Let us change variables in the integral as follows: $y_i = (x_i - x_i')/\sqrt{x'}$. Since the degree of homogeneity of the delta-function equals -1, we obtain that limit (21) coincides with

$$\frac{1}{\sqrt{(2\pi)^{n-1}\prod_{i=1}^{n} p_i}} \int_{\mathbb{R}^n} \delta\left(\langle \mathbf{a}, \mathbf{y}\rangle\right) \exp\left\{ -\frac{\langle \mathscr{B}\mathbf{y}, \mathbf{y}\rangle}{2} \right\} d\mathbf{y}, \tag{39}$$

where $\mathscr{B}$ is $n \times n$ matrix, whose all elements equal -1, except diagonal components which are greater by $1/p_i$.

3.2. Calculation of the Determinant

Lemma 5. *Let $n \geq 2$. Consider $n \times n$ matrix B, where all nondiagonal elements equal 1, while $b_{ii} = 1 + k_i$. Then*

(1) *the determinant of this matrix equals*

$$\prod_{i=1}^{n} k_i \left(1 + \sum_{j=1}^{n} \frac{1}{k_j}\right); \tag{40}$$

(2) *the algebraic complement of the element with indices (i, j), $i \neq j$, equals*

$$-\prod_{\ell \in [n]\setminus\{i,j\}} k_\ell, \quad \text{where } [n] = \{1, \ldots, n\}. \tag{41}$$

Corollary 6. *The matrix $\mathscr{B}$ in formula (39) is degenerate.*

Proof of Lemma 5. Note that the first item of Lemma 5 defines the value of the algebraic complement of the diagonal element of such a matrix. Let us prove the theorem by induction.

With $n = 2$ in the formula in item (2) we get the product over the empty set; it is accepted that this product equals 1. The formula in item (1) remains valid with $n = 1$. In the induction step we assume that the formula in item (1) is proved for all dimensions less than n and has to be proved for the case when the dimension equals n, while the formula in item (2) is proved for all dimensions not greater than n and has to be proved for $(n + 1) \times (n + 1)$ matrix.

For proving item (1) we can use the expansion by the last row. Multiplying the algebraic complement by the diagonal element $k_n + 1$, we get the sum

$$\prod_{i=1}^{n} k_i \left(1 + \sum_{j=1}^{n-1} \frac{1}{k_j}\right) + \prod_{i=1}^{n-1} k_i \left(1 + \sum_{j=1}^{n-1} \frac{1}{k_j}\right) = \prod_{i=1}^{n} k_i \left(1 + \sum_{j=1}^{n-1} \frac{1}{k_j}\right) + \prod_{i=1}^{n-1} k_i + \sum_{j=1}^{n-1} \prod_{\ell \in [n]\setminus\{n,j\}} k_\ell. \tag{42}$$

The expansion by the entire last row, taking into account the induction hypothesis for item (2), make the third part in row (42) vanish. First two terms in formula (42) together give the desired sum.

In order to prove item (2), let us expand the determinant considered in this item (algebraic complement of the element with (i, j) indices of the matrix B with $(n + 1) \times (n + 1)$ dimension) by the row whose number in the initial matrix of B was equal to j. Generally speaking, for clarity, we use the same indices as in the numeration of the initial matrix. Since the algebraic complement considered in this item and the occurring algebraic complement for the element with indices (j, i) (obtained by the expansion by a row of the determinant under consideration) have opposite signs, the value added by the element with indices (j, i) equals

$$-\prod_{r \in [n+1]\setminus\{i,j\}} k_r \left(1 + \sum_{\ell \in [n+1]\setminus\{i,j\}} \frac{1}{k_\ell}\right) \tag{43}$$

(here we have used the induction hypothesis for item (1)). The difference from the desired formula consists in the last term which equals (taking into account the first multiplier)

$$-\sum_{\ell \in [n+1]\setminus\{i,j\}} \prod_{r \in [n+1]\setminus\{i,j,\ell\}} k_r. \tag{44}$$

It vanishes, when taking into account the contribution of the remaining $n - 1$ elements in the jth row of the considered matrix. □

Lemma 7. *Let B_1 be the matrix mentioned in Lemma 5 (its dimension is $n \times n$, $n \geq 2$). Assume that $b_{ii} = 1 - 1/p_i$, $i = 1, \ldots, n$, where p_i are arbitrary nonzero numbers. Denote by B_2 a matrix of the same dimension in the form $a^T a$, where $a = (a_1, \ldots, a_n)$ is an arbitrary numeric row and T is the transposition sign. Let s be an arbitrary real number. Then*

$$\det(sB_2 - B_1) = \det(-B_1) + \frac{s\left(\left(\sum_{i=1}^{n} a_i p_i\right)^2 - \left(\sum_{j=1}^{n} p_j - 1\right)\sum_{i=1}^{n} a_i^2 p_i\right)}{\prod_{\ell=1}^{n} p_\ell}. \tag{45}$$

Corollary 8. *Let a vector* $\mathbf{p} = (p_1, \ldots, p_n)$ *satisfy additional constraints* $p_i > 0$, $\sum_{i=1}^n p_i = 1$ *(i.e.,* $-B_1 = \mathscr{B}$*), while* $a_i = -\ln p_i$*. Then*

$$\sqrt{s \det\left(s^{-1}B_2 - B_1\right)} = \frac{H(\mathbf{p})}{\sqrt{\prod_{\ell=1}^n p_\ell}}. \tag{46}$$

Proof of Lemma 7. By the differentiation rule for determinants, the derivative of the determinant of $n \times n$ matrix equals the sum of determinants of n matrices such that in the ith one all elements of the ith row are replaced with their derivatives. We obtain that $\partial^2 \det(sB_2 - B_1)/\partial s^2$ is the sum of determinants of matrices each one of which contains either the zero row or two various rows of the matrix B_2. Since rank $B_2 = 1$, we get $\partial^2 \det(sB_2 - B_1)/\partial s^2 = 0$.

Thus, $\det(sB_2 - B_1)$ is a linear function of s, whose free term evidently equals $\det(-B_1)$. It is clear that for calculating the coefficient $\det(sB_2 - B_1)$ at s it suffices to summate products of each element of the matrix B_2 by the algebraic complement of the corresponding element of the matrix $-B_1$. If an element has indices (i, j), $i \neq j$, then by item (2) of Lemma 5 this product equals $a_i a_j p_i p_j / \prod_{\ell=1}^n p_\ell$.

Let us explain the positive sign in the last formula. We calculate an algebraic complement of the $-B_1$ matrix element. The matrix has $n \times n$ dimension, and therefore the found algebraic complement differs from the algebraic complement of the corresponding B_1 matrix element for $(-1)^{n-1}$ times. According to item (2) of Lemma 5, the algebraic complement of the corresponding B_1 matrix element is a "minus" product of $n - 2$ multipliers k_i. In the given case each of k_i factors is negative (equals $-1/p_i$) which results in positive sign of the last formula in the above paragraph.

Assume that this formula is valid for all (i, j). Then we get the sum

$$\frac{\sum_{i,j=1}^n a_i a_j p_i p_j}{\prod_{\ell=1}^n p_\ell} = \frac{\left(\sum_{i=1}^n a_i p_i\right)^2}{\prod_{\ell=1}^n p_\ell}. \tag{47}$$

However by item (1) of Lemma 5 the algebraic complement of the diagonal element b_{ii} of the matrix $-B_1$ equals

$$(-1)^{n-1}\left(\prod_{j:j\neq i}\left(\frac{-1}{p_j}\right) + \sum_{j:j\neq i}\prod_{\ell\notin\{i,j\}}\left(\frac{-1}{p_\ell}\right)\right) \tag{48}$$

(here and below we omit the evident requirement that values of all indices belong to the set $[n]$).

Multiplying the first term in parentheses, that is, $\prod_{j:j\neq i}(-1/p_j)$, by $(-1)^{n-1}a_i^2$ and summing over all i, we get $\sum_{i=1}^n a_i^2 p_i / \prod_{\ell=1}^n p_\ell$. Let us multiply the resting term in parentheses (48) by $(-1)^{n-1}a_i^2$, sum over all i, and subtract the value

$$\frac{\sum_{i=1}^n a_i^2 p_i^2}{\prod_{\ell=1}^n p_\ell} \tag{49}$$

from the obtained result (note that the subtrahend was "illegally" included in formula (47)). It gives the overall contribution of the second term in formula (48), which equals

$$\frac{-\sum_{j=1}^n p_j \sum_{i=1}^n a_i^2 p_i}{\prod_{\ell=1}^n p_\ell}. \tag{50}$$

Taking into account all the calculation elements of the determinant $\det(sB_2 - B_1)$ allows completing the proof of Lemma 7. □

For completing the proof of Theorem 4 let us use Corollary 8. Let us replace the δ-function in integral (39) (as was proved earlier, this integral equals the limit considered in Theorem 4): $\delta(t) = \lim_{\sigma\to 0}(1/\sqrt{2\pi}\sigma)\exp\{-t^2/2\sigma^2\}$. Treating the limit multiplied by the coefficient at the exponent as a multiplier in the integral, we come to the limit of the Gaussian integral

$$\lim_{\sigma\to 0}\frac{\int_{\mathbb{R}^n}\exp\left\{-\left\langle\left(\sigma^{-2}B_2 + \mathscr{B}\right)\mathbf{y}, \mathbf{y}\right\rangle/2\right\}d\mathbf{y}}{\sigma\sqrt{(2\pi)^n\prod_{i=1}^n p_i}}, \tag{51}$$

that is,

$$\lim_{\sigma\to 0}\frac{1}{\sigma\sqrt{\prod_{i=1}^n p_i \det\left(\sigma^{-2}B_2 + \mathscr{B}\right)}}; \tag{52}$$

Immediately applying Corollary 8, we get desired $H^{-1}(\mathbf{p})$. This completes the proof.

4. The Ratio between the Sum and the Integral

What remains is to prove that, under assumptions of Theorem 3, the ratio of the integral of the function M calculated over the domain $S(z)$ to the sum of values of this function at integer points of this domain tends to 1 as $z \to \infty$. For comparing the integral of the function and the sum of its values in the same domain one usually applies the Koksma-Hlawka inequality (see [17]). Note that usually one considers the integral over a fixed domain (as a rule, the cube $[0, 1]^n$), whereas the domain in the case under consideration is varying. However, we intend only to prove the convergence of the fraction to 1 and do not need to estimate the asymptotic difference between the integral and the sum, which simplifies the task.

Evidently, it suffices to calculate the limit of the ratio for an arbitrary infinite increasing sequence $z_1, z_2, \ldots$, such that $z_i \to \infty$.

Theorem 9. *Let* $\Omega_1, \Omega_2, \ldots$ *be a sequence of Jordan measurable sets such that* $\Omega_i \subset \Omega_{i+1}$ *for all* $i = 1, 2, \ldots$. *Assume that* $f(x)$, $x \in \Omega$, *where* $\Omega = \bigcup_i \Omega_i$, *is an integrable and bounded on each of the domains* Ω_i *function such that* $f(x) \geq 0$ *and* $\int f(x)d\Omega_i \to \infty$ *as* $i \to \infty$. *Assume also that* K *is a countable set of points from* Ω *such that each of the sets* $K_i = K \cap \Omega_i$ *is finite. Then if for any sufficiently small* $\alpha > 0$ *there exists a partition of* Ω *onto a countable number of Jordan measurable*

sets $X_j = X_j(\alpha)$, $j = 1, 2, \ldots$, *such that* $\Omega_i = \bigcup_{j=1}^{n_i} X_j$ *for some* $n_i = n_i(\alpha)$, *while*

$$\frac{\sup_{x\in X_j} f(x)}{\inf_{x\in X_j} f(x)} < 1 + \alpha \quad \text{starting with some } j, \tag{53}$$

$$\frac{\left|K \cap X_j\right|}{\mu X_j} \longrightarrow 1 \quad \text{as } j \longrightarrow \infty, \tag{54}$$

then in this case there exists the limit

$$\lim_{i\to\infty} \frac{\int f(x)\, d\Omega_i}{\sum_{x\in K_i} f(x)} = 1. \tag{55}$$

Proof. Evidently,

$$\mu X_j \inf_{x\in X_j} f(x) \le \int f(x)\, dX_j \le \mu X_j \sup_{x\in X_j} f(x). \tag{56}$$

Therefore, in view of (53) we conclude that starting with some j it holds that

$$\frac{\int f(x)\, dX_j/\mu X_j}{\sum_{x\in K\cap X_j} f(x) / \left|K \cap X_j\right|} \in (1-\alpha, 1+\alpha) \tag{57}$$

with $\alpha < 1$. In accordance with (54) we conclude that $\mu X_j/|K \cap X_j| \in (1-\alpha, 1+\alpha)$ for all j, except a finite number of values of the index. Therefore, there exists ℓ such that, with all $j > n_\ell$,

$$\frac{\int f(x)\, dX_j}{\sum_{x\in K\cap X_j} f(x)} \in \left((1-\alpha)^2, (1+\alpha)^2\right). \tag{58}$$

Representing this correlation as a double inequality and summing it over all j from $n_\ell + 1$ to n_i, we obtain

$$\frac{\int f(x)\, d\left(\Omega_i \setminus \Omega_\ell\right)}{\sum_{x\in K_i\setminus K_\ell} f(x)} \in \left((1-\alpha)^2, (1+\alpha)^2\right) \tag{59}$$

with $i > \ell$.

Note that by condition the numerator in the latter fraction (different from the integral $\int f(x) d\Omega_i$ by a constant value) tends to infinity. Then the same is true for the denominator. Note that the denominator differs from $\sum_{x\in K_i} f(x)$ by a constant value.

Therefore we conclude that all limit points of the sequence $\int f(x) d\Omega_i / \sum_{x\in K_i} f(x)$ lie inside the interval $((1-\alpha)^2, (1+\alpha)^2)$. Due to the arbitrariness of the choice of positive α Theorem 9 is proved. □

Corollary 10 (completion of the proof of Theorem 1). *Let* $f(z)$ *be the function mentioned in assumptions of Theorem 4 and let* $\widetilde{Q}(z)$ *obey formula (13). Then if at least one of the ratios* a_i/a_k, $i, k \in \{1, \ldots, n\}$, $i \ne k$, *is irrational, then*

$$\lim_{z\to\infty} \frac{f(z)}{\widetilde{Q}(z)} = 1. \tag{60}$$

Proof. For clarity we denote by z the parameter that defines the boundary of the considered domain, and do by ζ the corresponding parameter of the hyperplane that contains a certain interior point $\mathbf{x}$ of this domain; that is, $\zeta(\mathbf{x}) = \langle \mathbf{a}, \mathbf{x}\rangle$.

First of all, note that considerations in Section 3.1 imply that both in the sum and in the integral we can replace $S(z)$ with the domain

$$\widehat{\Lambda}(z) = S(z) \cap \Lambda_{\varepsilon(\zeta)}, \quad \text{where } \varepsilon(\zeta) = \zeta^{-1/2+\delta}, \tag{61}$$

and replace the function $M(\mathbf{x})$ with $\widetilde{M}(\mathbf{x})$ defined by formula (34). Therefore, we need to prove that

$$\frac{\int_{\mathbf{x}\in\widehat{\Lambda}(z)} \widetilde{M}(\mathbf{x})\, d\mathbf{x}}{\sum_{\mathbf{k}\in\widehat{\Lambda}(z)} \widetilde{M}(\mathbf{k})} \longrightarrow 1 \tag{62}$$

(or that the difference of logarithms of the numerator and denominator tends to zero).

In view of Theorem 4 the logarithm of the numerator in the latter fraction is a uniformly continuous function of z, while the logarithm of the denominator evidently is a nondecreasing function. Therefore for proving the existence of the limit with $z \to \infty$ it suffices to prove the existence of the limit for a sequence in the form $z_n = \kappa n$, $n = 1, 2, \ldots$, where κ is an arbitrarily small positive value (as the difference between the numerator and denominator of the logarithms in an arbitrary point slightly differs from the value of difference in the nearest points z_n in this sequence). Namely, just for this fixed sequence we consider the ratio from the right-hand side of (62).

In order to apply Theorem 9, for an arbitrary sufficiently small positive α we construct a partition of $\Lambda_{\varepsilon(\zeta)}$ onto domains X_j satisfying assumptions of the theorem. Namely, we construct this partition by dividing of an infinite quantity of "flapjacks" located between neighboring hyperplanes in the forms $\zeta(\mathbf{x}) = c_r$ and $\zeta(\mathbf{x}) = c_{r+1}$, $r = 1, 2, \ldots$, where $c_{r+1} = c_r + \text{Const}$, onto a finite number of domains X_j.

Evidently, for any $\alpha \le 2\kappa$ we can choose a sequence c_r such that

$$c_{r+1} - c_r = \text{Const} < \frac{\alpha}{2}; \quad \text{for any } n\ \exists r : z_n = c_r. \tag{63}$$

To this end, it suffices to put $c_r = \text{Const}\, r$, where $\text{Const} = \kappa/\lceil 2\kappa/\alpha\rceil$ (here $\lceil\cdot\rceil$ is an upward rounding to the nearest integer).

Let $C_r = \{\mathbf{x} : c_r \le \zeta(\mathbf{x}) < c_{r+1}\}$. Denote by F_r the rth "flapjack" $C_r \cap \Lambda_{\varepsilon(\zeta)}$. We are going to "cut" F_r onto a finite number of domains X_j. We numerate the countable number of domains X_j, $j = 1, 2, \ldots$, so as to make domains X_j obtained by "cutting" F_r with the least r have lesser numbers, while the order of numbering inside the partition of F_r plays no role.

Since $\varepsilon(\zeta) = o(\zeta)$, with $\mathbf{x}, \mathbf{y} \in F_r$, it holds that $y_i = x_i + o(x_i)$ (cf. with (37)). Consequently, with $r \to \infty$ we get $\ln y_i - \ln x_i \to 0$ and $\ln y - \ln x \to 0$.

By formula (33),

$$\ln \widetilde{M}(\mathbf{x}) = \text{const} + g(\mathbf{x}) + \frac{\ln(x)}{2} - \frac{\sum_{i=1}^n \ln(x_i)}{2}, \tag{64}$$

where

$$g(\mathbf{x}) = xH(\mathbf{q}) = \sum_{i=1}^{n} x_i \ln x_i - \left(\sum_{i=1}^{n} x_i\right) \ln\left(\sum_{j=1}^{n} x_i\right). \quad (65)$$

We get grad $g = \ln \mathbf{q} = (\ln q_1, \ldots, \ln q_n)$ and

$$\frac{\partial^2 g}{\partial x_i \partial x_j} = O\left(\frac{1}{x}\right), \quad i, j \in \{1, \ldots, n\}. \quad (66)$$

Using expansion in a series $\ln \widetilde{M}$ with evaluation of the second-order terms and considerations of the previous paragraph we obtain the following important observation. If $\mathbf{x}, \mathbf{y} \in F_r$ and

$$|x_i - y_i| = o(\sqrt{x}) = o(\sqrt{c_r}), \quad i = 1, \ldots, n, \quad (67)$$

then with sufficiently large r it holds that

$$\ln \widetilde{M}(\mathbf{x}) - \ln \widetilde{M}(\mathbf{y}) < |\langle \ln \mathbf{q}, \mathbf{x} - \mathbf{y} \rangle| + \frac{\alpha}{10}. \quad (68)$$

Since $\mathbf{q} \to \mathbf{p}$ as $r \to \infty$, with sufficiently large r it holds that

$$|\langle \ln \mathbf{q}, \mathbf{x} - \mathbf{y} \rangle| < |\langle \mathbf{a}, \mathbf{x} - \mathbf{y} \rangle| + \frac{\alpha}{20} < (c_{r+1} - c_r) + \frac{\alpha}{20}. \quad (69)$$

As a result, we obtain that with sufficiently small α, starting with some r, it holds that

$$\frac{\widetilde{M}(\mathbf{x})}{\widetilde{M}(\mathbf{y})} < 1 + \alpha. \quad (70)$$

Therefore, dividing F_r onto domains X_j so as to fulfill correlation (67) for all points $\mathbf{x}, \mathbf{y}$ that belong to one domain, we guarantee the validity of assumption (53) in Theorem 9. Note that it suffices to fulfill condition (67) for all indices i except one, because the validity of this condition for the remaining index follows from the fact that $\mathbf{x}, \mathbf{y} \in C_r$.

Finally, let us use the irrationality of a_{i^*}/a_{k^*} for some $i^* \neq k^*$. Let us denote by I_{k^*} the set $\{1, \ldots, n\} \setminus \{k^*\}$ and do by $I_{i^*k^*}$ the set $\{1, \ldots, n\} \setminus \{i^*, k^*\}$. We are going to prove that, defining domains X_j by inequalities

$$l_{ji} \le x_i < L_{ji}, \quad i \in I_{k^*}, \text{ where } L_{ji} - l_{ji} > \text{const}\, c_r^{1/2-\delta}, \quad (71)$$

we fulfill condition (54) (with $K = \mathbb{Z}^n$). Here, as usual, δ is a sufficiently small real positive value, though in this case we can choose δ as any number in the interval $(0, 1/2)$ (roughly speaking, it is sufficient that the radius of the pieces X_j used to divide "flapjacks" F_r tends to infinity at $r \to \infty$).

Evidently, we can divide "almost all" F_r onto domains X_j so as to simultaneously fulfill inequalities (67) and conditions (71) on l and L (the remaining "cuttings" on the edges of the domain F_r which occur due to the inconsistency between the inequality $l_{ji} \le x_i < L_{ji}$, $i \in I_{k^*}$ and the definition of the boundary of the domain $\Lambda_{\varepsilon(z)}$ are asymptotically small).

Evidently, $\mu X_j = \prod_{i \in I_{k^*}} (L_{ji} - l_{ji}) \times (c_{r+1} - c_r)/a_{k^*}$. Since the difference $(L_{ji} - l_{ji})$ grows as $j \to \infty$, *the asymptotics* of the number of ways for choosing integer x_i such that $l_{ji} \le x_i < L_{ji}$ for $i \in I_{i^*k^*}$ coincide with $\prod_{i \in I_{i^*k^*}} (L_{ji} - l_{ji})$. Here and below we understand the asymptotics as a function of j such that the ratio of the considered quantity to this function tends to 1 as $j \to \infty$. In order to complete the proof of Corollary 10, what remains is to prove the following lemma.

Lemma 11. *Let the ratio a_{i*}/a_{k^*} be irrational and $(L_{ji^*} - l_{ji^*}) \to \infty$. Assume also that the ratio $(c_{r+1} - c_r)/a_{k^*}$ equals a constant value lesser than 1 which is independent of r. Then for fixed x_i, $i \in I_{i^*k^*}$, the asymptotics of the number of ways to choose integer x_i, $i \in \{i^*, k^*\}$, such that $l_{ji^*} \le x_{i^*} < L_{ji^*}$ and $c_r \le \zeta(\mathbf{x}) < c_{r+1}$ simultaneously, equal $(L_{ji} - l_{ji}) \times (c_{r+1} - c_r)/a_{k^*}$.*

Proof of Lemma 11. In what follows we need standard denotations for the fractional part $\{\cdot\}$, floor $\lfloor \cdot \rfloor$, and ceil $\lceil \cdot \rceil$ of a number.

Let $c' = \sum_{i \in I_{i^*k^*}} a_i x_i$, $d_r = (c_r - c')/a_{k^*}$, $D_r = (c_{r+1} - c')/a_{k^*}$, and $\theta = a_{i*}/a_{k^*}$. The condition $c_r \le \zeta(\mathbf{x}) < c_{r+1}$ is equivalent to the condition

$$\theta x_{i^*} + x_{k^*} \in [d_r, D_r). \quad (72)$$

If the difference $D_r - d_r$ (it equals $(c_{r+1} - c_r)/a_{k^*}$) is less than 1 (this inequality obviously holds for sufficiently small α) then with fixed x_{i^*} the integer value x_{k^*} satisfying condition (72) is defined uniquely, provided that it exists. Therefore, we need to estimate the quantity of values x_{i^*} in the interval $[l_{ji^*}, L_{ji^*})$ such that $\{\theta x_{i^*}\} \in [\{d_r\}, \{D_r\})$; here the latter correlation is understood in the sense of an interval on the unit circle, and the length of the considered interval is independent of r.

Recall the definition of a well-distributed sequence [17, section 1.5]. □

Let (y_n) $n = 1, 2, \ldots$, be a sequence of real numbers. For integers $N \ge 1$ and $k \ge 0$ and a subset E of $[0, 1)$, let $A(E, N, k)$ be the number of terms among $\{y_{k+1}\}, \{y_{k+2}\}, \ldots, \{y_{k+N}\}$ that are lying in E.

The sequence (y_n) $n = 1, 2, \ldots$, is said to be *well-distributed mod 1* if for all pairs a, b of real numbers with $0 \le a < b \le 1$ we have

$$\lim_{N \to \infty} \frac{A([a, b); N, k)}{N} = b - a \quad \text{uniformly in } k = 0, 1, 2, \ldots. \quad (73)$$

Example. The sequence $(n\theta)$ $n = 1, 2, \ldots$, with θ irrational is well-distributed mod 1.

The latter fact would have proved Lemma 11, if the interval of the unit circle $[\{d_r\}, \{D_r\})$ was independent of r. Let us clarify this property in the case of the inequality $\{D_r\} > \{d_r\}$. In what follows we always assume that this inequality is valid (evidently, as in the definition of the well-distribution

property, this leads to no loss of generality). Really, if k equals $\lceil l_{ji^*} \rceil - 1$ and N does the difference $\lfloor L_{ji^*} \rfloor - \lceil l_{ji^*} \rceil + 1$, then we obtain the uniform (in j) convergence

$$\lim_{N\to\infty} \frac{A\left(\left[\{d\}, \{D\}\right); N, \left\lceil l_{ji^*} \right\rceil - 1\right)}{N} = D - d, \tag{74}$$

which is equivalent to the assertion of the lemma with the fixed value of $\{d_r\}$, $\{D_r\}$.

Note that if with fixed j equality (74) is valid for any subinterval in $[0, 1)$, then we say that the corresponding sequence is *uniformly distributed modulo 1*. This property follows from the property of the *well-distribution modulo 1*. It is well known that (see [17, section 2.1]) for any sequence uniformly distributed modulo 1 the convergence is uniform with respect to all subintervals in $[0, 1)$. Consequently, we get the uniform (in j) convergence

$$\lim_{N\to\infty} \frac{A\left(\left[\{d_r\}, \{D_r\}\right); N, \left\lceil l_{ji^*} \right\rceil - 1\right)}{N} = \Delta, \tag{75}$$

where the *constant* Δ equals $D_r - d_r$. Therefore,

$$\lim_{j\to\infty} \frac{A\left(\left[\{d_r\}, \{D_r\}\right); \left\lfloor L_{ji^*} \right\rfloor - \left\lceil l_{ji^*} \right\rceil + 1, \left\lceil l_{ji^*} \right\rceil - 1\right)}{\left(L_{ji^*} - l_{ji^*}\right)\Delta} = 1, \tag{76}$$

which coincides with the lemma assertion in a general case. This completes the proof.

5. Conclusion

We have proved that in the monkey model the probability of words in the sorted list has the *exact* power asymptotics, provided that the ratio of logarithms of probabilities of certain letters is irrational.

Note that this condition is not only sufficient but also necessary. Really, otherwise logarithms of probabilities $a_i = -\ln p_i$, $i = 1, \ldots, n$, allow the representation $a_i = m_i v$, where m_i are natural numbers and v is independent of i. In this case formula (10) defines a linear recurrent correlation on a grid with the step of v. This does not affect the initial constancy of the function $\widetilde{Q}$ in cells of the grid with the mentioned step with any value of the argument. Such constancy piecewise of the function $\widetilde{Q}$ contradicts the existence of a finite limit for the ratio of $p(r)/r^{-\gamma}$.

It should be noted that using the expression for terms of linear recurring sequences via the corresponding powers of roots of the characteristic equation allows clear analysis of rate of convergence to the power law of the function $\widetilde{Q}$ (with a step of v on the grid) in this degenerate case. It would be more interesting to conduct such studies for more general case to which the main theorem of this paper is devoted.

A generalization of results obtained in this paper to the case of the Markov dependence is of even more interest. In this case an analog of the vector $\mathbf{p}^\gamma$ is a substochastic matrix of transition probabilities where the row and column that correspond to the absorbing state are deleted, and all elements of this matrix are raised to a power of γ such that its spectral radius equals 1. Denote this matrix by $\mathbf{P}^\gamma$. In the case considered above all rows of the matrix $\mathbf{P}^\gamma$ coincide with $\mathbf{p}^\gamma$. In a typical case, when the strong power law takes place (see Introduction), the matrix $\mathbf{P}$ is irreducible and the matrix transposed with respect to $\mathbf{P}^\gamma$ has a positive eigenvector that corresponds to the unit eigenvalue. Let us norm this vector so as to make the sum of its components equal 1 and denote the result by $\mathbf{w}$. In the case of the Markov chain with the transition probability matrix $\mathbf{P}^\gamma$ this vector defines an ergodic distribution.

If all rows of the considered matrix coincide with $\mathbf{p}^\gamma$, then one can easily see that $\mathbf{w}$ coincides with $\mathbf{p}^\gamma$. It is possible that, in the case of the Markov dependence with the irreducible matrix $\mathbf{P}$, an analog of Theorem 1 takes place. The role of the entropy of the vector $\mathbf{p}^\gamma$ in this case plays the conditional entropy of the matrix $\mathbf{P}^\gamma$ rows with the weights equal to the corresponding components of the vector $\mathbf{w}$. We will discuss this fact in another publication.

It should be noted that mean values defined by other type recurrent relations occur in the process of analyzing the digital trees (cf. formula (10) and the recurrent relation for A_N, where N is a natural number, in [18, p. 404]). Nevertheless, the results for these values almost wholly coincide with Theorem 2 (see [19]). These results were obtained using the Mellin transform. The Mellin transform may also be useful for our case but it is a discussible problem.

Conflicts of Interest

The authors declare that there are no conflicts of interest regarding the publication of this paper.

Acknowledgments

This work was supported by the Russian Foundation for Basic Research, Grant no. 15-06-07402. The research of the first author was supported by the Russian Government Program of Competitive Growth of Kazan Federal University.

References

[1] R. Durrett, *Random Graph Dynamics*, Cambridge Series in Statistical and Probabilistic Mathematics, Cambridge University Press, Cambridge, UK, 2007.

[2] M. Mitzenmacher, "A brief history of generative models for power law and lognormal distributions," *Internet Mathematics*, vol. 1, no. 2, pp. 226–251, 2004.

[3] R. H. Baayen, *Word Frequency Distributions*, vol. 18 of *Text, Speech and Language Technology*, Kluwer Academic, Dordrecht, Netherlands, 2001.

[4] G. K. Zipf, *Human Behavior and the Principle of Least Effort: An Introduction to Human Ecology*, Addison-Wesley, Cambridge, Mass, USA, 1949.

[5] B. Mandelbrot, "An informational theory of the statistical structure of languages," in *Communication Theory*, W. B. Jackson, Ed., pp. 486–502, 1953.

[6] B. Mandelbrot, "On recurrent noise limiting coding, in Proceedings of the symposium on information networks," in *Proceedings of the Symposium on Information Networks*, pp. 205–221, Polytechnic Institute of Brooklyn, New York, NY, USA, April 1954.

[7] G. A. Miller, "Some effects of intermittent silence," *The American Journal of Psychology*, vol. 70, no. 2, pp. 311–314, 1957.

[8] W. Li, "Random texts exhibit Zipf's-law-like word frequency distribution," *IEEE Transactions on Information Theory*, vol. 38, no. 6, pp. 1842–1845, 1992.

[9] R. Perline and R. Perline, "Two universality properties associated with the monkey model of Zipf's law," *Entropy*, vol. 18, no. 3, article 89, 2016.

[10] B. Conrad and M. Mitzenmacher, "Power laws for monkeys typing randomly: the case of unequal probabilities," *IEEE Transactions on Information Theory*, vol. 50, no. 7, pp. 1403–1414, 2004.

[11] V. V. Bochkarev and E. Yu. Lerner, "The Zipf law for random texts with unequal letter probabilities and the Pascal pyramid," *Izvestiya Vysshikh Uchebnykh Zavedenii. Matematika*, vol. 56, no. 12, pp. 30–33, 2012.

[12] R. Edwards, E. Foxall, and T. J. Perkins, "Scaling properties of paths on graphs," *Electronic Journal of Linear Algebra*, vol. 23, pp. 966–988, 2012.

[13] V. V. Bochkarev and E. Yu. Lerner, "Strong power and subexponential laws for an ordered list of trajectories of a Markov chain," *Electronic Journal of Linear Algebra*, vol. 27, pp. 534–556, 2014.

[14] V. V. Bochkarev and E. Yu. Lerner, "Zipf and non-Zipf laws for homogeneous Markov chain," https://arxiv.org/abs/1207.1872.

[15] E. Artin, *The Gamma Function*, Translated by Michael Butler. Athena Series: Selected Topics in Mathematics, Holt, Rinehart and Winston, New York, NY, USA, 1964.

[16] Yu. Suhov and M. Kelbert, *Probability and statistics by example. II*, Markov Chains: A Primer in Random Processes and Their Applications, Cambridge University Press, Cambridge, UK, 2008.

[17] L. Kuipers and H. Niederreiter, *Uniform Distribution of Sequences*, Pure and Applied Mathematics, Wiley-Interscience [John Wiley & Sons], New York, NY, USA, 1974.

[18] R. Sedgewick and P. Flajolet, *An Introduction to the Analysis of Algorithms*, Addison-Wesley, Boston, Mass, USA, 1995.

[19] P. Flajolet, M. Roux, and B. Vallee, "Digital trees and memoryless sources: from arithmetics to analysis," in *Proceedings of the 21st International Meeting on Probabilistic, Combinatorial, and Asymptotic Methods in the Analysis of Algorithms (AofA '10)*, Vienna, Austria, 2010.

On Shift-Dependent Cumulative Entropy Measures

Farsam Misagh

Department of Mathematics and Statistics, Tabriz Branch, Islamic Azad University, Tabriz, Iran

Correspondence should be addressed to Farsam Misagh; misagh@iaut.ac.ir

Academic Editor: Vladimir V. Mityushev

Measures of cumulative residual entropy (CRE) and cumulative entropy (CE) about predictability of failure time of a system have been introduced in the studies of reliability and life testing. In this paper, cumulative distribution and survival function are used to develop weighted forms of CRE and CE. These new measures are denominated as weighted cumulative residual entropy (WCRE) and weighted cumulative entropy (WCE) and the connections of these new measures with hazard and reversed hazard rates are assessed. These information-theoretic uncertainty measures are shift-dependent and various properties of these measures are studied, including their connections with CRE, CE, mean residual lifetime, and mean inactivity time. The notions of weighted mean residual lifetime (WMRL) and weighted mean inactivity time (WMIT) are defined. The connections of weighted cumulative uncertainties with WMRL and WMIT are used to calculate the cumulative entropies of some well-known distributions. The joint versions of WCE and WCRE are defined which have the additive properties similar to those of Shannon entropy for two independent random lifetimes. The upper boundaries of newly introduced measures and the effect of linear transformations on them are considered. Finally, empirical WCRE and WCE are proposed by virtue of sample mean, sample variance, and order statistics to estimate the new measures of uncertainty. The consistency of these estimators is studied under specific choices of distributions.

1. Introduction

The concept of entropy was originally introduced in Shannon [1] in the context of communication theory. Since then, it has been of great theoretical and applied interest. Shannon characterized the properties of information sources and of communication channels to analyze the outputs of these sources. Statisticians have played a crucial role in the development of information theory and have shown that it provides a framework for dealing with a wide variety of problems in reliability.

Let X be a nonnegative absolutely continuous random variable describing a component failure time. The probability density function of X is denoted as $f(x)$, the failure distribution is denoted as $F(x) = P(X \leq x)$, and the survival function is denoted as $\overline{F}(x) = 1 - F(x)$. The Shannon entropy of X, which has been shown by $H(X)$ in the literature of communication, is defined as

$$H(X) = -\int_0^\infty f(x) \log f(x)\, dx, \tag{1}$$

where log denotes the natural logarithm. Entropy (1) is not scale invariant because $H(cX) = \log|c| + H(X)$, but it is translation invariant, so that $H(c + X) = H(X)$ for some constant c. The latter property can be interpreted as the shift independence of Shannon information.

Let X be random lifetime of a system with support set $(0, \infty)$; the Shannon entropy can be rewritten as

$$H(X) = 1 - E\left[\log(r(X))\right] = 1 - E\left[\log(\tau(X))\right]. \tag{2}$$

Recall that hazard rate (HR) and reversed hazard rate (RHR) of random lifetime X are defined as $r(t) = f(t)/(\overline{F}(t))$ and $\tau(t) = f(t)/F(t)$, respectively. The HR and RHR have been used in the literature of reliability in both theory and applications of them.

The notion of cumulative residual entropy (CRE) as an alternative measure of uncertainty was introduced in Wang et al. [2]. This measure is based on survival function and is defined as follows:

$$\mathscr{E}(X) = -\int_0^\infty \overline{F}(x) \log \overline{F}(x)\, dx = E\left(m_F(X)\right), \tag{3}$$

where

$$m_F(t) = E(X - t \mid X \geq t) = \frac{1}{\overline{F}(t)} \int_t^\infty \overline{F}(x)\, dx \qquad (4)$$

is the mean residual life (MRL) of X for $t \geq 0$. CRE has been applied to reliability engineering and computer vision in Rao et al. [3] and Wang et al. [2].

The role of CRE in residual lifetimes was considered in Asadi and Zohrevand [4]. The dynamic cumulative residual entropy (DCRE) of lifetime X at time $t \geq 0$ is defined by

$$\begin{aligned} \mathcal{E}(X;t) &= -\int_t^\infty \frac{\overline{F}(x)}{\overline{F}(t)} \log \frac{\overline{F}(x)}{\overline{F}(t)} dx \\ &= -\frac{1}{\overline{F}(t)} \int_t^\infty \overline{F}(x) \log \overline{F}(x)\, dx \\ &\quad + m_F(t) \log \overline{F}(t). \end{aligned} \qquad (5)$$

Entropy (5) is, in fact, the CRE for residual lifetime distribution of X at time $t > 0$.

Recently, the cumulative entropy (CE) has been proposed in Di Crescenzo and Longobardi [5] with properties similar to those of CRE. Formally, the cumulative entropy of a nonnegative random lifetime X is defined as

$$\mathcal{CE}(X) = -\int_0^\infty F(x) \log F(x)\, dx = E\left(\mu_F(X)\right), \qquad (6)$$

where

$$\mu_F(t) = E(t - X \mid X \leq t) = \frac{1}{F(t)} \int_0^t F(x)\, dx \qquad (7)$$

is the mean inactivity time (MIT) of X for $t \geq 0$. Entropy (6) measures the uncertainty about the inactivity time of X, which is the time elapsing between the failure time of a system and the time when it is found to be down. In other words, $\mathcal{CE}(X)$ is a suitable measure of information when the uncertainty is related to the past.

Furthermore, Di Crescenzo and Longobardi [5] introduced the dynamic cumulative past entropy (DCPE) in past lifetimes. DCPE of lifetime X at time $t \geq 0$ is defined by

$$\begin{aligned} \mathcal{CE}(X;t) &= -\int_0^t \frac{F(x)}{F(t)} \log \frac{F(x)}{F(t)} dx \\ &= -\frac{1}{F(t)} \int_0^t F(x) \log F(x)\, dx \\ &\quad + \mu_F(t) \log F(t). \end{aligned} \qquad (8)$$

Entropy (8) measures the uncertainty about a system which is observed only at deterministic inspection times and is found to be down at time t; then the uncertainty relies on which instant in $(0, t)$ it has failed.

This paper is aimed at defining and assessing the weighted forms of CRE and CE. In Section 2, some properties of newly introduced measures are discussed, including the connections with reliability notions and determined various bounds. Section 3 is devoted to estimation of proposed measures by means of empirical distribution function and order statistics. Some conclusions are given in Section 4.

Throughout the remaining of this paper, all random variables are assumed as absolutely continuous.

2. Weighted Cumulative Measures of Information

In this section, two new measures of uncertainty are presented in nonnegative random variables and then some properties are discussed about these new measures.

In some practical situations of reliability and neurobiology, a shift-dependent measure of uncertainty is desirable. The notion of weighted entropy addresses this requirement. An important feature of the human visual system is that it can recognize objects in a scale- and transformation-invariant manner. To intercept or avoid moving objects successfully, a visual system must compensate for the sensorimotor delays associated with visual processing and motor movement. In spite of straightforwardness in the case of constant velocity motion, it is unclear how humans compensate for accelerations, as our visual system is relatively poor at detecting changes in velocity (see Wallis [6] and de Rugy et al. [7]). Neurophysiological evidence shows that some neurons in the macaque temporal cortical visual areas have responses which are invariant with respect to the position, size, and view of faces and objects and that these neurons show rapid processing and rapid learning. Wallis and Rolls [8] propose that neurons in these visual areas use a modified rule with a short-term memory trace to capture whatever can be captured at each stage which is invariant about objects as the object changes in retinal position, size, rotation, and view. Transformation-invariant measures have been attracted by researchers from finance and industry. In robotics and machinery analysis, line and screw systems are singular at particular geometric configurations. Otherwise, measures that describe how far they are from being so are required. Hartley and Kerr [9] proposed a new measure whose outcome is strictly invariant with respect to coordinate frame, origin, and unit of length. Kerr and Hartley [10] describe a general analytical method for determining the proximity to linear dependence of any system of lines and screws. Their method gives invariant scalars for n-system of screws. The robustness of optimal portfolio with respect to the choice of risk measure has been investigated in Adam et al. [11]. Argenti et al. [12] studied filtering of generalized signal-dependent noise which is performed and estimated in shift-invariant wavelet domains. They address the scheme which filtered pixel values obtaining as adaptive combinations of raw and local average values, driven by locally computed statistics. Ghosh et al. [13] analyze experimental data in order to characterize strange attractors in terms of invariant measures such as correlation, embedding, Lyapunov dimensions, and entropy. Misagh and Yari [14] studied some theoretic uncertainty measures which are shift-dependent. They introduced the weighted differential information measure for two-sided truncated random variables which is generalization of dynamic entropy measures.

In analogy with (3) and (6), Misagh et al. [15] defined the notions of weighted cumulative residual entropy (WCRE) and weighted cumulative entropy (WCE). The measures WCRE and WCE are defined for nonnegative random lifetime X as

$$\mathcal{E}^{\omega}(X) = -\int_0^{\infty} x\overline{F}(x)\log\overline{F}(x)\,dx, \tag{9}$$

$$\mathcal{CE}^{\omega}(X) = -\int_0^{\infty} xF(x)\log F(x)\,dx, \tag{10}$$

respectively. The designation of (9) and (10) as weighted entropies arises from coefficient x which emphasizes the importance of the occurrence of events $\{X > x\}$ and $\{X \le x\}$, respectively.

The definitions given in (9) and (10) are suitable modifications of the notions of weighted entropy functions introduced in Di Crescenzo and Longobardi [16]. Misagh et al. [15] studied various properties of these measures, including their connections with CRE and CE. They showed that, in some cases, there is a direct relation between variance and WCE. In such cases WCE may be used instead of variance. In addition, some extensions of weighted cumulative entropy are presented in Suhov and Yasaei Sekeh [17]. Furthermore, they defined the notion of weighted Kullback-Leibler divergence between two random lifetimes.

Remark 1. Due to (9) and (10), it can be shown that $0 \le \mathcal{E}^{\omega}(X)$ and $\mathcal{CE}^{\omega}(X) \le \infty$, with $\mathcal{E}^{\omega}(X) = 0$ or $\mathcal{CE}^{\omega}(X) = 0$, if and only if X follows a degenerate distribution.

Example 2. Suppose X and Y be random lifetimes of two systems with common support $(0, \infty)$ and density functions $f(x) = (1/3)\exp(-x/3)$ and $f(y) = (4\times3^4)/(3+4x)^4$, respectively. From (3), $\mathcal{E}(X) = \mathcal{E}(Y) = 3$. Therefore, the expected cumulative residual uncertainties in the predictability of the residual lifetimes of X and Y are identical. By simple calculations, $\mathcal{E}^{\omega}(X) = 0.097$ and $\mathcal{E}^{\omega}(Y) = 0.73$. Hence, even though $\mathcal{E}(X) = \mathcal{E}(Y)$, the expected weighted cumulative residual uncertainty of the predictability of the failure time of component Y is larger than that of X.

The forthcoming proposition is analogous to (3) and (6); the proof is given in Misagh et al. [15] and here it is omitted. First definitions of weighted mean residual lifetime (WMRL) and weighted mean inactivity time (WMIT) are given.

Definition 3. The WMRL and WMIT of a nonnegative random variable X are given by

$$m_F^*(t) = \frac{1}{\overline{F}(t)}\int_t^{\infty} x\overline{F}(x)\,dx, \tag{11}$$

$$\mu_F^*(t) = \frac{1}{F(t)}\int_0^{t} xF(x)\,dx, \tag{12}$$

respectively.

Proposition 4. *Let X be a nonnegative random variable with WMRL $m_F^*(t)$ and WMIT $\mu_F^*(t)$. Then*

(a) $\mathcal{E}^{\omega}(X) = E(m_F^*(X))$,

(b) $\mathcal{CE}^{\omega}(X) = E(\mu_F^*(X))$.

Example 5. (i) If X is distributed as exponential with mean λ, then $m_F^*(t) = \lambda t + \lambda^2$. Hence, $\mathcal{E}^{\omega}(X) = 2\lambda^2$.

(ii) If X has power distribution with density function,

$$f(x) = \begin{cases} \left(\frac{\beta}{\alpha}\right)\cdot\left(\frac{x}{\alpha}\right)^{\beta-1}, & 0 \le x \le \alpha,\ \alpha > 0,\ \beta > 0, \\ 0, & \text{otherwise}, \end{cases} \tag{13}$$

then $\mu_F^*(t) = t^2/(\beta+2)$ and $\mathcal{CE}^{\omega}(X) = (1/(\beta+2))E(X^2) = \beta(\alpha/(\beta+2))^2$.

(iii) If X is distributed uniformly on $(0, a)$, $a > 0$, then $m_F^*(t) = (1/2)a(a+t) - (1/3)(a^2 + at + t^2)$ and $\mu_F^*(t) = (1/3)t^3$. From Proposition 4, $\mathcal{E}^{\omega}(X) = (1/4)a^2 - (1/9)a^3$ and $\mathcal{CE}^{\omega}(X) = (1/9)a^2$.

WCRE is based on survival function and then a close relationship between it and mean residual life is expected. The same can be argued about WCE and MIT.

Proposition 6. *For nonnegative random variable X, there holds*

(a) $\mathcal{E}^{\omega}(X) = \int_0^{\infty}\overline{F}(t)(\mathcal{E}(X;t) - m_F(t)\log\overline{F}(t))dt$,

(b) $\mathcal{CE}^{\omega}(X) = \int_0^{\infty}F(t)(\mathcal{CE}(X;t) - \mu_F(t)\log F(t))dt$.

Proof. Part (a) is proven in Misagh et al. [15]. The second part is proven in a similar way. □

For independent random variables X and Y, $H(X,Y) = H(X) + H(Y)$, where $H(X,Y) = -E(\log f(X,Y))$ is the two-dimensional Shannon entropy. In the following proposition, similar properties are presented for weighted cumulative entropies.

Proposition 7. *Let X and Y be two nonnegative independent random variables with finite WMRL and WMIT. Then*

(a) $\mathcal{E}^{\omega}(X,Y) = (\int_0^{\infty} x\overline{F}_X(x)dx)\mathcal{E}^{\omega}(Y) + (\int_0^{\infty} y\overline{F}_Y(y)dy)\mathcal{E}^{\omega}(X)$,

(b) $\mathcal{CE}^{\omega}(X,Y) = (\int_0^{\infty} xF_X(x)dx)\mathcal{CE}^{\omega}(Y) + (\int_0^{\infty} yF_Y(y)dy)\mathcal{CE}^{\omega}(X)$.

Proof. The proof is straightforward. For part (a),

$$\begin{aligned}\mathcal{E}^{\omega}(X,Y) &= -\iint_0^{\infty} xy\overline{F}(x,y)\log\overline{F}(x,y)\,dx\,dy \\ &= -\iint_0^{\infty} xy\overline{F}_X(x)\overline{F}_Y(y)\log\overline{F}_X(x)\,dx\,dy \\ &\quad -\iint_0^{\infty} xy\overline{F}_X(x)\overline{F}_Y(y)\log\overline{F}_Y(y)\,dx\,dy,\end{aligned} \tag{14}$$

where the second equality comes from the independence of random variables. □

Remark 8. If the support sets of X and Y are limited to finite sets (a_X, b_X) and (a_Y, b_Y), respectively, from Proposition 7,

$$\begin{aligned}\mathcal{E}^{\omega}(X,Y) &= m_F^*(a_X)\,\mathcal{E}^{\omega}(Y) + m_G^*(a_Y)\,\mathcal{E}^{\omega}(X),\\ \mathcal{CE}^{\omega}(X,Y) &= \mu_F^*(b_X)\,\mathcal{CE}^{\omega}(Y) + \mu_G^*(b_Y)\,\mathcal{CE}^{\omega}(X).\end{aligned} \tag{15}$$

Furthermore, for

$$\begin{aligned}m_G^*(a_Y) &= m_F^*(a_X) = m^*,\\ \mu_G^*(b_Y) &= \mu_F^*(b_X) = \mu^*,\end{aligned} \tag{16}$$

it is obtained that

$$\begin{aligned}\mathcal{E}^{\omega}(X,Y) &= m^*\left(\mathcal{E}^{\omega}(Y) + \mathcal{E}^{\omega}(X)\right),\\ \mathcal{CE}^{\omega}(X,Y) &= \mu^*\left(\mathcal{CE}^{\omega}(Y) + \mathcal{CE}^{\omega}(X)\right),\end{aligned} \tag{17}$$

which is similar to the property of Shannon entropy for two independent random variables. For instance, if X and Y have same uniform distribution in the interval $(0, \sqrt{3})$, then $\mu^* = 1$ and $\mathcal{CE}^{\omega}(X,Y) = \mathcal{CE}^{\omega}(X) + \mathcal{CE}^{\omega}(Y)$.

In the following proposition, alternative expressions to (9) and (10) are provided in terms of double integrals of hazard and reversed hazard rates. A similar result for CE has been considered in Di Crescenzo and Longobardi [5].

Proposition 9. *Let X be a nonnegative random variable with finite WCE and WCRE; then*

(a) $\mathcal{E}^{\omega}(X) = E((X - 1/r(X))\widetilde{T}^2(X))$,

(b) $\mathcal{CE}^{\omega}(X) = E((X + 1/\tau(X))T^2(X))$,

where

$$\begin{aligned}\widetilde{T}^2(x) &= -\int_0^x \log\overline{F}(t)\,dt = \int_0^x\int_0^t r(u)\,du\,dt,\\ T^2(x) &= -\int_x^{\infty} \log F(t)\,dt = \int_x^{\infty}\int_t^{\infty} \tau(u)\,du\,dt.\end{aligned} \tag{18}$$

Proof. By recalling (9),

$$\begin{aligned}\mathcal{E}^{\omega}(X) &= -\int_0^{\infty} x\overline{F}(x)\log\overline{F}(x)\,dx\\ &= \int_0^{\infty}\left(\int_x^{\infty}\left(\overline{F}(t) - tf(t)\right)dt\right)\log\overline{F}(x)\,dx\\ &= \int_0^{\infty}\int_0^t \overline{F}(t)\log\overline{F}(x)\,dx\,dt\\ &\quad - \int_0^{\infty}\int_0^t tf(t)\log\overline{F}(x)\,dx\,dt\\ &= \int_0^{\infty}\overline{F}(t)\left(\int_0^t \log\overline{F}(x)\,dx\right)dt\\ &\quad - \int_0^{\infty} tf(t)\left(\int_0^t \log\overline{F}(x)\,dx\right)dt\\ &= -\int_0^{\infty} f(t)\,\frac{\overline{F}(t)}{f(t)}\widetilde{T}^2(t)\,dt\\ &\quad + \int_0^{\infty} tf(t)\,\widetilde{T}^2(t)\,dt\\ &= E\left(\left(X - \frac{\overline{F}(X)}{f(X)}\right)\widetilde{T}^2(X)\right).\end{aligned} \tag{19}$$

Part (b) is proven in a similar way. Note that

$$\begin{aligned}\mathcal{CE}^{\omega}(X) &= -\int_0^{\infty} xF(x)\log F(x)\,dx\\ &= -\int_0^{\infty}\left(\int_0^x \left(F(t) + tf(t)\right)dt\right)\log F(x)\,dx;\end{aligned} \tag{20}$$

this completes the proof. □

Example 10. (i) Let X be exponentially distributed with mean λ; then $\widetilde{T}^2(x) = x^2/2\lambda$ and $r(x) = 1/\lambda$. From Proposition 9, $\mathcal{E}^{\omega}(X) = E[(X-\lambda)(X^2/2\lambda)] = (1/2\lambda)E(X^3) - (1/2)E(X^2) = 2\lambda^2$.

(ii) Consider the random variable X with the following density function:

$$f(x) = \frac{2\alpha}{x^3}\exp\left(-\frac{\alpha}{x^2}\right), \quad x > 0,\ \alpha > 0. \tag{21}$$

Then $T^2(x) = \alpha/x$ and $\tau(x) = 2\alpha/x^3$ and, from Proposition 9, it is obtained that

$$\mathcal{CE}^{\omega}(X) = \alpha + \frac{1}{2}E\left(X^2\right) = \alpha + \frac{1}{2}\alpha Ei\left(1, \frac{\alpha}{x^2}\right), \tag{22}$$

where

$$Ei(a,z) = \int_1^{\infty} x^a e^{-zx}dx \tag{23}$$

is the exponential integral function (see Abramowitz and Stegun [18]).

Proposition 11. *Let X be a random variable with finite support set (α, β) with $\beta > \alpha > 0$. Then, for θ in $(0, 1]$,*

(a) $\mathcal{E}^{\omega}(X) \le \theta((\beta^2 - \alpha^2)/2) - m_F^*(\alpha)\log(\theta e)$,

(b) $\mathcal{CE}^{\omega}(X) \le \theta((\beta^2 - \alpha^2)/2) - \mu_F^*(\beta)\log(\theta e)$.

Proof. From Taylor expansion (see Walker [19]), it can be seen that, for all θ in $(0, 1]$,

$$-x\log x \le \theta - x\left(1 + \log\theta\right). \tag{24}$$

Now, from (9),

$$\begin{aligned}\mathcal{E}^{\omega}(X) &\le \int_{\alpha}^{\beta} x\left(\theta - \overline{F}(x)\left(1+\log\theta\right)\right)dx \\ &= \theta\int_{\alpha}^{\beta} x\,dx - \left(1+\log\theta\right)\int_{\alpha}^{\beta} x\overline{F}(x)\,dx \\ &= \theta\frac{\beta^2-\alpha^2}{2} - m_F^*(\alpha)\log(\theta e).\end{aligned} \tag{25}$$

Similarly, from (10),

$$\begin{aligned}\mathcal{CE}^{\omega}(X) &\le \theta\int_{\alpha}^{\beta} x\,dx - \left(1+\log\theta\right)\int_{\alpha}^{\beta} xF(x)\,dx \\ &= \theta\frac{\beta^2-\alpha^2}{2} - \mu_F^*(\beta)\log(\theta e).\end{aligned} \tag{26}$$

This completes the proof. □

Remark 12. From Proposition 11, we get, for all θ in $(0, 1]$,

$$\begin{aligned}\mathcal{E}^{\omega}(X) + \mathcal{CE}^{\omega}(X) \le{}& \theta\left(\beta^2-\alpha^2\right) \\ &- \left[m_F^*(\alpha) + \mu_F^*(\beta)\right]\log(\theta e).\end{aligned} \tag{27}$$

Remark 13. The right-hand sides of (a) and (b) in Proposition 11 are minimized at the points $\theta = 2m_F^*(\alpha)/(\beta^2-\alpha^2)$ and $\theta = 2\mu_F^*(\beta)/(\beta^2-\alpha^2)$, respectively.

The following proposition considers the effect of linear transformations on WCE and WCRE.

Proposition 14. *Let X be a nonnegative random variable. Then, for positive constants a and b,*

(a) $\mathcal{E}^{\omega}(aX+b) = a^2\mathcal{E}^{\omega}(X) + ab\mathcal{E}(X)$,

(b) $\mathcal{CE}^{\omega}(aX+b) = a^2\mathcal{CE}^{\omega}(X) + ab\mathcal{CE}(X)$.

Proof. The proof is straightforward. Note that

$$\begin{aligned}&\mathcal{E}^{\omega}(aX+b) \\ &= -\int_b^{\infty} yP\left(X > \frac{y-b}{a}\right)\log P\left(X > \frac{y-b}{a}\right)dy \\ &= -\int_0^{\infty} a(ax+b)\,P(X>x)\log P(X>x)\,dx \\ &= -a^2\int_0^{\infty} x\overline{F}(x)\log\overline{F}(x)\,dx \\ &\quad - ab\int_0^{\infty}\overline{F}(x)\log\overline{F}(x)\,dx.\end{aligned} \tag{28}$$

Part (b) is proven in a similar way. □

According to Proposition 14, it is realized that there may exist a close relation between WCE, WCRE, and variance.

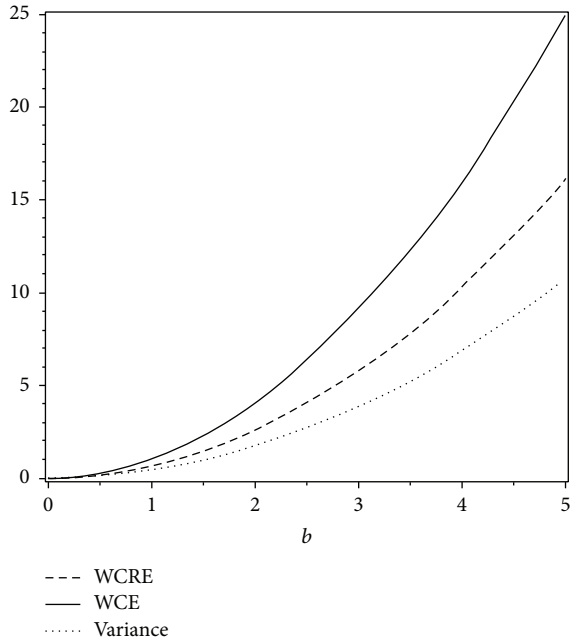

Figure 1: WCRE, WCE, and variance for Weibull distribution.

Example 15. Let X be a nonnegative random variable with Weibull distribution with scale parameter b and shape parameter 2. Its probability density function is given by

$$f(x) = \frac{x}{b^2}e^{-1/2}\exp\left(\frac{x^2}{b^2}\right), \quad b>0,\ x>0. \tag{29}$$

The plot of $\mathrm{Var}(X) = (2-(1/2)\pi)b^2$, $\mathcal{E}^{\omega}(X)$, and $\mathcal{CE}^{\omega}(X)$ are given in Figure 1 which shows a direct relation between variance and cumulative entropies. Furthermore, $\mathrm{Var}(X) \le \mathcal{CE}^{\omega}(X) \le \mathcal{E}^{\omega}(X)$. In such cases, WCRE and WCE may be used instead of variance as a discrepancy measure. It should be noticed that as b grows, the tendency of WCE and WCRE to overestimate the variance of X increases.

Hereafter, the weighted cumulative measures of information are studied when the lifetimes have proportional hazard (PH) and reversed proportional hazard (RPH) rates.

Two random variables X and Y with survival functions $\overline{F}$ and $\overline{G}$ are said to have PH model if there exists $\theta > 0$ such that $\overline{G}(x) = [\overline{F}(x)]^{\theta}$. The PH model, introduced by Cox [20], plays an important role in reliability and survival analysis. The RPH model is based on the assumption that the cumulative distribution functions of X and Y are related with $G(x) = [F(x)]^{\theta}$ with $\theta > 0$. Some results on these models are presented in Ebrahimi and Kirmani [21], Di Crescenzo [22], R. C. Gupta and R. D. Gupta [23], and Gupta et al. [24].

Proposition 16. *Let X and Y be two nonnegative random variables; then, for $\theta \ge 1$ and for PH and RPH models, $\mathcal{E}^{\omega}(Y) \le \mathcal{E}^{\omega}(\sqrt{\theta}X)$ and $\mathcal{CE}^{\omega}(Y) \le \mathcal{CE}^{\omega}(\sqrt{\theta}X)$, respectively. For $0 < \theta < 1$, the inequalities are reversed.*

Proof. The proof is easy and is omitted. Note that $F(x) \ge [F(x)]^{\theta}$ and $\overline{F}(x) \ge [\overline{F}(x)]^{\theta}$, $x \ge 0$, when $\theta > 1$. □

Example 17. Let $Y_1 = \min\{X_1, X_2, \ldots, X_n\}$ and $Y_n = \max\{X_1, X_2, \ldots, X_n\}$, where X_i, $i = 1, 2, \ldots, n$, are nonnegative independently and identically distributed with common distribution F. Suppose also that Y_j, $j = 1, 2$, has distribution function G_j, $j = 1, 2$, where $\overline{G}_1(x) = [\overline{F}(x)]^n$ and $G_n(x) = [F(x)]^n$. From Proposition 16, it is obtained that $\mathcal{E}^{\omega}(Y_1) \leq \mathcal{E}^{\omega}(\sqrt{n}X)$ and $\mathcal{CE}^{\omega}(Y_n) \leq \mathcal{CE}^{\omega}(\sqrt{n}X)$.

3. Empirical WCRE and WCE

Suppose $X_1, X_2, \ldots, X_n$ be a random sample with distribution F. The empirical distribution is a discrete probability distribution with probability function generated from the given sample. The empirical distribution and survival functions of random sample $X_1, X_2, \ldots, X_n$ at point x are given by $F_n(x) = (1/n)\sum_{i=1}^{n} I\{X_i \leq x\}$ and $\overline{F}_n = 1 - F_n$, respectively, where

$$I\{X \leq x\} = \begin{cases} 1, & X \leq x, \\ 0, & X > x \end{cases} \tag{30}$$

is the indicator function of event $\{X \leq x\}$.

Definition 18. Let $X_1, X_2, \ldots, X_n$ be a random sample drawn from a population having distribution function $F(x)$. The empirical WCRE (EWCRE) and empirical WCE (EWCE) are defined as

$$\mathcal{E}^{\omega}(F_n) = -\int_0^{\infty} x\overline{F}_n(x)\log\overline{F}_n(x)\,dx, \tag{31}$$

$$\mathcal{CE}^{\omega}(F_n) = -\int_0^{\infty} xF_n(x)\log F_n(x)\,dx, \tag{32}$$

respectively.

The following proposition presents alternative expressions of (31) and (32) in terms of sample mean $\overline{X} = (1/n)\sum_{i=1}^{n} X_i$, sample variance $S^2 = (1/(n-1))\sum_{i=1}^{n}(X_i - \overline{X})^2$, and order statistics.

Proposition 19. *Let $X_1, X_2, \ldots, X_n$ be a random sample drawn from a population having order statistics $X_{(1)} \leq X_{(2)} \leq \cdots \leq X_{(n)}$; then*

(a)

$$\mathcal{E}^{\omega}(F_n) = \left[\overline{X}^2 - X_{(1)}^2 + \left(1 - \frac{1}{n}\right)S^2\right]\log\sqrt{n} - \sum_{j=1}^{n-1} C_j(n-j)\log(n-j), \tag{33}$$

(b)

$$\mathcal{CE}^{\omega}(F_n) = \left(X_{(n)}^2 - \overline{X}^2 - \left(1 - \frac{1}{n}\right)S^2\right)\log\sqrt{n} - \sum_{j=1}^{n-1} C_j j\log j, \tag{34}$$

where $C_j = (1/2)(X_{(j+1)}^2 - X_{(j)}^2)$.

Proof. From (31), we get

$$\mathcal{E}^{\omega}(F_n) = -\sum_{j=1}^{n-1}\int_{X_{(j)}}^{X_{(j+1)}} x\overline{F}_n(x)\log\overline{F}_n(x)\,dx. \tag{35}$$

Recalling that, for $X_{(j)} \leq x < X_{(j+1)}$,

$$\overline{F}_n(x) = 1 - \frac{j}{n}, \quad j = 1, 2, \ldots, n-1, \tag{36}$$

so

$$\begin{aligned}\mathcal{E}^{\omega}(F_n) &= -\sum_{j=1}^{n-1}\int_{X_{(j)}}^{X_{(j+1)}} x\left(\frac{n-j}{n}\right)\log\left(\frac{n-j}{n}\right)dx \\ &= -\sum_{j=1}^{n-1}\left(\frac{X_{(j+1)}^2 - X_{(j)}^2}{2}\right)\left(\frac{n-j}{n}\right)\log\left(\frac{n-j}{n}\right) \\ &= -\frac{1}{n}\sum_{j=1}^{n-1} C_j(n-j)\log\left(\frac{n-j}{n}\right),\end{aligned} \tag{37}$$

where $C_j = (1/2)(X_{(j+1)}^2 - X_{(j)}^2)$.

In addition,

$$\begin{aligned}\sum_{j=1}^{n-1} C_j(n-j) &= \frac{n}{2}\sum_{j=1}^{n-1}\left(X_{(j+1)}^2 - X_{(j)}^2\right) \\ &\quad - \frac{1}{2}\sum_{j=1}^{n-1} j\left(X_{(j+1)}^2 - X_{(j)}^2\right) \\ &= \frac{n}{2}\left(\overline{X^2} - X_{(1)}^2\right),\end{aligned} \tag{38}$$

where

$$\overline{X^2} = \frac{1}{n}\sum_{j=1}^{n} X_{(j)}^2 = \frac{1}{n}\sum_{j=1}^{n} X_j^2. \tag{39}$$

Now, by virtue of $(1 - 1/n)S^2 = \overline{X^2} - \overline{X}^2$, (33) is obtained. Part (b) is proven in a similar way. Note that $\sum_{j=1}^{n-1} C_j j = (n/2)(X_{(n)}^2 - \overline{X^2})$. □

Here, the consistency of EWCRE and EWCE is studied under specific choices of function F. According to (33) and (34), the estimators $\mathcal{E}^{\omega}(F_n)$ and $\mathcal{CE}^{\omega}(F_n)$ are calculated for $n = 100$ simulated observations of distribution F and the process is repeated for 1000 times. Table 1 shows mean and mean squares of errors (MSE) of EWCRE and EWCE. Relevant values of $E[\mathcal{E}^{\omega}(F_{100})]$ and $E[\mathcal{CE}^{\omega}(F_{100})]$ are the mean of $\mathcal{E}^{\omega}(F_{100})$ and $\mathcal{CE}^{\omega}(F_{100})$ values generated in every step of simulation process. The numbers in brackets indicate the corresponding real values of $\mathcal{E}^{\omega}(X)$ and $\mathcal{CE}^{\omega}(X)$ calculated from (9) and (10). The MSE values are the mean of squared errors between empirical and real entropies. According to Table 1, the estimates are almost equal to real values of weighted cumulative information measures and MSE values are nearly zero.

Table 1: Mean and MSE of the empirical cumulative entropy for random samples of some familiar distributions.

Distribution	Survival function	$E[\mathcal{CE}^{\omega}(F_{100})]$	$E[\mathcal{E}^{\omega}(F_{100})]$	$\mathrm{MSE}[\mathcal{CE}^{\omega}(F_{100})]$	$\mathrm{MSE}[\mathcal{E}^{\omega}(F_{100})]$
Finite range	$(1-(1/2)x)^3$, $0<x<2$	0.15377 (0.15477)	0.26319 (0.27)	0.00087	0.00127
Uniform	$1-x$, $0<x<1$	0.11018 (0.11111)	0.13698 (0.13889)	0.00005	0.00004
Power	$1-(x/5)^2$, $0<x<5$	3.10340 (3.125)	3.09780 (3.125)	0.01958	0.01778
Exponential	$\exp(-2x)$, $x>0$	0.21012 (0.21175)	0.46532 (0.5)	0.00271	0.02267

4. Conclusion

Reliability and survival analysis is a branch of statistics which deals with death in biological organisms and failure in mechanical systems. There are several uncertainty measures that play a central role in understanding and describing reliability. Most of these information measures do not take into account the values of a random variable. Two shift-dependent measures of uncertainty are considered related to cumulative distribution and survival functions so that higher weight is assigned to large values of observed random variables. These measures are called weighted cumulative residual entropy (WCRE) and weighted cumulative entropy (WCE) with properties similar to those of the legacy entropies. Several propositions and examples for WCRE and WCE have been presented, some of which parallel those for results presented in Asadi and Zohrevand [4] and Di Crescenzo and Longobardi [5, 16]. It must be remarked that the empirical WCRE and WCE and the relationship with well-known statistics have been assessed. Of course, many properties of these measures are still waiting to be discovered.

Competing Interests

The author declares that there are no competing interests.

Acknowledgments

The author would like to thank Tabriz Branch, Islamic Azad University, for the financial support of this research, which is based on a research project contract.

References

[1] C. E. Shannon, "A mathematical theory of communication," *The Bell System Technical Journal*, vol. 27, pp. 379–423, 1948.

[2] F. E. Wang, B. C. Vemuri, M. Rao, and Y. Chen, "A new and robust information theoretic measure and its application to image alignment," in *Proceedings of the International Conference on Information Processing in Medical Imaging*, pp. 3880–4000, Springer, Ambleside, UK, 2003.

[3] M. Rao, Y. Chen, B. C. Vemuri, and F. Wang, "Cumulative residual entropy: a new measure of information," *IEEE Transactions on Information Theory*, vol. 50, no. 6, pp. 1220–1228, 2004.

[4] M. Asadi and Y. Zohrevand, "On the dynamic cumulative residual entropy," *Journal of Statistical Planning and Inference*, vol. 137, no. 6, pp. 1931–1941, 2007.

[5] A. Di Crescenzo and M. Longobardi, "On cumulative entropies," *Journal of Statistical Planning and Inference*, vol. 139, no. 12, pp. 4072–4087, 2009.

[6] G. Wallis, "Using spatio-temporal correlations to learn invariant object recognition," *Neural Networks*, vol. 9, no. 9, pp. 1513–1519, 1996.

[7] A. de Rugy, W. Marinovic, and G. Wallis, "Neural prediction of complex accelerations for object interception," *Journal of Neurophysiology*, vol. 107, no. 3, pp. 766–771, 2012.

[8] G. Wallis and E. T. Rolls, "Invariant face and object recognition in the visual system," *Progress in Neurobiology*, vol. 51, no. 2, pp. 167–194, 1997.

[9] D. M. Hartley and D. R. Kerr, "Invariant measures of the closeness to linear dependence of six lines or screws," *Proceedings of the Institution of Mechanical Engineers, Part C: Journal of Mechanical Engineering Science*, vol. 215, no. 10, pp. 1145–1151, 2001.

[10] D. R. Kerr and D. M. Hartley, "Invariant measures of closeness to linear dependency of screw systems," *Proceedings of the Institution of Mechanical Engineers, Part C*, vol. 220, no. 7, pp. 1033–1043, 2006.

[11] A. Adam, M. Houkari, and J.-P. Laurent, "Spectral risk measures and portfolio selection," *Journal of Banking and Finance*, vol. 32, no. 9, pp. 1870–1882, 2008.

[12] F. Argenti, G. Torricelli, and L. Alparone, "MMSE filtering of generalised signal-dependent noise in spatial and shift-invariant wavelet domains," *Signal Processing*, vol. 86, no. 8, pp. 2056–2066, 2006.

[13] A. Ghosh, M. V. Badiger, P. S. Tapadia, V. Ravi Kumar, and B. D. Kulkarni, "Characterization of chaotic dynamics-I: dynamical invariants of sheared polymer solutions," *Chemical Engineering Science*, vol. 56, no. 19, pp. 5635–5642, 2001.

[14] F. Misagh and G. H. Yari, "On weighted interval entropy," *Statistics and Probability Letters*, vol. 81, no. 2, pp. 188–194, 2011.

[15] F. Misagh, Y. Panahi, G. H. Yari, and R. Shahi, "Weighted cumulative entropy and its estimation," in *Proceedings of the IEEE International Conference on Quality and Reliability (ICQR '11)*, pp. 477–480, Bangkok, Thailand, September 2011.

[16] A. Di Crescenzo and M. Longobardi, "On cumulative entropies," *Journal of Statistical Planning and Inference*, vol. 139, no. 12, pp. 4072–4087, 2009.

[17] Y. Suhov and S. Yasaei Sekeh, "Weighted cumulative entropies: an extension of CRE and CE," http://arxiv.org/abs/1507.07051v1.

[18] M. Abramowitz and I. Stegun, *Handbook of Mathematical Functions*, Dover, New York, NY, USA, 1995.

[19] P. L. Walker, *Examples and Theorems in Analysis*, Springer, 2004.

[20] D. R. Cox, "Regression models and life-tables," *Journal of the Royal Statistical Society. Series B. Methodological*, vol. 34, pp. 187–220, 1972.

[21] N. Ebrahimi and S. N. U. A. Kirmani, "A measure of discrimination between two residual life-time distributions and its applications," *Annals of the Institute of Statistical Mathematics*, vol. 48, no. 2, pp. 257–265, 1996.

[22] A. Di Crescenzo, "Some results on the proportional reversed hazards model," *Statistics & Probability Letters*, vol. 50, no. 4, pp. 313–321, 2000.

[23] R. C. Gupta and R. D. Gupta, "Proportional reversed hazard rate model and its applications," *Journal of Statistical Planning and Inference*, vol. 137, no. 11, pp. 3525–3536, 2007.

[24] R. C. Gupta, R. D. Gupta, and P. L. Gupta, "Modeling failure time data by Lehman alternatives," *Communications in Statistics-Theory and Methods*, vol. 27, no. 4, pp. 887–904, 1998.

Arithmetical Functions Associated with the k-ary Divisors of an Integer

Joseph Vade Burnett, Sam Grayson, Zachary Sullivan, Richard Van Natta, and Luke Bang

The University of Texas at Dallas, 800 W Campbell Rd, Richardson, TX, USA

Correspondence should be addressed to Joseph Vade Burnett; joseph.burnett@utdallas.edu

Academic Editor: Pentti Haukkanen

The k-ary divisibility relations are a class of recursively defined relations beginning with standard divisibility and culminating in the so-called infinitary divisibility relation. We examine the summatory functions corresponding to the k-ary analogues of various popular functions in number theory, proving various results about the structure of the k-ary divisibility relations along the way.

1. Introduction

Let n be a positive integer and denote the set of divisors of n by $D(n)$. The set of unitary divisors of n, denoted by $D^1(n)$, are the divisors d of n which satisfy $D(d) \cap D(n/d) = \{1\}$; in other words, $(d, n/d) = 1$. The biunitary divisors of n are the divisors d of n which satisfy $D^1(d) \cap D^1(n/d)$. This differs from some definitions of biunitary divisibility in the literature (e.g., [1]) but is consistent with others (e.g., [2]). In general, we may define the k-ary divisors of an integer n to be the set

$$\begin{aligned} D^k(n) &:= \left\{ d \in D(n) \mid D^{k-1}(d) \cap D^{k-1}\left(\frac{n}{d}\right) = \{1\} \right\} \\ &= \left\{ d \in D(n) \mid \left(d, \frac{n}{d}\right)_{k-1} = 1 \right\}, \end{aligned} \tag{1}$$

where we define the greatest common k-ary divisor of m and n by

$$(m,n)_k := \max\left\{ D^k(m) \cap D^k(n) \right\}. \tag{2}$$

We write $d|_k n$ if $d \in D^k(n)$.

The k-ary divisibility relations as defined above were first introduced by Cohen [3] and have been studied more recently by Haukkanen [2] and Steuding et al. [4]. An alternative definition can be seen in Suryanarayana [5].

One easily verifies the following basic properties:

(i) $1 \in D^k(n)$ and $n \in D^k(n)$ for all n.

(ii) If n and m are coprime, then $D^k(nm) = D^k(n) \cdot D^k(m)$, where $A \cdot B := \{ab \mid a \in A, b \in B\}$.

(iii) If $d \in D^k(n)$, then $n/d \in D^k(n)$.

For example, the set of unitary divisors of a prime power p^a are $D^1(p^a) = \{1, p^a\}$. On the other hand, the biunitary divisors of a prime power p^a are given by $D(p^a)$ when a is odd and $D(p^a) \setminus \{p^{a/2}\}$ when a is even. We may then form the unitary and biunitary divisors of a positive integer n by "multiplying" the prime-power divisor sets that form the prime decomposition of n.

By viewing the sets D^k as representing some of the A-convolutions of Narkiewicz [6], we may define the k-ary convolution of arithmetic functions f and g:

$$(f \star_k g)(n) := \sum_{d|_k n} f(d)\, g\left(\frac{n}{d}\right). \tag{3}$$

The following properties of k-ary convolution can be found in [2]:

(i) The k-ary convolution is commutative.

(ii) The function $\iota(n)$, which takes on value of 1 if $n = 1$ and 0 otherwise, is the identity under k-ary convolution.

(iii) If an arithmetic function f satisfies $f(1) \neq 0$, then f possesses a unique inverse under k-ary convolution.

(iv) If f and g are multiplicative functions, then $f \star_k g$ is multiplicative as well.

By choosing f and g appropriately, we may obtain multiplicative k-ary analogues to the following classical functions from number theory in terms of the k-ary convolution:

(i) Let $f(n) = g(n) = 1$ for all n. Then $\tau_k(n) \coloneqq (f \star_k g)(n)$ is the number of k-ary divisors of n.

(ii) Let $f(n) = n$ and $g(n) = 1$ for all n. Then $\sigma_k(n) \coloneqq (f \star_k g)(n)$ is the sum of the k-ary divisors of n.

(iii) Let $f(n) = n$ and $g(n) = \mu_k(n)$ for all n, where μ_k is the unique inverse of the function $U(n) = 1$ under the k-ary convolution. Then $\varphi_k(n) \coloneqq (f \star_k g)(n)$ is the analogue of the Euler totient function.

(iv) Let $f(n) = n$ and $g(n) = |\mu_k(n)|$. Then $\psi_k(n) \coloneqq (f \star_k g)(n)$ is the analogue of the Dedekind ψ-function.

Note that while $\varphi(n)$ counts the totatives of n, in general φ_k does not count the k-ary totatives of n.

In this paper, we prove results concerning the structure of k-ary divisibility relations and use that to obtain formulae for the number of integers m less than or equal to n which satisfy $(m, n)_k = 1$. We then apply this result to obtain asymptotics for the summatory functions of k-ary generalizations of the classical functions mentioned above.

2. The Behavior of k-Ary Divisibility Relations

Let $D^\infty(n)$ be the set of infinitary divisors of n introduced and studied by Cohen [3, 7]. The infinitary divisibility relation can be thought of as the end behavior of the recursion defining the k-ary divisibility relations. It satisfies

(i) All properties of k-ary divisibility relations listed above

(ii) $d \in D^\infty(n)$ if and only if $D^\infty(d) \cap D^\infty(n/d) = \{1\}$

(iii) D^∞ being transitive; that is, for all n, if $d \in D^\infty(n)$, then $D^\infty(d) \subseteq D^\infty(n)$.

Additionally, the following reformulation of Theorem 1 from [3] characterizes in what sense k-ary divisibility relations "approach" the infinitary divisibility relation as k increases.

Theorem 1. *Let $k \geqslant 0$ be given, and suppose that $n \in \mathbb{N}$ is such that, for every prime p, $\nu_p(n) \leqslant k + 1$, where $\nu_p(n)$ is the exponent of the prime p in the prime decomposition of n (0 if p does not divide n). Then $D^k(n) = D^\infty(n)$.*

Proof. We proceed by induction on k. We need to only show the result for prime powers p^a, since by the second property listed above we obtain our theorem by multiplicative construction, akin to the treatment of multiplicative arithmetical functions. Therefore, we may speak of a set prime p and consider p^a, with $a \leqslant k+1$. For $k = 0$, we have $D^\infty(p) = D(p)$ and $D^\infty(1) = D(1)$.

Now assume that the result holds up to some $K - 1$. Then consider $D^K(p^a) = \{d \in D(p^a) \mid D^{K-1}(d) \cap D^{K-1}(p^a/d) = \{1\}\}$, with a such that $a \leqslant K + 1$. Notice that all divisors d of p^a, except p^a itself, satisfy $d = p^b$, with $b \leqslant K - 1$. Then, for $d \neq p^a$, we have $D^{K-1}(d) = D^\infty(d)$ and, for $d \neq 1$, we have $D^{K-1}(p^a/d) = D^\infty(p^a/d)$. So, for d not equal to 1 or p^a, $d \in D^K(p^a) \iff D^\infty(d) \cap D^\infty(p^a/d)$. But 1 and p^a are in $D^K(p^a)$ as well, so $D^K(p^a) = D^\infty(p^a)$, and by the second property of D^k and D^∞ listed above, we are done. □

Additionally, we observe the following.

Theorem 2. *For all $n \in \mathbb{N}$, $k \geqslant 0$, $D^\infty(n) \subseteq D^{2k+2}(n) \subseteq D^{2k}(n)$, and $D^{2k+1}(n) \subseteq D^{2k+3}(n) \subseteq D^\infty(n)$.*

Proof. We will again use induction. One can immediately verify that $D^\infty(n) \subseteq D^2(n) \subseteq D(n)$ and $D^1(n) \subseteq D^3(n) \subseteq D^\infty(n)$; $D^3(p^a)$ only differs from $D^1(p^a)$ at $a = 3$ and $a = 6$, where we have $D^3(p^3) = D^\infty(p^3)$ and $D^3(p^6) = D^\infty(p^6)$. Assuming that the theorem holds up to some K, observe that for each divisor d of n the condition $D^{2K+3}(d) \cap D^{2K+3}(n/d) = \{1\}$ implies that $D^{2K+1}(d) \cap D^{2K+1}(n/d) = \{1\}$ on account of $D^{2K+1}(d) \subseteq D^{2K+3}(d)$ for each d. Then $D^{2K+4}(n) \subseteq D^{2K+2}(n)$. But then, by the same reasoning, $D^{2K+3}(n) \subseteq D^{2K+5}(n)$.

To see that $D^\infty(n)$ is ordered according to the theorem, consider the statement $D^\infty(n) \subseteq D(n)$ for all n. Using the argument from above and the fact that $D^\infty(n) = \{d \in D(n) \mid D^\infty(d) \cap D^\infty(n/d) = \{1\}\}$, we conclude that, for all k, $D^{2k+1}(n) \subseteq D^\infty(n) \subseteq D^{2k}(n)$ and hence our relations hold. □

We observe that when looking at the k-ary divisors of the powers of a specific prime number, there is always an integer after which, for each a, the k-ary divisors of p^a will be either $D^2(p^a)$ or $D^1(p^a)$.

Theorem 3. *Let $k > 2$ be given. Then there is an integer N_k such that, for all $a > N_k$ and all primes p, $D^k(p^a) = D^1(p^a)$ if k is odd, and $D^k(p^a) = D^2(p^a)$ if k is even.*

Proof. We note first that, for $k = 1$ and $k = 2$, we have that $N_1 = 1$ and $N_2 = 3$ trivially suffice for bounds. Now assume that such an N_k exists for all $k = M - 1$. We consider the cases even M and odd M, respectively.

For even M, take $a > 2N_{M-1}$ and let $b \leqslant a/2$. Then $D^k(p^{a-b}) \cap D^k(p^b) = \{1\}$, since $D^k(p^{a-b}) = D^1(p^{a-b})$ and $b < a - b$. For $2b = a$, we have $p^b \notin D^M(p^a)$ as desired. Since k-ary divisions are symmetric, this argument holds for $b' = a - b$ as well. We see then that we may take $N_M = 2N_{M-1}$ for even M.

For odd M, take $a > 3N_{M-1}$. Let b be such that $0 \leqslant b \leqslant (2/3)a$. Then $D^{M-1}(p^{a-b}) \cap D^{M-1}(p^b) = \{1\}$ if $p^b \in D^{M-1}(p^{a-b})$. This occurs for all b and a satisfying $a \neq 3b$. If $a = 3b$, then $b > N_{M-1}$, so $D^k(p^b) = D^2(p^b)$. In either case, $D^{M-1}(p^{a-b}) \cap D^{M-1}(p^b) = \{1\}$, so that $D^{M-1}(p^a) = D^1(p^a)$. We then see that we may take $N_M > 3N_{M-1}$ for odd M. □

Definition 4. We denote by $N_k^\star$ the least N_k for a given k.

Our next section concerns itself with k-ary analogues of some classical results on summatory functions.

3. Summatory Functions

Let $k > 0$ be given and let $f(n)$ be an arithmetical function constructed as follows:

$$f(n) \coloneqq \sum_{d \in D^k(n)} g(d) \left(\frac{n}{d}\right)^r, \tag{4}$$

where r is a positive integer and $g(n)$ is a function such that $g(n) = \mathcal{O}(n^{r-1})$. We wish to explore the end behavior of the summatory function of f:

$$S(f)(x) \coloneqq \sum_{n \leqslant x} f(n) \tag{5}$$

We will employ techniques already used in [7, 8] to derive the result for the infinitary and unitary cases, respectively.

Definition 5. Let $k \geqslant 0$ and $r > 0$. We introduce the following function:

$$\varphi_{k,r}(x,n) \coloneqq \sum_{\substack{m \leqslant x \\ (m,n)_k = 1}} m^r. \tag{6}$$

For $r = 0$, this function counts the number of integers m that are less than x and k-ary coprime to n. It is known that, for $k = 0$, $\varphi_{0,0}(x,n) = x(\varphi(n)/n) + \mathcal{O}(\tau(n))$. The summatory functions for $\varphi_{k,0}$ may be broken into the case of even k or odd k, in accordance with whether $D^k(n) \subseteq D^\infty(n)$ or $D^\infty(n) \subseteq D^k(n)$.

Theorem 6. *Let $k > 0$ be an integer. Then, for even k, $\varphi_{k,0}(x, n) = x(\varphi(n)/n)K_k(n) + \mathcal{O}(\widetilde{\tau}_k(n)\tau(n))$, with*

$$K_k(n) = \prod_{p|n} \left(\sum_{\substack{b=0 \\ (p^b, p^{\nu_p(n)})_k = 1}}^{\infty} \frac{1}{p^b} \right) \tag{7}$$

and

$$\widetilde{\tau}_k(n) = \prod_{p|n} \left(\sum_{\substack{b=0 \\ (p^b, p^{\nu_p(n)})_k = 1}}^{\infty} 1 \right); \tag{8}$$

for odd k,

$$\varphi_{k,0}(x,n) = x\left(1 - \sum_{d \in D^1(n)} \frac{\varphi(d)\mu_1(d)}{d} K_k(d)\right) + \mathcal{O}\left(\widetilde{\tau}_k(n)\tau_1(n)\tau(n)\right), \tag{9}$$

with the following:

(i) *$\tau_1(n)$ is the number of elements (divisors) in $D^1(n)$.*

(ii) *$\mu_1(n)$ is the Möbius function corresponding to D^1: $\mu_1(n) = (-1)^{\omega(n)}$, where $\omega(n)$ is the number of distinct prime factors of n, counted without multiplicity.*

(iii)

$$K_k(n) = \prod_{p|n} \left(\sum_{\substack{b=0 \\ (p^b, p^{\nu_p(n)})_k > 1}} \frac{1}{p^b} \right). \tag{10}$$

(iv)

$$\widetilde{\tau}_k(n) = \prod_{p|n} \left(\sum_{\substack{b=0 \\ (p^b, p^{\nu_p(n)})_k > 1}} 1 \right). \tag{11}$$

Proof. First note that $K_k(n)$ and $\widetilde{\tau}_k(n)$ are well defined: by Theorem 3, for even k, the number of integers m satisfying the condition $(m,n)_k = 1$ for a given integer n must be finite, whereas for odd k and for each maximal prime power dividing n, the number of integers satisfying $(p^b, p^{\nu_p(n)})_k > 1$ must be finite, and hence the product over sums of prime powers k-ary-coprime to n must be finite. Therefore, the sums are finite. We will prove the result for even k first.

Let k be even and consider

$$\varphi_{k,0}(x,n) = \sum_{\substack{m \leqslant x \\ (m,n)_k = 1}} 1 = \sum_{\substack{m \leqslant x \\ m = m_1 m_2 \\ (m_1,n)=1 \\ (m_2,n)_k = 1 \\ \mathrm{core}(m_2)|n}} 1, \tag{12}$$

where

$$\mathrm{core}(m_2) \coloneqq \prod_{p|m_2} p \tag{13}$$

is the square-free part of the integer m_2, from [8]. Here we have split each m uniquely into a part that has no common divisor with n and a part whose prime decomposition uses only the primes of n (note that there is no restriction on the prime powers used; e.g., $m_2 = n^2$ may appear in this decomposition for large enough x).

We proceed:

$$\begin{aligned} \sum_{\substack{m \leqslant x \\ m = m_1 m_2 \\ (m_1,n)=1 \\ (m_2,n)_k = 1 \\ \mathrm{core}(m_2)|n}} 1 &= \sum_{\substack{m_2 : \mathrm{core}(m_2)|n \\ (m_2,n)_k = 1}} \sum_{\substack{m_1 \leqslant x/m_2 \\ (m_1,n)=1}} 1 \\ &= \sum_{\substack{m_2 : \mathrm{core}(m_2)|n \\ (m_2,n)_k = 1}} \varphi_{0,0}\left(\frac{x}{m_2}, n\right) \\ &= \sum_{\substack{m_2 : \mathrm{core}(m_2)|n \\ (m_2,n)_k = 1}} \left(x\frac{\varphi(n)}{n m_2} + \mathcal{O}(\tau(n)) \right), \end{aligned} \tag{14}$$

using the fact that the behavior of $\varphi_{0,0}(x,n)$ is known. Pulling out the constants with respect to the sum then immediately gives us our result.

For odd k, we proceed in a different manner:

$$\sum_{\substack{m\leqslant x\\(m,n)_k=1}} = [x] - \sum_{\substack{m\leqslant x\\(m,n)_k>1}} 1. \tag{15}$$

We then analyze the term

$$\sum_{\substack{m\leqslant x\\(m,n)_k>1}} 1 : \tag{16}$$

We wish to split m into m_1m_2 as before. However, this should be done in such a way as to be both unique and useful in dealing with the requirement that $(m,n)_k > 1$. For each divisor d of n, let $m = m_1m_2$, with $\text{core}(m_2) \mid d \mid n$, $(m_1,n) = 1$, and $(m_2, p^{\nu_p(d)})_k > 1$ for each $p \mid d$. We invoke the principle of inclusion-exclusion, enabling us to write

$$\begin{aligned}
\sum_{\substack{m\leqslant x\\(m,n)_k>1}} &= \sum_{\substack{m\leqslant x\\m=m_1m_2\\(m_1,p_1^{\nu_{p_1}(n)})=1\\\text{core}(m_2)\mid p_1^{\nu_{p_1}(n)}\\(m_2,p_1^{\nu_{p_1}(n)})_k>1}} 1 + \sum_{\substack{m\leqslant x\\m=m_1m_2\\(m_1,p_2^{\nu_{p_2}(n)})=1\\\text{core}(m_2)\mid p_2^{\nu_{p_2}(n)}\\(m_2,p_2^{\nu_{p_2}(n)})_k>1}} 1 + \cdots \\
&+ \sum_{\substack{m\leqslant x\\m=m_1m_2\\(m_1,p_s^{\nu_{p_s}(n)})=1\\\text{core}(m_2)\mid p_s^{\nu_{p_s}(n)}\\(m_2,p_s^{\nu_{p_s}(n)})_k>1}} 1 - \left(\sum_{\substack{m\leqslant x\\m=m_1m_2\\(m_1,p_1^{\nu_{p_1}(n)}p_2^{\nu_{p_2}(n)})=1\\\text{core}(m_2)\mid p_1^{\nu_{p_1}(n)}p_2^{\nu_{p_2}(n)}\\(m_2,p_1^{\nu_{p_1}(n)})_k>1\\(m_2,p_2^{\nu_{p_2}(n)})_k>1}} 1 \right. \\
&+ \sum_{\substack{m\leqslant x\\m=m_1m_2\\(m_1,p_1^{\nu_{p_1}(n)}p_3^{\nu_{p_3}(n)})=1\\\text{core}(m_2)\mid p_1^{\nu_{p_1}(n)}p_3^{\nu_{p_3}(n)}\\(m_2,p_1^{\nu_{p_1}(n)})_k>1\\(m_2,p_3^{\nu_{p_3}(n)})_k>1}} 1 + \cdots \\
&\left. + \sum_{\substack{m\leqslant x\\m=m_1m_2\\(m_1,p_{s-1}^{\nu_{p_{s-1}}(n)}p_s^{\nu_{p_s}(n)})=1\\\text{core}(m_2)\mid p_{s-1}^{\nu_{p_{s-1}}(n)}p_s^{\nu_{p_s}(n)}\\(m_2,p_{s-1}^{\nu_{p_{s-1}}(n)})_k>1\\(m_2,p_s^{\nu_{p_s}(n)})_k>1}} 1 \right) + \cdots + (-1)^s \\
&\cdot \left(\sum_{\substack{m\leqslant x\\m=m_1m_2\\(m_1,n)=1\\\text{core}(m_2)\mid n\\(m_2,p_1^{\nu_{p_1}(n)})_k>1\\(m_2,p_2^{\nu_{p_2}(n)})_k>1\\\vdots\\(m_2,p_s^{\nu_{p_s}(n)})_k>1}} 1 \right),
\end{aligned} \tag{17}$$

where

$$n = \prod_{l=1}^{s} p_l^{\nu_{p_l}(n)}, \tag{18}$$

with p_l being an appropriately indexed set of primes, and we use the fact that, for d = 1, the sum is 0.

This simplifies to

$$\begin{aligned}
&- \sum_{d\in D^1(n)} \mu_1(d) \sum_{\substack{m_2:\text{core}(m_2)\mid d\\\forall p\mid d,(m_2,p^{\nu_p(d)})_k>1}} \sum_{\substack{m_1\leqslant x/m_2\\(m_1,d)=1}} 1 \\
&= - \sum_{d\in D^1(n)} \mu_1(d) \sum_{\substack{m_2:\text{core}(m_2)\mid d\\\forall p\mid d,(m_2,p^{\nu_p(d)})_k>1}} \varphi_{0,0}\left(\frac{x}{m_2}, d\right) == \\
&- \sum_{d\in D^1(n)} \mu_1(d) \\
&\cdot \sum_{\substack{m_2:\text{core}(m_2)\mid d\\\forall p\mid d,(m_2,p^{\nu_p(d)})_k>1}} \left(x\frac{\varphi(d)}{dm_2} + \mathcal{O}(\tau(d)) \right) == \\
&- x \sum_{d\in D^1(n)} \mu_1(d) \frac{\varphi(d)}{d} \sum_{\substack{m_2:\text{core}(m_2)\mid d\\\forall p\mid d,(m_2,p^{\nu_p(d)})_k>1}} \frac{1}{m_2} \\
&+ \mathcal{O}\left(\sum_{d\in D^1(n)} \mu_1(d)\tau(d)\frac{\varphi(d)}{d} \right. \\
&\left. \cdot \sum_{\substack{m_2:\text{core}(m_2)\mid d\\\forall p\mid d,(m_2,p^{\nu_p(d)})_k>1}} 1 \right) == \\
&- \sum_{d\in D^1(n)} \frac{\varphi(d)\mu_1(d)}{d} K_k(d) + \mathcal{O}\left(\widetilde{\tau}_k(n)\tau_1(n)\tau(n)\right),
\end{aligned} \tag{19}$$

and our result follows. □

We let $L_k(n)$ be the coefficient appearing in front of the "x" term in $\varphi_{k,0}(x,n)$ and let $E_k(n)$ be the function in the error term, so that $\varphi_{k,0}(x,n) = xL_k(n) + \mathcal{O}(E(n))$.

Remark 7. Regarding the function $\widetilde{\tau}_k(n)$, we may estimate that $\widetilde{\tau}_k(n) \leqslant N_k^\star$ through the following reasoning: for even k, consider $a \leqslant N_k^\star$ (see Definition 4). If $b \leqslant N_k^\star$, then $(p^b, p^a)_k = 1$ for at most $N_k^\star - 1$ such b (excluding $b = a$). If $b > N_k^\star$, then $(p^b, p^a)_k = 1$ for at most 1 such b (the case of $D^k(p^a) = \{1, p^a\}$ and $b = 2a > N_k^\star$, as here $D^k(p^b) = D^2(p^b)$). Thus, $\widetilde{\tau}_k(p^a) \leqslant N_k^\star$ for $a \leqslant N_k^\star$. For $a > N_k^\star$, $D^k(p^a) = D^2(p^a)$, and so $(p^b, p^a)_k = 1$ for at most 2 such b by the above comments.

For odd k, a similar argument gives $(p^b, p^a)_k > 1$ for at most $N_k^\star$ choices of b when $a \leqslant N_k^\star$, and precisely 2 choices of b when $a > N_k^\star$; namely, $b = 0$ and $b = a$. So $N_k^\star$ bounds $\widetilde{\tau}_k(p^a)$ for all a.

Now, $\tau_k(p) = 2$ for all k, and for some $B_k \leqslant N_k^\star$, $2^{B_k} \geqslant N_k^\star \geqslant \widetilde{\tau}_k(n)$. Thus, since $\tau_k(p^a) \geqslant 2$ for all $a > 0$, we have that $\tau_k(n)^{B_k} \geqslant \widetilde{\tau}_k(n)$. In particular, there is a least B_k such that, for all n, $\tau_k(n)^{B_k} \geqslant \widetilde{\tau}_k(n)$. We will use this B_k in our asymptotic estimates.

We immediately get the following result as a consequence of Theorem 6.

Corollary 8. *$\varphi_{k,r}(x,n) = (x^r/(r+1))\varphi_{k,0}(x,n)$ for $r \in \mathbb{N}$.*

Proof. The case $r = 0$ is trivially true. We prove for each $r > 0$ using Stieltjes Integration. Then

$$\begin{aligned}
&\left(\sum_{\substack{m\leqslant x\\(m,n)_k=1}} m^r\right) + \mathcal{O}\left(x^r\right)\\
&= r\int_0^x \left(\sum_{\substack{m\leqslant y\\(m,n)_k=1}} m^{r-1}\right) dy\\
&= r\int_0^x \left(y^r \frac{\varphi(n)}{n} K_k(n) + \mathcal{O}\left(y^{r-1}E_k(n)\right)\right) dy\\
&= \frac{x^{r+1}}{r+1}\frac{\varphi(n)}{n}K_k(n) + \mathcal{O}\left(x^r E_k(n)\right)\\
&= \frac{x^r}{r+1}\varphi_{k,0}(x,n),
\end{aligned} \tag{20}$$

where the error term from the integral is absorbed by $\mathcal{O}(x^r E_k(n))$. □

Theorem 9. *Let $k \geqslant 0$. Suppose that an arithmetical function f is of the form*

$$f(n) = \sum_{d|_k n} g(d)\left(\frac{n}{d}\right)^r, \tag{21}$$

with $k > 0$ and $r \in \mathbb{N}$ and $g(n)$ is $\mathcal{O}(n^s)$, with $s \leqslant r-1$. Then

$$\sum_{n\leqslant x} f(n) = \frac{x^{r+1}}{r+1}\sum_{n=1}^{\infty}\frac{g(n)L_k(n)}{n^{r+1}} + \mathcal{O}\left(x^r(\log x)^{B_k+2}\right) \tag{22}$$

Proof. Let k, r, and s be given. Then

$$\begin{aligned}
\sum_{n\leqslant x} f(n) &= \sum_{n\leqslant x}\sum_{d|_{k+1}n} g(d)\left(\frac{n}{d}\right)^r\\
&= \sum_{n\leqslant x}\sum_{\substack{dd'=n\\(d,d')_k=1}} g(d)\left(\frac{n}{d}\right)^r\\
&= \sum_{\substack{dd'\leqslant x\\(d,d')_k=1}} g(d)\left(\frac{n}{d}\right)^r\\
&== \sum_{d\leqslant x} g(d)\sum_{\substack{d'\leqslant x/d\\(d,d')_k=1}}\left(d'\right)^r\\
&= \sum_{d\leqslant x} g(d)\,\varphi_{k,r}\left(\frac{x}{d},d\right)\\
&= \sum_{d\leqslant x} g(d)\,\varphi_{k,r}\left(\frac{x}{d},d\right)\\
&== \frac{x^{r+1}}{r+1}\sum_{d\leqslant x}\frac{g(d)L_k(d)}{d^{r+1}}\\
&\quad + \mathcal{O}\left(\sum_{d\leqslant x} x^r g(d)\frac{E_k(d)}{d^r}\right).
\end{aligned} \tag{23}$$

By our remark above, we may find B_k such that $\widetilde{\tau}_k(n) \leqslant (\tau_k(n))^{B_k}$ for all n, which enables us to estimate

$$\begin{aligned}
\mathcal{O}\left(x^r\sum_{n\leqslant x}\frac{g(n)E_k(n)}{n^r}\right) &\leqslant \mathcal{O}\left(x^r\sum_{n\leqslant x}\frac{(\tau(n))^{B_k+2}}{n}\right)\\
&= \mathcal{O}\left(x^r(\log x)^{B_k+2}\right),
\end{aligned} \tag{24}$$

where we use the fact that g is $\mathcal{O}(n^s)$ with $s \leqslant r-1$. Also,

$$\begin{aligned}
\frac{x^{r+1}}{r+1}\sum_{n\leqslant x}\frac{g(n)L_k(n)}{n^{r+1}} &= \frac{x^{r+1}}{r+1}\sum_{n=1}^{\infty}\frac{g(n)L_k(n)}{n^{r+1}}\\
&\quad - \frac{x^{r+1}}{r+1}\sum_{n>x}\frac{g(n)L_k(n)}{n^{r+1}},
\end{aligned} \tag{25}$$

and since g is $\mathcal{O}(n^s)$ and $L_k(n)$ is bounded, the infinite sums converge, but

$$\frac{x^{r+1}}{r+1}\sum_{n>x}\frac{g(n)L_k(n)}{n^{r+1}} = \mathcal{O}\left(x^{s+1}\right), \tag{26}$$

and $s < r$, so this is absorbed into our error term and we have our result. □

Note that, for each k and for all $\epsilon > 0$, we may state our error term for the summatory function as $\mathcal{O}(x^{r+\epsilon})$, where the multiplicative constant implied by the Big-Oh notation depends only on ϵ and k. This enables us to achieve roughly the same error as Cohen [7], albeit not as asymptotically strong as $x^r(\log x)^{B_k}$. However, as k tends to infinity, our error becomes unbounded, and so we cannot achieve Cohen's result for the infinitary case.

We recall that μ_k, the k-ary analogue of the Möbius function, is defined recursively via

$$\begin{aligned} \mu_k\left(p^0\right) &= 1, \\ \sum_{p^b \mid_k p^a} \mu_k\left(p^b\right) &= 0, \end{aligned} \tag{27}$$

which is extended to all n by making μ_k multiplicative. We then have the following.

Lemma 10. *Let k be given. Then there is a constant C_k depending only on k such that, for each k, $|\mu_k(n)| \leqslant \tau(n)^{C_k}$.*

Proof. By Theorem 3, for each prime p and each k, there is an $N_k^\star$ that ensures $D^k(p^a) = D^1(p^a)$ or $D^2(p^a)$, depending on the parity of k, for all $a > N_k^\star$. The values of $|\mu_k(p^a)|$ for $a \leqslant 2N_k^\star$ are finite, being generated from a finite recursion. For odd k with $a > N_k^\star$, $\mu_k(p^a) = -1$. For even k and even a, with $a > 2N_k^\star + 1$,

$$\begin{aligned} -\mu_k\left(p^a\right) &= \sum_{\substack{p^b \mid_k p^a \\ b \neq a}} \mu_k\left(p^b\right) \\ &= \sum_{p^b \mid_k p^{a-1}} \mu_k\left(p^b\right) - \mu_k\left(p^{a/2}\right), \end{aligned} \tag{28}$$

since $D^k(p^a) = D^2(p^a)$ and $D^k(p^{a-1}) = D^2(p^{a-1}) = D(p^{a-1})$, as $a - 1$ is odd. But

$$\sum_{p^b \mid_k p^{a-1}} \mu_k\left(p^b\right) = 0, \tag{29}$$

so $\mu_k(p^a) = \mu_k(p^{a/2})$. Also,

$$\begin{aligned} -\mu_k\left(p^{a+1}\right) &= \sum_{\substack{p^b \mid_k p^{a+1} \\ b \neq a+1}} \mu_k\left(p^b\right) \\ &= \sum_{p^b \mid_k p^a} \mu_k\left(p^b\right) + \mu_k\left(p^{a/2}\right) = \mu_k\left(p^{a/2}\right), \end{aligned} \tag{30}$$

so

$$\mu_k\left(p^a\right) = \mu_k\left(p^{a/2}\right) = -\mu_k\left(p^{a+1}\right) \tag{31}$$

for even a. Hence, $\mu_k(p^a)$ is bounded in absolute value for each k—call this bound 2^{C_k}—and so $|\mu_k(n)| \leqslant 2^{C_k\omega(n)} = \tau_1(n)^{C_k} \leqslant \tau(n)^{C_k}$ and we are done. □

We will analyze the summatory functions for the k-ary analogues of several well-known families of arithmetical functions:

(i) The k-ary divisor sum functions:

$$\sigma_{k,r}(n) \coloneqq \sum_{d \mid_k n} d^r \tag{32}$$

(ii) The k-ary Jordan totient functions:

$$J_{k,r}(n) \coloneqq \sum_{d \mid_k n} \mu_k\left(\frac{n}{d}\right) d^r \tag{33}$$

(iii) The k-ary Dedekind functions:

$$\psi_{k,r}(n) \coloneqq \sum_{d \mid_k n} \left|\mu_k\left(\frac{n}{d}\right)\right| d^r \tag{34}$$

Here r denotes a positive integer. By Lemma 10, we may apply Theorem 9 to the Jordan and Dedekind functions of order $r > 0$ without issue, since $\mu_k(n)$ is logarithmic in n; the summatory functions for the divisor sum functions carry no special restriction on r aside from it being a positive integer:

(i)

$$S\left(\sigma_{k,r}\right)(x) = \frac{x^{r+1}}{r+1} \sum_{n=1}^{\infty} \frac{L_k(n)}{n^{r+1}} + \mathcal{O}\left(x^r (\log x)^{B_k}\right) \tag{35}$$

(ii)

$$\begin{aligned} S\left(J_{k,r}\right)(x) = \frac{x^{r+1}}{r+1} \sum_{n=1}^{\infty} \frac{\mu_k(n) L_k(n)}{n^{r+1}} \\ + \mathcal{O}\left(x^r (\log x)^{B_k}\right) \end{aligned} \tag{36}$$

(iii)

$$\begin{aligned} S\left(\psi_{k,r}\right)(x) = \frac{x^{r+1}}{r+1} \sum_{n=1}^{\infty} \frac{\left|\mu_k(n)\right| L_k(n)}{n^{r+1}} \\ + \mathcal{O}\left(x^r (\log x)^{B_k}\right) \end{aligned} \tag{37}$$

By Theorems 2 and 3, for each n, the sequence $\{L_{2k}(n)\}_{k=0}^{\infty}$ (resp., $\{L_{2k+1}(n)\}_{k=0}^{\infty}$) is monotonically increasing (resp., decreasing). Both sequences must have the same limit, $L_\infty(n)$, which one can identify with the function $K_\infty(n)$ from Cohen's manuscript. However, we cannot obtain the function $\varphi_{\infty,0}(x,n)$ via a limit as k tends to infinity of $\varphi_{k,0}(x,n)$, as the error term grows without bound in k. A new approach will likely be needed in order to unify the infinite case with the finite cases.

Conflicts of Interest

The authors declare that they have no conflicts of interest.

Acknowledgments

The authors would like to acknowledge the Department of Mathematical Sciences at The University of Texas at Dallas for providing them with funding for this endeavor. They would also like to thank Dr. Paul Stanford for his numerous revisions and for inspiring and teaching them all.

References

[1] P. Haukkanen, "Basic properties of the bi-unitary convolution and the semi-unitary convolution," *Indian Journal of Mathematics*, vol. 40, no. 3, pp. 305–315, 1998.

[2] P. Haukkanen, "On the *k*-ary Convolution of Arithmetical Functions," *The Fibonacci Quarterly*, vol. 38, no. 5, pp. 440–445, 2000.

[3] G. L. Cohen, "On an integer's infinitary divisors," *Mathematics of Computation*, vol. 54, no. 189, pp. 395–411, 1990.

[4] R. Steuding, J. Steuding, and L. Tóth, "A modified Möbius μ-function. Rendiconti del Circolo Matematico di Palermo," *Rendiconti del Circolo Matematico di Palermo Serie II*, vol. 60, no. 1-2, pp. 13–21, 2011.

[5] D. Suryanarayana, "The number of *k*-ary divisors of an integer," *Monatshefte für Mathematik*, vol. 72, pp. 445–450, 1968.

[6] W. Narkiewicz, "On a class of arithmetical convolutions," *Colloquium Mathematicum*, vol. 10, pp. 81–94, 1963.

[7] G. L. Cohen and J. Hagis, "Arithmetic functions associated with the infinitary divisors of an integer," *International Journal of Mathematics and Mathematical Sciences*, vol. 16, no. 2, pp. 373–383, 1993.

[8] E. Cohen, "Arithmetical functions associated with the unitary divisors of an integer," *Mathematische Zeitschrift*, vol. 74, pp. 66–80, 1960.

The Multiresolving Sets of Graphs with Prescribed Multisimilar Equivalence Classes

Varanoot Khemmani and Supachoke Isariyapalakul

Department of Mathematics, Srinakharinwirot University, Sukhumvit 23, Bangkok 10110, Thailand

Correspondence should be addressed to Supachoke Isariyapalakul; supachoke.isa@g.swu.ac.th

Academic Editor: Dalibor Froncek

For a set $W = \{w_1, w_2, \ldots, w_k\}$ of vertices and a vertex v of a connected graph G, the multirepresentation of v with respect to W is the k-multiset $mr(v \mid W) = \{d(v, w_1), d(v, w_2), \ldots, d(v, w_k)\}$, where $d(v, w_i)$ is the distance between the vertices v and w_i for $i = 1, 2, \ldots, k$. The set W is a multiresolving set of G if every two distinct vertices of G have distinct multirepresentations with respect to W. The minimum cardinality of a multiresolving set of G is the multidimension $\dim_M(G)$ of G. It is shown that, for every pair k, n of integers with $k \geq 3$ and $n \geq 3(k-1)$, there is a connected graph G of order n with $\dim_M(G) = k$. For a multiset $\{a_1, a_2, \ldots, a_k\}$ and an integer c, we define $\{a_1, a_2, \ldots, a_k\} + \{c, c, \ldots, c\} = \{a_1 + c, a_2 + c, \ldots, a_k + c\}$. A multisimilar equivalence relation R_W on $V(G)$ with respect to W is defined by $u \, R_W \, v$ if $mr(u \mid W) = mr(v \mid W) + \{c_W(u, v), c_W(u, v), \ldots, c_W(u, v)\}$ for some integer $c_W(u, v)$. We study the relationship between the elements in multirepresentations of vertices that belong to the same multisimilar equivalence class and also establish the upper bound for the cardinality of a multisimilar equivalence class. Moreover, a multiresolving set with prescribed multisimilar equivalence classes is presented.

1. Introduction

The *distance* $d(u, v)$ between two vertices u and v in a connected graph G is the length of a shortest $u - v$ path in G. For an ordered set $W = \{w_1, w_2, \ldots, w_k\} \subseteq V(G)$ and a vertex v of G, the k-vector

$$r(v \mid W) = \left(d(v, w_1), d(v, w_2), \ldots, d(v, w_k)\right) \quad (1)$$

is referred to as the *representation of v with respect to W*. The ordered set W is called a *resolving set* of G if every two distinct vertices of G have distinct representations with respect to W. A resolving set of a minimum cardinality is called a *minimum resolving set* or a *basis* of G and this cardinality is the *dimension* $\dim(G)$ of G.

To illustrate these concepts, consider a connected graph G of Figure 1 with $V(G) = \{u, v, w, x, y, z\}$. Considering the ordered set $W_1 = \{w, z\}$, there are six representations of the vertices of G with respect to W_1:

$$\begin{aligned} r(u \mid W_1) &= (2, 3), \\ r(v \mid W_1) &= (3, 2), \\ r(w \mid W_1) &= (0, 3), \\ r(x \mid W_1) &= (1, 2), \\ r(y \mid W_1) &= (2, 1), \\ r(z \mid W_1) &= (3, 0). \end{aligned} \quad (2)$$

Since there is no 1-element resolving set of G, it follows that W_1 is a basis of G, and so $\dim(G) = 2$.

The concepts of resolving sets and minimum resolving sets have previously appeared in [1–4]. Slater in [3, 4] introduced these ideas and used a *locating set* for what we

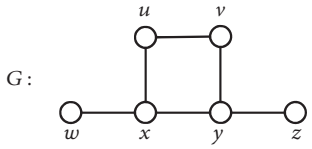

Figure 1: A connected graph G.

have called a resolving set. He referred to the cardinality of a minimum resolving set in a connected graph as its *locating number*. He described the usefulness of these ideas when working with US sonar and coast guard LORAN (long range aids to navigation) stations. Harary and Melter [2] discovered these concepts independently as well but used the term *metric dimension* rather than locating number, the terminology that we have adopted. These concepts were rediscovered by Johnson [5] of the Pharmacia Company while attempting to develop a capability of large datasets of chemical graphs. More applications of these concepts to navigation of robots in networks and other areas are discussed in [6–9].

A *multiset* is a generalization of the concept of a set, which is like a set except that its members need not to be distinct. For example, the set $\{1, 1, 2\}$ is the same as the set $\{1, 2\}$ but not so for the multiset. The multiset $M = \{5, 5, 6, a, a, a, a, b, b, b\}$ has 10 elements of 4 different types: 2 of type 5, 1 of type 6, 4 of type a, and 3 of type b. So, the multiset is usually indicated by specifying the number of times different types of elements occur in it. Therefore, the multiset M can be written by $M = \{2 \cdot 5, 1 \cdot 6, 4 \cdot a, 3 \cdot b\}$. The numbers 2, 1, 4, and 3 are called the *repetition numbers* of the multiset M. In particular, a set is a multiset having all repetition numbers equal to 1.

As described in [1], all connected graphs G contain an ordered set W such that each vertex of G is distinguished by a k-vector, known as a representation, consisting of its distance from the vertices in W. It may also occur that some graph contains a set W' with property that the vertices of graph have uniquely distinct k-multisets containing their distances from each of the vertices in W'. The goal of this paper is to study the existence of such a set of connected graphs.

For a set $W = \{w_1, w_2, \ldots, w_k\}$ of vertices and a vertex v of a connected graph G, we refer to the k-multiset

$$mr(v \mid W) = \{d(v, w_1), d(v, w_2), \ldots, d(v, w_k)\} \quad (3)$$

as the *multirepresentation of v with respect to W*. The set W is called a *multiresolving set* of G if every two distinct vertices have distinct multirepresentations with respect to W. A multiresolving set of a minimum cardinality is called a *minimum multiresolving set* or a *multibasis* of G and this cardinality is the *multidimension* $\dim_M(G)$ of G.

For example, consider a connected graph G of Figure 1. As we know $W_1 = \{w, z\}$ is a basis of G. However, W_1 is not a multiresolving set of G since $mr(u \mid W_1) = \{2, 3\} = mr(v \mid W_1)$. In fact, the set $W_2 = \{w, x, z\}$ is a multiresolving set of G with the following multirepresentations of the vertices of G with respect to W_2:

$$\begin{aligned} mr(u \mid W_2) &= \{1, 2, 3\}, \\ mr(v \mid W_2) &= \{2, 2, 3\}, \\ mr(w \mid W_2) &= \{0, 1, 3\}, \\ mr(x \mid W_2) &= \{0, 1, 2\}, \\ mr(y \mid W_2) &= \{1, 1, 2\}, \\ mr(z \mid W_2) &= \{0, 2, 3\}. \end{aligned} \quad (4)$$

It is routine to verify that there are no 1-element and 2-element multiresolving sets of G. Hence, W_2 is a multibasis of G, and so $\dim_M(G) = 3$.

Not all connected graphs have a multiresolving set and also $\dim_M(G)$ is not defined for all connected graphs G. For example, the complete graph K_3 has no multiresolving set. Thus, $\dim_M(K_3)$ is not defined. However, if G is a connected graph of order n, for which $\dim_M(G)$ is defined, and then every multiresolving set of G is a resolving set of G, and so

$$1 \leq \dim(G) \leq \dim_M(G) \leq n. \quad (5)$$

For every set W of vertices of a connected graph G, the vertices of G whose multirepresentations with respect to W contain 0 are vertices in W. On the other hand, the multirepresentations of vertices of G which do not belong to W have elements, all of which are positive. In fact, to determine whether a set W is a multiresolving set of G, the vertex set $V(G)$ can be partitioned into W and $V(G) - W$ to examine whether the vertices in each subset have distinct multirepresentations with respect to W.

The multiresolving set of a connected graph was introduced by Saenpholphat [10] who showed that there is no connected graph G such that $\dim_M(G) = 2$. Moreover, the multidimensions of complete graphs, paths, cycles, and bipartite graphs were determined. Simanjuntak, Vetrík, and Mulia [11] discovered this concept independently and used a notation $md(G)$ for a multidimension of a connected graph G.

2. The Multidimension of a Connected Graph

Two vertices u and v of a connected graph G are *distance-similar* if $d(u, x) = d(v, x)$ for all $x \in V(G) - \{u, v\}$. Certainly, distance similarity in G is an equivalence relation on $V(G)$. For example, consider a complete bipartite graph $K_{r,s}$ with partite sets U and V. Every pair of vertices in the same partite set are distance-similar. Then the distance-similar equivalence classes in $K_{r,s}$ are its partite sets U and V. The following results were obtained in [10] showing the usefulness of the distance-similar equivalence class to determine the multidimensions of connected graphs.

Theorem 1 (see [10]). *Let G be a connected graph such that $\dim_M(G)$ is defined. If U is a distance-similar equivalence class in G with $|U| = 2$, then every multiresolving set of G contains exactly one vertex of U.*

Theorem 2 (see [10]). *If U is a distance-similar equivalence class in a connected graph G with $|U| \geq 3$, then $\dim_M(G)$ is not defined.*

It was shown in [10, 11] that a path is the only one of connected graphs with multidimension 1, and any multiresolving sets of a connected graph cannot contain only two vertices. We state these results in the following theorems.

Theorem 3 (see [10, 11]). *Let G be a connected graph. Then $\dim_M(G) = 1$ if and only if $G = P_n$, the path of order n.*

Theorem 4 (see [10, 11]). *A connected graph has no multiresolving set of cardinality* 2.

Last, we are able to determine all pairs k, n of positive integers with $k \geq 3$ and $n \geq 3(k-1)$ which are realizable as the multidimension and the order of some connected graph. In order to do this, we present an additional notation. For integers a and b, let $[a, b]$ be a multiset such that

$$[a,b] = \begin{cases} \{a, a+1, \ldots, b-1, b\} & \text{if } a < b \\ \{a\} & \text{if } a = b \\ \emptyset & \text{if } a > b. \end{cases} \quad (6)$$

Such a multiset is referred to as a *consecutive multiset* of integers a and b.

Theorem 5. *For every pair k, n of integers with $k \geq 3$ and $n \geq 3(k-1)$, there is a connected graph G of order n with $\dim_M(G) = k$.*

Proof. Let k and n be integers with $k \geq 3$ and $n \geq 3(k-1)$. We consider two cases.

Case 1 ($n = 3(k-1)$). Let G be a graph obtained from the path $P_{k-1} = (u_1, u_2, \ldots, u_{k-1})$ by adding the $2(k-1)$ vertices v_i and w_i for $1 \leq i \leq k-1$ and joining v_i and w_i to u_i, as it is shown in Figure 2. Then the order of G is $n = 3(k-1)$. First, we claim that there is no multiresolving set of G with cardinality at most $k-1$. Assume, to the contrary, that there is a multiresolving set S of G such that $|S| \leq k-1$. Since a set $V_i = \{v_i, w_i\}$ for $1 \leq i \leq k-1$ is a distance-similar equivalence class in G, it follows by Theorem 1 that S contains exactly one vertex of V_i. Without loss of generality, let $w_i \in S$ for $1 \leq i \leq k-1$. Thus, $|S| = k-1$. Since $d(w_1, w_i) = d(w_{k-1}, w_{k-i})$ for all $1 \leq i \leq k-1$, it follows that $mr(w_1 \mid S) = mr(w_{k-1} \mid S)$ and so a set $S = \{w_1, w_2, \ldots, w_{k-1}\}$ is not a multiresolving set of G, thereby producing a contradiction. Hence, $\dim_M(G) \geq k$. Next, we claim that a set $W = \{w_1, w_2, \ldots, w_{k-1}\} \cup \{u_1\}$ is a multiresolving set of G. For a vertex $x \in W$, the multirepresentation of x with respect to W is

$$mr(x \mid W) = \begin{cases} \{0, i\} \cup [3, i+1] \cup [3, k-i+1] & \text{if } x = w_i \ (1 \leq i \leq k-1) \\ [0, k-1] & \text{if } x = u_1. \end{cases} \quad (7)$$

For $2 \leq i \leq k-1$, the multirepresentation of u_i with respect to W is

$$mr(u_i \mid W) = \{1, i-1\} \cup [2, i] \cup [2, k-i]. \quad (8)$$

For $1 \leq i \leq k-1$, the multirepresentation of v_i with respect to W is

$$mr(v_i \mid W) = \{2, i\} \cup [3, i+1] \cup [3, k-i+1]. \quad (9)$$

Therefore, W is a multiresolving set of G with $|W| = k$. Hence, $\dim_M(G) = k$.

Case 2 ($n > 3(k-1)$). Let H be a graph obtained from the graph G in Case 1 by adding the path $P = (x_1, x_2, \ldots, x_{n-3(k-1)})$ and joining x_1 to v_{k-1} and w_{k-1}, as it is shown in Figure 3. By a similar argument to the one used in Case 1, it is shown that there is no l−multiresolving set of H with $1 \leq l \leq k-1$. We claim that a set $W = \{w_1, w_2, \ldots, w_{k-1}\} \cup \{u_1\}$ is a multiresolving set of H. For vertices in $V(H) - \{x_1, x_2, \ldots, x_{n-3(k-1)}\}$, their multirepresentations with respect to W are the same as in Case 1. For $1 \leq i \leq n-3(k-1)$, the multirepresentation of x_i with respect to W is

$$mr(x_i \mid W) = \{i, i+k-1\} \cup [i+3, i+k]. \quad (10)$$

Hence, W is a multiresolving set of H with $|W| = k$, and so $\dim_M(H) = k$. □

3. Multisimilar Equivalence Relation

In this section, we investigate another equivalence relation on a vertex set of a connected graph. First, we need some additional definitions and notations. Let $A = \{\{a_1, a_2, \ldots, a_k\} \mid a_i \in \mathbb{Z} \text{ for } 1 \leq i \leq k\}$ be a collection of multisets. For an integer c, we define

$$\{a_1, a_2, \ldots, a_k\} + \{c, c, \ldots, c\} = \{a_1 + c, a_2 + c, \ldots, a_k + c\}, \quad (11)$$

where $\{a_1, a_2, \ldots, a_k\} \in A$. Let W be a set of vertices of a connected graph G and let u and v be vertices of G. A *multisimilar relation* R_W with respect to W on a vertex set $V(G)$ is defined by $u R_W v$ if there is an integer $c_W(u, v)$ such that

$$mr(u \mid W) = mr(v \mid W) + \{c_W(u,v), c_W(u,v), \ldots, c_W(u,v)\}. \quad (12)$$

An integer $c_W(u, v)$ satisfying (12) is called a *multisimilar constant of $u R_W v$* or simply a *multisimilar constant*. Clearly, R_W is an equivalence relation on $V(G)$. For each vertex u in $V(G)$, let $[u]_W$ denote the multisimilar equivalence class of u with respect to W. Then

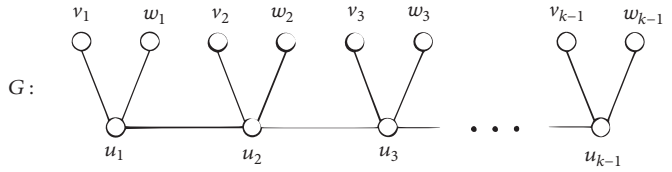

Figure 2: A connected graph G in Case 1.

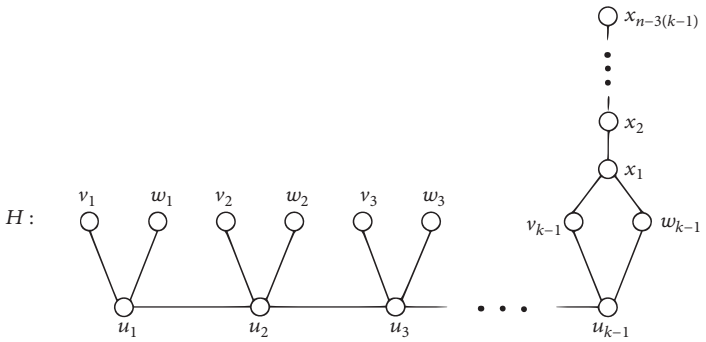

Figure 3: A connected graph H in Case 2.

$$x \in [u]_W \quad \text{if and only if } mr(x \mid W) = mr(u \mid W) + \{c_W(x,u), c_W(x,u), \ldots, c_W(x,u)\}, \tag{13}$$

where $c_W(x,u)$ is a multisimilar constant. Observe that if $x \in [u]_W$, then there is a multisimilar constant $c_W(x,u)$ with a property that, for every vertex $w \in W$, there is a corresponding vertex $w' \in W$ such that

$$d(x,w) = d(u,w') + c_W(x,u). \tag{14}$$

With this observation, we may as well say that $x \in [u]_W$ if and only if there are multisimilar constant $c_W(x,u)$ and a bijective function f on W defined as

$$f(w) = w' \quad \text{whenever } d(x,w) = d(u,w') + c_W(x,u). \tag{15}$$

The function f is called a *multisimilar function of* $x\ R_W\ u$ or a *multisimilar function* if there is no ambiguity. Consequently, it is not surprising that an inverse function f^{-1} is also multisimilar function of $v\ R_W\ u$ with a multisimilar constant $c_W(v,u) = -c_W(u,v)$.

To illustrate these concepts, consider a vertex u in a connected graph G of Figure 1 and the set $W = \{w, y, z\}$. There is only one vertex x in $V(G) - \{u\}$ such that x is related to u by a multisimilar relation R_W with a multisimilar constant $c_W(x,u) = -1$; that is,

$$mr(x \mid W) = mr(u \mid W) + \{-1, -1, -1\}. \tag{16}$$

Therefore, $[u]_W = \{u, x\}$. Thus, a multisimilar function f of $x\ R_W\ u$ is defined by

$$f(w) = y, \quad f(y) = w \quad \text{and } f(z) = z. \tag{17}$$

Moreover, there is another multisimilar function f' of $x\ R_W\ u$; that is,

$$f'(w) = w, \quad f'(y) = y \quad \text{and } f'(z) = z. \tag{18}$$

The example just described shows an important point that the multisimilar function of any two vertices in the same multisimilar equivalence class with respect to a set W is not necessarily unique.

More generally, for a vertex u and a set W of vertices of a connected graph G, let $mr(u \mid W) = \{r_1 \cdot a_1, r_2 \cdot a_2, \ldots, r_l \cdot a_l\}$, where $a_1 < a_2 < \cdots < a_l$ and r_i is a repetition number of type a_i for each i with $1 \le i \le l$. If $u \in [v]_W$, where $v \in V(G)$, then it follows by (13) and (14) that, for each type of $mr(u \mid W)$, there is a corresponding type of $mr(v \mid W)$ such that their repetition numbers are equal. Therefore, we may assume that $mr(v \mid W) = \{r_1 \cdot b_1, r_2 \cdot b_2, \ldots, r_l \cdot b_l\}$, where $b_1 < b_2 < \cdots < b_l$. For each integer i with $1 \le i \le l$, let $A_i = \{w \in W \mid d(u,w) =$

$a_i\}$ and $B_i = \{w \in W \mid d(v,w) = b_i\}$. Then the types of $mr(u \mid W)$ partition W into l sets $A_1, A_2, \ldots, A_l$. On the other hand, W is also partitioned into l sets $B_1, B_2, \ldots, B_l$ depending on the types of $mr(v \mid W)$. Hence, the multisimilar function f of $u\ R_W\ v$ has the property that, for every vertex $w \in A_i$, there is a vertex $w' \in B_i$ such that

$$f(w) = w', \tag{19}$$

where $1 \le i \le l$. Indeed, there are $r_1!r_2!\cdots r_l!$ distinct multisimilar functions of $u\ R_W\ v$. These observations yield the following result.

Theorem 6. *Let W be a set of vertices of a connected graph G and let u and v be vertices of G such that $u \in [v]_W$. Suppose that $mr(u \mid W) = \{r_1 \cdot a_1, r_2 \cdot a_2, \ldots, r_l \cdot a_l\}$, where $a_1 < a_2 < \cdots < a_l$ and r_i is a repetition number of type a_i for each i with $1 \le i \le l$. Then*

(i) *$mr(v \mid W) = \{r_1 \cdot b_1, r_2 \cdot b_2, \ldots, r_l \cdot b_l\}$ for some integers $b_1, b_2, \ldots, b_l$ with $b_1 < b_2 < \cdots < b_l$,*

(ii) *there is a multisimilar function f of $u\ R_W\ v$ such that $f(w_i) = w_i'$, where $d(u, w_i) = a_i$ and $d(v, w_i') = b_i$ for each i with $1 \le i \le l$,*

(iii) *there are $r_1!r_2!\cdots r_l!$ distinct multisimilar functions of $u\ R_W\ v$.*

By Theorem 6, the following result is obtained.

Corollary 7. *Let W be a set of vertices of a connected graph G and let u and v be vertices of G such that $u \in [v]_W$ with a multisimilar constant $c_W(u,v)$. Then*

(i) *if M_1 and M_2 are the maximum elements of $mr(u \mid W)$ and $mr(v \mid W)$, respectively, then $M_1 = M_2 + c_W(u,v)$,*

(ii) *if m_1 and m_2 are the minimum elements of $mr(u \mid W)$ and $mr(v \mid W)$, respectively, then $m_1 = m_2 + c_W(u,v)$.*

Proof. Suppose that $u \in [v]_W$. Let $mr(u \mid W) = \{r_1 \cdot a_1, r_2 \cdot a_2, \ldots, r_l \cdot a_l\}$ and $mr(v \mid W) = \{r_1 \cdot b_1, r_2 \cdot b_2, \ldots, r_l \cdot b_l\}$, where $a_1 < a_2 < \cdots < a_l$ and $b_1 < b_2 < \cdots < b_l$. Since M_1 and M_2 are the maximum elements of $mr(u \mid W)$ and $mr(v \mid W)$, respectively, there are vertices w and w' in W such that $M_1 = d(u,w) = a_l$ and $M_2 = d(v,w') = b_l$. It follows by Theorem 6 that there is a multisimilar function f of $u\ R_W\ v$ such that $f(w) = w'$. Then $d(u,w) = d(v,w') + c_W(u,v)$, where $c_W(u,v)$ is a multisimilar constant. Thus, (i) holds. For (ii), the statement may be proven in the same way as (i), and therefore such proof is omitted. □

Next, we are prepared to establish the upper bound for the cardinality of a multisimilar equivalence class of a vertex in a connected graph. To show this, let us present a useful proposition as follows.

Proposition 8. *Let W be a set of vertices of a connected graph G and let u and v be vertices of G such that $u \in [v]_W$. Then $mr(u \mid W)$ and $mr(v \mid W)$ have the same minimum (or maximum) element if and only if $mr(u \mid W) = mr(v \mid W)$.*

Proof. If $mr(u \mid W) = mr(v \mid W)$, then the minimum (and maximum) elements of $mr(u \mid W)$ and $mr(v \mid W)$ are the same. For the converse, assume that m_1 and m_2 are the minimum elements of $mr(u \mid W)$ and $mr(v \mid W)$, respectively, such that $m_1 = m_2$. Since $u \in [v]_W$, there is a multisimilar constant $c_W(u,v)$ such that

$$\begin{aligned} mr(u \mid W) &= mr(v \mid W) \\ &\quad + \{c_W(u,v), c_W(u,v), \ldots, c_W(u,v)\}. \end{aligned} \tag{20}$$

By Corollary 7 (ii), it follows that $m_1 = m_2 + c_W(u,v)$. Thus, $c_W(u,v) = 0$. Hence, $mr(u \mid W) = mr(v \mid W)$. Similarly, if $mr(u \mid W)$ and $mr(v \mid W)$ have the same maximum element, then $mr(u \mid W) = mr(v \mid W)$. □

Theorem 9. *If W is a multiresolving set of a connected graph G, then the cardinality of multisimilar equivalence class of each vertex of G with respect to W is at most* $\mathrm{diam}(G) + 1$.

Proof. Assume, to the contrary, that there is a vertex v of G such that $[v]_W$ has the cardinality at least $\mathrm{diam}(G) + 2$. Since the minimum elements of multirepresentations of vertices in $[v]_W$ with respect to W have at most $\mathrm{diam}(G) + 1$ distinct values, there are at least two vertices x and y in $[v]_W$ having the same value of the minimum element of $mr(x \mid W)$ and $mr(y \mid W)$. It follows by Proposition 8 that $mr(x \mid W) = mr(y \mid W)$, contradicting the fact that W is a multiresolving set of G. □

We can show that the upper bound in Theorem 9 is sharp. Consider the path $P_n = (v_1, v_2, \ldots, v_n)$. We have that $\mathrm{diam}(P_n) = n-1$ and the set $W = \{v_1\}$ is a multiresolving set of P_n. Thus, $[v_1]_W$ contains all vertices of P_n, and so $|[v_1]_W| = n$.

In the last result, we describe the properties of a multisimilar equivalence classes with respect to a set of vertices.

Theorem 10. *Let u and v be vertices of a connected graph G and let W be a set of vertices of G. Then*

(i) *if $[u]_W \ne [v]_W$, then $mr(x \mid W) \ne mr(y \mid W)$ for all $x \in [u]_W$ and $y \in [v]_W$,*

(ii) *if $[u]_W = \{u\}$ for all $u \in V(G)$, then W is a multiresolving set of G.*

Proof. (i) Assume, to the contrary, that there exist two distinct vertices $x \in [u]_W$ and $y \in [v]_W$ such that $mr(x \mid W) = mr(y \mid W)$. Then there are multisimilar constants $c_W(x,u)$ and $c_W(y,v)$ such that $mr(x \mid W) = mr(u \mid W) + \{c_W(x,u), c_W(x,u), \ldots, c_W(x,u)\}$ and $mr(y \mid W) = mr(v \mid W) + \{c_W(y,v), c_W(y,v), \ldots, c_W(y,v)\}$. Therefore,

$$\begin{aligned} &mr(u \mid W) + \{c_W(x,u), c_W(x,u), \ldots, c_W(x,u)\} \\ &\quad = mr(v \mid W) \\ &\qquad + \{c_W(y,v), c_W(y,v), \ldots, c_W(y,v)\}. \end{aligned} \tag{21}$$

Thus, $mr(u \mid W) = mr(v \mid W) + \{c_W(y,v) - c_W(x,u), c_W(y,v) - c_W(x,u), \ldots, c_W(y,v) - c_W(x,u)\}$. Hence, u belongs to $[v]_W$, which is a contradiction.

(ii) Assume, to the contrary, that W is not a multiresolving set of G. Then there exist two distinct vertices x and y such that $mr(x \mid W) = mr(y \mid W)$. Hence, y belongs to $[x]_W$, producing a contradiction. □

4. Final Remarks

The complete graph K_n is only one graph that its dimension is $n-1$ but not so for multidimensions. It follows by [10, 11] that the multidimension of complete graph is not defined. Thus, (5) leads us to the conjecture:

> If G is a connected graph such that $\dim_M(G)$ is defined, then $\dim_M(G) \leq n-2$.

Conflicts of Interest

The authors declare that they have no conflicts of interest.

Acknowledgments

This work was funded by the Faculty of Science, Srinakharinwirot University.

References

[1] G. Chartrand, L. Eroh, M. A. Johnson, and O. R. Oellermann, "Resolvability in graphs and the metric dimension of a graph," *Discrete Applied Mathematics*, vol. 105, no. 1-3, pp. 99–113, 2000.

[2] F. Harary and R. A. Melter, "On the metric dimension of a graph," *Ars Combinatoria*, vol. 2, pp. 191–195, 1976.

[3] P. J. Slater, "Leaves of trees," *Congressus Numerantium*, vol. 14, pp. 549–559, 1975.

[4] P. J. Slater, "Dominating and reference sets in a graph," *Journal of Mathematical and Physical Sciences*, vol. 22, no. 4, pp. 445–455, 1988.

[5] M. Johnson, "Browsable structure-activity datasets," in *Advances in Molecular Similarity Volume 2*, vol. 2 of *Advances in Molecular Similarity*, pp. 153–170, Elsevier, 1999.

[6] B. L. Hulme, A. W. Shiver, and P. J. Slater, *FIRE, a subroutine for fire protection network analysis (SAND 81–1261)*, Sandia National Laboratories, New Mexico, 1981.

[7] B. L. Hulme, A. W. Shiver, and P. J. Slater, *Computing minimum cost fire protection (SAND 820809*, Sandia National Laboratories, New Mexico, 1982.

[8] B. L. Hulme, A. W. Shiver, and P. J. Slater, "A Boolean Algebraic Analysis of Fire Protection," *North-Holland Mathematics Studies*, vol. 95, no. C, pp. 215–227, 1984.

[9] S. Khuller, B. Rsghavachari, and A. Rosenfeld, *Localization in graphs (CS-TR-3326)*, University of Maryland, Maryland, 1994.

[10] V. Saenpholphat, "On multiset dimension in graphs," *Academic SWU*, vol. 1, pp. 193–202, 2009.

[11] R. Simanjuntak, T. Vetrík, and P. B. Mulia, "The multiset dimension of graphs," *Discrete Applied Mathematics*.

Permissions

 Every chapter published in this book has been scrutinized by our experts. Their significance has been extensively debated. The topics covered herein carry significant findings which will fuel the growth of the discipline. They may even be implemented as practical applications or may be referred to as a beginning point for another development.

The contributors of this book come from diverse backgrounds, making this book a truly international effort. This book will bring forth new frontiers with its revolutionizing research information and detailed analysis of the nascent developments around the world.

We would like to thank all the contributing authors for lending their expertise to make the book truly unique. They have played a crucial role in the development of this book. Without their invaluable contributions this book wouldn't have been possible. They have made vital efforts to compile up to date information on the varied aspects of this subject to make this book a valuable addition to the collection of many professionals and students.

This book was conceptualized with the vision of imparting up-to-date information and advanced data in this field. To ensure the same, a matchless editorial board was set up. Every individual on the board went through rigorous rounds of assessment to prove their worth. After which they invested a large part of their time researching and compiling the most relevant data for our readers.

The editorial board has been involved in producing this book since its inception. They have spent rigorous hours researching and exploring the diverse topics which have resulted in the successful publishing of this book. They have passed on their knowledge of decades through this book. To expedite this challenging task, the publisher supported the team at every step. A small team of assistant editors was also appointed to further simplify the editing procedure and attain best results for the readers.

Apart from the editorial board, the designing team has also invested a significant amount of their time in understanding the subject and creating the most relevant covers. They scrutinized every image to scout for the most suitable representation of the subject and create an appropriate cover for the book.

The publishing team has been an ardent support to the editorial, designing and production team. Their endless efforts to recruit the best for this project, has resulted in the accomplishment of this book. They are a veteran in the field of academics and their pool of knowledge is as vast as their experience in printing. Their expertise and guidance has proved useful at every step. Their uncompromising quality standards have made this book an exceptional effort. Their encouragement from time to time has been an inspiration for everyone.

The publisher and the editorial board hope that this book will prove to be a valuable piece of knowledge for researchers, students, practitioners and scholars across the globe.

List of Contributors

Shaibu Osman
Department of Mathematics, Pan African University, Institute for Basic Sciences, Technology and Innovations, Nairobi, Kenya

Oluwole Daniel Makinde
Faculty of Military Science, Stellenbosch University, Saldanha 7395, South Africa

Asmiati and I. Ketut Sadha Gunce Yana
Mathematics Department, Faculty of Mathematics and Natural Sciences, Lampung University, Jl. Brodjonegoro No.1 Bandar Lampung, Indonesia

Lyra Yulianti
Mathematics Department, Faculty of Mathematics and Natural Sciences, Andalas University, Kampus UNAND Limau Manis, Padang 25163, Indonesia

Paul Bracken
Department of Mathematics, University of Texas, Edinburg, TX 78540, USA

Fumio Hiroshima
Faculty of Mathematics, Kyushu University, Fukuoka 819-0385, Japan

Susumu Osawa
Faculty of Science, Department of Mathematics, Hokkaido University, Sapporo, Hokkaido 060-0810, Japan

Zeraoulia Rafik
University Batna, Algeria

Alvaro H. Salas
Universidad Nacional de Colombia, Colombia

David L. Ocampo
Universidad Nacional de Colombia, Colombia
Universidad de Caldas-Colombia, Colombia

Wayan Somayasa and Gusti N. Adhi Wibawa
Department of Mathematics, Haluoleo University, Kendari, Indonesia

La Hamimu and La Ode Ngkoimani
Department of Geological Engineering, Haluoleo University, Kendari, Indonesia

Patcharapan Jumnongnit and Kittikorn Nakprasit
Department of Mathematics, Faculty of Science, Khon Kaen University, Khon Kaen 40002, Thailand

Jairos Kahuru and Yaw Nkansah-Gyekye
School of Computational and Communication Science and Engineering, Nelson Mandela African Institution of Science and Technology, Arusha, Tanzania

Livingstone S. Luboobi
School of Computational and Communication Science and Engineering, Nelson Mandela African Institution of Science and Technology, Arusha, Tanzania
Department of Mathematics, Makerere University, Kampala, Uganda

Mohammad Imam Utoyo, Windarto and Aminatus Sa'adah
Department of Mathematics, Faculty of Science and Technology, Universitas Airlangga, Indonesia

Sung Myung
Department of Mathematics Education, Inha University, 253 Yonghyun-dong, Nam-gu, Incheon 402-751, Republic of Korea

Gargi Tyagi and Shalini Chandra
Department of Mathematics & Statistics, Banasthali University, Rajasthan 304022, India

Fatmawati, Endrik Mifta Shaiful and Mohammad Imam Utoyo
Department of Mathematics, Faculty of Science and Technology, Universitas Airlangga, Surabaya 60115, Indonesia

Somphong Jitman and Chakrit Phongthai
Department of Mathematics, Faculty of Science, Silpakorn University, Nakhon Pathom 73000, Thailand

Litegebe Wondie and Satish Kumar
Department of Mathematics, College of Natural and Computational Science, University of Gondar, Gondar, Ethiopia

Ngurah Anak Agung Gede
Department of Civil Engineering, Universitas Merdeka Malang, Jl. Taman Agung No. 1, Malang 65146, Indonesia

Adiwijaya
School of Computing, Telkom University, Jl. Telekomunikasi No. 1, Bandung 40257, Indonesia

James E. Marengo, David L. Farnsworth and Lucas Stefanic
School of Mathematical Sciences, Rochester Institute of Technology, Rochester, NY 14623, USA

Titus Okello Orwa, Rachel Waema Mbogo and Livingstone Serwadda Luboobi
Institute of Mathematical Sciences, Strathmore University Nairobi, Kenya

Nur Inayah
Mathematics Department, Faculty of Sciences and Technology, State Islamic University of Syarif Hidayatullah, Jakarta, Indonesia

I. Wayan Sudarsana, Selvy Musdalifah and Nurhasanah Daeng Mangesa
Combinatorial and Applied Mathematics Research Group (CAMRG), Department of Mathematics, Faculty of Mathematics and Natural Sciences, Tadulako University, Palu, Indonesia

Agus Suryanto, Isnani Darti and Syaiful Anam
Department of Mathematics, Brawijaya University, Jl. Veteran, Malang 65145, Indonesia

Yuliang Yin and Bingbing Wang
School of Economics, Beijing Technology and Business University, Beijing 100048, China

Vladimir Bochkarev and Eduard Lerner
Kazan (Volga Region) Federal University, 18 St. Kremlevskaya, Kazan 420008, Russia

Farsam Misagh
Department of Mathematics and Statistics, Tabriz Branch, Islamic Azad University, Tabriz, Iran

Joseph Vade Burnett, Sam Grayson, Zachary Sullivan, Richard Van Natta and Luke Bang
The University of Texas at Dallas, 800WCampbell Rd, Richardson, TX, USA

Varanoot Khemmani and Supachoke Isariyapalakul
Department of Mathematics, Srinakharinwirot University, Sukhumvit 23, Bangkok 10110, Thailand

Index